หนังสือภาษาอังกฤษ

รายงานวิจัยฉบับสมบูรณ์

สูตรที่เหมาะสมต่อพฤติกรรมทางกลและการคืบของวัสดุผสมพอลิโพรพิลีนรีไซเคิลและผงไม้ยางพารา

Optimal Formulation of Recycled Polypropylene/Rubberwood Flour Composites on Mechanical and Creep Behaviors

ผู้ช่วยศาสตราจารย์ ดร.ธเนศ รัตนวิไล ภาควิชาวิศวกรรมอุตสาหการ คณะวิศวกรรมศาสตร์
รองศาสตราจารย์ ดร.วิริยะ ทองเรือง ภาควิชาวิศวกรรมเครื่องกล คณะวิศวกรรมศาสตร์
ผู้ช่วยศาสตราจารย์ ดร.สุกฤทธิรา รัตนวิไล ภาควิชาวิศวกรรมเคมี คณะวิศวกรรมศาสตร์

โครงการวิจัยนี้ได้รับทุนสนับสนุนจาก งบประมาณแผ่นดิน
มหาวิทยาลัยสงขลานครินทร์
ประจำปีงบประมาณ 2555 รหัสโครงการ ENG5500285

บทคัดย่อ

วัสดุผสมไม้พลาสติกถูกผลิตโดยการใช้พอลิโพรพิลีนรีไซเคิลและผงไม้ยางพารา พอลิโพรพิลีนที่ผ่านการใช้งานและวัสดุเหลือใช้ไม้ยางพาราถูกใช้เป็นวัสดุหลัก ในบางสูตรของวัสดุผสมถูกผลิตโดยพอลิโพรพิลีนบริสุทธิ์เพื่อการศึกษาเปรียบเทียบ ในการขึ้นรูปวัสดุผสมทำการผลิตโดยใช้เครื่องอัดรีดแบบเกลียวคู่ และสูตรที่ใช้ผลิตมาจากการออกแบบการทดลองแบบผสม (Mixture experimental design) ซึ่งประกอบด้วยส่วนผสมของพอลิโพรพิลีน ผงไม้ยางพารา สารคู่ควบ สารต้านทานรังสียูวี และสารหล่อลื่น จากนั้นศึกษาสมบัติทางกล ทางสัณฐานวิทยา ความคงทน และการเสถียรทางรูปร่างของวัสดุผสม สมบัติเหล่านี้ของวัสดุผสมถูกศึกษาเพื่อหาปริมาณที่เหมาะสมของส่วนผสม และเพื่อประเมินผลกระทบของส่วนผสม นอกจากนี้เพื่อพัฒนาวัสดุผสมเป็นผลิตภัณฑ์ทางการก่อสร้าง พฤติกรรมการคืบ การทำนายอายุการใช้งาน และผลกระทบของความหนาแน่นที่อัดรีดถูกศึกษาเช่นเดียวกัน

การทดสอบแช่น้ำระยะยาว (10 สัปดาห์) ของวัสดุผสมพบว่า การดูดซับน้ำและการบวมเพิ่มขึ้นตามปริมาณผงไม้ที่เพิ่มขึ้นในวัสดุผสม และวัสดุผสมพอลิโพรพิลีนรีไซเคิลดูดซับน้ำและบวมมากกว่าวัสดุผสมพอลิโพรพิลีนบริสุทธิ์ในส่วนผสมที่มีผงไม้ 45 เปอร์เซ็นต์โดยน้ำหนัก (wt%) การเติมสารคู่ควบ 3 wt% ลดการดูดซับน้ำและการบวม แต่การเติม 1 wt% ของสารต้านทานรังสียูวีเพิ่มการดูดซับน้ำและการบวม ความแข็งแรงและมอดูลัสดัดของวัสดุผสมลดลงอย่างมีนัยสำคัญตามการดูดซับน้ำ อย่างไรก็ตามการดูดซับน้ำน้อยกว่า 3% มีผลกระทบอย่างไม่มีนัยสำคัญต่อความแข็งแรงดัด นอกจากนี้จากการทดสอบวัสดุผสมในสภาวะสภาพแวดล้อมทางธรรมชาติ (Natural weathering test) พบว่า ค่าความเป็นสีขาว (Lightness) และการเปลี่ยนสีของวัสดุผสมมีการเปลี่ยนแปลงอย่างชัดเจน เช่นเดียวกันค่าความแข็งแรงและมอดูลัสดัดมีการสูญเสียอย่างช้าๆ หลังจากทดสอบในสภาพแวดล้อมทางธรรมชาติ วัสดุผสมพอลิโพรพิลีนบริสุทธิ์มีการเปลี่ยนแปลงค่าความเป็นสีขาวและการสูญเสียค่าความแข็งและสมบัติการดัดที่น้อยกว่าวัสดุผสมพอลิโพรพิลีนรีไซเคิล ในขณะที่การเพิ่มขึ้นของปริมาณผงไม้ในวัสดุผสมจาก 25 ถึง 45 wt% พบว่า เพิ่มการเปลี่ยนแปลงค่าความเป็นสีขาวและการสูญเสียสมบัติการดัด อย่างไรก็ตามการเติมสารต้านทานรังสียูวี 1 wt% ลดการเปลี่ยนแปลงค่าความเป็นสีขาวและการสูญเสียของค่าความแข็ง ความแข็งแรงดัด มอดูลัสดัด และความเครียดสูงสุด

การคืบลดลงเมื่อปริมาณผงไม้ในวัสดุผสมเพิ่มขึ้น และวัสดุผสมระหว่างพอลิโพรพิลีนบริสุทธิ์และผงไม้ยางพาราแสดงการคืบที่ต่ำกว่าวัสดุผสมพอลิโพรพิลีนรีไซเคิล ในขณะที่การเติม 5 wt% ของสารคู่ควบ และ 1 wt% ของสารต้านทานรังสียูวีพบว่า เพิ่มการคืบของวัสดุผสม นอกจากนี้ความแข็งแรงดัด อัด และดึงของวัสดุผสมพอลิโพรพิลีนรีไซเคิลและผงไม้ยางพาราเพิ่มขึ้น

เมื่อเติมผงไม้เกิน 25 wt% ในขณะที่ค่ามอดูลัสและความแข็งเพิ่มขึ้นอย่างเป็นเส้นตรงตามปริมาณผงไม้ที่เพิ่มขึ้น และวัสดุผสมพอลิโพรพิลีนรีไซเคิลแสดงสมบัติทางกลที่ต่ำกว่าวัสดุผสมพอลิโพรพิลีนบริสุทธิ์ การเติมสารคู่ควบ 4 wt% ในวัสดุผสมถูกแนะนำเพื่อประโยชน์ทางความประหยัดและสมบัติทางกลที่ดี อย่างไรก็ตามการเติมสารต้านทานรังสียูวี 1 wt% ลดค่าความแข็ง ความแข็งแรง และมอดูลัสของวัสดุผสม นอกจากนั้นพบว่าสูตรที่เหมาะสมของวัสดุผสมบนพื้นฐานของสมบัติทางกลประกอบด้วย พอลิโพรพิลีนรีไซเคิล 50.3 wt% ผงไม้ยางพารา 44.5 wt% สารคู่ควบ 3.9 wt% สารต้านทานรังสียูวี 0.2 wt% และสารหล่อลื่น 1 wt% ซึ่งมีความหนาแน่น 1.085 g/cm^3 สูตรวัสดุผสมที่ได้ถูกนำมาใช้เพื่อศึกษาการคืบ การทำนายอายุการใช้งาน ผลกระทบของความหนาแน่นที่อัดรีดและการประมาณต้นทุน จากการทดลองพบว่า การคืบเพิ่มขึ้นตามเวลา อุณหภูมิ และความเค้นที่เพิ่มขึ้น และ Burger, Power law และ HRZ models สามารถทำนายพฤติกรรมการคืบได้เป็นอย่างดี อย่างไรก็ตามที่ระดับอุณหภูมิและความเค้นสูงๆ Power law และ HRZ models ทำนายการคืบได้ไม่ดีนัก นอกจากนี้หลักการซ้อนทับกันระหว่างเวลาและอุณหภูมิ (Time-temperature superposition; TTS) และระหว่างเวลาและความเค้น (Time-stress superposition; TSS) ถูกนำมาใช้เช่นเดียวกันเพื่อทำนายพฤติกรรมการคืบระยะยาว เส้นโค้งการคืบหลักจาก TTS และ TSS แสดงพฤติกรรมการคืบที่ไม่แตกต่างกัน เช่นเดียวกัน TSS ทำนายอายุการใช้งานโดยการคืบระยะยาวเกินกว่า 10 ปี เมื่อวัสดุผสมรองรับโหลด 15 MPa ที่อุณหภูมิ 25 องศาเซลเซียส นอกจากนั้นสมบัติความแข็ง การดัด การดึง การอัด และความแข็งแรงที่ถอนสกรูและตะปูพบว่า ลดลงเมื่อความหนาแน่นของวัสดุผสมลดลง และเมื่อประมาณต้นทุนของผลิตภัณฑ์แผ่นเรียบจากวัสดุผสมพอลิโพรพิลีนรีไซเคิลและผงไม้ยางพาราขนาด 25 มม × 50 มม × 1000 มม มีราคาประมาณ 388 บาทต่อท่อน

ABSTRACT

Wood-plastic composites (WPCs) were made from recycled polypropylene (rPP) and rubberwood flour (RWF) as reinforcement. Post-consumer polypropylene and rubberwood waste were used as main materials. Some formulations of WPCs were also produced with virgin polypropylene (vPP) for comparative studies. WPC panels were manufactured by using twin-screw extruder based on formulations designed with mixture experiment, the components being rPP, RWF, maleic anhydride-grafted polypropylene (MAPP), ultraviolet (UV) stabilizer, and lubricant (Lub). Mechanical properties, morphology, durability, and dimensional stability of WPCs were studied. These characterizations of WPCs were investigated to optimize the mixture ratios for composites made from rPP and RWF, and to assess effect of compositions. Likewise, to develop composites as building products creep, lifetime prediction, and extruded density effect were also examined.

Long-term water immersion test of the PP/RWF composites over a period of 10 weeks revealed that both water absorption (WA) and thickness swelling (TS) increased with wood flour content. rPP gave higher WA and TS than vPP, for the composites with 45 wt% RWF. An addition of MAPP at 3 wt% reduced WA and TS, with no further benefit reached at 5 wt% MAPP. In contrast, addition of 1 wt% UV stabilizer increased the WA and TS of composites. The flexural strength (MOR) and modulus (MOE) of composites reduced significantly with moisture uptake; however, at WA less than 3% its effects on MOR were not significant. From natural weathering test, PP/RWF composites sharply changed lightness (L^*) and discoloration, and slightly lost in MOR and MOE after the weathering. vPP gave lower percentage change of L^* and loss percentage of hardness, MOR and MOE than rPP. Increasing RWF content from 25 to 45 wt% in composites increased the change of L^* and loss of MOR, MOE, and maximum strain. Addition of 1 wt% UV stabilizer reduced change of L^* and loss of hardness, MOR, MOE, and maximum strain.

Creep reduced as the wood flour level increased. The neat vPP and composites based on vPP exhibited lower creep than those based on rPP. The additions of 5 wt% MAPP and 1 wt% UV stabilizer contents increased the creep strain

of composites. Furthermore, strengths (flexure, compression, and tension) of RWF reinforced rPP composites could be enhanced with increasing wood flour contents beyond 25 wt%. The modulus and hardness of composites (both virgin and recycled plastics) increased linearly with wood flour loadings in range of 25-45 wt%. The unfilled rPP and composites based on rPP exhibited lower mechanical properties than those based on vPP. The addition level of 4.0 wt% MAPP in the rPP/RWF composites is suggested for economical benefit and good mechanical properties. The strength, modulus, and hardness of composites were reduced by an addition of 1 wt% UV stabilizer content. Besides, the optimal formulation based on the mechanical properties found was 50.3 wt% rPP, 44.5 wt% RWF, 3.9 wt% MAPP, 0.2 wt% UV stabilizer, and 1.0 wt% lubricant. This optimal composite formulation was used to investigate creep, lifetime prediction, extruded density effect, and cost estimation. Creep increased with time, temperature, and stress. The Burger, Power law, and HRZ models fit the creep profiles well in general, but at high temperature and stress levels the Power law and HRZ models could not performed well. Time-temperature superposition (TTS) and time-stress superposition (TSS) principles were used to model long-term creep. The master curves from TTS and TSS principles were in good agreement with each other. TSS predicted that the lifetime limitation by long-term creep exceeds 10 years for 15 MPa stress at 25 $^{\circ}$C. In addition, properties of hardness, flexure, tension, compression, and screw and nail withdrawal strengths decreased with the decrease of extruded density. Estimated cost of decking product with dimension of 25 mm x 50 mm x 1000 mm is approximately 388 baht per piece.

ACKNOWLEDGEMENTS

We would like to acknowledge the Department of Industrial Engineering and Department of Mechanical Engineering, Prince of Songkla University, for the machine supports. And, we would like to acknowledge all the technical staffs, academic staffs, and colleagues at Department of Industrial Engineering for their invaluable assistances during my research work. In addition, special thank goes to Faculty of Science and Technology, Prince of Songkla University, Pattani Campus and Mr. Somkit Srisuwan for their offering the twin-screw extruder machine and their friendly hospitality during my visit.

We are also immensely grateful the financial support from the graduate school of Prince of Songkla University, the Government budget Fund (Research Grant Code: 2555A11502062), and Rubberwood Technology and Management Research Group (ENG-54-27-11-0137-S) of Faculty of Engineering, Prince of Songkla University.

Thanate Ratanawilai

Wiriya Thongruang

Sukritthira Ratanawilai

CONTENTS

CONTENTS (cont.)

CONTENTS (cont.)

CONTENTS (cont.)

CONTENTS (cont.)

CONTENTS (cont.)

CONTENTS (cont.)

CONTENTS (cont.)

CONTENTS (cont.)

LIST OF TABLES

LIST OF TABLES(cont.)

LIST OF TABLES(cont.)

LIST OF TABLES(cont.)

LIST OF FIGURES

LIST OF FIGURES (cont.)

LIST OF FIGURES (cont.)

LIST OF FIGURES (cont.)

LIST OF FIGURES (cont.)

LIST OF FIGURES (cont.)

LIST OF FIGURES (cont.)

LIST OF FIGURES (cont.)

CHAPTER 1

Introduction

1.1 Background

Nowadays, wood-plastic composites (WPCs) have become popular due to recyclability, low density, low cost, low maintenance, and eco-friendliness with good mechanical properties. WPCs are produced by mixing wood fiber into molten plastic matrices as well as coupling agents or the other additives, and then composite materials form through various processing methods such as compression, extrusion or injection molding [1]. WPCs are extensively used in automotive industry as door inner panels, seat backs, and headliners; in construction business as decking, cladding, and fencing; and in infrastructure as marina and boardwalk. Moreover, softwood lumber is increasingly replaced as WPCs and plastic lumber in applications of deck-building because of having better durability than softwood lumber [2, 3], and demand of WPCs is also expected to expand nearly 12% each year between 2000 and 2010 in the United States [3]. Likewise, in comparing the decking demand produced from wood, WPCs, and neat plastic in Table 1.1, it was found that tendency clearly increased the demand of WPCs decking but steadily decreased in the demand of wood decking due to ability to resist water absorption, and providing positive response to environmental issues of WPCs materials [4-6]. As comparing to the neat plastics, WPCs exhibited better thermal stability, mechanical properties, and more degradable resistance to the ultraviolet light [1, 7]. Therefore, they have stimulated a great interest in developing WPC materials for structural applications.

Wood fiber is one of the major materials in WPCs. There are many species of wood that found to produce WPCs such as pine, jute, oil palm empty fruit bunch, bamboo, curaua, including rubberwood. Rubber tree (*Hevea brasiliensis*) is widely planted in the South and the Northeast of Thailand. It is major economic important plant because the latex extracted from the tree is the primary source of

natural rubber. However, when it becomes unproductive at about 25 years of age, it is cut down [8]. The cut rubber tree is generally produced as wood wastes about 34% and plantation wastes about 54%. Only 12% of the rubberwood ends up as the goods [9, 10]. In addition, rubberwood lumber and root could be mainly utilized to manufacture furniture, toys, and packing materials. In these rubberwood industries, a large amount of wood waste in the forms of flour, sawdust, and chips is generated at different stages of processing. Generally, some of the wood waste can be used as raw material to manufacture plywood, particleboard, and medium-density fiberboard [11], but most of such waste is disposed in landfills (dump in space areas) or burning, resulting in pollution issues. Therefore, the utilization of rubberwood waste as filler in polymer composites is great interest, which decreases environmental impacts but increases value of waste. The wastes in the forms of flour, sawdust, and chips have primarily been used as inexpensive filler in plastic industries, to reduce raw material costs and to increase the strength and modulus of various thermoplastics. Moreover, the rubberwood waste reinforced thermoplastics also offers many advantages including biodegradability, renewable character, absence of associated health hazards, and low equipment wear during their processings [12], when compared to synthetic fillers.

Table 1.1 Percentage of decking demand by material [5]

Year	Market ($ billions)	Share of percentage		
		Wood	WPCs	Neat plastic
1992	2.3	97	2	1
2002	3.4	91	7	2
2005	5.1	77	19	4
2006	5.5	73	22	5
2011 (Forecast)	6.5	66	30	4

The other major material of WPCs is plastic acting as a matrix. It was found that the global production of plastics was approximately 1.5 million tons in 1950 but reached 245 million tons in 2008 [13], resulting in a significant contribution

to municipal solid waste. For example, in 2008 post-consumer plastics were generated at least 33.6 million tons in the United States, of which 28.9 million tons went to landfills, 2.6 million tons to combustion and energy recovery, and only 2.2 million tons to recycling [14, 15] – only a tiny fraction of plastic wastes is recycled. The most plastic wastes are typically consisted of polyethylene (PE), polypropylene (PP), polyvinyl chloride (PVC), polyethylene terephthalate (PET), and polystyrene (PS) [16]. Of all these plastic types, PE and PP are large component in landfills and have similarities in their structures and properties [17]; however, when PE (virgin and recycled) was blended with sawdust, it showed lower stiffness and strength than PP (virgin and recycled) mixed the sawdust [18]. In addition, the increasing worldwide production and consumption of plastics have caused serious public concerns about effective and safe disposal [19]; however, plastic wastes could be a promising raw material source for WPCs [18]. The use of recycled plastics for producing WPCs would not only offer an effective disposal of plastic wastes, but also reduces the consumption of natural resources [14, 20]. Therefore, increasing the use of recycled plastics by blending with rubberwood wastes provides the chance of lessening wastes going to landfill, decreasing solid waste disposals, and reducing the costs of making the WPCs [19, 21]. However, to have an effective study, experimental design has to be adopted.

A D-optimal mixture experimental design is a special type of statistical approach to experimentally find the individual effect and interaction of components in a mixture, and the fitted models can be used to find the optimal formulation of a composite material [22]. A D-optimal design can considerably reduce the number of experiments needed for scientific and technical information on the composition ratio. However, recent several publications have assessed the effects of each material component on the thermal and mechanical properties. Mixture designs and factorial designs have been rarely used in experiments on WPCs. For example, a four-factor central composite design was applied to develop a response surface model and to study the foamability of rigid PVC/wood-flour composites [23]. A 2^4 factorial design was used to determine the effects of two hindered amine light stabilizers, a colorant,

an ultraviolet absorber, and their interactions on the photostabilization of wood flour/high-density polyethylene composites [24]. A Box-Behnken design with response surface method was adopted to determine variables influenced board performance significantly [25]. Prior studies on the component effects and interactions, and optimization of the formulation for WPCs, seem not to have used a D-optimal mixture design. Therefore, a D-optimal design was applied to model mechanical and physical characteristics of WPCs.

The usage of WPCs is mostly limited to non-structural interior applications due to the decrease of WPCs stability when exposed to exterior conditions [1]. The main factors affected WPCs properties are humidity, sunlight, and temperature, resulting in change of physical and chemical properties [1, 26, 27]. Due to the hydrophilic nature of lignocellulosic filler, this is a disadvantage impacting the performance of the WPCs [28, 29]. The water absorption characteristics WPCs limit their end-use applications [30], as several mechanical and physical properties, such as dimensional stability, are affected. In addition, the environmental parameters, such as temperature, are the most important variables influenced the creep behavior of WPCs due to the temperature accelerating the creep deformation of WPCs that are subjected a constant load for long term. The evaluation of the creep deformation with temperature is necessary because most polymeric materials exhibit different behaviors under different temperatures [31]. Therefore, when WPCs are applied in different environmental conditions, they are necessary to study the durability and stability of WPCs products as well as effects of the material compositions and environmental conditions [1].

In this research, development of new material for building products needs to be examined the mechanical, physical, dimensional stability, and durability properties of WPCs. The effects of material compositions (including different grades of plastic and the contents of rubberwood flour, coupling agent, and UV stabilizer) on the mechanical and physical properties of composites were also investigated. The new information will facilitate informed decisions regarding manufacture of

composites and helps target the most suitable end-use applications of such composites.

1.2 Objectives

The specific objectives of the research explained in this work are to:

1) Find the optimal mixture ratio of recycled polypropylene/rubberwood flour composites.

2) Predict the creep behavior of recycled polypropylene/rubberwood flour composites.

3) Analyze the effect of extruded density on mechanical and physical properties of recycled polypropylene/rubberwood flour composites.

1.3 Scopes of research

The scopes of the research described in this work are:

1) The ranges of compositions applied in this research were recycled polypropylene 50-70 wt%, rubberwood flour 25-45 wt%, coupling agent 3-5 wt%, ultraviolet stabilizer 0-1 wt%, and lubricant 1 wt%.

2) Mixture experimental design and response surface methodology were used to statistically optimize the formulation of composites and to statistically evaluate the effect of compositions. The design and analysis were generated by Design-Expert software (8.0.6, Stat-Ease, Inc.), according to D-optimal mixture design.

3) Optimal formulation based on the mechanical properties was used to predict the creep behavior for long terms, to analyze the effect of extruded density, and to produce the product of the recycled polypropylene/rubberwood flour composites.

4) Testing for creep behavior prediction of temperature dependence was applied at temperatures of 25, 35, 45, 55, and 65 $^{\circ}$C with constant loads 19 MPa, which calculates from 40 percentage of ultimate flexural strength. Likewise, testing of load dependence applied at loads was 3, 7, 11, 15, 19, 23, 27, 31, 35, and 39 MPa with temperature at 25 $^{\circ}$C. The time duration used of each test was 100 minutes.

5) The optimal formulation based on each property, such as water absorption, weathering resistance, creep behavior, and mechanical properties, was produced using a twin-screw extruder (Model SHJ-36 from En Mach Co., Ltd, Nonthaburi, Thailand). The extruding conditions were as follows: (1) temperature profiles: 130–190 °C; (2) screw rotating speed: 50 rpm; (3) vacuum venting at 9 temperature zones: 0.022 MPa; and (4) melt pressure: 0.10–0.20 MPa. The samples were extruded through a rectangular die with the dimensions of 9 mm × 22 mm and cooled in ambient air.

The overview of this research to the responses and results associated to each stage and chapter is shown in Figure 1.1, as explained below:

1) **Stage 1:** to study the effect of rubberwood flour content and cooling rate on mechanical and physical properties of recycled polypropylene (rPP)/ rubberwood flour (RWF) composites. The formulations for the investigation included with the recycled polypropylene and rubberwood flour, as shown in Figure 1.1. Then each formulation was produced using a twin-screw extruder, which extruded through a rectangular die with the dimensions of 9 mm × 22 mm and cooled in ambient air and water.

2) Test the mechanical and thermal properties, such as flexure, tension, differential scanning calorimeter (DSC), and dynamic mechanical thermal analysis (DMTA) of rPP/RWF composites.

3) Conclude the effects of rubberwood flour content reinforced rPP composites on the mechanical and physical properties.

4) **Stage 2:** to investigate the optimal mixture ratio of rPP/RWF composites on water absorption, weathering resistance, creep behavior, and mechanical properties.

5) Design the experiment by using a D-optimal mixture design principle. The experimental D-optimal mixture design and statistical analysis were done with Design-Expert software (version 8.0.6, Stat-Ease, Inc.). The experimental optimized design had mixture compositions for the manufacture of WPCs, the components being rPP, RWF, maleic anhydride-grafted polypropylene (MAPP), ultraviolet (UV)

stabilizer, and lubricant. The ranges of rPP and RWF contents were used to experimental design obtained from preliminary study and the other compositions were determined following the literature review. Then the software generated the formulations for the experiment.

6) Produce the panel samples following the designed formulations. They were manufactured using the twin-screw extruder, which extruded through a rectangular die with the dimensions of 9 mm × 22 mm and cooled in ambient air.

7) Test the properties of water absorption, thickness swelling, and flexure to optimize formulation based on the water absorption.

8) Test the properties of color change, hardness, and flexure after the specimens exposed to the weathering, and then optimized the formulation based on the weathering resistance.

9) Test creep property of the composites for 100 minutes under a constant stress of 19 MPa and temperature 25 °C, and then optimized the formulation based on the creep behavior.

10) Test the properties of flexure, compression, tension, and hardness, and then optimized the formulation based on the mechanical properties.

11) Conclude the optimal formulation of each property. The application of WPCs always decides based on the mechanical properties, so the optimal formulation based on the mechanical properties was used to study in the next stage.

12) **Stage 3:** to examine creep behavior and effect of extruded density of optimal formulation based on mechanical properties. The evaluation of creep behavior and extruded density is necessary in application for long term and in expanding the product to large sizes, respectively.

13) To investigate the creep behavior at different stress and temperature levels as well as predicting the long-term creep, the panel samples were produced using a twin-screw extruder, which extruded through a rectangular die with the dimensions of 9 mm × 22 mm and cooled in ambient air.

14) The creep tests were conducted at 25 °C ambient temperature at ten different stress levels: 3, 7, 11, 15, 19, 23, 27, 31, 35, and 39 MPa. Five levels of

temperature in the range from 25 to 65 $^{\circ}C$ were used with constant 19 MPa stress to assess temperature effects.

15) The Burger, Power law, and HRZ models were used to fit the creep curves. Likewise, the time-temperature superposition (TTS) and the time-stress superposition (TSS) principles were used to model long-term creep.

16) To investigate the effects of extruded density, the panel samples were produced using a twin-screw extruder, which extruded through rectangular 9 mm × 22 mm, 17 mm × 36 mm, and 25 mm × 50 mm dies with density of 1.085 g/cm^3, 1.029 g/cm^3, and 0.963 g/cm^3, respectively.

17) Test the mechanical and physical properties, such as flexure, tension, compression, hardness, and screw withdrawal strength of rPP/RWF composites.

18) Conclude the effects of the different stress and temperature levels on the creep behavior and the extruded density on the mechanical and physical properties.

19) **Stage 4:** to estimate the cost of rPP/RWF composites. When the new materials are successfully developed, the cost calculation of the products manufactured from such materials is necessary. This research particularly explores the direct material cost and energy cost in processing of decking board produced from new composite materials with dimensions of 25 mm × 50 mm × 1000 mm.

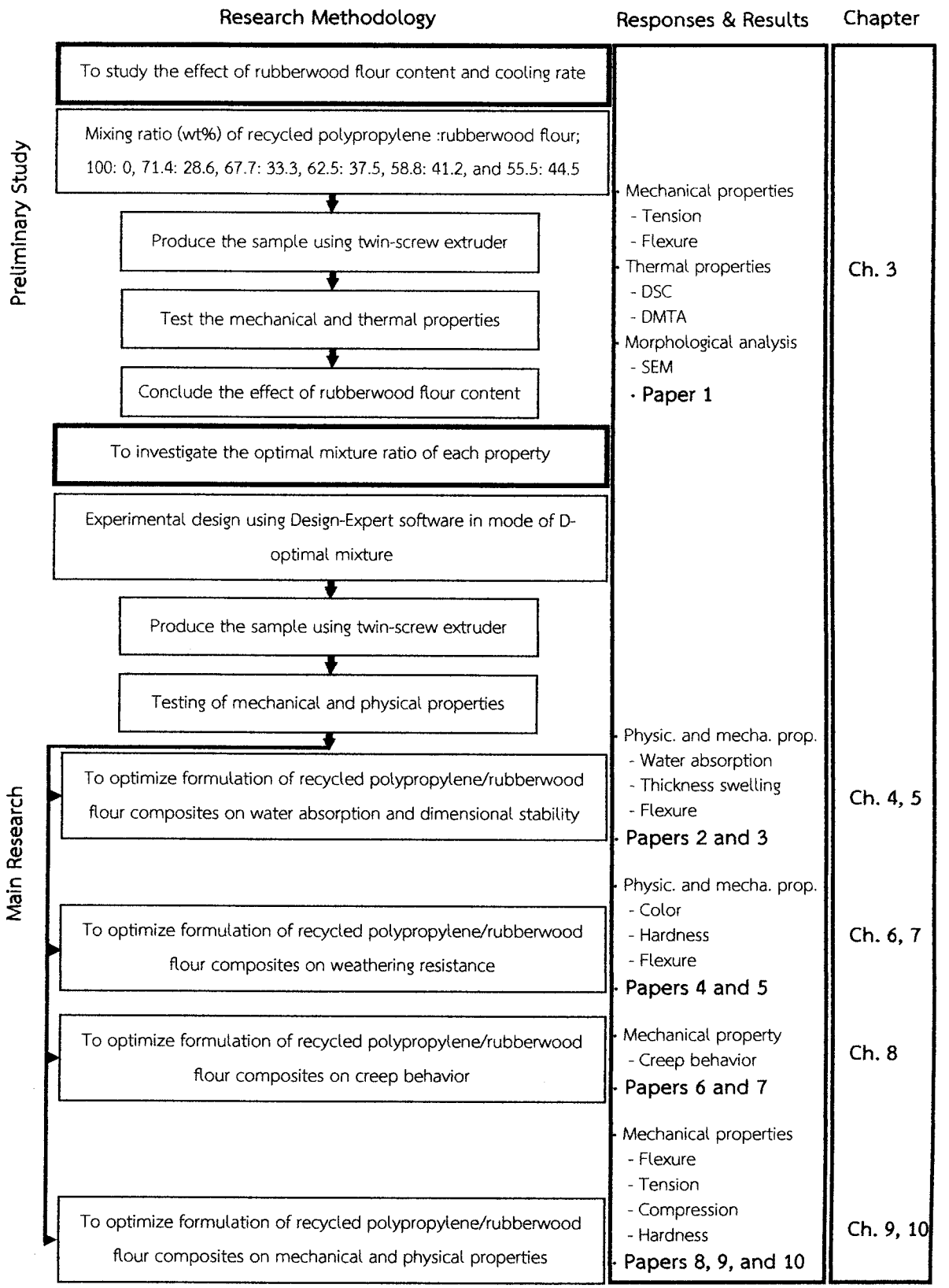

Figure 1.1 The overview of research to the responses and results associated to each stage and chapter

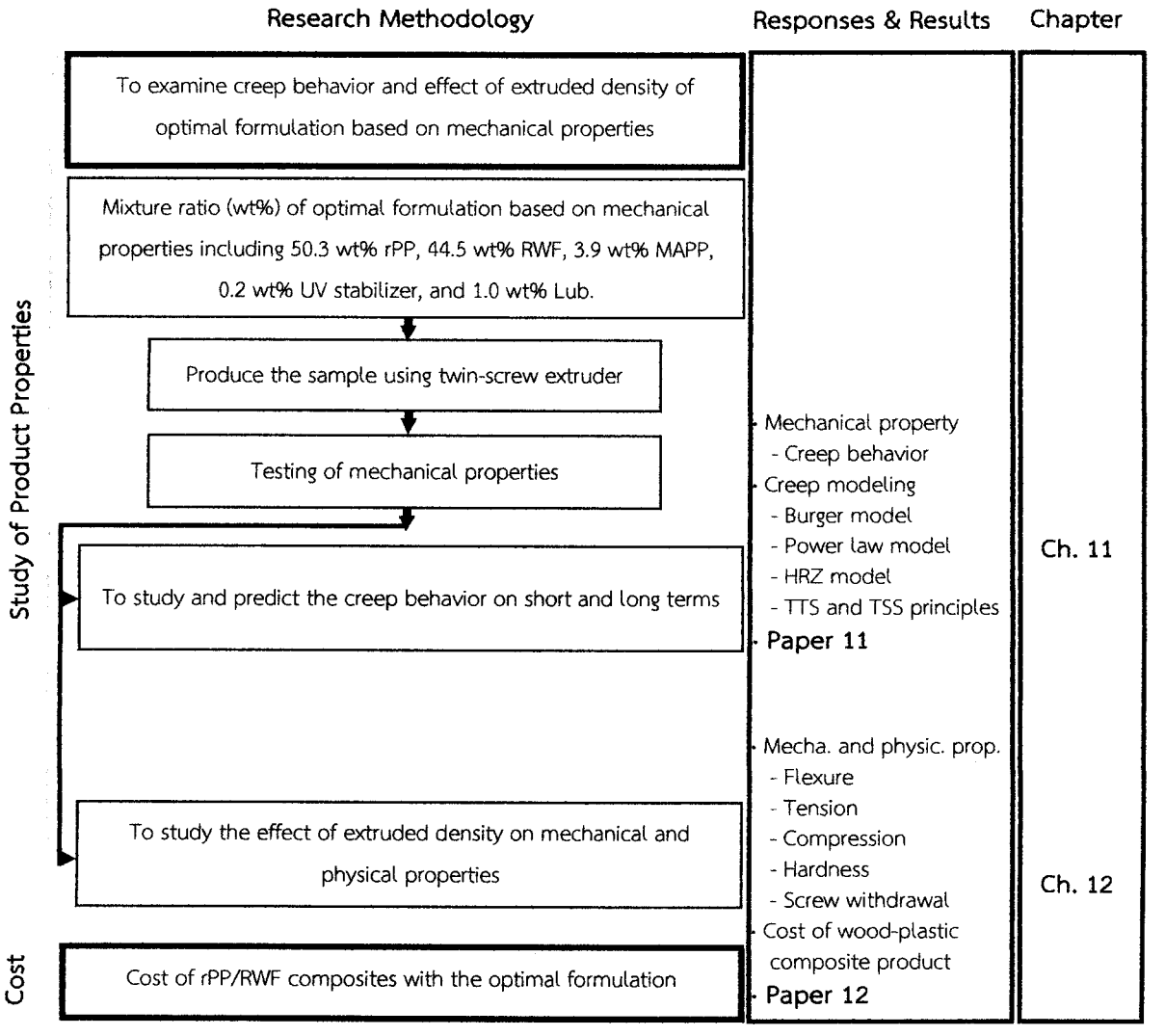

Figure 1.1 The overview of research to the responses and results associated to each stage and chapter (cont.)

1.4 References

[1] K.B. Adhikary. "Development of Wood Flour-Recycled Polymer Composite Panels as Building Materials." Ph.D. dissertation, University of Canterbury, New Zealand, 2008.

[2] D.R. Carroll, R.B. Stone, A.M. Sirignano, R.M. Saindon, S.C. Gose, and M.A. Friedman. "Structural Properties of Recycled Plastic/Sawdust Lumber Decking Planks." *Resources, Conservation and Recycling*, vol. 31, pp. 241–251, 2011.

[3] I. Ganguly and I.L. Eastin. "Trends in the US Decking Market: A National Survey of Deck and Home Builders." *The Forestry Chronicle*, vol. 85, pp. 82–90, 2009.

[4] S. Tamrakar, R.A. Lopez-Anido, A. Kiziltas, and D.J. Gardner. "Time and Temperature Dependent Response of a Wood-Polypropylene Composite." *Composites Part A: Applied Science and Manufacturing*, vol. 42, pp. 834–842, 2011.

[5] A.A. Klyosov. *Wood-Plastic Composites*. Hoboken, New Jersey: John Wiley & Son, Inc., 2007.

[6] T. Ratanawilai, P. Lekanukit, and S. Urapantamas. "Effect of Rubberwood and Palm Oil Content on the Properties of Wood-Polyvinyl Chloride Composites." *Journal of Thermoplastic Composite Materials*, Epub ahead of print 9 August 2012. DOI: 10.1177/0892705712454863.

[7] Optimat Ltd and MERL Ltd. "Wood Plastic Composites Study-Technology and UK Market Opportunities." *The Waste and Resources Action Programme*, pp. 1–100, 2003.

[8] S. Rimdusit, W. Smittakorn, S. Jittarom, and S. Tiptipakorn. "Highly Filled Polypropylene Rubber Wood Flour Composites." *Engineering Journal*, vol. 15, pp. 17–30, 2011.

[9] S. Prasertsan and P. Vanapruk. "Rubber Plantations: An Overlooked Dendropower Option." Food and Agriculture Organazation of the United Nations, Manila, 1998.

[10] P. Petchpradab, T. Yoshida, T. Charinpanitkul, and Y. Matsumura. "Hydrothermal Pretreatment of Rubber Wood for the Saccharification Process." *Industrial and Engineering Chemistry Research*, vol. 48, pp. 4587–4591, 2009.

[11] C. Homkhiew, T. Ratanawilai, and W. Thongruang. "Composites from Recycled Polypropylene and Rubberwood Flour: Effects of Composition on Mechanical Properties." *Journal of Thermoplastic Composite Materials*, Epub ahead of print 14 February 2013. DOI: 10.1177/0892705712475019.

[12] S.L. Favaro, M.S. Lopes, A.G.V.d.C. Neto, R.R.d. Santana, and E. Radovanovic. "Chemical, Morphological, and Mechanical Analysis of Rice Husk/Post-Consumer Polyethylene Composites." *Composites Part A: Applied Science and Manufacturing*, vol. 41, pp. 154–160, 2010.

[13] Plastics Europe. "An Analysis of Plastic Production, Demand and Recovery for 2008 in Europe, the Compelling Facts about Plastics." Brussels: Association of Plastics Manufacturers, 2009.

[14] T. Ratanawilai, N. Thanawattanasirikul, and C. Homkhiew. "Mechanical and Thermal Properties of Oil Palm Wood Sawdust Reinforced Post-Consumer Polyethylene Composites." *ScienceAsia*, vol. 38, pp. 289–294, 2012.

[15] N.J. Themelis, M.J. Castaldi, J. Bhatti, and L. Arsova. "Energy and Economic Value of Non-recycled Plastics and Municipal Solid Wastes that are Currently Landfilled in the Fifty States." *EEC Study of Non-recycled Plastics*, Earth Engineering Center, Columbia University, 2011.

[16] S.E. Selke and I. Wichman. "Wood Fiber/Polyolefin Composites." *Composites Part A: Applied Science and Manufacturing*, vol. 35, pp. 321–326, 2004.

[17] Y. Kazemi, A. Cloutier, and D. Rodrigue. "Mechanical and Morphological Properties of Wood Plastic Composites Based on Municipal Plastic Waste." *Polymer Composites*, vol. 34, pp. 487–493, 2013.

[18] S.K. Najafi, E. Hamidinia, and M. Tajvidi. "Mechanical Properties of Composites from Sawdust and Recycled Plastics." *Journal of Applied Polymer Science*, vol. 100, pp. 3641–3645, 2006.

[19] A. Ashori and S. Sheshmani. "Hybrid Composites made from Recycled Materials: Moisture Absorption and Thickness Swelling Behavior." *Bioresource Technology*, vol. 101, pp. 4717–4720, 2010.

[20] Z.A. Khan, S. Kamaruddin, and A.N. Siddiquee. "Feasibility Study of Use of Recycled High Density Polyethylene and Multi Response Optimization of Injection Moulding Parameters Using Combined Grey Relational and Principal Component Analyses." *Materials and Design*, vol. 31, pp. 2925–2931, 2010.

[21] K.B. Adhikary, S. Pang, and M.P. Staiger. "Dimensional Stability and Mechanical Behaviour of Wood-Plastic Composites based Recycled and Virgin High-Density Polyethylene." *Composites Part B: Engineering*, vol. 39, pp. 807–815, 2008.

[22] Y.B. Khosrowshahi and A. Salem. "Influence of Polyvinyl Alcohol and Carboxymethyl Cellulose on the Reliability of Extruded Ceramic Body: Application of Mixture Design Method in Fabricating Reliable Ceramic Raschig Rings." *International Journal of Applied Ceramic Technology*, vol. 8, pp. 1334–1343, 2011.

[23] L.M. Matuana and F. Mengeloglu. "Manufacture of Rigid PVC/Wood-Flour Composite Foams Using Moisture Contained in Wood as Foaming Agent." *Journal of Vinyl & Additive Technology*, vol. 8, pp. 264–270, 2002.

[24] N.M. Stark and L.M. Matuana. "Ultraviolet Weathering of Photostabilized Wood-Flour-Filled High-Density Polyethylene Composites." *Journal of Applied Polymer Science*, vol. 90, pp. 2609–2617, 2003.

[25] Z. Jun, W. Xiang-Ming, C. Jian-Min, and Z. Kai. "Optimization of Processing Variables in Wood–Rubber Composite Panel Manufacturing Technology." *Bioresource Technology*, vol. 99, pp. 2384–2391, 2008.

[26] A. Wechsler and S. Hiziroglu. "Some of the Properties of Wood–Plastic Composites." *Building and Environment*, vol. 42, pp. 2637–2644, 2007.

[27] D.J. Pooler. "The Temperature Dependent Non-Linear Response of a Wood Plastic Composite." M.S. thesis, Washington State University, United States, 2001.

[28] K.B. Adhikary, S. Pang, and M.P. Staiger. "Long-Term Moisture Absorption and Thickness Swelling Behavior of Recycled Thermoplastics Reinforced with Pinus Radiata Sawdust." *Chemical Engineering Journal*, vol. 142, pp. 190–198, 2008.

[29] D.D. Stokke and D.J. Gardner. "Fundamental Aspects of Wood as a Component of Thermoplastic Composites." *Journal of Vinyl and Additive Technology*, vol. 9, pp. 96–104, 2003.

[30] T.T. Law and Z.A.M. Ishak. "Water Absorption and Dimensional Stability of Short Kenaf Fiber-Filled Polypropylene Composites Treated with Maleated

Polypropylene." *Journal of Applied Polymer Science*, vol. 120, pp. 563–572, 2011.

[31] F.C. Chang, F. Lam, and J.F. Kadla. "Using Master Curves based on Time–Temperature Superposition Principle to Predict Creep Strains of Wood–Plastic Composites." *Wood Science and Technology*, vol. 47, pp. 571–584, 2013.

CHAPTER 2

Theory and Literature Review

2.1 Theory

2.1.1 Natural fiber reinforced plastics

A composite is a combination of two or more materials, which properties of components are different such as polymer: ductile and wood: rigidity, and they are made to become a single material [1]. In composite systems including plastics (both thermoplastic and thermoset) and natural fiber materials, plastic molecules have the role in close contact with surfaces of natural fiber, and then there are some interactions between the surfaces of the two materials [2]. Basically, the reinforcing fibers are the main load-carrying component in the composites, which offers high strength and stiffness as well as resistance to bending and breaking under the applied stress [3]. However, the nature of plastics is nonpolar, which is not compatible with polar wood fibers, thus poor adhesion between plastic and fiber in wood-plastic composites (WPCs) is a result [4]. The strong adhesion between the surfaces of the materials is one of great important factors, which affects the mechanical, physical, and thermal properties. The interface bonding between the plastic matrix and natural fiber can be improved by using coupling agents to achieve the required properties [3]. Another problem affected the properties of WPCs is the processing temperature. Plant fibers are consisted of various chemical components (cellulose, hemicelluloses, and lignin) and therefore their thermal treatments contribute to the changes of physical and chemical properties [4]. Thermal degradation of those fibers affects poor organoleptic properties such as odor and colors and deterioration of their mechanical properties of the composites [4]. In addition, to achieve the desired properties and high performance of the composites, the properties of both the fibers and the matrix are very important factors [3] to be concerned before applying.

2.1.2 Thermoplastic matrices

Nowadays, thermoplastics are considered to be the most important class of plastic materials commercially available [5] in which their consumptions are approximately 80% or more of the total plastic consumption [6]. They have chemical independent macromolecules and the simplest molecular structure [6]. Thermoplastics are softened or melted when heated to a flowable state, and under high pressure they can be pushed or transferred into a cool mold [7]. Thermoplastics do not cure or set, they can be repeated the cycles of heating and cooling without severe damage and allow reprocessing and recycling [6, 7]. In addition, the thermoplastics are often added the additives or fillers to improve specific properties such as mechanical and thermal properties, UV resistance, etc [6].

The thermoplastics have many advantages including recyclability, very short processing cycles, ease of processing, and the melting or softening by heating allowing thermoforming and welding [6]. In contrast, the disadvantages are a decrease in strength and stiffness and high creep and relaxation behaviors with increasing temperature. However, the thermoplastics are popular in the application with WPCs including polyethylene, polypropylene, and polyvinyl chloride.

2.1.2.1 Polyethylene (PE)

Polyethylene is one of the polyolefin family resins and the best-known thermoplastic [7]. It is very few crystalline plastics and will float on water [8]. Polyethylene has excellent chemical resistance, high toughness and ductility, low water vapor permeability, and very low water absorption [7]. Its density is in range of 0.91 to 0.96 g/cm^3 [8], and the increasing density of polyethylene increases the stiffness, yield strength, and melt temperature [7, 9]. However, polyethylene is limited by its low modulus, yield stress, and melting point (melt at 105-130 $^{\circ}$C) [7], which an increase of temperature reduces their properties [9]. Applications of the polyethylene are generally used to make packaging film, bottles, bags, pails, and crates, etc. Furthermore, the most of polyethylene grades is commercially manufactured in three main types: low-density polyethylene, linear low-density

polyethylene, and high-density polyethylene [9]. Chain molecular structures of each polyethylene type are shown in Figure 2.1 [7].

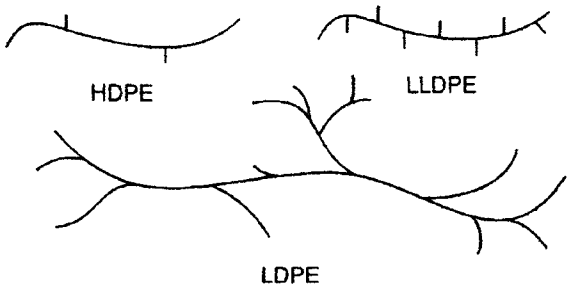

Figure 2.1 Chain molecular structures of each polyethylene type [7]

Low-density polyethylene (LDPE) has macromolecules including numerous short branches, which reduce the crystallinity, melting point, and tensile strength [6]. Its property combines high impact strength, ductility, and toughness, it has therefore used widely in the packaging film industries such as shrink film, thin film for automatic packaging, heavy sacking, and multilayer films [7].

Linear low-density polyethylene (LLDPE) has higher toughness, tensile strength, elongation at break, and puncture resistance than LDPE for the same density [5, 7]. Likewise, LLDPE also has higher production economies than LDPE due to lower temperatures and polymerization pressures [7]. Generally, LLDPE has long linear chain without long side chains or branches, and the density of LLDPE is in range of 0.915 to 0.940 g/cm^3 [7], and it is produced to use in film applications [5].

High-density polyethylene (HDPE) is one of plastics produced the highest-volume goods [7]. Products produced from all polyethylene are approximate 86% having applications of HDPE as raw materials [6]. The most methods of processing HDPE are extrusion, injection molding, compression molding, and blow molding; for example, blow molding is used to manufacture house wares, bottles, drums, bags, toys, pails, and automotive gas tanks and injection molded is used to produce food containers, house wares, garbage pails, toys, and milk cases [7].

2.1.2.2 Polypropylene (PP)

Polypropylene exhibits a similar chemical structure to polyethylene but has better strength, stiffness, and heat resistance [7]. At lower temperatures its impact strength is quite poor [9]. The density of PP is in range of 0.900 to 0.915 g/cm^3, which has the lowest value when compared with the other plastic materials [7].

The properties of the PP will generally depend on the size and type of crystal structure formed, which controlled by varying the rate of cooling and by the incorporation of nucleating agents [5]. Polypropylene has the marked properties such as chemical resistance, dimensional stability, heat resistance, rigidity, toughness, surface gloss, and low cost [7]. However, pure PP generally is not appropriate for use in load-bearing applications due to rapid plastic creeps [7]. In addition, the specific heat of PP is lower than polyethylene. Therefore, the plasticizing capacity of an injection molding machine using PP is higher than a HDPE [5]. Further, due to their excellent quality and versatility, the PP provides the manufacture of products through injection molding, extrusion, and compression molding [7]. PP has extensively used in the textile industry, and the largest use of PP extruded is in thin-film packaging [7].

2.1.2.3 Polyvinyl chloride (PVC)

Polyvinyl chloride is plastics extensively used in the vinyl family and is produced by the polymerization of vinyl chloride in a free radical reaction [7]. In theory the PVC contained by chlorine content is approximate 57% [6] and has the main linear chain branches, but short chain branches may lightly remain [7]. Besides, the glass transition temperature of PVC varies in range of 60 to 80 $^{\circ}$C, which depends on the polymerization method [7].

The raw PVCs are usually unsuitable for desired applications. Therefore, it is necessary to compound the raw PVCs with numerous additives such as fillers, plasticizers, stabilizers, pigment, and lubricant, to satisfy the requirements of customers and applications [1, 6]. PVC has many applications in the field of flame

resistant wire, cable, reinforced hose, conveyor belting and heavy-duty fabrics [1, 7]. In addition, PVC can be generally distinguished into two basic forms: plasticized and rigid. Plasticized PVC is improved by the filling of low-molecular-weight plasticizers to increase flexibility of the polymer. It is used in applications such as floor mats, flexible tubing, garden hose, bottles, and shrink wrap [7]. Rigid PVC exhibits higher rigidity, stronger and stiffer than polypropylene and polyethylene, and therefore is mainly used in products such as extruded pipe, house siding, and thermoformed and injection-molded parts [7].

2.1.3 Natural fiber reinforcement

Natural fibers have been used as reinforcement for over 3000 years, which combine with polymeric materials [10]. They are generally divided into two main types: from animals and plants. Animal fibers are composed of proteins while plant fibers consist of cellulose [4]. Plant fibers are subdivided into three main categories, which depend on the part of the plant: (1) leaf fibers (sisal, henequen, banana, istle, manila hemp, piassava, pine apple, etc.); (2) seed or fruit fibers (cotton, sponge gourd, coir, kapok, oil palm, etc.); and (3) stem or bast fibers (jute, roselle, flax, isora, hemp, nettle, ramie, kenaf, etc.) [10]. Nowadays, many types of natural fibers are popular to reinforce plastic matrix such as pine, jute, oil palm empty fruit bunch, bamboo, curaua, pineapple, rubberwood, etc. Because they offer several advantages including biodegradability, nonabrasive nature, low density, low cost, ecological character, safe fiber handling, high possible filling levels, and low energy consumption [4], when compared with inorganic fillers such as glass fiber and carbon fibers [11].

The natural fiber is one of the great important factors affecting the mechanical, physical, and thermal properties of the WPCs due to the various fiber species, which consist of different contents and components such as cellulose, hemicelluloses, and lignin [12]. The property of each component affects the overall properties of the fiber [13]. The cellulose in the form of cellulose microfibrils presents the framework substance, the hemicelluloses are the matrix substances,

which link between cellulose microfibrils, and the lignin is the encrusting substance of the cell wall associated with the matrix substances [2]. The roles of these three chemical substances in the cell wall are compared to the reinforced plastic in which cellulose, hemicellulose, and lignin corresponds, respectively, to the natural fiber core, plastic matrix, and coupling agent to improve their adhesions [2]. Therefore, the effects of the natural fibers due to species, size, and content are important factor to examine. However, most of the experiment on composite formulations is still conducted by changing the contents of each composition at a time, and the other compositions are constantly fixed in order to investigate the effects of such specific composition. To achieve this study, statistical experimental design is an efficient tool to investigate the effect and interaction of the compositions in WPCs, and it also decreases the number of experiments but increases the scientific information of compositions [14, 15].

2.1.4 Mixture experimental design

A mixture experiment is a special method of response surface experiment in which the variables are the compositions or ingredients of a mixture [16]. The mixture experimental designs are appropriate when the fractions of components in a mixture cannot be changed independently, and their amounts must add up to 100% [17]. For example, if $x_1, x_2,..., x_l$ denote the fractions of l components of a mixture, then [18]

$$0 \le x_i \le 1 \qquad i = 1, 2,..., l$$

and

$$x_1 + x_2 +....+ x_l = 1 \qquad \text{(i.e., 100 percent)}$$

Figure 2.2 shows the constrained experimental region on trilinear coordinate system of three components of the mixture [18]. Each of the three sides of the graph is a mixture, and the nine grid lines in each direction mark off 10% increments in the respective components [16].

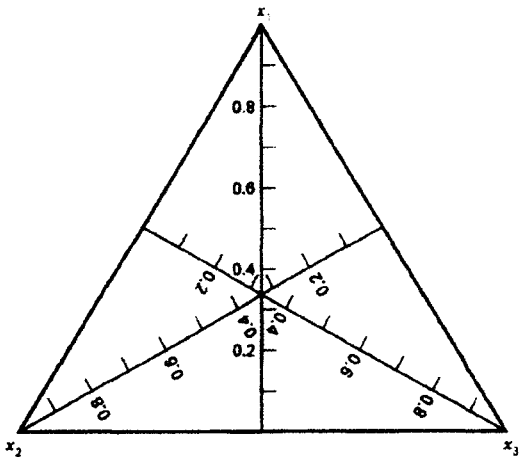

Figure 2.2 Constrained experimental region for a simplex mixture design [18]

In addition, the mixture models differ from the general polynomials applied in response surface work due to the constraint $\sum x_i = 1$ [18]. The standard mixture models of linear, quadratic, full cubic, and special cubic are expressed in equations 2.1, 2.2, 2.3, and 2.4, respectively [16].

$$Y = \sum_{i=1}^{l} \beta_i x_i \tag{2.1}$$

$$Y = \sum_{i=1}^{l} \beta_i x_i + \sum \sum_{i<j}^{l} \beta_{ij} x_i x_j \tag{2.2}$$

$$Y = \sum_{i=1}^{l} \beta_i x_i + \sum \sum_{i<j}^{l} \beta_{ij} x_i x_j + \sum \sum_{i<j}^{l} \delta_{ij} x_i x_j (x_i - x_j) + \sum \sum_{i<j<k} \sum \beta_{ijk} x_i x_j x_k \tag{2.3}$$

$$Y = \sum_{i=1}^{l} \beta_i x_i + \sum \sum_{i<j}^{l} \beta_{ij} x_i x_j + \sum \sum_{i<j<k} \sum \beta_{ijk} x_i x_j x_k \tag{2.4}$$

where Y is the predicted response, β_i is the model response to a pure component in the blend, each β_{ij} scales an interaction between components, each β_{ijk} scales an interaction of three components, x_i, x_j..., x_l are the fractions of components, and x_ix_j, x_ix_k..., x_kx_l are the quadratic interactions of the fractions.

2.1.5 Manufacturing processes

Manufacturing processes are methods converting raw materials into products. The processes used to manufacture the wood-plastic composites have several methods; however, the processes are popular and important in the applications including compression molding, injection molding, and extrusion.

2.1.5.1 Compression molding

Compression molding of thermoplastics includes four stages. The first, thermoplastic material is placed in an open heated mold. The second, thermoplastic is compressed at high pressure to fill the hot cavity space between the two parts of the heated mold and is softened and shaped, and then the mold is cooled to solidify [6]. Finally, the upper mold as shown in Figure 2.3 is opened to remove the product. In addition, the compression molding process has advantages such as no sprues or runners in compression molding and few investments. However, it also has some disadvantages including small outputs, high labor costs, and low output rates because of the long time needed to heat and then to cool the thermoplastic parts before demolding [6, 19].

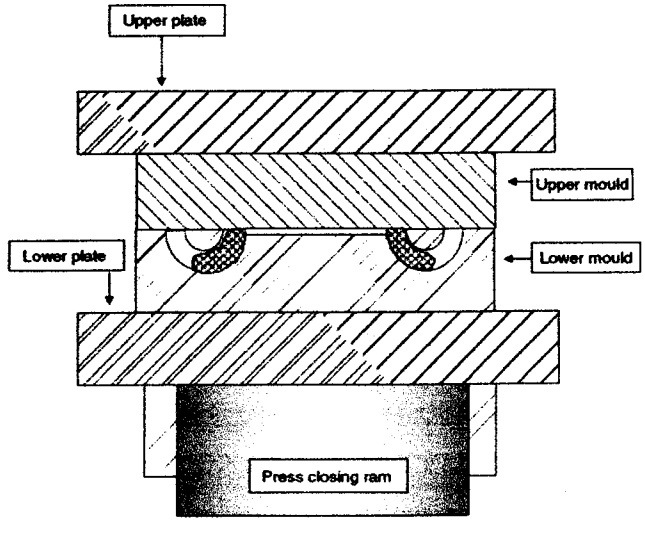

Figure 2.3 Compression molding machine [6]

2.1.5.2 Injection molding

During the injection molding process, the softened or melted thermoplastic is forced into a mould cavity, and then cooled until the melt solidifies as the shape of the cavity [6, 7]. When the melted plastic is sufficiently cooled, the mold is opened, the solid plastic is then pushed from the mold, and the mold is again closed to repeat this cycle [7]. The injection molding process has several advantages such as automatic process, high output rates, the cheapest labor costs, and good finishing surface, but it has the highest mold and press prices and is difficult to optimize the process parameters [6]. An injection-molding machine is shown in Figure 2.4 [6].

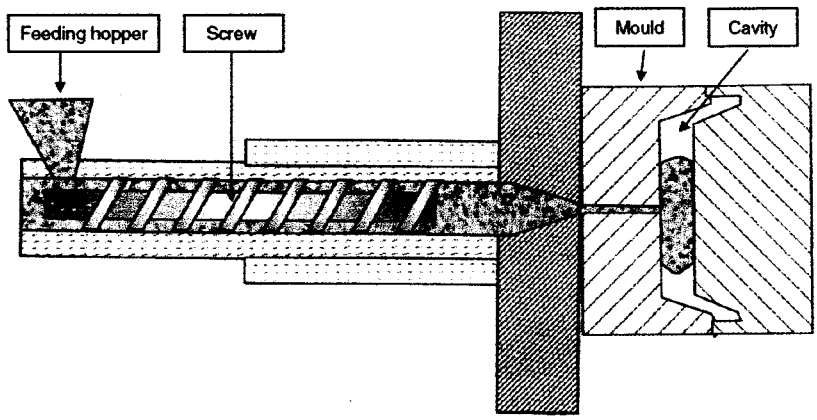

Figure 2.4 Injection molding machine [6]

2.1.5.3 Extrusion

Extrusion is a process used to create objects fixed cross-sectional profiles. In the extrusion process, plastic or polymer is continuously pushed with a screw through regions of high temperature and pressure [7], and then melted plastics are forced through a die shaped to give the final section of the profile [6, 7]. The extruder machine in Figure 2.5 has many types for applications in plastic industries, for example, single-screw used commonly to extrude profiles and multiple-screw used typically to compound and to extrude the profile in a single step [6]. Generally, an extrusion line included the important equipment is [6]:

1) the extruder including a rotating screw, heats, plasticizes, homogenizes and pressurizes [6].

2) the die and the punch or internal mandrel, which will produce the desired form of the profiles [6].

3) the cooling fixtures that precisely and permanently define the shape of the profiles [6].

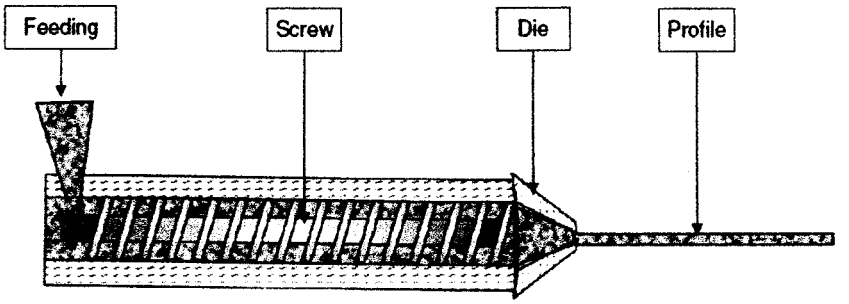

Figure 2.5 Extrusion machine [6]

In this study, the extrusion was adopted because of its continuous process to produce longer WPC panels which were focused in this research.

2.1.6 Mechanical properties

The mechanical properties are the most important properties because all service conditions and the majority of end-use applications relate some degree of mechanical loading [8]. The mechanical properties of plastic materials depend on the type of plastic, rate of crystallization, molecular structure, molecular weight, reinforcements, chemical additives, type and amount of colorant, and impact modifier [20]. Likewise, they also depend on the test procedures, testing methods, reporting of the property values, and manufacturing process of the plastic materials [20]. In addition, the mechanical properties are considered in the design of goods and process of material selection because almost all applications require the resistance of the mechanical loading. The plastic materials responding the mechanical properties within a region of elasticity are generally applied [20]. The design and selection of material for various applications are often considered based on

mechanical properties such as tensile properties, flexural properties, and compressive properties.

2.1.6.1 Tensile properties

Measurements of tensile strength and modulus are the most important indications of stiffness in a material and are the widely specified properties of plastic materials [8]. Tensile test is a measurement of the ability of a material to withstand forces that tend to pull it apart and to determine what extent the material stretches before breaking [8]. To operate a tensile test, the specimen is gripped at each end and pulled apart [21]. The pulling is continuously done for measuring the force that develops as the test specimen is elongated at a constant rate of extension [20]. From this test a stress-strain curve is generated which serves to define the following terms such as tensile stress and strain, percentage of elongation, yield point, proportional limit, yield strength, and modulus of elasticity [20], as shown in Figure 2.6. However, the grips hold the specimen by exerting a clamping force, they always punish some damage to the specimen [21]. Further, an increase in pulling speed typically results in an increase of yield point and ultimate strength [1]. The ultimate tensile strength and the tensile modulus are calculated:

$$\text{Ultimate tensile strength} = \frac{\text{Maximum load}}{\text{Cross-section area}} \quad \left(\frac{N}{mm^2}\right) \qquad (2.5)$$

$$\text{Tensile modulus} = \frac{\text{Tensile stress}}{\text{Tensile strain}} \quad \left(\frac{N}{mm^2}\right) \qquad (2.6)$$

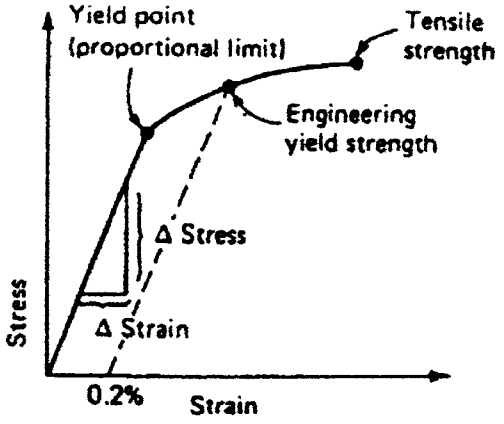

Figure 2.6 Stress-strain curve of tensile test [20]

2.1.6.2 Flexural properties

Flexure of plastic materials is interest to designers as well as plastic manufacturers [8]. Flexural test is a measurement of the ability of a material to withstand bending forces applied perpendicular to its longitudinal axis and is a combination of tensile and compressive stresses [8, 20] as shown in Figure 2.7. When a specimen is subjected under load, the side of the material opposite the loading undergoes the tensile stress, but the side of the specimen being loaded undergoes compressive stress [1]. These stresses linearly reduce to the center of the specimen; therefore, a flexural specimen is not in a state of uniform stress on the specimen. Theoretically, the center is a plane, called the neutral axis, which is not the stress [1]. Flexural properties are calculated and reported in terms of the maximum stress and strain that occur at the outside surface of the testing specimen, and many plastics do not break under flexure even after a large deflection [8]. Simple beam equations used to determine the flexural stress and modulus are:

$$\text{Ultimate flexural strength} = \frac{3P_{max}L}{2bd^2} \quad \left(\frac{N}{mm^2}\right) \tag{2.7}$$

$$\text{Flexural modulus} = \frac{P_{pl}L^3}{4\delta_{pl}bd^3} \quad \left(\frac{N}{mm^2}\right) \tag{2.8}$$

where P_{max} is the maximum load (N), L is the span (mm), b is the width of the specimen (mm) and d is the thickness of the specimen (mm), P_{pl} is the incremental load in the range of linear line of graph (N), and δ_{pl} is the incremental bending distance in the range of linear line of graph (mm) [22].

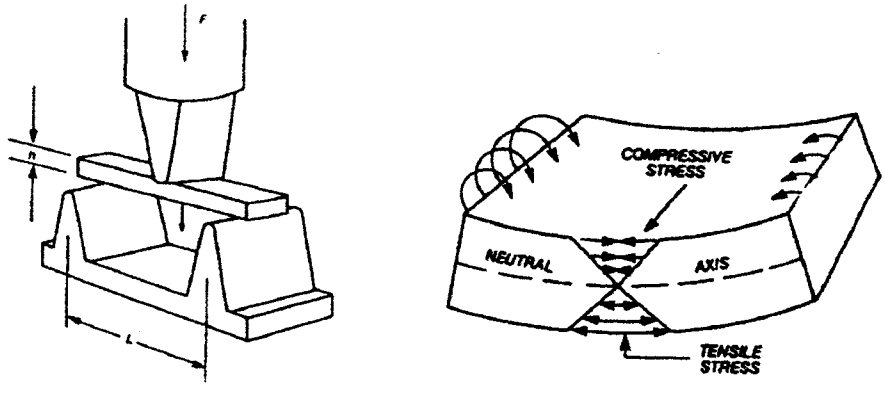

Figure 2.7 Three-point bending test and tensile and compressive stresses occurred on a flexural specimen [1]

2.1.6.3 Compressive properties

The compressive properties of plastic materials are very important for product design analysis, and one of the basic product design rules is the application of compressive structural loads and distribution of the loads uniformly across the entire product structural area [20]. Compressive properties are the behavior of a material, subjected under a compressive load at a uniform rate of loading, which tends to crush or squeeze the specimen [8, 20], as shown in Figure 2.8. For plastics that do not damage by shattering fracture, the compressive strength is an arbitrary value and not a fundamental property of the material tested [23]. Likewise, when there is no brittle failure, compressive strength is reported at a particular deformation level such as 1 or 10% [23]. In addition, the compressive properties include compressive strength, modulus, yield stress, deformation beyond yield point, and compressive strain; however, compressive strength and modulus are the only two values most widely specified in product design [8, 20]. The ultimate compressive strength and compressive modulus are calculated:

$$\text{Ultimate compressive strength} = \frac{\text{Maximum load}}{\text{Cross-section area}} \quad \left(\frac{N}{mm^2}\right) \quad (2.9)$$

$$\text{Compressive modulus} = \frac{\text{Compressive stress}}{\text{Compressive strain}} \quad \left(\frac{N}{mm^2}\right) \quad (2.10)$$

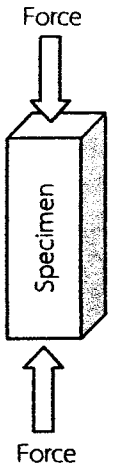

Figure 2.8 Compressive test

2.1.7 Thermal properties

The thermal properties of plastic and wood-plastic composite materials are equally as important as the mechanical properties because plastics are very sensitive to changes in temperature [8]. Therefore, in designing a plastic part or selecting a plastic material for applications, the study in effects of temperature on the properties of plastic material are necessary [8]. The design and selection of plastics and wood-plastic composites for various applications are often considered the thermal properties such as differential scanning calorimeter, thermogravimetric analysis, and dynamic mechanical thermal analysis.

2.1.7.1 Differential scanning calorimeter (DSC)

Differential scanning calorimeter is thermal analysis technique widely used to measure the energy absorbed (endotherm) or produced (exotherm) as a function of time or temperature [8, 23]. It is commonly used to measure

crystallization, melting, loss of solvents, resin curing, and other processes involving an energy change [23]. In addition, DSC measurements can be regularly operated in two methods. Firstly, the electrical heaters located or placed below the pans necessary to maintain the two pans at the same temperature [23]. Secondly, the heat flow measurement (heat flux) occurs as a function of sample temperature [23].

2.1.7.2 Thermogravimetric analysis (TGA)

Thermogravimetric analysis is a test procedure that involves measurement of the weight gain or loss of a material as a function of temperature and time [8, 23]. The components of a polymer or polymer composite formulation volatilize or decompose at different temperatures, which lead to weight-loss steps [8]. The applications of TGA are mostly used to assess the thermal stability of the materials [23]. Likewise, TGA can also be applied to measure moisture, volatile, and filler contents, to examine the effects of additives, and to separate some compositions [23].

2.1.7.3 Dynamic mechanical thermal analysis (DMTA)

Dynamic mechanical thermal analysis is normally used to assess the viscoelastic properties of polymer materials [23]. From this test can be calculated the storage and loss modulus, viscosity, and compliance, which show a function of applied frequency, stress, and strain as well as temperature [8]. Measurements of DMTA can be operated in several modes including flexure, tension, compression, shear, and torsion [23]. Moreover, DMTA is not regularly used as a failure analysis technique, but it offers information of valuable materials [23].

2.1.8 Creep behavior

Nowadays, designers have accepted that understanding in the deformation behavior of plastics and WPCs under varying temperatures and long-term load is importance, which such behavior is creep properties [8]. Creep is the time-dependent deformation of plastic and WPCs when it is subjected under a

constant load or stress at room temperature for long terms. Continuous loading slowly leads strain accumulation in creep as the chain molecular structure of the polymer rotates and unwinds to accommodate the load [24]. WPCs that have significant time sensitivity at the temperature of use will have limited value for structural applications [25]. The creep curves will depend not only on stress but also on: (1) temperature; (2) humidity; (3) type of stress; and (4) presence of solvents in the atmosphere [5]. In addition, the general creep behavior of plastics and WPCs is composed of four continuous stages in Figure 2.9 [8]. Initially, when the stress is applied, the instantaneous elastic deformation occurs in the first stage (OP), and then strain occurs rapidly but at a decreasing rate in the second stage (PQ), which is referred as primary creep. The third stage (QR) is considered constant strain rate (straight portion of the curve; steady state). The final stage (RS) represents an increase of creep rate until the creep fracture occurs (tertiary stage) [8].

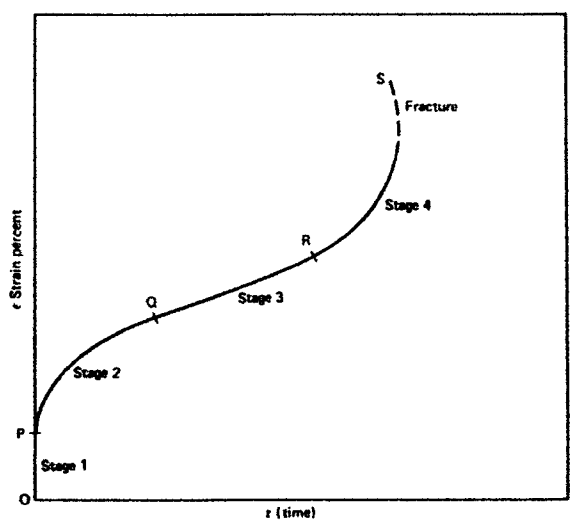

Figure 2.9 Generalized creep curve of plastic and WPCs [8]

2.1.9 Time-temperature superposition principle

Basically, the behavior of polymeric materials such as plastics and WPCs is dependent on time, temperature, and stress [26]. The determination of the long-term performance of such materials has limited by cost and time used in the experiments [27]. Therefore, a time-temperature superposition principle (TTSP) is

utilized to predict lifetime using a master curve that is constructed from short-term testing creep data at different temperatures and shifting of the measured curves on the log-time scale to generate a long-term master curve [24], as shown in Figure 2.10. At a reference temperature 120 °C each curve above 120 °C is shifted to the right, whereas below 120 °C is shifted to the left so as to form a continuation of longer time for the 120 °C compliance curve [24]. The TTSP was initially developed in the mid-1950s for solid plastics, and then in 1970's this theory was applied with fiber-reinforced composites [27-29]. By the principle of TTS, the effect of temperature on the time-dependent behavior of materials is assumed as equivalence for stretching or shrinking of the real time of the creep response by a certain shift factor [27, 30].

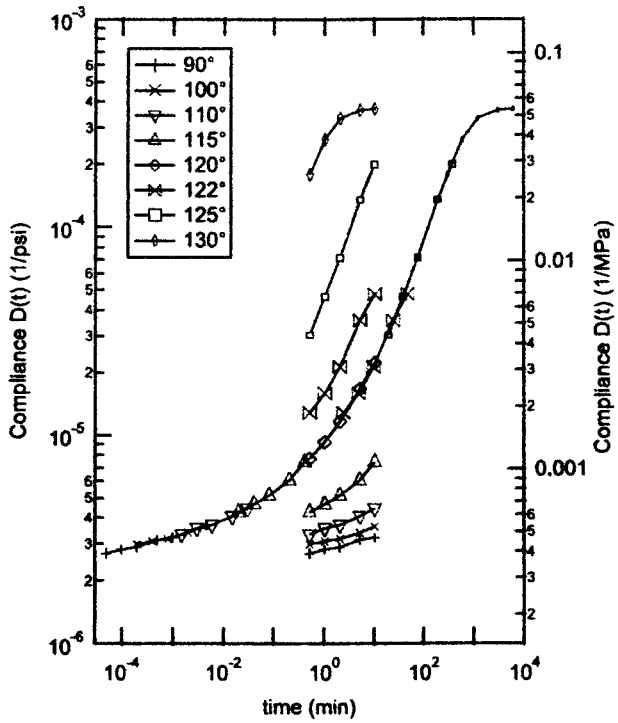

Figure 2.10 Creep compliance master curve for an epoxy at 120 °C [24]

2.2 Literature review

2.2.1 Wood-plastic composites

Wood-plastic composites have been extensively developed and used for non-structural application [31]. WPCs are manufactured by mixing wood flour and

plastics, which can use the same process as 100% plastic-based products [32]. Normally, the plastic matrix (either thermoplastics or thermoset) is the material that holds the reinforcements (wood or other natural fibers) together and has lower strength and stiffness than the reinforcements [3]. WPCs have found commercial applications including profiles, sheathings, decking, roof tiles, parquet flooring, and window trims [32, 33]. Other commercial items include billiard cues, golf clubs, archery bows, musical instruments, knife handles, and office equipments [33]. Over the last decade, the applications of WPCs have been increasingly seen in construction industry due to their high specific strength and stiffness and lower density [34]. Further, due to low cost of the composite materials, WPCs are being considered as a replacement to the conventional steel in reinforced concrete structures [34]. In addition, comparing to wood, WPCs exhibit better dimensional stability and durability, require less maintenance and lower water absorption, and provide superior fungal resistance [35-37]. However, WPCs is not suitable for applications where strength and stiffness are critical due to having lower mechanical properties than solid wood [3].

2.2.2 Applied polymer in wood-plastic composites

Polymers applied extensively in WPC industries are typically virgin thermoplastics such as PP, PVC, polystyrene (PS), and PE both high density and low density. Bledzki et al. [38] studied the potential of grain by-product such as barley husk, coconut shell as reinforcements for polypropylene. Kociszewski et al. [39] assessed the effect of particle size on the mechanical properties of softwood-PVC composites, and found that the flexural and tensile properties as well as the impact strength reduced with increasing cross-section size and enhanced with an increase of particle size. Petchwattana et al. [40] investigated the influences of rice hull (RH) contents and particle sizes on the mechanical properties of HDPE/RH composites. They found that the flexural and tensile strengths were increased upon raising the silica-rich RH contents, whereas the addition of RH in the composites became brittle as was reflected by the lower impact strength. However, few studies of WPCs based

on recycled plastic have been revealed. Lisperguer et al. [41] compared WPCs manufactured from wood flour and virgin and/or recycled PS. They reported that the mechanical properties of the composites based on virgin PS were not better than those based on recycled PS. Najafi et al. [42] studied the mechanical properties of WPCs produced from sawdust and virgin or recycled plastics, namely HDPE and PP. The composites containing HDPE (recycled and virgin) exhibited lower stiffness and strength than those made from PP. Ashori and Sheshmani [43] investigated the effects of weight fraction of fibers in hybrid composites made from combinations of recycled newspaper fiber, poplar wood flour, and recycled PP. The composites with a high fraction of recycled newspaper fiber showed maximum water absorption during the whole duration of immersion. Nourbakhsh et al. [44] also concluded that PP waste and wood waste are promising alternative raw materials for making low cost WPCs. In addition, PP is one of the most well-known plastics that have been widely used in plastic industries due to its high strength and ease of manufacturing and recycling. Hence, both virgin and recycled PP has become popular for blending with natural fibers. For example, Ndiaye et al. [45] studied PP-wood flour composites that were blended with different contents of maleic anhydride-grafted polypropylene (MAPP) and clay. They found that the addition of MAPP or clay in the formulation greatly improved the dispersion of the wood flour in the composites. Butylina et al. [46] examined the effect of wood fiber source on the physical and mechanical properties of wood fiber-PP composites and found that the density of the composites was a key factor governing water absorption and thickness swelling. Ghahri et al. [47] improved the impact strength of wood flour–recycled PP composites and found that the addition of ethylene vinyl acetate up to 9 wt% doubly increased the impact strengths of the composites made with PP recycled. Spinace et al. [48] studied the mechanical and thermal properties of composites made from curaua fibers and post-consumer PP and found that the properties of composites based on recycled PP are similar to those of composites using virgin PP.

2.2.3 Applied wood fillers in wood-plastic composites

Natural organic fibers are potential replacements for glass or carbon fibers, inorganic fillers, and other traditional materials in composites [49, 50]. The several advantages of natural fibers include low cost, low density, low energy consumption, biodegradability, and non-abrasive nature [49, 51]. Likewise, they improve the specific strength and modulus, allowing the production of low-density composites with high filler content [52, 53]. Recent advances in natural fillers create opportunities for improved materials from renewable resources and supporting global sustainability [54]. There have been numerous studies on producing thermoplastic composites with plant fibers, plant flour, or wood flour: including eastern red cedar [55], flax [56], maple [57], oak [55], pine [58], and rubberwood [59]. However, the type of natural fibers is also an important factor affecting the mechanical, physical, and thermal properties of the WPCs. Because its pore penetration, surface roughness, surface morphology, and chemical compositions, such as cellulose, hemi-cellulose, lignin, ash, may seriously affect the extent of interaction between the matrix and filler phases in a composite [12, 22, 55, 60]. Hence, several researchers investigated the effect of natural fibers on the mechanical, physical, and thermal properties of the WPCs. Yemele et al. [61] mixed bark and HDPE to examine the effect of species and fiber content on flexural and tensile properties. They found that black spruce bark composites gave better strength than aspen bark composites. The result also showed that increasing the fiber proportion decreased the tensile strength. Prachayawarakorn et al. [62] investigated the effect of rubberwood sawdust loading in PVC/LDPE blend on mechanical properties. They reported that elastic and flexural moduli of the composite materials increased with increasing sawdust loading, but tensile and flexural strengths slowly decreased. Panthapulakkal and Sain [63] used agro-residues such as wheat straw, cornstalk, and corncob as reinforcement for HDPE. They reported that the wheat straw reinforced HDPE exhibited superior tensile and flexural strengths and also tensile and flexural modulus compared with cornstalk and corncob. Rahman et al. [64] also investigated the effects of jute fiber content on the

mechanical properties of reinforced PP. The tensile strength of the composites decreased with an increasing jute fiber loading, but the Young's modulus decreased only slowly. Reddy et al. [65] reported that an increase in the wheat straw and clay contents in a PP hybrid composite increased the flexural modulus and water absorption.

2.2.4 Improvement of interfacial adhesion in wood-plastic composites

Major limitation of using natural fibers as reinforcement in plastic matrices is poor interfacial bonding between the polar-hydrophilic natural fibers and the nonpolar-hydrophobic plastics [66, 67], which affected negatively the mechanical and physical properties of the composite materials [48]. The interfacial adhesion between fiber and polymer can be improved through modification of either the fiber surfaces or the polymeric matrix [48]. A few studies have treated the fillers or wood fibers using the chemical modifications. Ichazo et al. [68] treated the wood flour with sodium hydroxide and vinil-tris-(2-metoxietoxi)-silane and found that the composites treated showed the same tendency to slightly increase the tensile strength and modulus, but they did not affect their melt flow indexes. Gwon et al. [69] investigated the effect of NaOH treatment of wood fibers on the mechanical strength of WPCs. NaOH treated wood fibers reduced the natural impurities (hemicellulose, lignin, and extractives) of the wood fibers and decreased the possible cracks and microvoids at the interfaces between the fibers and polymer matrix. Furthermore, a coupling agent is generally used to improve the interfacial bonding of the composite materials. Kuo et al. [35] reported that addition of maleic anhydride-grafted polypropylene (MAPP) 3-4.5 wt% gave the optimal increase in mechanical properties of the WPCs. Bengtsson et al. [70] found that the addition of MAPP in the composites increased significantly the stiffness and strength but decreased the elongation break due to an improvement in dispersion of the cellulose fibers in the polypropylene matrix. Adhikary et al. [58] reported that both the stability and mechanical properties were significantly improved by addition of MAPP 3–5 wt% in the composite formulation. Increasing the polymer content or addition of coupling agent can

improve the dimensional stability and strength properties of the composites. Nachtigall et al. [71] explained that the degradation temperature of PP/wood-fiber composites increased with the addition of coupling agents. However, the commercial coupling agents give the different effect on WPC performances. The important parameters that determine the efficiency of the additive are the molecular weight and amount of maleic grafted [72]. Therefore, the selection of coupling agent used is very important to application and processing requirement of the WPCs [72].

2.2.5 Production of wood-plastic composites

Usually, the composite materials based on thermoplastic are manufactured through a two-stage process: (1) compounding of the natural fiber and the plastic with the additives and (2) injection molding, compression molding, or extrusion of the mixing compositions to produce the products [58, 73]. For example, Doan et al. [74] compounded jute yarn, PP granules, and MAPP granules on a co-rotating twin-screw extruder into WPC granules, and then an injection molding machine was used to make the specimens. Gao et al. [75] dried the wood fibers to the moisture content below 1% before the extrusion process. Wood fiber, PP/PE blends, and additives were compounded in a high speed mixer, and then mixed in a co-rotating twin screw extruder to manufacture the WPC pellets, and finally the pellets were extruded by using a single screw extruder machine through a rectangular die. Wechsler and Hiziroglu [32] compounded the compositions of the composites by using mixer rotating. Mixed samples then were pressed in a compression molding. The press was cooled off while the samples were still under compression before removal. Adhikary et al. [58] compounded wood flour and HDPE granulates in a co-rotating twin-screw extruder, and the extruded strand passed through a water bath and was subsequently palletized. Before producing the WPC panels, the mixed pellets were dried to reduce the moisture content. The WPC pellets were then molded in a heated compression and transferred to a cold press. Bouafif et al. [76] produced the WPCs in a two-step process. In the first step, wood particle and HDPE were compounded using a co-rotating twin-screw extruder. In the

second stage, WPC specimens were produced using an injection molding machine. From the literature reviews, the compounding and producing of the WPC materials was used the various and different methods. The hot platen compression system is appropriate for manufacturing flat and curved composite panels [3], whereas the extruder system is suitable for producing the continuous long composite panels. Therefore, the appropriate mixing of wood filler and plastic matrix with additives and suitable manufacturing process of the WPCs is very important to each application.

2.3 References

[1] D. Rosato and D. Rosato. *Reinforced Plastics Handbook.* Elsevier Science & Technology Books, 2004.

[2] D.N.S. Hon and N. Shiraishi. *Wood and Cellulosic Chemistry.* Marcel Dekker, Madison Avenue, New York, NY, 2001.

[3] K.B. Adhikary. "Development of Wood Flour-Recycled Polymer Composite Panels as Building Materials." Ph.D. dissertation, University of Canterbury, New Zealand, 2008.

[4] A. Ashori. "Wood–Plastic Composites as Promising Green-Composites for Automotive Industries!." *Bioresource Technology,* vol. 99, pp. 4661–4667, 2008.

[5] J.A. Brydson. *Plastics Materials.* Butterworth-Heinemann. Jordan hill, Oxford, 1999.

[6] M. Biron. *Thermoplastics and Thermoplastic Composites.* Elsevier Ltd. Linacre House, Jordan Hill, Oxford, 2007.

[7] C.A. Harper and E.M. Petrie. *Plastics Materials and Processes: A Concise Encyclopedia.* John Wiley & Sons, Inc., Hoboken, New Jersey, 2003.

[8] V. Shah. *Handbook of Plastics Testing and Failure Analysis.* John Wiley & Sons, Inc., Hoboken, New Jersey, 2007.

[9] A.K.v.d. Vegt. *From Polymers to Plastics.* Delft University Press, Delft, Netherlands, 2002.

[10] M. Jawaid and H.P.S.A. Khalil. "Cellulosic/Synthetic Fibre Reinforced Polymer Hybrid Composites: A Review." *Carbohydrate Polymers*, vol. 86, pp. 1–18, 2011.

[11] Y. Xie, C.A.S. Hill, Z. Xiao, H. Militz, and C. Mai. "Silane Coupling Agents Used for Natural Fiber/Polymer Composites: A Review." *Composites Part A: Applied Science and Manufacturing*, vol. 41, pp. 806–819, 2010.

[12] B. Li, H. Jiang, L. Guo, and H. Shi. "Comparative Study on the Effect of Manchurian Ash and Larch Wood Flour on Mechanical Property, Morphology, and Rheology of HDPE/Wood Flour Composites." *Journal of Applied Polymer Science*, vol. 107, pp. 2520–2530, 2008.

[13] S. Kalia, B.S. Kaith, and I. Kaur. *Cellulose Fibers: Bio- and Nano-Polymer Composites*, Springer Heidelberg Dordrecht, London, New York, 2011.

[14] Y.B. Khosrowshahi and A. Salem. "Influence of Polyvinyl Alcohol and Carboxymethyl Cellulose on the Reliability of Extruded Ceramic Body: Application of Mixture Design Method in Fabricating Reliable Ceramic Raschig Rings." *International Journal of Applied Ceramic Technology*, vol. 8, pp. 1334–1343, 2011.

[15] R.C.S. John. "Experiments with Mixtures, Ill-Conditioning, and Ridge Regression." *Journal of Quality Technology*, vol. 16, pp. 81–96, 1984.

[16] R.H. Myers, D.C. Montgomery, and C.M. Anderson-Cook. *Response Surface Methodology: Process and Product Optimization Using Designed Experiments*. John Wiley & Sons, Inc., Hoboken, New Jersey, 2009.

[17] F. Mirjalili, S. Moradian, and F. Ameri. "Attaining Optimal Dyeability and Tensile Properties of Polypropylene/Poly(ethylene terephthalate) Blends with a Special Cubic Mixture Experimental Design." *Journal of Applied Polymer Science*, vol. 121, pp. 3201–3210, 2011.

[18] D.C. Montgomery. *Design and Analysis of Experiments*. John Wiley & Sons, Inc., 2009.

[19] J.G. Bralla. *Handbook of Manufacturing Processes: How Products, Components and Materials are Made*. Industrial Press Inc., New York, 2007.

[20] E.A. Campo. *Selection of Polymeric Materials: How to Select Design Properties from Different Standards*. Williani Andrew Inc., Norwich, NY, 2008.

[21] S.B. Driscoll. *The Basics of Testing Plastics: Mechanical Properties, Flame Exposure, and General Guidelines*. American Society for Testing and Materials, West Conshohocken, PA., 1998.

[22] T. Ratanawilai, P. Lekanukit, and S. Urapantamas. "Effect of Rubberwood and Palm Oil Content on the Properties of Wood-Polyvinyl Chloride Composites." *Journal of Thermoplastic Composite Materials*, Epub ahead of print 9 August 2012. DOI: 10.1177/0892705712454863.

[23] S. Lampman, B. Sanders, N. Hrivnak, J. Kinson, and C. Polakowski. *Characterization and Failure Analysis of Plastics*. ASM International, 2003.

[24] H.F. Brinson and L.C. Brinson. *Polymer Engineering Science and Viscoelasticity; An Introduction*. Springer Science+Business Media, New York, 2008.

[25] L.W. McKeen. The Effect of Creep and Other Time Related Factors on Plastics and Elastomers. Linacre House, Jordan Hill, Oxford, UK, Elsevier Inc., 2009.

[26] D.J. Pooler. "The Temperature Dependent Non-Linear Response of a Wood Plastic Composite." M.S. thesis, Washington State University, United States, 2001.

[27] S.I. Farid. "Viscoelastic Properties of Wood-Fiber Reinforced Polyethylene: Stress Relaxation, Creep and Threaded Joints." M.S. thesis, University of Toronto, Canada, 2000.

[28] M.L. William, R.F. Landel, and J.D. Ferry. "The Temperature Dependence of Relaxation Mechanism in- Amorphous Polymer and Other Glass-Liquids." *Journal of the American Chemical Society*, vol. 77, pp. 370, 1955.

[29] Y.T. Yeow. "The Time-Temperature Behavior of a Undirectional Graphite/ Epoxy Composite Materials." VPI-E-78-4, 1978.

[30] W.K. Goertzen and M.R. Kessler. "Creep Behavior of Carbon Fiber/Epoxy Matrix Composites." *Materials Science and Engineering A*, vol. 421, pp. 217–225, 2006.

[31] S. Tamrakar, R.A. Lopez-Anido, A. Kiziltas, and D.J. Gardner. "Time and Temperature Dependent Response of a Wood-Polypropylene Composite." *Composites Part A: Applied Science and Manufacturing*, vol. 42, pp. 834–842, 2011.

[32] A. Wechsler and S. Hiziroglu. "Some of the Properties of Wood–Plastic Composites." *Building and Environment*, vol. 42, pp. 2637–2644, 2007.

[33] U.C. Yildiz, S. Yildiz, and E.D. Gezer. "Mechanical Properties and Decay Resistance of Wood–Polymer Composites Prepared from Fast Growing Species in Turkey." *Bioresource Technology*, vol. 96, pp. 1003–1011, 2005.

[34] S.S. Pendhari, T. Kant, and Y.M. Desai. "Application of Polymer Composites in Civil Construction: A General Review." *Composite Structures*, vol. 84, pp. 114–124, 2008.

[35] P.Y. Kuo, S.Y. Wang, J.H. Chen, H.C. Hsueh, and M.J. Tsai. "Effects of Material Compositions on the Mechanical Properties of Wood–Plastic Composites Manufactured by Injection Molding." *Materials and Design*, vol. 30, pp. 3489–3496, 2009.

[36] C. Clemons. "Wood-Plastic Composites in the United States." *Forest Products Journal*, vol. 52, pp. 10–18, 2002.

[37] N. Rocha, A. Kazlauciunas, M.H. Gil, P.M. Goncalves, and J.T. Guthrie. "Poly(Vinyl Chloride)–Wood Flour Press Mould Composites: The Influence of Raw Materials on Performance Properties." *Composites Part A: Applied Science and Manufacturing*, vol. 40, pp. 653–661, 2009.

[38] A.K. Bledzki, A.A. Mamun, and J. Volk. "Barley Husk and Coconut Shell Reinforced Polypropylene Composites: The Effect of Fibre Physical, Chemical and Surface Properties." *Composites Science and Technology*, vol. 70, pp. 840–846, 2010.

[39] M. Kociszewski, C. Gozdecki, A. Wilczynski, S. Zajchowski, and J. Mirowski. "Effect of Industrial Wood Particle Size on Mechanical Properties of Wood-Polyvinyl Chloride Composites." *European Journal of Wood and Wood Products*, vol. 70, pp. 113–118, 2012.

[40] N. Petchwattana, S. Covavisaruch, and S. Chanakul. "Mechanical Properties, Thermal Degradation and Natural Weathering of High Density Polyethylene/Rice Hull Composites Compatibilized with Maleic Anhydride Grafted Polyethylene." *Journal of Polymer Research*, vol. 19, pp. 1–9, 2012.

[41] J. Lisperguer, X. Bustos, and Y. Saravia. "Thermal and Mechanical Properties of Wood Flour-Polystyrene Blends from Postconsumer Plastic Waste." *Journal of Applied Polymer Science*, vol. 119, pp. 443–451, 2011.

[42] S.K. Najafi, E. Hamidinia, and M. Tajvidi. "Mechanical Properties of Composites from Sawdust and Recycled Plastics." *Journal of Applied Polymer Science*, vol. 100, pp. 3641–3645, 2006.

[43] A. Ashori and S. Sheshmani. "Hybrid Composites Made from Recycled Materials: Moisture Absorption and Thickness Swelling Behavior." *Bioresource Technology*, vol. 101, pp. 4717–4720, 2010.

[44] A. Nourbakhsh, A. Ashori, H.Z. Tabari, and F. Rezaei. "Mechanical and Thermo-Chemical Properties of Wood-Flour/Polypropylene Blends." *Polymer Bulletin*, vol. 65, pp. 691–700, 2010.

[45] D. Ndiaye, L.M. Matuana, S.M. Therias, L. Vidal, A. Tidjani, and J.L. Gardette, "Thermal and Mechanical Properties of Polypropylene/Wood-Flour Composites." *Journal of Applied Polymer Science*, vol. 119, pp. 3321–3328, 2011.

[46] S. Butylina, O. Martikka, and T. Kärki. "Properties of Wood Fibre-Polypropylene Composites: Effect of Wood Fibre Source." *Applied Composite Materials*, vol. 18, pp. 101–111, 2011.

[47] S. Ghahri, S.K. Najafi, B. Mohebby, and M. Tajvidi. "Impact Strength Improvement of Wood Flour–Recycled Polypropylene Composites." *Journal of Applied Polymer Science*, vol. 124, pp. 1074–1080, 2012.

[48] M.A.S. Spinace, K.K.G. Fermoseli, and M.A.D. Paoli. "Recycled Polypropylene Reinforced with Curaua Fibers by Extrusion." *Journal of Applied Polymer Science*, vol. 112, pp. 3686–3694, 2009.

[49] A. Kaymakci, N. Ayrilmis, F. Ozdemir, and T. Gulec. "Utilization of Sunflower Stalk in Manufacture of Thermoplastic Composite." *Journal of Polymers and the Environment*, Epub ahead of print 18 December 2012. DOI: 10.1007/s10924-012-0564-9.

[50] T.T. Law and Z.A.M. Ishak. "Water Absorption and Dimensional Stability of Short Kenaf Fiber-Filled Polypropylene Composites Treated with Maleated Polypropylene." *Journal of Applied Polymer Science*, vol. 120, pp. 563–572, 2011.

[51] B. Mirzaei, M. Tajvidi, R.H. Falk, and C. Felton. "Stress-Relaxation Behavior of Lignocellulosic High-Density Polyethylene Composites." *Journal of Reinforced Plastics and Composites*, vol. 30, pp. 875–881, 2011.

[52] A. Ashori and A. Nourbakhsh. "Performance Properties of Microcrystalline Cellulose as a Reinforcing Agent in Wood Plastic Composites." *Composites Part B: Engineering*, vol. 41, pp. 578–581, 2010.

[53] W. Liu, L.T. Drzal, A.K. Mohanty, and M. Misra. "Influence of Processing Methods and Fiber Length on Physical Properties of Kenaf Fiber Reinforced Soy Based Biocomposites." *Composites Part B: Engineering*, vol. 38, pp. 352–359, 2007.

[54] H.Y. Cheung, M.P. Ho, K.T. Lau, F. Cardona, and D. Hui. "Natural Fibre-Reinforced Composites for Bioengineering and Environmental Engineering Applications." *Composites Part B: Engineering*, vol. 40, pp. 655–663, 2009.

[55] J.W. Kim, D.P. Harper, and A.M. Taylor. "Effect of Wood Species on the Mechanical and Thermal Properties of Wood–Plastic Composites." *Journal of Applied Polymer Science*, vol. 112, pp. 1378–1385, 2009.

[56] N.M. Barkoula, S.K. Garkhail, and T. Peijs. "Effect of Compounding and Injection Molding on the Mechanical Properties of Flax Fiber Polypropylene Composites." *Journal of Reinforced Plastics and Composites*, vol. 29, pp. 1366–1385, 2010.

[57] T. Li and N. Yan. "Mechanical Properties of Wood Flour/HDPE/Ionomer Composites." *Composites Part A: Applied Science and Manufacturing*, vol. 38, pp. 1–12, 2007.

[58] K.B. Adhikary, S. Pang, and M.P. Staiger. "Dimensional Stability and Mechanical Behaviour of Wood-Plastic Composites based Recycled and Virgin High-Density Polyethylene." *Composites Part B: Engineering*, vol. 39, pp. 807–815, 2008.

[59] C. Homkhiew, T. Ratanawilai, and W. Thongruang. "Effect of Wood Flour Content and Cooling Rate on Properties of Rubberwood Flour/Recycled Polypropylene Composites." *Advanced Materials Research*, vol. 488–489, pp. 495-500, 2012.

[60] W. Gacitúa and M. Wolcott. "Morphology of Wood Species Affecting Wood-Thermoplastic Interaction: Microstructure and Mechanical Adhesion." *Maderas: Ciencia Y Tecnología*, vol. 11, pp. 217–231, 2009.

[61] M.C.N. Yemele, A. Koubaa, A. Cloutier, P. Soulounganga, and M. Wolcott. "Effect of Bark Fiber Content and Size on the Mechanical Properties of Bark/HDPE Composites." *Composites Part A: Applied Science and Manufacturing*, vol. 41, pp. 131–137, 2010.

[62] J. Prachayawarakorn, J. Khamsri, K. Chaochanchaikul, and N. Sombatsompop. "Effects of Compatibilizer Type and Rubber-Wood Sawdust Content on the Mechanical, Morphological, and Thermal Properties of PVC/LDPE Blend." *Journal of Applied Polymer Science*, vol. 102, pp. 598–606, 2006.

[63] S. Panthapulakkal and M. Sain. "Agro-Residue Reinforced High-density Polyethylene Composites: Fiber Characterization and Analysis of Composite Properties." *Composites Part A: Applied Science and Manufacturing*, vol. 38, pp. 1445–1454, 2007.

[64] M.R. Rahman, M.M. Huque, M.N. Islam, and M. Hasan. "Improvement of Physico-Mechanical Properties of Jute Fiber Reinforced Polypropylene Composites by Post-Treatment." *Composites Part A: Applied Science and Manufacturing*, vol. 39, pp. 1739–1747, 2008.

[65] C.R. Reddy, A.P. Sardashti, and L.C. Simon. "Preparation and Characterization of Polypropylene–Wheat Straw–Clay Composites." *Composites Science and Technology*, vol. 70, pp. 1674–1680, 2010.

[66] P.W. Balasuriya, L. Ye, and Y.W. Mai. "Mechanical Properties of Wood Flake-Polyethylene Composites. Part I: Effects of Processing Methods and Matrix Melt Flow Behaviour." *Composites Part A: Applied Science and Manufacturing*, vol. 32, pp. 619–629, 2001.

[67] D. Moldas, B. Kokta, R. Raj, and C. Daneault. "Improvement of the Mechanical Properties of Sawdust Wood Fibre-Polystyrene Composites by Chemical Treatment." *Polymer*, vol. 29, pp. 1255–1265, 1988.

[68] M.N. Ichazo, C. Albano, J. Gonzalez, R. Perera, and M.V. Candal. "Polypropylene/Wood Flour Composites: Treatments and Properties." *Composite Structures*, vol. 54, pp. 207–214, 2001.

[69] J.G. Gwon, S.Y. Lee, S.J. Chun, G.H. Doh, and J.H. Kim. "Effects of Chemical Treatments of Hybrid Fillers on the Physical and Thermal Properties of Wood Plastic Composites." *Composites Part A: Applied Science and Manufacturing*, vol. 41, pp. 1491–1497, 2010.

[70] M. Bengtsson, M.L. Baillif, and K. Oksman. "Extrusion and Mechanical Properties of Highly Filled Cellulose Fibre–Polypropylene Composites." *Composites Part A: Applied Science and Manufacturing*, vol. 38, pp. 1922–1931, 2007.

[71] S.M.B. Nachtigall, G.S. Cerveira, and S.M.L. Rosa. "New Polymeric-Coupling Agent for Polypropylene/Wood-Flour Composites." *Polymer Testing*, vol. 26, pp. 619–628, 2007.

[72] H.P. San, L.A. Nee, and H.C. Meng. "Physical and Bending Properties of Injection Moulded Wood Plastic Composites Boards." *ARPN Journal of Engineering and Applied Sciences*, vol. 3, pp. 13–19, 2008.

[73] F. Mantia. *Handbook of Plastics Recycling*, Rapra Technology, 2002.

[74] T.T.L. Doan, S.L. Gao, and E. Mader. "Jute/Polypropylene Composites I. Effect of Matrix Modification." *Composites Science and Technology*, vol. 66, pp. 952–963, 2006.

[75] H. Gao, Y.M. Song, Q.W. Wang, Z. Han, and M.L. Zhang. "Rheological and Mechanical Properties of Wood Fiber-PP/PE Blend Composites." *Journal of Forestry Research*, vol. 19, p. 315–318, 2008.

[76] H. Bouafif, A. Koubaa, P. Perre, and A. Cloutier. "Effects of Fiber Characteristics on the Physical and Mechanical Properties of Wood Plastic Composites." *Composites Part A: Applied Science and Manufacturing*, vol. 40, pp. 1975–1981, 2009.

CHAPTER 3

Effect of Wood Flour Content and Cooling Rate on Properties of Recycled Polypropylene/Rubberwood Flour Composites

3.1 Chapter summary

The present chapter summarizes an experimental study on the mechanical and thermal properties of recycled polypropylene composites reinforced with rubberwood flour. Different compositions were varied to investigate mechanical strengths, melting temperature, storage modulus, and loss modulus. It was observed that the tensile and flexural strengths decreased with an increase of wood flour content. Furthermore, the air cooled composites showed an improvement of properties in comparison with the water cooled composites. The melting and crystallization temperature results presented a weak influence of increasing wood flour content on composites; however, dynamic mechanical thermal analysis showed an increase in the storage and loss modulus.

3.2 Introduction

Fiber reinforced polymers is significantly growing in construction-materials due to their light weight, ease of installation, low maintenance, tailor made properties, and corrosion resistance [1]. Wood flour has been primarily used by the plastic industries as an inexpensive filler to increase the strength and stiffness of thermoplastic and to reduce raw material costs [2]. However, the use of wood flour reinforced plastics affects mechanical and thermal properties. Polypropylene is one of the most well-known plastics that have been widely used in wood-plastic composite (WPCs) industries because of its high strength and ease of manufacturing and recycling. Extrusion is basically used to fabricate WPCs. The extruder of the plastic is heated to a temperature above its glass transition point before extruding through the open die. The extrudate is consequently cooled down to lower its

transition temperature while the molecules are still under stress. The molecules will become frozen whilst in an oriented state. Such an orientation significantly affects the properties of the extruded plastic [3].

There are numbers of published studies on the reinforcement of virgin polypropylene (PP) with wood flour relating to the results of mechanical and thermal properties; however, studies on WPCs based on recycled PP are very limited. Ndiaye et al. [4] studied PP/wood flour composites that were blended with different contents of maleic anhydride-grafted polypropylene (MAPP) and clay. They found that the addition of MAPP or clay in the formulation greatly improved the dispersion of the wood flour in the composites. Lisperguer et al. [5] showed that the glass transition values of the recycled polystyrene (rPS) and rPS/wood composites were higher than those of the virgin PS and virgin PS/wood composites. The use of rPS increased the stiffness and flexural modulus of the composites. Adhikary et al. [6] found that mechanical properties of wood-based recycled plastics of high-density polyethylene (HDPE) were as good as the composites made from virgin-based HDPE. Therefore, wood flour content and oriented state of cooling significantly affect on the properties of composites. This research aims to study the use of rubberwood flour (RWF) and Post-Consumer Recycled PP (PCR-PP) for the production of the composites. The effects of the RWF content and the oriented state of cooling on the mechanical and thermal properties were also investigated.

3.3 Experimental

3.3.1 Materials and sample preparation

Rubberwood flour from S.T.A Furniture Group Co., Ltd (Songkhla, Thailand) was used as lignocellulosic filler. The important chemical compositions are listed in Table 3.1. The recycled PP was supplied by Withaya Intertrade Co., Ltd (Samutprakarn, Thailand) in the pellet form. Prior to blending, the RWF was sieved through 80 mesh and dried in an oven at 110 $^{\circ}$C for 8 h. The dried wood flour was stored in a sealed plastic container to prevent the absorption of water vapor. Each formulation in Table 3.2 was weighed and stirred for 5 min to obtain uniform

dispersion. A twin-screw extruder (Model SHJ-36 from En Mach Co., Ltd, Nonthaburi, Thailand) was used to produce the WPC panels with dimensions of 9 mm × 22 mm. The temperature profiles in the extruding process were 145-180 °C with a screw rotating speed of 100 rpm. The temperatures of extruding composites were lower down in atmospheric air cooling (AC) and water cooling (WC). Subsequently, the specimens were machined corresponding to ASTM for mechanical testing.

Table 3.1 Chemical compositions of rubberwood [7]

Chemical constituent	Cellulose	Hemicellulose	Lignin	Ash
Composition (%)	39	29	28	4

Table 3.2 Compositions of the wood-plastic composites

Sample ID	rPRWF0	rPRWF28	rPRWF33	rPRWF37	rPRWF41	rPRWF44
rPP (wt%)	100	71.4	66.7	62.5	58.8	55.5
RWF (wt%)	0	28.6	33.3	37.5	41.2	44.5

3.3.2 Mechanical testing

The tensile and flexural properties were measured on the Instron Universal Testing Machine (Model 5582 from Instron Corporation, Massachusetts, USA). Tensile tests were carried out according to ASTM D638-91 Type I at a testing speed of 5 mm/min. Three-point bending tests were performed in accordance to ASTM D790-92. Tests were conducted at a cross-head speed of 2 mm/min. All the tests were carried out at room temperature (25 °C) with five replications.

3.3.3 Morphological observation

The state of dispersion, interfacial adhesion, and voids of the wood flour in the polymeric matrix was analyzed with scanning electron microscope (SEM). A FEI Quanta 400 microscope (FEI Company, Oregon, USA) working at 15 kV was used to obtain microphotographs of the composite surfaces.

3.3.4 Thermal testing

The effects of filler concentration on melting and crystallization temperatures (T_m and T_c, respectively), and the heat of fusion (Δh_f) were ascertained from differential scanning calorimetry (DSC-7, PerkinElmer, Massachusetts, USA). The DSC was typically operated at heating and cooling rates of 10 °C/min, respectively. The dynamic mechanical thermal analysis (Rheometric scientific DMTA V, USA) was also performed to measure storage (E′) and loss (E″) modulus as a function of temperature at small strain amplitudes and a fixed frequency of 10 Hz in the linear viscoelastic limit. The specimen size of 10 mm × 35 mm × 3 mm was prepared and investigated.

3.4 Results and discussion

3.4.1 Mechanical properties

The effect of different amounts of wood flour on the mechanical properties of rPP/rubberwood composites was shown in Table 3.3 and Figure 3.1. It was found that an increase of rubberwood flour content resulted in a decrease of tensile strength (TS) and flexural strength (MOR) for both in air and water cooling. The result is in good agreement with Prachayawarakorn et al. [8] and Sombatsompop et al. [9]. The decreases in the tensile and flexural strengths, due to the addition of wood flour, were associated with poor dispersion and weak adhesion of the wood particles in the plastic matrix. From the SEM micrographs shown in Figure 3.2, it was clearly seen that the wood particles (fibers) tended to cling together due to strong interfiber hydrogen bonding and resist dispersion as an individual fiber while the fiber content was increased from 28.6 to 44.5 wt% [9]. Likewise, the enlarging wood flour content increased the poor interfacial adhesion and void amounts, and thus reduced mechanical strengths of the composites.

The tensile modulus (TM) and flexural modulus (MOE), as shown in Table 3.3 and Figure 3.1, of the composites enhanced with an increase of RWF content. The increase of the modulus with wood flour content was caused by the fact that the wood flour is more rigid phase compared to the polymer matrix [8].

Furthermore, the air cooled composites appeared to give higher mechanical properties (both tensile and flexural properties) than that of the water cooled composites. The reason is the polypropylene matrix instantaneously cooled below its glass transition temperature while the molecule was still under stress. The molecules therefore became frozen whilst in an oriented state [3]. Likewise, the composites cooled in the air revealed higher crystallinity than cooling in the water, as shown in Table 3.4.

Table 3.3 Effects of rubberwood flour loading on the mechanical properties

	Air cooling (AC)				Water cooling (WC)			
Wood flour content (wt%)	TS (MPa)	TM (MPa)	MOR (MPa)	MOE (MPa)	TS (MPa)	TM (MPa)	MOR (MPa)	MOE (MPa)
0	25.9	317	44.8	1446	22.6	308	41.2	1387
28.6	22.3	420	39.1	1927	20.2	356	36.4	1619
33.3	20.9	586	38.2	1959	17.8	431	34.8	1644
37.5	19.5	626	34.9	2171	17.4	442	31.1	1760
41.2	18.6	773	34.1	2403	17.0	524	31.6	1854
44.5	18.2	708	30.5	2583	16.0	557	30.5	2004

3.4.2 Morphological analysis

The SEM micrographs of rPRWF28, rPRWF37, and rPRWF44 composites are given in Figures 3.2(a), 3.2(b), and 3.2(c), respectively. It clearly showed that rubberwood flour exhibited the shape of irregular short fibers in the composites. The analysis of the rubberwood flour dispersion shows that the addition of higher wood flour content to rPP matrix [Figures 3.2(b) and 3.2(c)] seems to present a higher number of agglomerations. This behavior probably means that poorer particle dispersion in the rPP matrix has occurred [10]. It is known that wood flour has a great tendency to form agglomerates, in fact, agglomeration is a well-known phenomenon, and its probability increases with decreasing particle size. The occurrence and extent of agglomeration are determined by the relative magnitude of the forces, which

either bind together the particles or try to separate them [11]. This result is in accordance with the mechanical results found in this work.

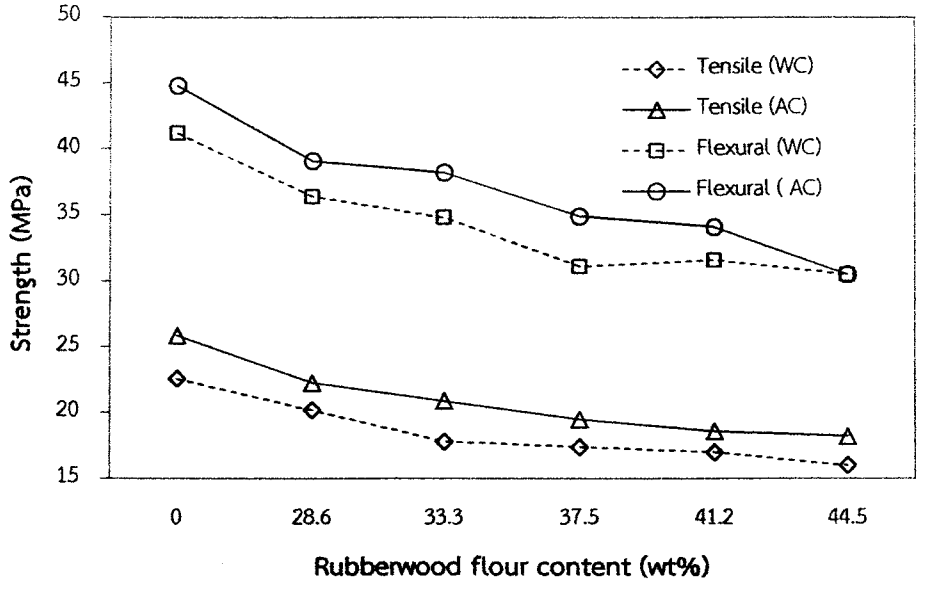

(a)

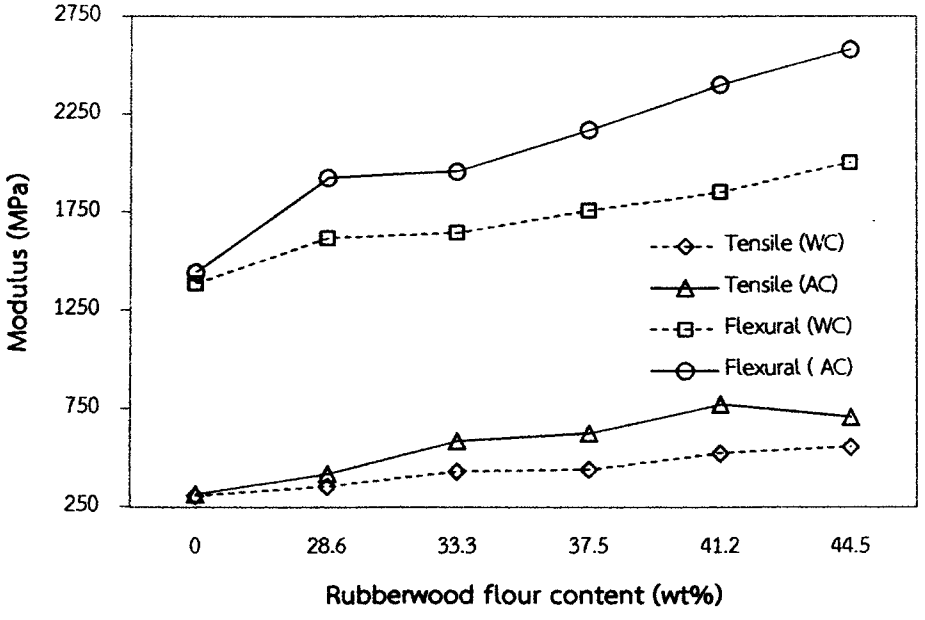

(b)

Figure 3.1 Mechanical properties of rPP/rubberwood flour composites versus different wood flour content (a) tensile and flexural strengths, (b) tensile and flexural modulus

than 5%. However, the crystallinity of the polypropylene was unaffected by wood flour content. In good agreement with the findings of Xu et al. [12] who studied ultra-high-molecular-weight polyethylene (UHMWPE) composites containing carbon black (CB), they reported that the crystallinity of UHMWPE was unaffected by the presence of CB and infer from these results that the polymer crystal size is independent of the filler loading level. Similar behavior was also observed in the present of HDPE/UHMWPE blends filled with CB, in which the crystallinity varies by less than 5% [13]. However, the cooling rate insignificantly affected T_m and T_c but significant crystallinity. The plastics that were heated to a temperature above its glass transition and then were slowly cooled below its transition temperature gain higher crystallinity than the instantaneous cooling.

Table 3.4 Thermal properties of the WPCs containing different concentrations of wood flour and cooling orientation state

Wood flour	T_m (°C)		T_c (°C)		Δh_f (J/g)		Crystallinity* (%)	
content (wt%)	AC	WC	AC	WC	AC	WC	AC	WC
0	160.2	156.8	119.9	116.8	77.2	68.5	46.8	41.5
28.6	160.0	159.2	119.9	119.3	56.6	52.4	48.0	44.5
37.5	159.7	159.2	119.3	119.3	45.4	42.5	44.0	41.2
44.5	159.8	158.7	119.3	118.8	44.3	39.0	48.4	42.6

*Calculated from the ratio of the measured Δh_f to that of a 100% crystalline polypropylene (165 J/g).

3.4.3.2 Dynamic mechanical thermal analysis

The variation of storage (E′) and loss modulus (E″) for unfilled rPP and rPP/RWF composites was shown in Figures 3.3(a) and 3.3(b), respectively. It showed that composites had higher E′ and E″ than unfilled rPP through the whole temperature range of the study due to the reinforcement effect of rubberwood flour. The wood flour can cautiously carry in decreasing of E′ and E″. Likewise, the enlarging wood flour content can increase the storage and loss modulus. This is consistent with the results reported in the literature [14]. The addition of wood flour leads to the increase in both elastic and viscous abilities of composites under the dynamic load [14]. The E′ and E″ gradually decreased in the range of 50 °C to 160 °C,

but instantaneously decreased at 160 °C to 210 °C. This was due to the melting effect of the PP matrix. Furthermore, WPCs with air cooling had higher storage and loss modulus than the one with water cooling. Because melting temperature and crystallinity of WPCs with air cooling affected greater than that of water cooling based on DSC analysis.

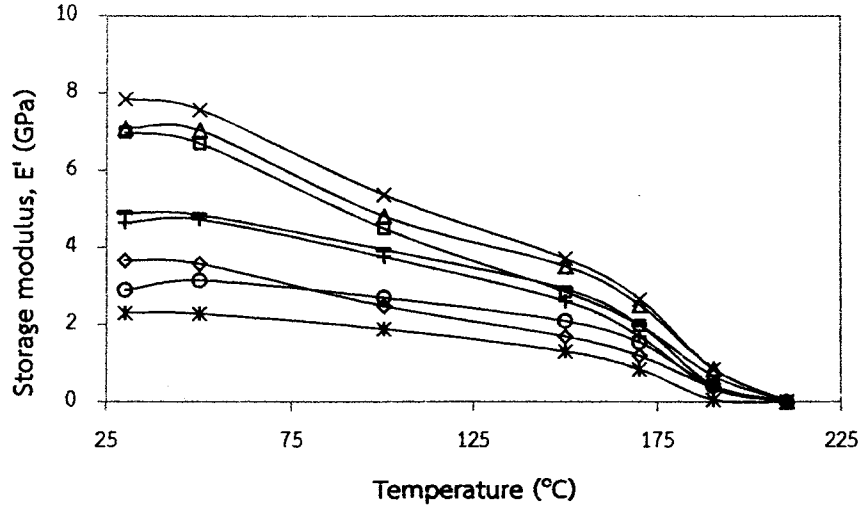

(a)

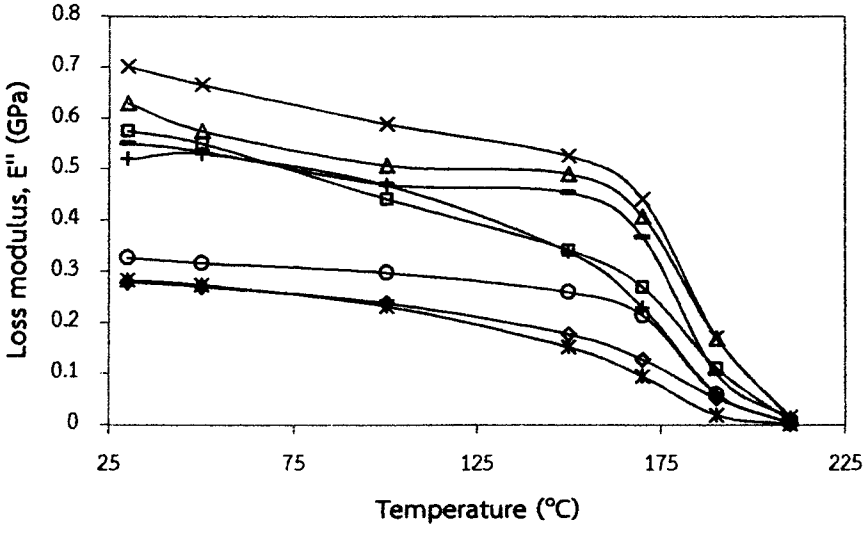

(b)

Figure 3.3 Variation of (a) storage and (b) loss modulus with temperature for air cooling; rPRWF0 (◊), rPRWF28 (□), rPRWF37 (Δ), rPRWF44 (×), and water cooling; rPRWF0 (*), rPRWF28 (O), rPRWF37 (+), and rPRWF44 (—), the solid lines serve to connect the data

3.5 Conclusions

Natural rubberwood flour can be simply blended with recycled polypropylene to produce cost-competitive and woodlike composites with satisfactory properties [15]. The mechanical and thermal properties of composites were affected by the concentration of rubberwood flour. It was found that the mechanical properties of rPP/RWF composites decreased with an increase of RWF loading due to poorer interfacial adhesion between the hydrophilic filler and the polymer matrix [16]. The mechanical results were corroborated with morphological evidence. DSC analysis also showed that the increase of rubberwood flour content insignificant affected the degree of crystallinity because of stability of the crystalline portion in the material. However, the degree of crystallinity was dependent on methods of the cooling. Furthermore, plots of storage and loss modulus with temperature showed an increase in the magnitude of the peaks with the enlarging wood flour reinforcement and air cooling. On the basis of these studies, it can be concluded that wood flour decreased mechanical properties of composites, but it increased the stability of composites. The cooling rate significantly affected the mechanical and thermal properties.

3.6 References

[1] A. Conroy, S. Halliwell, and T. Reynolds. "Composite Recycling in the Construction Industry." *Composites Part A: Applied Science and Manufacturing*, vol. 37, pp. 1216–1222, 2006.

[2] M.C.N. Yemele, A. Koubaa, A. Cloutier, P. Soulounganga, and M. Wolcott. "Effect of Bark Fiber Content and Size on the Mechanical Properties of Bark/HDPE Composites." *Composites Part A: Applied Science and Manufacturing*, vol. 41, pp. 131–137, 2010.

[3] J.A. Brydson. *Plastics Materials*. Butterworth-Heinemann, Jordan hill, Oxford, 1999.

[4] D. Ndiaye, L.M. Matuana, S.M. Therias, L. Vidal, A. Tidjani, and J.L. Gardette. "Thermal and Mechanical Properties of Polypropylene/Wood-Flour

Composites." *Journal of Applied Polymer Science*, vol. 119, pp. 3321–3328, 2011.

[5] J. Lisperguer, X. Bustos, and Y. Saravia. "Thermal and Mechanical Properties of Wood Flour-Polystyrene Blends from Postconsumer Plastic Waste." *Journal of Applied Polymer Science*, vol. 119, pp. 443–451, 2011.

[6] K.B. Adhikary, S. Pang, and M.P. Staiger. "Dimensional Stability and Mechanical Behaviour of Wood-Plastic Composites based Recycled and Virgin High-Density Polyethylene." *Composites Part B: Engineering*, vol. 39, pp. 807–815, 2008.

[7] P. Petchpradab, T. Yoshida, T. Charinpanitkul, and Y. Matsumura. "Hydrothermal Pretreatment of Rubber Wood for the Saccharification Process." *Industrial and Engineering Chemistry Research*, vol. 48, pp. 4587–4591, 2009.

[8] J. Prachayawarakorn, J. Khamsri, K. Chaochanchaikul, and N. Sombatsompop. "Effects of Compatibilizer Type and Rubber-Wood Sawdust Content on the Mechanical, Morphological, and Thermal Properties of PVC/LDPE Blend." *Journal of Applied Polymer Science*, vol. 102, pp. 598–606, 2006.

[9] N. Sombatsompop, K. Chaochanchaikul, C. Phromchirasuk, and S. Thongsang. "Effect of Wood Sawdust Content on Rheological and Structural Changes, and Thermo-Mechanical Properties of PVC/Sawdust Composites." *Polymer International*, vol. 52, pp. 1847–1855, 2003.

[10] S.C.S. Teixeira, M.C.G. Rocha, and F.M.B. Coutinho. "Composites of High Density Polyethylene and Different Grades of Calcium Carbonate: Mechanical, Rheological, Thermal, and Morphological Properties." *Journal of Applied Polymer Science*, vol. 101, pp. 2559–2564, 2006.

[11] R.H. Elleithy, I. Ali, M.A. Ali, and S.M. Al-Zahrani. "High Density Polyethylene/Micro Calcium Carbonate Composites: A Study of the Morphological, Thermal, and Viscoelastic Properties." *Journal of Applied Polymer Science*, vol. 117, pp. 2413–2421, 2010.

[12] C. Xu, Y. Agari, and M. Matsuo. "Mechanical and Electric Properties of Ultra-High-Molecular Weight Polyethylene and Carbon Black Particle Blends." *Polymer Journal*, vol. 30, pp. 372–380, 1998.

[13] W. Thongruang, C.M. Balik, and R.J. Spontak. "Volume-Exclusion Effects in Polyethylene Blends Filled with Carbon Black, Graphite, or Carbon Fiber." *Journal of Polymer Science: Polymer Physics*, vol. 40, pp. 1013–1023, 2002.

[14] H. Jiang and D.P. Kamdem. "Thermal and Dynamic Mechanical Behavior of Poly(Vinyl Chloride)/Wood Flour Composites." *Journal of Applied Polymer Science*, vol. 107, pp. 951–957, 2008.

[15] X.C. Ge, X.H. Li, and Y.Z. Meng. "Tensile Properties, Morphology, and Thermal Behavior of PVC Composites Containing Pine Flour and Bamboo Flour." *Journal of Applied Polymer Science*, vol. 93, pp. 1804–1811, 2004.

[16] M.A. Syed, B. Ramaraj, S. Akhtar, and A.A. Syed. "Development of Environmentally Friendly High-Density Polyethylene and Turmeric Spent Composites: Physicomechanical, Thermal, and Morphological Studies." *Journal of Applied Polymer Science*, vol. 118, pp. 1204–1210, 2010.

CHAPTER 4

Long-Term Water Absorption and Dimensional Stability of Composites from Recycled Polypropylene and Rubberwood Flour

4.1 Chapter summary

This study aims to investigate the moisture absorption of polypropylene/rubberwood flour (RWF) composites and its effects on dimensional stability. The compositions included different grades of plastic (virgin and recycled); and the amounts of wood flour, maleic anhydride-grafted polypropylene (MAPP) and ultraviolet (UV) stabilizer were varied. The composite materials were manufactured into panels by using a twin-screw extruder. Long-term water absorption (WA), long-term thickness swelling (TS) and failure of flexural properties of the composites were studied for a range of water immersion times. The WA and TS increased with RWF content and immersion time. Recycled polypropylene (rPP) gave higher WA and TS than virgin polypropylene (vPP), for the composites with 45 wt% RWF. Increasing MAPP content from 3 wt% to 5 wt% had no significant effect on WA and TS, but the addition of 1 wt% UV stabilizer did. A MAPP content of 3 wt% is recommended for moisture resistance, while the amount of UV stabilizer should be kept as low as possible. Flexural strength and modulus of composites also decreased with moisture uptake; however less than 3% WA did not significantly affect the flexural strength. In contrast, the maximum strain of composites consistently increased with WA.

4.2 Introduction

Natural organic fibers are potential replacements for glass or carbon fibers, inorganic fillers, and other traditional materials in composites [1, 2]. The advantages of natural fibers include low cost, low density, low energy consumption, biodegradability, and non-abrasive nature [1, 3]. Likewise, they can have high specific strength and modulus, allowing the production of low-density composites with high

filler content [4, 5]. Recent advances in natural fillers create opportunities to improve materials from renewable resources, supporting global sustainability [6]. Natural wood fibers in the forms of flour, sawdust and chips are available as waste streams from sawmills and furniture factories. In plastics industries, they have been primarily used as inexpensive reinforcement to enhance the modulus of several thermoplastics, and as fillers substituting for more costly raw materials. There have been numerous studies on producing thermoplastic composites with plant fibers, plant flour, or wood flour: including eastern red cedar [7], flax [8], maple [9], oak [7], pine [10], and rubberwood [11]. In addition, the increasing global production and consumption of plastics significantly contributes to municipal solid waste [12]. In 2008, at least 33.6 million tons of post-consumer plastics were generated in the United States, of which 85.8% went to landfills, 7.7% to combustion and energy recovery, and only 6.5% to recycling [13, 14] – only a tiny fraction of plastic wastes are recycled. Effective and safe disposal has also become a serious public concern [15]; however, plastic wastes could be raw materials for wood-plastic composites (WPCs) [16]. Increasing the opportunities to make use of plastic wastes has motivated the current study. The WPCs produced from recycled plastic would not only provide effective disposal of plastic wastes, but also the consumption of energy and natural resources would be reduced [13, 17]. There is clearly potential for both environmental and economic benefits in recycling combinations of wood and plastic wastes [10, 15].

Rubberwood (*Hevea brasiliensis*) is used in large amounts by sawmills and furniture industry in southern Thailand, and these produce large quantities of waste in the forms of sawdust and wood chips. In these industries only 12% of the rubberwood ends up in the products, while the rest is wood waste (about 34%) and plantation wastes (about 54%) [18]. Most of the wood waste (sawdust) is used to produce medium-density fiberboard and particleboard [19]. However, the utilization of wood waste as reinforcement in plastic composites is great interest, with both environmental and economic benefits. Wood as reinforcement of plastic composites has many advantages over synthetic fillers [20], but its hydrophilic nature is a disadvantage impacting the performance of the WPCs [12, 21]. The water absorption

characteristics WPCs limit their end-use applications [2], as several mechanical and physical properties, for example, an effect of dimensional stability. The water absorption of the WPCs varies by the wood species, partly because they have different contents of cellulose, lignin, hemicelluloses, and extractants [22]. Hence, the effects of filler (rubberwood flour; RWF) and grade of plastic (virgin or recycled) on the composite properties need to be characterized. The goal of current work is to determine the effects of material compositions (including different grades of plastic; and contents of RWF, coupling agent, and ultraviolet stabilizer) on the long-term water absorption, and the thickness swelling and failure of flexural properties, of RWF reinforced polypropylene composites. The new information would help target the most suitable end-use applications of such composites.

4.3 Experimental

4.3.1 Materials

Rubberwood flour supplied by a local furniture factory (Songkhla, Thailand) was used as reinforcement. The main chemical constituents were: cellulose (39%), hemicellulose (29%), lignin (28%), and ash (4%) [18]. The wood flour was sieved through a standard sieve of mesh size 80 (passing particles smaller than 180 μm) and was dried in an oven at 110 °C for 8 h before compounding. Recycled polypropylene (rPP) pellets, WT170 with a melt flow index of 11 g/10 min at 230 °C, were supplied by Withaya Intertrade Co., Ltd (Samutprakarn, Thailand). Virgin polypropylene (vPP) granules, HIPOL J600 with a melt flow index of 7 g/10 min at 230 °C, were procured from Mitsui Petrochemical Industries Co., Ltd (Tokyo, Japan). The coupling agent used was maleic anhydride-grafted polypropylene (MAPP), supplied by Sigma-Aldrich (Missouri, USA), with 8-10% of maleic anhydride. Hindered amine light stabilizer additive, chosen as the UV stabilizer (UV), was supplied by TH Color Co., Ltd (Samutprakarn, Thailand) under the trade name MEUV008. A paraffin wax lubricant (Lub) was purchased from Nippon Seiro Co., Ltd (Yamaguchi, Japan).

4.3.2 Composite preparation

WPCs were manufactured in a two-stage process. In the first stage to produce WPC pellets, rubberwood flour and polypropylene were mixed and pelletized using a twin-screw extruder (Model SHJ-36 from En Mach Co., Ltd, Nonthaburi, Thailand). Barrel temperatures of the ten zones were controlled at 130-170 °C from feeding to die zones, to reduce degradation of the compositions, while the screw rotation speed was controlled at 70 rpm. In the second stage to produce WPC panels, the WPC pellets were carefully dried prior to use, in an oven at 110 °C for 8 h. The WPC pellets, MAPP, UV stabilizer, and lubricant (formulations in Table 4.1) were then dry-mixed and added into the feeder of a twin-screw extruder. The extruding conditions were as follows: (1) temperature profiles: 130-190 °C; (2) screw rotating speed: 50 rpm; (3) vacuum venting at 9 temperature zones: 0.022 MPa; and (4) melt pressure: 0.10-0.20 MPa depending on wood flour content. The samples were extruded through a rectangular die with the dimensions of 9 mm × 22 mm and cooled in ambient air. After cooling the specimens were cut according to ASTM for physical and mechanical tests

Table 4.1 Wood-plastic composite formulations (percent by weight)

Composite sample code	rPP	vPP	RWF	MAPP	UV	Lub	Density (g/cm^3)
rP100	100						0.886 (0.065)*
vP100		**100**					**0.816 (0.092)**
rP70R25M3U1	70		25	3	1	1	0.986 (0.070)
vP70R25M3U1		**70**	**25**	**3**	**1**	**1**	**0.953 (0.069)**
rP60R35M3U0.5	60.3		35.3	3	0.5	1	1.015 (0.036)
vP60R35M3U0.5		**60.3**	**35.3**	**3**	**0.5**	**1**	**0.985 (0.063)**
rP50R45M3U1	50		45	3	1	1	1.085 (0.033)
vP50R45M3U1		**50**	**45**	**3**	**1**	**1**	**1.009 (0.060)**
rP68R25M5U1	68		25	5	1	1	0.972 (0.089)
rP69R25M5U0	69		25	5	0	1	0.914 (0.072)

Note; The sample codes summarize the formulation, as in rP70R25M3U1 having 70 wt% rPP, 25 wt% RWF, 3 wt% MAPP, and 1 wt% UV. *The values in parentheses are standard deviations from five replications.

4.3.3 Testing

Density. All samples were oven-dried at 50 °C for 24 h. After oven drying, the samples were cooled in a desiccator containing calcium chloride and then weighed (a precision of 0.001 g). After that, the dimensions of the composite samples were measured using a digital vernier caliper (a precision of 0.01 mm) and the volume were calculated. The full dry density of PP/RWF composites was computed using Equation (4.1).

$$\text{Density} = \frac{M_0}{V_0} \quad \left(\frac{g}{cm^3}\right) \tag{4.1}$$

where M_0 is the full dry weight (g) and V_0 is the volume (cm^3) of the composites.

Water absorption and dimensional stability. Water absorption test was carried out according to ASTM D570-88 specification. Specimens (4.8 mm × 13 mm × 26 mm) were cut from the extruded panels and used to measure the water absorption and thickness swelling. Five specimens of each formulation were dried in an oven at 50 °C for 24 h. The weight and thickness of dried specimens were measured to a precision of 0.001 g and 0.01 mm, respectively. The specimens were then immersed in water at ambient room temperature. After one week, soaked specimens were removed from the water, thoroughly dried with tissue papers, and immediately weighed and measured to determine the weight and thickness. Then the specimens were immersed in water again and stored at ambient room temperature for ten weeks. The data collection was weekly repeated. The percentage of water absorption (WA) can be calculated using equation (4.2):

$$WA_t = \frac{W_t - W_0}{W_0} \times 100 \quad (\%) \tag{4.2}$$

where WA_t is the water absorption at time t, W_0 is the initial dry weight, and W_t is the soaked weight of specimen at a given time t.

The percentage of thickness swelling (TS) was calculated using equation (4.3):

$$TS_t = \frac{T_t - T_0}{T_0} \times 100 \quad (\%) \tag{4.3}$$

where TS_t is the thickness swelling at any time t, T_0 is the initial dry thickness, and T_t is the soaked thickness of specimen at a given time t.

Flexure testing. Three-point flexure test was carried out on an Instron Universal Testing Machine (Model 5582 from Instron Corporation, Massachusetts, USA) at a cross-head speed of 2 mm/min with nominal dimensions of 4.8 mm × 13 mm × 100 mm, a span of 80 mm in accordance with ASTM D790-92. The testing was performed at ambient room temperature of 25 °C with five samples of each formulation to obtain an average value. In addition, the measurements of flexural strength and modulus were weekly repeated. The failure of the flexural properties was determined for a total of six weeks, at which time the samples were water saturated and no longer absorbing.

4.3.4 Analysis

Morphological analysis. Morphological studies with a scanning electron microscope (SEM) were carried out to assess the interfacial adhesion and phase dispersion of wood flour in the polymeric matrix. SEM imaging with a FEI Quanta 400 microscope (FEI Company, Oregon, USA) used an accelerating voltage of 20 kV. Prior to SEM observations, all samples were sputter-coated with gold to prevent electrical charging during the imaging. Specimens were imaged at magnifications of 150× and 1000×.

Statistical analysis. The effects of water absorption on the bending properties of RWF reinforced polypropylene composites were evaluated by analysis of variance (ANOVA) and Tukey's multiple comparison test. The ANOVA revealed significant differences between water absorption amounts, failure of flexural properties in each week, and a comparison of the mean values was done with Tukey's multiple comparison test. Results, such as mean values and standard deviations from five samples of each test, were statistically analyzed. All the statistical analyses used a 5% significance level ($\alpha = 0.05$).

4.4 Results and discussion

4.4.1 Density of wood-plastic composites

Densities of the WPCs at various mix ratios and different plastic grades are shown in Figure 4.1. The density of the composites ranges from 0.816 g/cm^3 for the entire vPP-panel to 1.085 g/cm^3 for the 45 wt% rubberwood-rPP composite panels with 3 wt% MAPP. The density of WPCs increased linearly with the wood fiber loading; the R^2 values of linear fits are 0.992 and 0.943 for virgin and recycled polypropylene composites, respectively. As the density of produced WPCs is over 0.8 g/cm^3, which is comparable to high-density fiberboard (0.8-1.040 g/cm^3). These are high-density boards that could be interest as structure materials, among other applications. Generally, the bulk density of most wood species is in the range of 0.32 to 0.72 g/cm^3. Wood with density exceeding 0.8 g/cm^3 is considered high density wood [23]. Furthermore, the WPCs from recycled polypropylene had higher densities than with virgin polypropylene at all mix ratios, although both types of polypropylene gave a similar trend for the density increase with wood flour loading. The effect of UV stabilizer was to increase the density of PP/RWF composites, at 1 wt% addition level. This is probably because the UV stabilizer has higher density than the recycled polypropylene.

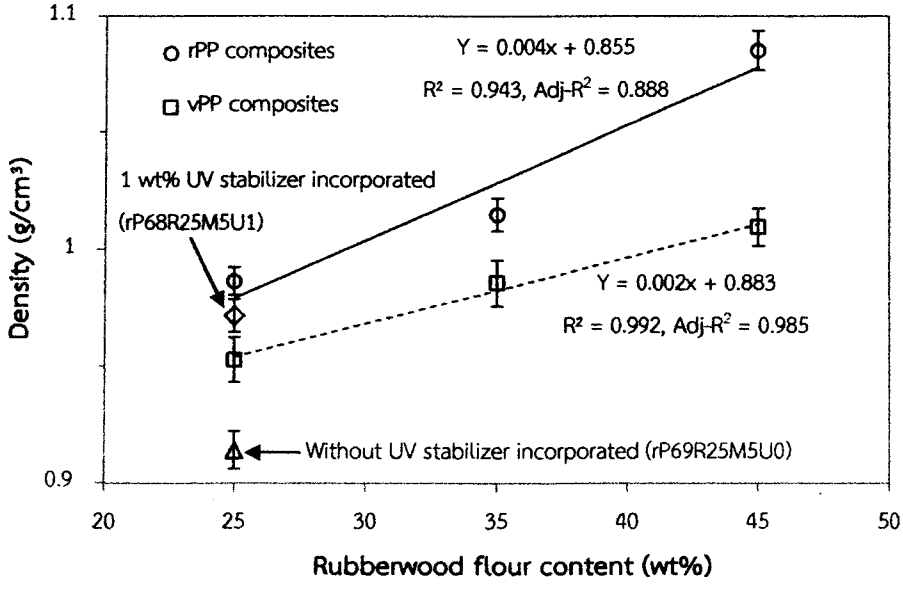

Figure 4.1 Averages of density as a function of wood flour loading, for the PP-rubberwood flour composites

4.4.2 Long-term water absorption behavior

The long-term water absorption of the PP/RWF composites was monitored by full water immersion over a period of 10 weeks (70 days) as shown in Figure 4.2. Composites made from virgin and recycled polypropylene with 45 wt% RWF absorbed the most water, having moisture ratios of 9.80% and 10.33% (relative to solids by weight), respectively, after 70 days. Generally, the water absorption increased with wood flour content [24] because of an increase of free OH groups with wood cellulose content. These free OH groups interact with polar water molecules, leading to the weight gain of the composites [12]. During immersion the wood flour absorbed a significant quantity of water, while the plastics absorbed very little [12]. At the same wood flour contents up to 35%, the composites based on virgin and recycled polypropylene had very similar water absorption. However, at 45 wt% RWF the two types of plastic seem to give different absorption behavior. This may be due to better encapsulation of wood flour into virgin polypropylene, with good dispersion and strong interfacial bonding between wood particles and polymer, and consequently slower water absorption. Theoretically, the penetration of moisture into wood-plastic composites takes place by three different mechanisms. The main processes are capillary transport of water in the pores, and flows at the interfaces between polymer and fibers, due to poor wettability and impregnation. The third common mechanism is the diffusion of water molecules in the micro gaps between polymer chains, and transport by microcracks in the matrix [25, 26].

The effects of MAPP and UV stabilizer contents on the water absorption are also shown in Figure 4.2. MAPP addition of 5 wt% in rPP/RWF composites containing 25 wt% RWF (rP68R25M5U1) gave a lower water absorption (not statistically significant) than the addition of 3 wt% MAPP (rP70R25M3U1). Similar results have been reported by Adhikary et al. [12]: the coupling agent increased adhesion in WPCs, by improving compatibility between the wood particles and the polymer. Then the plastic can cover more of the wood surfaces, resulting in lower water absorption. Furthermore, adding 1 wt% UV stabilizer (rP68R25M5U1) increased the equilibrium moisture content (EMC) to 3.13%, from 2.78% without UV stabilizer (rP69R25M5U0), as shown in Figure 4.3. This may be attributed to the nonuniform

spatial distribution of wood flour, polymer, and UV stabilizer [19, 27], which results in higher water absorption. In Figure 4.3, the linear correlation between EMC and wood flour content is high, for both virgin and recycled polypropylene composites (R^2 = 0.995 and 0.999, respectively). However, the relationship between composite board density and EMC is low, with the R^2 value being 0.781. The water absorption behavior is complex and can be influenced by several factors, for example wood content, virgin or recycled plastics, UV stabilizer, and coupling agent.

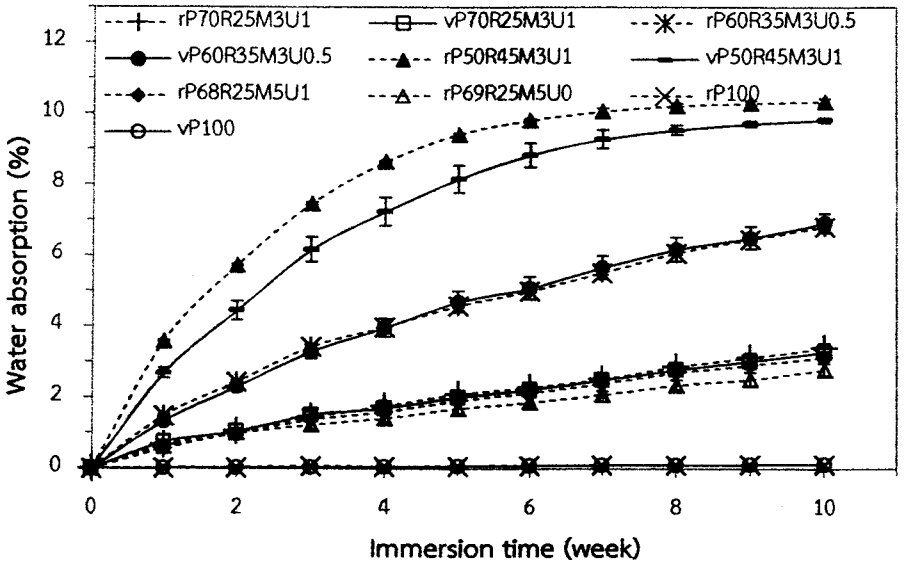

Figure 4.2 Effect of composition contents and plastic grades on long-term water absorption for PP-rubberwood flour composites

4.4.3 Long-term thickness swelling behavior

The thickness swelling (TS) of virgin and recycled polypropylene composites with various contents of rubberwood flour is represented in Figure 4.4. The TS of virgin and recycled composites was the highest with 45 wt% RWF at 3.20% and 3.51%, respectively, corresponding also to the highest water absorption. However, the recycled polypropylene composites containing 45 wt% RWF had more thickness swelling than the virgin polypropylene composites. These results can be compared to the scanning electron micrographs of PP composites with 45 wt% RWF in Figure 4.5; Figures 4.5(a) and (b) for vPP and Figures 4.5(c) and (d) for rPP. Irregular

short fibers were spread in the plastic matrix. The rPP composites showed less homogenous morphological structure, poorer dispersion of the fibers in the matrix and weaker interfacial bonding between the wood flour and the polymer matrix, than the vPP composites. Therefore, the rPP composites allow easier access of water to the cellulose [12]. With a similar trend to the water absorption, the TS of rPP/RWF composites increased with wood flour content and immersion time, until saturation at equilibrium. For example, the rPP composites containing 25, 35, and 45 wt% RWF with addition of 3 wt% MAPP displayed equilibrium thickness swelling (ETS) values of 0.89%, 1.73%, and 3.51%, respectively. Likewise, the TS of vPP/RWF showed the same trends and qualitative behavior; the equilibrium TS of vPP composites with 25, 35, and 45 wt% RWF were 0.69%, 2.0%, and 3.20%, respectively.

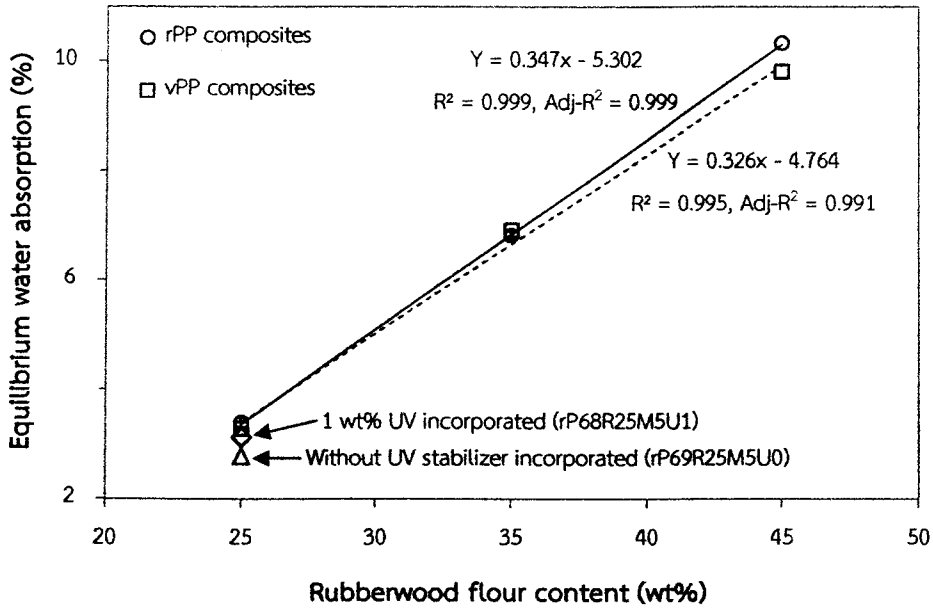

Figure 4.3 Averages of equilibrium water absorption is a practically linear function of wood flour loading, for the PP-rubberwood flour composites

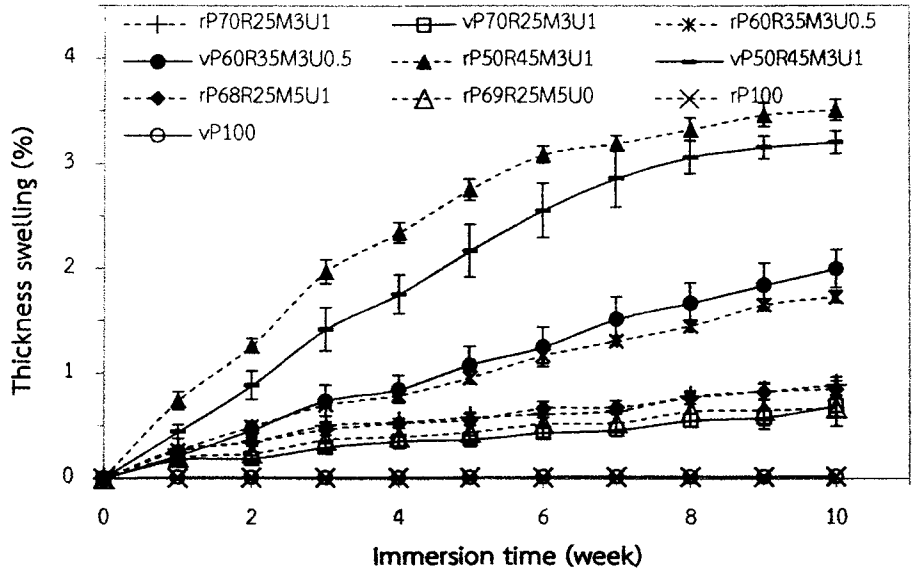

Figure 4.4 Thickness swelling as function of water immersion time, for PP-rubberwood flour composites. Solid and dashed lines represent virgin and recycled polymer, respectively

The effects of MAPP and UV stabilizer contents on the thickness swelling of WPCs are also shown in Figure 4.4. As can be seen, the rPP/RWF composites with 3 wt% MAPP (rP70R25M3U1) yielded the same thickness swelling as the composites with 5 wt% MAPP (rP68R25M5U1), and had similar water absorption trends. In the range 3-5 wt%, changes in MAPP content had no effect on the water absorption and thickness swelling of rPP/RWF composites, so using MAPP in excess of 3 wt% may be unnecessary. However, at the same wood flour content, the WA and TS significantly decreased with addition of 3-5 wt% coupling agent to the composites, compared to the composites without MAPP [12, 26]. The coupling agent improves the interfacial adhesion between wood flour and polymer matrix, and this restricts the water absorption and thickness swelling of the composites [28]. In addition, the change in the thickness swelling with different UV stabilizer concentrations is similar to that found in the water absorption. The composites with 25 wt% RWF show an insignificant increase in ETS with an increase in UV stabilizer from 0 wt% (rP69R25M5U0) to 1 wt% (rP68R25M5U1), as shown in Figure 4.6. The mechanisms causing this phenomenon were discussed earlier in relation to water

absorption. Using 1 wt% of UV stabilizer may be unnecessary, and to reduce the negative effects on the TS and WA, the amount of UV stabilizer should be minimized.

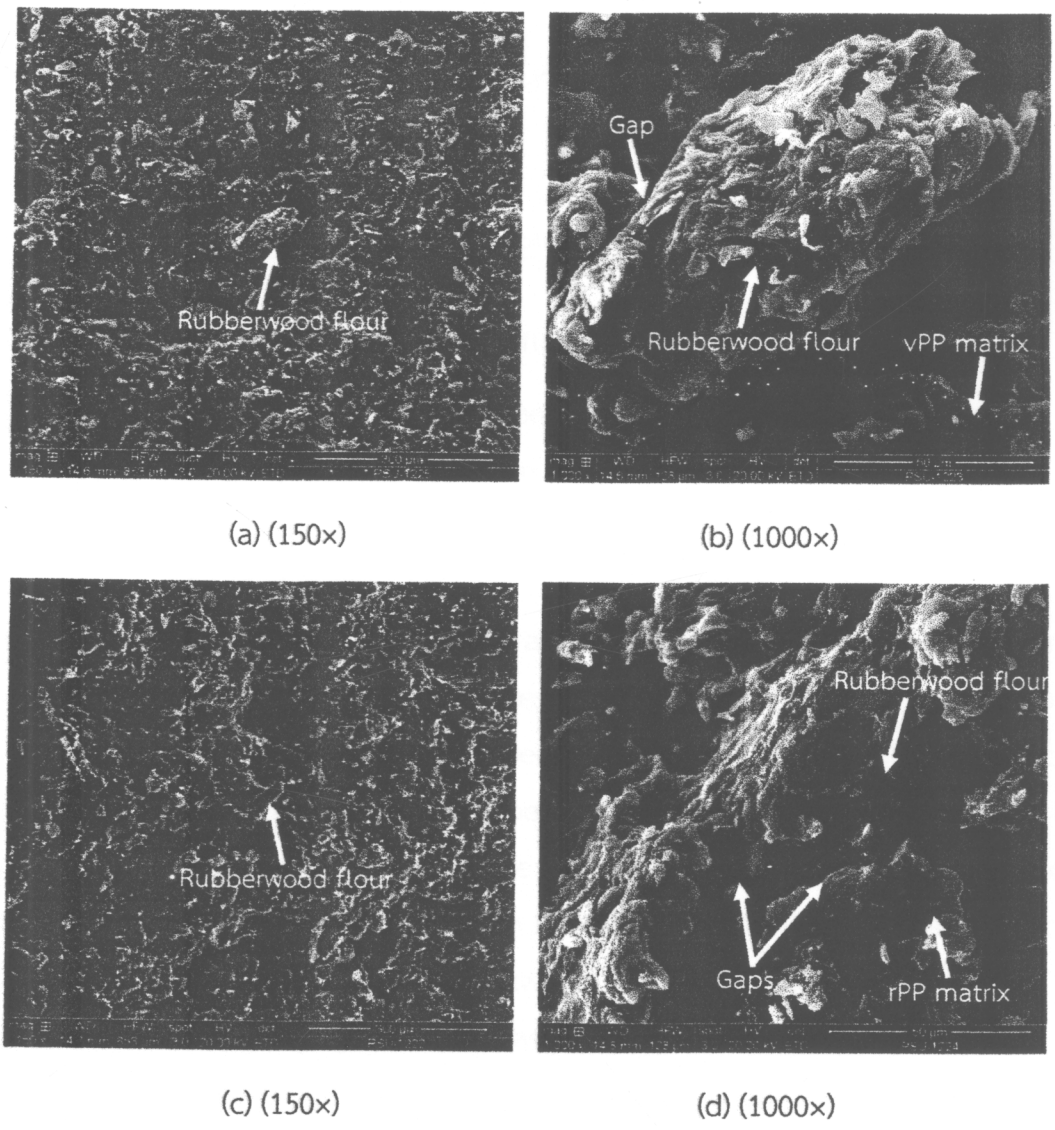

(a) (150×) (b) (1000×)

(c) (150×) (d) (1000×)

Figure 4.5 Scanning electron micrographs of 45 wt% RWF composites based on (a), (b) virgin polypropylene; and (c), (d) recycled polypropylene. Magnifications 150× and 1000× from left to right

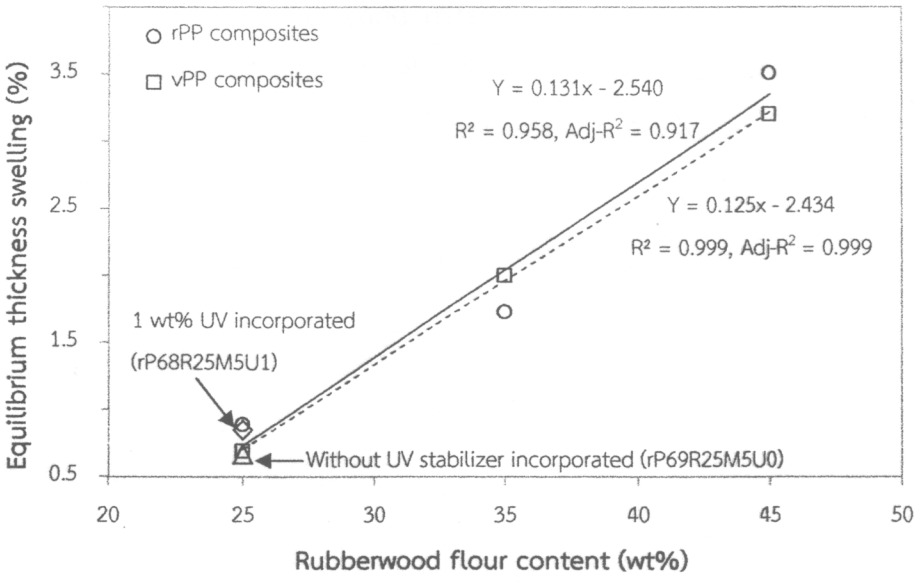

Figure 4.6 Averages of equilibrium thickness swelling of the PP-rubberwood flour composites as a function of wood flour loadings

The relationships between ETS and wood flour content of the virgin and recycled polypropylene composites are also shown in Figure 4.6, with strong linear correlations (R^2 = 0.999 and 0.958, respectively). When the wood flour content in the composites is increased, the number of free OH groups contributed by wood cellulose is also increased. Therefore, the water absorption increases, resulting in increased thickness swelling [2, 12, 29]. The relationship between the ETS and EMC of the PP/RWF composites is also linear with R^2 value of 0.997. The empirical equation obtained from the linear correlation between equilibrium thickness swelling (ETS) and equilibrium water absorption (EMC) was:

$$ETS\ (\%) = 0.334EMC(\%) - 0.208 \quad (\text{for } EMC > 0.63\%) \qquad (4.4)$$

Since the ETS should be positive value, the minimum EMC should be greater than 0.63%.

4.4.4 Failure in mechanical properties

The flexural properties are important for decision-making on WPCs applications. The failure of flexural strength and modulus of the composites, with

virgin or recycled polypropylene and different amounts of rubberwood flour, are shown in Figures 4.7 and 4.8. Both the flexural strength and modulus of vPP or rPP/RWF composites decreased with immersion time and moisture uptake. Moreover, the composites with high wood flour contents lost flexural properties sharply. The water molecules reduced the strength of interfacial adhesion between rubberwood flour and polypropylene [2]. When water molecules infiltrate into the composites, the wood flour tends to swell, resulting in localized yielding of the polymer matrix and loss of adhesion between the wood flour and matrix [2, 30]. The flexural modulus also decreased, more significantly than the strength. In fact, wood flour as hard filler in comparison to the plastic matrix increased the stiffness of the composites. When wood flour plasticizes and becomes ductile, the stiffness of composites is decreased [30].

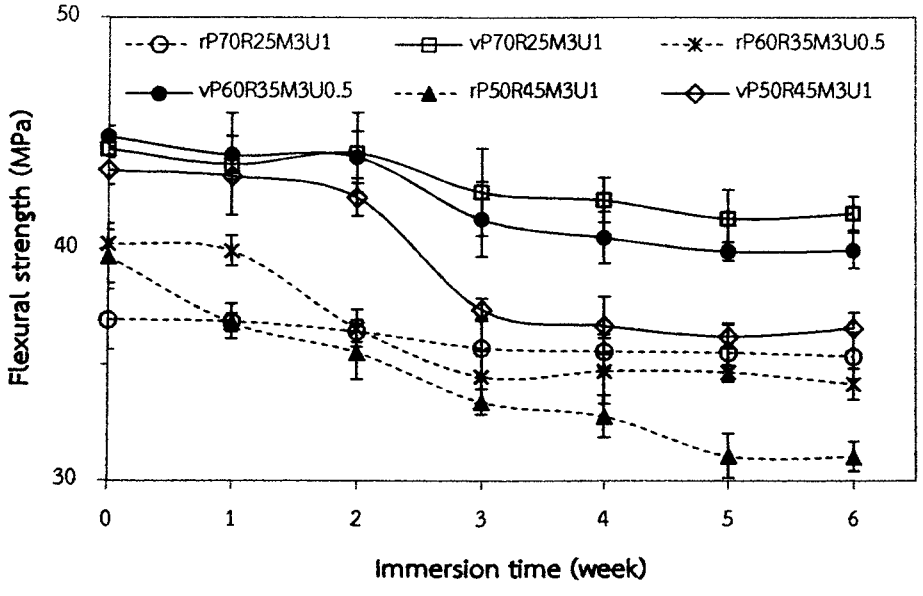

Figure 4.7 Effect of water immersion time on flexural strength of virgin (solid lines) and recycled (dashed lines) PP composites containing different RWF loadings

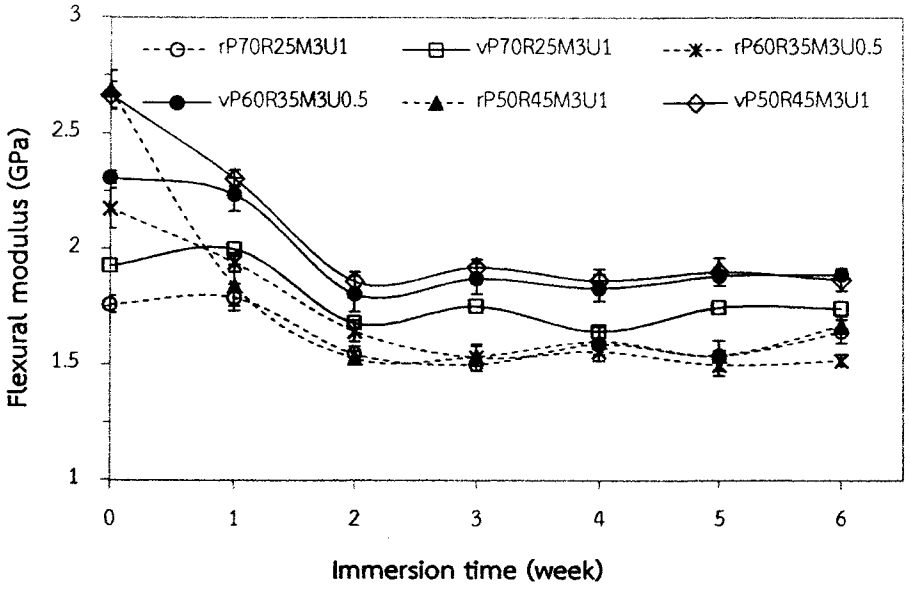

Figure 4.8 Effect of water immersion time on flexural modulus of virgin and recycled PP composites containing different RWF loadings

These qualitative observations were assessed for statistical validity by analysis of variance (ANOVA). According to one-way ANOVA of data in Tables 4.2 and 4.3, the water absorption does not significantly affect the flexural strength of vPP or rPP composites containing 25 wt% RWF. In contrast, with 35 and 45 wt% RWF the flexural strength is significantly affected by water absorption. Initially for up to 2 weeks, the flexural strength decreases only slightly (not statistically significant), but after 2 weeks it decreases significantly and then stabilizes. The flexural strength depends on crack formation or fracture mechanisms of the composites. When WPCs are soaked in water, the wood flour absorbs water and swells, while polypropylene hardly absorbs water or swells [30]. Hence, the swelling of wood flour mainly causes microcracks, and reduces adhesion of wood particles to the plastic matrix. However, the initial water absorption (for up to 2 weeks) is only around 1-3%, and the swelling of wood flour is not sufficient to generate microcracks [30]; in the current study, less than 3% absorption did not significantly affect flexural strength. Tukey's test in Table 4.3 also indicates that, for vPP composites with 45 wt% RWF (vP50R45M3U1), for up to 2 weeks the decrease in flexural strength was not significant (suffix a), but these

initial flexural strengths were significantly higher than that of the value at 3 to 6 weeks (suffix b).

An increase of maximum strain (max. ε) of the vPP or rPP composites with different amounts of rubberwood flour is also shown in Figure 4.9. The maximum strain increased significantly with immersion time and water absorption: the initial increase was rapid, and then stabilized after two weeks. The reason for this phenomenon is probably similar as described earlier. When wood flour wets, it plasticizes and becomes ductile [30], and this increases the maximum strain. The composites with high wood flour contents have sharper increases in the maximum strain because of this. The composites based on vPP had higher maximum strains than those based on rPP, at equal wood contents. Virgin polypropylene being stiffer than recycled polypropylene may be the reason for this. The molecular weight of recycled plastic decreases with repeated recycling. Short chains have more chain ends per mass than long chains, and these ends act as crystal defects that initiate failure during flexural loading, at comparatively lower elongation [31].

Table 4.2 Effect of moisture content on flexural properties of the rPP-rubberwood flour composites

	rP70R25M3U1				rP60R35M3U0.5				rP50R45M3U1			
Time (week)	WA (%)	MOR (MPa)	MOE (GPa)	Max. ε (%)	WA (%)	MOR (MPa)	MOE (GPa)	Max. ε (%)	WA (%)	MOR (MPa)	MOE (GPa)	Max. ε (%)
0	0	36.9^{a}	1.76^{ab}	3.09^{a}	0	40.2^{a}	2.18^{a}	2.79^{a}	0	39.7^{a}	2.69^{a}	2.07^{a}
1	0.67^{a}	36.9^{a}	1.79^{a}	3.38^{ab}	1.48^{a}	39.9^{a}	1.94^{b}	3.15^{bc}	3.58^{a}	36.8^{ab}	1.84^{b}	3.07^{b}
2	1.06^{b}	36.4^{a}	1.55^{bc}	3.76^{abc}	2.44^{b}	36.6^{ab}	1.64^{c}	3.82^{ab}	5.71^{b}	35.5^{b}	1.53^{c}	3.45^{c}
3	1.46^{c}	35.7^{a}	1.50^{c}	4.30^{c}	3.43^{c}	34.5^{b}	1.53^{c}	4.00^{bc}	7.46^{c}	33.4^{bc}	1.53^{c}	3.60^{bc}
4	1.76^{d}	35.6^{a}	1.59^{abc}	4.26^{bc}	3.98^{cd}	34.7^{b}	1.56^{c}	4.07^{bc}	8.63^{cd}	32.8^{bc}	1.60^{bc}	3.60^{bc}
5	2.10^{e}	35.5^{a}	1.54^{bc}	4.31^{c}	4.58^{de}	34.7^{b}	1.50^{c}	4.29^{c}	9.41^{d}	31.1^{c}	1.54^{c}	3.51^{bc}
6	2.28^{f}	35.4^{a}	1.64^{abc}	4.15^{abc}	5.00^{e}	34.2^{b}	1.52^{c}	4.14^{bc}	9.80^{d}	31.0^{c}	1.67^{bc}	3.46^{bc}
p-value	0.000	0.879	0.001	0.000	0.000	0.000	0.000	0.000	0.000	0.000	0.000	0.000

Note; Means within each column with the same letter are not significantly different (Tukey's test, $\alpha = 0.05$).

Table 4.3 Effect of moisture content on flexural properties of the vPP-rubberwood flour composites

	vP70R25M3U1				vP60R35M3U0.5				vP50R45M3U1			
Time (week)	WA (%)	MOR (MPa)	MOE (GPa)	Max. ε (%)	WA (%)	MOR (MPa)	MOE (GPa)	Max. ε (%)	WA (%)	MOR (MPa)	MOE (GPa)	Max. ε (%)
0	0	44.3^{a}	1.93^{a}	3.99^{a}	0	44.8^{a}	2.31^{a}	3.23^{a}	0	43.4^{a}	2.66^{a}	2.36^{a}
1	0.74^{a}	43.7^{a}	2.00^{a}	4.18^{ab}	1.33^{a}	44.1^{ab}	2.24^{a}	3.72^{a}	2.67^{a}	43.1^{a}	2.31^{b}	3.42^{b}
2	1.05^{a}	44.1^{a}	1.68^{b}	4.66^{abc}	2.30^{b}	44.0^{abc}	1.81^{b}	4.44^{b}	4.44^{b}	42.2^{a}	1.86^{c}	4.00^{c}
3	1.51^{b}	42.4^{a}	1.75^{bc}	4.86^{bc}	3.28^{c}	41.3^{abc}	1.87^{b}	4.56^{b}	6.15^{c}	37.4^{b}	1.92^{c}	3.92^{c}
4	1.70^{bc}	42.1^{a}	1.64^{b}	5.16^{c}	3.96^{cd}	40.5^{bc}	1.83^{b}	4.60^{b}	7.23^{cd}	36.7^{b}	1.86^{c}	3.90^{bc}
5	2.01^{cd}	41.3^{a}	1.75^{bc}	4.99^{c}	4.69^{de}	39.9^{c}	1.88^{b}	4.59^{b}	8.15^{de}	36.2^{b}	1.90^{c}	3.77^{bc}
6	2.22^{d}	41.5^{a}	1.74^{bc}	5.20^{c}	5.07^{e}	39.9^{bc}	1.89^{b}	4.46^{b}	8.82^{e}	36.6^{b}	1.87^{c}	3.87^{bc}
p-value	0.000	0.050	0.001	0.000	0.000	0.001	0.000	0.000	0.000	0.000	0.000	0.000

Note; Means within each column with the same letter are not significantly different (Tukey's test, $\alpha = 0.05$).

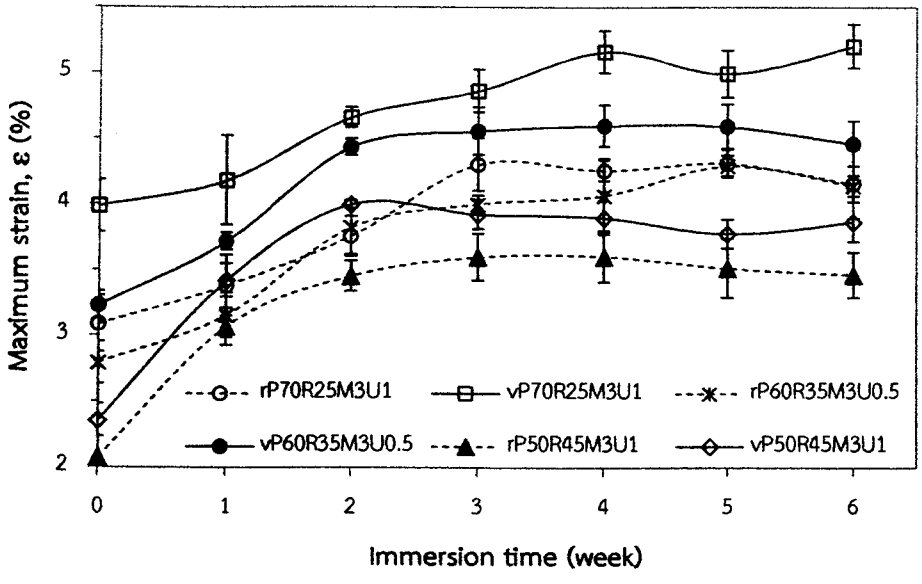

Figure 4.9 Effect of water immersion time on maximum strain of virgin and recycled PP composites containing different RWF loadings

4.5 Conclusions

Wood-polymer composites (WPCs) were prepared from rubberwood flour (RWF) and recycled or virgin polypropylene (rPP or vPP). The density of WPCs

increased linearly with wood flour content, because these natural fibers have a higher density than the polymer matrix. Long-term water absorption (WA) and thickness swelling (TS) behavior of vPP or rPP/RWF were experimentally observed. Both WA and TS increased with wood flour content because wood cellulose absorbs water while the plastic matrix in the composites does not. At 45 wt% RWF, the rPP composites had initially higher WA and TS than the vPP composites; however, after 6 weeks of immersion the vPP and rPP composites had closely similar saturation values. The initial absorption rate difference between the two types of plastic was attributed to poorer encapsulation of wood flour into the rPP matrix, with poor dispersion and weak interfacial adhesion. The coupling agent MAPP at 3 wt% reduced WA and TS, with no further benefit reached at 5 wt% MAPP: using more than 3 wt% MAPP may be unnecessary and uneconomical. The WA and TS of composites were increased by an addition of 1 wt% UV stabilizer. These negative effects of the UV stabilizer on the WA and TS of the composites should be minimized, by minimal use of the stabilizer. The flexural strength and modulus of composites decreased significantly with moisture uptake; however, at WA less than 3% its effects on flexural strength were not significant. The composites with high wood flour loadings suffered a sharp decrease in the flexural properties with absorption of water, which reduced the interfacial adhesion between wood flour and plastic matrix. The maximum strain of composites significantly increased with absorption due to the water plasticizing wood particles.

4.6 References

[1] A. Kaymakci, N. Ayrilmis, F. Ozdemir, and T. Gulec. "Utilization of Sunflower Stalk in Manufacture of Thermoplastic Composite." *Journal of Polymers and the Environment*, Epub ahead of print 18 December 2012. DOI: 10.1007/s10924-012-0564-9.

[2] T.T. Law and Z.A.M. Ishak. "Water Absorption and Dimensional Stability of Short Kenaf Fiber-Filled Polypropylene Composites Treated with Maleated Polypropylene." *Journal of Applied Polymer Science*, vol. 120, pp. 563–572, 2011.

[3] B. Mirzaei, M. Tajvidi, R.H. Falk, and C. Felton. "Stress-Relaxation Behavior of Lignocellulosic High-Density Polyethylene Composites." *Journal of Reinforced Plastics and Composites*, vol. 30, pp. 875–881, 2011.

[4] A. Ashori and A. Nourbakhsh. "Performance Properties of Microcrystalline Cellulose as a Reinforcing Agent in Wood Plastic Composites." *Composites Part B: Engineering*, vol. 41, pp. 578–581, 2010.

[5] W. Liu, L.T. Drzal, A.K. Mohanty, and M. Misra. "Influence of Processing Methods and Fiber Length on Physical Properties of Kenaf Fiber Reinforced Soy based Biocomposites." *Composites Part B: Engineering*, vol. 38, pp. 352–359, 2007.

[6] H.Y. Cheung, M.P. Ho, K.T. Lau, F. Cardona, and D. Hui. "Natural Fibre-Reinforced Composites for Bioengineering and Environmental Engineering Applications." *Composites Part B: Engineering*, vol. 40, pp. 655–663, 2009.

[7] J.W. Kim, D.P. Harper, and A.M. Taylor. "Effect of Wood Species on the Mechanical and Thermal Properties of Wood–Plastic Composites." *Journal of Applied Polymer Science*, vol. 112, pp. 1378–1385, 2009.

[8] N.M. Barkoula, S.K. Garkhail, and T. Peijs. "Effect of Compounding and Injection Molding on the Mechanical Properties of Flax Fiber Polypropylene Composites." *Journal of Reinforced Plastics and Composites*, vol. 29, pp. 1366–1385, 2010.

[9] T. Li and N. Yan. "Mechanical Properties of Wood Flour/HDPE/Ionomer Composites." *Composites Part A: Applied Science and Manufacturing*, vol. 38, pp. 1–12, 2007.

[10] K.B. Adhikary, S. Pang, and M.P. Staiger. "Dimensional Stability and Mechanical Behaviour of Wood-Plastic Composites based Recycled and Virgin High-Density Polyethylene." *Composites Part B: Engineering*, vol. 39, pp. 807–815, 2008.

[11] C. Homkhiew, T. Ratanawilai, and W. Thongruang. "Effect of Wood Flour Content and Cooling Rate on Properties of Rubberwood Flour/Recycled Polypropylene Composites." *Advanced Materials Research*, vol. 488–489, pp. 495-500, 2012.

[12] K.B. Adhikary, S. Pang, and M.P. Staiger. "Long-Term Moisture Absorption and Thickness Swelling Behaviour of Recycled Thermoplastics Reinforced with Pinus Radiata Sawdust." *Chemical Engineering Journal*, vol. 142, pp. 190–198, 2008.

[13] T. Ratanawilai, N. Thanawattanasirikul, and C. Homkhiew. "Mechanical and Thermal Properties of Oil Palm Wood Sawdust Reinforced Post-Consumer Polyethylene Composites." *ScienceAsia*, vol. 38, pp. 289–294, 2012.

[14] N.J. Themelis, M.J. Castaldi, J. Bhatti, and L. Arsova. "Energy and Economic Value of Non-recycled Plastics and Municipal Solid Wastes that are Currently Landfilled in the Fifty States." *EEC Study of Non-recycled Plastics*, Earth Engineering Center, Columbia University, 2011.

[15] A. Ashori and S. Sheshmani. "Hybrid Composites Made from Recycled Materials: Moisture Absorption and Thickness Swelling Behavior." *Bioresource Technology*, vol. 101, pp. 4717–4720, 2010.

[16] S.K. Najafi, E. Hamidinia, and M. Tajvidi. "Mechanical Properties of Composites from Sawdust and Recycled Plastics." *Journal of Applied Polymer Science*, vol. 100, pp. 3641–3645, 2006.

[17] Z.A. Khan, S. Kamaruddin, and A.N. Siddiquee. "Feasibility Study of Use of Recycled High Density Polyethylene and Multi Response Optimization of Injection Moulding Parameters Using Combined Grey Relational and Principal Component Analyses." *Materials and Design*, vol. 31, pp. 2925–2931, 2010.

[18] P. Petchpradab, T. Yoshida, T. Charinpanitkul, and Y. Matsumura. "Hydrothermal Pretreatment of Rubber Wood for the Saccharification Process." *Industrial and Engineering Chemistry Research*, vol. 48, pp. 4587–4591, 2009.

[19] C. Homkhiew, T. Ratanawilai, and W. Thongruang. "Composites from Recycled Polypropylene and Rubberwood Flour: Effects of Composition on Mechanical Properties." *Journal of Thermoplastic Composite Materials*, Epub ahead of print 14 February 2013.DOI: 10.1177/0892705712475019.

[20] S. Mishra and H. Aireddy. "Evaluation of Dielectric Behavior of Bio-Waste Reinforced Polymer Composite." *Journal of Reinforced Plastics and Composites*, vol. 30, pp. 134–141, 2011.

[21] D.D. Stokke and D.J. Gardner. "Fundamental Aspects of Wood as a Component of Thermoplastic Composites." *Journal of Vinyl and Additive Technology*, vol. 9, pp. 96–104, 2003.

[22] B. Li, H. Jiang, L. Guo, and H. Shi. "Comparative Study on the Effect of Manchurian Ash and Larch Wood Flour on Mechanical Property, Morphology, and Rheology of HDPE/Wood Flour Composites." *Journal of Applied Polymer Science*, vol. 107, pp. 2520–2530, 2008.

[23] T. Ratanawilai, P. Lekanukit, and S. Urapantamas. "Effect of Rubberwood and Palm Oil Content on the Properties of Wood-Polyvinyl Chloride Composites." *Journal of Thermoplastic Composite Materials*, Epub ahead of print 9 August 2012. DOI: 10.1177/0892705712454863.

[24] H. El-Saied, A.H. Basta, M.E. Hassanen, H. Korte, and A. Helal. "Behaviour of Rice-Byproducts and Optimizing the Conditions for Production of High Performance Natural Fiber Polymer Composites." *Journal of Polymers and the Environment*, vol. 20, pp. 838–847, 2012.

[25] Q. Lin, X. Zhou, and J. Dai. "Effect of Hydrothermal Environment on Moisture Absorption and Mechanical Properties of Wood Flour-Filled Polypropylene Composites." *Journal of Applied Polymer Science*, vol. 85, pp. 2824–2832, 2002.

[26] A. Shakeri and A. Ghasemian. "Water Absorption and Thickness Swelling Behavior of Polypropylene Reinforced with Hybrid Recycled Newspaper and Glass Fiber." *Applied Composite Materials*, vol. 17, pp. 183–193, 2010.

[27] A. Wechsler and S. Hiziroglu. "Some of the Properties of Wood–Plastic Composites." *Building and Environment*, vol. 42, pp. 2637–2644, 2007.

[28] H.S. Yang, H.J. Kim, H.J. Park, B.J. Lee, and T.S. Hwang. "Water Absorption Behavior and Mechanical Properties of Lignocellulosic Filler–Polyolefin Bio-Composites." *Composite Structures*, vol. 72, pp. 429–437, 2006.

[29] M. Tajvidi and A. Takemura. "Recycled Natural Fiber Polypropylene Composites: Water Absorption/Desorption Kinetics and Dimensional Stability." *Journal of Polymers and the Environment*, vol. 18, pp. 500–509, 2010.

[30] S. Tamrakar and R.A. Lopez-Anido. "Water Absorption of Wood Polypropylene Composite Sheet Piles and Its Influence on Mechanical Properties." *Construction and Building Materials*, vol. 25, pp. 3977–3988, 2011.

[31] J. Aurrekoetxea, M.A. Sarrionandia, I. Urrutibeascoa, and M.L. Maspoch. "Effects of Recycling on the Microstructure and the Mechanical Properties of Isotactic Polypropylene." *Journal of Materials Science*, vol. 36, pp. 2607–2613, 2001.

CHAPTER 5

Optimizing the Formulation of Polypropylene and Rubberwood Flour Composites for Moisture Resistance by Mixture Design

5.1 Chapter summary

D-optimal mixture experimental design was used to determine the optimal mixture of composites from rubberwood flour (RWF) and recycled polypropylene (rPP) and to systematically analyze the effects of composition, namely of rPP, RWF, maleic anhydride-grafted polypropylene (MAPP), and ultraviolet (UV) stabilizer fractions. The overall compositions significantly affected water absorption, thickness swelling, flexural strength and modulus, and maximum strain. Water absorption and thickness swelling increased with the fraction of RWF. At long immersion times, flexural strength and modulus decreased but maximum strain increased with high fraction of RWF. The fraction of MAPP only slightly affected water absorption and flexural properties while the UV stabilizer fraction had a clear negative effect increasing water absorption and decreasing flexural properties. The models fitted were used for optimization of a desirability score, substituting for the multiple objectives modeled. The optimal formulation found was 68.9 wt% rPP, 25.0 wt% RWF, 5.0 wt% MAPP, 0.1 wt% UV stabilizer, and 1.0 wt% lubricant.

5.2 Introduction

In recent decades, plastic waste has globally become a significant contributor to municipal solid waste [1]. In 2008, at least 33.6 million tons of post-consumer plastics were generated in the United States, of which 28.9 million tons went to landfills, 2.6 million tons to combustion and energy recovery, and only 2.2 million tons to recycling [2]. The plastic waste typically includes polyethylene (PE), polypropylene (PP), polyvinyl chloride (PVC), polyethylene terephthalate (PET), and polystyrene (PS) [3]. Of all these plastic types PE and PP significantly contribute to

landfills and have similarities in their structure and properties [4]. However, when PE (virgin or recycled) was blended with sawdust, it had lower stiffness and strength than similar composites with PP (virgin or recycled) [5]. Due to availability of plastic waste and increased environmental awareness, there have been many studies on natural fiber reinforced recycled thermoplastics. For example, Cui et al. [1] fabricated composites from post-consumer high density polyethylene and wood fiber, and found that wood fiber content affected the flexural strength, modulus, and impact strength. Kazemi et al. [4] produced composites from wood sawdust and post-consumer PE and PP. The wood flour in composites increased tensile, flexural, and torsion moduli in comparison to the recycled plastic blends. Nourbakhsh et al. [8] also concluded that polypropylene waste and wood waste are promising alternative raw materials for making low cost wood-plastic composites (WPCs). Hence, the use of recycled plastics may effectively dispose of plastic waste and also reduce the cost of products [6].

The rubberwood industries of Thailand generate a large amount of wood waste in the forms of flour, sawdust, and chips at different stages of wood processing. Generally, rubberwood waste is dumped in landfills or burned, but some is used in medium-density fiberboard and particleboard [7]. Rubberwood waste as reinforcement in plastic composites is great interest, both for economic and for environmental reasons. Natural fiber (wood waste) reinforced thermoplastics also offers many advantages including biodegradability, renewable character, low cost, absence of associated health hazards, and low wear of processing equipment [8-10], when compared with synthetic fillers [11]. Natural fibers have successfully improved the mechanical properties of plastic composites, as the following examples demonstrate. Homkhiew et al. [7] investigated the effects of rubberwood flour content on the mechanical properties of recycled PP composites and found that the modulus and hardness of composites increased linearly with wood flour loadings in range of 25-45 wt%. Karmarkar et al. [12] also reported that the tensile strength and modulus linearly increased with an increase from 10 to 50 wt% wood fiber in PP composites. However, the hygroscopic nature of natural fibers is a disadvantage influencing the performance of the WPCs, when exposed to environmental

conditions. The water absorption characteristics WPCs limit their end-use applications [13], as several mechanical and physical properties, such as dimensional stability, are affected. The water absorption of WPCs varies by the wood species, partly because they have different contents of cellulose, lignin, hemicelluloses, and extractants [14]. Hence, the effects of filler on the composite properties need to be characterized, and this has not been done previously for rubberwood flour (RWF) in relation to moisture resistance.

Designs of statistical experiment, such as mixture design, factorial design, and Taguchi method, is a well-established concept for planning and execution of informative experiments [15]. Recently, WPCs have been studied with designed experiments. For example, Jun et al. [16] used a Box-Behnken design with response surface method to determine which variables influenced board performance significantly. Matuana et al. [17] used a four-factor central composite design to develop a response surface model and to study the foamability of rigid PVC/wood-flour composites. Stark et al. [18] applied a 2^4 factorial design to determine the effects of two hindered amine light stabilizers, a colorant and an ultraviolet absorber, and their interactions on the photostabilization of wood flour/high-density polyethylene composites. However, the fractions of components in a mixture cannot be changed independently since they must add up to 100%, and the methods for mixture designs have been created with this in mind [19]. Mixture designs have been successful in many applications, particularly in food and pharmaceutical industries, whereas prior studies on WPCs seem not to use a mixture design.

Experiments with mixture design enable statistical estimation of individual effects and interactions of components in a mixture, and the fitted models can be used to find the optimal formulation of a composite material [20]. Hence, this work used a mixture experimental design to model selected physical and mechanical characteristics of WPCs. The main objective of this work is to optimize the mixture ratios for composites made from recycled polypropylene and rubberwood flour, based on experimentally determined water absorption and flexural failure.

5.3 Experimental

5.3.1 Materials

Recycled polypropylene (rPP) pellets, WT170 with a melt flow index of 11 g/10 min at 230 °C, were purchased from Withaya Intertrade Co., Ltd (Samutprakarn, Thailand) and used as the polymer matrix. Rubberwood flour obtained from the cutting process in local furniture industry (Songkhla, Thailand) was used as reinforcement. Maleic anhydride-grafted polypropylene (MAPP) with 8-10% of maleic anhydride was supplied by Sigma-Aldrich (Missouri, USA) and used as a coupling agent to improve the interfacial adhesion between filler and matrix. Hindered amine light stabilizer (MEUV008) was purchased from TH Color Co., Ltd (Samutprakarn, Thailand), chosen as ultraviolet (UV) stabilizer. Paraffin wax was procured from Nippon Seiro Co., Ltd (Yamaguchi, Japan), and used as lubricant (Lub).

5.3.2 Experimental design to optimize formulation

The region of interest for the current experiments has constraints imposed on the component fractions [19], and these can be incorporated in a D-optimal mixture design. The experimental results were used to statistically evaluate the effects of component fractions on water absorption and flexural failure, and the identified models were used to optimize the formulation. The experimental D-optimal mixture design and statistical analysis were done with Design-Expert software (version 8.0.6, Stat-Ease, Inc.). The formulations for the manufacture of WPCs were defined by component fractions for rPP (x_1), RWF (x_2), MAPP (x_3), UV stabilizer (x_4), and Lub (x_5). The upper and lower limits of experimental range are shown in Table 5.1. The ranges of rPP and RWF contents obtained from preliminary study (Chapter 3) and the other compositions were determined following the literature review. For example, Kuo et al. [8] reported that the optimal content of MAPP was 3-4.5 wt%. Despite the fraction of Lub being held constant, it is included as a variable because it contributes to the 100% in the mixture. The design included 15 different formulations and 5 replications to evaluate reproducibility and variances. Thus, the total number of runs was 20, as shown in Tables 5.2 and 5.3. After data collection,

linear, quadratic, and special cubic models (see equations 2.1, 2.2, and 2.4) were used to model the responses.

Table 5.1 Constraints for the mixture design of experiments

Component	Fraction restrictions (wt%)
rPP (x_1)	$50 \leq x_1 \leq 70$
RWF (x_2)	$25 \leq x_2 \leq 45$
MAPP (x_3)	$3 \leq x_3 \leq 5$
UV stabilizer (x_4)	$0 \leq x_4 \leq 1$
Lub (x_5)	$= 1$

5.3.3 Preparation of composites

Prior to compounding, the wood flour was sieved through a standard sieve of mesh size 80 (passing particles smaller than 180 μm) and was dried in an oven at 110 °C for 8 h, to minimize the moisture content. The WPCs were then manufactured in a two-stage process. In the first stage WPC pellets were produced: rPP and RWF were dry-blended and melt-blended into wood-plastic composite pellets using a twin-screw extruder (Model SHJ-36 from En Mach Co., Ltd, Nonthaburi, Thailand). The 10 temperature zones of the extruder were set to a profile in range of 130-170 °C, to reduce degradation of the mixture components, while the screw rotating speed was maintained at 70 rpm. The extruded strand passed through a water bath and was subsequently pelletized. In the second stage WPC panels were produced: the WPC pellets were again dried at 110 °C for 8 h. WPC pellets, MAPP, UV stabilizer, and lubricant compositions indicated in Table 5.2 and 5.3 were then dry-mixed and fed into the twin-screw extruder. The processing conditions for extruding were as follows: (1) temperature profiles: 130-190 °C; (2) screw rotating speed: 50 rpm; (3) melt pressure: 0.10-0.20 MPa depending on wood flour content; and (4) vacuum venting at 9 temperature zones: 0.022 MPa. The WPC panels were extruded through a 9 mm × 22 mm rectangular die and cooled in ambient air. These specimens were machined following the standards of American Society for Testing and Materials (ASTM) for physical and mechanical testing.

Table 5.2 Compositions based on mixture experimental design and responses of WA and TS at 1, 5, and 10 weeks

Run	Mixture component fraction (wt%)					Water absorption (%)			Thickness swelling (%)		
No.	x_1	x_2	x_3	x_4	x_5	W1	W5	W10	W1	W5	W10
1	63.9	29.9	4.5	0.7	1.0	0.97	2.97	4.77	0.24	0.70	1.28
2	70.0	25.0	3.0	1.0	1.0	0.77	2.22	3.64	0.28	0.58	0.89
3	50.0	43.0	5.0	1.0	1.0	2.65	7.28	9.87	0.49	1.63	2.72
4	54.9	38.9	4.5	0.7	1.0	1.99	6.12	8.59	0.43	1.39	2.60
5	59.5	34.5	5.0	0.0	1.0	2.06	5.13	7.56	0.30	1.00	1.99
6	55.4	39.9	3.5	0.2	1.0	1.94	5.80	8.34	0.50	1.43	2.53
7	59.5	34.5	4.0	1.0	1.0	1.06	4.67	6.90	0.40	1.11	1.91
8*	59.5	34.5	5.0	0.0	1.0	1.55	4.75	7.10	0.31	1.17	2.15
9	50.0	44.3	4.3	0.5	1.0	2.58	7.14	9.45	0.66	1.92	3.07
10	68.0	25.0	5.0	1.0	1.0	0.56	1.91	3.13	0.26	0.56	0.85
11	50.0	45.0	3.0	1.0	1.0	3.39	8.92	10.50	0.75	2.39	3.15
12*	50.0	43.0	5.0	1.0	1.0	3.08	8.05	9.70	0.43	1.92	2.63
13	60.3	35.3	3.0	0.5	1.0	1.48	4.58	6.81	0.27	0.96	1.73
14	64.9	30.4	3.5	0.2	1.0	0.97	3.39	5.28	0.29	0.89	1.60
15*	70.0	25.0	3.0	1.0	1.0	0.67	2.10	3.39	0.23	0.58	0.93
16	51.0	45.0	3.0	0.0	1.0	2.70	7.77	10.02	0.60	2.11	3.37
17*	51.0	45.0	3.0	0.0	1.0	2.91	8.12	10.31	0.61	2.27	3.47
18*	50.0	45.0	3.0	1.0	1.0	3.58	9.41	10.33	0.74	2.75	3.51
19	70.0	25.0	4.0	0.0	1.0	0.68	1.80	2.95	0.28	0.48	0.75
20	69.0	25.0	5.0	0.0	1.0	0.61	1.69	2.78	0.20	0.44	0.67

Note; *duplicate experiments

5.3.4 Water absorption and dimensional stability tests

Water absorption and thickness swelling tests were carried out according to ASTM D570-88 specification. Before testing, five replication specimens of each formulation were dried in an oven at 50 °C for 24 h. The weight and thickness of each specimen were measured to a precision of 0.001 g and 0.01 mm, respectively. The specimens were then submerged in water at ambient room temperature. After 1, 5, and 10 weeks, soaked specimens were removed from the

water, thoroughly surface dried with tissue papers, and immediately weighed and measured to determine the weight and thickness. The percentage of water absorption (WA) at any given time was calculated following equation 4.2. Likewise, the percentage of thickness swelling (TS) at any given time was calculated following equation 4.3.

Table 5.3 Compositions based on mixture experimental design and responses of flexural properties at 1 and 6 weeks

Run	Mixture component fraction (wt%)					MOR (MPa)		MOE (GPa)		Max. ε (%)	
No.	x_1	x_2	x_3	x_4	x_5	W1	W6	W1	W6	W1	W6
1	63.9	29.9	4.5	0.7	1.0	38.7	36.8	1.90	1.67	3.23	3.80
2	70.0	25.0	3.0	1.0	1.0	37.2	35.8	1.76	1.65	3.03	3.81
3	50.0	43.0	5.0	1.0	1.0	37.5	29.7	2.10	1.63	2.92	3.11
4	54.9	38.9	4.5	0.7	1.0	39.7	34.2	2.03	1.62	3.12	3.66
5	59.5	34.5	5.0	0.0	1.0	41.9	32.5	1.87	1.50	3.52	3.74
6	55.4	39.9	3.5	0.2	1.0	40.7	32.5	1.96	1.59	3.41	3.61
7	59.5	34.5	4.0	1.0	1.0	36.3	32.8	1.94	1.49	2.82	3.67
8*	59.5	34.5	5.0	0.0	1.0	40.1	31.9	1.82	1.47	3.63	3.79
9	50.0	44.3	4.3	0.5	1.0	40.3	33.5	2.04	1.70	3.09	3.60
10	68.0	25.0	5.0	1.0	1.0	36.8	36.6	1.75	1.65	3.14	3.78
11	50.0	45.0	3.0	1.0	1.0	35.9	30.7	1.85	1.65	2.97	3.20
12*	50.0	43.0	5.0	1.0	1.0	37.4	28.6	2.10	1.64	2.75	2.77
13	60.3	35.3	3.0	0.5	1.0	39.9	34.2	1.94	1.52	3.15	4.14
14	64.9	30.4	3.5	0.2	1.0	40.8	37.0	1.86	1.53	3.70	4.42
15*	70.0	25.0	3.0	1.0	1.0	36.9	35.4	1.79	1.64	3.38	4.15
16	51.0	45.0	3.0	0.0	1.0	44.6	33.3	2.12	1.63	3.49	3.90
17*	51.0	45.0	3.0	0.0	1.0	43.1	34.6	2.11	1.65	3.50	3.94
18*	50.0	45.0	3.0	1.0	1.0	36.8	31.0	1.84	1.67	3.07	3.46
19	70.0	25.0	4.0	0.0	1.0	38.9	38.9	1.81	1.54	3.50	4.81
20	69.0	25.0	5.0	0.0	1.0	38.6	38.1	1.83	1.75	3.59	4.90

Note; *duplicate experiments

5.3.5 Flexural test of wood-plastic composites

Flexural properties of the samples were determined with an Instron Universal Testing Machine (Model 5582 from Instron Corporation, Massachusetts, USA) in accordance with ASTM D790-92. In the destructive flexural tests (three point bending) specimens with nominal dimensions of 4.8 mm × 13 mm × 100 mm, a span of 80 mm, and a cross-head speed of 2 mm/min were used. The testing was performed at ambient room temperature of 25 $^{\circ}$C with five samples of each formulation to obtain an average value. The measurements of flexural strength (MOR), modulus of elasticity (MOE), and maximum strain (max. ε) at maximum stress, were done at 1 and 6 weeks, and at the latter time water absorption had reached its equilibrium so further testing was considered unnecessary.

5.4 Results and discussion

The D-optimal mixture design of experiments, with five fractions as (mutually dependent) variables (that sum to one), had 20 runs in a randomized order. The twelve determined responses were the values of the water absorption and thickness swelling at 1, 5, and 10 weeks; and flexural strength, modulus, and maximum strain at 1 and 6 weeks. The results are summarized in Tables 5.2 and 5.3.

5.4.1 Statistical analysis of the response models

Analysis of variance (ANOVA) of the alternative types of response models revealed that WA at 1, 5, and 10 weeks, TS at 1 and 5 weeks, and MOR at 1 and 6 weeks were best fit with quadratic models, instead of linear, special cubic, or cubic models, whereas MOE at both 1 and 6 weeks was best fit with special cubic model. The MOE at 6 weeks is shown as an example in Table 5.4. The sequential model sums of squares for quadratic and special cubic models are significant ($p<0.05$), but not for the other model types. Moreover, the lack of fit is clearly insignificant for the special cubic model, suggesting this model performs well. It also has the highest adjusted coefficient of determination (adj-R^2 = 0.9726) and predicted coefficient of determination (pred-R^2 = 0.9484), further indicating good fit.

Table 5.4 Fitted model summary for MOE at 6 weeks

Source	Sequential p-value	Lack of fit p-value	Adj-R^2	Pred-R^2	
Linear	0.6971	0.0002*	-0.0884	-0.4177	
Quadratic	0.0056*	0.0023*	0.6382	-0.6377	
Special cubic	0.0004*	0.9391	0.9726	0.9484	Suggested
Cubic	0.9391	-	0.9672	-	Aliased

*P-value less than 0.05 is considered significant.

The detailed ANOVAs in Tables 5.5 and 5.6 document the significant quadratic or cubic terms in models for each response, in terms of their p-values. The ANOVA shows statistical significance ($p<0.05$) of these terms supplementing linear models of the fractions, namely of rPP, RWF, MAPP, and UV stabilizer. No interaction term was significant in models of WA, MOR, and MOE at 1 week, or TS at 5 weeks. However, other modeled responses had significant interactions, for example, between MAPP and UV stabilizer for WA at 5 weeks and between rPP and RWF, rPP and UV stabilizer, RWF and UV stabilizer, MAPP and UV stabilizer for MOR at 6 weeks. The frequent interactions with UV stabilizer might indicate that UV stabilizer reacted chemically with the other components, or affected its distribution and interaction. In addition, the ANOVA also showed that lack of fit was not significant for any of the response surface models at 95% confidence level. The regression models fit the data in a statistically sound manner.

Table 5.5 Analysis of variance and model adequacy for WA and TS responses

	Water absorption			Thickness swelling		
Source	W1	W5	W10	W1	W5	W10
Model	<0.0001*	<0.0001*	<0.0001*	<0.0001*	<0.0001*	<0.0001*
Linear Mixture	<0.0001*	<0.0001*	<0.0001*	<0.0001*	<0.0001*	<0.0001*
x_1x_2	0.1380	0.9034	0.0042*	0.0005*	0.0925	-
x_1x_3	0.1107	0.3851	0.4548	0.0007*	0.6560	-
x_1x_4	0.7164	0.0701	0.0246*	0.1941	0.2073	-
x_2x_3	0.1097	0.3679	0.5153	0.0010*	0.7388	-
x_2x_4	0.7422	0.0746	0.0242*	0.1839	0.2088	-
x_3x_4	0.2698	0.0205*	0.0065*	0.2339	0.1190	-
Lack of Fit	0.4366	0.4456	0.2319	0.1650	0.5991	0.2126
R^2	0.9703	0.9906	0.9959	0.9810	0.9749	0.9727
Adj-R^2	0.9435	0.9821	0.9921	0.9639	0.9524	0.9675
Pred-R^2	0.8245	0.9526	0.9800	0.8801	0.8898	0.9584
C.V. %	13.29	6.65	3.54	8.14	11.79	8.39

*P-value less than 0.05 is considered significant.

Tables 5.5 and 5.6 also include the coefficient of determination (R^2), adj-R^2, pred-R^2, and coefficient of variation (C.V.). The R^2 values of the twelve response fits are in the range from 0.8354 to 0.9959. The R^2 values of maximum strain at 1 week (0.8354) and WA at 10 weeks (0.9959) indicate that only 16.46% and 0.41%, respectively, of the total variability in observations are not explained by the models; R^2 values close to 1 indicate good fits [21]. Also the adj-R^2 values in the range from 0.8045 to 0.9921 suggest good fits; and the same goes for pred-R^2 values. The pred-R^2 value of WA at 10 weeks was 0.9800 meaning that the fitted model would explain about 98% of the variability in new data. The coefficients of variation of all response fits based on the replications of experiments show low values in the range from 0.78 to 13.29%. The low C.V. values indicate that the determinations of material characteristics had a good precision, and could serve the fitting of parametric models.

Table 5.6 Analysis of variance and model adequacy for flexural properties

	MOR		MOE		Max. ε	
Source	W1	W6	W1	W6	W1	W6
Model	<0.0001*	<0.0001*	<0.0001*	<0.0001*	<0.0001*	<0.0001*
Linear Mixture	<0.0001*	<0.0001*	<0.0001*	0.0018*	<0.0001*	<0.0001*
x_1x_2	0.9169	0.0067*	0.1091	0.5197	-	-
x_1x_3	0.2973	0.0726	0.3808	0.2568	-	-
x_1x_4	0.1474	0.0124*	0.2373	0.0007*	-	-
x_2x_3	0.3236	0.0952	0.3308	0.5825	-	-
x_2x_4	0.1700	0.0127*	0.2523	0.0008*	-	-
x_3x_4	0.0968	0.0020*	0.8386	0.7737	-	-
$x_1x_2x_3$	-	-	0.5757	0.3760	-	-
$x_1x_2x_4$	-	-	0.0619	0.0039*	-	-
$x_1x_3x_4$	-	-	0.7685	0.5580	-	-
$x_2x_3x_4$	-	-	0.6719	0.3347	-	-
Lack of Fit	0.6701	0.1192	0.7600	0.9391	0.6122	0.2335
R^2	0.9499	0.9514	0.9936	0.9913	0.8354	0.8382
Adj-R^2	0.9048	0.9077	0.9799	0.9726	0.8045	0.8079
Pred-R^2	0.8310	0.8449	0.7753	0.9484	0.7360	0.7354
C.V. %	1.86	2.51	0.91	0.78	3.86	5.90

*P-value less than 0.05 is considered significant.

5.4.2 Model adequacy checking

Model adequacy checking is performed to verify that the fitted model is an appropriate approximation [22]. Figure 5.1(a) displays normal probability plots of the residuals for water absorption at 10 weeks (WAW10). The good linear fit in this plot indicates that the residuals (approximation errors remaining in the model) are close to normally distributed. Normally distributed residuals are a requirement for validity of least squares regression, so the model is adequate. Likewise, there is no indication of possible outliers, such as faulty experiment cases with particularly large residuals [19]. The plot of residuals vs. predicted values in Figure 5.1(b) exhibits no obvious patterns that would suggest adding a term to the model, to account for that pattern. If the residuals had such structure, the model would not appropriate [19].

Figure 5.1(c) shows model predictions vs. observations. The model outputs fit the actual observations quite well, with WAW10 model deviating from actual by less than about 5%. These adequacy checks of the WAW10 response model indicated no problems with the model type or its fit to data. Similar checking for the other modeled responses gave no indications of problems with the fitted models either. This type of checking cannot guarantee predictive capability, but suggests that the models are able to approximately interpolate within the experimental range.

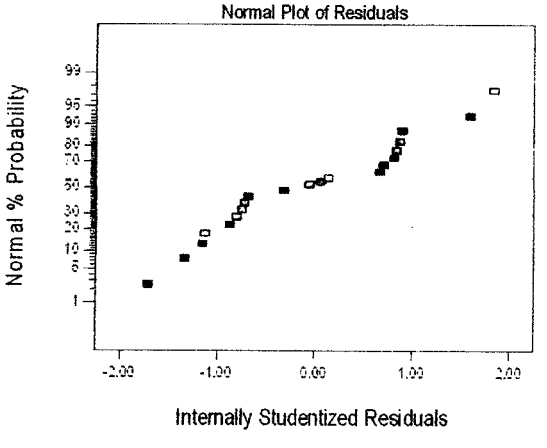

(a)

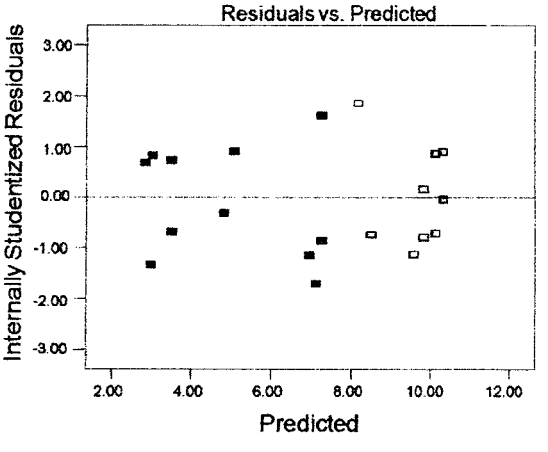

(b)

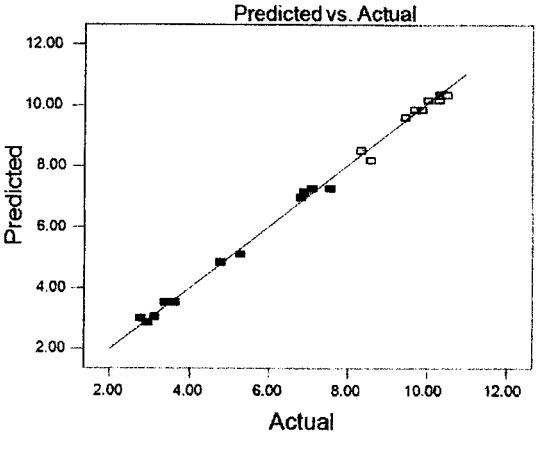

(c)

Figure 5.1 Model adequacy checking for water absorption at 10 weeks; (a) normal probability plot of residuals, (b) plot of residuals versus predicted values, and (c) plot of predicted versus actual values

5.4.3 Effect of composition on the water absorption and optimal formulation

The quadratic regression models for WAW1, WAW5, and WAW10 were:

$$\text{WAW1} = 0.73x_1 + 2.99x_2 + 120.23x_3 + 115.96x_4 - 1.18x_1x_2 - 129.92x_1x_3 - 121.13x_1x_4 - 129.82x_2x_3 - 109.74x_2x_4 - 346.98x_3x_4 \quad (5.1)$$

$$\text{WAW5} = 1.8x_1 + 8.23x_2 + 91.78x_3 + 907.58x_4 + 0.13x_1x_2 - 96.75x_1x_3 - 942.92x_1x_4 - 100.05x_2x_3 - 926.36x_2x_4 - 1171.62x_3x_4 \quad (5.2)$$

$$\text{WAW10} = 2.99x_1 + 10.38x_2 + 57.33x_3 + 861.54x_4 + 2.80x_1x_2 - 60x_1x_3 - 890.01x_1x_4 - 51.83x_2x_3 - 894.58x_2x_4 - 1056.74x_3x_4 \quad (5.3)$$

These equations show a positive coefficient for all the individual components, namely rPP (x_1), RWF (x_2), MAPP (x_3), and UV stabilizer (x_4), and the coefficients of rPP and RWF increased with immersion time. The rPP has the smallest coefficient in the fit for the water absorption due to hydrophobicity of this matrix polymer. Contour plots of WAW1 and WAW10 are shown in Figures 5.2(a) and 5.2(b), respectively. In these triangular plots the three pure components (rPP, RWF, and MAPP) are represented by the corners, while the additive levels were fixed (UV stabilizer at 0.5 wt%, and Lub at 1 wt%). The contours in the colored areas that include the experimental observations, present the WAW1 and WAW10 regression fits varying from 0.5 to 2.5% and 2.9 to 9.5%, respectively. Both WAW1 and WAW10 clearly increase with an increase of the RWF content; the free OH groups of RWF cellulose increase the water absorption of the composites [23]. Increasing the MAPP addition from 3 to 5 wt% slightly affects the water absorption. This is because the coupling agent increases bonding in WPCs, by improving compatibility between the wood particles and the polymer. Then the plastic can cover more of the wood surfaces, resulting in a lower water absorption [24]. Furthermore, adding 1 wt% UV stabilizer increased the moisture content in the rPP/RWF composites. This may be attributed to nonuniform spatial distribution of wood flour, polymer, and UV stabilizer [7, 25]. Figure 5.3 displays the numerically optimized composition, based on these model fits. Since three models are optimized simultaneously, the software actually uses a

single surrogate called "desirability" to balance them. This is reasonable because the three characteristics are not competing, but are in a good mutual agreement. The model-based optimal formulations are shown in Table 5.7, and the "overall" water absorption represented by the desirability was minimized by 69.3 wt% rPP, 25.0 wt% RWF, 4.6 wt% MAPP, 0.1 wt% UV stabilizer, and 1 wt% Lub, with a high desirability score of 0.992 that indicates the agreement of the multiple objectives.

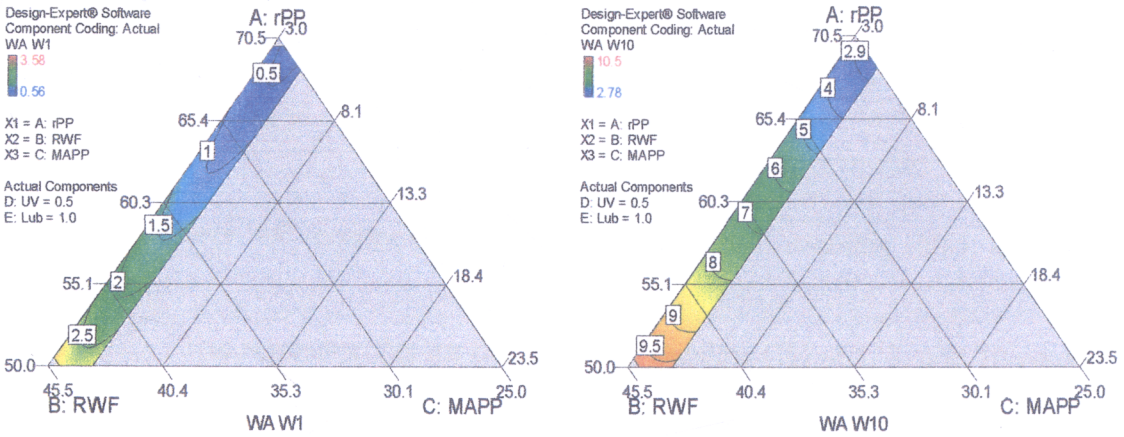

(a) (b)

Figure 5.2 Contour plots for effects of the compositions on water absorption at (a) 1 and (b) 10 weeks, with UV stabilizer fixed at 0.5 wt% and Lub at 1 wt%

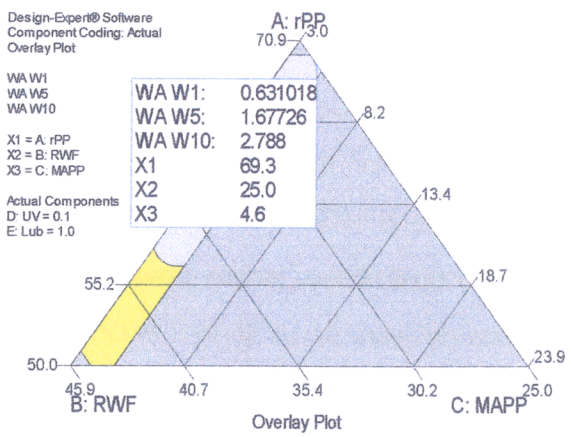

Figure 5.3 The optimal formulation for water absorption

Table 5.7 Predicted optimal formulations and their responses, from multiobjective optimizations. For example, the formulation in first row is optimal for a desirability score that balances WA at times W1, W5, and W10

	Mixture component fraction (wt%)					Predicted response				
Property	x_1	x_2	x_3	x_4	x_5	W1	W5	W6	W10	Desirability
WA (%)	69.3	25.0	4.6	0.1	1.0	0.63	1.67	-	2.78	0.992
TS (%)	68.9	25.0	5.0	0.1	1.0	0.22	0.49	-	0.78	0.969
MOR (MPa)	69.4	26.4	3.1	0.1	1.0	40.4	-	37.7	-	0.678
MOE (GPa)	50.0	44.1	4.2	0.7	1.0	2.03	-	1.74	-	0.862
Max. ε (%)	69.8	26.2	3.0	0.0	1.0	3.70	-	4.77	-	0.968

5.4.4 Effect of composition on the thickness swelling and optimal formulation

The regression fits for the thickness swelling (TS) at 1, 5, and 10 weeks were:

$$TSW1 = 0.093x_1 + 0.67x_2 - 43.45x_3 + 63.68x_4 - 0.52x_1x_2 + 49.74x_1x_3 - 63.11x_1x_4 + 47.51x_2x_3 - 64.78x_2x_4 - 52.62x_3x_4 \quad (5.4)$$

$$TSW5 = 0.33x_1 + 2.33x_2 - 17.17x_3 + 273.76x_4 - 0.87x_1x_2 + 21.95x_1x_3 - 281.51x_1x_4 + 16.33x_2x_3 - 280.74x_2x_4 - 326.17x_3x_4 \quad (5.5)$$

$$TSW10 = 0.95x_1 + 3.45x_2 - 0.71x_3 - 1.10x_4 \quad (5.6)$$

The equations of TS at all immersion times show positive coefficients for fraction of rPP (x_1) and RWF (x_2) but negative coefficient for fraction of MAPP (x_3), so MAPP addition should be maximized. When the positive coefficients between rPP and RWF were compared, the RWF showed higher coefficients than the rPP due to the hydrophilic filler. Figure 5.4 shows that TS at 10 week (in range of 1 to 3%) increases with an increase of the rubberwood flour fraction. The wood flour expands and keeps absorbing water until the cell walls are saturated [13]. The addition of MAPP from 3 to 5 wt% affected the thickness swelling of composites, so that the swelling decreased with MAPP fraction. The reason is probably similar to what was discussed in relation to the water absorption. The optimal formulation based on these

numerical models, combined by a desirability score for optimization, is also included in Table 5.7.

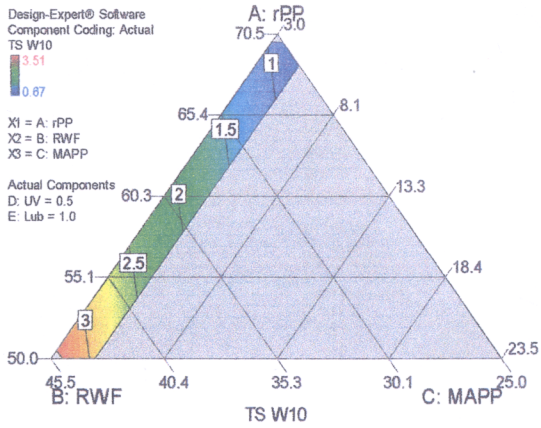

Figure 5.4 Triangular contour plots for effects of composition on thickness swelling at 10 week, with UV stabilizer fixed at 0.5 wt% and Lub at 1 wt%

5.4.5 Effect of composition on the flexural strength and optimal formulation

The quadratic regression models fitted for the flexural strength (MOR) at 1 and 6 weeks were:

$$\text{MOR W1} = 40.35x_1 + 43.78x_2 + 247.09x_3 - 1498.46x_4 + 0.24x_1x_2 - 247.39x_1x_3 + 1542.49x_1x_4 - 232.7x_2x_3 + 1453.86x_2x_4 + 1649.2x_3x_4 \quad (5.7)$$

$$\text{MOR W6} = 37.82x_1 + 33.70x_2 - 437.66x_3 - 3328.49x_4 - 8.79x_1x_2 + 526.16x_1x_3 + 3484.81x_1x_4 + 481.2x_2x_3 + 3468.82x_2x_4 + 4344.19x_3x_4 \quad (5.8)$$

The coefficients of rPP (x_1), RWF (x_2), MAPP (x_3), and UV stabilizer (x_4) decrease with immersion time. The UV stabilizer fraction has the largest negative coefficients in the model fits, so it should be minimized. UV stabilizer in WPCs is known to decrease the flexural properties due to non-homogeneous spatial distribution of wood flour, polymer, and UV stabilizer [25]. The triangular contour plots in Figures 5.5(a) and 5.5(b) illustrate that an increase of wood flour loading slowly increased MOR at 1 week but greatly decreased MOR at 6 weeks, respectively. The water molecules reduced interfacial adhesion between rubberwood flour and polypropylene [13].

When water molecules infiltrate into the composites, the wood flour tends to swell, resulting in localized yielding of the polymer matrix and loss of adhesion between the wood flour and matrix [13, 26]. The optimal composition based on the quadratic regression models is shown numerically in Table 5.7.

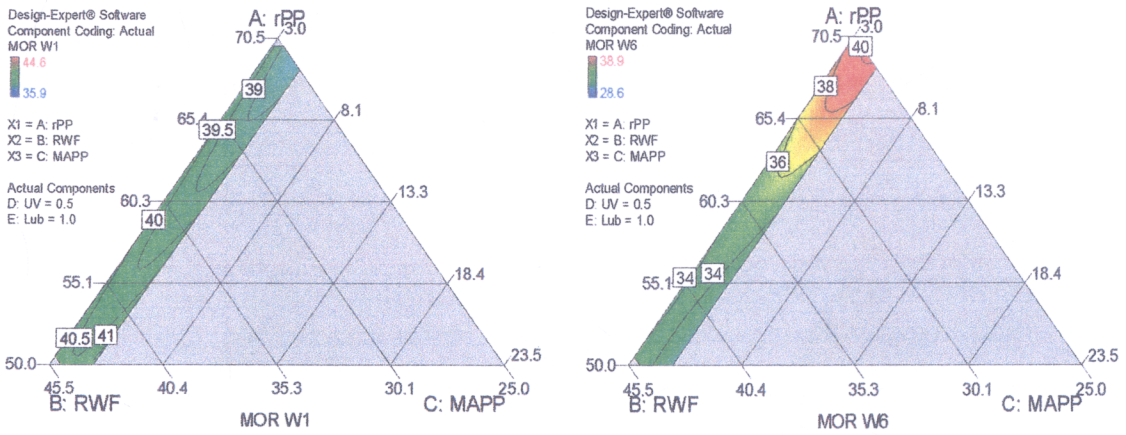

(a) (b)

Figure 5.5 Triangular contour plots for effects of composition on MOR at (a) 1 and (b) 6 weeks, with UV stabilizer fixed at 0.5 wt% and Lub at 1 wt%

5.4.6 Effect of composition on the flexural modulus and optimal formulation

The special cubic models fitted for the flexural modulus MOE at 1 and 6 weeks were:

$$\text{MOE W1} = 1.88x_1 + 2.15x_2 + 19.67x_3 - 64.10x_4 - 0.43x_1x_2 - 20.28x_1x_3 + 66.89x_1x_4 - 21.35x_2x_3 + 62.9x_2x_4 - 149.38x_3x_4 + 1.61x_1x_2x_3 + 16.71x_1x_2x_4 + 235.95x_1x_3x_4 + 332.38x_2x_3x_4 \quad (5.9)$$

$$\text{MOE W6} = 1.24x_1 + 1.67x_2 - 10.92x_3 - 211.79x_4 - 0.11x_1x_2 + 19.33x_1x_3 + 232.57x_1x_4 + 8.43x_2x_3 + 224.01x_2x_4 - 151.98x_3x_4 + 1.87x_1x_2x_3 - 23.9x_1x_2x_4 + 341.82x_1x_3x_4 + 563.41x_2x_3x_4 \quad (5.10)$$

These equations show kind of coefficients as flexural strength (MOR), decreasing with immersion time. Figure 5.6(a) shows that MOE at 1 week (in range of 1.85 to 2.05 GPa) increased for high fractions of wood flour, and high fractions of MAPP at about 4-5

wt%, giving high flexural modulus. However, in Figure 5.6(b) when composites were soaked in water for 6 weeks, MOE at high 45 wt% RWF fraction was comparable to composites with 25 wt% RWF. The wood flour as hard filler, in comparison to the plastic matrix, increased the stiffness of the composites. However, when wood flour plasticizes and becomes ductile, the stiffness of composites is decreased [26]. Figure 5.7 shows the optimal formulation based on the special cubic models for MOE, and a desirability score combining their outputs. The optimal formulation is also included in Table 5.7.

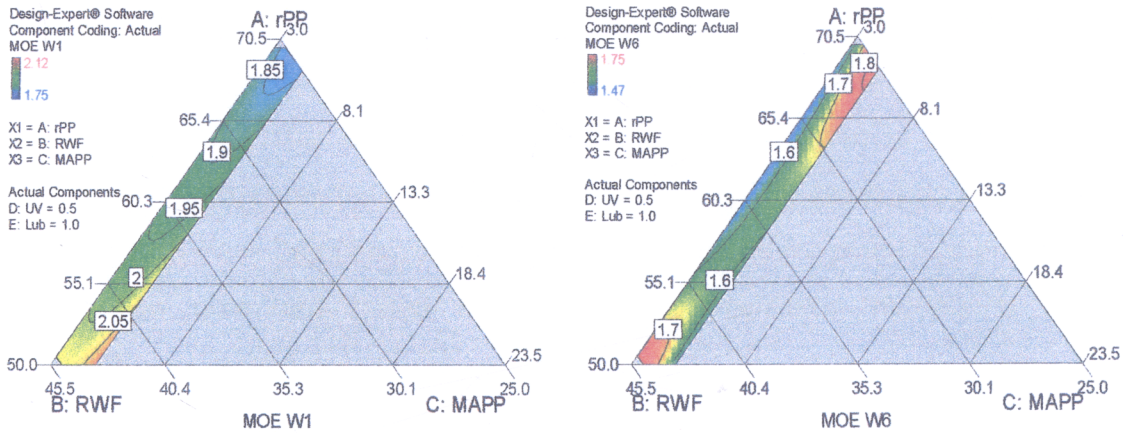

(a) (b)

Figure 5.6 Triangular contour plots for effects of composition on MOE at (a) 1 and (b) 6 weeks, with UV stabilizer fixed at 0.5 wt% and Lub at 1 wt%

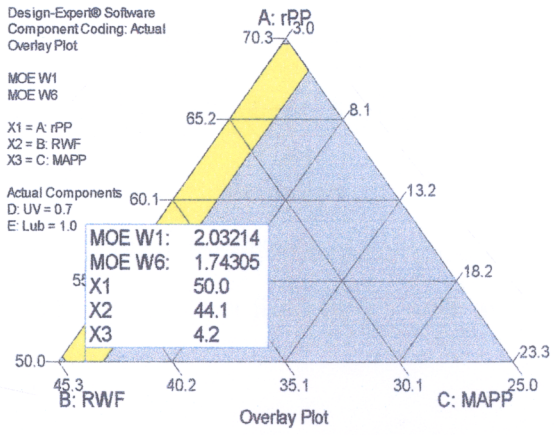

Figure 5.7 The optimal formulation for MOE

5.4.7 Effect of composition on the maximum strain and optimal formulation

The linear regression models for the max. ε at 1 and 6 weeks were:

$$\text{Max. } \varepsilon \text{ W1} = 3.72x_1 + 3.48x_2 + 2.63x_3 - 7.75x_4 \quad (5.11)$$

$$\text{Max. } \varepsilon \text{ W6} = 4.82x_1 + 3.87x_2 + 1.23x_3 - 9.29x_4 \quad (5.12)$$

The fraction of rPP (x_1) has the largest coefficients in the fit, so the maximum strain increases with high fraction of rPP. In contrast, it decreases with the fraction of UV stabilizer (x_4) that has a negative coefficient. Again the maximum strain increases with the water absorption and immersion time. The reason for this is probably similar as described earlier: ductile wet wood increases the maximum strain. Figure 5.8 shows that the maximum strain decreases with RWF content. This is due to increases in the stiffness and brittleness reducing the maximum strain. The stress concentrations at the fiber ends have been recognized as the leading cause for embrittlement [6]. The composition optimized based on these linear regression models is shown numerically in Table 5.7.

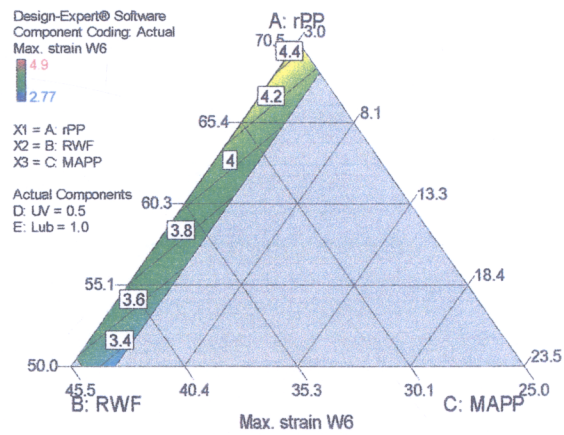

Figure 5.8 Triangular contour plots for effects of composition on the maximum strain at 6 weeks, with UV stabilizer fixed at 0.5 wt% and Lub at 1 wt%

5.4.8 Optimal formulation of the overall properties based on water absorption

An optimal formulation for rPP/RWF composites was determined to minimize water absorption and thickness swelling, and maximize flexural strength, modulus, and maximum strain. This multiobjective optimization, using all of the regression models, was performed with the Design-Expert software by constructing a desirability score that balances all of the fitted models. The plot in Figure 5.9 shows the formulation that was optimal, along with contours of the desirability score. The optimal formulation was 68.9 wt% rPP, 25.0 wt% RWF, 5.0 wt% MAPP, 0.1 wt% UV stabilizer, and 1.0 wt% Lub. The optimal formulation is given in Table 5.8, along with the model based responses. The formulations in Table 5.7 overall closely agree with this optimum.

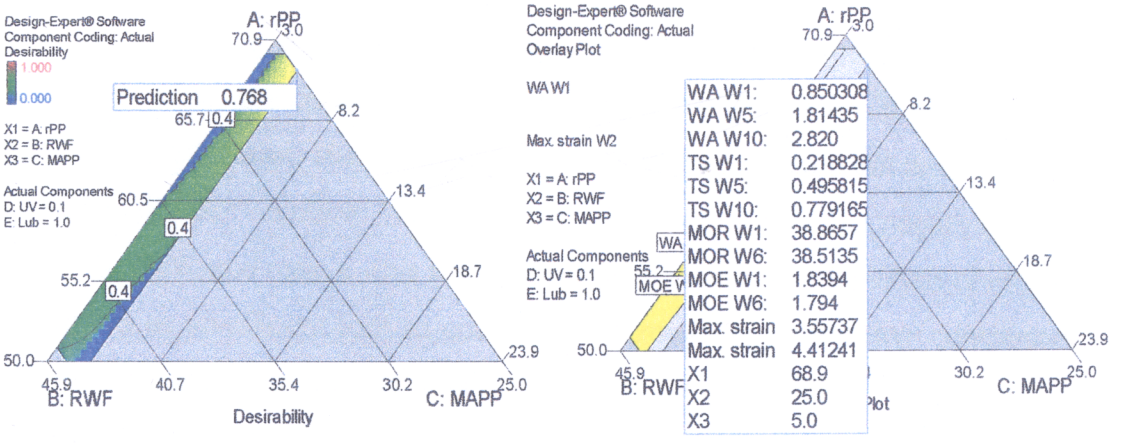

Figure 5.9 The optimal formulation for overall desirability

Table 5.8 Predicted responses with the formulation optimized jointly for all properties

	Mixture component fractions (wt%)					Predicted response			
Property	x_1	x_2	x_3	x_4	x_5	W1	W5	W6	W10
WA (%)						0.85	1.81	-	2.82
TS (%)						0.22	0.50	-	0.78
MOR (MPa)	68.9	25.0	5.0	0.1	1.0	38.9	-	38.5	-
MOE (GPa)						1.84	-	1.79	-
Max. ε (%)						3.56	-	4.41	-

5.5 Conclusions

Mixture experimental design, statistical modeling, and optimization were used to quantify the effects of rPP/RWF composite formulation, and to optimize the formulation for moisture resistance. Analysis of variance revealed that all the component fractions experimentally varied, namely of rPP, RWF, MAPP, and UV stabilizer, significantly affected the water absorption, thickness swelling, flexural strength and modulus, and maximum strain. In general, a high fraction of RWF increased the WA and TS across immersion times. The free OH groups in wood flour contribute to WA [23]. When the composites were soaked in water for 1 week, high fractions of RWF increased MOR and MOE but reduced maximum strain. In contrast, at 6 weeks the MOR and MOE decreased but maximum strain increased with RWF loading. At the longer immersion time water reduced the interfacial adhesion between RWF and rPP, and moisture plasticized the wood flour making it ductile: this decreased strength and stiffness but increased the maximum strain of composites [13, 26]. Therefore, the optimum found had 25 wt% RWF which was the minimum in the experimental design. The compatibilizer MAPP slightly affected WA and TS, which decreasd with MAPP content. The fraction of UV stabilizer also had negative effects on the WA, MOR, and max. ε. This study demonstrated design and analysis of mixture experiments as an efficient tool to optimize the formulation of rPP/RWF composites, for minimum water absorption and for maximum flexural properties.

5.6 References

[1] Y. Cui, S. Lee, B. Noruziaan, M. Cheung, and J. Tao. "Fabrication and Interfacial Modification of Wood/Recycled Plastic Composite Materials." *Composites Part A: Applied Science and Manufacturing*, vol. 39, pp. 655–661, 2008.

[2] N.J. Themelis, M.J. Castaldi, J. Bhatti, and L. Arsova. "Energy and Economic Value of Non-recycled Plastics and Municipal Solid Wastes that are Currently Landfilled in the Fifty States." *EEC Study of Non-recycled Plastics*, Earth Engineering Center, Columbia University, 2011.

[3] S.E. Selke and I. Wichman. "Wood Fiber/Polyolefin Composites." *Composites Part A: Applied Science and Manufacturing*, vol. 35, pp. 321–326, 2004.

[4] Y. Kazemi, A. Cloutier, and D. Rodrigue. "Mechanical and Morphological Properties of Wood Plastic Composites Based on Municipal Plastic Waste." *Polymer Composites*, vol. 34, pp. 487–493, 2013.

[5] S.K. Najafi, E. Hamidinia, and M. Tajvidi. "Mechanical Properties of Composites from Sawdust and Recycled Plastics." *Journal of Applied Polymer Science*, vol. 100, pp. 3641–3645, 2006.

[6] K.B. Adhikary, S. Pang, and M.P. Staiger. "Dimensional Stability and Mechanical Behaviour of Wood-Plastic Composites based Recycled and Virgin High-Density Polyethylene." *Composites Part B: Engineering*, vol. 39, pp. 807–815, 2008.

[7] C. Homkhiew, T. Ratanawilai, and W. Thongruang. "Composites from Recycled Polypropylene and Rubberwood Flour: Effects of Composition on Mechanical Properties." *Journal of Thermoplastic Composite Materials*, Epub ahead of print 14 February 2013.DOI: 10.1177/0892705712475019.

[8] P.Y. Kuo, S.Y. Wang, J.H. Chen, H.C. Hsueh, and M.J. Tsai. "Effects of Material Compositions on the Mechanical Properties of Wood–Plastic Composites Manufactured by Injection Molding." *Materials and Design*, vol. 30, pp. 3489–3496, 2009.

[9] S.L. Favaro, M.S. Lopes, A.G.V.d.C. Neto, R.R.d. Santana, and E. Radovanovic. "Chemical, Morphological, and Mechanical Analysis of Rice Husk/Post-Consumer Polyethylene Composites." *Composites Part A: Applied Science and Manufacturing*, vol. 41, pp. 154–160, 2010.

[10] N. Petchwattana and S. Covavisaruch. "Influences of Particle Sizes and Contents of Chemical Blowing Agents on Foaming Wood Plastic Composites Prepared from Poly(Vinyl Chloride) and Rice Hull." *Materials and Design*, vol. 32, pp. 2844–2850, 2011.

[11] M. Khalid, C.T. Ratnam, T.G. Chuah, S. Ali, and T.S.Y. Choong. "Comparative Study of Polypropylene Composites Reinforced with Oil Palm Empty Fruit Bunch Fiber and Oil Palm Derived Cellulose." *Materials and Design*, vol. 29, pp. 173–178, 2008.

[12] A. Karmarkar, S.S. Chauhan, J.M. Modak, and M. Chanda. "Mechanical Properties of Wood–Fiber Reinforced Polypropylene Composites: Effect of a

Novel Compatibilizer with Isocyanate Functional Group." *Composites Part A: Applied Science and Manufacturing*, vol. 38, pp. 227–233, 2007.

[13] T.T. Law and Z.A.M. Ishak. "Water Absorption and Dimensional Stability of Short Kenaf Fiber-Filled Polypropylene Composites Treated with Maleated Polypropylene." *Journal of Applied Polymer Science*, vol. 120, pp. 563–572, 2011.

[14] B. Li, H. Jiang, L. Guo, and H. Shi. "Comparative Study on the Effect of Manchurian Ash and Larch Wood Flour on Mechanical Property, Morphology, and Rheology of HDPE/Wood Flour Composites." *Journal of Applied Polymer Science*, vol. 107, pp. 2520–2530, 2008.

[15] T. Martinello, T.M. Kaneko, M.V.R. Velasco, M.E.S. Taqueda, and V.O. Consiglieri. "Optimization of Poorly Compactable Drug Tablets Manufactured by Direct Compression Using the Mixture Experimental Design." *International Journal of Pharmaceutics*, vol. 322, pp. 87–95, 2006.

[16] Z. Jun, W. Xiang-Ming, C. Jian-Min, and Z. Kai. "Optimization of Processing Variables in Wood–Rubber Composite Panel Manufacturing Technology." *Bioresource Technology*, vol. 99, pp. 2384–2391, 2008.

[17] L.M. Matuana and F. Mengeloglu. "Manufacture of Rigid PVC/Wood-Flour Composite Foams Using Moisture Contained in Wood as Foaming Agent." *Journal of Vinyl & Additive Technology*, vol. 8, pp. 264–270, 2002.

[18] N.M. Stark and L.M. Matuana. "Ultraviolet Weathering of Photostabilized Wood-Flour-Filled High-Density Polyethylene Composites." *Journal of Applied Polymer Science*, vol. 90, pp. 2609–2617, 2003.

[19] D.C. Montgomery. *Design and Analysis of Experiments*. John Wiley & Sons, Inc., 2009.

[20] Y.B. Khosrowshahi and A. Salem. "Influence of Polyvinyl Alcohol and Carboxymethyl Cellulose on the Reliability of Extruded Ceramic Body: Application of Mixture Design Method in Fabricating Reliable Ceramic Raschig Rings." *International Journal of Applied Ceramic Technology*, vol. 8, pp. 1334–1343, 2011.

[21] M. Amini, H. Younesi, N. Bahramifar, A.A.Z. Lorestani, F. Ghorbani, A. Daneshi, and M. Sharifzadeh. "Application of Response Surface Methodology for Optimization of Lead Biosorption in an Aqueous Solution by Aspergillus Niger." *Journal of Hazardous Materials*, vol. 154, pp. 694–702, 2008.

[22] R.H. Myers, D.C. Montgomery, and C.M. Anderson-Cook. *Response Surface Methodology: Process and Product Optimization Using Designed Experiments*. John Wiley & Sons, Inc., Hoboken, New Jersey, 2009.

[23] A. Shakeri and A. Ghasemian. "Water Absorption and Thickness Swelling Behavior of Polypropylene Reinforced with Hybrid Recycled Newspaper and Glass Fiber." *Applied Composite Materials*, vol. 17, pp. 183–193, 2010.

[24] K.B. Adhikary, S. Pang, and M.P. Staiger. "Long-Term Moisture Absorption and Thickness Swelling Behaviour of Recycled Thermoplastics Reinforced with Pinus Radiata Sawdust." *Chemical Engineering Journal*, vol. 142, pp. 190–198, 2008.

[25] A. Wechsler and S. Hiziroglu. "Some of the Properties of Wood–Plastic Composites." *Building and Environment*, vol. 42, pp. 2637–2644, 2007.

[26] S. Tamrakar and R.A. Lopez-Anido. "Water Absorption of Wood Polypropylene Composite Sheet Piles and Its Influence on Mechanical Properties." *Construction and Building Materials*, vol. 25, pp. 3977–3988, 2011.

CHAPTER 6

Effects of Natural Weathering on the Properties of Recycled Polypropylene Composites Reinforced with Rubberwood Flour

6.1 Chapter summary

The effects of natural weathering on the physical and mechanical properties of polypropylene (PP)/rubberwood flour (RWF) composites were investigated for various compositions, with different grades of plastic (virgin and recycled) and varied contents of wood flour and ultraviolet (UV) stabilizer. Composite panels were manufactured using a twin-screw extruder. Weathering sharply changed lightness (L^*) and discoloration, and slightly reduced flexural strength (MOR) and modulus (MOE) of the PP/RWF composites. Virgin PP had smaller relative changes of lightness and smaller relative loss of hardness, MOR, and MOE than recycled PP (rPP), both in composites and as unfilled plastic. Increasing RWF content from 25 to 45 wt% in composites increased the change of L^* and loss of MOR, MOE, and maximum strain. Addition of 1 wt% UV stabilizer reduced change of L^* and loss of hardness, MOR, MOE, and maximum strain, compared to composites without UV stabilizer.

6.2 Introduction

Wood-plastic composites (WPCs) have been gaining popularity in several applications, including door inner panels, seat backs, and headliners in automotive industry; decking, cladding, and fencing in construction; and in infrastructure as marina and boardwalk. Among these, structural applications are the largest and fastest-growing market for WPCs [1, 2] that offer low density, low cost, low maintenance, recyclability, and eco-friendliness with good mechanical properties. Moreover, softwood lumber is increasingly replaced by WPCs and plastic lumber in applications of deck-building because this improves durability [3, 4], and

the demand for WPCs is expected to have increased nearly 12% annually between 2000 and 2010 in the United States [4].

The increasing use of WPCs in construction has resulted in concerns about long-term weatherability and durability [5]. Generally, the WPC products that are used in ground contact or in aboveground exterior are subjected to accelerated material deterioration [1]. In ground contact, biological agents such as fungi and subterranean termites affect degradation [1, 6], while in aboveground exterior there is exposure to ultraviolet (UV) rays and moisture [1, 7]. Likewise, WPCs have been reported to discolor when exposed to weathering, affecting aesthetics, and to lose mechanical properties critical to performance [8-12]. The loss of mechanical properties can stem from matrix crystallinity changes, composite surface oxidation, and interfacial degradation caused by moisture absorption [13]. Therefore, when a new WPC material is developed, it is important to evaluate changes in its properties under a variety of environmental conditions, to assess effects influencing useful service life [1, 14].

A number of studies on the properties of WPCs under service conditions have focused on weathering (e.g. aging effects of temperature, moisture, UV light, and biological decay), and its relation to wood content, processing method, and type and content of UV stabilizer and pigments [9, 11, 14, 15]. The addition of wood flour (WF) into plastics accelerates the photodegradation of WPCs [14]. This is attributed to the deterioration of wood's components (namely lignin, cellulose, hemicellulose, and extractives) [15, 16]. Likewise, the UV component of sunlight affects primarily the photodegradation of wood. The degradation rates of wood components greatly depend on their abilities to absorb UV light [17]. Because most wood chromophores are in lignin, it accounts for 80-95% of light absorption by wood, making its photodegradation a significant contributor to wood discoloration [17, 18]. In addition, when WPCs are exposed long-term in outdoor applications, moisture or water negatively affects their properties. Moisture can accelerate photo-oxidation and mechanical property loss in WPCs by causing the wood fibers to swell, facilitating deeper light penetration into the wood, and inducing cracks in the plastic matrix [11, 14]. As a result the flexural strength and modulus decrease with the

deterioration of interfacial bonding between natural fibers and the matrix [14, 19]. Moisture absorption can be influenced by the wood flour loading, wood particle size, and wood species [19].

Chaochanchaikul et al. [14] studied the effects of natural and accelerated weathering conditions on the structural and physical characteristics of polyvinyl chloride (PVC) and wood/polyvinyl chloride (WPVC) composites. The PVC and WPVC composites had more photodegradation under accelerated weathering conditions than under natural weathering conditions. Stark and Matuana [8] investigated the influence of UV radiation with and without water spray on the photodegradation and mechanical properties of WF-filled high-density polyethylene (HDPE) composites, and found that the composites were more photobleached and lost more flexural strength and modulus, than when exposed to UV radiation without water spray. Du et al. [20] examined the effects of color pigments on the durability of HDPE/WF composites, and found that the composites containing pigments exhibited less deterioration, less surface discoloration, and less cracks on surface than those without pigment. Zhang et al. [21] also reported that the changes in lightness of HDPE/WF composites decreased with an increase of pigment dosage. Beg and Pickering [22] studied degradation of unbleached and bleached kraft fiber reinforced polypropylene (PP) composites under accelerated weathering conditions. Tensile strength and Young's modulus as well as thermal stability of both unbleached and bleached fiber composites decreased with accelerated weathering. Selden et al. [12] also found that the color of PP/WF composite plates changed from brown to chalky white. Although the photodegradation and mechanical property loss of WF-reinforced plastics have been extensively examined, little information is available on WF-reinforced polypropylene, and there is no prior report on the photodegradation and mechanical property loss of rubberwood flour (RWF) reinforced postconsumer polypropylene that was the focus of this research.

Rubber tree (*Hevea brasiliensis*) is widely planted in South and Northeast Thailand. It is major economic importance because the latex extracted from these trees is the primary source of natural rubber. However, the trees become unproductive at about 25 years of age and are cut down [23]. Rubberwood lumber

and root are mainly utilized to manufacture furniture, toys, and packing materials. In these rubberwood industries, a large amount of wood waste in the forms of flour, sawdust, and chips is generated at different stages of processing. Generally, rubberwood waste is dumped in landfills or burned, resulting in pollution issues, but some of the waste is also used to produce medium-density fiberboard and particleboard [24]. The utilization of rubberwood waste as a reinforcement in polymer composites could decrease environmental impacts from the waste, as well as increase value of the waste material. Moreover, rubberwood waste reinforced thermoplastics also offer advantages including biodegradability, renewable character, absence of associated health hazards, and low equipment wear during their processing [25], when compared to synthetic fillers.

The quality of filler (wood flour or wood fiber) is an important factor affecting the photodegradation and mechanical properties of WPCs, because different wood species have different contents of cellulose, lignin, hemicelluloses, and extractants [26]. Hence, the effects of filler (rubberwood flour) and the selected grade of plastic (virgin or recycled PP) on the composites need to be characterized. The ultimate goal of this work is to determine the effects of material compositions (including different grades of plastic; and contents of RWF and UV stabilizer) on the physical and mechanical properties of RWF reinforced PP composites exposed to weathering tests. The new information helps target the most suitable end-use applications of such composites.

6.3 Experimental

6.3.1 Materials

Recycled polypropylene (rPP) pellets, WT170 with a melt flow index of 11 g/10 min at 230 °C, were purchased from Withaya Intertrade Co., Ltd (Samutprakarn, Thailand). Virgin polypropylene (vPP) granules, HIPOL J600 with a melt flow index of 7 g/10 min at 230 °C, were supplied by Mitsui Petrochemical Industries Co., Ltd (Tokyo, Japan). Rubberwood flour obtained from the cutting process in local furniture industry (Songkhla, Thailand) was used as reinforcement. Its main chemical constituents were cellulose (39%), hemicellulose (29%), lignin (28%),

and ash (4%) [27]. Before compounding, the RWF was sieved through a standard sieve of mesh size 80 (passing particles smaller than 180 μm) and was dried in an oven at 110 °C for 8 h. Maleic anhydride-grafted polypropylene (MAPP) with 8-10% of maleic anhydride was supplied by Sigma-Aldrich (Missouri, USA), and used as a coupling agent to improve the interfacial adhesion between filler and matrix. Hindered amine light stabilizer (HALS) additive, chosen as the UV stabilizer, was supplied by TH Color Co., Ltd (Samutprakarn, Thailand) under the trade name MEUV008. A paraffin wax lubricant (Lub) was purchased from Nippon Seiro Co., Ltd (Yamaguchi, Japan).

6.3.2 Composite processing

WPCs were produced in a two-stage process. In the first stage to produce WPC pellets, RWF and PP were dry-blended, melt-blended, and pelletized into wood-plastic composite pellets using a twin-screw extruder (Model SHJ-36 from En Mach Co., Ltd, Nonthaburi, Thailand). The 10 temperature zones of the extruder were controlled at 130-170 °C from feeding to die zone, to reduce degradation of the compositions, while the screw rotating speed was maintained at 70 rpm. In the second stage to produce WPC panels, the WPC pellets were again dried prior to use, in an oven at 110 °C for 8 h. The WPC pellets, MAPP, UV stabilizer, and lubricant (formulations in Table 6.1) were then dry-mixed and fed into the twin-screw extruder. The processing conditions for extruding were as follows: (1) temperature profiles: 130-190 °C; (2) screw rotating speed: 50 rpm; (3) melt pressure: 0.10-0.20 MPa depending on wood flour content; and (4) vacuum venting at 9 temperature zones: 0.022 MPa. The WPC samples were extruded through a rectangular die with the dimensions of 9 mm × 22 mm and cooled in ambient air. After cooling, the specimens were cut according to American Society for Testing and Materials (ASTM) for physical and mechanical testing.

6.3.3 Natural weathering testing

The unfilled PP and PP/RWF composite specimens were cut from extrudates to dimensions dependent on the type of testing. The composite

specimens were placed on the roof of 4th floors building in Hat Yai, Songkhla, Thailand, for 360 days (from July 1st 2012 to June 25th 2013). All the specimens were placed on wood exposure racks according to ASTM D1435-03, and were attached on the racks at a 45° angle, facing in a southerly direction [14]. The samples were then removed for characterizations after 60, 120, 180, 240, 300, and 360 days.

Table 6.1 Wood-plastic composite formulation (percent by weight)

Composite sample code	rPP	vPP	RWF	MAPP	UV	Lub
rP100	100					
vP100		**100**				
rP70R25M3U1	70		25	3	1	1
vP70R25M3U1		**70**	**25**	**3**	**1**	**1**
rP60R35M3U0.5	60.3		35.3	3	0.5	1
vP60R35M3U0.5		**60.3**	**35.3**	**3**	**0.5**	**1**
rP50R45M3U1	50		45	3	1	1
vP50R45M3U1		**50**	**45**	**3**	**1**	**1**
rP51R45M3U0	51		45	3	0	1

Note; The selected formulations from the mixture experimental design were carried out. The rP70R25M3U1 means 70 wt% rPP, 25 wt% RWF, 3 wt% MAPP, and 1 wt% UV stabilizer.

6.3.4 Characterizations

Color measurements. A Hunterlab Color Standard (Hunter Associates Laboratory, Inc., Virginia, USA) was used to measure color parameters of the unfilled PP and PP/RWF composite samples before and after weathering, according to the CIE $L^*a^*b^*$ color system. L^* represents the lightness, whereas a^* and b^* are the chromaticity coordinates. A higher L^* -value means an increase in lightness. The a^* coordinate represents red-green hue, while b^* coordinate represents yellow-blue hue. Three replications of each formulation and time condition were measured, and each specimen was measured at three locations. The total color changes or discolorations (ΔE) of the un-weathered and weathered PP and PP/RWF composite specimens were measured by Euclidean distance in the parameter space:

$$\Delta E = \sqrt{(L_2^* - L_1^*)^2 + (a_2^* - a_1^*)^2 + (b_2^* - b_1^*)^2} \quad (6.1)$$

where subscript 1 denotes the values of unexposed PP and PP/RWF composite specimens, and subscript 2 denotes the values of exposed PP and PP/RWF composite specimens. These discoloration comparisons with equation (6.1) were only done to contrast between exposed and unexposed, for otherwise similar samples at similar age.

Hardness. Hardness measurements were performed according to ASTM D2240-91 specification, using two Durometers (Shore D scales) for the composites. The dimensions of the specimens tested were approximately 16 mm × 16 mm × 6.5 mm. The measurements were performed at room temperature (25 °C).

Flexure testing. Before testing, the specimens were dried in an oven at 50 °C for 24 h. Three-point flexure test was carried out on an Instron Universal Testing Machine (Model 5582 from Instron Corporation, Massachusetts, USA) at a cross-head speed of 2 mm/min, with nominal sample dimensions of 4.8 mm × 13 mm × 100 mm, and a span of 80 mm in accordance with ASTM D790-92. The testing was performed at ambient room temperature of 25 °C, with five specimens of each formulation at each aging time, to obtain an average value. The flexural properties of composite samples were determined both before exposure and after outdoor exposure for 60, 120, 180, 240, 300, and 360 days. The maximum stress, modulus of elasticity, and maximum strain at maximum stress were calculated according to the above-mentioned standard.

6.3.5 Analysis

Morphological analysis. Morphological studies with a scanning electron microscope (SEM) were carried out to assess the formation of surface cracks. SEM imaging with FEI Quanta 400 microscope (FEI Company, Oregon, USA) used an accelerating voltage of 20 kV. Prior to SEM observations, all samples were dried in an oven at 50 °C for 24 h and were sputter-coated with gold to prevent electrical charging during the imaging. All specimens were imaged perpendicular to the surface with a 150× magnification.

Statistical analysis. The effects of weathering on the color change, hardness, flexural strength and modulus, and maximum strain of unfilled PP and PP/RWF composites were evaluated by Student's *t*-test using a 5% significance level (α = 0.05). Results, such as mean values and standard deviations from three and five samples for color measurements and flexural properties, respectively, of each formulation and time condition, were statistically analyzed. Comparisons were only conducted within each formulation between unexposed and exposed (360 day) samples. Superscript letters were used to denote significance in tabulations: if the letters are the same, the means that are not significantly different; different superscripts indicate significant difference [28].

6.4 Results and discussion

6.4.1 Color analysis

The physical appearances of unfilled PP and PP/RWF composites with and without UV stabilizer, after exposure to natural weathering for a total of 360 days, were evaluated from lightness and discoloration. Figure 6.1 shows an overall increase in lightness (L^*) for all formulations (based on virgin and recycled PP), but this increase was not monotonic with exposure time for filled samples. The highest L^* -values were at 60 days of exposure, then they gradually decreased up to 180 days, but again increased slightly after 240 days for filled samples. However, for unfilled rPP lightness L^* steadily increased with exposure time. Photographs of virgin and recycled PP with different RWF contents are shown in Figure 6.2. Discoloration occurred in three stages. The samples were quickly photobleached by exposure to weathering for 60 days, then darkened up to approximately 180 days, and finally the composites again lightened with further exposure. The photobleaching mainly affected the wood component, particularly lignin [8], while darkening may have been caused by surface oxidation [29]. An increase in RWF content from 25 to 45 wt% in vPP and rPP composites increased the lightness (in Figure 6.1), and increased the percentage change in Table 6.2. With a high wood flour content, some of it was exposed at the sample surface where complete encapsulation by the matrix is less likely [29]. Furthermore, the composites based on vPP show lower lightness than

those based on rPP, for the same plastic to wood ratio. This may be due to better encapsulation of wood flour in virgin polypropylene, with good dispersion and strong interfacial bonding between wood flour and polymer, and consequently slower photobleaching of the wood component. For the effect of UV stabilizer, it was observed that the addition of 1 wt% UV stabilizer (rP50R45M3U1) in rPP/RWF composites decreased the L^* value, when compared with the composites without UV stabilizer (rP51R45M3U0). This is because UV stabilizer (HALS) prevents photodegradation in polymer [15].

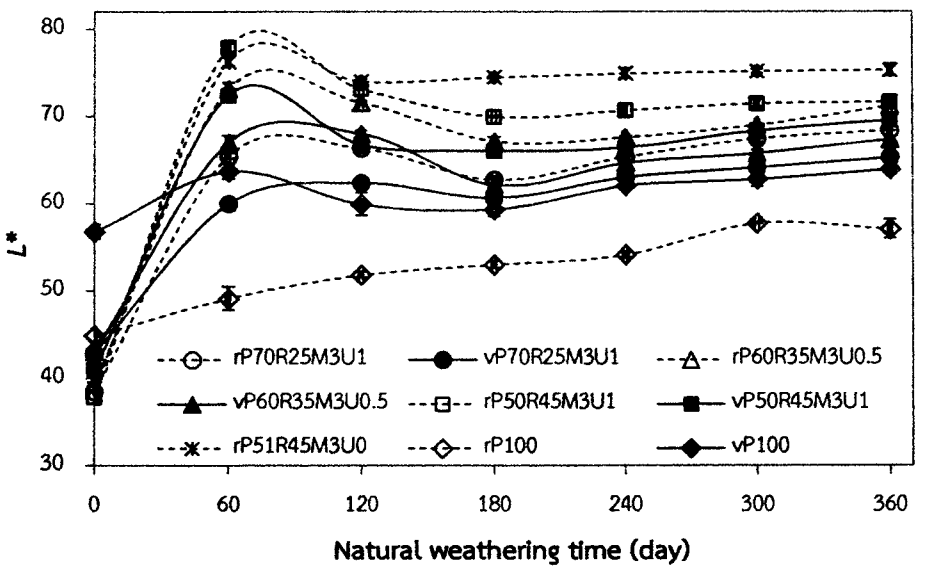

Figure 6.1 Effect of weathering on lightness of unfilled PP and PP composites (both virgin and recycled) with various RWF loadings, with and without UV stabilizer

The effects of the natural weathering on lightness were also verified by statistical analysis, and Student's *t*-test is shown in Table 6.2. With all the formulations (based on virgin and recycled PP) lightness was significantly increased by 360 days exposure, with the exception of unfilled vPP that had an insignificant increase.

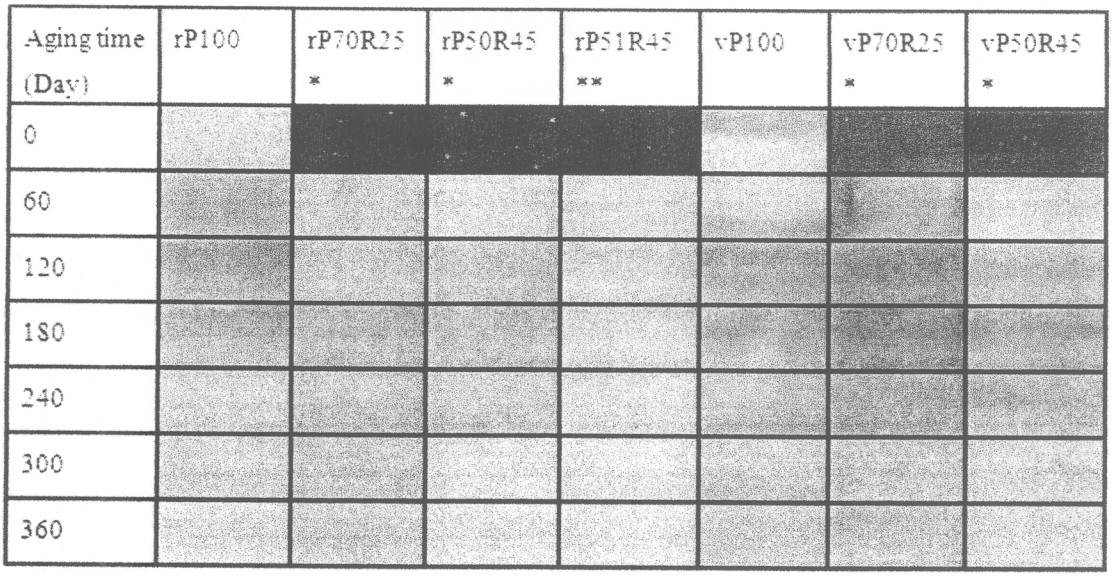

*The composites were fixed MAPP at 3 wt% and UV stabilizer at 1 wt%. **The composites were fixed MAPP at 3 wt% and without UV stabilizer.

Figure 6.2 Digital photographs of virgin and recycled polypropylene containing various RWF loadings

Table 6.2 Effects of weathering on physical properties of unfilled PP and PP composites with various RWF loadings

	*L**			Hardness (shore D)		
Formulation	0D**	360D***	% change	0D**	360D***	% loss
rP100	44.9^{a}	57.1^{b}	27.20	72.5^{a}	60.4^{b}	16.69
vP100	**56.8^{a}**	**64.0^{a}**	**12.65**	**75.6^{a}**	**65.9^{b}**	**12.82**
rP70R25M3U1	38.5^{a}	68.4^{b}	77.72	73.2^{a}	69.2^{b}	5.49
vP70R25M3U1	**42.9^{a}**	**65.3^{b}**	**52.28**	**76.4^{a}**	**72.3^{b}**	**5.32**
rP60R35M3U0.5	39.4^{a}	71.2^{b}	80.92	74.3^{a}	70.6^{b}	5.00
vP60R35M3U0.5	**43.0^{a}**	**67.4^{b}**	**56.69**	**77.8^{a}**	**74.5^{b}**	**4.67**
rP50R45M3U1	37.9^{a}	71.7^{b}	89.26	75.2^{a}	72.7^{a}	3.29
vP50R45M3U1	**41.0^{a}**	**69.6^{b}**	**69.81**	**78.3^{a}**	**74.8^{a}**	**4.47**
rP51R45M3U0	38.9^{a}	75.3^{b}	93.82	76.1^{a}	72.0^{b}	5.41

Note; Means within each formulation with the same letter are not significantly different (Student's *t*-test, α = 0.05). 0D** unexposed and 360D*** exposed for 360 days.

The total color changes or discolorations are shown in Figure 6.3. The trend is similar to lightness. The ΔE sharply increased up to 60 days of weathering and then clearly decreased up to 180 days, after which it slowly increased. Switching vPP to rPP increases ΔE. This is probably due to stronger structure (chains) of virgin polypropylene. During exposure to natural weathering water facilitated the removal of degraded wood components and formation of cracks [17], and a stronger structural plastic reduces these effects. Likewise, the vPP (vP100) gave the lowest ΔE value with insignificant change in ΔE, but rPP composites containing 45 wt% RWF without UV stabilizer (rP51R45M3U0) had the highest ΔE value with significant change by weathering. This is caused by high wood flour content and omission of UV stabilizer.

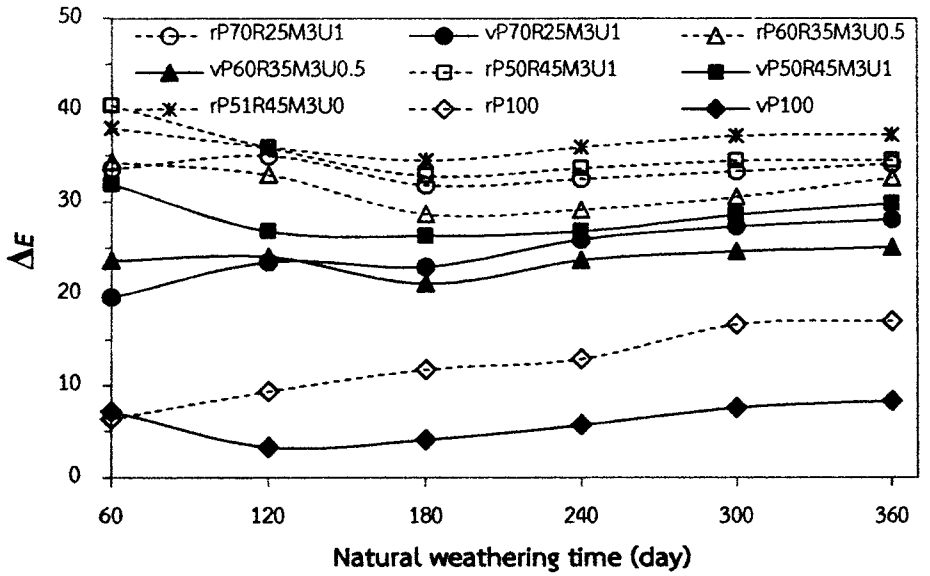

Figure 6.3 Effects of weathering on discoloration of unfilled PP and PP composites with various RWF loadings, with and without UV stabilizer

6.4.2 Hardness analysis

Hardness generally decreased with weathering as shown in Figure 6.4. The hardness of unfilled vPP was only insignificantly reduced at 60 days of weathering, and decreased significantly after 120 days, whereas the hardness of unfilled rPP decreased significantly with exposure time. This was caused by polymer

chain scission, which results in surface cracks, and the number of chain scissions increased with the exposure time [20]. In addition, the vPP and rPP composites with RWF loading lose less hardness with exposure time than unfilled vPP and rPP. These results indicate that the addition of wood flour can efficiently improve the degradation resistance of plastic composites. Besides, unfilled vPP and composites based on vPP show higher hardness than those based on rPP for the same plastic to wood ratio, through the experimental duration. This is probably because vPP has lower melt flow index than rPP, leading to lower flexibility. Usually, composites with a less flexible matrix have a higher hardness [24, 30]. Furthermore, the loss percentage of hardness after 360 day exposure to weathering is also shown in Table 6.2. An increase in RWF content decreases the relative loss of hardness. This is because the number of polymer chain scissions on the surface decreases. Likewise, the composites with 1 wt% UV stabilizer (3.29 %loss) lost less hardness than that the composites without the UV stabilizer (5.41 %loss). Student's *t*-test (in Table 6.2) demonstrates that the effects of exposure to weathering for 360 days were statistically significant, except with 45 wt% RWF (loss less than 5%).

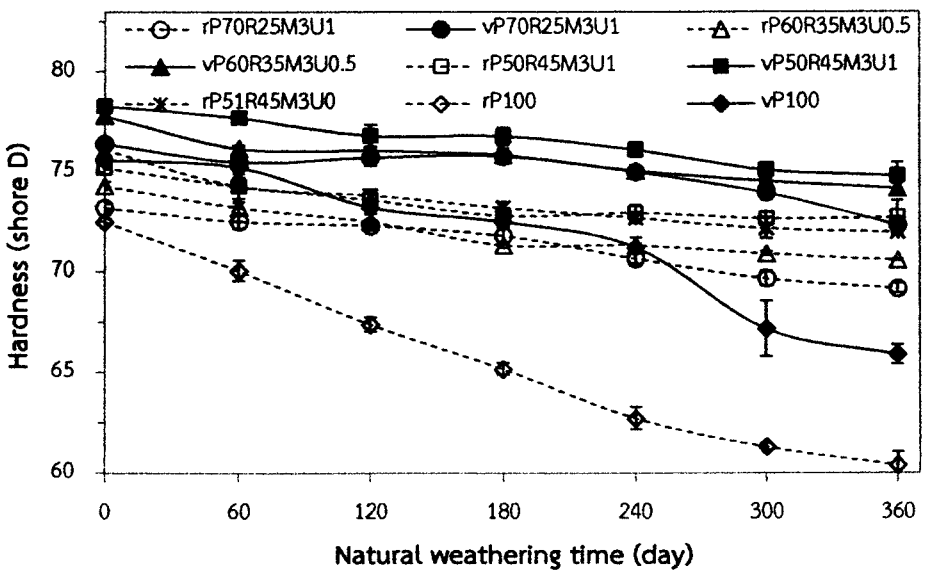

Figure 6.4 Effects of weathering on hardness of unfilled PP and PP composites with various RWF loadings, with and without UV stabilizer

6.4.3 SEM morphological analysis

Microphotographs of unexposed and exposed vPP and rPP composites are shown in Figure 6.5. Prior to exposure, the vPP and rPP composites with different wood flour loading [Figures 6.5(a), (c), (e), (g), (i)] have smooth surfaces. The composites with 45 wt% RWF [Figures 6.5(c), (g), (i)] have more RWF on the surface than the composites with 25 wt% RWF [Figures 6.5(a), (e)]. This substantiates that a larger amount of wood flour was exposed on the surfaces of WPCs with high filler loading [29]. Moreover, the vPP and rPP composites exposed for 360 days [Figures 6.5(b), (d), (f), (h), (j)] show large surface cracks. The cracks are related to polymer chain scission, which results from wetting and drying cycles [5]. Fabiyi et al. demonstrated three main stages of WPC degradation. First the surface was eroded with many cavities, second the size and frequency of cavities increased, and finally small cracks on the weathered surface developed following the second stage [5]. The composites with 25 wt% RWF [Figures 6.5(b), (f)] clearly exhibit less surface cracks than the composites with 45 wt% RWF [Figures 6.5(d), (h), (j)]. The WPCs with high wood flour content had strong swelling when exposed to moisture or water. As cracks accumulate, they contribute also to deeper light penetration [8]. In addition, rPP composites show higher cracking on the surfaces than those based on vPP, for the same plastic to wood ratio. This is probably due to the virgin plastic being stiffer than recycled plastic. The recycled plastic had a lower melt viscosity, which is attributed to decreased molecular weight [24, 31] and shorter polymer chains. Furthermore, on comparing the rPP composites with 45 wt% RWF with and without UV stabilizer, deeper cracking was found without UV stabilizer [Figure 6.5(j)] than with UV stabilizer [Figure 6.5(h)]. The UV stabilizer as a free radical scavenger reduces photodegradation of plastic [15].

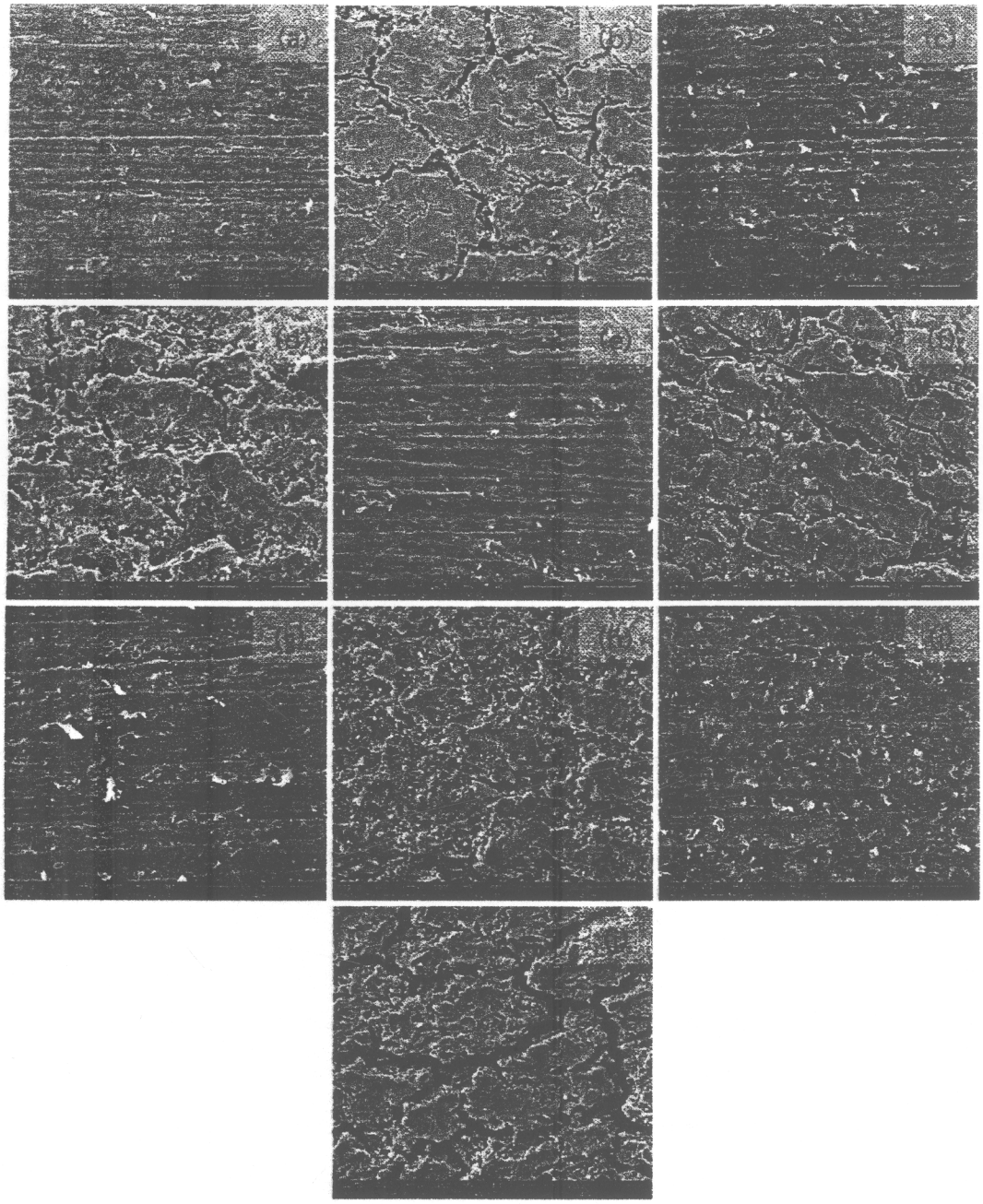

Figure 6.5 SEM (150×) images of WPC surfaces before and after weathering for 360 days: vPP composites with 25 wt% RWF (a and b) and with 45 wt% RWF (c and d), rPP composites with 25 wt% RWF (e and f) and with 45 wt% RWF (g and h), and rPP composites containing 45 wt% RWF without UV stabilizer (i and j)

6.4.4 Flexural property analysis

When the product is in service, flexural strength (MOR) and modulus (MOE) are critical for the composite's performance [32]. Figure 6.6 shows that MOR of unfilled vPP and rPP strongly decreased with exposure time, and MOR of the composites based on rPP slightly decreased up to 120 days and then clearly decreased after 180 days. For composites based on vPP, MOR decreased slightly after 120 days. Stark and Matuana [8] explained that crystallinity of the composites initially increases during exposure to UV light and water, and then decreases with continued exposure [13] because chain scissions occur when PP is exposed to UV light. Initially, the more mobile shorter chains recrystallize [8, 33]. When chain scission continues further, the crystalline regions are affected and crystallinity decreases [8]. It is expected that after 120 days of exposure, the crystallinity of PP decreases, decreasing MOR. Further, the composites without UV stabilizer had sharp decreases after 120 days, and bigger loss of MOR than with 1 wt% UV stabilizer, as shown in Table 6.3. Table 6.3 also reveals that loss of MOR increased with RWF content increased from 25 to 45 wt%, both for vPP and rPP. This may be due to increased swelling with RWF content that causes microcracks in the matrix and decreases the efficiency of stress transfer from wood flour to plastic matrix, decreasing MOR [8, 21]. Student's *t*-test (in Table 6.3) also verifies that the exposure to weathering for 360 days significantly affected MOR, except for the vPP composites with 25 and 35 wt% RWF.

Figure 6.7 shows changes in MOE of unfilled PP (both virgin and recycled) and the PP composites. The trends are similar to the MOR, clearly decreasing after 180 days. Likewise, the loss of MOE (in Table 6.3) increases with RWF content, and is statistically significant at 360 days for all formulations. The loss of MOE is partly due to the negative effects of moisture penetration during exposure [8, 34].

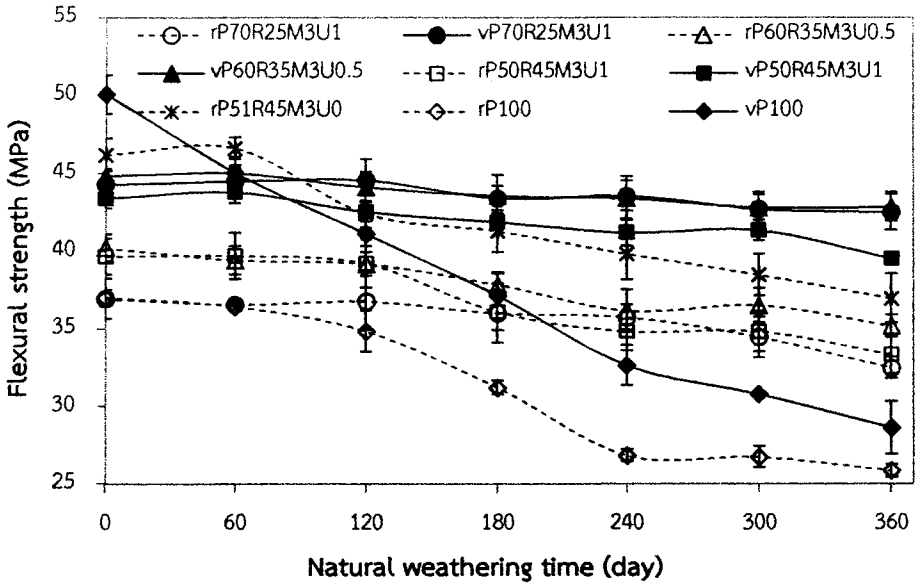

Figure 6.6 Effects of weathering on flexural strength of unfilled PP and PP composites with various RWF loadings, with and without UV stabilizer

Table 6.3 Effects of weathering on mechanical properties of unfilled PP and PP composites with various RWF loadings

	MOR (MPa)			MOE (GPa)			Maximum strain (%)		
Formulation	0D*	360D**	% loss	0D*	360D**	% loss	0D*	360D**	% loss
rP100	37.0^{a}	25.8^{b}	30.19	1.27^{a}	0.98^{b}	42.03	6.20^{a}	1.47^{b}	67.48
vP100	**50.1^{a}**	**28.6^{b}**	**42.85**	**1.67^{a}**	**0.97^{b}**	**23.22**	**6.95^{a}**	**2.26^{b}**	**76.25**
rP70R25M3U1	36.9^{a}	32.5^{b}	12.08	1.76^{a}	1.50^{b}	15.00	3.09^{a}	2.90^{a}	6.06
vP70R25M3U1	**44.3^{a}**	**42.5^{a}**	**4.09**	**1.93^{a}**	**1.73^{b}**	**10.26**	**3.99^{a}**	**3.53^{a}**	**11.39**
rP60R35M3U0.5	40.2^{a}	35.2^{b}	12.55	2.18^{a}	1.80^{b}	17.44	2.79^{a}	2.58^{a}	7.55
vP60R35M3U0.5	**44.8^{a}**	**42.9^{a}**	**4.40**	**2.31^{a}**	**2.06^{b}**	**10.63**	**3.23^{a}**	**2.84^{a}**	**12.09**
rP50R45M3U1	39.7^{a}	33.3^{b}	15.95	2.69^{a}	2.08^{b}	22.54	2.07^{a}	1.88^{a}	9.38
vP50R45M3U1	**43.4^{a}**	**39.5^{b}**	**8.95**	**2.66^{a}**	**2.23^{b}**	**16.30**	**2.36^{a}**	**2.04^{a}**	**13.39**
rP51R45M3U0	46.2^{a}	37.0^{b}	20.01	2.60^{a}	1.98^{b}	23.84	2.40^{a}	1.96^{a}	18.24

Note; Means within each formulation with the same letter are not significantly different (Student's *t*-test, α = 0.05). 0D* unexposed and 360D** exposed for 360 days.

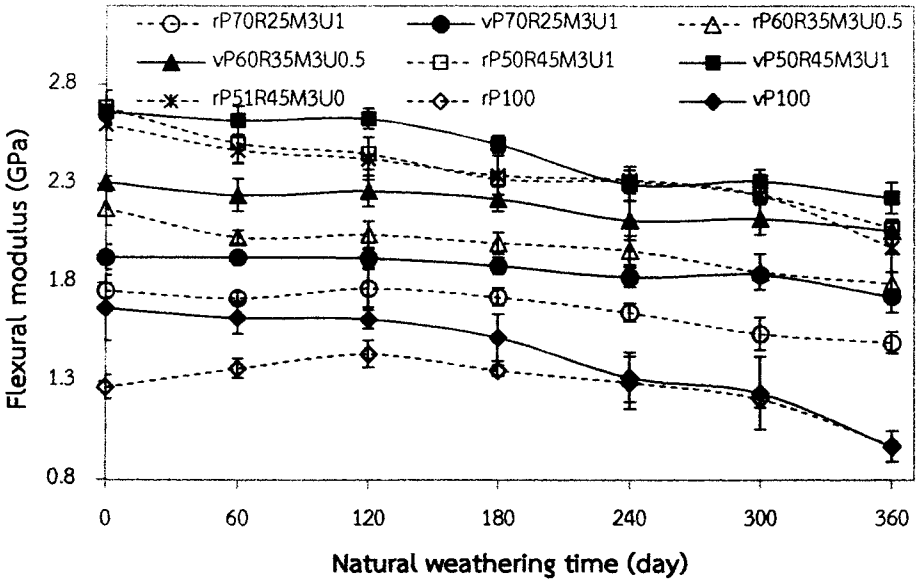

Figure 6.7 Effects of weathering on flexural modulus of unfilled PP and PP composites with various RWF loadings, with and without UV stabilizer

Figure 6.8 illustrates the effects of exposure on the maximum strain of the composites. The maximum strain of unfilled vPP and rPP sharply decreases after 240 days, and then stabilizes. The significant drop in maximum strain indicates that the PP (both virgin and recycled) became more brittle during weathering [35]. However, the vPP and rPP composites only have insignificant decreases of maximum strain, which increase with RWF loading (in Table 6.3). The reason may again be increased swelling with RWF content, when exposed to water, deteriorating mechanical properties [8]. Stark and Matuana [36] revealed that exposure to UV light causes surface cracking of the plastic matrix and deterioration of lignin in wood flour. Exposure to water causes swelling of wood flour, creates microcracks in the matrix, and also washes loose wood flour and degraded lignin to the wood surface [17].

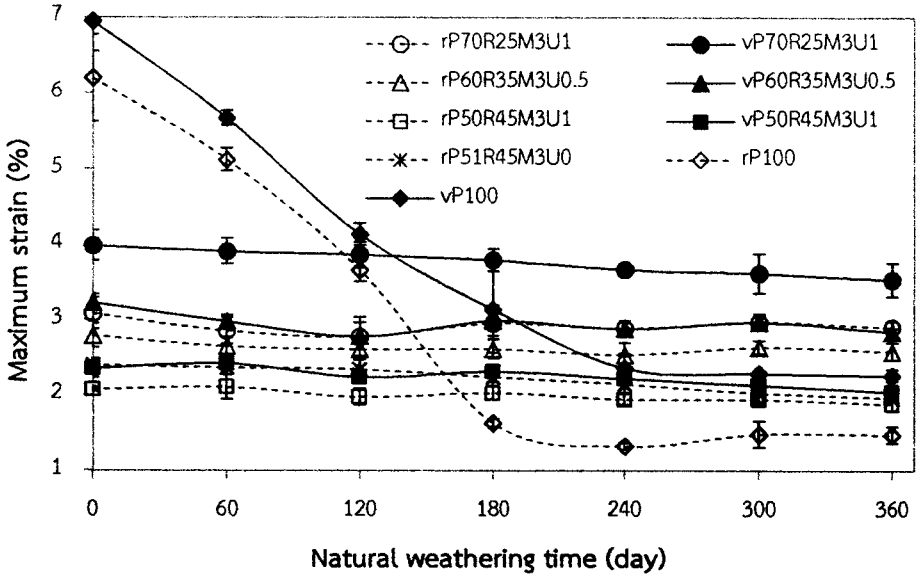

Figure 6.8 Effects of weathering on maximum strain of unfilled PP and PP composites with various RWF loadings, with and without UV stabilizer

6.5 Conclusions

The effects of plastic grades (virgin and recycled) and contents of wood flour and UV stabilizer on the physical and mechanical properties of RWF reinforced PP composites exposed to the weathering were examined. The vPP and rPP composites filled with RWF experienced changes in physical properties and loss of mechanical properties due to weathering. The lightness and discoloration of unfilled PP and PP/RWF composites sharply increased after 60 days, and then clearly decreased up to 180 days, further increasing slightly after 240 days. The composites based on vPP had smaller percentage changes of L^* and smaller loss of hardness, MOR and MOE than those based on rPP, at equal plastic to wood ratios, due to better encapsulation of wood flour in virgin polypropylene. Increasing the RWF content from 25 to 45 wt% in vPP and rPP composites increased the percentage change of lightness and relative loss of MOR, MOE, and maximum strain. This increased the exposure of wood flour on the sample surface [29], increased microcracks, and decreased the efficiency of stress transfer from wood flour to plastic matrix [8]. The rPP/RWF composites with 1 wt% UV stabilizer had smaller changes in lightness and smaller relative loss of hardness, MOR, MOE, and maximum

strain than without UV stabilizer, due to reduced photodegradation of polymer [15]. The overall result highlights effects of composition and new information to facilitate development of engineering performance of composite materials, applying in exterior environments.

6.6 References

[1] J.M. Pilarski and L.M. Matuana. "Durability of Wood Flour-Plastic Composites Exposed to Accelerated Freeze–Thaw Cycling. Part I. Rigid PVC Matrix." *Journal of Vinyl and Additive Technology*, vol. 11, pp. 1–8, 2005.

[2] P. Mapleston. "It's One Hot Market for Profile Extruders." *Modern Plastics*, vol. June, pp. 49–52, 2001.

[3] D.R. Carroll, R.B. Stone, A.M. Sirignano, R.M. Saindon, S.C. Gose, and M.A. Friedman. "Structural Properties of Recycled Plastic/Sawdust Lumber Decking Planks." *Resources, Conservation and Recycling*, vol. 31, pp. 241–251, 2011.

[4] I. Ganguly and I.L. Eastin. "Trends in the US Decking Market: A National Survey of Deck and Home Builders." *The Forestry Chronicle*, vol. 85, pp. 82–90, 2009.

[5] J.S. Fabiyi, A.G. McDonald, M.P. Wolcott, and P.R. Griffiths. "Wood Plastic Composites Weathering: Visual Appearance and Chemical Changes." *Polymer Degradation and Stability*, vol. 93, pp. 1405–1414, 2008.

[6] M. Mankowski and J.J. Morrell. "Patterns of Fungal Attack in Wood Plastic Composites Following Exposure in a Soil Block Test." *Wood and Fiber Science*, vol. 32, pp. 340–345, 2000.

[7] L.M. Matuana and D.P. Kamdem. "Accelerated Ultraviolet Weathering of PVC/Wood-Flour Composites." *Polymer Engineering and Science*, vol. 42, pp. 1657–1666, 2002.

[8] N.M. Stark and L.M. Matuana. "Influence of Photostabilizers on Wood Flour-HDPE Composites Exposed to Xenon-Arc Radiation with and without Water Spray." *Polymer Degradation and Stability*, vol. 91, pp. 3048–3056, 2006.

[9] L.M. Matuana, D.P. Kamdem, and J. Zhang. "Photoaging and Stabilization of Rigid PVC/Wood-Fiber Composites." *Journal of Applied Polymer Science*, vol. 80, pp. 1943–1950, 2001.

[10] N.M. Stark and L.M. Matuana. "Ultraviolet Weathering of Photostabilized Wood-Flour-Filled High-Density Polyethylene Composites." *Journal of Applied Polymer Science*, vol. 90, pp. 2609–2617, 2003.

[11] N.M. Stark. "Effect of Weathering Cycle and Manufacturing Method on Performance of Wood Flour and High-Density Polyethylene Composites." *Journal of Applied Polymer Science*, vol. 100, pp. 3131–3140, 2006.

[12] R. Selden, B. Nystrom, and R. Langstrom. "UV Aging of Poly(Propylene)/ Wood-Fiber Composites." *Polymer Composites*, vol. 25, pp. 543–553, 2004.

[13] N.M. Stark, L.M. Matuana, and C.M. Clemons. "Effect of Processing Method on Surface and Weathering Characteristics of Wood–Flour/HDPE Composites." *Journal of Applied Polymer Science*, vol. 93, pp. 1021–1030, 2004.

[14] K. Chaochanchaikul, V. Rosarpitak, and N. Sombatsompop. "Photodegradation Profiles of PVC Compound and Wood/PVC Composites under UV Weathering." *Express Polymer Letters*, vol. 7, pp. 146–160, 2013.

[15] M. Muasher and M. Sain. "The Efficacy of Photostabilizers on the Color Change of Wood Filled Plastic Composites." *Polymer Degradation and Stability*, vol. 91, pp. 1156–1165, 2006.

[16] C.W. Dence. *The Determination of Lignin: Methods in Lignin Chemistry.* Springer–Verlag, 1992.

[17] L.M. Matuana, S. Jin, and N.M. Stark. "Ultraviolet Weathering of HDPE/Wood-Flour Composites Coextruded with a Clear HDPE Cap Layer." *Polymer Degradation and Stability*, vol. 96, pp. 97–106, 2011.

[18] U. Müller, M. Ratzsch, M. Schwanninger, M. Steiner, and H. Zöbl. "Yellowing and IR-Changes of Spruce Wood as Result of UV-Irradiation." *Journal of Photochemistry and Photobiology B: Biology*, vol. 69, pp. 97–105, 2003.

[19] N.M. Stark and L.M. Matuana. "Surface Chemistry and Mechanical Property Changes of Wood-Flour/High-Density-Polyethylene Composites after Accelerated Weathering." *Journal of Applied Polymer Science*, vol. 94, pp. 2263–2273, 2004.

[20] H. Du, W. Wang, Q. Wang, Z. Zhang, S. Sui, and Y. Zhang. "Effects of Pigments on the UV Degradation of Wood-Flour/HDPE Composites." *Journal of Applied Polymer Science*, vol. 118, pp. 1068–1076, 2010.

[21] Z.M. Zhang, H. Du, W. Hong, and Q.W. Wang. "Property Changes of Wood-Fiber/HDPE Composites Colored by Iron Oxide Pigments after Accelerated UV Weathering." *Journal of Forestry Research*, vol. 21, pp. 59–62, 2010.

[22] M.D.H. Beg and K.L. Pickering. "Accelerated Weathering of Unbleached and Bleached Kraft Wood Fibre Reinforced Polypropylene Composites." *Polymer Degradation and Stability*, vol. 93, pp. 1939–1946, 2008.

[23] S. Rimdusit, W. Smittakorn, S. Jittarom, and S. Tiptipakorn. "Highly Filled Polypropylene Rubber Wood Flour Composites." *Engineering Journal*, vol. 15, pp. 17–30, 2011.

[24] C. Homkhiew, T. Ratanawilai, and W. Thongruang. "Composites from Recycled Polypropylene and Rubberwood Flour: Effects of Composition on Mechanical Properties." *Journal of Thermoplastic Composite Materials*, Epub ahead of print 14 February 2013.DOI: 10.1177/0892705712475019.

[25] S.L. Favaro, M.S. Lopes, A.G.V.d.C. Neto, R.R.d. Santana, and E. Radovanovic. "Chemical, Morphological, and Mechanical Analysis of Rice Husk/Post-Consumer Polyethylene Composites." *Composites Part A: Applied Science and Manufacturing*, vol. 41, pp. 154–160, 2010.

[26] B. Li, H. Jiang, L. Guo, and H. Shi. "Comparative Study on the Effect of Manchurian Ash and Larch Wood Flour on Mechanical Property, Morphology, and Rheology of HDPE/Wood Flour Composites." *Journal of Applied Polymer Science*, vol. 107, pp. 2520–2530, 2008.

[27] P. Petchpradab, T. Yoshida, T. Charinpanitkul, and Y. Matsumura. "Hydrothermal Pretreatment of Rubber Wood for the Saccharification Process." *Industrial and Engineering Chemistry Research*, vol. 48, pp. 4587–4591, 2009.

[28] N.M. Stark and S.A. Mueller. "Improving the Color Stability of Wood-Plastic Composites through Fiber Pre-Treatment." *Wood and Fiber Science*, vol. 40, pp. 271–278, 2008.

[29] K.B. Adhikary. "Development of Wood Flour-Recycled Polymer Composite Panels as Building Materials." Ph.D. dissertation, University of Canterbury, New Zealand, 2008.

[30] M.R. Rahman, M.M. Huque, M.N. Islam, and M. Hasan. "Mechanical Properties of Polypropylene Composites Reinforced with Chemically Treated Abaca." *Composites Part A: Applied Science and Manufacturing*, vol. 40, pp. 511–517, 2009.

[31] J. Lisperguer, X. Bustos, and Y. Saravia. "Thermal and Mechanical Properties of Wood Flour-Polystyrene Blends from Postconsumer Plastic Waste." *Journal of Applied Polymer Science*, vol. 119, pp. 443–451, 2011.

[32] J.L. Lopez, M. Sain, and P. Cooper. "Performance of Natural-Fiber–Plastic Composites under Stress for Outdoor Applications: Effect of Moisture, Temperature, and Ultraviolet Light Exposure." *Journal of Applied Polymer Science*, vol. 99, pp. 2570–2577, 2006.

[33] G. Wypych. *Handbook of Material Weathering*. Toronto, Ontario: Chem–Tec Publishing, 1995.

[34] D. Hon. *Wood and Cellulose Chemistry*. New York, Marcel Dekker, 2001.

[35] K. Chaochanchaikul and N. Sombatsompop. "Stabilizations of Molecular Structures and Mechanical Properties of PVC and Wood/PVC Composites by Tinuvin and TiO_2 Stabilizers." *Polymer Engineering & Science*, vol. 51, pp. 1354–1365, 2011.

[36] N.M. Stark and L.M. Matuana. "Characterization of Weathered Wood-Plastic Composite Surfaces Using FTIR Spectroscopy, Contact Angle, and XPS." *Polymer Degradation and Stability*, vol. 92, pp. 1883–1890, 2007.

CHAPTER 7

Optimizing the Formulation of Recycled Polypropylene and Rubberwood Flour Composites for Weathering Resistance by Mixture Design

7.1 Chapter summary

D-optimal mixture design was used in this study to determine the optimal mixture of composites from rubberwood flour (RWF) and recycled polypropylene (rPP), for resistance against weathering. The effects on physical and mechanical properties of component fractions, namely of rPP, RWF, maleic anhydride-grafted polypropylene (MAPP), and ultraviolet (UV) stabilizer, were systematically analyzed. The mixed materials were formed into panels using an extruder. The overall composition significantly affected weathering effects on color (L^*), discoloration (ΔE), hardness, flexural strength (MOR) and modulus (MOE), and maximum strain. L^*, ΔE, hardness, MOR, and MOE increased with the fraction of RWF. At long weathering exposure times hardness, MOR, and MOE decreased. The fraction of MAPP only slightly affected L^*, hardness, and MOR, while the UV stabilizer fraction had clear positive effects decreasing L^* and ΔE, but negative effects decreasing flexural properties. The models fitted were used to optimize a desirability score that balanced multiple physical and mechanical properties. The model-based optimal formulation found was 61.9 wt% rPP, 33.9 wt% RWF, 3.1 wt% MAPP, 0.2 wt% UV stabilizer, and 1.0 wt% lubricant.

7.2 Introduction

The use of wood flour or fiber in composites with thermoplastic matrix, such as polyethylene (PE), polypropylene (PP), polyvinyl chloride (PVC), or polystyrene (PS), is increasing rapidly, particularly in the United states, Japan, and China [1]. Recently, wood-plastic composites (WPCs) have been widely developed

and used for non-structural applications [2]: in automotive industry as door inner panels, seat backs, and headliners; in construction business as decking, cladding, and fencing; and in infrastructure as marina and boardwalk. Likewise, WPCs have been replaced softwood lumber in some deck building applications, due to improved durability over softwood lumber [3, 4]. The demand of WPCs is expected to have expanded nearly 12% each year from 2000 to 2010 in the United States [4]. The WPCs offer low cost, low density, low maintenance, recyclability, and eco-friendliness with good mechanical properties, and can address some environmental issues.

The increased application of WPCs in construction faces concerns about long-term durability and weatherability [5], because WPCs can deteriorate quickly with discoloration and their physical and mechanical properties worsen [6, 7] when exposed to natural weathering. Likewise, WPCs applied in aboveground exterior environments are degraded by ultraviolet (UV) rays in sunlight [8, 9], or in ground contact by biological agents such as fungi and subterranean termites [8, 10]. Furthermore, when WPCs are exposed long-term in outdoor applications, water or moisture negatively influences their properties. Moisture can accelerate photo-oxidation and mechanical property loss in WPCs by swelling wood fibers, facilitating deeper light penetration into the wood, and causing cracks in the plastic matrix [11, 12]. This reduces flexural strength and modulus, by loss of interfacial bonding between natural fibers and matrix [11, 13]. Moisture absorption can be influenced by wood flour loading, wood particle size, and wood species [13]. A number of studies on the properties of WPCs under service conditions have focused on weathering, and how it is influenced by processing method, wood content, and type and content of UV stabilizer and pigments [7, 11, 12, 14]. Du et al. [15] studied the effects of color pigments on the durability of wood-flour/high-density polyethylene (HDPE) composites, and found that the addition of pigments to the composites results in less weather-related damage. Matuana et al. [16] examined the effects of co-extruding a clear HDPE cap layer onto HDPE/wood-flour composites on the discoloration. The uncapped composites lightened quickly under accelerated weathering, with loss of yellowness and redness, and were more discolored than co-

extruded composites. Najafi and Englund [17] investigated the influence of highly degraded HDPE on mechanical properties of HDPE-wood flour composites. The mechanical properties of composites containing highly degraded HDPEs were similar to composites with virgin HDPE, with the exception of impact strength. Butylina et al. [18] examined the effects of outdoor weathering on the properties of wood-PP composites with and without pigments, and found that dark colored pigments improved color stability, while high moisture absorption decreased Charpy impact strength. Therefore, when a new WPC material is developed, it is important to evaluate the effects of weathering, as this relates to product durability [8, 11].

Statistical experimental designs, such as mixture design, factorial design, and taguchi method, are well-established as a bases of informative experiments [19]. However, the fractions of components in a mixture cannot be changed independently since they must add to 100%, and for these cases the mixture designs are an appropriate method [20]. A D-optimal mixture experimental design can be used to experimentally find the individual effects of components in a mixture, and the fitted models to optimize the formulation of a composite material [21]. A D-optimal design can considerably reduce the number of experiments needed for scientific and technical information on the composition effects. It allows restricting the ranges of component fractions, and within this range of formulations helps fit the mathematical models, used to improve the characteristics of final goods [21, 22]. Moreover, this method is appropriate for non-linear models [23].

Recent studies of WPCs have naturally employed designed experiments. For example, Stark et al. [24] applied a 2^4 factorial design to determine the effects of two hindered amine light stabilizers, a colorant and an ultraviolet absorber, and their interactions on the photostabilization of wood flour/high-density polyethylene composites. Matuana et al. [25] used a four-factor central composite design to develop a response surface model and to study the foamability of rigid PVC/wood-flour composites. Jun et al. [26] used a Box-Behnken design with response surface method to determine which variables influenced board performance significantly. Likewise, mixture designs are widely used in pharmacy and food industries to assess the effects of composition and to find an optimal formulation,

whereas prior studies on weathering of WPCs seem not to have used D-optimal mixture designs. Hence, a D-optimal mixture design was applied to model physical and mechanical characteristics of WPCs during weathering. The ultimate objective of this work is to optimize the mixture ratios for composites made from recycled polypropylene and rubberwood flour, based on experimentally determined color change and flexural failure. The new information will facilitate informed decisions regarding manufacture of such composites.

7.3 Experimental

7.3.1 Materials

Recycled polypropylene (rPP) pellets, WT170 with a melt flow index of 11 g/10 min at 230 °C, were supplied by Withaya Intertrade Co., Ltd (Samutprakarn, Thailand). Rubberwood flour (RWF) obtained from the cutting process in local furniture industry (Songkhla, Thailand) was used as reinforcement. The main chemical constituents were: cellulose (39%), hemicellulose (29%), lignin (28%), and ash (4%) [27]. Before compounding, the wood flour was sieved through a standard sieve of mesh size 80 (passing particles smaller than 180 μm) and was dried in an oven at 110 °C for 8 h. The coupling agent used was maleic anhydride-grafted polypropylene (MAPP), supplied by Sigma-Aldrich (Missouri, USA), with 8-10% of maleic anhydride. Hindered amine light stabilizer (HALS) additive, chosen as the UV stabilizer, was supplied by TH Color Co., Ltd (Samutprakarn, Thailand) under the trade name MEUV008. A paraffin wax lubricant (Lub) was purchased from Nippon Seiro Co., Ltd (Yamaguchi, Japan).

7.3.2 Experimental design to optimize formulation

The region of interest for the current experiments has constraints imposed on the component fractions [20], and these can be incorporated in a D-optimal mixture design. The experimental results were used to statistically evaluate the effects of component fractions on color change and flexural failure, and the identified models were used to optimize the formulation. The D-optimal mixture experimental design and statistical analysis were done with Design-Expert software

(version 8.0.6, Stat-Ease, Inc.). The formulations for the manufacture of WPCs were defined by component fractions for rPP (x_1), RWF (x_2), MAPP (x_3), UV stabilizer (x_4), and Lub (x_5). The upper and lower limits of experimental range are shown in Table 5.1. Despite the fraction of Lub being held constant, it is included as a variable because it contributes to the 100% in the mixture. The design included 15 different formulations and 5 replications to evaluate reproducibility and variances. Thus, the total number of runs was 20, as shown in Tables 7.1 and 7.2.

7.3.3 Preparation of composites

The WPCs were manufactured in a two-stage process. In the first stage WPC pellets were produced: rPP and RWF were dry-blended and melt-blended into wood-plastic composite pellets using a twin-screw extruder (Model SHJ-36 from En Mach Co., Ltd, Nonthaburi, Thailand). The 10 temperature zones of the extruder were set to a profile in range 130-170 °C, to reduce degradation of the mixture components, while the screw rotating speed was maintained at 70 rpm. The extruded strand was passed through a water bath and was subsequently pelletized. In the second stage WPC panels were produced: the WPC pellets were again dried at 110 °C for 8 h. WPC pellets, MAPP, UV stabilizer, and lubricant compositions indicated in Tables 7.1 and 7.2 were then dry-mixed and fed into the twin-screw extruder. The processing conditions for extruding were as follows: (1) temperature profiles: 130-190 °C; (2) screw rotating speed: 50 rpm; (3) melt pressure: 0.10-0.20 MPa depending on wood flour content; and (4) vacuum venting at 9 temperature zones: 0.022 MPa. The WPC panels were extruded through a 9 mm × 22 mm rectangular die and cooled in ambient air. These specimens were machined following the standards of American Society for Testing and Materials (ASTM) for physical and mechanical testing.

Table 7.1 Experimental compositions based on mixture experimental design and measured responses: L^*, ΔE, and hardness at 60 and 360 days

Run	Mixture component fraction (wt%)					L^*		ΔE		Hardness (shore D)	
No.	x_1	x_2	x_3	x_4	x_5	D60	D360	D60	D360	D60	D360
1	63.9	29.9	4.5	0.7	1.0	75.1	73.0	44.0	42.4	73.9	70.3
2	70.0	25.0	3.0	1.0	1.0	64.4	70.8	35.5	33.5	72.9	69.9
3	50.0	43.0	5.0	1.0	1.0	77.3	75.0	43.0	42.1	74.7	71.9
4	54.9	38.9	4.5	0.7	1.0	75.9	73.9	40.4	38.8	73.9	71.2
5	59.5	34.5	5.0	0.0	1.0	76.0	75.0	41.5	39.8	73.9	71.2
6	55.4	39.9	3.5	0.2	1.0	76.6	74.5	42.7	40.9	75.0	71.6
7	59.5	34.5	4.0	1.0	1.0	75.8	73.8	44.6	39.9	73.9	71.5
8**	59.5	34.5	5.0	0.0	1.0	75.0	73.4	39.3	38.6	73.1	69.6
9	50.0	44.3	4.3	0.5	1.0	77.5	77.0	48.5	44.3	76.1	72.4
10	68.0	25.0	5.0	1.0	1.0	65.3	67.6	34.0	33.7	73.1	69.7
11	50.0	45.0	3.0	1.0	1.0	77.9	71.7	41.5	44.5	74.6	72.7
12**	50.0	43.0	5.0	1.0	1.0	76.1	75.3	45.9	44.3	74.8	71.7
13	60.3	35.3	3.0	0.5	1.0	73.2	71.2	34.3	36.6	73.2	70.6
14	64.9	30.4	3.5	0.2	1.0	73.8	72.8	43.1	42.6	74.4	69.9
15**	70.0	25.0	3.0	1.0	1.0	66.0	68.4	32.6	31.1	72.5	69.2
16	51.0	45.0	3.0	0.0	1.0	76.1	75.3	38.0	40.3	74.3	72.0
17**	51.0	45.0	3.0	0.0	1.0	77.5	74.2	45.7	43.9	74.1	71.9
18**	50.0	45.0	3.0	1.0	1.0	77.1	73.2	47.1	44.0	75.4	72.0
19	70.0	25.0	4.0	0.0	1.0	73.5	71.1	35.7	33.9	71.9	67.9
20	69.0	25.0	5.0	0.0	1.0	74.3	71.8	35.3	32.4	72.2	68.8

Note; **duplicate experiments

7.3.4 Natural weathering testing

The rPP/RWF composite specimens were cut from extrudates to dimensions dependent on the types of testing. The composite specimens were placed on the roof of a 4-floor building in Hat Yai, Songkhla, Thailand, for 360 days (from July 1st 2012 to June 25th 2013). All the specimens were placed on wood exposure racks according to ASTM D1435-03 and were attached on the racks at a 45^{o}

angle, facing in a southerly direction [11]. The samples were then removed for characterizations after 60 and 360 days.

Table 7.2 The experimental compositions and measured flexural properties

Run	Mixture component fraction (wt%)					MOR (MPa)		MOE (GPa)		Max. strain (%)	
No.	x_1	x_2	x_3	x_4	x_5	D60	D360	D60	D360	D60	D360
1	63.9	29.9	4.5	0.7	1.0	39.9	35.6	1.96	1.76	2.72	2.71
2	70.0	25.0	3.0	1.0	1.0	36.4	33.3	1.73	1.57	2.80	2.68
3	50.0	43.0	5.0	1.0	1.0	35.9	33.7	2.29	2.12	1.94	1.90
4	54.9	38.9	4.5	0.7	1.0	40.9	37.3	2.25	1.88	2.41	2.56
5	59.5	34.5	5.0	0.0	1.0	43.4	38.4	2.08	1.92	2.78	2.69
6	55.4	39.9	3.5	0.2	1.0	42.2	39.4	2.33	2.06	2.51	2.75
7	59.5	34.5	4.0	1.0	1.0	39.9	34.8	2.07	1.88	2.60	2.43
8**	59.5	34.5	5.0	0.0	1.0	38.5	36.6	1.89	1.68	2.87	3.02
9	50.0	44.3	4.3	0.5	1.0	40.8	36.7	2.53	2.19	1.90	2.23
10	68.0	25.0	5.0	1.0	1.0	36.5	32.1	1.81	1.64	2.66	2.50
11	50.0	45.0	3.0	1.0	1.0	39.7	33.3	2.51	2.08	2.11	1.88
12**	50.0	43.0	5.0	1.0	1.0	37.1	33.7	2.46	2.08	1.87	1.96
13	60.3	35.3	3.0	0.5	1.0	39.4	35.2	2.03	1.80	2.65	2.58
14	64.9	30.4	3.5	0.2	1.0	40.6	36.5	1.92	1.68	2.94	2.94
15**	70.0	25.0	3.0	1.0	1.0	36.5	32.5	1.72	1.50	2.89	2.90
16	51.0	45.0	3.0	0.0	1.0	46.6	37.0	2.47	1.98	2.37	1.96
17**	51.0	45.0	3.0	0.0	1.0	44.6	39.6	2.53	2.13	2.48	2.48
18**	50.0	45.0	3.0	1.0	1.0	40.4	36.4	2.56	2.25	2.07	2.10
19	70.0	25.0	4.0	0.0	1.0	38.9	36.4	1.68	1.62	3.27	3.02
20	69.0	25.0	5.0	0.0	1.0	40.9	37.0	1.70	1.68	3.44	3.03

Note; **duplicate experiments

7.3.5 Characterizations

Color measurements. A Hunterlab Color Standard (Hunter Associates Laboratory, Inc., Virginia, USA) was used to measure color changes of the rPP/RWF composite samples before and after weathering according to CIE $L^*a^*b^*$ color system. L^* represents the lightness, whereas a^* and b^* are the chromaticity

coordinates. Higher L^* value means an increased lightness. The a^* coordinate represents the red-green hue while b^* coordinate represents the yellow-blue hue. Three replications of each formulation and aging time were measured, and each specimen was measured at three locations. The total color changes or discolorations (ΔE) of the un-weathered and weathered rPP/RWF composite specimens were quantitated in equation 6.1.

Hardness. Hardness measurements of the samples exposed were performed according to ASTM D2240-91 specification, using two Durometers (Shore D scales) for the plastic composites. The dimensions of the specimens tested were approximately 16 mm × 16 mm × 6.5 mm. The measurements were performed at room temperature (25 °C).

Flexure testing. Before testing, the specimens were dried in an oven at 50 °C for 24 h. Three-point flexural test was carried out on an Instron Universal Testing Machine (Model 5582 from Instron Corporation, Massachusetts, USA) at a cross-head speed of 2 mm/min, with nominal dimensions of 4.8 mm × 13 mm × 100 mm, and a span of 80 mm in accordance with ASTM D790-92. The testing was performed at ambient room temperature of 25 °C with five specimens of each formulation and age to obtain an average value. The flexural properties were measured before and after outdoor exposure for 60 and 360 days. The maximum stress, modulus of elasticity, and maximum strain at maximum stress were calculated according to the above-mentioned standard.

Morphological analysis. Prior to imaging with a scanning electron microscope (SEM), all samples were dried in an oven at 50 °C for 24 h and were sputter-coated with gold to prevent electrical charging during the imaging. Morphological studies were carried out to assess the formation of surface cracks. SEM imaging with FEI Quanta 400 microscope (FEI Company, Oregon, USA) used an accelerating voltage of 20 kV. All specimens were imaged perpendicular to the surface with 100× magnification.

7.4 Results and discussion

The D-optimal mixture design of experiments, with five fractions as (mutually dependent) variables (that sum to one), had 20 runs in a randomized order. The twelve determined responses were the values of lightness, discoloration, hardness, flexural strength and modulus, and maximum strain, after weathering for 60 and 360 days. The results are summarized in Tables 7.1 and 7.2.

7.4.1 Statistical analysis of the response models

Analysis of variance (ANOVA) of the alternative types of response models revealed that all the responses after weathering for 60 and 360 days were best fit with linear model, instead of quadratic, special cubic, or cubic models, except for lightness and maximum strain at 60 days that were best fit with quadratic model. The MOE at 60 days is shown as an example in Table 7.3. The sequential model sums of squares for linear model are significant ($p<0.05$), but not for the other model types. Moreover, the lack of fit is clearly insignificant for the linear model, suggesting this model performs well. It also has high adjusted coefficient of determination (adj-R^2 = 0.9500) and the highest predicted coefficient of determination (pred-R^2 = 0.9329), further indicating good fit.

Table 7.3 Fitted model summary for MOE at 60 days

Source	Sequential p-value	Lack of fit p-value	Adj-R^2	Pred-R^2	
Linear	<0.0001*	0.8141	0.9500	0.9329	Suggested
Quadratic	0.2785	0.9653	0.9576	0.9166	
Special cubic	0.9027	0.9528	0.9392	0.9015	
Cubic	0.9528	-	0.9271	-	Aliased

*P-value less than 0.05 is considered significant.

The detailed ANOVAs in Tables 7.4 and 7.5 document the significant linear or quadratic terms in models for each response, in terms of their p-values. The ANOVA shows statistical significance ($p<0.05$) of these terms supplementing linear

models of the fractions, namely of rPP, RWF, MAPP, and UV stabilizer. For quadratic terms, modeled responses had significant interactions, for example, between rPP and MAPP, RWF and MAPP for lightness at 60 days and between rPP and RWF for maximum strain at 60 days. In addition, the ANOVA also showed that lack of fit was not significant for any of the response surface models at 95% confidence level. This suggests the regression models fit the data well.

Table 7.4 Analysis of variance and model adequacy of L^*, ΔE and hardness responses

	L^*		ΔE		Hardness	
Source	D60***	D360****	D60***	D360****	D60***	D360****
Model	<0.0001**	<0.0001**	0.0006**	0.0001**	0.0001**	<0.0001**
Linear Mixture	<0.0001**	<0.0001**	0.0006**	0.0001**	0.0001**	<0.0001**
x_1x_2	0.1193	-	-	-	-	-
x_1x_3	0.0384**	-	-	-	-	-
x_1x_4	0.5343	-	-	-	-	-
x_2x_3	0.0420**	-	-	-	-	-
x_2x_4	0.5950	-	-	-	-	-
x_3x_4	0.8741	-	-	-	-	-
Lack of Fit	0.0869	0.2708	0.0961	0.0919	0.1032	0.8639
R^2	0.9447	0.7247	0.6531	0.7103	0.7114	0.8821
Adj-R^2	0.8949	0.6730	0.5881	0.6560	0.6572	0.8599
Pred-R^2	0.6485	0.5484	0.5123	0.5837	0.5918	0.8134
C.V. %	1.80	1.84	7.64	6.57	0.85	0.70

P-value less than 0.05 is considered significant. D60* exposed for 60 days and D360**** exposed for 360 days.

Coefficients of determination (R^2), adj-R^2, pred-R^2, and coefficient of variation (C.V.) are also included in Tables 7.4 and 7.5. The R^2 values of the twelve response fits are in the range from 0.6531 to 0.9749. The R^2 values of discoloration (0.6531) and maximum strain at 60 days (0.9749) indicate that only 34.69% and 2.51%, respectively, of the total variability in observations are not explained by the models; R^2 value close to 1 indicates good fits [28]. Likewise, the adj-R^2 values in the range from 0.5881 to 0.9523 suggest good fits; and the same goes for pred-R^2 values. The pred-R^2 value of MOE at 60 days was 0.9329 meaning that the fitted model

would explain about 93.29% of the variability in new data. The coefficients of variation of all response fits based on the replications of experiments show low values in the range from 0.70 to 7.64%. The low C.V. values indicate that the determinations of material characteristics had a good precision, and can serve the fitting of parametric models. Basically, the coefficient of variation was used to measure the residual variation in the data [20].

Table 7.5 Analysis of variance and model adequacy for flexural properties

	MOR		MOE		Max. strain	
Source	D60***	D360****	D60***	D360****	D60***	D360****
Model	0.0001**	<0.0001**	<0.0001**	<0.0001**	<0.0001**	<0.0001**
Linear Mixture	0.0001**	<0.0001**	<0.0001**	<0.0001**	<0.0001**	<0.0001**
x_1x_2	-	-	-	-	0.0373**	-
x_1x_3	-	-	-	-	0.8442	-
x_1x_4	-	-	-	-	0.0891	-
x_2x_3	-	-	-	-	0.9162	-
x_2x_4	-	-	-	-	0.0959	-
x_3x_4	-	-	-	-	0.0597	-
Lack of Fit	0.6342	0.7996	0.8141	0.8964	0.0720	0.7885
R^2	0.7135	0.7435	0.9579	0.8872	0.9749	0.8132
Adj-R^2	0.6598	0.6954	0.9500	0.8661	0.9523	0.7781
Pred-R^2	0.5549	0.6087	0.9329	0.8230	0.8397	0.6932
C.V. %	4.10	3.34	3.34	4.45	3.70	7.34

P-value less than 0.05 is considered significant. D60* exposed for 60 days and D360**** exposed for 360 days.

7.4.2 Model adequacy checking

Model adequacy checking is always necessary with a fitted model [29]. Figure 7.1(a) displays normal probability plots of the residuals for MOE after weathering for 60 days (MOE D60). The good linear fit in this plot indicates that the residuals (approximation errors remaining in the model) are close to normally distributed. Normally distributed residuals are a requirement for validity of least squares regression, and this condition is satisfied. Likewise, there is no indication of possible outliers, such as faulty experiment cases with particularly large residuals [20]. The plot of residuals vs. predicted values in Figure 7.1(b) exhibits no obvious

patterns that would suggest adding a term to the model, to account for that pattern. If the residuals had such structure, the model would not be appropriate [20]. Figure 7.1(c) shows model predictions vs. observations. The model outputs fit the actual observations quite well, with MOE D60 model deviating from actual by less than about 10%. These adequacy checks of the MOE D60 response model indicate a good fit to data. Similar checking for the other modeled responses showed qualitatively similar normal probability plots, residuals vs. predicted values, and predicted values vs. actual data. This type of checking cannot guarantee predictive capability, but suggests the models are sound approximations for interpolating within the experimental range.

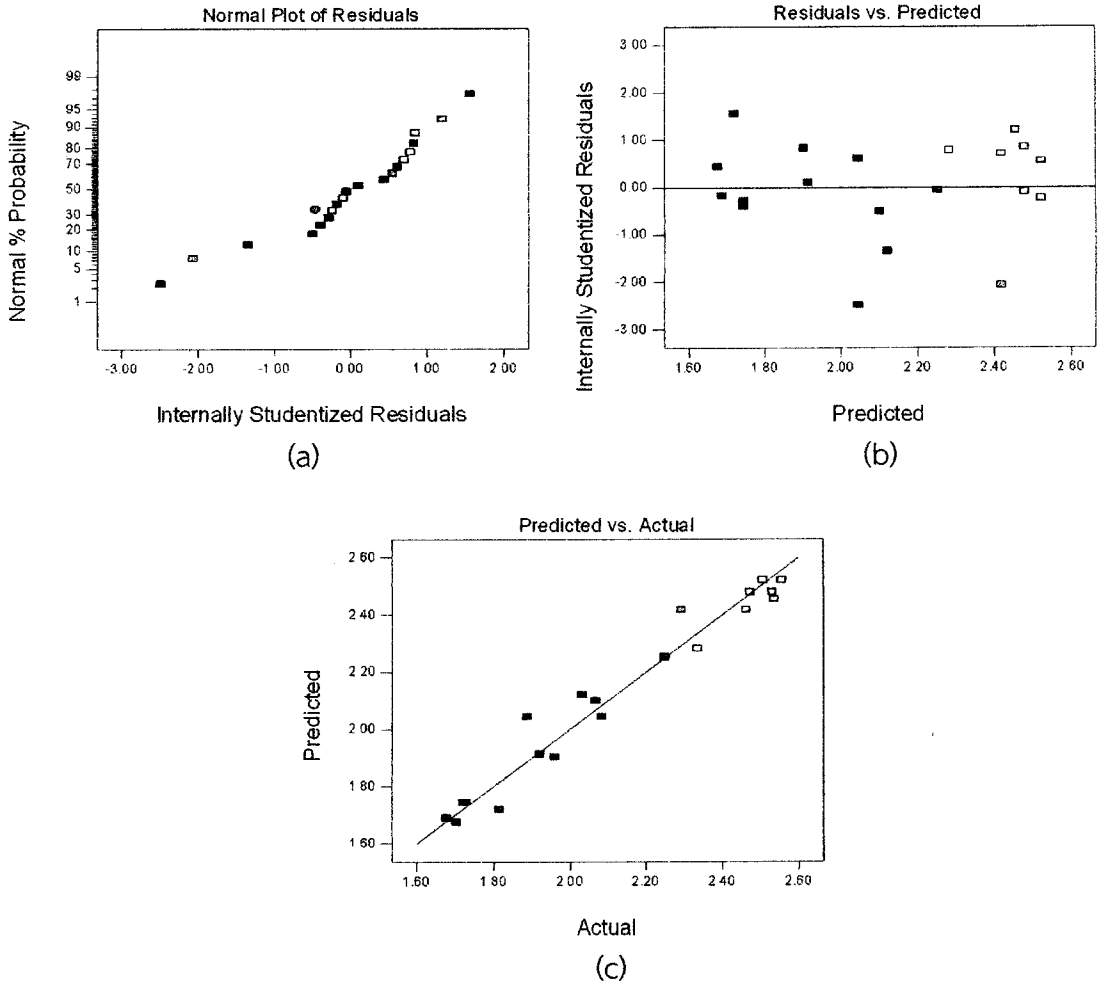

Figure 7.1 Model adequacy checking for MOE after exposing 60 days; (a) normal probability plot of residuals, (b) plot of residuals versus predicted values, and (c) plot of predicted versus actual values

7.4.3 Effect of composition on the lightness and optimal formulation

The regression fits for the lightness (L^*) after weathering for 60 and 360 days were:

$$L^* \text{ D60} = 70.79x_1 + 76.16x_2 - 793.51x_3 + 1053.12x_4 + 6.91x_1x_2 + 982.79x_1x_3 - 1158.85x_1x_4 + 957.41x_2x_3 - 989.52x_2x_4 - 268.09x_3x_4 \quad (7.1)$$

$$L^* \text{ D360} = 70.49x_1 + 75.45x_2 + 68.00x_3 + 37.33x_4 \quad (7.2)$$

The coefficients for fractions of rPP (x_1), RWF (x_2), and UV stabilizer (x_4) are positive. RWF has larger coefficients than rPP due to high photobleaching of the wood components, particularly lignin [30]. The covered experimental regions of L^* D60 and L^* D360 are shown in Figures 7.2(a) and 7.2(b), respectively. In these triangular plots the three pure components (rPP, RWF, and MAPP) are represented by the corners, while the additive levels were fixed (UV stabilizer at 0.5 wt% and Lub at 1 wt%). The contours in the colored areas, that include the experimental observations, present the L^* D60 and L^* D360 regression fits varying from 70 to 78 and 71 to 75, respectively. The lightness evidently increases with RWF content. With increased RWF fraction in the composites, more wood flour was exposed at the sample surface where complete encapsulation by the matrix was less likely [31]. Likewise, the rPP/RWF composites weathered for 60 days were lighter colored after 360 days. This is because the color change of the composites occurred in three stages. The composites quickly lightened after weathering for 60 days and then darkened. Lastly, they again got lighter with further exposure. In addition, high fractions of MAPP at 3-5 wt% gave high lightness. This may be caused by weakened interfacial adhesion at high MAPP contents. The photodegradation of wood components on the surface of the composites was accelerated by weak adhesion between the wood flour and plastic matrix [13, 16]. Furthermore, adding 1 wt% UV stabilizer decreased the lightness of the rPP/RWF composites. This may be attributed to UV stabilizer (HALS) preventing photodegradation of polymer [14]. Figure 7.3 displays the numerically optimized composition, based on these model fits. Since two models are optimized simultaneously, the software actually uses a single surrogate called "desirability" to

balance them. The model-based optimal formulation is shown in Table 7.6, with minimum lightness found for 70.0 wt% rPP, 25.0 wt% RWF, 3.0 wt% MAPP, 1.0 wt% UV stabilizer, and 1 wt% Lub, with a high desirability score of 0.908.

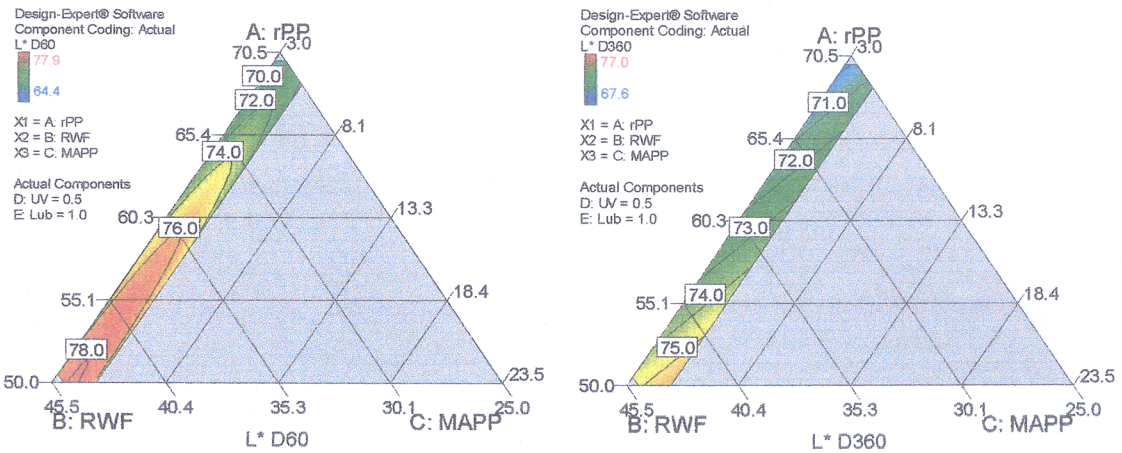

(a) (b)

Figure 7.2 Triangular contour plots for effects of the compositions on lightness at (a) 60 and (b) 360 days, with UV stabilizer fixed at 0.5 wt% and Lub at 1 wt%

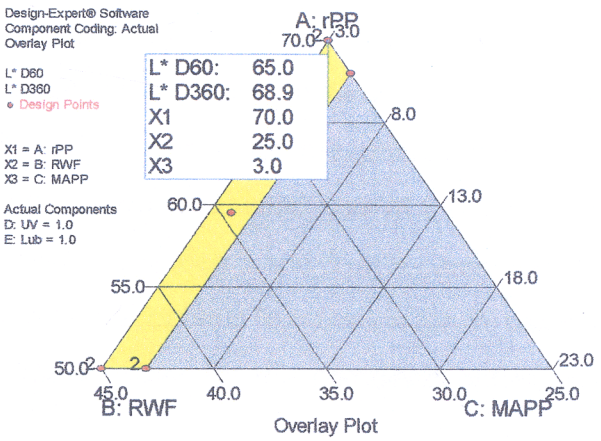

Figure 7.3 The optimal formulation for lightness

Table 7.6 Predicted optimal formulations and their responses from multiobjective optimizations. For example, the formulation in first row is optimal for a desirability score that balances L^* at 60 and 360 days

	Mixture component fraction (wt%)					Predicted response		
Property	x_1	x_2	x_3	x_4	x_5	D60	D360	Desirability
L^*	70.0	25.0	3.0	1.0	1.0	65.0	68.9	0.908
ΔE	69.8	25.0	3.2	1.0	1.0	35.3	34.0	0.809
Hardness (shore D)	50.0	45.0	3.0	1.0	1.0	75.1	72.5	0.853
MOR (MPa)	51.9	43.4	3.4	0.2	1.0	43.0	37.9	0.713
MOE (GPa)	50.0	45.0	3.0	1.0	1.0	2.52	2.12	0.892
Max. strain (%)	69.0	25.0	4.9	0.1	1.0	3.23	3.09	0.931

7.4.4 Effect of composition on the discoloration and optimal formulation

The linear regression models for discoloration (ΔE) after weathering for 60 and 360 days were:

$$\Delta E \text{ D60} = 34.68x_1 + 45.29x_2 + 50.19x_3 + 44.67x_4 \quad (7.3)$$

$$\Delta E \text{ D360} = 33.67x_1 + 43.66x_2 + 44.73x_3 + 39.09x_4 \quad (7.4)$$

The coefficients decreased with exposure time, indicating reduced discoloration. Figure 7.4 shows that ΔE at 360 days (in range of 36 to 42) increased for high fractions of wood flour. The reason for this phenomenon is probably similar as described earlier, namely exposure of wood flour at the sample surface [31]. Besides, the choice of MAPP content between 3 and 5 wt% barely affected the discoloration of composites at 360 days. The optimal formulation for ΔE based on these numerical models, and the desirability score for this combined optimization, are included in Table 7.6.

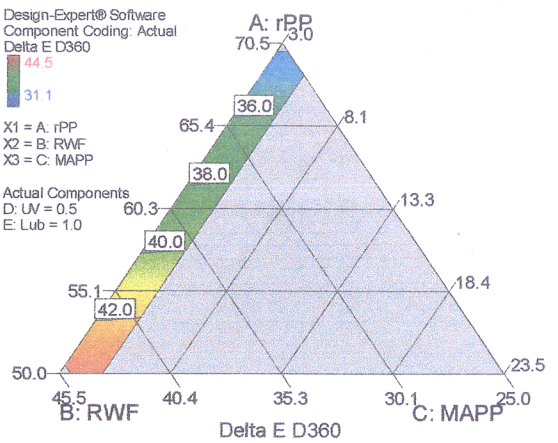

Figure 7.4 Triangular contour plots for effects of composition on ΔE at 360 days, with UV stabilizer fixed at 0.5 wt% and Lub at 1 wt%

7.4.5 Effect of composition on the hardness and optimal formulation

The linear regression fits for hardness after 60 and 360 days exposure were:

$$\text{Hardness D60} = 72.37x_1 + 74.74x_2 + 74.30x_3 + 81.46x_4 \quad (7.5)$$

$$\text{Hardness D360} = 68.87x_1 + 72.03x_2 + 68.38x_3 + 82.51x_4 \quad (7.6)$$

The coefficients of rPP (x_1), RWF (x_2), and MAPP (x_3) decrease with increasing exposure time from 60 to 360 days. This is because of polymer chain scission, which results in surface cracks as well as facilitates the removal of degraded wood component through the cracks [16], and the chain scissions accumulated over the exposure time [15]. The UV stabilizer fraction has the largest positive coefficients in the model fits, so it should be maximized. UV stabilizer as free radical scavenger prevents photodegradation in plastics [14]. Figure 7.5 shows that hardness at 360 days (in range of 70 to 72 shore D) increases with rubberwood flour fraction. This is because rubberwood filler has considerably higher hardness than weak polymer matrix [32-34], so flexibility was reduced by increase of RWF content, resulting in more rigid composites [34-36]. The addition of MAPP from 3 to 5 wt% affected the hardness of the composites, so that hardness increased with MAPP fraction. The wood flour was

better dispersed in the plastic matrix, with minimum voids [33, 35, 36]. The optimal formulation for hardness, based on the numerical models, is also shown in Table 7.6.

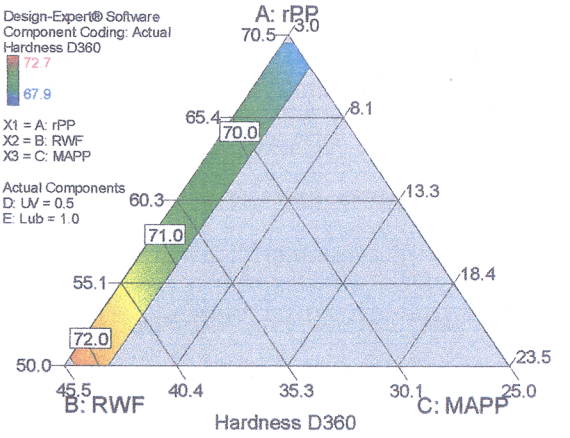

Figure 7.5 Triangular contour plots for effects of composition on hardness at 360 days, with UV stabilizer fixed at 0.5 wt% and Lub at 1 wt%

7.4.6 Effect of composition on the flexural strength and optimal formulation

The linear regression models fitted for flexural strength (MOR) at 60 and 360 days were:

$$\text{MOR D60} = 41.54x_1 + 44.64x_2 + 25.13x_3 - 51.72x_4 \quad (7.7)$$

$$\text{MOR D360} = 36.96x_1 + 38.92x_2 + 35.59x_3 - 45.41x_4 \quad (7.8)$$

The fraction of RWF (x_2) has the largest positive coefficients in the fits, so the flexural strength increases with fraction of RWF. In contrast, MOR decreases with the fraction of UV stabilizer (x_4) that has a negative coefficient, so UV stabilizer fraction should be minimized. This is probably due to non-homogeneous spatial distribution of wood flour, polymer, and UV stabilizer [37]. Figures 7.6(a) and 7.6(b) display the covered experimental regions of MOR after exposure for 60 and 360 days, respectively. The contours in the colored areas present the MOR at 60 and 360 days varying from 38 to 42 MPa and 35 to 36.5 MPa, respectively. MOR at 60 days clearly increases with RWF content. This is due to the reinforcing effect of the wood flour in continuous plastic matrix [38], whereas MOR at 360 days increases only insignificantly with RWF

content. This reveals that loss of MOR increased with RWF content, with the longer exposure. When WPCs were exposed to water, the swelling of wood flour caused microcracks in the matrix, and thus the efficiency of stress transfer from wood flour to plastic matrix decreased [30, 39]. In addition, MOR of the composites clearly reduced with exposure time due to increased polymer chain scission and cracking in WPCs. These results can be substantiated by the SEM micrographs in Figure 7.7 [Figures 7.7(a), 7.7(b) for 25 wt% RWF and 7.7(c), 7.7(d) for 45 wt% RWF]. The composites with 25 wt% RWF [Figure 7.7(a)] have less RWF on the surface than the composites with 45 wt% RWF [Figure 7.7(c)], in agreement with prior work [31]. Furthermore, the rPP/RWF composites exposed for 360 days [Figure 7.7(b), (d)] show large surface cracking due to polymer chain scission, which results from cycles of wetting and drying [5]. The composites with 25 wt% RWF [Figure 7.7(b)] obviously display less surface cracking than the composites with 45 wt% RWF [Figures 7.7(d)]. When WPCs were exposed to water, the swelling increased with RWF content, and led to increased cracking [30]. The optimal composition based on the linear regression models is shown numerically in Table 7.6.

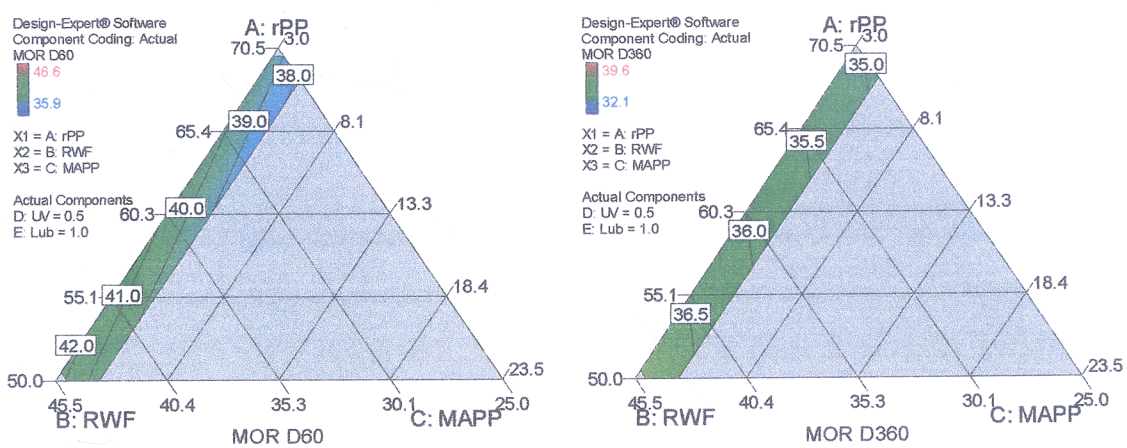

(a) (b)

Figure 7.6 Triangular contour plots for effects of composition on MOR at (a) 60 and (b) 360 days, with UV stabilizer fixed at 0.5 wt% and Lub at 1 wt%

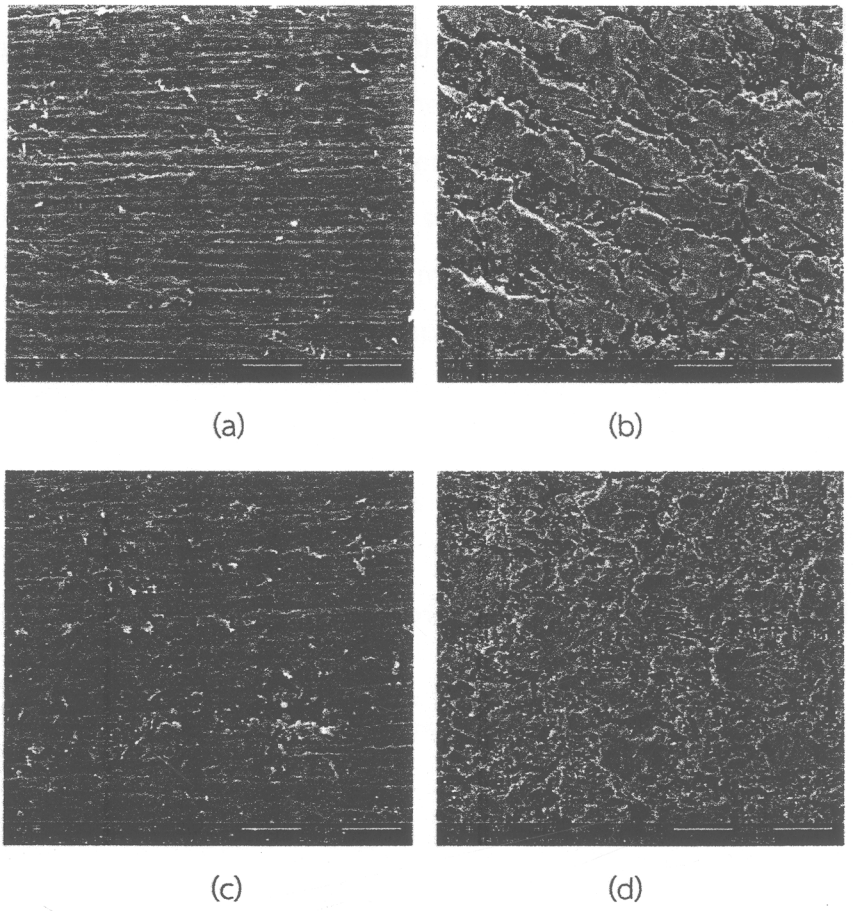

Figure 7.7 SEM (100×) images of WPC surfaces before (left column) and after exposure for 360 days (right column): rPP composites with 25 wt% RWF (a and b) and with 45 wt% RWF (c and d)

7.4.7 Effect of composition on the flexural modulus and optimal Formulation

The linear regression models fitted for the flexural modulus (MOE) at 60 and 360 days were:

$$\text{MOE D60} = 1.70x_1 + 2.52x_2 + 1.43x_3 + 2.61x_4 \quad (7.9)$$

$$\text{MOE D360} = 1.54x_1 + 2.11x_2 + 2.10x_3 + 2.21x_4 \quad (7.10)$$

By these equations, all the component fractions, namely of rPP (x_1), RWF (x_2), MAPP (x_3), and UV stabilizer (x_4), increase the MOE after weathering for 60 and 360 days; all terms containing these variables have positive coefficients. The UV stabilizer fraction

has the largest coefficient in each fit. Furthermore, the coefficients of rPP, RWF, and UV stabilizer decrease with exposure time. The swelling of wood cell walls when penetrated by water facilitates light penetration, and contributes to failure of mechanical properties [30, 40]. The UV stabilizer could not protect against water absorption, which may have contributed more to degradation than UV exposure [6]; the UV photodegradation may mostly impact the surfaces [6]. In addition, RWF has higher coefficients than rPP. This implies that RWF contributes more to MOE than rPP, because wood flour is stiffer than the neat plastic [41]. The composition optimized based on these linear regression models is shown numerically in Table 7.6.

7.4.8 Effect of composition on the maximum strain and optimal formulation

The regression fits for the maximum strain after exposures for 60 and 360 days were:

$$\text{Maximum strain D60} = 3.31x_1 + 2.30x_2 - 2.02x_3 + 222.05x_4 + 0.69x_1x_2 + 5.90x_1x_3 - 240.37x_1x_4 + 3.14x_2x_3 - 234.86x_2x_4 - 248.36x_3x_4 \quad (7.11)$$

$$\text{Maximum strain D360} = 3.16x_1 + 2.36x_2 + 2.69x_3 - 5.36x_4 \quad (7.12)$$

The fraction of rPP (x_1) has larger positive coefficients than RWF (x_2) in the fit, so the maximum strain increases with high fraction of rPP. Besides, increasing exposure time reduced the coefficient of rPP because it became more brittle with weathering [6], whereas the coefficient of RWF grew with exposure time. The wood flour absorbed water during exposure, and this led to softening of the WPCs [6]. The optimal formulation based on these numerical models, combined by a desirability score for optimization, is also included in Table 7.6.

7.4.9 Optimal overall resistance to natural weathering

An optimal formulation for rPP/RWF composites was determined to minimize lightness and discoloration, and maximize hardness, flexural strength and modulus, and maximum strain. This multiobjective optimization, using all of the

regression models, was performed with the Design-Expert software by constructing a desirability score that balances all of the fitted models. The plot in Figure 7.8 shows the formulation that was optimal, along with contours of the desirability score. The optimal formulation was 61.9 wt% rPP, 33.9 wt% RWF, 3.1 wt% MAPP, 0.2 wt% UV stabilizer, and 1.0 wt% Lub. The optimal formulation is given in Table 7.7, along with the model based responses.

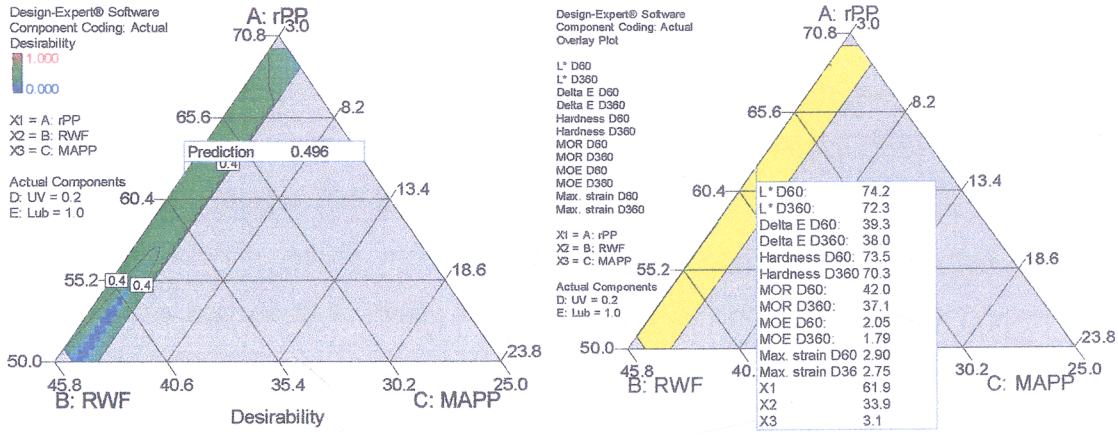

Figure 7.8 The optimal formulation for overall desirability

Table 7.7 Predicted responses with the formulation optimized jointly for all properties

	Mixture component fractions (wt%)					Predicted response	
Property	x_1	x_2	x_3	x_4	x_5	D60	D360
L^*	61.9	33.9	3.1	0.2	1.0	74.2	72.3
ΔE						39.3	38.0
Hardness (shore D)						73.5	70.3
MOR (MPa)						42.0	37.1
MOE (GPa)						2.05	1.79
Max. strain (%)						2.90	2.75

7.5 Conclusions

Mixture experimental design, statistical modeling, and response surface methodology were used to determine the influences of rPP/RWF composite

formulation, and to optimize the formulation for weathering resistance. Analysis of variance revealed that all the component fractions experimentally varied, namely of rPP, RWF, MAPP, and UV stabilizer, significantly affected the lightness, discoloration, hardness, flexural strength and modulus, and maximum strain. In general, a high fraction of RWF increased L^* and ΔE across exposure times. The lignin in wood flour contributes to the L^* and ΔE. When the composites were exposed to the natural weathering for 60 and 360 days, high fractions of RWF increased hardness, MOR, and MOE but reduced maximum strain. However, hardness, MOR, and MOE clearly degraded with exposure time. At the longer exposure time, the wetting and drying cycles caused microcracks in the matrix, and thus the efficiency of stress between wood flour and plastic matrix decreased [30, 39]. The MAPP slightly affected L^*, hardness, and MOR, which increasesd with MAPP content. The fraction of UV stabilizer also had positive effects on the L^* and ΔE, due to it (HALS) preventing photodegradation of polymer [14]. In addition, SEM micrographs of the composites exposed for 360 days show larger surface cracking than in unexposed composites. High fractions of RWF increased the surfaces cracking on the WPCs. This study demonstrated design and analysis of mixture experiments as an efficient tool to optimize the formulation of rPP/RWF composites, for minimum color changes and for maximum hardness and flexural properties.

7.6 References

[1] R. Selden, B. Nystrom, and R. Langstrom. "UV Aging of Poly(Propylene)/ Wood-Fiber Composites." *Polymer Composites*, vol. 25, pp. 543–553, 2004.

[2] S. Tamrakar, R.A. Lopez-Anido, A. Kiziltas, and D.J. Gardner. "Time and Temperature Dependent Response of a Wood-Polypropylene Composite." *Composites Part A: Applied Science and Manufacturing*, vol. 42, pp. 834–842, 2011.

[3] D.R. Carroll, R.B. Stone, A.M. Sirignano, R.M. Saindon, S.C. Gose, and M.A. Friedman. "Structural Properties of Recycled Plastic/Sawdust Lumber Decking Planks." *Resources, Conservation and Recycling*, vol. 31, pp. 241–251, 2011.

[4] I. Ganguly and I.L. Eastin. "Trends in the US Decking Market: A National Survey of Deck and Home Builders." *The Forestry Chronicle*, vol. 85, pp. 82–90, 2009.

[5] J.S. Fabiyi, A.G. McDonald, M.P. Wolcott, and P.R. Griffiths. "Wood Plastic Composites Weathering: Visual Appearance and Chemical Changes." *Polymer Degradation and Stability*, vol. 93, pp. 1405–1414, 2008.

[6] K. Chaochanchaikul and N. Sombatsompop. "Stabilizations of Molecular Structures and Mechanical Properties of PVC and Wood/PVC Composites by Tinuvin and TiO_2 Stabilizers." *Polymer Engineering & Science*, vol. 51, pp. 1354–1365, 2011.

[7] L.M. Matuana, D.P. Kamdem, and J. Zhang. "Photoaging and Stabilization of Rigid PVC/Wood-Fiber Composites." *Journal of Applied Polymer Science*, vol. 80, pp. 1943–1950, 2001.

[8] J.M. Pilarski and L.M. Matuana. "Durability of Wood Flour-Plastic Composites Exposed to Accelerated Freeze–Thaw Cycling. Part I. Rigid PVC Matrix." *Journal of Vinyl and Additive Technology*, vol. 11, pp. 1–8, 2005.

[9] L.M. Matuana and D.P. Kamdem. "Accelerated Ultraviolet Weathering of PVC/Wood-Flour Composites." *Polymer Engineering and Science*, vol. 42, pp. 1657–1666, 2002.

[10] M. Mankowski and J.J. Morrell. "Patterns of Fungal Attack in Wood Plastic Composites Following Exposure in a Soil Block Test." *Wood and Fiber Science*, vol. 32, pp. 340–345, 2000.

[11] K. Chaochanchaikul, V. Rosarpitak, and N. Sombatsompop. "Photodegradation Profiles of PVC Compound and Wood/PVC Composites under UV Weathering." *Express Polymer Letters*, vol. 7, pp. 146–160, 2013.

[12] N.M. Stark. "Effect of Weathering Cycle and Manufacturing Method on Performance of Wood Flour and High-Density Polyethylene Composites." *Journal of Applied Polymer Science*, vol. 100, pp. 3131–3140, 2006.

[13] N.M. Stark and L.M. Matuana. "Surface Chemistry and Mechanical Property Changes of Wood-Flour/High-Density-Polyethylene Composites after Accelerated Weathering." *Journal of Applied Polymer Science*, vol. 94, pp. 2263–2273, 2004.

[14] M. Muasher and M. Sain. "The Efficacy of Photostabilizers on the Color Change of Wood Filled Plastic Composites." *Polymer Degradation and Stability*, vol. 91, pp. 1156–1165, 2006.

[15] H. Du, W. Wang, Q. Wang, Z. Zhang, S. Sui, and Y. Zhang. "Effects of Pigments on the UV Degradation of Wood-Flour/HDPE Composites." *Journal of Applied Polymer Science*, vol. 118, pp. 1068–1076, 2010.

[16] L.M. Matuana, S. Jin, and N.M. Stark. "Ultraviolet Weathering of HDPE/Wood-Flour Composites Coextruded with a Clear HDPE Cap Layer." *Polymer Degradation and Stability*, vol. 96, pp. 97–106, 2011.

[17] S.K. Najafi and K.R. Englund. "Effect of Highly Degraded High-Density Polyethylene (HDPE) on Processing and Mechanical Properties of Wood Flour-HDPE Composites." *Journal of Applied Polymer Science*, vol. 129, pp. 3404–3410, 2013.

[18] S. Butylina, M. Hyvärinen, and T. Kärki. "A Study of Surface Changes of Wood-Polypropylene Composites as the Result of Exterior Weathering." *Polymer Degradation and Stability*, vol. 97, pp. 337-345, 2012.

[19] T. Martinello, T.M. Kaneko, M.V.R. Velasco, M.E.S. Taqueda, and V.O. Consiglieri. "Optimization of Poorly Compactable Drug Tablets Manufactured by Direct Compression Using the Mixture Experimental Design." *International Journal of Pharmaceutics*, vol. 322, pp. 87-95, 2006.

[20] D.C. Montgomery. *Design and Analysis of Experiments*. John Wiley & Sons, Inc., 2009.

[21] Y.B. Khosrowshahi and A. Salem. "Influence of Polyvinyl Alcohol and Carboxymethyl Cellulose on the Reliability of Extruded Ceramic Body: Application of Mixture Design Method in Fabricating Reliable Ceramic Raschig Rings." *International Journal of Applied Ceramic Technology*, vol. 8, pp. 1334–1343, 2011.

[22] R.C.S. John. "Experiments with Mixtures, Ill-Conditioning, and Ridge Regression." *Journal of Quality Technology*, vol. 16, pp. 81–96, 1984.

[23] A. Mannarswamy, S.H. Munson-McGee, and P.K. Andersen. "D-optimal Designs for the Cross Viscosity Model Applied to Guar Gum Mixtures." *Journal of Food Engineering*, vol. 97, pp. 403–409, 2010.

[24] N.M. Stark and L.M. Matuana. "Ultraviolet Weathering of Photostabilized Wood-Flour-Filled High-Density Polyethylene Composites." *Journal of Applied Polymer Science*, vol. 90, pp. 2609–2617, 2003.

[25] L.M. Matuana and F. Mengeloglu. "Manufacture of Rigid PVC/Wood-Flour Composite Foams Using Moisture Contained in Wood as Foaming Agent." *Journal of Vinyl and Additive Technology*, vol. 8, pp. 264-270, 2002.

[26] Z. Jun, W. Xiang-Ming, C. Jian-Min, and Z. Kai. "Optimization of Processing Variables in Wood–Rubber Composite Panel Manufacturing Technology." *Bioresource Technology*, vol. 99, pp. 2384–2391, 2008.

[27] P. Petchpradab, T. Yoshida, T. Charinpanitkul, and Y. Matsumura. "Hydrothermal Pretreatment of Rubber Wood for the Saccharification Process." *Industrial and Engineering Chemistry Research*, vol. 48, pp. 4587–4591, 2009.

[28] M. Amini, H. Younesi, N. Bahramifar, A.A.Z. Lorestani, F. Ghorbani, A. Daneshi, and M. Sharifzadeh. "Application of Response Surface Methodology for Optimization of Lead Biosorption in an Aqueous Solution by Aspergillus Niger." *Journal of Hazardous Materials*, vol. 154, pp. 694-702, 2008.

[29] R.H. Myers, D.C. Montgomery, and C.M. Anderson-Cook. *Response Surface Methodology: Process and Product Optimization Using Designed Experiments*. John Wiley & Sons, Inc., Hoboken, New Jersey, 2009.

[30] N.M. Stark and L.M. Matuana. "Influence of Photostabilizers on Wood Flour-HDPE Composites Exposed to Xenon-Arc Radiation with and without Water Spray." *Polymer Degradation and Stability*, vol. 91, pp. 3048–3056, 2006.

[31] K.B. Adhikary. "Development of Wood Flour-Recycled Polymer Composite Panels as Building Materials." Ph.D. dissertation, University of Canterbury, New Zealand, 2008.

[32] B. Kord. "Effect of Wood Flour Content on the Hardness and Water Uptake of Thermoplastic Polymer Composites." *World Applied Sciences Journal*, vol. 12, pp. 1632-1634, 2011.

[33] C. Homkhiew, T. Ratanawilai, and W. Thongruang. "Composites from Recycled Polypropylene and Rubberwood Flour: Effects of Composition on Mechanical Properties." *Journal of Thermoplastic Composite Materials*, Epub ahead of print 14 February 2013.DOI: 10.1177/0892705712475019.

[34] C. Homkhiew, T. Ratanawilai, and W. Thongruang. "Optimal Formulation of Recycled Polypropylene/Rubberwood Flour Composites on Hardness Property." *Applied Mechanics and Materials*, vol. 368-370, pp. 785-790, 2013.

[35] M.R. Rahman, M.M. Huque, M.N. Islam, and M. Hasan. "Improvement of Physico-Mechanical Properties of Jute Fiber Reinforced Polypropylene Composites by Post-Treatment." *Composites Part A: Applied Science and Manufacturing*, vol. 39, pp. 1739–1747, 2008.

[36] M.R. Rahman, M.M. Huque, M.N. Islam, and M. Hasan. "Mechanical Properties of Polypropylene Composites Reinforced with Chemically Treated Abaca." *Composites Part A: Applied Science and Manufacturing*, vol. 40, pp. 511–517, 2009.

[37] A. Wechsler and S. Hiziroglu. "Some of the Properties of Wood–Plastic Composites." *Building and Environment*, vol. 42, pp. 2637–2644, 2007.

[38] S. Mohanty, S.K. Verma, S.K. Nayak, and S.S. Tripathy. "Influence of Fiber Treatment on the Performance of Sisal–Polypropylene Composites." *Journal of Applied Polymer Science*, vol. 94, pp. 1336–1345, 2004.

[39] Z.M. Zhang, H. Du, W. Hong, and Q.W. Wang. "Property Changes of Wood-Fiber/HDPE Composites Colored by Iron Oxide Pigments after Accelerated UV Weathering." *Journal of Forestry Research*, vol. 21, pp. 59–62, 2010.

[40] D. Hon. *Wood and Cellulose Chemistry*. New York, Marcel Dekker, 2001.

[41] M. Garcia, J. Hidalgo, I. Garmendia, and J. Garcia-Jaca. "Wood–Plastics Composites with Better Fire Retardancy and Durability Performance." *Composites Part A: Applied Science and Manufacturing*, vol. 40, pp. 1772-1776, 2009.

CHAPTER 8

Minimizing the Creep of Recycled Polypropylene/Rubberwood Flour Composites with Mixture Design Experiments

8.1 Chapter summary

Composites of rubberwood flour (RWF) and recycled polypropylene (rPP) were produced into panel samples by using a twin-screw extruder. The effects of mixture ratios, including rPP, RWF, maleic anhydride-grafted polypropylene (MAPP), and ultraviolet (UV) stabilizer, on creep behavior were studied in a D-optimal mixture design. Creep was significantly affected by the composition. Increasing the fraction of RWF decreased creep, but the increasing additions of MAPP and UV stabilizer increased creep. The models fitted were used to optimize a desirability score that balanced multiple creep characteristics. The model-based optimal formulation 50.5 wt% rPP, 44.9 wt% RWF, 3.5 wt% MAPP, 0.1 wt% UV stabilizer, and 1.0 wt% lubricant, was experimentally validated to have low creep closely matching the model predictions. In addition, virgin polypropylene gave lower creep strain than recycled polypropylene, both in composites and as unfilled plastic. Four-element Burger model offered a good fitting on the creep behavior of each composite formulation.

8.2 Introduction

Wood-plastic composites (WPCs) have been extensively developed and used in non-structural applications [1]. For example, WPCs are increasingly used to replace softwood lumber in deck-building, to improve durability [2, 3]. The advantages of WPCs include high specific strength and stiffness, resistance to water absorption, and positive impact on environmental issues. These have stimulated the development of WPC materials for structural applications [1, 4, 5]. However, these composites are poorly suited for some applications due to long-term creep under

loading. This study aims to evaluate and improve the creep characteristics of specific WPCs.

Raw materials were focused on waste that is locally available in southern Thailand. This gives both environmental benefits, and low-cost raw materials. Rubberwood (*Hevea brasiliensis*) waste is mainly produced by sawmills and furniture industry, both prevalent in southern Thailand. Of their total wood intake, these industries generally generate about 34% wood wastes and about 54% rejects of plantation wastes, while only 12% of the rubberwood ends up in the products [6]. Most of the wood waste can be used in medium-density fiberboard and particleboard [7]. However, the use of wood waste as reinforcement in plastic composites is great interest, with environmental and economic benefits. The advantages of wood particles include biodegradability, low health hazard during handling, and non-abrasive nature [8, 9], when substituted for synthetic fillers such as glass fiber, carbon fiber, and inorganic filler. In addition, plastic waste is one of the major constituents of global municipal solid waste [10]. In 2008, at least 33.6 million tons post-consumer plastics were generated in the United States, of which 28.9 million tons went to landfills, 2.6 million tons to combustion and energy recovery, and only 2.2 million tons to recycling [11, 12] – only a tiny fraction of plastic wastes are recycled. Blending post-consumer plastics with wood flour to create value-added products could increase the value of plastic waste and impact its re-use practices [11]. Plastic waste is a promising raw material for WPCs because of low cost [10] and similar properties to virgin materials. For example, composites made from recycled high-density polyethylene (rHDPE) have similar or, in some cases, better mechanical properties than composites made from virgin HDPE [13, 14]. The mechanical properties of composites are not better with virgin polystyrene than with recycled polystyrene [15]. In another study, no statistically significant differences were found in mechanical properties of composites, on comparing recycled plastics (HDPE and polypropylene) with virgin plastics [16]. Polypropylene waste and wood waste are promising alternative raw materials for making low cost WPCs [17]. To reduce solid waste disposal in landfills and have low cost WPC products [13] with good

mechanical properties and low creep deformation, suitable WPC formulations need to be developed.

Design of experiments contributes efficiently to find the best formulation. Typical designs include taguchi method, factorial design, and mixture design [18]. The fractions of components in a mixture cannot be changed independently because they must add up to 100%, and mixture designs make use of this fact [18]. A D-optimal mixture experimental design allows to fit model that can be used to optimize the formulation of a composite material [19]. It also allows placing restrictions on the formulations, such as lower or upper limits on the fractions of some components [19, 20]. Mixture designs have recently been applied in food and pharmaceutical industries to find optimal formulation, because they appear efficient in providing useful models with a comparatively small number of experiments. However, prior studies on WPCs seem not to have used D-optimal mixture designs. A four-factor central composite design was applied to develop a response surface model, and to study the foamability of rigid PVC/wood-flour composites [21]. A 2^4 factorial design was used to determine the effects of two hindered amine light stabilizers, a colorant, an ultraviolet absorber, and their interactions, on the photostabilization of wood flour/high-density polyethylene composites [22]. A Box-Behnken design with response surface method was adopted to determine which variables influenced board performance significantly [23]. In the current study, a D-optimal mixture design was used to model the creep of WPCs. The ultimate goal of this work is to optimize the composite formulation using recycled polypropylene and rubberwood flour, for minimal creep, and to investigate the effect of plastic grades on the creep behavior.

8.3 Experimental

8.3.1 Materials

Recycled polypropylene (rPP) pellets, with a melt flow index of 11 g/10 min at 230 °C, were purchased from Withaya Intertrade Co., Ltd (Samutprakarn, Thailand). Rubberwood flour (RWF), used as a natural reinforcement, was collected from a local furniture factory (Songkhla, Thailand). Its chemical composition (by dry

weight) was: cellulose 39%; hemicellulose 29%; lignin 28%; ash 4% [6]. The interfacial bonding between wood flour filler and polymer matrix was also modified, using maleic anhydride-grafted polypropylene (MAPP) with 8-10% of maleic anhydride, supplied by Sigma-Aldrich (Missouri, USA). Hindered amine light stabilizer (HALS) additive under the trade name MEUV008, chosen as the ultraviolet (UV) stabilizer, was supplied by TH Color Co., Ltd (Samutprakarn, Thailand). Paraffin wax, chosen as the lubricant (Lub), was purchased from Nippon Seiro Co., Ltd (Yamaguchi, Japan).

8.3.2 Experimental design to optimize formulation

The D-optimal design of mixture experiments was created with Design-Expert software (version 8.0.6, Stat-Ease, Inc.), to statistically evaluate and model the effects of component fractions on creep properties, and to optimize the formulation. The optimal experimental design of WPC formulations specified the component fractions of rPP (x_1), RWF (x_2), MAPP (x_3), UV stabilizer (x_4), and Lub (x_5). The upper and lower limits of experimental range for the compositions are shown in Table 5.1. Despite the fraction of Lub being held constant it is included as a variable, because it contributes to the 100% in the mixture. The total number of runs was 20, as shown in Table 8.1, including 15 different formulations and 5 duplications to evaluate reproducibility or variances.

8.3.3 Composites processing

Before compounding, the rubberwood flour was sieved through an 80 mesh standard sieve (particles smaller than 180 μm pass), and dried in an oven at 110 °C for 8 h to minimize moisture content. WPCs were then produced in a two-stage process. In the first stage WPC pellets were produced: rPP and RWF were dry-blended, and then melt-blended into wood-plastic composite pellets using a twin-screw extruder machine (Model SHJ-36 from En Mach Co., Ltd, Nonthaburi, Thailand). The extrusion barrel with 10 temperature zones was controlled at 130-170 °C to avoid degradation of the components, while the screw rotating speed was maintained at 70 rpm. The extruded strand passed through a water bath and was

subsequently pelletized. In the second stage WPC panels were produced: the WPC pellets were again dried at 110 °C for 8 h. WPC pellets, MAPP, UV stabilizer, and lubricant compositions indicated in Table 8.1 were then dry-mixed, and added into the feeder of the twin-screw extruder. The temperature profile for extruding was 130-190 °C, with 50 rpm screw feed. Melt pressure at the die varied between 0.10-0.20 MPa, depending on wood flour content. Vacuum venting at 9 temperature zones was also used to purge volatile compounds. The samples were extruded through a rectangular 9 mm × 22 mm die and cooled in atmospheric air. The specimens were machined for flexural creep testing, following the standard of American Society for Testing and Materials (ASTM).

8.3.4 Characterization

Three-point bending creep tests of rPP/RWF composites were carried out on an Instron Universal Testing Machine (Model 5582 from Instron Corporation, Massachusetts, USA) in Figure 8.1, according to ASTM D2990-01 standard. All the tests were performed on 13 mm × 4.8 mm × 100 mm (width × thickness × length) rectangular samples, and a test span of 80 mm. Before the creep tests the specimens were equilibrated in testing room at a temperature of 25 °C (ambient conditions) for 15 min, and then the tests were conducted. The total time of the testing was 100 min (6000 sec), under a constant stress of 19 MPa. In addition, modulus of elastic (MOE) was also measured in a three-point flexural test at a cross-head speed of 2 mm/min, according to ASTM D790-92 standard. Five replications of each formulation were tested.

8.3.5 Creep modeling

Basically, creep strain, $\varepsilon(\sigma, t, T)$, depends on stress ($\sigma$), time ($t$), and temperature ($T$) [24]. It consists of three main elements: (1) elastic deformation (stress-temperature dependence) $\varepsilon_e(\sigma, T)$; (2) viscoelastic deformation (stress-time-temperature dependence) $\varepsilon_{ve}(\sigma, t, T)$; and (3) viscoplastic deformation (stress-time-temperature dependence) $\varepsilon_p(\sigma, t, T)$ [24]:

$$\varepsilon(\sigma, t, T) = \varepsilon_e(\sigma, T) + \varepsilon_{ve}(\sigma, t, T) + \varepsilon_p(\sigma, t, T) \quad (8.1)$$

To describe and predict the short-term creep behavior, many models were developed and applied by using the constitutive relation of polymeric materials [25]. The four-element Burger model (Figure 8.2) is a mathematical model that has been revealed to give a satisfactory prediction and description [25-27]. This model is combinations of Maxwell and Kelvin-Voigt models, which consists of elastic and viscous elements [25, 27]. The mathematical equation for Burger model can be expressed as follows:

$$\varepsilon(t) = \frac{\sigma}{E_M} + \frac{\sigma}{E_K}\left[1 - \exp\left(-t\frac{E_K}{\eta_K}\right)\right] + t\frac{\sigma}{\eta_M} \quad (8.2)$$

where ε is strain accumulated following time (t), when a certain stress (σ) is employed. E_M represents the elastic modulus of the spring in the Maxwell element, which defines the instantaneous elastic deformation that can be immediately recovered when stress is removed. E_K and η_K represent the elastic modulus of the spring and the viscosity of the dashpot, respectively, in the Kelvin element, which associate with the stiffness and viscous or oriented flow of amorphous polymer chains in the short term. η_M represents the viscosity of the dashpot in the Maxwell element, which defines the viscous flow [28].

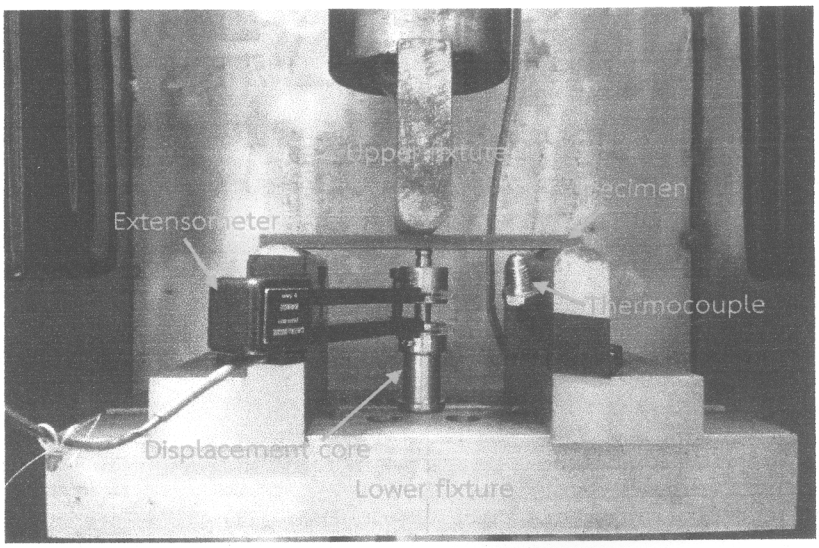

Figure 8.1 Test apparatus of three-point bending creep

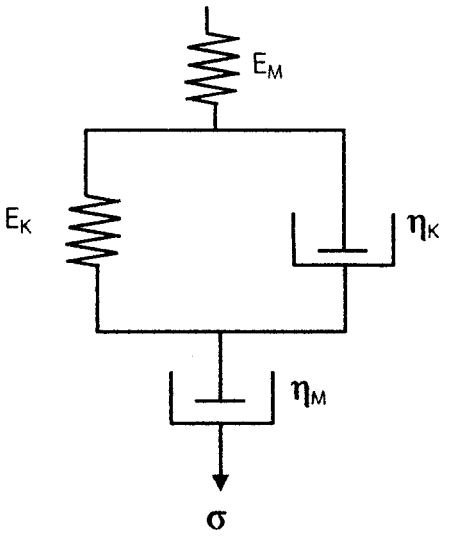

Figure 8.2 Schematic of the four-element Burger model

8.4 Results and discussion

The D-optimal mixture design of experiments, with five fractions as (mutually dependent) variables (that sum to one), had 20 runs in a randomized order. The three determined responses were the values of the instantaneous creep strain (C_e), of the viscoelastic creep strain after 6000 s (C_{ve6000}), and of the total creep strain after 6000 s (C_{t6000}). The results are summarized in Table 8.1.

8.4.1 Statistical analysis of the response surface model

The data for C_e, C_{ve6000}, and C_{t6000} were fit with linear model by multiple linear regressions, with no statistical need for quadratic, special cubic and cubic models. For example, a summary of modeling the C_{t6000} response is shown in Table 8.2. The sequentially fit linear model is significant (p-value less than $\alpha = 0.05$), but the higher order terms are not. The adjusted coefficient of determination (adj-R^2) and predicted coefficient of determination (pred-R^2) shown in Table 8.3 have the fairly good values 0.8780 and 0.8413, respectively. The values in Table 8.3 came from an analysis of variance (ANOVA) on the significant effects relative to the creep responses. The ANOVA shows statistical significance of these linear models, indicated by p-values less than α ($\alpha = 0.05$). This result implies that each modeled output, C_e,

C_{ve6000}, and C_{t6000}, was significantly affected by at least one of the four controlled variables. The R^2 value for C_{ve6000} is relatively poor, partly because its determination was "noisy" with a high C.V.

Table 8.1 Experimental compositions in mixture experimental design and measured responses

Run	Mixture component proportion (wt%)					Creep strain (%)		
no.	x_1	x_2	x_3	x_4	x_5	C_e	C_{ve6000}	C_{t6000}
1	63.9	29.9	4.5	0.7	1.0	0.98	0.33	1.31
2	70.0	25.0	3.0	1.0	1.0	1.03	0.42	1.45
3	50.0	43.0	5.0	1.0	1.0	0.77	0.27	1.04
4	54.9	38.9	4.5	0.7	1.0	0.75	0.25	1.00
5	59.5	34.5	5.0	0.0	1.0	0.80	0.37	1.17
6	55.4	39.9	3.5	0.2	1.0	0.74	0.29	1.03
7	59.5	34.5	4.0	1.0	1.0	0.78	0.31	1.09
8*	59.5	34.5	5.0	0.0	1.0	0.89	0.38	1.27
9	50.0	44.3	4.3	0.5	1.0	0.67	0.27	0.94
10	68.0	25.0	5.0	1.0	1.0	1.07	0.43	1.50
11	50.0	45.0	3.0	1.0	1.0	0.70	0.25	0.95
12*	50.0	43.0	5.0	1.0	1.0	0.71	0.36	1.07
13	60.3	35.3	3.0	0.5	1.0	0.88	0.34	1.22
14	64.9	30.4	3.5	0.2	1.0	0.90	0.38	1.28
15*	70.0	25.0	3.0	1.0	1.0	1.03	0.40	1.43
16	51.0	45.0	3.0	0.0	1.0	0.70	0.32	1.02
17*	51.0	45.0	3.0	0.0	1.0	0.69	0.26	0.95
18*	50.0	45.0	3.0	1.0	1.0	0.73	0.25	0.98
19	70.0	25.0	4.0	0.0	1.0	0.94	0.42	1.36
20	69.0	25.0	5.0	0.0	1.0	0.96	0.33	1.29

Note; *duplicate experiment

Table 8.2 Fit summary of C_{t6000} response

Source	Sequential p-value	Lack of fit p-value	Adj-R^2	Pred-R^2	
Linear	<0.0001*	0.1125	0.8780	0.8413	Suggested
Quadratic	0.2092	0.1415	0.9045	0.7242	
Special cubic	0.2454	0.1161	0.9279	-13.77	
Cubic	0.1161	-	0.9497	-	Aliased

*P-value less than 0.05 indicate model terms are significant.

Table 8.3 P-values from analysis of variance and model adequacy indicators for each modeled response

Source	C_e (%)	C_{ve6000} (%)	C_{t6000} (%)
Model	linear	linear	linear
	<0.0001*	0.0006*	<0.0001*
Linear Mixture	<0.0001*	0.0006*	<0.0001*
Lack of Fit	0.3331	0.3590	0.1125
R^2	0.9143	0.6555	0.8973
Adj-R^2	0.8982	0.5909	0.8780
Pred-R^2	0.8742	0.4296	0.8413
C.V. (%)	4.99	12.03	5.52

*P-value less than 0.05 indicate model terms are significant.

The R^2 values of the C_e, C_{ve6000}, and C_{t6000} are 0.9143, 0.6555, and 0.8973, indicating that 8.57%, 34.45%, and 10.27%, respectively, of the total variability in observations is not explained by the models; R^2 values close to 1 indicate good fits [29]. R^2 values will always increase when a variable is added to the model [30], and the computed adj-R^2 should be close to R^2 value of the model selected. This indeed is the case for the fitted models, indicating it is unlikely that the models have insignificant terms included [31]. The pred-R^2 value of C_e was 0.8742, meaning that the fitted model is estimated to explain about 87% of variability in new cases, and this is in reasonable agreement with the adj-R^2 of 0.8982. For C_{ve6000} all of R^2, adj-R^2, and pred-R^2, have relatively low or poor values, because

C_{ve6000} was calculated as C_{t6000}-C_e and this increased its relative inaccuracy. The coefficients of variation (C.V.), of C_e, C_{ve6000}, and C_{t6000}, were estimated at 4.99%, 12.03%, and 5.52%, respectively, based on the residual variation. Low C.V. values indicate good precision of the determinations.

8.4.2 Model adequacy checking

Model adequacy checking is always necessary with a fitted model [31]. Figure 8.3(a) displays normal probability plots of the residuals for elastic creep strain C_e, and the visually good fit with a straight line suggests that the residuals are about normally distributed. The interpretation is that the residuals are Gaussian measurement noise, while the explanatory variables (fractions of rPP, RWF, MAPP, and UV stabilizer) explain the deterministic part of the relationship. Likewise, there is no strong indication of presence of outliers, as such a failed experiment would give a large residual disabling the good straight line fit in a probability plot [18]. A plot of the residuals vs. the predicted values for the model of C_e is shown in Figure 8.3(b). There is no obvious patterns remaining, and therefore no suggestion for adding some nonlinear terms to the fit [18]. Figure 8.3(c) shows the C_e model predictions vs. observations. The model outputs fit the actual observations quite well, with C_e model deviating from actual by less than about 5%, in alignment with the estimated C.V. The model adequacy was similarly checked for C_{ve6000} and C_{t6000}, with essentially similar conclusions.

8.4.3 Effect of composition on the elastic creep strain and optimal formulation

The linear regression model fitted to experimental C_e value was:

$$C_e = 0.99x_1 + 0.66x_2 + 0.89x_3 + 1.78x_4 \quad (8.3)$$

in which all coefficients are positive. RWF (x_2) has the smallest coefficient so it should be maximized to minimize creep. The UV stabilizer (x_4) has the largest coefficient, so its addition should be as small as possible. The experimentally covered formulations are shown in Figures 8.4(a) and 8.4(b), with color coding for the modeled C_e. In the

triangular contour plot of Figure 8.4(a) the three pure components (rPP, RWF, and MAPP) are represented by the corners, while the additive levels were fixed (UV stabilizer at 0.5 wt% and Lub at 1 wt%). The contours in the colored areas, that include the experimental observations, present the C_e regression fits varying from 0.7 to 1%. The creep C_e clearly decreases with increasing rubberwood flour content. High wood flour content increases the modulus of elasticity (MOE) of composites [32], so that higher stress is required for the same deformation [7, 33]. The choice of MAPP content between 3 and 5 wt% barely affected the C_e. Generally, the addition of coupling agent in the WPCs decreases the creep strain due to the improved filler dispersion and improved interfacial adhesion between wood flour and polymer matrix [34-36], whereas too much MAPP relative to wood flour will cause self-entanglement, resulting in slippage with the PP molecules [7, 37]. The triangular contour plot in Figure 8.4(b) also shows that addition of 1 wt% UV stabilizer slightly increased the elastic creep strain from 0.82 to 0.88%. UV stabilizer is known to reduce the flexural properties but to increase creep strain, due to non-homogeneous spatial distribution of wood flour, polymer, and UV stabilizer [38]. Using 1 wt% of UV stabilizer may be unnecessary, and its fraction should be minimized to decrease creep.

The numerically optimized compositions for each creep characteristic, based on fitted models, are shown in Table 8.4. In all three cases the formulations have about 50.0 wt% of rPP and 45.0 wt% of RWF, with minor variation in MAPP and UV stabilizer fractions. Since the requirements of optimizing the different creep characteristics are not in much of a conflict, they can be approximately optimized simultaneously.

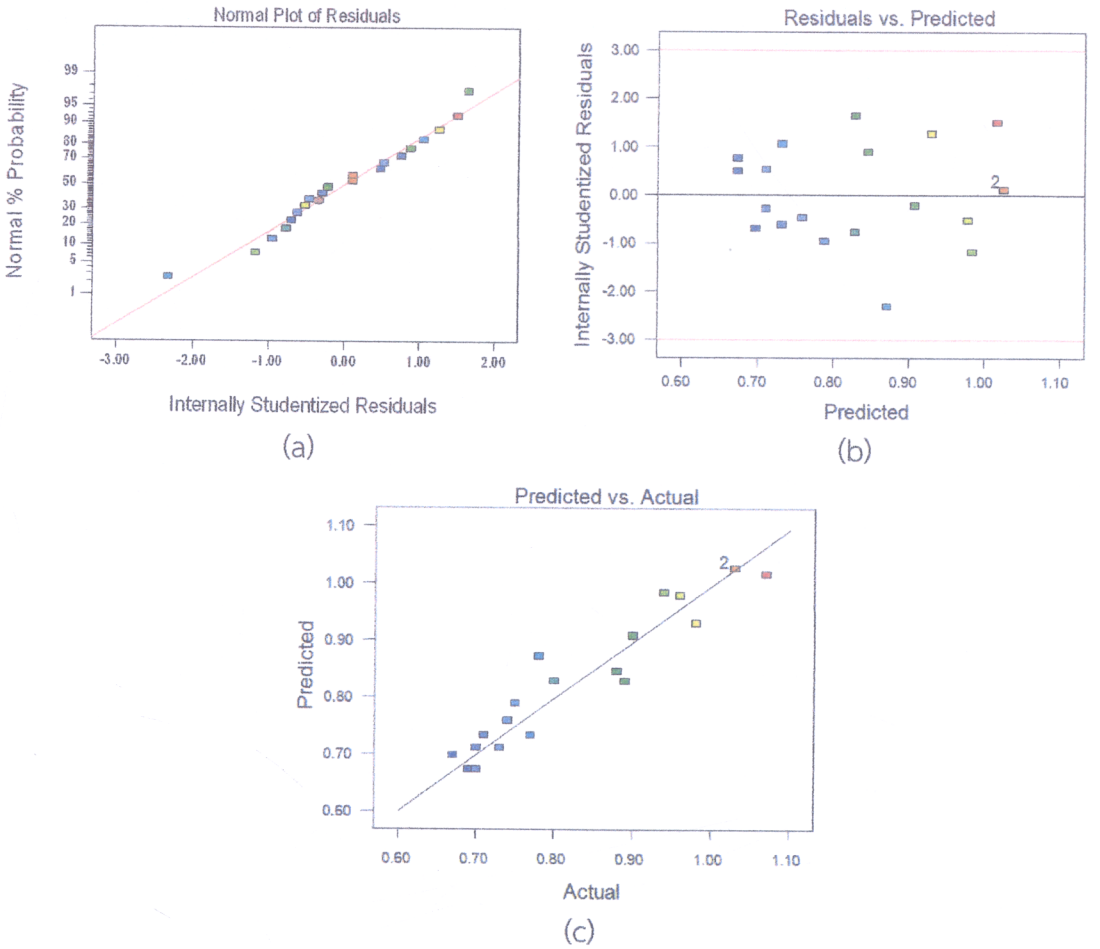

Figure 8.3 Model adequacy checking for elastic creep strain; (a) normal probability plot of residuals, (b) plot of residuals versus predicted values, and (c) plot of predicted versus actual values

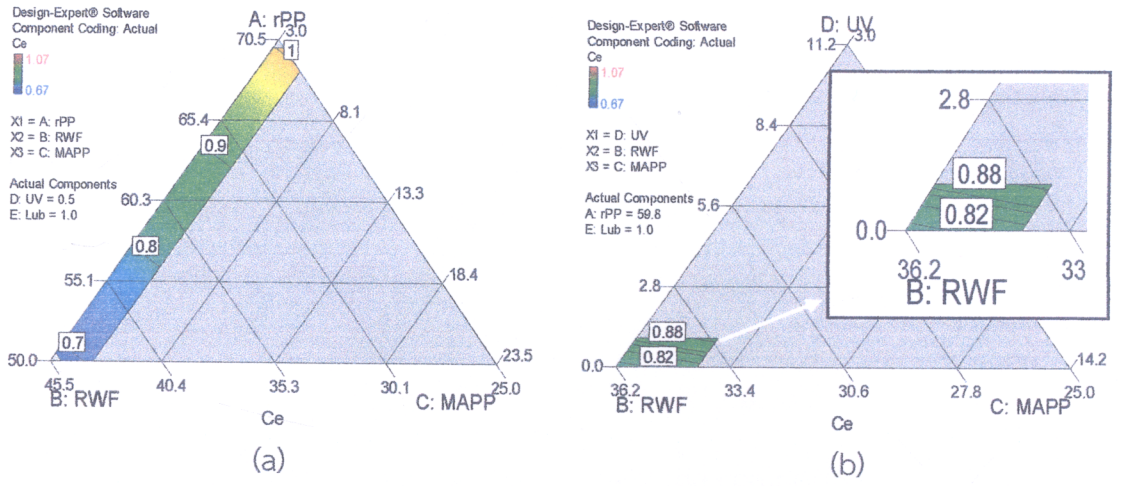

Figure 8.4 Contour plots for effects of compositions on elastic creep strain (a) fixed UV stabilizer at 0.5 wt%, Lub at 1 wt% and (b) fixed rPP at 59.8 wt%, Lub at 1 wt%

Table 8.4 The optimal formulations that minimize each creep characteristic, with predicted responses

Property (%)	Mixture component proportion (wt%)					Predicted response	Desirability
	x_1	x_2	x_3	x_4	x_5		
C_e	50.0	45.0	3.9	0.1	1.0	0.67	0.996
C_{ve6000}	50.0	45.0	3.0	1.0	1.0	0.26	0.906
C_{t6000}	50.1	45.0	3.5	0.3	1.0	0.95	0.962

8.4.4 Effect of composition on the viscoelastic creep strain and optimal formulation

The linear regression model for the viscoelastic creep strain (C_{ve6000}) was:

$$C_{ve6000} = 0.40x_1 + 0.27x_2 + 0.45x_3 + 0.26x_4 \quad (8.4)$$

with positive coefficients. In Figure 8.5 C_{ve6000} (in the range of 0.28 to 0.40%) increases for high fractions of recycled polypropylene, because the mobility of polymer chains increased in the wood-plastic composites and contributed to viscoelasticity. The concentration effect of MAPP on C_{ve6000} was insignificant similar to elastic creep strain. The optimal composition minimizing viscoelastic creep strain coincided with formulation 11, see Table 8.4.

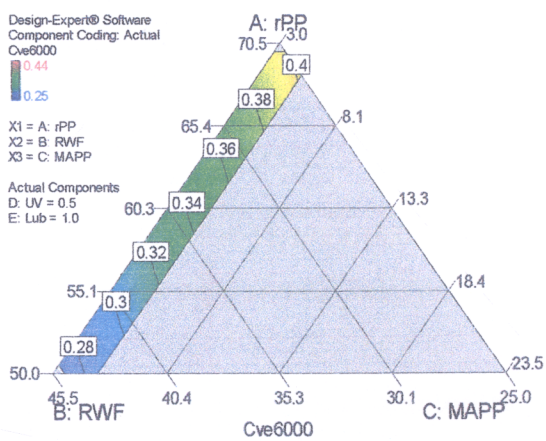

Figure 8.5 Triangular contour plot for effects of the compositions on viscoelastic creep strain. Constant fractions of UV stabilizer at 0.5 wt% and Lub at 1 wt%

8.4.5 Effect of composition on the total creep strain and optimal formulation

The linear regression fit for the total creep strain (C_{t6000}) was:

$$C_{t6000} = 1.39x_1 + 0.93x_2 + 1.33x_3 + 2.04x_4 \quad (8.5)$$

with positive coefficients. RWF (x_2) has the lowest coefficient, while UV stabilizer (x_4) has the largest coefficient. Figure 8.6(a) shows that total creep strain varies in range of 1.0 to 1.3% and decreases with rubberwood flour loading. Rubberwood flour had a lower coefficient than recycled polypropylene because wood flour is stiffer than the neat plastic [39]. Figure 8.6(b) presents the effect of MAPP and UV stabilizer contents on the total creep strain. The total creep strain slightly increases with MAPP and UV stabilizer concentrations, with reasons similar to what was discussed in relation to C_e. The optimal formulation based on the numerical model is also shown in Table 8.4.

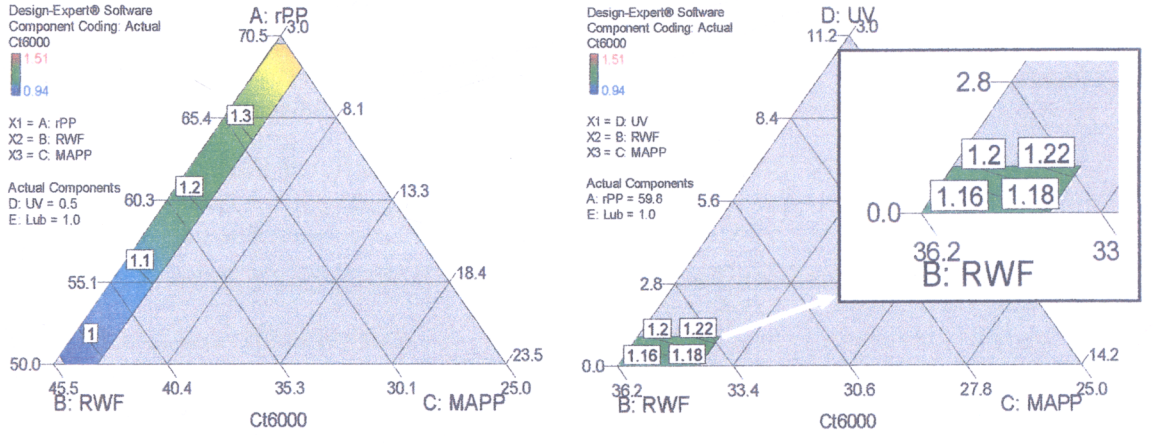

Figure 8.6 Contour plots for effects of the compositions on total creep strain (a) fixed UV stabilizer at 0.5 wt%, Lub at 1 wt% and (b) fixed rPP at 59.8 wt%, Lub at 1 wt%

8.4.6 Optimal formulation for all creep characteristics

Multiobjective optimization using all of the regression models was performed with the Design-Expert software, using its default settings to construct a desirability score that balances all of the fitted models. The plot in Figure 8.7 shows

the formulation that was considered optimal, along with contours of the desirability score. The optimal formulation found was 50.5 wt% rPP, 44.9 wt% RWF, 3.5 wt% MAPP, 0.1 wt% UV stabilizer, and 1.0 wt% Lub, corresponding to a high desirability of 0.945. All the previous optima, in Table 8.4, were at practically the same formulation. The model predictions were validated experimentally, and the results are in Table 8.5 for the jointly optimal formulation. The maximum deviations between model predictions and experimental averages are the same order as the earlier estimated C.V. accuracies of determinations.

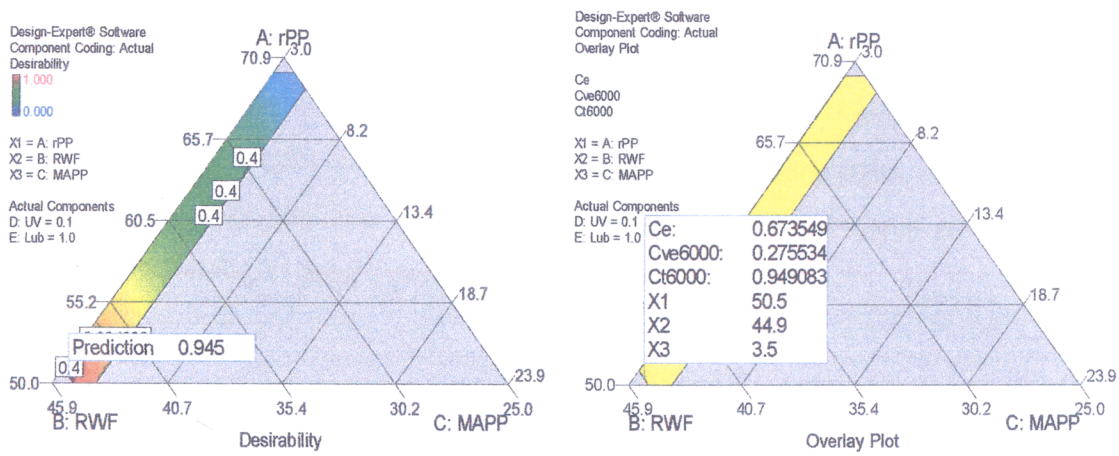

Figure 8.7 The optimal formulation for overall desirability

Table 8.5 Predicted and observed responses with the formulation optimized jointly for all the creep characteristics

	Mixture component proportion (wt%)					Creep strain (%)		
	x_1	x_2	x_3	x_4	x_5	C_e	C_{ve6000}	C_{t6000}
Predicted	50.5	44.9	3.5	0.1	1.0	0.67	0.27	0.95
Observed						0.71	0.29	1.00
						(0.01)*	(0.02)	(0.03)

*The values in parentheses are standard deviations from five replications.

8.4.7 Effect of plastic grades on creep behavior

The short-term flexural creep behavior of unfilled PP and PP/RWF composites with different RWF content is shown in Figure 8.8, while the values of the

C_e, C_{ve6000}, and C_{t6000} are also exhibited in Table 8.6. As can be seen in Figure 8.8, the neat PP (both virgin and recycled) presented the highest creep in the duration of testing, and an increase of rubberwood flour content in the composites showed the decreased creep tendency. This behavior is probably due to an increase in modulus of elastic (MOE) of composites with high wood flour content [32], as shown in Table 8.7. The MOE of composites (both virgin and recycled plastics) increased with wood flour loadings. Since RWF is a high modulus material compared to the plastic matrix, composites with higher wood flour content require a higher stress for the same deformation [7, 33]. MOE thus has positive effect on decreasing deformation and effective improvement in creep behavior. In addition, unfilled rPP and composites based on rPP show higher creep strain than those based on vPP, for the same plastic to wood ratio. This is probably because of the virgin plastic being stiffer than recycled plastics [7]. However, the two types of plastic with 45 wt% RWF seem to have the same creep behavior, in good agreement with the values of MOE.

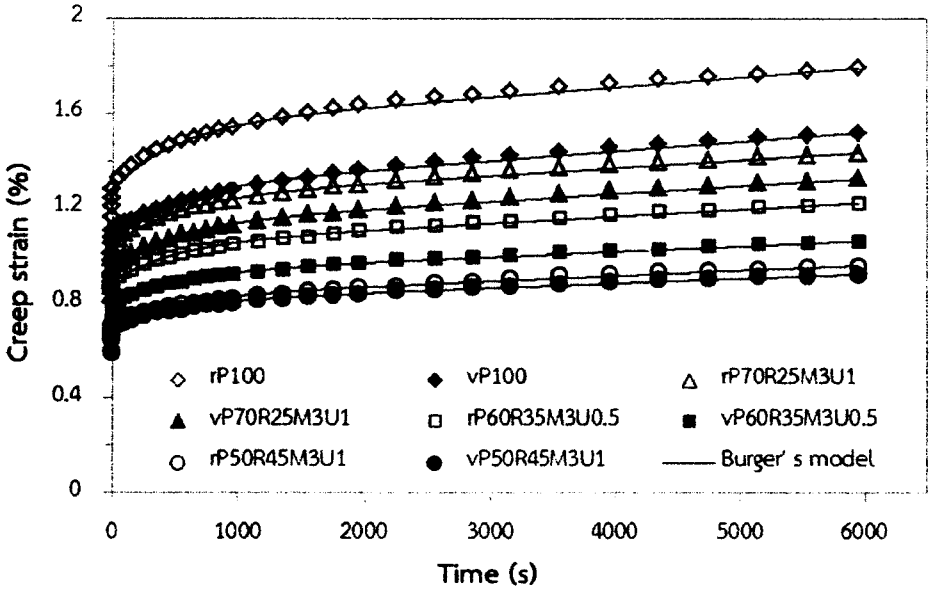

Figure 8.8 Creep strain (dot) as a function of time at 25 °C affected by plastic grades and rubberwood flour contents; solid lines represent Burger model fit

Table 8.6 Wood-plastic composite formulation (percent by weight) and creep strain of unfilled PP and PP/RWF composites (T = 25 °C, σ = 19 MPa)

Composite	Mixture component proportion (wt%)						Creep strain (%)		
sample code	rPP	vPP	RWF	MAPP	UV	Lub	C_e	C_{ve6000}	C_{t6000}
rP100	100						1.27	0.52	1.79
vP100		**100**					**1.07**	**0.44**	**1.51**
rP70R25M3U1	70		25	3	1	1	1.03	0.40	1.43
vP70R25M3U1		**70**	**25**	**3**	**1**	**1**	**0.94**	**0.38**	**1.32**
rP60R35M3U0.5	60.3		35.3	3	0.5	1	0.88	0.34	1.22
vP60R35M3U0.5		**60.3**	**35.3**	**3**	**0.5**	**1**	**0.78**	**0.27**	**1.05**
rP50R45M3U1	50		45	3	1	1	0.70	0.25	0.95
vP50R45M3U1		**50**	**45**	**3**	**1**	**1**	**0.68**	**0.23**	**0.91**

Table 8.7 Modulus of elastic and Burger's model parameters

Composite sample code	MOE (GPa)	E_M (MPa)	E_K (MPa)	η_M (MPa·s)	η_K (MPa·s)
rP100	1.27 (0.06)*	1489	7142	4.55E+ 07	3.57E + 06
vP100	**1.67 (0.06)**	**1764**	**9547**	**4.67E + 07**	**4.77E + 06**
rP70R25M3U1	1.76 (0.03)	1832	9595	5.73E + 07	4.79E + 06
vP70R25M3U1	**1.93 (0.06)**	**2012**	**10326**	**5.82E + 07**	**5.16E + 06**
rP60R35M3U0.5	2.17 (0.08)	2146	11801	6.49E + 07	5.90E + 06
vP60R35M3U0.5	**2.31 (0.02)**	**2420**	**13868**	**8.25E + 07**	**6.93E + 06**
rP50R45M3U1	2.68 (0.08)	2702	16239	8.31E + 07	8.11E + 06
vP50R45M3U1	**2.66 (0.05)**	**2773**	**16521**	**9.50E + 07**	**8.26E + 06**

*The values in parentheses are standard deviations from five replications.

8.4.8 Creep modeling analysis

Figure 8.8 also shows fit of creep curves using Burger model with the solid lines. It can be seen that Burger model provided a good fitting with the experimental data of each formulation. Similar results were found in the work of Liu et al. [26] and Tamrakar et al. [27] who reported that the Burger model offered a good fitting for the creep curves of the composites. The first instantaneous creep arises from the elastic modulus or the spring (E_M) and later time-dependent deflection

participates with the spring (E_K) and dashpot (η_K), and last time-dependent deformation comes from the viscous dashpot flow (η_M) [25]. The short-term creep curves were modeled with the Burger equation and the parameters are summarized in Table 8.7. According to these results, viscosity increased with an increase of the rubberwood flour content, and lower flow occurred in the dashpot, and thus permanent deflection reduced. In the Maxwell spring part, the modulus (E_M) of composites from both virgin and recycled plastics exhibited the enhanced values with the wood flour loading. This is attributed to the stiffness of the composite materials with higher RWF content, and thus reduced the instantaneous elastic deformation during creep experiments. The viscous flow (η_M) values tend to also enhance with the increase of the wood flour content. This is caused by the fact that increasing additions of wood flour content reduced the amount of polymer chains in the plastic composites, resulting in the increase of the viscosity. The retardant elasticity (E_K) and viscosity (η_K) revealed a similar trend on wood flour content, increasing with wood flour content. It could be concluded that the deformation of the Kelvin-Voigt element decreased with increasing wood flour content.

8.5 Conclusions

Design and analysis of D-optimal mixture experiments were used to efficiently obtain the optimal formulation of rPP/RWF composites that minimizes creep. All the component fractions which experimentally varied, namely of rPP, RWF, MAPP, and UV stabilizer, significantly affected all the creep characteristics (C_e, C_{ve6000}, and C_{t6000}). In general, a high fraction of RWF reduced all of these, and the optima found had 45 wt% RWF which was the maximum in the experimental design. At this wood flour loading, the modulus of elasticity was maximized, so that a comparatively high stress is required for a given creep deformation. Increasing the fraction of MAPP from 3 to 5 wt% only slightly affected the creep strain, lacking statistical significance. The addition of 1 wt% UV stabilizer slightly increased creep. The approximately optimal formulation minimizing jointly all creep characteristics was 50.5 wt% rPP, 44.9 wt% RWF, 3.5 wt% MAPP, 0.1 wt% UV stabilizer, and 1.0 wt% Lub. The joint optimization maximized a desirability score that balanced the multiple

objectives, and the jointly optimal formulation was experimentally validated to produce low creep nearly as predicted.

In addition, the plastic grades and rubberwood flour contents showed a large impact on the creep behavior of the composites. The neat vPP and composites based on vPP exhibited lower creep deformation than those based on rPP, for the same plastic to wood ratio. The unfilled PP (both virgin and recycled) demonstrated the highest creep strain in range of time studied. The creep strain reduced as the wood flour level increased, due to the resulting increase in stiffness [40]. It was clearly revealed that the addition of rubberwood flour in PP composites can be efficiently improved the poor creep stability of polyolefin. Besides, the short-term flexural creep behavior could be well fitted by using the Burger model, and the data of modeling offered an understanding of the deformation mechanism for three elements: elastic, viscoelastic, and viscoplastic deformation.

8.6 References

[1] S. Tamrakar, R.A. Lopez-Anido, A. Kiziltas, and D.J. Gardner. "Time and Temperature Dependent Response of a Wood-Polypropylene Composite." *Composites Part A: Applied Science and Manufacturing*, vol. 42, pp. 834–842, 2011.

[2] D.R. Carroll, R.B. Stone, A.M. Sirignano, R.M. Saindon, S.C. Gose, and M.A. Friedman. "Structural Properties of Recycled Plastic/Sawdust Lumber Decking Planks." *Resources, Conservation and Recycling*, vol. 31, pp. 241–251, 2011.

[3] I. Ganguly and I.L. Eastin. "Trends in the US Decking Market: A National Survey of Deck and Home Builders." *The Forestry Chronicle*, vol. 85, pp. 82–90, 2009.

[4] A.A. Klyosov. *Wood-Plastic Composites*. Hoboken, New Jersey: John Wiley & Son, Inc., 2007.

[5] T. Ratanawilai, P. Lekanukit, and S. Urapantamas. "Effect of Rubberwood and Palm Oil Content on the Properties of Wood-Polyvinyl Chloride Composites." *Journal of Thermoplastic Composite Materials*, Epub ahead of print 9 August 2012. DOI: 10.1177/0892705712454863.

[6] P. Petchpradab, T. Yoshida, T. Charinpanitkul, and Y. Matsumura. "Hydrothermal Pretreatment of Rubber Wood for the Saccharification Process." *Industrial and Engineering Chemistry Research*, vol. 48, pp. 4587–4591, 2009.

[7] C. Homkhiew, T. Ratanawilai, and W. Thongruang. "Composites from Recycled Polypropylene and Rubberwood Flour: Effects of Composition on Mechanical Properties." *Journal of Thermoplastic Composite Materials*, Epub ahead of print 14 February 2013. DOI: 10.1177/0892705712475019.

[8] X. Peng, M. Fan, J. Hartley, and M. Al-Zubaidy. "Properties of Natural Fiber Composites Made by Pultrusion Process." *Journal of Composite Materials*, vol. 46, pp. 237–246, 2011.

[9] G. Francucci, E.S. Rodriguez, and A. Vazquez. "Experimental Study of the Compaction Response of Jute Fabrics in Liquid Composite Molding Processes." *Journal of Composite Materials*, vol. 46, pp. 155–167, 2011.

[10] Y. Cui, S. Lee, B. Noruziaan, M. Cheung, and J. Tao. "Fabrication and Interfacial Modification of Wood/Recycled Plastic Composite Materials." *Composites Part A: Applied Science and Manufacturing*, vol. 39, pp. 655–661, 2008.

[11] T. Ratanawilai, N. Thanawattanasirikul, and C. Homkhiew. "Mechanical and Thermal Properties of Oil Palm Wood Sawdust Reinforced Post-Consumer Polyethylene Composites." *ScienceAsia*, vol. 38, pp. 289–294, 2012.

[12] N.J. Themelis, M.J. Castaldi, J. Bhatti, and L. Arsova. "Energy and Economic Value of Non-recycled Plastics and Municipal Solid Wastes that are Currently Landfilled in the Fifty States." *EEC Study of Non-recycled Plastics*, Earth Engineering Center, Columbia University, 2011.

[13] K.B. Adhikary, S. Pang, and M.P. Staiger. "Dimensional Stability and Mechanical Behaviour of Wood-Plastic Composites based Recycled and Virgin High-Density Polyethylene." *Composites Part B: Engineering*, vol. 39, pp. 807–815, 2008.

[14] S.E. Selke and I. Wichman. "Wood Fiber/Polyolefin Composites." *Composites Part A: Applied Science and Manufacturing*, vol. 35, pp. 321–326, 2004.

[15] J. Lisperguer, X. Bustos, and Y. Saravia. "Thermal and Mechanical Properties of Wood Flour-Polystyrene Blends from Postconsumer Plastic Waste." *Journal of Applied Polymer Science*, vol. 119, pp. 443–451, 2011.

[16] S.K. Najafi, E. Hamidinia, and M. Tajvidi. "Mechanical Properties of Composites from Sawdust and Recycled Plastics." *Journal of Applied Polymer Science*, vol. 100, pp. 3641–3645, 2006.

[17] A. Nourbakhsh, A. Ashori, H.Z. Tabari, and F. Rezaei. "Mechanical and Thermo-Chemical Properties of Wood-Flour/Polypropylene Blends." *Polymer Bulletin*, vol. 65, pp. 691–700, 2010.

[18] D.C. Montgomery. *Design and Analysis of Experiments*. John Wiley & Sons, Inc., 2009.

[19] Y.B. Khosrowshahi and A. Salem. "Influence of Polyvinyl Alcohol and Carboxymethyl Cellulose on the Reliability of Extruded Ceramic Body: Application of Mixture Design Method in Fabricating Reliable Ceramic Raschig Rings." *International Journal of Applied Ceramic Technology*, vol. 8, pp. 1334–1343, 2011.

[20] R.C.S. John. "Experiments with Mixtures, Ill-Conditioning, and Ridge Regression." *Journal of Quality Technology*, vol. 16, pp. 81–96, 1984.

[21] L.M. Matuana and F. Mengeloglu. "Manufacture of Rigid PVC/Wood-Flour Composite Foams Using Moisture Contained in Wood as Foaming Agent." *Journal of Vinyl & Additive Technology*, vol. 8, pp. 264–270, 2002.

[22] N.M. Stark and L.M. Matuana. "Ultraviolet Weathering of Photostabilized Wood-Flour-Filled High-Density Polyethylene Composites." *Journal of Applied Polymer Science*, vol. 90, pp. 2609–2617, 2003.

[23] Z. Jun, W. Xiang-ming, C. Jian-min, and Z. Kai. "Optimization of Processing Variables in Wood–Rubber Composite Panel Manufacturing Technology." *Bioresource Technology*, vol. 99, pp. 2384–2391, 2008.

[24] A. Dorigato, A. Pegoretti, and J. Kolarik. "Nonlinear Tensile Creep of Linear Low Density Polyethylene/Fumed Silica Nanocomposites:Time-Strain Superposition and Creep Prediction." *Polymer Composites*, vol. 31, pp. 1947–1955, 2010.

[25] K. Banik, J. Karger-Kocsis, and T. Abraham. "Flexural Creep of All-Polypropylene Composites: Model Analysis." *Polymer Engineering and Science*, vol. 48, pp. 941–948, 2008.

[26] H. Liu, F. Yao, Y. Xu, and Q. Wu. "A Novel Wood Flour-Filled Composite based on Microfibrillar High-Density Polyethylene (HDPE)/Nylon-6 Blends." *Bioresource Technology*, vol. 101, pp. 3295–3297, 2010.

[27] S. Tamrakar, R.A. Lopez-Anido, A. Kiziltas, and D.J. Gardner. "Time and Temperature Dependent Response of a Wood-Polypropylene Composite." *Composites Part A: Applied Science and Manufacturing*, vol. 42, pp. 834–842, 2011.

[28] G. Gong, J. Pyo, A.P. Mathew, and K. Oksman. "Tensile Behavior, Morphology and Viscoelastic Analysis of Cellulose Nanofiber-Reinforced Polyvinyl Acetate." *Composites Part A: Applied Science and Manufacturing*, vol. 42, pp. 1275–1282, 2011.

[29] M. Amini, H. Younesi, N. Bahramifar, A.A.Z. Lorestani, F. Ghorbani, A. Daneshi, and M. Sharifzadeh. "Application of Response Surface Methodology for Optimization of Lead Biosorption in an Aqueous Solution by Aspergillus Niger." *Journal of Hazardous Materials*, vol. 154, pp. 694–702, 2008.

[30] I. Eren and F. Kaymak-Ertekin. "Optimization of Osmotic Dehydration of Potato Using Response Surface Methodology." *Journal of Food Engineering*, vol. 79, pp. 344–352, 2007.

[31] R.H. Myers, D.C. Montgomery, and C.M. Anderson-Cook. *Response Surface Methodology: Process and Product Optimization Using Designed Experiments.* John Wiley & Sons, Inc., Hoboken, New Jersey, 2009.

[32] N.E. Marcovich and M.A. Villar. "Thermal and Mechanical Characterization of Linear Low-Density Polyethylene/Wood Flour Composites." *Journal of Applied Polymer Science*, vol. 90, pp. 2775–2784, 2003.

[33] M.R. Rahman, M.M. Huque, M.N. Islam, and M. Hasan. "Improvement of Physico-Mechanical Properties of Jute Fiber Reinforced Polypropylene Composites by Post-Treatment." *Composites Part A: Applied Science and Manufacturing*, vol. 39, pp. 1739–1747, 2008.

[34] J. Mingyin, X. Ping, Z. Yongsheng, and W. Kejian. "Creep Behaviour of Wood Flour/Poly(Vinyl Chloride) Composites." *Journal of Wuhan University of Technolotgy-Mater*, vol. 24, pp. 440–447, 2009.

[35] M. Bengtsson, P. Gatenholm, and K. Oksman. "The Effect of Crosslinking on the Properties of Polyethylene/Wood Flour Composites." *Composites Science and Technology*, vol. 65, pp. 1468–1479, 2005.

[36] A.J. Nunez, P.C. Sturm, J.M. Kenny, M.I. Aranguren, N.E. Marcovich, and M.M. Reboredo. "Mechanical Characterization of Polypropylene–Wood Flour Composites." *Journal of Applied Polymer Science*, vol. 88, pp. 1420–1428, 2003.

[37] S. Mohanty, S.K. Verma, S.K. Nayak, and S.S. Tripathy. "Influence of Fiber Treatment on the Performance of Sisal–Polypropylene Composites." *Journal of Applied Polymer Science*, vol. 94, pp. 1336–1345, 2004.

[38] A. Wechsler and S. Hiziroglu. "Some of the Properties of Wood–Plastic Composites." *Building and Environment*, vol. 42, pp. 2637–2644, 2007.

[39] M. Garcia, J. Hidalgo, I. Garmendia, and J. Garcia-Jaca. "Wood–Plastics Composites with Better Fire Retardancy and Durability Performance." *Composites Part A: Applied Science and Manufacturing*, vol. 40, pp. 1772–1776, 2009.

[40] S.Y. Lee, H.S. Yang, H.J. Kim, C.S. Jeong, B.S. Lim, and J.N. Lee. "Creep Behavior and Manufacturing Parameters of Wood Flour Filled Polypropylene Composites." *Composite Structures*, vol. 65, pp. 459–469, 2004.

CHAPTER 9

Composites from Recycled Polypropylene and Rubberwood Flour: Effects of Composition on Mechanical Properties

9.1 Chapter summary

The mechanical properties of composites from recycled plastic waste and sawdust waste are interest on trying to convert these waste streams to useful products. The development of these composites from natural fiber is therefore receiving widespread attention due to the growing environmental awareness. Effects of compositions were investigated including different grades of plastic (virgin and recycled) and amounts of wood flour, coupling agent, and UV stabilizer on mechanical and physical properties of polypropylene/rubberwood flour composites. Virgin polypropylene gave better mechanical properties than recycled (rPP), both in composites and as unfilled plastic. Rubberwood flour (RWF) content exceeding 25 wt% enhanced the strength of RWF reinforced rPP composites. The modulus and hardness of composites increased linearly with wood flour loadings. Maleic anhydride -grafted polypropylene (MAPP) as a coupling agent increased the strength, modulus, and hardness of the composites. However, an addition of 1 wt% UV stabilizer degraded the mechanical properties. This research suggests that using 4.0 wt% MAPP content is good mechanical properties in rPP/RWF composites, while the amount of UV stabilizer should be as small as possible to avoid its negative influence.

9.2 Introduction

Nowadays, wood-plastic composites (WPCs) have become popular. They are extensively used in automotive industry as door inner panels, seat backs, and headliners; in construction business as decking, cladding, and fencing; and in infrastructure as marina and boardwalk. This is due to recyclability, low density, low cost, low maintenance, and eco-friendliness with good mechanical properties.

Moreover, softwood lumber is increasingly replaced as WPCs and plastic lumber in applications of deck-building because of having better durability than softwood lumber [1, 2], and demand of WPCs is also expected to expand nearly 12% each year between 2000 and 2010 in the United States [2].

Numerous investigators have recently studied the thermal and mechanical properties of virgin plastics filled with cellulosic fibers in an attempt to reduce the cost and improve the properties of plastics [3, 4], whereas the utilization of post-consumer plastics in WPCs has been rarely studied. Lisperguer et al. [5] compared WPCs manufactured from wood flour and virgin and/or recycled polystyrene (rPS). They reported that the mechanical properties of the composites based on virgin polystyrene were not better than those based on rPS. Najafi et al. [6] studied the mechanical properties of WPCs produced from sawdust and virgin or recycled plastics, namely high-density polyethylene (HDPE) and polypropylene (PP). The composites containing HDPE (recycled and virgin) exhibited lower stiffness and strength than those made from PP. Ashori and Sheshmani [7] investigated the effects of weight fraction of fibers in hybrid composites made from combinations of recycled newspaper fiber, poplar wood flour, and recycled polypropylene. The composites with a high fraction of recycled newspaper fiber showed maximum water absorption during the whole duration of immersion. Nourbakhsh et al. [8] also concluded that polypropylene waste and wood waste are promising alternative raw materials for making low cost WPCs.

Plastic wastes are the major constituent of municipal solid waste and a promising raw material source for WPCs [6]. Using recycled plastics to produce WPCs would not only decrease the consumption of energy and natural resources, but also offers an effective method of disposing plastic waste [9]. The development of new composites from post-consumer polymers, and a better understanding of the effects of composition on the physical and mechanical properties, will facilitate economic application of these composites in consumer products, and accordingly decrease environmental impacts [10, 11].

Application of fiber waste as reinforcement or filler is increasing in WPCs. These fibers offer several advantages including biodegradability, renewable

character, low cost, ease of fiber surface modification, absence of associated health hazards, and low equipment wear during their processings [10, 12]. Natural fibers have been extensively popularized and successfully used to improve the mechanical properties of plastic composites, with bagasse, bamboo, banana, flax, hemp, jute, kenaf, oil palm, pineapple, sisal, wood, and other wastes as examples [13, 14]. Yemele et al. [15] mixed bark with HDPE and examined the effects of wood species on mechanical properties. They found that black spruce bark composites had better strength than aspen bark composites. Rahman et al. [16] also investigated the effects of jute fiber content on the mechanical properties of reinforced PP. The tensile strength of the composites decreased with an increasing jute fiber loading, but the Young's modulus decreased only slowly. Reddy et al. [17] reported that an increase in the wheat straw and clay contents in a polypropylene hybrid composite increased the flexural modulus and water absorption. Despite extensive research in the area of natural fiber reinforced plastics, few studies have used rubberwood flour to reinforce virgin plastics, and there is no prior report on rubberwood flour reinforced post-consumer polypropylene.

The rubberwood (*Hevea brasiliensis*) flour is much fiber waste generated from sawmills and furniture industries, such as local factories in Thailand. In these industries are generally produced wood wastes about 34% and plantation wastes about 54%. Only 12% of the rubberwood ends up as the goods [18]. Most of the wood waste can be used as raw material to manufacture particleboard and medium-density fiberboard (MDF). However, there is a great deal of interest in utilizing the fibers waste as reinforcement of plastic composites. The fillers (wood flour or wood fiber) are also a more important factor affecting the mechanical properties of the WPCs because of the different wood species consisted of different content and components, such as cellulose, hemicellulose, lignin, and extractants [19]. Hence, the effect of filler (rubberwood flour) and grade of plastic (virgin and recycled polypropylene) on the composites is needed to be further studied. In the current work, the effects of material compositions (including different grades of plastic and the contents of rubberwood flour, coupling agent, and UV stabilizer) on the mechanical and physical properties of composites were investigated. The goal of

this research is to determine the effects of composition on the mechanical and physical properties, for rubberwood flour reinforced recycled polypropylene. The new information will facilitate informed decisions regarding manufacture of such composites.

9.3 Experimental

9.3.1 Materials

Recycled polypropylene (rPP) pellets were obtained from Withaya Intertrade Co., Ltd (Samutprakarn, Thailand) under the trade name WT170. The material has a melt flow index of 11 g/10 min at 230 °C. Virgin polypropylene (vPP), HIPOL J600 with a melt flow index of 7 g/10 min at 230 °C was supplied by Mitsui Petrochemical Industries Co., Ltd (Tokyo, Japan). Rubberwood flour (RWF), used as a lignocellulosic filler, was supplied by S.T.A Furniture Group Co., Ltd (Songkhla, Thailand). Its chemical composition (by weight) was: cellulose 39%; hemicellulose 29%; lignin 28%; ash 4% [18]. The interfacial adhesion between filler and matrix was also modified using as a coupling agent maleic anhydride-grafted polypropylene (MAPP), supplied by Sigma-Aldrich (Missouri, USA) with 8-10% of maleic anhydride. HALS additive, chosen as the UV stabilizer (UV), was supplied by TH Color Co., Ltd (Samutprakarn, Thailand) under the trade name MEUV008. A lubricant (Lub), paraffin wax, was purchased from Nippon Seiro Co., Ltd (Yamaguchi, Japan).

9.3.2 Preparation of the composites

Prior to compounding, the rubberwood flour was sieved (80 mesh) and dried in an oven at 110 °C for 8 h. WPCs were then produced in a two-stage process. In the first stage WPC pellets were produced: polypropylene and wood particles were compounded into wood-plastic composite pellets using a twin-screw extruder (Model SHJ-36 from En Mach Co., Ltd, Nonthaburi, Thailand). The barrel with 10 temperature zones was controlled at 130-170 °C to reduce degradation of the compositions, while the screw rotation speed was fixed at 70 rpm. In the second stage WPC panels were produced: the WPC pellets were again dried at 110 °C for 8 h. WPC pellets, MAPP, UV stabilizer, and lubricant (formulations in Table 9.1) were

then dry-mixed and fed into a twin-screw extruder. The temperature profile in the extruding process was 130-190 °C, with 50 rpm. Melt pressure at the die varied between 0.10-0.20 MPa, depending on wood flour content. Vacuum venting at 9 temperature zones was also used to purge volatile compounds. The samples were then extruded through a rectangular 9 mm × 22 mm die and cooled in atmospheric air. Subsequently, the specimens were machined according to ASTM for mechanical and physical testing.

Table 9.1 Wood-plastic composite formulation (percent by weight)

Composite sample code	rPP	vPP	RWF	MAPP	UV	Lub
rP100	100					
vP100		**100**				
rP70R25M3U1	70		25	3	1	1
vP70R25M3U1		**70**	**25**	**3**	**1**	**1**
rP60R35M3U0.5	60.3		35.3	3	0.5	1
vP60R35M3U0.5		**60.3**	**35.3**	**3**	**0.5**	**1**
rP50R45M3U1	50		45	3	1	1
vP50R45M3U1		**50**	**45**	**3**	**1**	**1**
rP51R45M3U0	51		45	3	0	1
rP70R25M4U0	70		25	4	0	1
rP69R25M5U0	69		25	5	0	1
rP68R25M5U1	68		25	5	1	1

Note; The selected formulations from the mixture experimental design were carried out. The rP70R25M3U1 means 70 wt% rPP, 25 wt% RWF, 3 wt% MAPP, and 1 wt% UV.

9.3.3 Testing

Mechanical properties. Tensile, compressive, and flexural tests were carried out on an Instron Universal Testing Machine (Model 5582 from Instron Corporation, Massachusetts, USA), according to ASTM standards D638-99, D6108-97, and D790-92, respectively. The cross-head speed used for the type-IV tensile specimens was 5 mm/min. The compressive test was also conducted using a constant displacement rate of 0.5 mm/min, and prism specimens were used to determine the compressive

strength and modulus. For the flexural test, specimens with nominal dimensions of 4.8 mm × 13 mm × 100 mm, a span of 80 mm, and a cross-head speed of 2 mm/min were used. All the mechanical tests were performed at room temperature (25 °C) with five replications.

Hardness testing. Hardness measurements were performed according to ASTM D2240-91 specification, using two Durometers (Shore D scales) for the composites. The dimensions of the specimens tested were approximately 16 mm × 16 mm × 6.5 mm. The measurements were performed at room temperature (25 °C).

9.3.4 Analysis

Morphological analysis. The interfacial morphology and phase dispersion of the wood flour in the polymeric matrix were analyzed with a scanning electron microscope (SEM). SEM imaging was performed using a FEI Quanta 400 microscope (Oregon, USA) at an accelerating voltage of 20 kV. The samples were sputter-coated with gold to prevent electrical charging during the observation. Specimens were imaged at magnifications of 150× and 1000×.

Statistical analysis. Results, such as mean values and standard deviations, from five samples of each test were statistically analyzed. The effects of composition on the wood-plastic composites' properties were evaluated by analysis of variance (ANOVA) and student's *t*-test. ANOVA indicated the significant differences between wood flour contents, and then a comparison of the means was done with Tukey's multiple comparison test. A two-sample *t*-test was also used to detect significant differences between levels of additives. All the statistical analyses used a 5% significance level ($\alpha = 0.05$).

9.4 Results and discussion

The specimens produced from blends of polypropylene and rubberwood flour were characterized. The mechanical and physical properties of WPCs are summarized in Tables 9.2 and 9.3. The average values and standard deviations of the flexural strength and modulus, compressive strength and modulus, tensile strength and modulus, and hardness, were calculated from five replications.

Table 9.2 Effects of rubberwood flour content on mechanical and physical properties of WPCs

Composite sample code	Flexural Strength (MPa)	Flexural Modulus (GPa)	Compressive Strength (MPa)	Compressive Modulus (GPa)	Tensile Strength (MPa)	Tensile Modulus (GPa)	Hardness (shore D)
rP100	37.02^{a}	1.27^{a}	10.10^{a}	0.79^{a}	24.12^{a}	0.55^{a}	72.5^{a}
vP100	**50.07^{A}**	**1.67^{A}**	**20.03^{A}**	**0.97^{A}**	**30.12^{A}**	**0.69^{A}**	**75.6^{A}**
rP70R25M3U1	36.94^{a}	1.76^{b}	8.25^{a}	0.71^{a}	23.00^{a}	0.65^{b}	73.2^{a}
vP70R25M3U1	**44.31^{B}**	**1.93^{A}**	**15.34^{B}**	**1.06^{A}**	**25.86^{B}**	**0.84^{B}**	**76.4^{A}**
rP50R45M3U1	39.66^{b}	2.68^{c}	13.59^{b}	1.20^{b}	23.97^{a}	0.99^{b}	75.2^{b}
vP50R45M3U1	**43.41^{B}**	**2.66^{B}**	**16.77^{B}**	**1.40^{B}**	**27.93^{C}**	**1.09^{C}**	**78.3^{B}**
rP60R35M3U0.5*	40.23	2.17	15.73	1.15	25.38	0.88	74.3
vP60R35M3U0.5*	**44.85**	**2.31**	**19.63**	**1.28**	**28.41**	**0.99**	**77.8**

Note; *rP60R35M3U0.5 and vP60R35M3U0.5 were not analyzed to compare the statistical effect of rubberwood content, but they were employed to show the trend of increasing RWF content. Means within each property with the same letter (suffixes a-c for rPP and A-C for vPP) are not significantly different (Tukey's test, α = 0.05).

Table 9.3 Effect of MAPP and UV stabilizer contents on mechanical and physical properties of WPCs

Composite sample code	Flexural Strength (MPa)	Flexural Modulus (GPa)	Compressive Strength (MPa)	Compressive Modulus (GPa)	Tensile Strength (MPa)	Tensile Modulus (GPa)	Hardness (shore D)
rP70R25M3U1	36.94^{a}	1.76^{a}	8.25^{a}	0.71^{a}	23.00^{a}	0.65^{a}	73.2^{a}
rP68R25M5U1	37.04^{a}	2.01^{b}	8.21^{a}	0.83^{a}	23.29^{a}	0.74^{b}	73.7^{b}
rP70R25M4U0	38.95^{a}	1.90^{a}	10.55^{a}	1.01^{a}	24.65^{a}	0.76^{a}	73.6^{a}
rP69R25M5U0	38.44^{a}	1.93^{a}	8.96^{b}	0.79^{b}	25.01^{a}	0.78^{a}	73.8^{a}
rP69R25M5U0	38.44^{a}	1.93^{a}	8.96^{a}	0.79^{a}	25.01^{a}	0.78^{a}	73.8^{a}
rP68R25M5U1	37.04^{a}	2.01^{a}	8.21^{a}	0.83^{a}	23.29^{b}	0.74^{b}	73.7^{a}
rP51R45M3U0	46.24^{a}	2.60^{a}	17.96^{a}	1.45^{a}	28.36^{a}	1.09^{a}	76.1^{a}
rP50R45M3U1	39.66^{b}	2.68^{a}	13.59^{b}	1.20^{b}	23.97^{b}	0.99^{a}	75.2^{b}

Note; Means within each couple of formulation with the same letter are not significantly different (student's *t*-test, α = 0.05).

9.4.1 Flexural properties

The flexural properties are important factors in decision making of WPCs applications. Figures 9.1(a) and 9.1(b) show the flexural strength and modulus, respectively, of the composites with virgin or recycled polypropylene and different amounts of rubberwood flour. Generally, an increase in the wood flour content (without the coupling agent) clearly decreases the flexural strength, but the flexural modulus slightly increases [20, 21]. It was found in the present work that an increase of RWF content in recycled polypropylene increased the flexural strength. This is because of the reinforcing effect of the wood flour that distributes a uniform stress from a continuous plastic matrix to a dispersed wood flour phase [22, 23]. Likewise, the flexural modulus of composites (both virgin and recycled plastics) linearly increased with wood flour loadings. Since RWF is a high modulus material compared to the plastic matrix, composites with higher wood flour concentration require a higher stress for the same deformation [16]. These results are verified by the statistical analysis of variance. According to the one-way ANOVA of the composites between RWF and rPP or vPP in Table 9.4, the RWF content significantly ($p<5\%$) affects the flexural strength and modulus of the composite materials. Tukey's test in Table 9.2 also indicates that unfilled rPP (suffix *a*) has insignificantly higher flexural strength than rPP composites with 25 wt% RWF (suffix *a*), but unfilled rPP and composites with 25 wt% RWF have significantly lower flexural strength than rPP composites with 45 wt% RWF (suffix b). Furthermore, unfilled vPP and composites based on vPP exhibit higher flexural properties than those based on rPP, for the same plastic to wood ratio. This is probably due to the virgin plastic being stiffer than recycled plastic. The recycled plastic has the lowering of the melt viscosity, which is attributed to decrease of molecular weight [24].

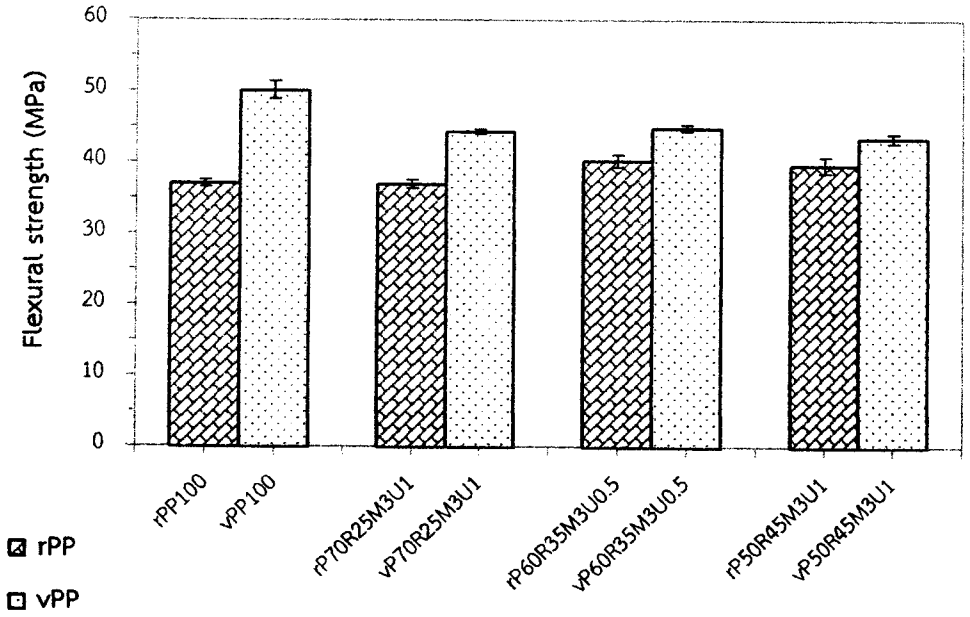

(a)

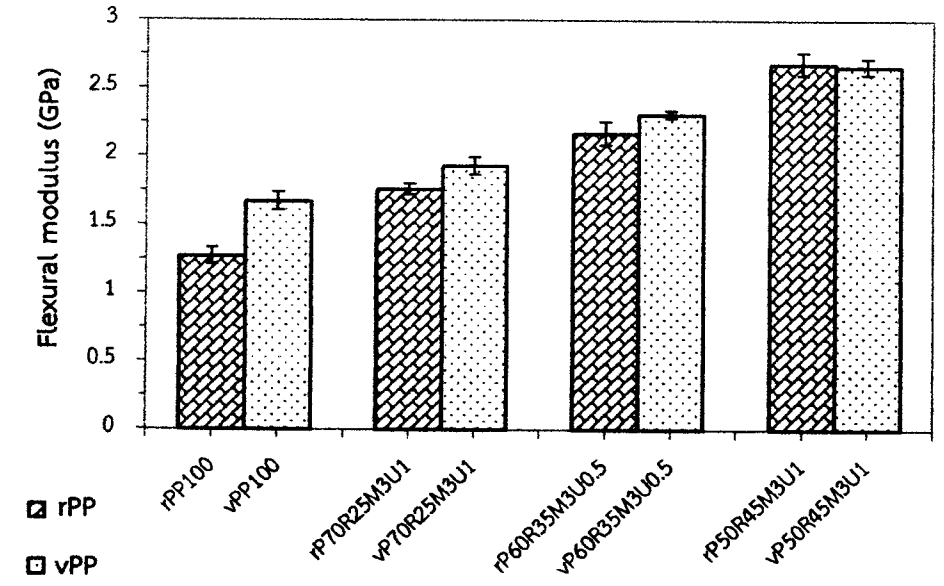

(b)

Figure 9.1 Effect of RWF content and plastic grade on (a) flexural strength and (b) flexural modulus for PP-rubberwood flour composites

Table 9.4 Results of one-way ANOVA for the effect of RWF content on mechanical and physical properties of PP-rubberwood flour composites

	rPP/RWF composites		vPP/RWF composites	
Property	F_0	p-value	F_0	p-value
Flexural strength	4.60	0.003*	22.99	0.000*
Flexural modulus	112.55	0.000*	38.75	0.000*
Compressive strength	10.46	0.003*	13.15	0.001*
Compressive modulus	19.69	0.000*	9.88	0.004*
Tensile strength	0.96	0.417	17.46	0.000*
Tensile modulus	20.82	0.000*	178.66	0.000*
Hardness	112.99	0.000*	23.35	0.000*

*The effect of RWF content is significant at $p < 0.05$.

The effects of different amounts of MAPP and UV stabilizer on the flexural strength and modulus are shown in Figures 9.2(a) and 9.2(b), respectively. The effects of 3 and 5 wt% MAPP additions on the flexural properties of rPP/RWF composites containing 25 wt% RWF show that the addition of 5 wt% MAPP gives higher flexural strength (not statistically significant) and modulus (significantly) than the 3 wt% MAPP addition. This was expected because MAPP can improve the compatibility between wood flour and rPP matrix [8, 21, 22], improving the stress transfer from polymer to wood particles [22]. However, comparing additions of 4 and 5 wt% MAPP, the composites adding 4 wt% MAPP show higher strength (not statistically significant) than composites adding 5 wt% MAPP in accordance with prior research [22, 25]. Too much MAPP relative to wood flour causes self-entanglement, and results in slippage with the PP molecules [22]. These trends conclude that addition of 3 wt% MAPP in composites shows lower flexural properties than those based on additions of 4 and 5 wt% MAPP, and addition of 5 wt% MAPP exhibits lower flexural strength than those based on additions of 4 wt% MAPP. Furthermore, adding 1 wt% UV stabilizer affects the flexural properties of the composites with 25 wt% RWF so that the strength is reduced (not statistically significant), but the modulus increases slightly. Again, composites with 45 wt% RWF showed a significant

decrease in strength with UV stabilizer content. This may be attributed to nonhomogeneous spatial distribution of wood flour, polymer, and UV stabilizer [26].

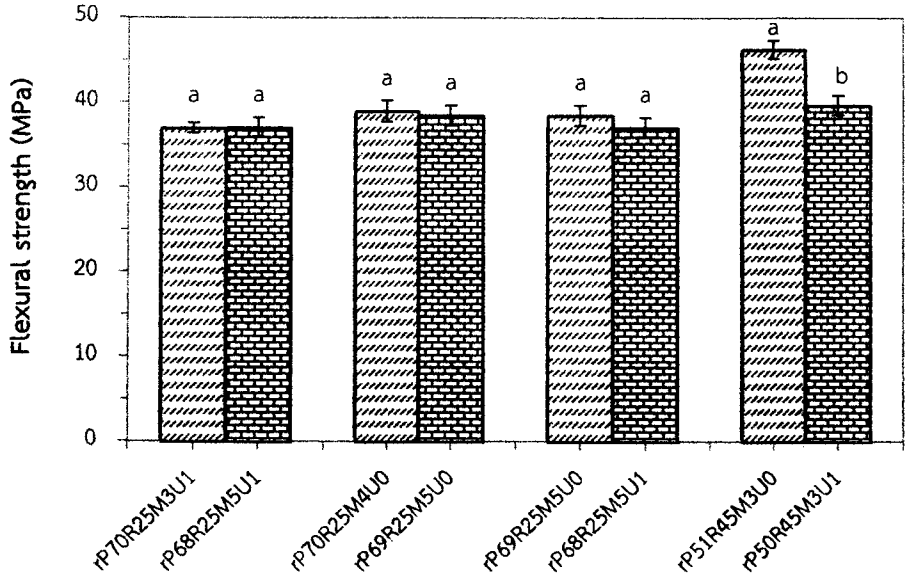

(a)

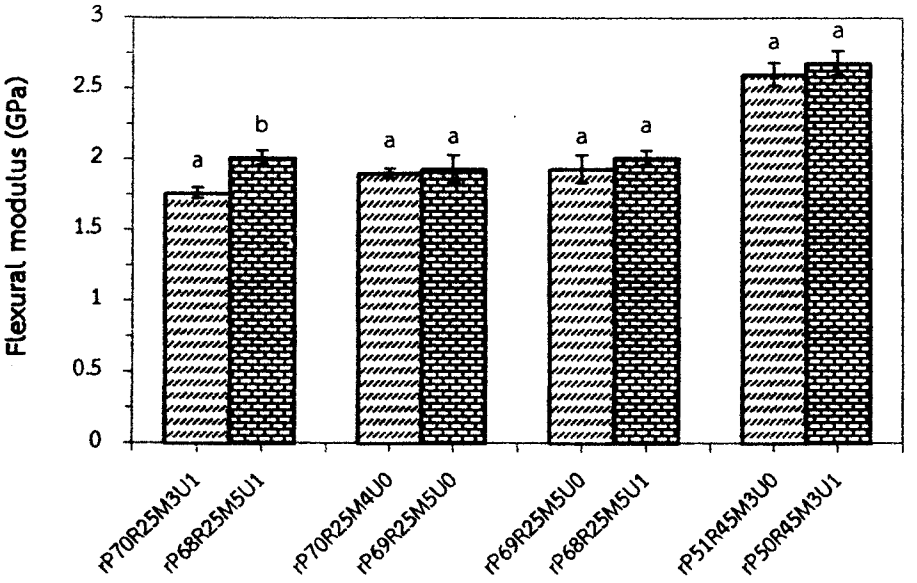

(b)

Figure 9.2 Influence of MAPP and UV stabilizer concentration on (a) flexural strength and (b) flexural modulus of rPP-rubberwood flour composites

9.4.2 Compressive properties

Figures 9.3(a) and 9.3(b) show variation of the compressive strength and modulus with different wood flour loadings, for PP/RWF composites with both virgin and recycled PP. Compressive strength of the composites decreases with the addition of 25 wt% RWF, but increases clearly with the further addition to 35.3 wt% RWF. However, it was observed that the increase of RWF content to 45 wt% exhibits a slight reduction of the compressive strength. This decrease is probably because of weak interfacial bonding of the wood within the polymer, with microcrack formation at the interface [22]. Besides, the compressive modulus exhibited a similar trend to the flexural modulus: the modulus increased progressively with wood flour content. Similar results were found by Garcia et al. [27], reporting that the increase of compressive modulus was caused the wood flour being stiffer than the neat plastics. In addition, composites based on vPP exhibit a similar trend to rPP/RWF composites with increased wood flour loading. The ANOVA results in Table 9.4 demonstrate that the effects of the wood flour concentration on the compressive properties are statistically significant, for both virgin and recycled PP composites.

The effects of MAPP and UV stabilizer contents on the compressive strength and modulus of WPCs are shown in Figures 9.4(a) and 9.4(b), respectively. As can be seen, the compressive properties (both strength and modulus) of composites with MAPP between 3 wt% and 5 wt% showed a similar trend to the flexural properties. However, for the coupling agent MAPP between 4 wt% and 5 wt%, both the strength and the modulus of composites decreased significantly. Furthermore, the change in the compressive strength and modulus with different UV stabilizer concentration, for 25 wt% RWF, is similar to that found in the flexural properties. The composites with 45 wt% RWF show a significant decrease of both strength and modulus with an increase (from 0 to 1 wt%) of UV stabilizer. The reason for this phenomenon is probably similar to that shown in the flexural properties. Using 1 wt% of UV stabilizer may be unnecessary, and to reduce the negative effects on the mechanical properties the amount of UV stabilizer should be minimized [26].

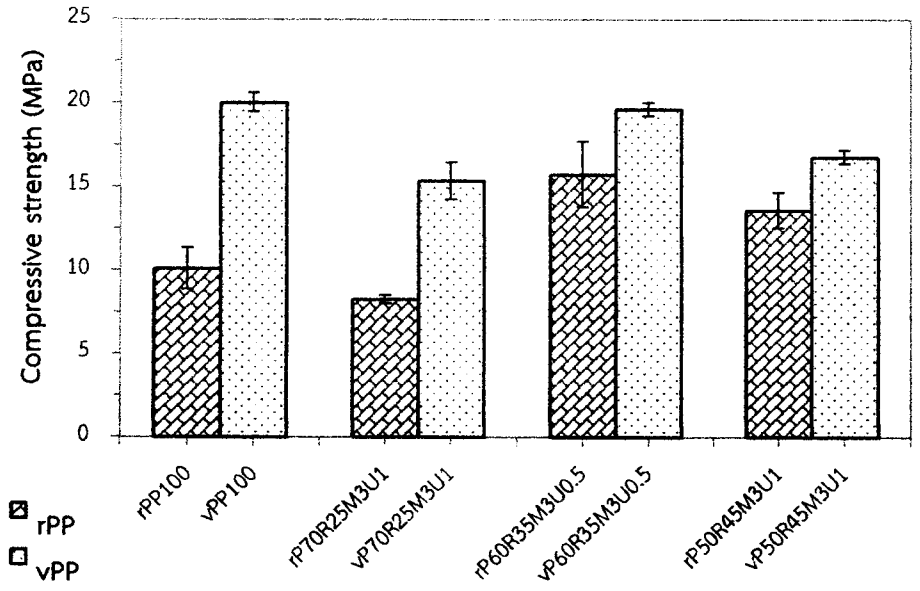

(a)

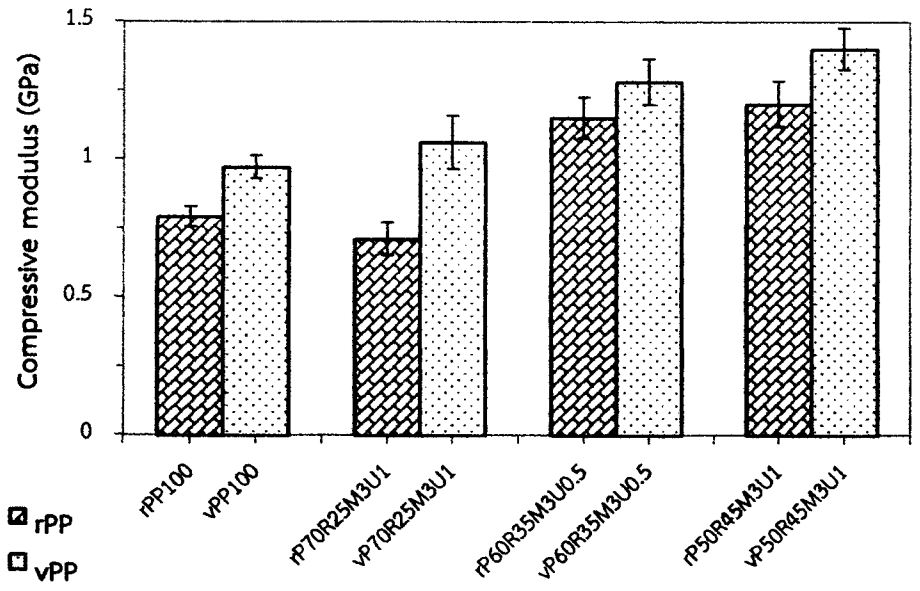

(b)

Figure 9.3 Effect of RWF content and plastic grade on (a) compressive strength and (b) compressive modulus for PP-rubberwood flour composites

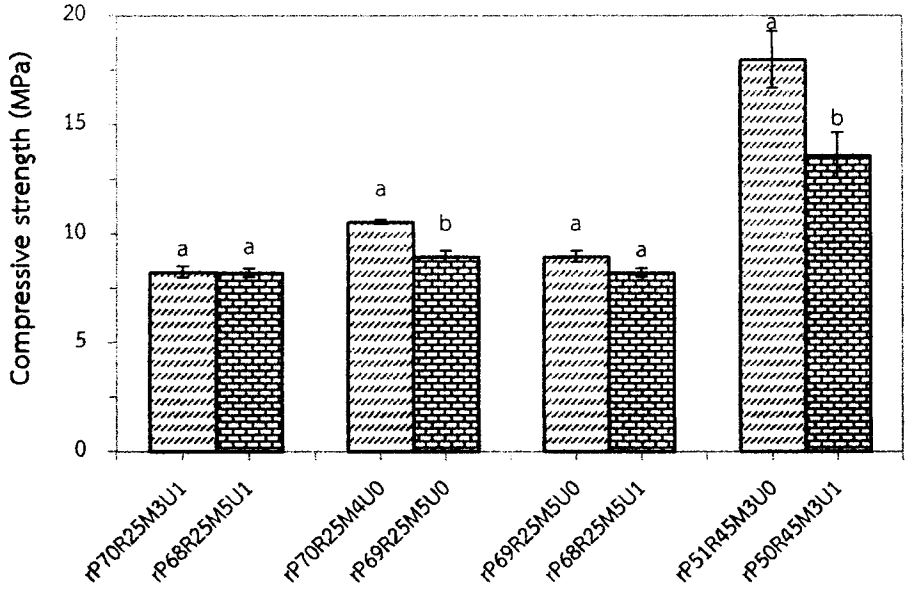

(a)

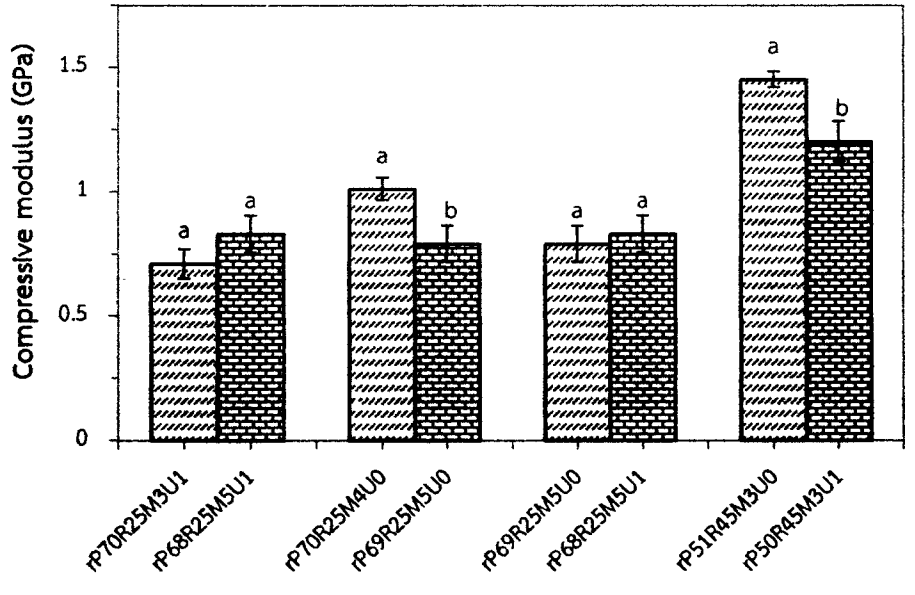

(b)

Figure 9.4 Influence of MAPP and UV stabilizer concentration on (a) compressive strength and (b) compressive modulus of rPP-rubberwood flour composites

9.4.3 Tensile properties

Figures 9.5(a) and 9.5(b) show the tensile strength and modulus of PP/wood flour composites with different rubberwood contents. Both the tensile

strength and modulus exhibited a similar behavior to the flexural properties, increasing slightly with wood flour content. These results can be substantiated by considering the SEM micrographs in Figure 9.6 [Figures 9.6(a), 9.6(b) for 25 wt% RWF and 9.6(c), 9.6(d) for 45 wt% RWF]. It could be seen that the shape of irregular short fibers shows in the composites. The composites containing 25 and 45 wt% RWF had few voids, good dispersion of the fibers in the matrix, and strong interfacial adhesion between the wood flour and the PP matrix. Hence, stress transfer is supported at these high wood flour contents. According to this SEM study, the coupling agent used in the composites improves the compatibility between the wood flour and the PP matrix of all the formulations, resulting in the good interfacial bonding and enhancement of mechanical properties. In contrast, the previous work [20] was found that rPP/RWF composites without the compatibilizer showed numerous cavities and weak interfacial adhesion, and these results in a decrease in the mechanical properties of the composites. Besides, the unfilled vPP and composites based on vPP exhibit higher tensile properties than those based on rPP, for the same plastic to wood flour ratio. Moreover, unfilled vPP has a higher tensile strength than the composites based on vPP. This is because high melt viscosity or low melt flow index (about 7 g/10 min) of vPP reduces the encapsulation of wood flour into the resin, resulting in poor dispersion and weak interfacial bonding between wood particles and polymer. The ANOVA results in Table 9.4 show a statistically significant effect of rubberwood flour content on the tensile properties of reinforced rPP or vPP, although the tensile strength that effects on composites with rPP is not significant at 5% level.

Figures 9.7(a) and 9.7(b) (tensile strength and modulus, respectively) show the influence of MAPP and UV concentrations on the tensile properties of rPP/rubberwood flour composites. The effects of these concentrations have similar trends as in the flexural and compressive properties. Increasing MAPP content between 3 and 5 wt% does not significantly increase the tensile strength but significantly enhances the tensile modulus. In contrast, an increase of UV stabilizer content reduced the tensile properties (both strength and modulus). Potential mechanisms causing these trends were discussed earlier for flexural properties.

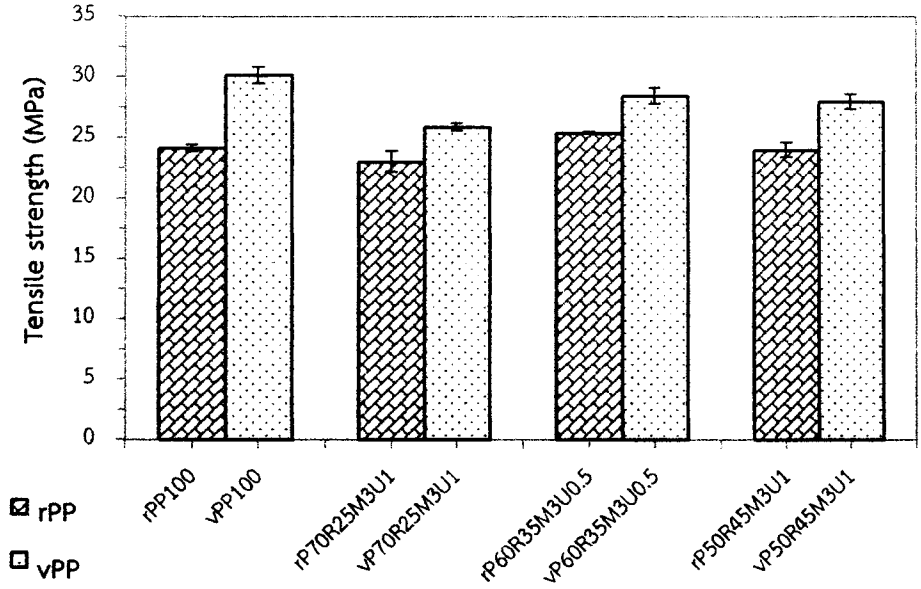

(a)

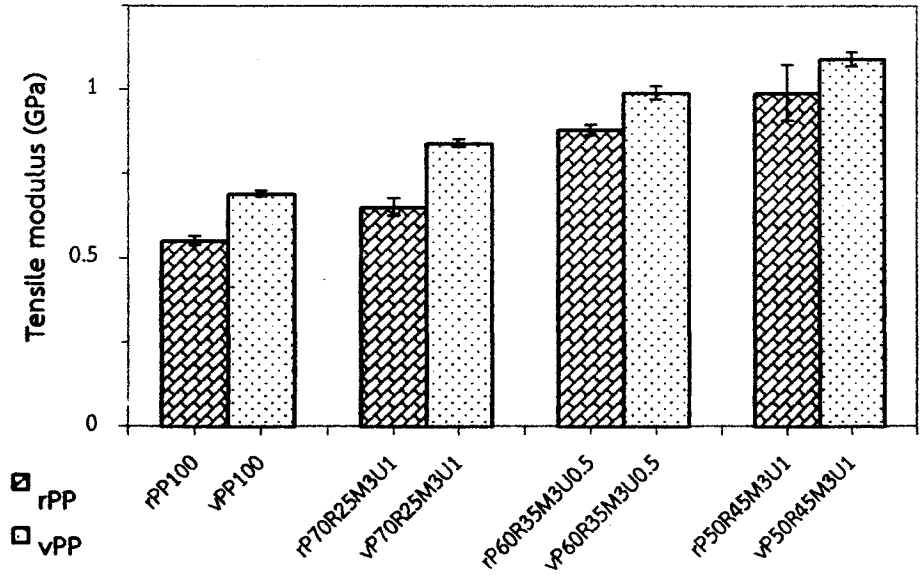

(b)

Figure 9.5 Effect of RWF content and plastic grade on (a) tensile strength and (b) tensile modulus for PP-rubberwood flour composites

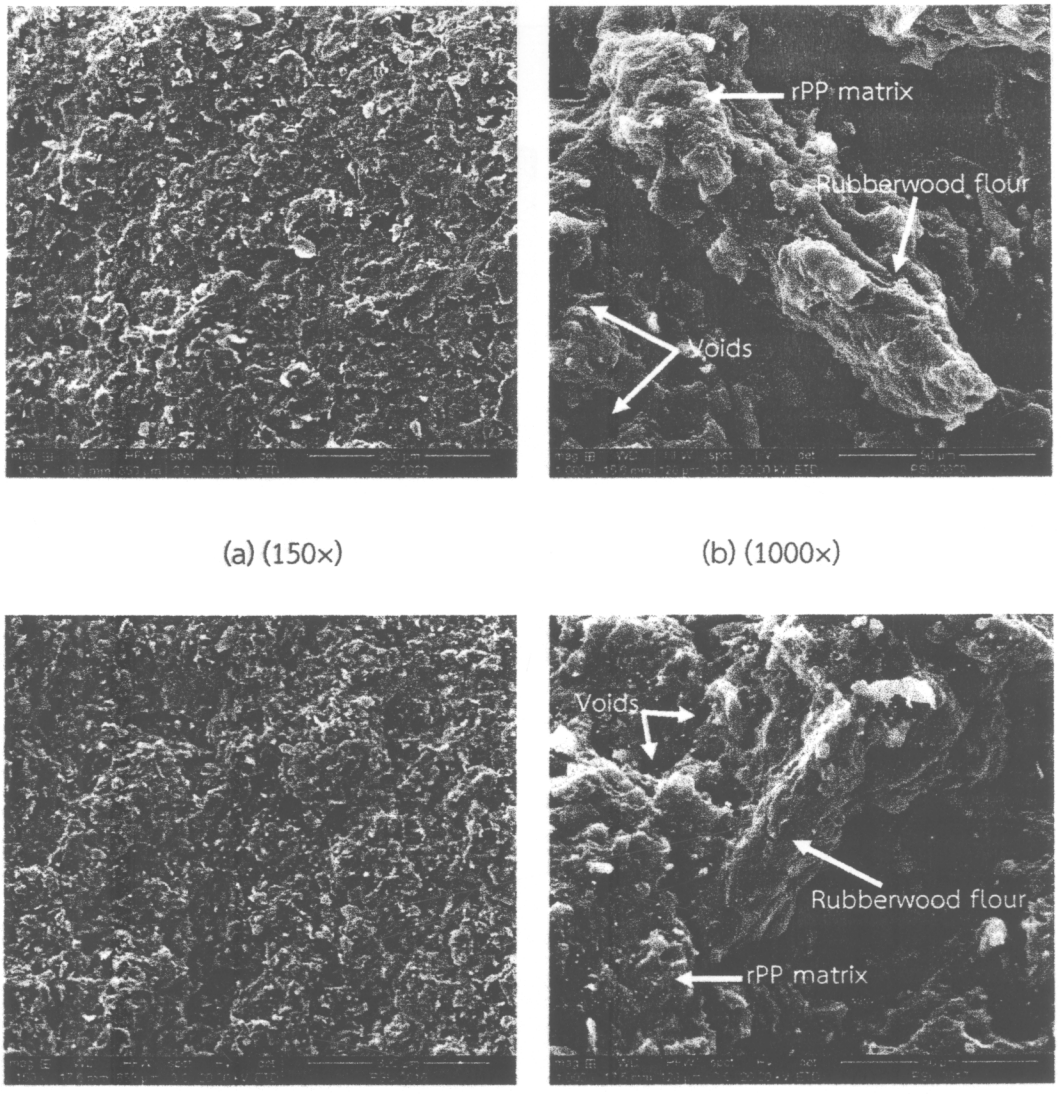

(a) (150×) (b) (1000×)

(c) (150×) (d) (1000×)

Figure 9.6 SEM micrographs of rPP-rubberwood flour composites showing voids, dispersion of the fibers in the matrix, and interfacial adhesion based on various formulations (Magnification 150× and 1000×): (a), (b) rP70R25M3U1 and (c), (d) rP50R45M3U1

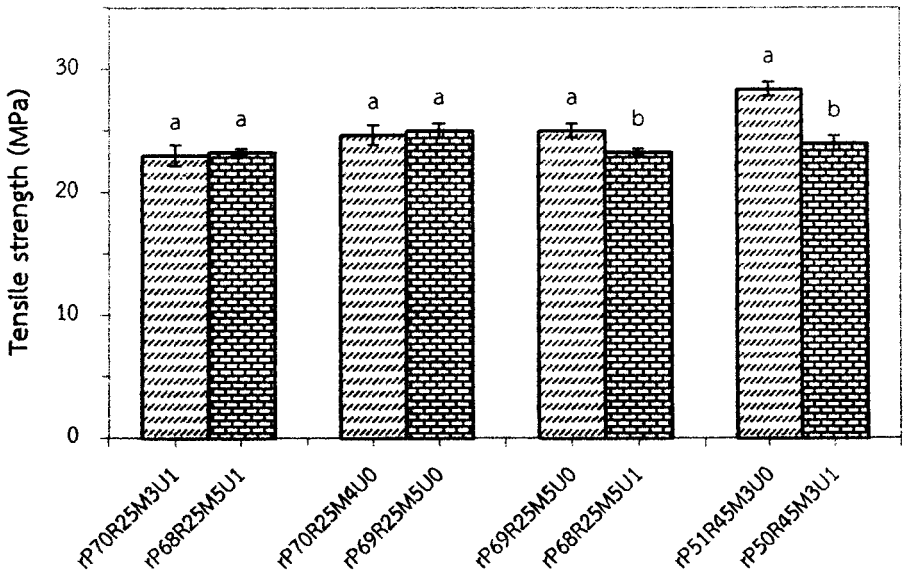

(a)

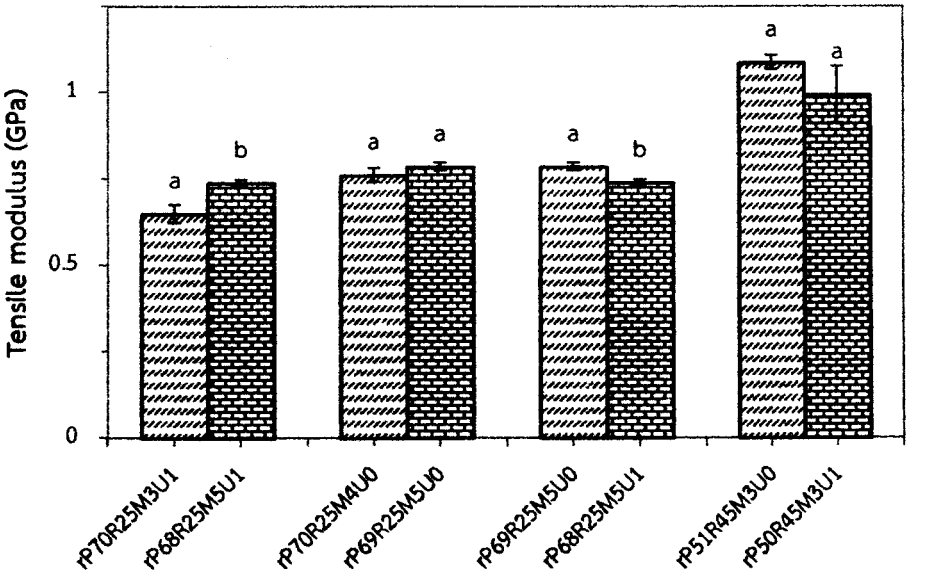

(b)

Figure 9.7 Influence of MAPP and UV stabilizer concentration on (a) tensile strength and (b) tensile modulus of rPP-rubberwood flour composites

9.4.4 Hardness

Figure 9.8 shows the hardness of both virgin and recycled PP/RWF composites with different amounts of wood flour. The average hardness (both for virgin and recycled PP) greatly increased with the reinforcing filler. This is caused by the fact that the wood filler has a considerably higher hardness than the weak plastic matrix [28], and adding RWF decreases flexibility resulting in more rigid composites [16, 29]. The virgin PP/RWF composites seem to have much higher hardness compared to the recycled PP since vPP has lower melt flow index than that of the rPP, leading to lower flexibility composites. Usually, composites with a less flexible matrix have a higher hardness [29]. Moreover, results of the analysis of variance (Table 9.4) show that the hardness of PP/RWF composites was significantly affected by wood flour content.

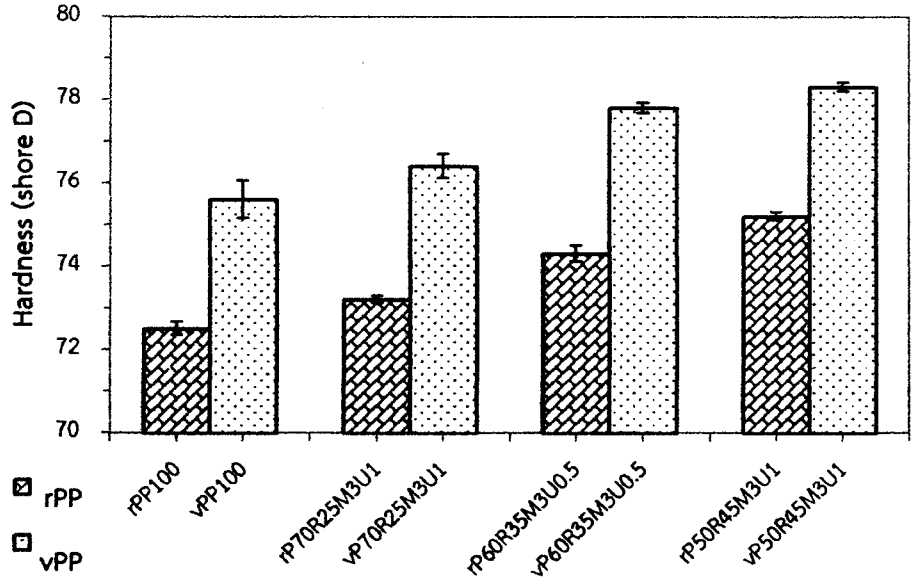

Figure 9.8 Effect of RWF content and plastic grade on hardness for PP-rubberwood flour composites

Hardness of rPP/RWF composites with different coupling agent and UV stabilizer contents are presented in Figure 9.9. The addition of coupling agent to composites based on 25 wt% RWF showed a significant increase of hardness with MAPP concentration. This could be attributed to both better dispersion of the wood

flour into the polymer with minimum voids, and stronger coupling between the RWF and rPP [16, 29]. When the UV stabilizer was added into the composites containing 45 wt% RWF, the hardness decreased significantly. This decrease is probably due to the negative interaction of mixtures (namely wood flour and UV stabilizer).

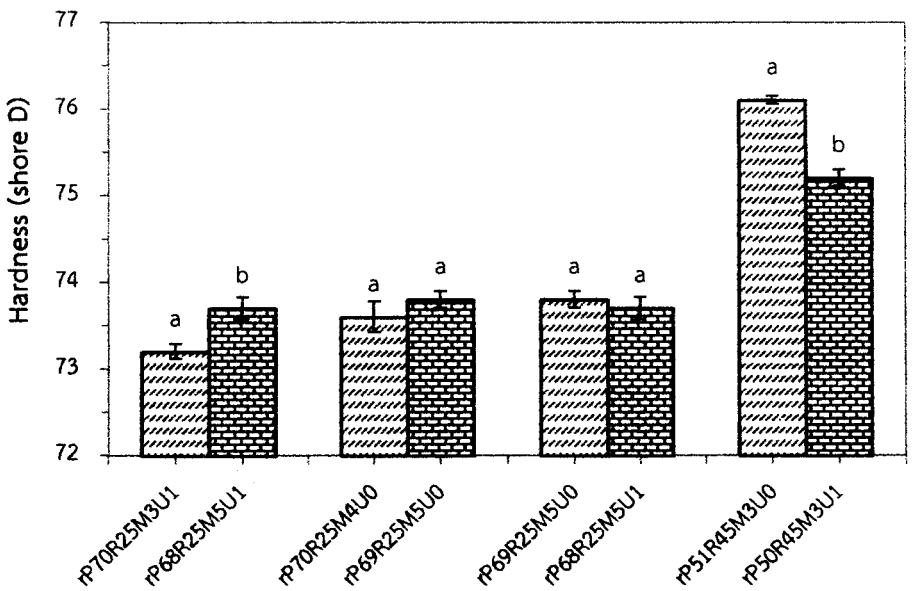

Figure 9.9 Influence of MAPP and UV stabilizer concentration on hardness of rPP-rubberwood flour composites

9.5 Conclusions

The influence of plastic grades (virgin and recycled) and contents of wood flour, coupling agent, and UV stabilizer on the mechanical and physical properties of PP/RWF composites was examined. The results demonstrated that the strengths (flexure, compression, and tension) of RWF reinforced rPP composites could be enhanced with increasing wood flour contents beyond 25 wt%, whereas those composites based on vPP show lower strengths than the unfilled vPP due to poorer encapsulation of wood flour into the resin. The modulus and hardness of composites (both virgin and recycled plastics) increased linearly with wood flour loadings due to the fact that wood flour is much stiffer than the PP matrices. The unfilled rPP and composites based on rPP exhibit lower mechanical properties than those based on vPP for the same plastic to wood ratio. The MAPP content affected on the

mechanical and physical properties of the composites; however, the addition level of 4.0 wt% MAPP in the rPP/wood flour composites is suggested for economical benefit and good mechanical properties. The strength, modulus, and hardness of composites were reduced by an addition of 1 wt% UV stabilizer content. To limit the negative effects of the UV stabilizer on the mechanical properties of the composites, its use should be minimized. The overall result highlights effects of composition and new information to facilitate development of engineering performance of composite materials, making use of wastes and by products from industry, and lending technology towards another effective environmental conservation.

9.6 References

[1] D.R. Carroll, R.B. Stone, A.M. Sirignano, R.M. Saindon, S.C. Gose, and M.A. Friedman. "Structural Properties of Recycled Plastic/Sawdust Lumber Decking Planks." *Resources, Conservation and Recycling*, vol. 31, pp. 241–251, 2011.

[2] I. Ganguly and I.L. Eastin. "Trends in the US Decking Market: A National Survey of Deck and Home Builders." *The Forestry Chronicle*, vol. 85, pp. 82–90, 2009.

[3] N. Sombatsompop, W. Prapruit, K. Chaochanchaikul, T. Pulngern, and V. Rosarpitak. "Effects of Cross Section Design and Testing Conditions on the Flexural Properties of Wood/PVC Composite Beams." *Journal of Vinyl and Additive Technology*, vol. 16, pp. 33–41, 2010.

[4] H. Bouafif, A. Koubaa, P. Perre, and A. Cloutier. "Effects of Fiber Characteristics on the Physical and Mechanical Properties of Wood Plastic Composites." *Composites Part A: Applied Science and Manufacturing*, vol. 40, pp. 1975–1981, 2009.

[5] J. Lisperguer, X. Bustos, and Y. Saravia. "Thermal and Mechanical Properties of Wood Flour-Polystyrene Blends from Postconsumer Plastic Waste." *Journal of Applied Polymer Science*, vol. 119, pp. 443–451, 2011.

[6] S.K. Najafi, E. Hamidinia, and M. Tajvidi. "Mechanical Properties of Composites from Sawdust and Recycled Plastics." *Journal of Applied Polymer Science*, vol. 100, pp. 3641–3645, 2006.

[7] A. Ashori and S. Sheshmani. "Hybrid Composites Made from Recycled Materials: Moisture Absorption and Thickness Swelling Behavior." *Bioresource Technology*, vol. 101, pp. 4717–4720, 2010.

[8] A. Nourbakhsh, A. Ashori, H.Z. Tabari, and F. Rezaei. "Mechanical and Thermo-Chemical Properties of Wood-Flour/Polypropylene Blends." *Polymer Bulletin*, vol. 65, pp. 691–700, 2010.

[9] Z.A. Khan, S. Kamaruddin, and A.N. Siddiquee. "Feasibility Study of Use of Recycled High Density Polyethylene and Multi Response Optimization of Injection Moulding Parameters Using Combined Grey Relational and Principal Component Analyses." *Materials and Design*, vol. 31, pp. 2925–2931, 2010.

[10] S.L. Favaro, M.S. Lopes, A.G.V.d.C. Neto, R.R.d. Santana, and E. Radovanovic. "Chemical, Morphological, and Mechanical Analysis of Rice Husk/Post-Consumer Polyethylene Composites." *Composites Part A: Applied Science and Manufacturing*, vol. 41, pp. 154–160, 2010.

[11] J. Dullius, C. Ruecker, V. Oliveira, R. Ligabue, and S. Einloft. "Chemical Recycling of Post-Consumer PET: Alkyd Resins Synthesis." *Progress in Organic Coatings*, vol. 57, pp. 123–127, 2006.

[12] S.M. Zabihzadeh. "Influence of Plastic Type and Compatibilizer on Thermal Properties of Wheat Straw Flour/Thermoplastic Composites." *Journal of Thermoplastic Composite Materials*, vol. 23, pp. 817–826, 2010.

[13] A. Ashori. "Wood–Plastic Composites as Promising Green-Composites for Automotive Industries!." *Bioresource Technology*, vol. 99, pp. 4661–4667, 2008.

[14] S. Nahar, R.A. Khan, K. Dey, B. Sarker, A.K. Das, and S. Ghoshal. "Comparative Studies of Mechanical and Interfacial Properties between Jute and Bamboo Fiber-Reinforced Polypropylene-Based Composites." *Journal of Thermoplastic Composite Materials*, vol. 25, pp. 15–32, 2012.

[15] M.C.N. Yemele, A. Koubaa, A. Cloutier, P. Soulounganga, and M. Wolcott. "Effect of Bark Fiber Content and Size on the Mechanical Properties of Bark/HDPE Composites." *Composites Part A: Applied Science and Manufacturing*, vol. 41, pp. 131–137, 2010.

[16] M.R. Rahman, M.M. Huque, M.N. Islam, and M. Hasan. "Improvement of Physico-Mechanical Properties of Jute Fiber Reinforced Polypropylene Composites by Post-Treatment." *Composites Part A: Applied Science and Manufacturing*, vol. 39, pp. 1739–1747, 2008.

[17] C.R. Reddy, A.P. Sardashti, and L.C. Simon. "Preparation and Characterization of Polypropylene–Wheat Straw–Clay Composites." *Composites Science and Technology*, vol. 70, pp. 1674–1680, 2010.

[18] P. Petchpradab, T. Yoshida, T. Charinpanitkul, and Y. Matsumura. "Hydrothermal Pretreatment of Rubber Wood for the Saccharification Process." *Industrial and Engineering Chemistry Research*, vol. 48, pp. 4587–4591, 2009.

[19] B. Li, H. Jiang, L. Guo, and H. Shi. "Comparative Study on the Effect of Manchurian Ash and Larch Wood Flour on Mechanical Property, Morphology, and Rheology of HDPE/Wood Flour Composites." *Journal of Applied Polymer Science*, vol. 107, pp. 2520–2530, 2008.

[20] C. Homkhiew, T. Ratanawilai, and W. Thongruang. "Effect of Wood Flour Content and Cooling Rate on Properties of Rubberwood Flour/Recycled Polypropylene Composites." *Advanced Materials Research*, vol. 488–489, pp. 495-500, 2012.

[21] K.B. Adhikary, S. Pang, and M.P. Staiger. "Dimensional Stability and Mechanical Behaviour of Wood-Plastic Composites based Recycled and Virgin High-Density Polyethylene." *Composites Part B: Engineering*, vol. 39, pp. 807–815, 2008.

[22] S. Mohanty, S.K. Verma, S.K. Nayak, and S.S. Tripathy. "Influence of Fiber Treatment on the Performance of Sisal–Polypropylene Composites." *Journal of Applied Polymer Science*, vol. 94, pp. 1336–1345, 2004.

[23] T. Ratanawilai, P. Lekanukit, and S. Urapantamas. "Effect of Rubberwood and Palm Oil Content on the Properties of Wood-Polyvinyl Chloride Composites." *Journal of Thermoplastic Composite Materials*, Epub ahead of print 9 August 2012. DOI: 10.1177/0892705712454863.

[24] J. Aurrekoetxea, M.A. Sarrionandia, I. Urrutibeascoa, and M.L. Maspoch. "Effects of Recycling on the Microstructure and the Mechanical Properties of Isotactic Polypropylene." *Journal of Materials Science*, vol. 36, pp. 2607–2613, 2001.

[25] P.Y. Kuo, S.Y. Wang, J.H. Chen, H.C. Hsueh, and M.J. Tsai. "Effects of Material Compositions on the Mechanical Properties of Wood–Plastic Composites Manufactured by Injection Molding." *Materials and Design*, vol. 30, pp. 3489–3496, 2009.

[26] A. Wechsler and S. Hiziroglu. "Some of the Properties of Wood–Plastic Composites." *Building and Environment*, vol. 42, pp. 2637–2644, 2007.

[27] M. Garcia, J. Hidalgo, I. Garmendia, and J. Garcia-Jaca. "Wood–Plastics Composites with Better Fire Retardancy and Durability Performance." *Composites Part A: Applied Science and Manufacturing*, vol. 40, pp. 1772–1776, 2009.

[28] B. Kord. "Effect of Wood Flour Content on the Hardness and Water Uptake of Thermoplastic Polymer Composites." *World Applied Sciences Journal*, vol. 12, pp. 1632–1634, 2011.

[29] M.R. Rahman, M.M. Huque, M.N. Islam, and M. Hasan. "Mechanical Properties of Polypropylene Composites Reinforced with Chemically Treated Abaca." *Composites Part A: Applied Science and Manufacturing*, vol. 40, pp. 511–517, 2009.

CHAPTER 10

The Optimal Formulation of Recycled Polypropylene/Rubberwood Flour Composites from Experiments with Mixture Design based on Mechanical Properties

10.1 Chapter summary

A mixture design was used in experiments, to determine the optimal mixture for composites of rubberwood flour (RWF) and reinforced recycled polypropylene (rPP). The mixed materials were extruded into panels. Effects of the mixture components rPP, RWF, maleic anhydride-grafted polypropylene (MAPP), and ultraviolet (UV) stabilizer, on the mechanical properties were determined. The overall compositions significantly affected flexural, compressive, tensile and hardness properties. The fractions of recycled polypropylene and rubberwood flour increased all the mechanical material properties; however, increasing one fraction must be balanced by decreasing the other, and the rubberwood flour fraction had a higher effect size. The fraction of MAPP was best kept in mid-range of the fractions tested, while the UV stabilizer fraction overall degraded the mechanical properties. This research suggests that the fraction of UV stabilizer should be as small as possible to minimize its negative influences. The models fitted were used for optimization of a desirability score, substituting for the multiple objectives modeled. The optimal formulation found was 50.3 wt% rPP, 44.5 wt% RWF, 3.9 wt% MAPP, 0.2 wt% UV stabilizer, and 1.0 wt% lubricant with density of 1.085 g/cm^3. The composite made with this formulation had good mechanical properties that closely matched the model predictions.

10.2 Introduction

Wood wastes are generated when wood is processed for various applications, such as in sawmills and in furniture making. The wastes in the forms of

flour, sawdust, and chips have primarily been used as inexpensive filler in plastic industries, to reduce raw material costs and to increase the strength and modulus of various thermoplastics. Likewise, the wood particles show high specific strength and modulus that allow the production of low-density composites with higher filler content [1, 2], and advantages associated with wood particles include their non-abrasive nature, low energy consumption, and biodegradability. Hence, these natural plant based fillers offer several benefits over synthetic fillers [1]. Recent advances in natural fillers may lead to improved materials using renewable resources; this trend would also support global sustainability [3]. The mechanical properties of environmentally friendly plastic composites have been improved with wood wastes from various tree species including eastern red cedar [4], maple [5], oak [4], pine [6], and rubberwood [7]. In addition, the increasing worldwide production and consumption of plastics has caused serious public concerns about effective and safe disposal [8]; however, plastic wastes could be a promising raw material source for wood-plastic composites (WPCs) [9]. The use of recycled plastics for producing WPCs would not only decrease the consumption of energy and natural resources, but also offers an effective way to dispose of plastic wastes [10]. Therefore, increasing the use of wood and plastic wastes could reduce solid waste, lessen the amounts going to landfills, and decrease the costs of making WPCs [6, 8].

A D-optimal mixture experimental design is a special type of statistical approach to experimentally find the individual effects and interactions of components in a mixture, and the fitted models can be used to find the optimal formulation of a composite material [11]. A D-optimal design can considerably reduce the number of experiments needed for scientific and technical information on the composition ratio. It allows restricting the ranges of component fractions, and within this range of formulations helps fit the mathematical models, used to improve the characteristics of final goods [11, 12]. Moreover, this method is appropriate for non-linear models [13].

The fractions of components in wood-plastic composites, such as polymer, filler and coupling agent, significantly affect their mechanical properties. Recently, several publications have assessed the effects of each material component

on the thermal and mechanical properties. Mixture designs and factorial designs have been used in experiments on WPCs. Matuana et al. [14] used a four-factor central composite design to develop a response surface model and to study the foamability of rigid PVC/wood-flour composites. Stark et al. [15] applied a 2^4 factorial design to determine the effects of two hindered amine light stabilizers, a colorant, an ultraviolet absorber, and their interactions on the photostabilization of wood flour/high-density polyethylene composites. Jun et al. [16] used a Box-Behnken design with response surface method to determine which variables influenced board performance significantly. Prior studies on the component effects and interactions, and optimization of the formulation for WPCs, seem not to have used a D-optimal mixture design. Here, a D-optimal mixture design was applied to model mechanical characteristics of WPCs. The main objective of this work is to optimize the mixture ratios for composites made from recycled polypropylene and rubberwood flour, based on mechanical properties determined experimentally. The new information will facilitate informed decisions regarding manufacture of such composites.

10.3 Experimental

10.3.1 Materials

Rubberwood flour (RWF) collected from local furniture factory was used as lignocellulosic filler, and the size of the wood flour particles was smaller than 180 μm, after sieving through a standard sieve of 80 mesh. The chemical composition of RWF was, by weight: cellulose 39%; hemicellulose 29%; lignin 28%; and ash 4% [17]. Recycled polypropylene (rPP) pellets with a melt flow index of 11 g/10 min at 230 °C were supplied by Withaya Intertrade Co., Ltd (Samutprakarn, Thailand) under the trade name WT170. The interfacial adhesion between wood flour and polymer was improved using maleic anhydride-grafted polypropylene (MAPP), supplied by Sigma-Aldrich (Missouri, USA) with 8-10% of maleic anhydride as a coupling agent. The ultraviolet (UV) stabilizer used was hindered amine light stabilizer additive, purchased from TH Color Co., Ltd (Samutprakarn, Thailand) under the trade name MEUV008. Paraffin wax chosen as a lubricant (Lub) was supplied by Nippon Seiro Co., Ltd (Yamaguchi, Japan).

10.3.2 Experimental design to optimize formulation

The responses of a process to various factors and parameters are effectively explored with designed experiments, using approaches such as the taguchi method, factorial design, and mixture design [18, 19]. The fractions of components in a mixture cannot be changed independently, and for these cases the mixture designs are appropriate. The nonnegative fractions must add up to 100%.

The region of interest for the current experiments is not this simplex but has additional constraints added [18], so a D-optimal design was used to statistically evaluate the effects of component fractions on the mechanical properties, and the identified models were used to optimize the formulation. The experimental optimized design had mixture compositions for the manufacture of WPCs, the components being rPP (x_1), RWF (x_2), MAPP (x_3), UV (x_4), and Lub (x_5). The upper and lower limits of experimental range for the compositions are shown in Table 5.1. Despite the fraction of Lub being held constant, it is included as a variable because it contributes to the 100% in the mixture. The experimental design and analysis were done with Design-Expert software (version 8.0.6, Stat-Ease, Inc.), according to D-optimal mixture design. The design included 15 different formulations and 5 replications to check the lack of fit. Thus, the total number of runs was 20, as shown in Tables 10.1 and 10.2. After data collection, linear and quadratic models following equations 2.1 and 2.2, respectively, were used to model the responses.

10.3.3 Composites processing

To minimize its moisture content, the rubberwood flour was carefully dried prior to use in an oven at 110 °C for 8 h. WPCs were then manufactured in a two-stage process. In the first stage to produce WPC pellets, rubberwood flour and recycled polypropylene were dry-blended, and then melt-blended into wood-plastic composite pellets using a twin-screw extruder machine (Model SHJ-36 from En Mach Co., Ltd, Nonthaburi, Thailand). The 10 temperature zones of the extruder were set to a profile in range 130-170 °C, to reduce degradation of the mixture components, while the screw rotating speed was controlled at 70 rpm. The extruded strand passed through a water bath and was subsequently pelletized. In the second stage

to produce WPC panels, the WPC pellets were again dried at 110 °C for 8 h. WPC pellets, MAPP, UV stabilizer, and lubricant compositions indicated in Tables 10.1 and 10.2 were then dry-mixed, and added into the feeder of a twin-screw extruder. The processing conditions for extruding were as follows: (1) barrel temperatures: 130-190 °C; (2) screw rotation speed: 50 rpm; (3) melt pressure: 0.10-0.20 MPa depending on wood flour content; and (4) vacuum venting at nine temperature zones: 0.022 MPa. The samples were extruded through a 9 mm × 22 mm rectangular die and cooled in atmospheric air. Consequently, the specimens were machined following the standards of American Society for Testing and Materials (ASTM) for flexural, compressive, tensile and hardness tests.

Table 10.1 Experimental compositions and hardness response based on mixture experimental design

	Mixture proportion (wt%)					Hardness		Mixture proportion (wt%)					Hardness
Run No.	x_1	x_2	x_3	x_4	x_5	(shore D)	Run No.	x_1	x_2	x_3	x_4	x_5	(shore D)
1	63.9	29.9	4.5	0.7	1.0	73.3 (0.40)**	11	50.0	45.0	3.0	1.0	1.0	75.2 (0.19)
2	70.0	25.0	3.0	1.0	1.0	73.2 (0.17)	12*	50.0	43.0	5.0	1.0	1.0	74.9 (0.44)
3	50.0	43.0	5.0	1.0	1.0	74.8 (0.38)	13	60.3	35.3	3.0	0.5	1.0	74.3 (0.39)
4	54.9	38.9	4.5	0.7	1.0	75.5 (0.40)	14	64.9	30.4	3.5	0.2	1.0	74.6 (0.10)
5	59.5	34.5	5.0	0.0	1.0	74.6 (0.53)	15*	70.0	25.0	3.0	1.0	1.0	72.9 (0.37)
6	55.4	39.9	3.5	0.2	1.0	74.7 (0.46)	16	51.0	45.0	3.0	0.0	1.0	76.1 (0.09)
7	59.5	34.5	4.0	1.0	1.0	74.9 (0.60)	17*	51.0	45.0	3.0	0.0	1.0	75.8 (0.24)
8*	59.5	34.5	5.0	0.0	1.0	75.0 (0.39)	18*	50.0	45.0	3.0	1.0	1.0	74.9 (0.33)
9	50.0	44.3	4.3	0.5	1.0	75.3 (0.51)	19	70.0	25.0	4.0	0.0	1.0	73.6 (0.36)
10	68.0	25.0	5.0	1.0	1.0	73.7 (0.26)	20	69.0	25.0	5.0	0.0	1.0	73.8 (0.19)

Note; *duplicate experiments, **the values in parentheses are standard deviations from five replications.

Table 10.2 Experimental compositions and responses based on mixture experimental design

Experiment	Mixture component fraction (wt%)					Response (MPa)					
						Flexure		Compression		Tension	
run No.	x_1	x_2	x_3	x_4	x_5	MOR	MOE	CS	CM	TS	TM
1	63.9	29.9	4.5	0.7	1.0	39.38	2120	12.43	978	24.86	833
2	70.0	25.0	3.0	1.0	1.0	36.84	1807	9.45	763	23.89	787
3	50.0	43.0	5.0	1.0	1.0	36.91	2429	8.89	1133	23.37	1058
4	54.9	38.9	4.5	0.7	1.0	41.62	2387	14.43	1018	26.17	967
5	59.5	34.5	5.0	0.0	1.0	42.51	1965	14.82	830	26.32	872
6	55.4	39.9	3.5	0.2	1.0	43.97	2472	16.44	1123	28.10	997
7	59.5	34.5	4.0	1.0	1.0	36.64	2119	9.03	945	23.79	961
8*	59.5	34.5	5.0	0.0	1.0	41.41	2040	15.61	915	27.42	867
9	50.0	44.3	4.3	0.5	1.0	40.44	2569	15.02	1287	26.84	1067
10	68.0	25.0	5.0	1.0	1.0	37.04	2007	8.21	826	23.29	738
11	50.0	45.0	3.0	1.0	1.0	39.66	2685	13.59	1202	23.97	993
12*	50.0	43.0	5.0	1.0	1.0	37.85	2485	10.23	1236	24.00	1083
13	60.3	35.3	3.0	0.5	1.0	40.23	2175	15.73	1151	25.38	879
14	64.9	30.4	3.5	0.2	1.0	41.01	1969	13.02	832	25.20	765
15*	70.0	25.0	3.0	1.0	1.0	36.94	1760	8.25	711	23.00	649
16	51.0	45.0	3.0	0.0	1.0	46.24	2601	17.96	1449	28.36	1087
17*	51.0	45.0	3.0	0.0	1.0	47.63	2740	18.20	1418	28.33	1074
18*	50.0	45.0	3.0	1.0	1.0	39.49	2676	11.74	1262	24.70	1024
19	70.0	25.0	4.0	0.0	1.0	38.95	1902	10.55	1006	24.65	760
20	69.0	25.0	5.0	0.0	1.0	38.44	1929	8.96	789	25.01	785

Note; *duplicate experiments

10.3.4 Mechanical properties

Flexural properties were measured in a three-point bending test at a cross-head speed of 2 mm/min, with nominal dimensions of 4.8 mm × 13 mm × 100 mm, and a span of 80 mm in accordance with ASTM D790-92. For compressive properties, prism specimens were used to determine the compressive strength and modulus. The displacement rate was a constant 0.5 mm/min, following ASTM

standard D6108-97. Type-IV tensile bar specimens with dimensions of 115 mm × 19 mm × 4 mm were cut and machined from the extruded composite panels. The cross-head speed of tensile test was 5 mm/min, according to ASTM standard D638-99. The flexural, compressive and tensile measurements were carried out on an Instron Universal Testing Machine (Model 5582 from Instron Corporation, Massachusetts, USA) and performed at ambient conditions of 25 °C. Five replications of each composite formulation were tested. Extrusion is directional and orients the fibers and polymer chains. The composite will not be similar in all directions (isotropic), instead it has a preferred direction. The span in flexural testing was in the extrusion direction, and the same for tensile testing. The compression tests, however, compressed normal to the extrusion direction.

10.3.5 Hardness

Hardness measurement of the composites was tested according to ASTM D2240-91 standard by using mechanical Shore D Durometer (Model GS-702G from Teclock Corporation, Nagano, Japan). The rectangular specimens with dimensions of 16 mm × 16 mm × 6.5 mm were tested. The test was characterized at room temperature (25 °C). Average of five specimens was measured and calculated.

10.4 Results and discussion

The D-optimal mixture design of experiments, with five fractions as (mutually dependent) variables (that sum to one), had 20 runs in a randomized order. The seven determined responses were flexural strength (MOR) and modulus (MOE), compressive strength (CS) and modulus (CM), tensile strength (TS) and modulus (TM), and hardness, and the results are summarized in Tables 10.1 and 10.2.

10.4.1 Statistical analysis of the response models

Analysis of variance (ANOVA) of the response surface models is revealed that quadratic model was best fit with MOR, MOE, CS, CM, and TS than linear and special cubic models except TM and hardness which was fit with linear model. It showed large insignificance of lack of fit, high adjusted coefficient of

determination (adj-R^2), and high predicted coefficient of determination (pred-R^2), when compared with the other models. For example in TS response, the lack of fit of quadratic, special cubic, and linear are 0.5874, 0.3987, and 0.1256 respectively, the adj-R^2 values are 0.9112, 0.9045, and 0.7747 respectively, and the pred-R^2 values are 0.8004, -5.8708, and 0.7051 respectively. The ANOVA analysis in Table 10.3 also shows statistical significance of these models, indicating by p-value less than α (α = 0.05). This result concludes that at least one of the four variables contributes each response. For the linear mixture, fractions of rPP, RWF, MAPP, and UV stabilizer significantly influence ($p<0.0001$) all the mechanical properties. No interaction between the components had a significant effect on MOR, CM, or TS; however, there were significant interactions between rPP and RWF and between MAPP and UV stabilizer for MOE. Regarding of the CS property, the interaction effects between rPP and UV stabilizer, RWF and UV stabilizer, MAPP and UV stabilizer are significant. The frequent interactions with UV stabilizer might indicate it has some chemical reactions with the other components. In addition, the ANOVA also showed that lack of fit was not significant for any of the response surface models at 95% confidence level. This concludes that the regression model fits the data.

The fit of models was also checked by the coefficient of determination (R^2), adj-R^2, pred-R^2, and coefficient of variation (C.V.), see Table 10.4. The R^2 values of the seven response fits are in the range from 0.8336 to 0.9838. The extreme R^2 values of hardness (0.8336) and MOE (0.9838) indicate that only 16.64% and 1.62%, respectively, of the total variability in observations is not explained by the models; R^2 values close to 1 indicate good fits [20]. Also the adj-R^2 values in the range from 0.8024 to 0.9693 suggest good fits; and the same goes for pred-R^2 values. The pred-R^2 value of MOE was 0.9237 meaning that the full model would explain about 92.37% of the variability in new data. The coefficients of variation, of MOR, MOE, CS, CM, TS, TM, and hardness, were estimated at 2.63%, 2.51%, 8.15%, 7.94%, 2.04%, 4.72%, and 0.53%, respectively, based on the replications of experiments. The low C.V. values indicate that the determinations of material characteristics had a good precision, and can serve the fitting of parametric models. Basically, the coefficient of variation was used to measure the residual variation in the data [18].

Table 10.3 P-values from analysis of variance, for the quadratic and linear models, and for the individual interaction terms included in the quadratic models

Resource	MOR	MOE	CS	CM	TS	TM	Hardness
Model	quadratic	quadratic	quadratic	quadratic	quadratic	linear	linear
	<0.0001*	<0.0001*	<0.0001*	0.0002*	<0.0001*	<0.0001*	<0.0001*
Linear Mixture	<0.0001*	<0.0001*	<0.0001*	<0.0001*	<0.0001*	<0.0001*	<0.0001*
x_1x_2	0.5289	0.0072*	0.1054	0.0958	0.9599	-	-
x_1x_3	0.8167	0.3759	0.3675	0.9867	0.3210	-	-
x_1x_4	0.6484	0.0844	0.0171*	0.4518	0.1583	-	-
x_2x_3	0.7577	0.5301	0.3433	0.9665	0.3374	-	-
x_2x_4	0.7047	0.0841	0.0196*	0.4440	0.1918	-	-
x_3x_4	0.5885	0.0195*	0.0273*	0.1605	0.1815	-	-
Lack of Fit	0.0628	0.4678	0.2521	0.0631	0.5874	0.6260	0.0510

*P-value less than 0.05 is considered significant.

Table 10.4 Model adequacy indicators for each response of rPP/RWF composites

Response	R^2	Adj-R^2	Pred-R^2	C.V.
MOR	0.9390	0.8841	0.5496	2.63
MOE	0.9838	0.9693	0.9237	2.51
CS	0.9490	0.9031	0.6751	8.15
CM	0.9258	0.8589	0.6135	7.94
TS	0.9533	0.9112	0.8004	2.04
TM	0.9153	0.8995	0.8577	4.72
Hardness	0.8336	0.8024	0.7663	0.53

10.4.2 Effect of composition on the flexural properties and optimal formulation

The quadratic regression models fitted to experimental MOR and MOE values were:

$$MOR = 39.04x_1 + 47.14x_2 + 107.71x_3 - 646.43x_4 + 2.09x_1x_2 - 77.5x_1x_3 + 668.48x_1x_4 - 102.86x_2x_3 + 555.13x_2x_4 + 728.26x_3x_4 \quad (10.1)$$

$$MOE = 1803.43x_1 + 2743.06x_2 - 11575.14x_3 - 136983x_4 - 573.4x_1x_2 + 16071.92x_1x_3 + 145070x_1x_4 + 11237.53x_2x_3 + 145344.6x_2x_4 + 192792.7x_3x_4 \quad (10.2)$$

The equation of MOR shows a negative coefficient for fraction of UV stabilizer (x_4), and MOE shows negative coefficients for MAPP (x_3) and UV stabilizer (x_4). However, since these are quadratic models, also the quadratic interaction terms must be inspected, for example at some reasonable values of the other fractions. This is why linear models are much more interpretable, and even on inspecting them, the dependency between the fractions (they must sum to one) makes model interpretation difficult. The addition of UV stabilizer in the wood-plastic composites is known to reduce the flexural properties due to non-homogeneous spatial distribution of wood flour, polymer, and UV stabilizer [21]. The covered experimental regions of MOR and MOE are shown in Figures 10.1(a) and 10.1(b), respectively. In these triangular plots the three pure components (rPP, RWF, and MAPP) are represented by the corners, while the additive levels were fixed (UV stabilizer at 0.5 wt% and Lub at 1 wt%). The contours in the colored areas, that include the experimental observations, present the MOR and MOE regression fits varying from 39 to 43 MPa and 2000 to 2600 MPa, respectively. MOR and MOE clearly increase with the rubberwood flour content, and its good interfacial adhesion to recycled polypropylene contributes to this. MAPP acts as a compatibilizer providing a hydrophobic rich layer attached to wood flour [22]. Generally, the strength and modulus of wood flour reinforced composites depend on the properties of constituents and the interfacial adhesion [22]. The MAPP addition of about 3-4 wt% is close to optimal for MOE, based on the regression fit. Similar results were found in the work of Kuo et al. [23] who reported that the optimal content of MAPP was 3-4.5 wt% because of the interfacial adhesion weakens at higher MAPP contents.

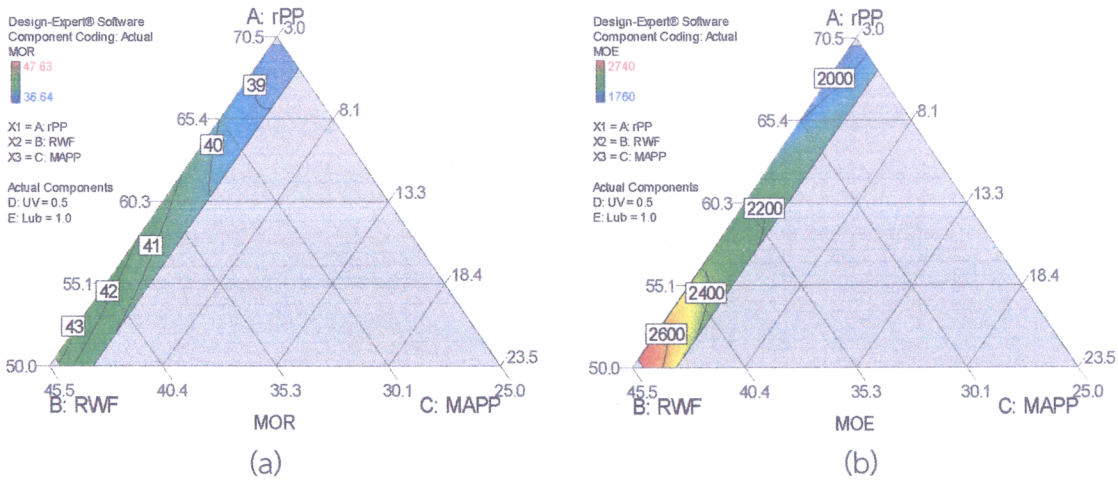

Figure 10.1 Triangular contour plots for composition effects at fixed UV stabilizer fraction of 0.5 wt%, and Lub fraction 1 wt%: (a) MOR, and (b) MOE. The contours represent the models fit to experimental data

Figures 10.2(a) and 10.2(b) show the MOR and MOE model predictions vs. observations. The model outputs fit the actual observations quite well, with MOR model deviating from actual by less than about 5%, and MOE model being slightly more accurate. These correlations verified that the equations 10.1 and 10.2 are adequate to predict the MOR and MOE responses. The numerically optimized composition, based on these model fits, is shown in Figure 10.3. Since two models are optimized simultaneously, the software actually uses a single surrogate called "desirability" to balance them. The model-based optimal formulation is included in Table 10.5.

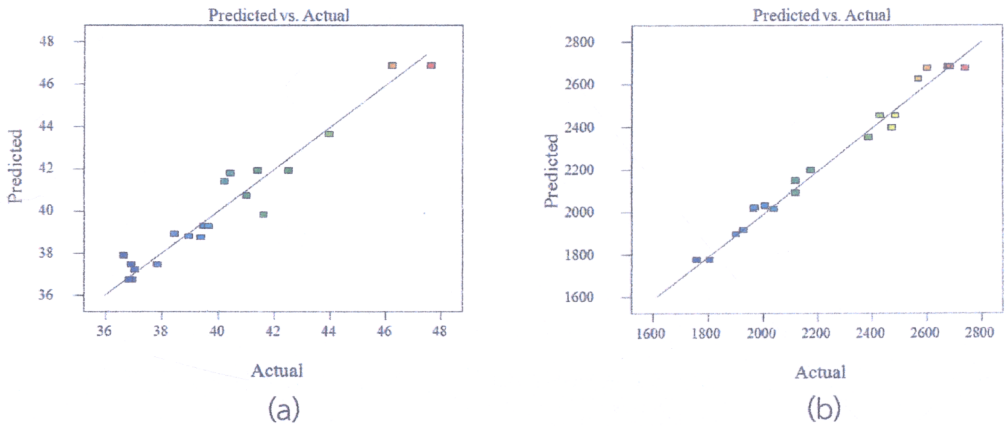

Figure 10.2 Comparisons of model outputs to the fitted observed values for rPP/RWF composites. Model output was (a) MOR and (b) MOE

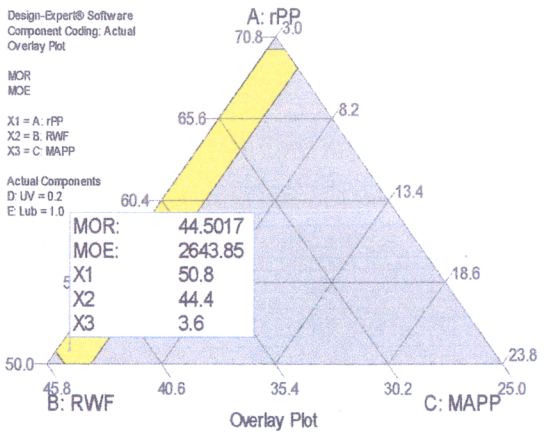

Figure 10.3 The optimal formulation for flexural properties

Table 10.5 Predicted responses with optimized formulation of each property

	Mixture proportion (wt%)					Predicted response			
Property	x_1	x_2	x_3	x_4	x_5	Strength	Modulus	Hardness	Desirability
Flexure (MPa)	50.8	44.4	3.6	0.2	1.0	44.50	2643	-	0.803
Compression (MPa)	51.2	44.2	3.4	0.2	1.0	17.51	1333	-	0.886
Tension (MPa)	50.0	44.8	4.0	0.2	1.0	28.47	1065	-	0.975
Hardness (shore D)	50.0	45.0	3.9	0.1	1.0	-	-	75.73	0.887

10.4.3 Effect of composition on the compressive properties and optimal formulation

The quadratic regression models for the compressive properties CS and CM were:

$$CS = 9.76x_1 + 18.28x_2 + 287.82x_3 - 3776.11x_4 + 5.56x_1x_2 - 299.68x_1x_3 + 3956.09x_1x_4 - 314.6x_2x_3 + 3852.86x_2x_4 + 3278.65x_3x_4 \quad (10.3)$$

$$CM = 1014.25x_1 + 1461.58x_2 - 1406.56x_3 - 87880.43x_4 - 462.14x_1x_2 + 435.39x_1x_3 + 87388.18x_1x_4 - 1096.7x_2x_3 + 89032x_2x_4 + 155014.6x_3x_4 \quad (10.4)$$

Again these equations do not lend themselves to easy interpretation, due to interaction terms and dependencies between the model input variables. This resorts to inspecting plots of the model outputs. Figure 10.4(a) shows that CS (in range of 16

to 10 MPa) decreases for high fractions of the UV stabilizer. The reason for this phenomenon is probably similar to what was discussed in relation to flexural properties. In Figure 10.4(b), the CM values vary in range of 900 to 1300 MPa and increase with wood flour loadings, since wood flour is stiffer than the neat plastic [24]. Likewise, the optimal addition of MAPP for the compressive modulus is approximately 3-4 wt%. Too much MAPP relative to wood flour will cause self-entanglement, resulting in slippage with the PP molecules [25]. Figures 10.5(a) and 10.5(b) display the values of CS and CM model prediction vs. actual observations, and show model precisions of the order 5% for CM and 10% for CS. Figure 10.6 shows the optimal formulation based on these numerical models, and a desirability score combining their outputs. The optimal formulation is included in Table 10.5.

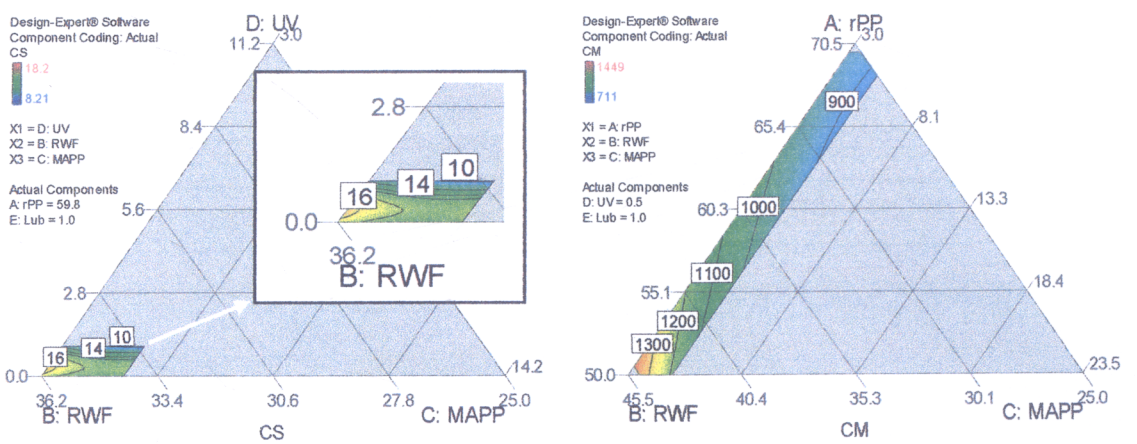

Figure 10.4 Triangular contour plots for effects of the compositions on (a) CS fixed rPP at 59.8 wt%, Lub at 1 wt% and (b) CM fixed UV stabilizer at 0.5 wt%, Lub at 1 wt%

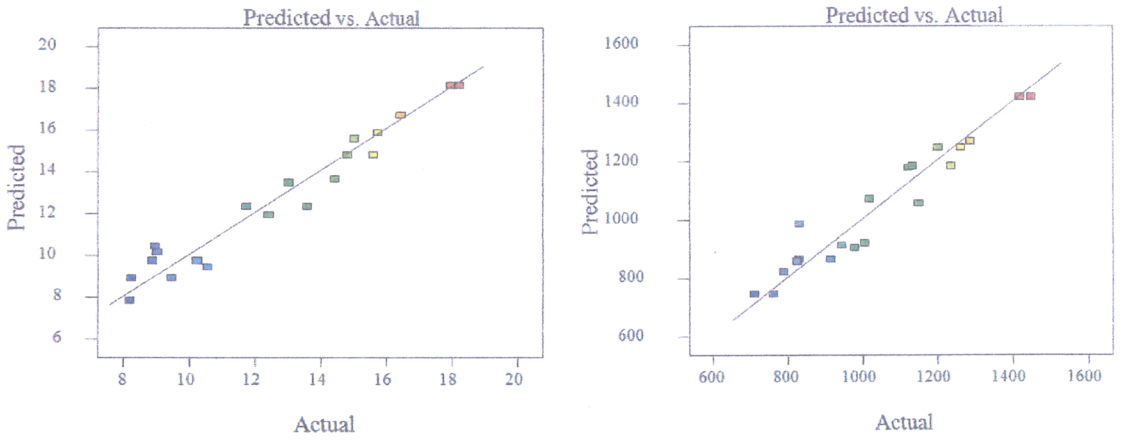

(a) (b)

Figure 10.5 Comparisons of model outputs to the fitted observed values for rPP/RWF composites. Model output was (a) CS and (b) CM

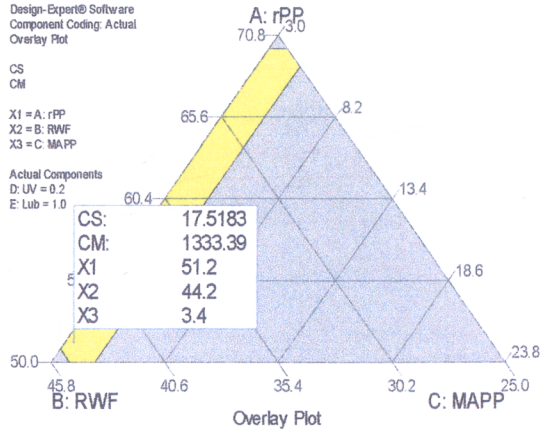

Figure 10.6 The optimal formulation for compressive properties

10.4.4 Effect of composition on the tensile properties and optimal formulation

The regression fits for the tensile strength (TS) and modulus (TM) were:

$$TS = 23.54x_1 + 28.64x_2 - 112.44x_3 - 989.02x_4 + 0.081x_1x_2 + 166.14x_1x_3 + 1059.37x_1x_4 + 159.72x_2x_3 + 973.37x_2x_4 + 914.15x_3x_4 \quad (10.5)$$

$$TM = 717.6x_1 + 1067.03x_2 + 1114.53x_3 + 687.04x_4 \quad (10.6)$$

By these equations, rPP (x_1) and RWF (x_2) increase the tensile properties; all terms containing these variables have positive coefficients. Of these two, RWF has the larger coefficient in the fit for TS and TM, so it should be maximized. The fractions of MAPP (x_3) and UV stabilizer (x_4) each have both positive and negative coefficients in the model for tensile strength, but both increase the tensile modulus. Figures 10.7(a) and 10.7(b) show that TS and TM increase with the rubberwood flour content. The composition optimized based on these regression models is shown graphically in Figure 10.8, and numerically in Table 10.5.

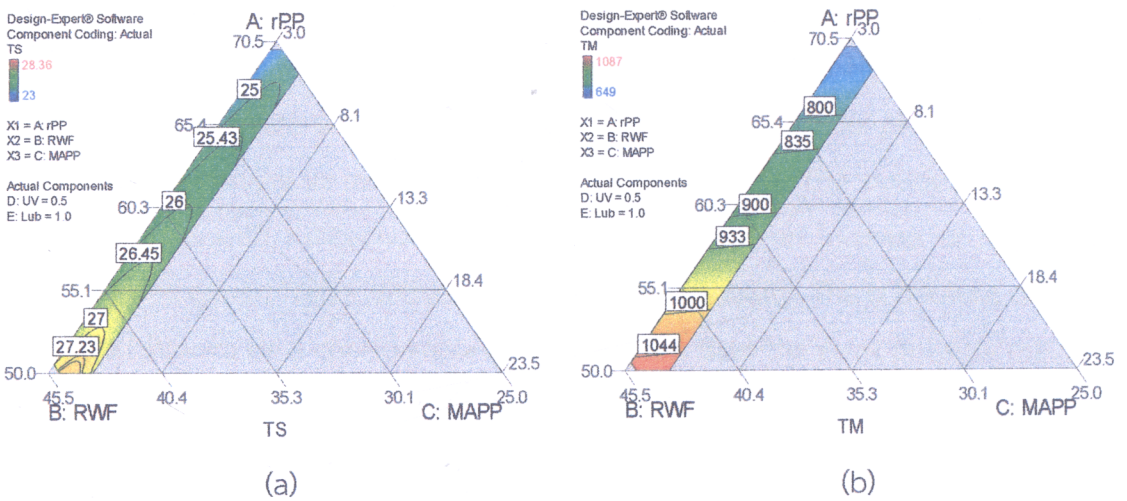

Figure 10.7 Composition effects on (a) TS and (b) TM. The fractions held fixed were UV stabilizer at 0.5 wt% and Lub at 1 wt%. The contours represent the numerical models fitted to experimental observations

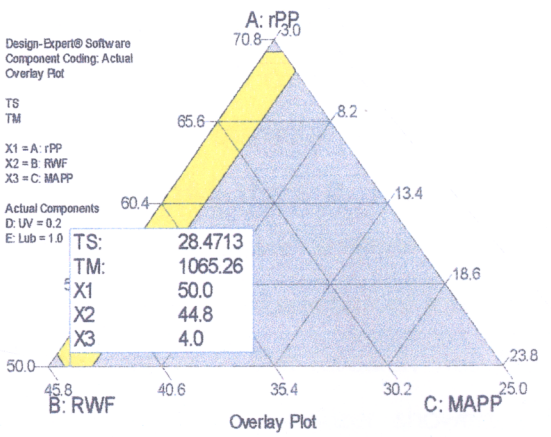

Figure 10.8 The optimal formulation for tensile properties

10.4.5 Effect of composition on the hardness property and optimal formulation

Linear significant model, the hardness property affected by the WPC compositions, was obtained from the hardness response. The equation calculated from the regression data was:

$$\text{Hardness} = 73.74x_1 + 75.82x_2 + 75.12x_3 + 62.02x_4 \quad (10.7)$$

The linear equation of hardness shows positive coefficient of all the compositions, revealing the positive effect on the hardness property. The rubberwood flour (x_2) yielded the highest positive effect as compared with the other compositions. The covered experimental regions of hardness property are shown in Figures 10.9(a) and 10.9(b). As seen in Figure 10.9(a), the clear area in triangular contour plot reveals the hardness values varying in range of 73.66 to 75.38 shore D. The average hardness greatly increased with rubberwood flour loading, whereas an increase of recycled polypropylene content highly decreased the hardness property. This is because of the rubberwood filler to be a considerably higher hardness than the weak polymer matrix [26, 27], and flexibility was reduced by an increase of RWF content, resulting in more rigid composites [28, 29]. The enhancing addition of MAPP (from 3 to 5 wt%) unaffected the hardness property as shown in the contour plot [Figure 10.9(a)]. Generally, addition of the coupling agent to the composites increases the hardness with MAPP concentration. This is due to both stronger coupling between the RWF and rPP and better dispersion of the wood flour into the plastic matrix with minimum voids [27-29]. Furthermore, the effect of UV stabilizer addition is also exhibited in the contour plot [Figure 10.9(b)], in which two compositions fixed were the rPP at 59.8 wt% and the Lub at 1 wt%. The area in triangular contour plot presents the hardness values varying in range of 74.2 to 74.8 shore D. The hardness value of rPP/RWF composites slightly reduced with increasing addition of the UV stabilizer. This decrease is attributed due to the negative interaction of mixtures (namely wood flour and UV stabilizer) [27]. In the chapter 9, this research was found that composites containing 45 wt% RWF and 1 wt% UV stabilizer showed a higher decrease of hardness value than composites with 25 wt% RWF and 1 wt% UV. The composition

optimized based on linear regression model is shown graphically in Figure 10.10, and numerically in Table 10.5.

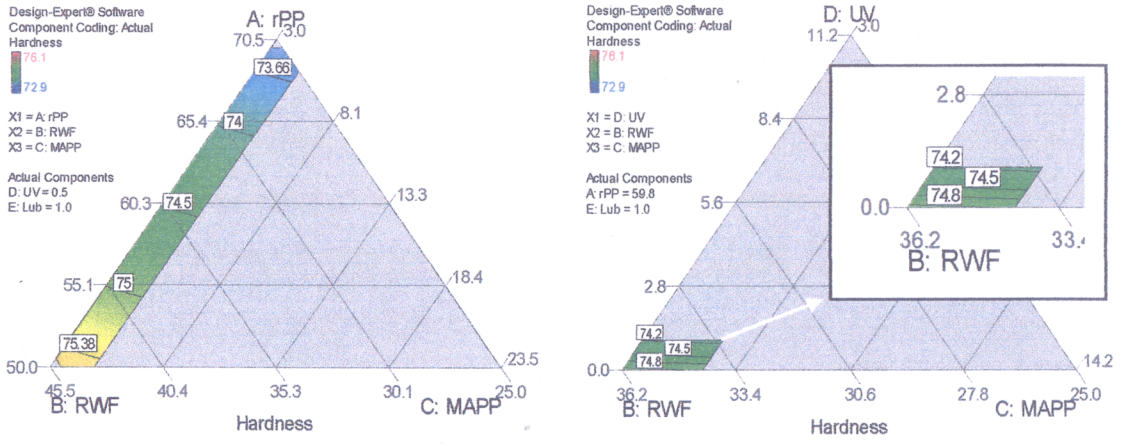

(a) (b)

Figure 10.9 Contour plots for effects of the compositions on hardness (a) fixed UV stabilizer at 0.5 wt%, Lub at 1 wt% and (b) fixed rPP at 59.8 wt%, Lub at 1 wt%

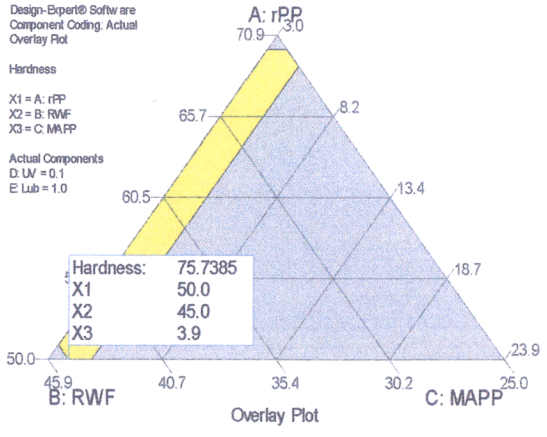

Figure 10.10 The optimal formulation for hardness property

10.4.6 Optimal formulation of the overall mechanical properties

Multiobjective optimization using all of the regression models was performed with the Design-Expert software, using its default settings to construct a desirability score that balances all of the fitted models. The plot in Figure 10.11 shows the formulation that was considered optimal, along with contours of the

desirability score. The optimal formulation is given in Table 10.6, and can be compared with the formulations in Table 10.5: all the previous optima were practical at the same formulation, so a reasonable desirability score must also give this formulation. Table 10.6 also shows the model predicted responses for this formulation. Test samples with five replications were prepared with this formulation, and the average material properties along with their standard deviations are also included in Table 10.6. The maximum deviation between model prediction and experimental average occurs for MOR and is the order 10%.

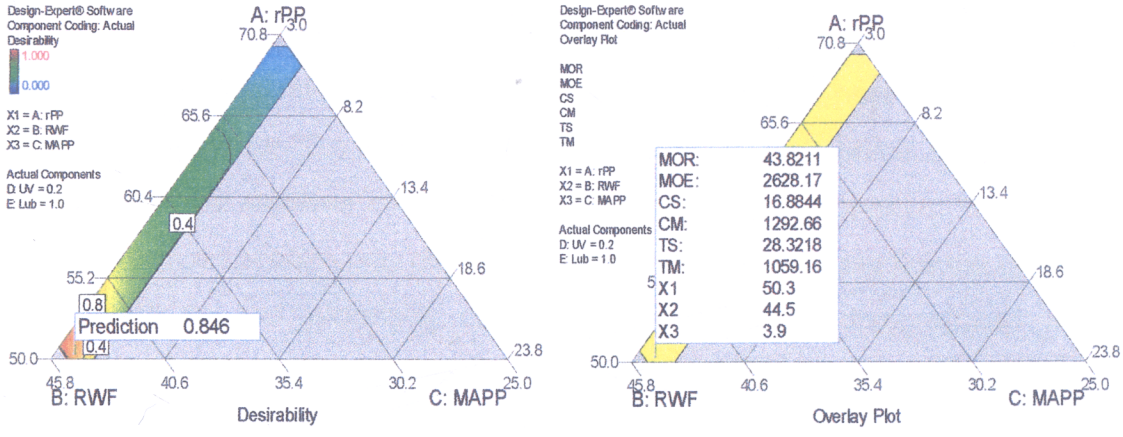

Figure 10.11 The optimal formulation for overall desirability

Table 10.6 Predicted and observed responses with the formulation optimized jointly for all the mechanical properties

	Mixture component proportion (wt%)					Response (MPa)					
						Flexure		Compression		Tension	
	x_1	x_2	x_3	x_4	x_5	MOR	MOE	CS	CM	TS	TM
Predicted	50.3	44.5	3.9	0.2	1.0	43.82	2628	16.88	1292	28.32	1059
Observed						47.28	2527	17.11	1369	27.68	1024
						(2.92)*	(112)	(2.72)	(109)	(2.41)	(128)

*The values in parentheses are standard deviations from five replications. The optimal formulation has the density of 1.085 g/cm^3.

10.5 Conclusions

Design and analysis of a D-optimal mixture experiment were used to obtain the optimal formulation of rPP/RWF composites. The formulation provides high values for all the material characteristics modeled. Analysis of variance revealed that all the component fractions experimentally varied, namely of rPP, RWF, MAPP, and UV stabilizer, significantly affected every one of the mechanical properties (MOR, MOE, CS, CM, TS, TM, and hardness). In general, a high fraction of RWF improved all of these, and the optima found had close to 45% RWF which was the maximum in the experimental design. At this wood flour loading stress transfer was still supported by good dispersion and surface contact with the polymer; and the wood flour is much stiffer than the rPP matrix. The compatibilizer MAPP had negative effects on MOE and CM, while for TS a middle of the range value seemed optimal [Figure 7(a)]. The fraction of UV stabilizer overall reduced the mechanical properties. While the actual optimal composition may depend on a variety of factors, including the quality of raw materials and processing conditions, this work has demonstrated the applicability of particular techniques to optimizing properties of composites. In this case, the optima for various mechanical properties agreed well, while in general the joint optimization of multiple responses will depend on their prioritization.

10.6 References

[1] A. Ashori and A. Nourbakhsh. "Performance Properties of Microcrystalline Cellulose as a Reinforcing Agent in Wood Plastic Composites." *Composites Part B: Engineering*, vol. 41, pp. 578–581, 2010.

[2] W. Liu, L.T. Drzal, A.K. Mohanty, and M. Misra. "Influence of Processing Methods and Fiber Length on Physical Properties of Kenaf Fiber Reinforced Soy Based Biocomposites." *Composites Part B: Engineering*, vol. 38, pp. 352–359, 2007.

[3] H.Y. Cheung, M.P. Ho, K.T. Lau, F. Cardona, and D. Hui. "Natural Fibre-Reinforced Composites for Bioengineering and Environmental Engineering Applications." *Composites Part B: Engineering*, vol. 40, pp. 655–663, 2009.

[4] J.W. Kim, D.P. Harper, and A.M. Taylor. "Effect of Wood Species on the Mechanical and Thermal Properties of Wood–Plastic Composites." *Journal of Applied Polymer Science*, vol. 112, pp. 1378–1385, 2009.

[5] T. Li and N. Yan. "Mechanical Properties of Wood Flour/HDPE/Ionomer Composites." *Composites Part A: Applied Science and Manufacturing*, vol. 38, pp. 1–12, 2007.

[6] K.B. Adhikary, S. Pang, and M.P. Staiger. "Dimensional Stability and Mechanical Behaviour of Wood-Plastic Composites based Recycled and Virgin High-Density Polyethylene." *Composites Part B: Engineering*, vol. 39, pp. 807–815, 2008.

[7] C. Homkhiew, T. Ratanawilai, and W. Thongruang. "Effect of Wood Flour Content and Cooling Rate on Properties of Rubberwood Flour/Recycled Polypropylene Composites." *Advanced Materials Research*, vol. 488–489, pp. 495-500, 2012.

[8] A. Ashori and S. Sheshmani. "Hybrid Composites Made from Recycled Materials: Moisture Absorption and Thickness Swelling Behavior." *Bioresource Technology*, vol. 101, pp. 4717–4720, 2010.

[9] S.K. Najafi, E. Hamidinia, and M. Tajvidi. "Mechanical Properties of Composites from Sawdust and Recycled Plastics." *Journal of Applied Polymer Science*, vol. 100, pp. 3641–3645, 2006.

[10] Z.A. Khan, S. Kamaruddin, and A.N. Siddiquee. "Feasibility Study of Use of Recycled High Density Polyethylene and Multi Response Optimization of Injection Moulding Parameters Using Combined Grey Relational and Principal Component Analyses." *Materials and Design*, vol. 31, pp. 2925–2931, 2010.

[11] Y.B. Khosrowshahi and A. Salem. "Influence of Polyvinyl Alcohol and Carboxymethyl Cellulose on the Reliability of Extruded Ceramic Body: Application of Mixture Design Method in Fabricating Reliable Ceramic Raschig Rings." *International Journal of Applied Ceramic Technology*, vol. 8, pp. 1334–1343, 2011.

[12] R.C.S. John. "Experiments with Mixtures, Ill-Conditioning, and Ridge Regression." *Journal of Quality Technology*, vol. 16, pp. 81–96, 1984.

[13] A. Mannarswamy, S.H. Munson-McGee, and P.K. Andersen. "D-optimal Designs for the Cross Viscosity Model Applied to Guar Gum Mixtures." *Journal of Food Engineering*, vol. 97, pp. 403–409, 2010.

[14] L.M. Matuana and F. Mengeloglu. "Manufacture of Rigid PVC/Wood-Flour Composite Foams Using Moisture Contained in Wood as Foaming Agent." *Journal of Vinyl and Additive Technology*, vol. 8, pp. 264–270, 2002.

[15] N.M. Stark and L.M. Matuana. "Ultraviolet Weathering of Photostabilized Wood-Flour-Filled High-Density Polyethylene Composites." *Journal of Applied Polymer Science*, vol. 90, pp. 2609–2617, 2003.

[16] Z. Jun, W. Xiang-Ming, C. Jian-Min, and Z. Kai. "Optimization of Processing Variables in Wood–Rubber Composite Panel Manufacturing Technology." *Bioresource Technology*, vol. 99, pp. 2384–2391, 2008.

[17] P. Petchpradab, T. Yoshida, T. Charinpanitkul, and Y. Matsumura. "Hydrothermal Pretreatment of Rubber Wood for the Saccharification Process." *Industrial and Engineering Chemistry Research*, vol. 48, pp. 4587–4591, 2009.

[18] D.C. Montgomery. *Design and Analysis of Experiments*. John Wiley & Sons, Inc., 2009.

[19] F. Mirjalili, S. Moradian, and F. Ameri. "Attaining Optimal Dyeability and Tensile Properties of Polypropylene/Poly(ethylene terephthalate) Blends with a Special Cubic Mixture Experimental Design." *Journal of Applied Polymer Science*, vol. 121, pp. 3201–3210, 2011.

[20] M. Amini, H. Younesi, N. Bahramifar, A.A.Z. Lorestani, F. Ghorbani, A. Daneshi, and M. Sharifzadeh. "Application of Response Surface Methodology for Optimization of Lead Biosorption in an Aqueous Solution by Aspergillus Niger." *Journal of Hazardous Materials*, vol. 154, pp. 694–702, 2008.

[21] A. Wechsler and S. Hiziroglu. "Some of the Properties of Wood–Plastic Composites." *Building and Environment*, vol. 42, pp. 2637–2644, 2007.

[22] A. Ashori and A. Nourbakhsh. "Mechanical Behavior of Agro-Residue-Reinforced Polypropylene Composites." *Journal of Applied Polymer Science*, vol. 111, pp. 2616–2620, 2009.

[23] P.Y. Kuo, S.Y. Wang, J.H. Chen, H.C. Hsueh, and M.J. Tsai. "Effects of Material Compositions on the Mechanical Properties of Wood-Plastic Composites Manufactured by Injection Molding." *Materials and Design*, vol. 30, pp. 3489-3496, 2009.

[24] M. Garcia, J. Hidalgo, I. Garmendia, and J. Garcia-Jaca. "Wood-Plastics Composites with Better Fire Retardancy and Durability Performance." *Composites Part A: Applied Science and Manufacturing*, vol. 40, pp. 1772-1776, 2009.

[25] S. Mohanty, S.K. Verma, S.K. Nayak, and S.S. Tripathy. "Influence of Fiber Treatment on the Performance of Sisal-Polypropylene Composites." *Journal of Applied Polymer Science*, vol. 94, pp. 1336-1345, 2004.

[26] B. Kord. "Effect of Wood Flour Content on the Hardness and Water Uptake of Thermoplastic Polymer Composites." *World Applied Sciences Journal*, vol. 12, pp. 1632-1634, 2011.

[27] C. Homkhiew, T. Ratanawilai, and W. Thongruang. "Composites from Recycled Polypropylene and Rubberwood Flour: Effects of Composition on Mechanical Properties." *Journal of Thermoplastic Composite Materials*, Epub ahead of print 14 February 2013. DOI: 10.1177/0892705712475019.

[28] M.R. Rahman, M.M. Huque, M.N. Islam, and M. Hasan. "Improvement of Physico-Mechanical Properties of Jute Fiber Reinforced Polypropylene Composites by Post-Treatment." *Composites Part A: Applied Science and Manufacturing*, vol. 39, pp. 1739-1747, 2008.

[29] M.R. Rahman, M.M. Huque, M.N. Islam, and M. Hasan. "Mechanical Properties of Polypropylene Composites Reinforced with Chemically Treated Abaca." *Composites Part A: Applied Science and Manufacturing*, vol. 40, pp. 511-517, 2009.

CHAPTER 11

Time-Temperature and Stress Dependent Behaviors of Composites between Recycled Polypropylene and Rubberwood Flour

11.1 Chapter summary

In previous chapter (Chapter 10), the optimal composite formulation on mechanical properties found was 50.3 wt% rPP, 44.5 wt% RWF, 3.9 wt% MAPP, 0.2 wt% UV stabilizer, and 1.0 wt% Lub with density 1.085 g/cm^3, flexural strength 47.28 MPa, and modulus 2527 MPa. Therefore, this chapter used such formulation to investigate the time-temperature and stress dependent behaviors of the composites. The effects of time, temperature, and stress on the flexural creep of composites from recycled polypropylene and rubberwood flour were experimentally investigated and modeled numerically. The composites were formed into panel samples with a twin-screw extruder. The creep increased with time, temperature, and stress. The Burger, Power law, and HRZ models fit the creep profiles well in general, but at high temperature and stress levels the Power law and HRZ models performed poorly. However, the HRZ model interpolated creep well across the applied stresses, or across the temperatures. The time-temperature superposition (TTS) and the time-stress superposition (TSS) principles were used to model long-term creep. The master curves from TTS and TSS principles were in good agreement with each other. They predicted that the lifetime limitation by long-term creep exceeds 10 years for 15 MPa stress at 25 °C, and is irrelevant for 3 MPa stress at the same temperature. All these results pertain to a specific formulation of rPP/RWF composites.

11.2 Introduction

In recent decades, reinforcing thermoplastics with inorganic fibers such as carbon, glass, graphite, and talc have successfully produced high performance composites [1]. Likewise, the reinforcement of organic fibers in plastic composites,

particularly use of wood flour, is great interest due to several potential advantages, such as low cost, biodegradability, low health hazard during handling, and non-abrasive nature [2]. Therefore, the use of wood flour to replace inorganic filler has an increasing trend in the plastic composite industries. Wood-plastic composites (WPCs) may have good moisture resistance and dimensional stability because of the continuous thermoplastic matrices [3]. They have been largely used as a replacement for softwood lumber as decking, railings, door and window frames, and other outdoor applications, where they have better durability than softwood lumber [4, 5].

Rubber tree (*Hevea brasiliensis*) is widely planted in Thailand for the production of latex, and is cut down when it becomes unproductive at about 25 years of age [6]. Rubberwood lumber is mainly used to produce furniture, toys, and packing materials. In these rubberwood industries, a large amount of wood waste in the forms of flour, sawdust, and chips is generated at different stages of processing. Generally, rubberwood waste is dumped in landfills or burned, but some of the waste is also used to produce medium-density fiberboard and particleboard [7]. The utilization of rubberwood waste as a filler in polymer composites could decrease environmental impacts from the waste, as well as add value when contributing to the composite properties.

The mechanical characteristics of WPCs include creep, i.e. time-dependent deformation under loading, due to their continuous thermoplastic matrices, and such creep is a critical issue in many engineering applications; for example biomedical, aerospace, and civil engineering infrastructure applications [8]. Hence, creep is an important material characteristic in the design of wood-plastic composite products, and relates to load-bearing capacity of end products. Likewise, durability and lifetime limitations of products, from intolerably large deformations, should be estimated at the design stage [9]. Environmental parameters, such as temperature and humidity, influence the creep of WPCs, because of temperature effects on the polymer and moisture effects on the wood filler [10]. Long term evaluation of creep would be prohibitively cost, so accelerated testing methods and mathematical models are used instead [10]. Acha et al. [8] investigated the effects of

modifying the interfacial adhesion between jute and polypropylene on the creep behavior, and used the time-temperature superposition (TTS) to predict long-term creep deformation. Mosiewicki et al. [11] experimentally evaluated the creep of composites made from linseed oil-based polyester thermoset, and compared the results with Power law and Burger models; both models fit the data well. Chevali et al. [12] studied flexural creep behavior of nylon 6/6, polypropylene, high-density polyethylene, and their long fiber thermoplastic composites. The HRZ (for Hadid, Rechak, and Zouani [13]) model provided an excellent fit to the experimental data, and the master curves obtained from TTS were able to predict the long-term creep. Banik et al. [14] investigated the influence of unidirectional and cross-ply polypropylene composites on the creep behavior, and both Burger and Findley power law models were satisfactory for fitting short-term creep behavior. Subramanian and Senthilvelan [15] experimentally evaluated the creep of leaf springs from glass-fiber-reinforced thermoplastic composites at various loads, and compared the results with the HRZ model. Despite extensive prior research on inorganic fiber and natural fiber reinforced plastics, only a few studies on creep behavior have used rubberwood flour (RWF) to reinforce virgin plastics, and there is no prior report on the creep of RWF-reinforced postconsumer plastics that this work focuses on.

In earlier chapter, the formulation of recycled polypropylene/RWF composites was optimized, based on mechanical properties, but creep deformation was not investigated. The evaluation of creep is indispensable for developing a new product subjected to long-term loading, when the materials are known to have viscoelastic time-dependent behavior. Therefore, creep must affect the design of WPCs and selecting their end-use applications. The objective of current work is to investigate the creep characteristic of composites from recycled polypropylene and rubberwood flour, in particular the effects of temperature and stress levels. The Burger, Power law, and HRZ models were fit to creep data. The time-temperature superposition and the time-stress superposition (TSS) principles were used to construct master curves of creep deformation to predict long-time creep.

11.3 Experimental

11.3.1 Materials

Rubberwood flour collected from local furniture factory was used as reinforcing filler. Before use it was sieved through a standard sieve of mesh size 80 (passing particles smaller than 180 μm) and dried in an oven at 110 °C for 8 h to minimize the moisture content. The main chemical constituents of rubberwood are: cellulose (39%), hemicellulose (29%), lignin (28%), and ash (4%) [16]. The matrix polymer was recycled polypropylene (rPP), purchased as pellets with a melt flow index of 11 g/10 min at 230 °C from Withaya Intertrade Co., Ltd (Samutprakarn, Thailand). Maleic anhydride-grafted polypropylene (MAPP) with 8-10% of maleic anhydride, used as a coupling agent to improve interfacial bonding between wood flour and plastic matrix, was supplied by Sigma-Aldrich (Missouri, USA). TH Color Co., Ltd (Samutprakarn, Thailand) supplied hindered amine light stabilizer additive, under the trade name MEUV008, chosen as the ultraviolet (UV) stabilizer. Paraffin wax used as lubricant (Lub) in processing was procured from Nippon Seiro Co., Ltd (Yamaguchi, Japan).

11.3.2 Preparation of composite samples

The WPCs were produced in a two-step process. In the first step to produce WPC pellets, RWF and rPP were blended into wood-plastic composite pellets using a twin-screw extruder (Model SHJ-36 from En Mach Co., Ltd, Nonthaburi, Thailand). Barrel temperatures in ten zones were set in the range 130-170 °C from feed to die, to limit degradation of the raw materials, while the screw rotating speed was controlled at 70 rpm. The extruded strand passed through a water bath and was subsequently pelletized. In the second step to produce WPC panels, the WPC pellets were again dried prior to use, in an oven at 110 °C for 8 h. The WPC pellets, MAPP, UV stabilizer, and lubricant were dry-mixed, and fed to the twin-screw extruder. The extruding conditions were as follows: (1) temperature profiles: 130–190 °C; (2) screw rotating speed: 50 rpm; (3) vacuum venting at 9 temperature zones: 0.022 MPa; and (4) melt pressure: 0.10-0.20 MPa. The samples were extruded through a rectangular 9 mm × 22 mm die and cooled in atmospheric air. Consequently, the

specimens were machined, following the flexural creep testing standard of American Society for Testing and Materials (ASTM).

11.3.3 Characterization

Short-term creep tests of rPP/RWF composites were carried out using an Instron Universal Testing Machine (Model 5582 from Instron Corporation, Massachusetts, USA) with three-point bending as shown in Figure 8.1, following ASTM D2990-01 standard. In all tests, the flexural strain was measured by an Instron extensometer with a travel of 5 mm and a gauge length of 10 mm. The specimens were 13 mm x 4.8 mm x 100 mm (width x thickness x length), and the test span was 80 mm in the direction of extrusion. To evaluate the effects of various stress levels, creep tests were conducted at 25 °C ambient temperature at ten different stress levels: 3, 7, 11, 15, 19, 23, 27, 31, 35, and 39 MPa. Five levels of temperature in the range from 25 to 65 °C were used with constant 19 MPa stress to assess temperature effects. This constant stress was approximately 40% of the ultimate flexural strength, from quasi-static tests at 25 °C. Before each creep test the specimens were equilibrated in an environmental chamber for 15 min. The loading duration of a test was 6000 sec (100 min), and there were five replications at each test condition.

11.3.4 Creep models

Creep is the slow deformation of a material under constant stress. It is important in applications with long-term loading. When a material subjected to constant load creeps, its deflection continuously accumulates with time [14, 17]. Wood-reinforced plastics show this type of viscoelastic behavior. The creep strain of polymers or wood-plastic composites, $\varepsilon(\sigma, t, T)$, mainly depends on stress (σ), time (t), and temperature (T) [18, 19]. Conceptually this strain has three main components: (i) elastic deformation (stress-temperature dependence, reversible) $\varepsilon_e(\sigma, T)$; (ii) viscoelastic deformation (stress-time-temperature dependence, reversible) $\varepsilon_{ve}(\sigma, t, T)$; and (iii) viscoplastic deformation (stress-time-temperature dependence, irreversible) $\varepsilon_p(\sigma, t, T)$ [18, 19]:

$$\varepsilon(\sigma,t,T) = \varepsilon_e(\sigma,T) + \varepsilon_{ve}(\sigma,t,T) + \varepsilon_p(\sigma,t,T) \quad (11.1)$$

The modeling of experimental data helps bridge the gap between material properties and engineering designs [17]. For applications to predicting the creep behavior of WPCs, several models developed from the constitutive relations of polymeric materials [14] can be explored. If reinforced polymer materials are tested within their linearly viscoelastic range, simple rheological models are appropriate [14]. A simple constitutive model, the four-element Burger model, has given satisfactory descriptions and predictions [14, 20, 21]. It combines Maxwell and Kelvin-Voigt models; instantaneous deformation comes from the Maxwell spring; viscoelastic deformation from Kelvin units; and viscoplastic deformation from the Maxwell dashpot [22]. Mathematical description for response to constant stress is:

$$\varepsilon(t) = \frac{\sigma}{E_M} + \frac{\sigma}{E_K}\left[1 - \exp\left(-t\frac{E_K}{\eta_K}\right)\right] + t\frac{\sigma}{\eta_M} \quad (11.2)$$

where ε is the strain at time t, with constant stress σ. E_M and E_K are the elastic moduli, and η_M and η_K are the viscosities, of the Maxwell and Kelvin bodies, respectively [21]. Especially with non-linear creep behavior, empirical mathematical models have often been applied with satisfactory prediction, despite simple forms [14, 23]. An example of such simple model is the Power law model. Subramanian and Senthilvelan [15] and Hadid et al. [13] used the Power law model for the three-point bending creep of glass fiber reinforced thermoplastics. Also the American Society of Civil Engineers (ASCE) recommend this model for the analysis of composite materials under long-term structural loading, in their structural plastics design manual [15, 24]. The Power law equation is:

$$\varepsilon(t) = r_0 t^n \quad (11.3)$$

where ε is the creep strain at time t, r_0 is a coefficient, and n is the Power law exponent [23].

The two Power law parameters, the coefficient and the exponent, are significantly affected by the stress level [15]. This model was modified by Hadid et al. [13] to incorporate also stress dependence. This HRZ model has the form:

$$\varepsilon(t) = a \cdot \sigma^{b} \cdot t^{c \cdot \exp(e \cdot \sigma)} \quad (11.4)$$

where the model parameters *a, b, c,* and *e* are fit to data by non-linear regression. Subramanian and Senthilvelan [15] and Chevali et al. [12] used the HRZ model to fit experimental data, finding excellent fit to short-time flexural creep over a wide range of stresses.

11.3.5 Time-temperature and stress superposition

Time-temperature and stress superposition principles are widely used with viscoelastic materials such as wood-reinforced plastics. They are empirical relationships between time and temperature, or time and stress [25], stating that the effect of a constant temperature or stress change on a time-dependent response equals a uniform shift in logarithmic time-scale [25]. Then a single master curve at a reference temperature (or stress), using a logarithmic time scale, includes the creep curves obtained at different temperatures (or stresses); these are superposed on the master curve by a horizontal shift [11]. The master curve can be used to predict creep response at large time scales, even if experiments are limited to short times.

11.4 Results and discussion

11.4.1 Effect of the various stress levels

In service the plastic composites may be subjected to long-term stresses. The logarithmic re-scaling of time, according to the superposition principles, suggests accelerated testing by use of elevated stresses and/or temperatures, so a range of each stress or temperature was experimented. The creep strain against time, with the specific composite formulation described earlier, is shown at different stress levels ranging from 3 MPa to 39 MPa in Figure 11.1. The creep of the rPP/RWF composites was clearly dependent on the test stress, and increased with the stress level as expected. At the highest applied 39 MPa stress (83% of ultimate strength) the rate of creep deformation was the highest. At stresses close to the 47.28 MPa ultimate strength the mobility of the macromolecular chains strongly increases, and this mobility leads to eventual failure of the test specimen.

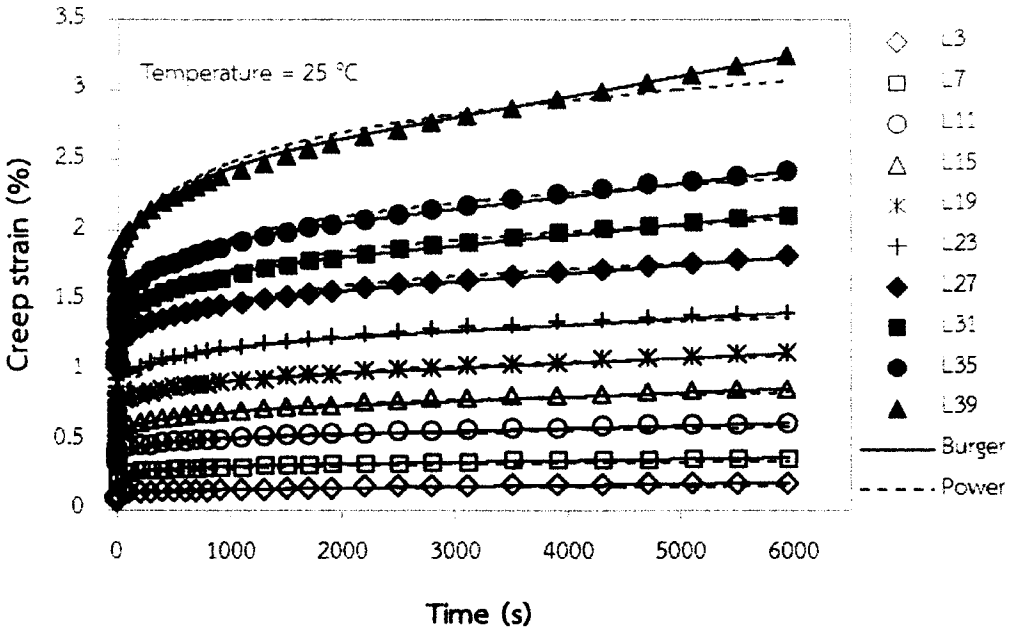

Figure 11.1 Short-term flexural creep at different stress levels, fitted with Burger model (solid lines) and Power law model (dashed lines)

The creep was modeled with equations (11.2) and (11.3), for Burger and Power law models. The solid and dashed lines represent the fit for each stress level of Burger and Power law models, respectively, while symbols in the legend represent experimental averages across replications. Both Burger and Power law models fit the experimental data overall well, but at 39 MPa stress level the Burger model is clearly better. This is not surprising since the Power law model is simpler with fewer parameters than the Burger model [11]. Also Hadid et al. [13] observed poorer fits at higher stress levels.

The four parameters of Burger model can be calculated as these steps:

1) The short-term creep curve was divided into three stages; instantaneous creep strain (C_e), viscoelastic creep strain (C_{ve}), and viscoplastic creep strain (C_t). For example, the creep curve of stress 39 MPa and temperature 25 °C was included with C_e 1.844139%, C_{ve} 0.525461%, and C_t 0.863364%.

2) The time intervals of C_e, C_{ve}, and C_t are 0, 450, and 5950 second, respectively.

3) Each parameter of Burger model can be expressed as follows:

$$E_M = \frac{\sigma}{\varepsilon_{Ce}} = \frac{39}{0.01844139} = 2115 \text{ MPa}$$

$$E_K = \frac{\sigma}{\varepsilon_{Cve}} = \frac{39}{0.00525461} = 7422 \text{ MPa}$$

$$\eta_M = \frac{\sigma(t_t)}{\varepsilon_{Ct}} = \frac{39(5950)}{0.00863364} = 26877423 \text{ MPa}$$

$$\eta_K = \frac{\sigma(t_{Cve})}{\varepsilon_{Cve}} = \frac{39(450)}{0.00525461} = 3339924 \text{ MPa}$$

The fitted parameters of Burger and Power law models obtained from the rPP/RWF composites are shown in Table 11.1. All parameters (E_M, E_K, η_M, and η_K) in the Burger model decrease with stress level. The moduli (E_M and E_K) decrease because new mechanisms of molecular bond breaking and slippage emerge as stress is increased. The viscosities (η_M and η_K) similarly decrease due to increased polymer chain mobility. The Power law parameter r_0 is for instantaneous strain (time-independent) and relates to the elastic initial response, while the parameter n relates to viscous creep response (time-dependent) [11]. Both parameters increase with the stress level for the same molecular mobility reasons discussed earlier.

11.4.2 Effects of temperature

The short-term bending creep responses of rPP/RWF composites at five different temperatures are shown in Figure 11.2. The creep curves were still in the secondary creep stage at the end of the tests for temperatures from 25 °C to 55 °C, but the highest 65 °C temperature produced failure after 1500 sec (25 min), before the end of the test duration, and showed the tertiary creep stage. This indicates that 65 °C is a critical temperature for the recycled polypropylene composites containing 44.5 wt% of rubberwood flour. Both the instantaneous deformation and viscous creep increase with temperature, see Figure 11.4. Normally, thermoplastic materials are softened by an increase in temperature and creep deformation of matrix-dominant composites increases [1].

Table 11.1 Parameters of Burger model and Power law model

		Burger model				Power law model	
σ (MPa)	T (°C)	E_M (MPa)	E_K (MPa)	η_M (MPa·s)	η_K (MPa·s)	r_0	n
3	25	2742	15268	6.62E + 07	7.83E + 06	0.079	0.089
7	25	2695	14815	6.27E + 07	7.41E + 06	0.158	0.091
11	25	2585	13679	5.79E + 07	6.84E + 06	0.260	0.095
15	25	2539	12714	5.53E + 07	6.36E + 06	0.358	0.098
19	25	2505	11970	5.35E + 07	5.49E + 06	0.457	0.101
23	25	2487	10705	5.09E + 07	4.82E + 06	0.561	0.103
27	25	2391	9879	4.51E + 07	4.45E + 06	0.722	0.105
31	25	2366	9847	4.04E + 07	4.43E + 06	0.814	0.108
35	25	2351	9025	3.85E + 07	4.06E + 06	0.903	0.111
39	25	2115	7422	2.69E + 07	3.34E + 06	1.108	0.117
19	**35**	**2065**	**8004**	**3.49E + 07**	**4.00E + 06**	**0.583**	**0.104**
19	**45**	**1508**	**7691**	**2.84E + 07**	**3.85E + 06**	**0.771**	**0.106**
19	**55**	**1215**	**7386**	**1.56E + 07**	**3.69E + 06**	**0.905**	**0.109**
19	**65**	**967**	**7276**	**2.37E + 06**	**7.28E + 05**	**1.305**	**0.115**

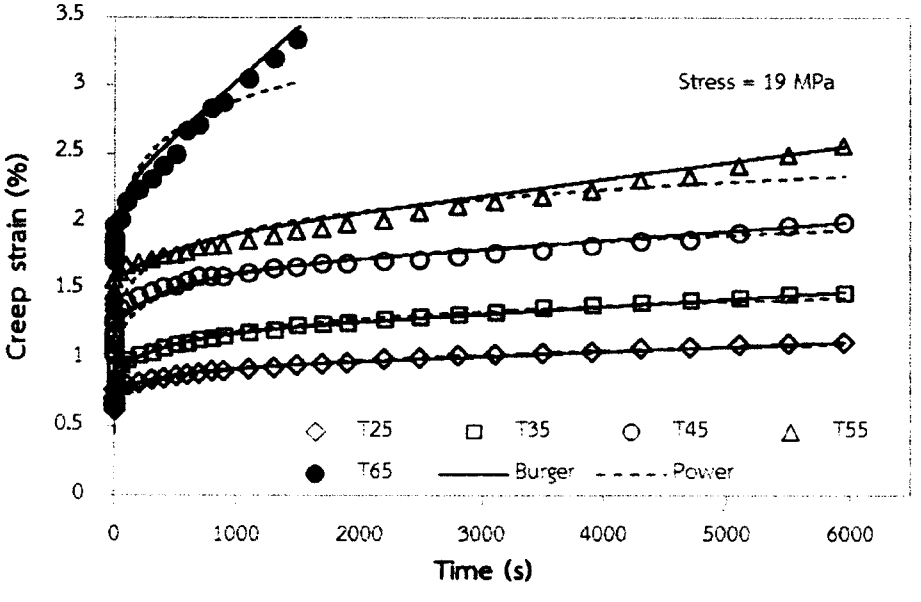

Figure 11.2 Short-term flexural creep at different temperatures fitted with Burger model (solid lines) and Power law model (dashed lines)

The curve fits with Burger and Power law models are included in Figure 11.2, with solid and dashed lines. The fits were otherwise good, but at high temperatures (55 °C and 65 °C) the Power law model performed poorly. The Power law model appears appropriate with low creep deformation only, while the Burger model fits all of the data well. This might be due to the better flexibility of Burger model, as it has more parameters, or because this model actually describes some of the mechanisms determining the constitutive behavior [14].

The Burger parameters listed in Table 11.1 decrease with temperature. The moduli may decrease due to softening of the composite materials [14]. Likewise, the viscosities decrease and contribute to creep deformation with increasing temperature [14]. This confirms increasing molecular mobility with temperature [11, 14]. The parameters of Power law model both increased with temperature due to the same reasons [11].

11.4.3 Empirical model for short-term creep

The creep of the rPP/RWF composites for stresses from 3 MPa to 39 MPa and temperatures ranging from 25 °C to 65 °C is shown in Figures 11.1 and 11.2. The Power law coefficient r_0 and the exponent n increase with stress and temperature levels. This agrees with prior works in Subramanian and Senthilvelan [15], and Hadid et al. [13].

Figures 11.3 and 11.4 show the curve fits of the type used in the HRZ model, of the Power law parameters. The found HRZ model parameters (*a, b, c,* and *e*) are shown in these figures and listed in Table 11.2. Parameters *a* and *b* are determined by the instantaneous elastic strain immediately after load application, and depend on the degree of crystallinity and glass transition temperature [12, 15, 26]. Parameters *c* and *e* describe how the creep depends on stress, testing time, and relaxation of the composites [12, 15]. The HRZ and Power law fits are shown in Figures 11.5 and 11.6. The HRZ model fits the data almost as well as the Power law fits of individual curve, but performs poorly at the highest stress level tested. Similar lack of fit at high stresses was found by Hadid et al. [13] and Subramanian and

Senthilvelan [15]. The HRZ model allows interpolation between the stresses and temperatures used experimentally.

Table 11.2 HRZ model parameters (*a, b, c,* and *e*) that allow interpolation of stress and temperature

Parameter	*a*	*b*	*c*	*e*
Stress dependence	0.023	1.034	0.087	0.0072
Temperature dependence	0.026	0.885	0.095	0.0025

11.4.4 Time-temperature and stress superposition

In order to predict the long-term creep behavior of the composites, the time-temperature superposition (TTS) and the time-stress superposition (TSS) principles were utilized, using master curves produced from the short-term creep tests accelerated by temperature and stress. In Figure 11.7, the short-term creep data from different temperatures are superposed by horizontal shifts of log time scale. The reference temperature chosen was 25 °C, and the master curve constructed reveals long-term behavior at this temperature, based on accelerated testing. Figure 11.8 has similarly constructed master curve from the various stress levels, with 19 MPa as the reference stress whose long-term creep is revealed.

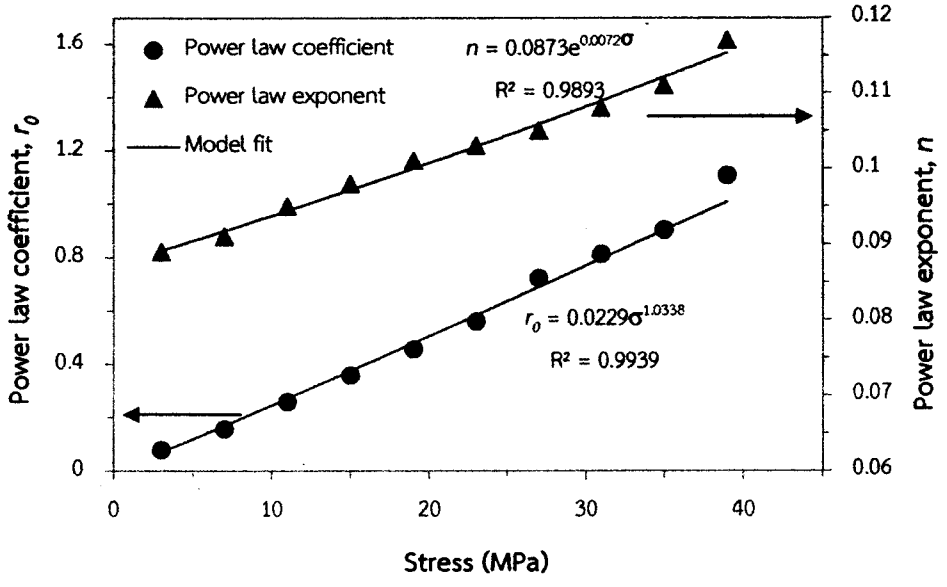

Figure 11.3 Variation of Power law coefficient and exponent with stress level

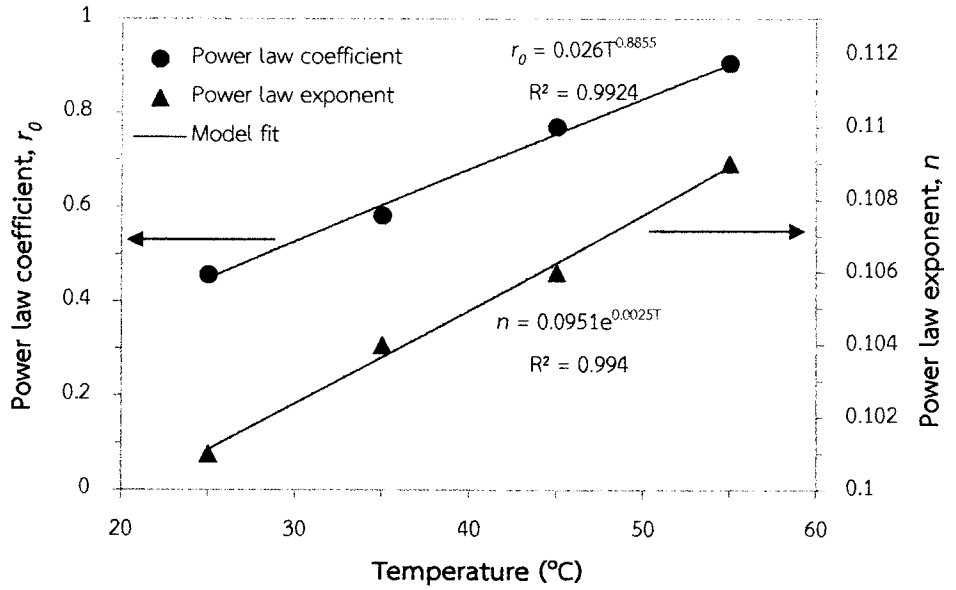

Figure 11.4 Variation of Power law coefficient and exponent with temperature

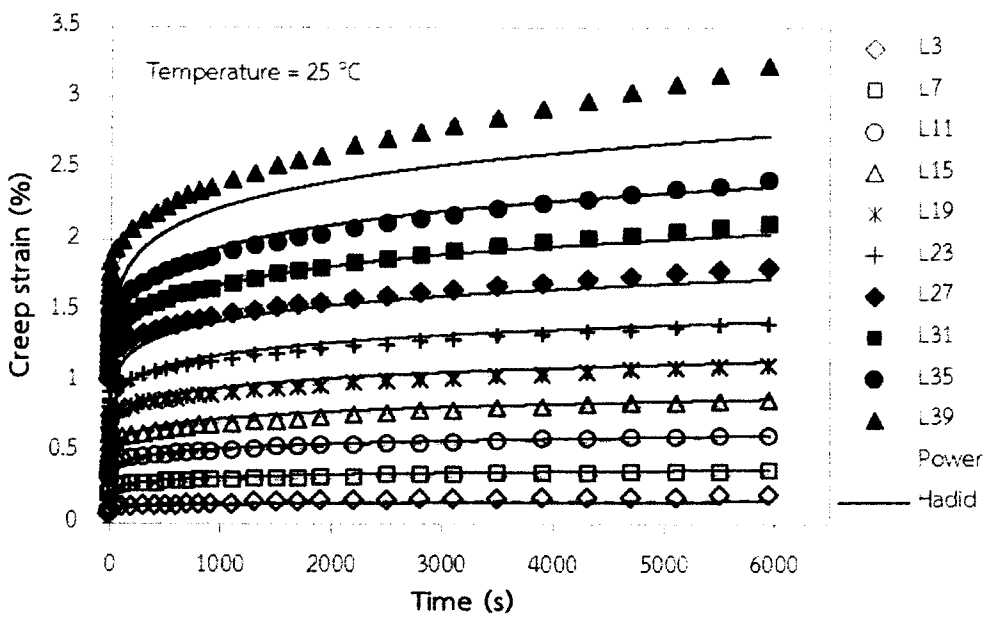

Figure 11.5 Power law and HRZ model fits to the flexural creep curves at different stress levels

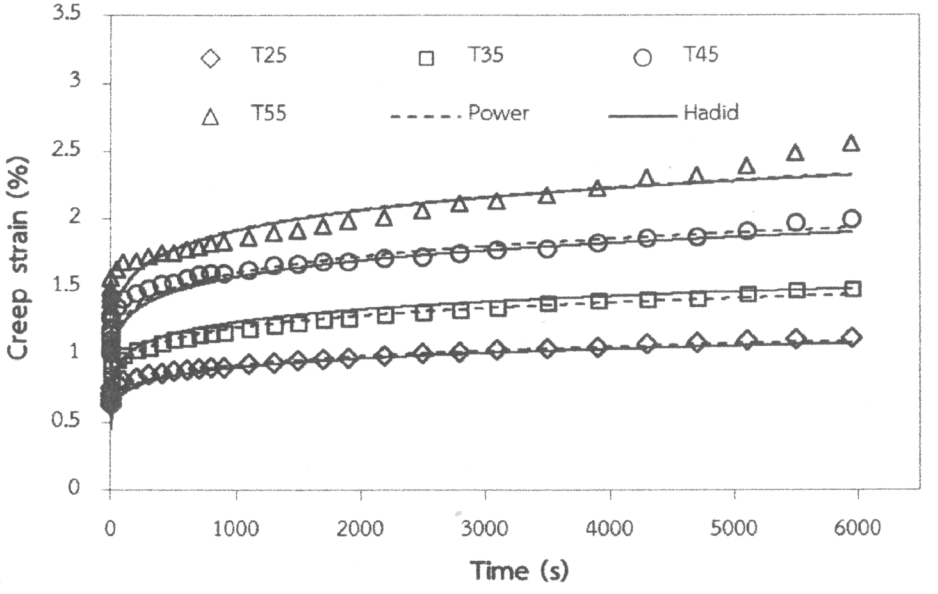

Figure 11.6 Power law and HRZ model fits to the flexural creep curves at different temperatures

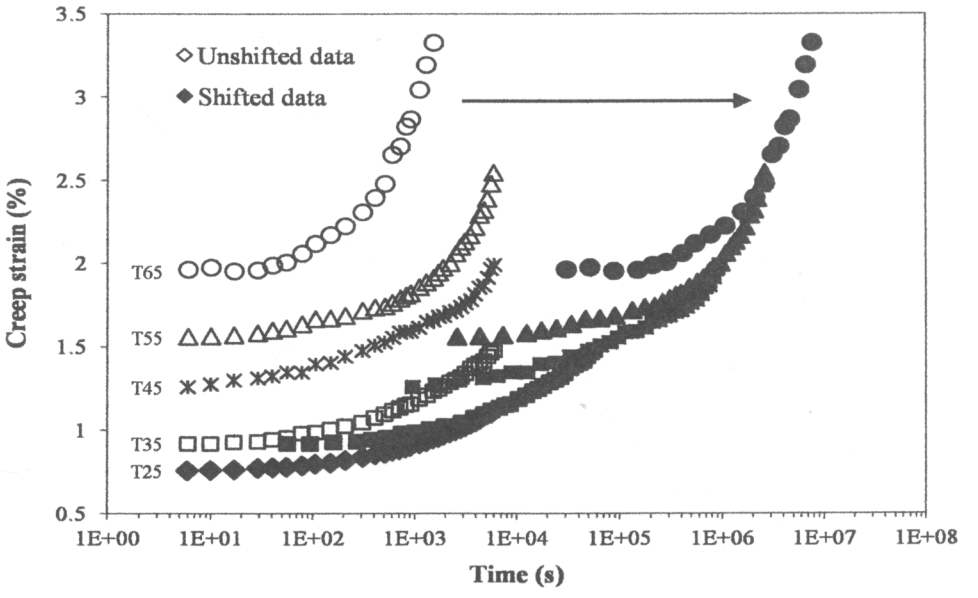

Figure 11.7 Short-term creep curves superposed to a master curve; the reference temperature is 25 °C

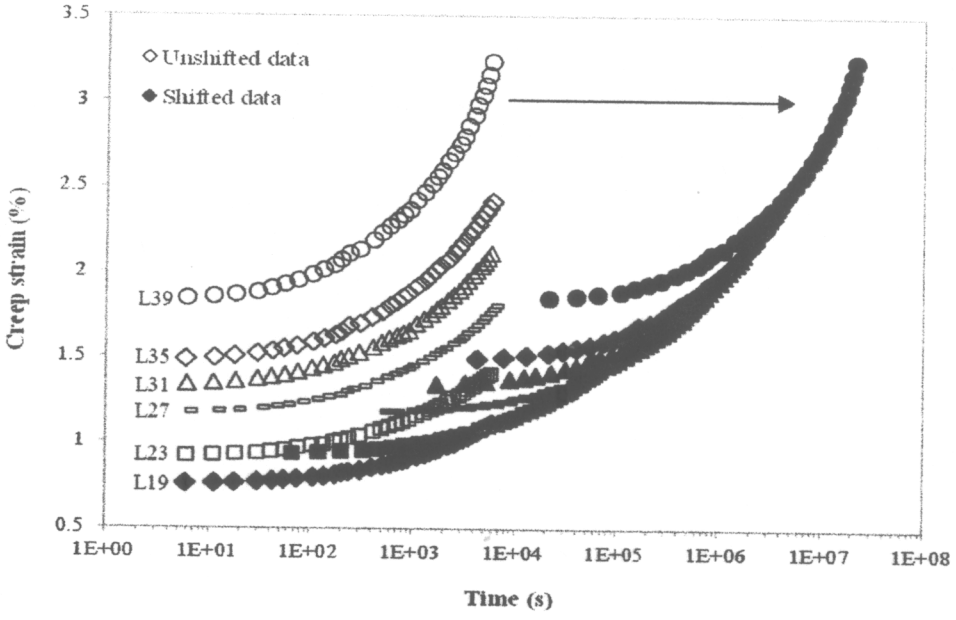

Figure 11.8 Short-term creep curves superposed to a master curve; the reference stress is 19 MPa

In order to show the lifetime creep deformation of rPP/RWF composites, Figure 11.9 displays master curves at reference temperature 25 °C with constant load 19 MPa as well as reference stresses at 3, 11, and 19 MPa with temperature fixed at 25 °C, with the vertical lines indicating 1, 10, 100, and 1000 years [27]. The two master curves, accelerated by temperature and stress, agree well at 25 °C and 19 MPa. The highest temperature tested affected the curve from temperature acceleration, causing deviation of the two master curves at high strain. The two master curves predict a lifetime of less than 1 year at this stress level. However, at lower stress levels and 25 °C the predicted lifetimes of rPP/RWF composites exceed 10 years for 15 MPa stress and 1000 years for 3 MPa stress. Low creep deformation at 3 MPa stress results the predicted lifetimes of rPP/RWF composites exceed 1000 years. However, the applications of the composites with very low stress level have been rarely limited.

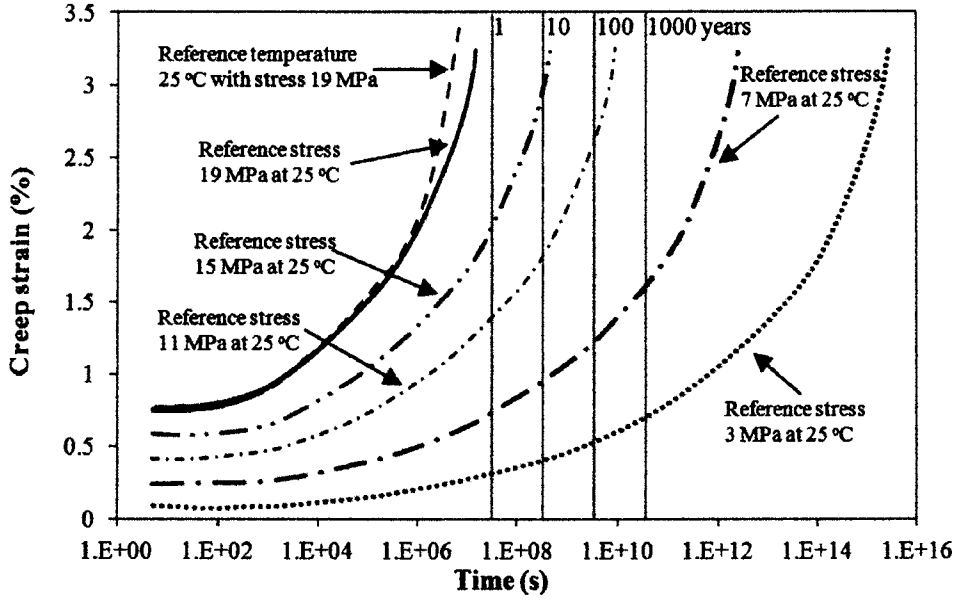

Figure 11.9 Creep master curves for three-point flexure predict lifetimes

11.5 Conclusions

Creep deformation is an important characteristic of a composite material, when the end products are subjected to loading. The creep of a specific composite formulation from recycled polypropylene and rubberwood flour was investigated experimentally and modeled numerically. The creep was dependent on both temperature and stress, increasing with both of these. The Burger and Power law models were both able to fit well the creep data in general, but at high temperature and stress levels the Power law gave the poorer fit to these models. The HRZ model provided an approximate interpolation across temperatures or stresses of the Power law fits, and also fit these data well in cases where the Power law performed well. The master curves from time-temperature and time-stress superpositions were in good agreement with each other. From the master curves the long-term creep was predicted with stresses 3 and 15 MPa at 25 $^{\circ}$C, suggesting that the creep-limited lifetime of rPP/RWF composites exceeds 10 years at the higher stress level, and is no longer a relevant limitation at the lower stress level.

11.6 References

[1] B.D. Park and J.J. Balatinecz. "Short-Term Flexural Creep Behavior of Wood-Fiber/Polypropylene Composites." *Polymer Composites*, vol. 19, pp. 377–382, 1998.

[2] X. Peng, M. Fan, J. Hartley, and M. Al-Zubaidy. "Properties of Natural Fiber Composites Made by Pultrusion Process." *Journal of Composite Materials*, vol. 46, pp. 237–246, 2011.

[3] G. Grubbstrom, A. Holmgren, and K. Oksman. "Silane-Crosslinking of Recycled Low-Density Polyethylene/Wood Composites." *Composites Part A: Applied Science and Manufacturing*, vol. 41, pp. 678–683, 2010.

[4] D.R. Carroll, R.B. Stone, A.M. Sirignano, R.M. Saindon, S.C. Gose, and M.A. Friedman. "Structural Properties of Recycled Plastic/Sawdust Lumber Decking Planks." *Resources, Conservation and Recycling*, vol. 31, pp. 241–251, 2011.

[5] I. Ganguly and I.L. Eastin. "Trends in the US Decking Market: A National Survey of Deck and Home Builders." *The Forestry Chronicle*, vol. 85, pp. 82–90, 2009.

[6] S. Rimdusit, W. Smittakorn, S. Jittarom, and S. Tiptipakorn. "Highly Filled Polypropylene Rubber Wood Flour Composites." *Engineering Journal*, vol. 15, pp. 17–30, 2011.

[7] C. Homkhiew, T. Ratanawilai, and W. Thongruang. "Composites from Recycled Polypropylene and Rubberwood Flour: Effects of Composition on Mechanical Properties." *Journal of Thermoplastic Composite Materials*, Epub ahead of print 14 February 2013. DOI: 10.1177/0892705712475019.

[8] B.A. Acha, M.M. Reboredo, and N.E. Marcovich. "Creep and Dynamic Mechanical Behavior of PP–Jute Composites: Effect of the Interfacial Adhesion." *Composites Part A: Applied Science and Manufacturing*, vol. 38, pp. 1507–1516, 2007.

[9] J. Lai and A. Bakker. "Analysis of the Non-Linear Creep of High-Density Polyethylene." *Polymer*, vol. 36, pp. 93–99, 1995.

[10] F.C. Chang, F. Lam, and J.F. Kadla. "Using Master Curves based on Time–Temperature Superposition Principle to Predict Creep Strains of Wood–Plastic Composites." *Wood Science and Technology*, vol. 47, pp. 571–584, 2013.

[11] M.A. Mosiewicki, N.E. Marcovich, and M.I. Aranguren. "Creep Behavior of Wood Flour Composites Made from Linseed Oil-based Polyester Thermosets." *Journal of Applied Polymer Science*, vol. 121, pp. 2626–2633, 2011.

[12] V.S. Chevali, D.R. Dean, and G.M. Janowski. "Flexural Creep Behavior of Discontinuous Thermoplastic Composites: Non-Linear Viscoelastic Modeling and Time-Temperature-Stress Superposition." *Composites Part A: Applied Science and Manufacturing*, vol. 40, pp. 870–877, 2009.

[13] M. Hadid, S. Rechak, and A. Zouani. "Empirical Nonlinear Viscoelastic Model for Injection Molded Thermoplastic Composite." *Polymer Composites*, vol. 2002, pp. 771–778, 2002.

[14] K. Banik, J. Karger-Kocsis, and T. Abraham. "Flexural Creep of All-Polypropylene Composites: Model Analysis." *Polymer Engineering and Science*, vol. 48, pp. 941–948, 2008.

[15] C. Subramanian and S. Senthilvelan. "Short-Term Flexural Creep Behavior and Model Analysis of a Glass-Fiber-Reinforced Thermoplastic Composite Leaf Spring." *Journal of Applied Polymer Science*, vol. 120, pp. 3679–3686, 2011.

[16] P. Petchpradab, T. Yoshida, T. Charinpanitkul, and Y. Matsumura. "Hydrothermal Pretreatment of Rubber Wood for the Saccharification Process." *Industrial and Engineering Chemistry Research*, vol. 48, pp. 4587–4591, 2009.

[17] A.J. Schildmeyer. "Temperature and Time Dependent Behaviors of a Wood-Polypropylene Composite." M.S. thesis, Washington State University, United States, 2006.

[18] A. Dorigato, A. Pegoretti, and J. Kolarik. "Nonlinear Tensile Creep of Linear Low Density Polyethylene/Fumed Silica Nanocomposites: Time-Strain Superposition and Creep Prediction." *Polymer Composites*, vol. 31, pp. 1947–1955, 2010.

[19] J. Kolarik, A. Pegoretti, L. Fambri, and A. Penati. "Prediction of Nonlinear Long-Term Tensile Creep of Heterogeneous Blends: Rubber-Toughened Polypropylene–Poly(Styrene-co-Acrylonitrile)." *Journal of Applied Polymer Science*, vol. 88, pp. 641–651, 2003.

[20] H. Liu, F. Yao, Y. Xu, and Q. Wu. "A Novel Wood Flour-Filled Composite based on Microfibrillar High-Density Polyethylene (HDPE)/Nylon-6 Blends." *Bioresource Technology*, vol. 101, pp. 3295–3297, 2010.

[21] S. Tamrakar, R.A. Lopez-Anido, A. Kiziltas, and D.J. Gardner. "Time and Temperature Dependent Response of a Wood-Polypropylene Composite." *Composites Part A: Applied Science and Manufacturing*, vol. 42, pp. 834–842, 2011.

[22] Y. Xu, Q. Wu, Y. Lei, and F. Yao. "Creep Behavior of Bagasse Fiber Reinforced Polymer Composites." *Bioresource Technology*, vol. 101, pp. 3280–3286, 2010.

[23] M. Hadid, S. Rechak, and A. Tati. "Long-Term Bending Creep Behavior Prediction of Injection Molded Composite Using Stress-Time Correspondence Principle." *Materials Science and Engineering A*, vol. 385, pp. 54–58, 2004.

[24] American Society of Civil Engineers. *Structural Plastic Design Manual*: ASCE Publications, New York, 1986.

[25] F.C. Chang, F. Lam, and J.F. Kadla. "Application of Time–Temperature–Stress Superposition on Creep of Wood–Plastic Composites." *Mechanics of Time-Dependent Materials*, Epub ahead of print 6 October 2012. DOI: 10.1007/s11043-012-9194-9.

[26] V.S. Chevali and G.M. Janowski. "Flexural Creep of Long Fiber-Reinforced Thermoplastic Composites: Effect of Processing-Dependent Fiber Variables on Creep Response." *Composites Part A: Applied Science and Manufacturing*, vol. 41, pp. 1253–1262, 2010.

[27] W.K. Goertzen and M.R. Kessler. "Creep Behavior of Carbon Fiber/Epoxy Matrix Composites." *Materials Science and Engineering A*, vol. 421, pp. 217–225, 2006.

CHAPTER 12

Effect of Extruded Density on Mechanical and Physical Properties of Recycled Polypropylene Composites Reinforced with Rubberwood Flour

12.1 Chapter summary

The effects of extruded density of composites from recycled polypropylene and rubberwood flour were experimentally investigated. The composite materials were manufactured by using twin-screw extruder into panels with three cross-section sizes: 9 mm × 22 mm; 17 mm × 36 mm; and 25 mm × 50 mm. Flexural strength, and tensile strength and modulus significantly decreased with a decrease of the extruded density, whereas hardness, flexural modulus, compressive strength and modulus, and screw and nail withdrawal strengths insignificantly reduced with a decrease of the extruded density from 1.085 g/cm^3 to 1.029 g/cm^3, but significantly decreased for the density 0.963 g/cm^3. Estimated cost of decking board product with dimensions of 25 mm × 50 mm × 1000 mm is 388 baht per piece.

12.2 Introduction

Rubber tree (*Hevea brasiliensis*) is widely planted in the South and the Northeast of Thailand. It is major economic important plant because the latex extracted from the tree is the primary source of natural rubber. However, when it becomes unproductive at about 25 years of age, it is cut down [1]. The cut rubberwood is generally produced as wood wastes about 34% and plantation wastes about 54%. Only 12% of the rubberwood ends up as the goods [2]. In addition, rubberwood lumber and root could be mainly utilized to manufacture furniture, toys, and packing materials. In these rubberwood industries, a large amount of wood waste in the forms of flour, sawdust, and chips is generated at different stages of

processing. Generally, some of the wood waste can be used as raw material to manufacture plywood, particleboard, and medium-density fiberboard [3], but most of such waste is disposed in landfills (dump in space areas) or burning, resulting in pollution issues. Therefore, the utilization of rubberwood waste as filler in polymer composites is great interest, which decreases environmental impacts but increases value of waste. The wastes in the forms of flour, sawdust, and chips have primarily been used as inexpensive filler in plastic industries, to reduce material costs and to increase the strength and modulus of various thermoplastics. Moreover, the rubberwood waste reinforced thermoplastics also offers many advantages including biodegradability, renewable character, absence of associated health hazards, and low equipment wear during their processings [4], compared to synthetic fillers.

Recently, wood-plastic composites (WPCs) have become popular. They are extensively investigated for applications in automotive industry, construction business, and infrastructure. Numerous researchers have studied the thermal, physical, and mechanical properties of thermoplastics filled with natural fibers in an attempt to reduce the cost and improve the properties of plastics [5, 6], whereas the utilization of rubberwood filler in WPCs has been rarely studied. Ghahri et al. [7] improved the impact strength of composites from recycled polypropylene (PP) and wood flour (beech; *Fagus orientalis*) through impact modification. The addition of ethylene vinyl acetate 9 wt% increased the impact strengths of the composites made with recycled PP up to two times. Butylina et al. [8] examined the effects of outdoor weathering on the properties of wood-polypropylene composites with and without pigments, and found that better color stability experienced with composites containing darker color pigments. Sombatsompop and Chaochanchaikul [9] assessed the effect of moisture content on mechanical properties and thermal and structural changes of polyvinyl chloride/wood sawdust composites. The tensile modulus decreased but elongation at break of the composites increased with increasing moisture content, while the glass transition temperature did not change with varying moisture content. Petchwattana et al. [10] investigated the influences of rice hull (RH) contents filled into high-density polyethylene composites on the

mechanical, physical, and thermal properties, and found that the flexural and the tensile strengths increased with increasing RH contents. Homkhiew et al. [3] studied the effects of different grades of plastic (virgin and recycled) and amounts of components on mechanical and physical properties of PP/rubberwood flour (RWF) composites. Virgin PP gave better mechanical properties than recycled PP, both in composites and as unfilled plastic, and the modulus and hardness of composites increased linearly with wood flour loadings in range of 25-45 wt%. Nourbakhsh et al. [11] also concluded that polypropylene waste and wood waste are promising alternative raw materials for making low cost WPCs.

The interfacial adhesion between fiber and polymer can be improved through modification of either the fiber surfaces or the polymeric matrix [12]. Ichazo et al. [13] treated the wood flour with sodium hydroxide and vinil-tris-(2-metoxietoxi)-silane, and found that the treated composites showed the same tendency to slightly increase the tensile strength and modulus. Bengtsson et al. [14] found that the addition of MAPP in the composites increased significantly the stiffness and strength but decreased the elongation break due to an improvement in dispersion of the cellulose fibers in the polypropylene matrix. Adhikary et al. [15] reported that both the stability and mechanical properties were significantly improved by addition of MAPP 3–5 wt% in the composite formulation. Likewise, Kuo et al. [16] reported that addition of MAPP 3-4.5 wt% gave the optimal increase in mechanical properties of the WPCs. The increasing polymer content or addition of coupling agent can improve the dimensional stability and strength properties of the composites. Nachtigall et al. [17] explained that the degradation temperature of the fibers was affected by the use of coupling agents. However, the commercial coupling agents gave the different effect on WPC performances, and the important parameters that determine the efficiency of the additive are the molecular weight and amount of maleic grafted [18].

From the recent literatures, most of the researches have been extensively published the experimental results related with the property developments and structure-property relationships of WPC products [5], but effects

of extruded density due to cross-section sizes were not investigated and still open for discussion. The evaluation of extruded density is necessary for expanding the product to large sizes. Therefore, the extruded density must affect the design and application of WPCs. The main objective of present work is to assess the effects of extruded density on physical and mechanical properties of recycled polypropylene/ rubberwood flour composites produced by a twin-screw extruder with Ø 36 mm and to estimate cost of decking board product with dimensions of 25 mm × 50 mm × 1000 mm. The experimental results in this work will provide the new information to facilitate informed decisions regarding designer and manufacturer of such composites.

12.3 Experimental

12.3.1 Materials

Recycled polypropylene (rPP) pellets, WT170 with a melt flow index of 11 g/10 min at 230 °C, were purchased from Withaya Intertrade Co., Ltd (Samutprakarn, Thailand). Rubberwood flour (RWF) obtained from the cutting process in local furniture industry (Songkhla, Thailand) was used as reinforcement. Maleic anhydride-grafted polypropylene (MAPP) with 8-10% of maleic anhydride was supplied by Sigma-Aldrich (Missouri, USA) and used as a coupling agent to improve the interfacial adhesion between filler and matrix. Hindered amine light stabilizer (HALS) additive, chosen as the UV stabilizer, was supplied by TH Color Co., Ltd (Samutprakarn, Thailand) under the trade name MEUV008. A paraffin wax lubricant (Lub) was purchased from Nippon Seiro Co., Ltd (Yamaguchi, Japan).

In chapter 10, the formulation of recycled polypropylene/RWF composites was optimized on mechanical properties. Thus, in the current work the composite formulation was held constant at 50.3 wt% rPP, 44.5 wt% RWF, 3.9 wt% MAPP, 0.2 wt% UV stabilizer, and 1.0 wt% Lub, which has flexural strength 47.28 MPa and modulus 2527 MPa.

12.3.2 Preparation of the composites

Prior to compounding, the RWF was sieved through a standard sieve of mesh size 80 (passing particles smaller than 180 μm) and was dried in an oven at 110 °C for 8 h. WPCs were produced in a two-stage process. In the first stage to produce WPC pellets, RWF and rPP were dry-blended, melt-blended, and pelletized into wood-plastic composite pellets using a twin-screw extruder (Model SHJ-36 from En Mach Co., Ltd, Nonthaburi, Thailand). The 10 temperature zones of the extruder were controlled at 130-170 °C from feeding to die zones, to reduce degradation of the compositions, while the screw rotating speed was maintained at 70 rpm. In the second stage to produce WPC panels, the WPC pellets were again dried prior to use, in an oven at 110 °C for 8 h. The WPC pellets, MAPP, UV stabilizer, and lubricant were then dry-mixed and fed into the twin-screw extruder. The temperature profiles in the extruding process were 130-190 °C, with 50 rpm. Melt pressure at the die varied between 0.05-0.15 MPa, depending on cross-section size. Vacuum venting at 9 temperature zones was also used to purge volatile compounds. The samples were then extruded through rectangular 9 mm × 22 mm, 17 mm × 36 mm, and 25 mm × 50 mm dies with density 1.085 g/cm^3, 1.029 g/cm^3, and 0.963 g/cm^3, respectively, as shown in Figure 12.1, and cooled in atmospheric air. Subsequently, the specimens were machined according to ASTM for mechanical and physical tests.

12.3.3 Characterizations

Hardness on the horizontal plane. Hardness measurements of rPP/RWF composite samples were performed according to ASTM D2240-91 specification, using two Durometers (Shore D scales) for the plastic composites. The dimensions of the specimens tested were approximately 16 mm × 16 mm × 6.5 mm. The measurements were performed at room temperature (25 °C).

Mechanical tests. Flexural properties were measured in a three-point bending test at a cross-head speed of 2 mm/min, with nominal dimensions of 4.8 mm × 13 mm × 100 mm, and a span of 80 mm in accordance with ASTM D790-92. For compressive properties, prism specimens were used to determine the

compressive strength and modulus. The displacement rate was a constant 0.5 mm/min, following ASTM standard D6108-97. Type-IV tensile bar specimens with dimensions of 115 mm x 19 mm x 4 mm were cut and machined from the extruded composite panels. The cross-head speed of tensile test was 5 mm/min, according to ASTM standard D638-99. The flexural, compressive, and tensile measurements were carried out on an Instron Universal Testing Machine (Model 5582 from Instron Corporation, Massachusetts, USA) and performed at ambient conditions of 25 °C. Five replications of each composite formulation were tested.

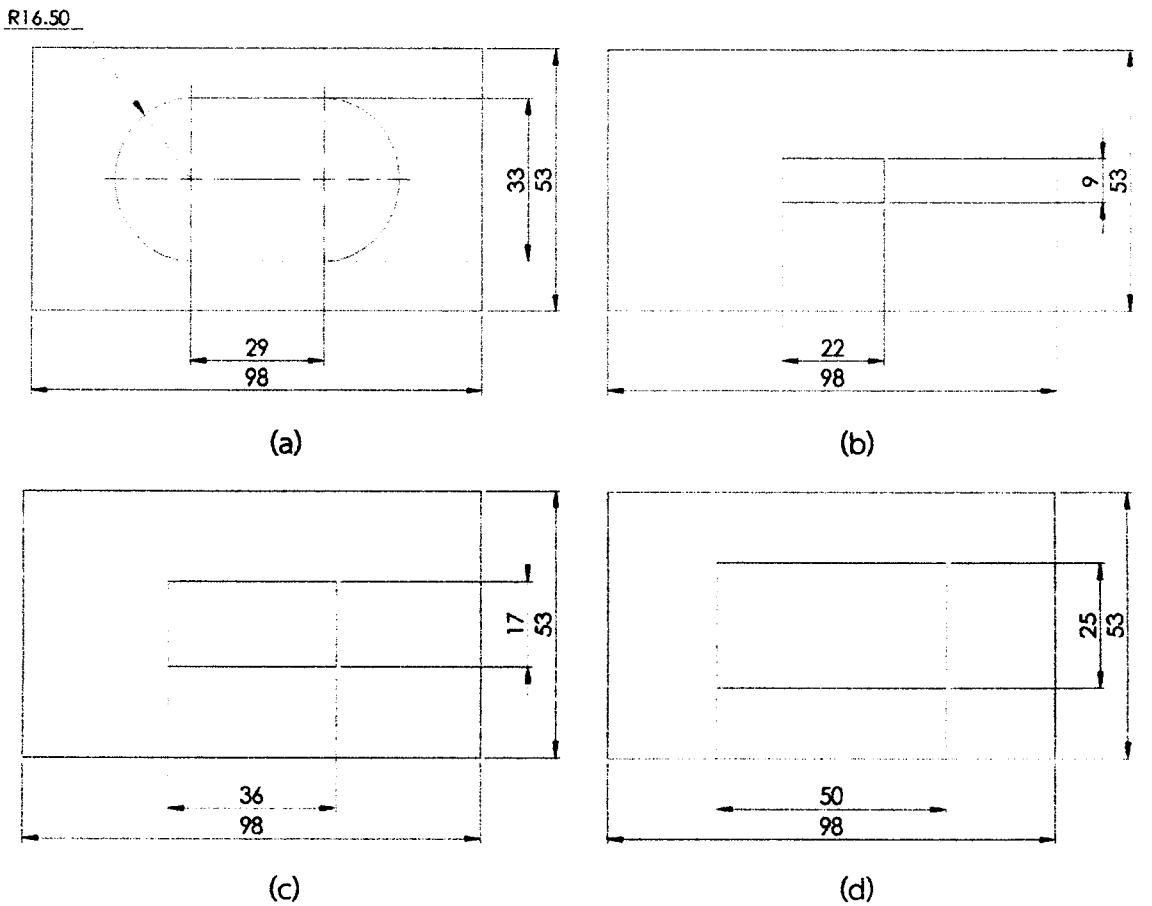

Figure 12.1 Cross-section of different die sizes (a) head die, (b) 9 mm x 22 mm, (c) 17 mm x 36 mm, and (d) 25 mm x 50 mm

Screw and nail withdrawal. Screw and nail withdrawal strengths are measured to determine maximum load required to pull a standard screw and nail from the panel specimens. These tests were carried out according to BS Standard (DD CEN/TS 15534-1:2007) [19]. Specimens' dimension for screw and nail withdrawal was 23 mm x 23 mm x 10 mm. The screws used in the study are sheet metal screws with diameter of 4.1 mm and length of 25 mm, and the nails have diameter of 3.0 mm and length of 60 mm. Each specimen of screw test was predrilled 5 mm (pilot hole) with diameter 3.5 mm, while nail test was predrilled 10 mm with diameter 1.5 mm. Then screw and nail were hand-driven 5 mm into the panel specimens. The cross-head speed of screw and nail withdrawal tests was set at 10 mm/min. The tests were carried out on an Instron Universal Testing Machine and performed at ambient conditions of 25 °C. Five replications of each composite formulation were tested. Screw and nail withdrawal strengths were determined using the following equation [20].

$$WR = \frac{P_{max}}{D} \qquad \left(\frac{N}{mm}\right) \tag{12.1}$$

where *WR* is withdrawal strength, P_{max} is ultimate load (N) required to pull out screw or nail from the panel specimen, and *D* is the depth (mm) of the screw or nail penetrated into specimen [20].

Statistical analysis. Results, such as mean values and standard deviations, from five samples of each test were statistically analyzed. The effects of extruded density on the WPCs' properties were evaluated by analysis of variance (ANOVA), and then a comparison of the means was done with Tukey's multiple comparison test. All the statistical analyses used a 5% significance level ($\alpha = 0.05$).

12.4 Results and discussion

12.4.1 Density and hardness analysis

Results for composite density are given in Figure 12.2. They are found that the density of the rPP/RWF composites ranges from 0.963 g/cm^3 to 1.085 g/cm^3, depending on the cross-section size. An increase of the cross section clearly

decreased the composite density. This is because of the decrease of compressive forces in the extruding as well as the increasing number of porosity.

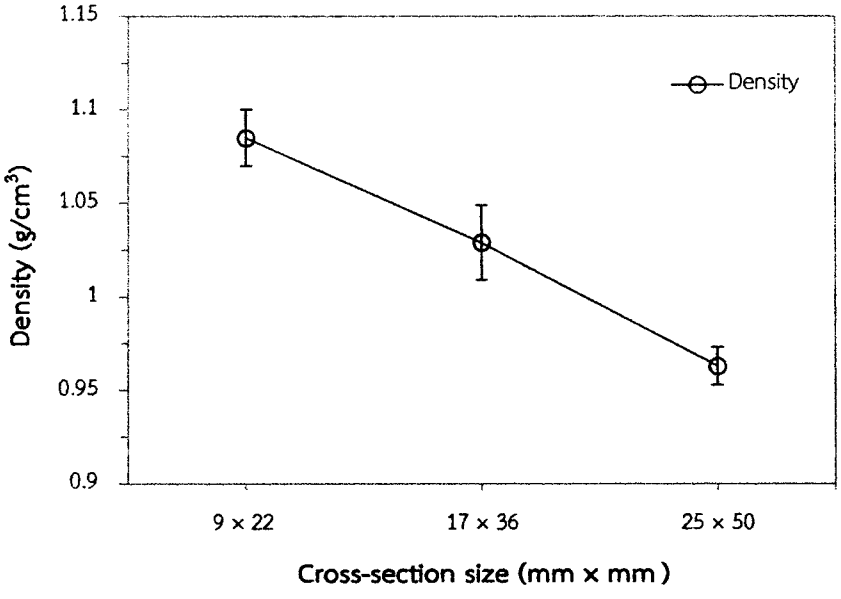

Figure 12.2 Effect of cross section on density of rPP/RWF composites

The hardness of rPP/RWF composites was found in the range of 72.65 to 75.56 shore D in Figure 12.3 and Table 12.1. The hardness steadily reduced with a decrease of extruded density. This is because the rPP/RWF composites with lower density allow easy access of indenter of the Durometer. In addition, these results are verified by the statistical analysis of variance (ANOVA). According to the one-way ANOVA of the rPP/RWF composites (in Table 12.1), the extruded density significantly affected the hardness of the composites. Tukey's test in Table 12.1 also indicates that the decreasing density of composites from 1.085 g/cm^3 (suffix a) to 1.029 g/cm^3 (suffix a) insignificantly reduced the density, but significantly decreased for the density 0.963 g/cm^3.

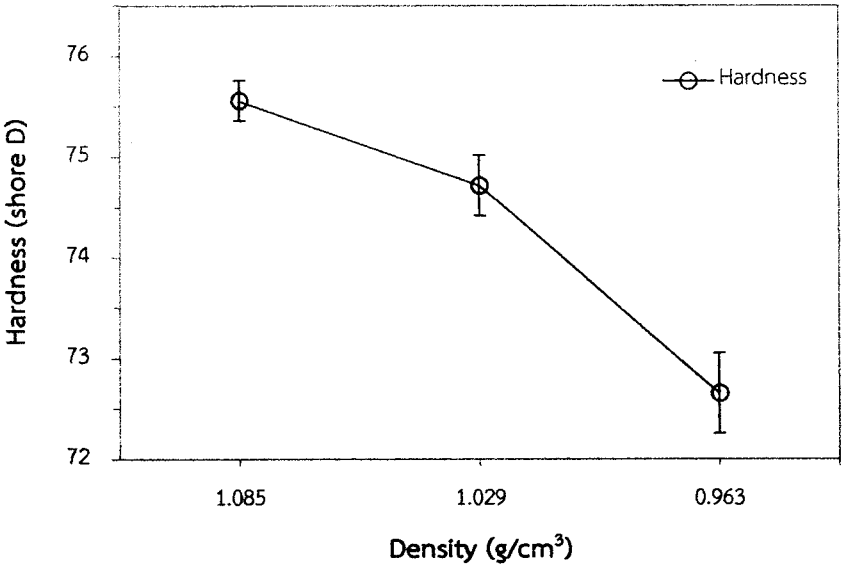

Figure 12.3 Effect of extruded density on hardness of rPP/RWF composites

Table 12.1 Effect of extruded density in physical and mechanical properties of the rPP/RWF composites

Property	Extruded density (g/cm^3)			p-value
	1.085	1.029	0.963	
Hardness (shore D)	75.56^{a}	74.72^{a}	72.65^{b}	0.028
Flexural strength (MPa)	47.28^{a}	37.55^{b}	25.29^{c}	0.001
Flexural modulus (GPa)	2.53^{a}	2.40^{a}	1.81^{b}	0.000
Compressive strength (MPa)	17.11^{a}	14.35^{ab}	10.76^{b}	0.000
Compressive modulus (GPa)	1.37^{a}	1.14^{ab}	0.95^{b}	0.001
Tensile strength (MPa)	27.68^{a}	16.23^{b}	9.11^{b}	0.001
Tensile modulus (GPa)	1.02^{a}	0.51^{b}	0.31^{b}	0.000
Screw withdrawal (N/mm)	122.09^{a}	120.85^{a}	93.54^{b}	0.008
Nail withdrawal (N/mm)	11.31^{a}	10.53^{ab}	8.94^{b}	0.031

Note; Means within each row with the same letter are not significantly different (Tukey's test, $\alpha = 0.05$).

12.4.2 Mechanical properties

Flexural strength and modulus of rPP/RWF composites with three different densities are shown in Figure 12.4. The flexural strength linearly reduced with a decrease of density, whereas the flexural modulus slowly reduced with the

decrease of density 1.029 g/cm^3 and sharply decreased with the further decrease of density 0.963 g/cm^3. This is because of the increasing number of porosity, resulting in poor stress transfer in the composite materials. This reason can be substantiated by considering in Figure 12.5. The rPP/RWF composites with lower density or higher cross-section size exhibited the increasing number of voids and larger porosity. Furthermore, the ANOVA results in Table 12.1 also revealed that the density significantly affected the flexural properties.

Figure 12.6 shows variation in the compressive strength and modulus with different density. Both compressive strength and modulus of the rPP/RWF composites reduced with the decrease of the density. The reason for this phenomenon is probably similar to that shown in the flexural properties. The ANOVA results in Table 12.1 demonstrated that the effects of the density on the compressive properties are statistically significant.

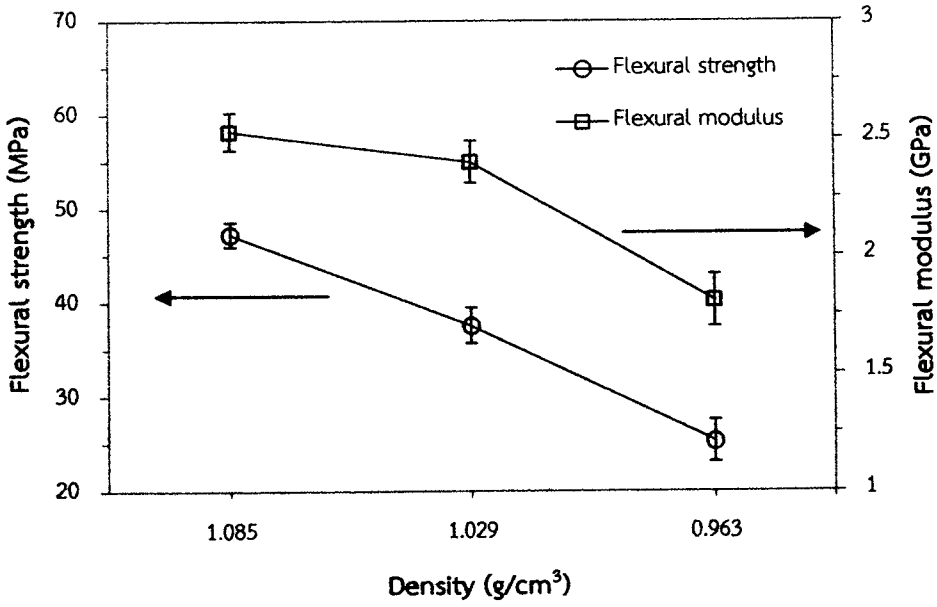

Figure 12.4 Effect of extruded density on flexural strength and modulus of rPP/RWF composites

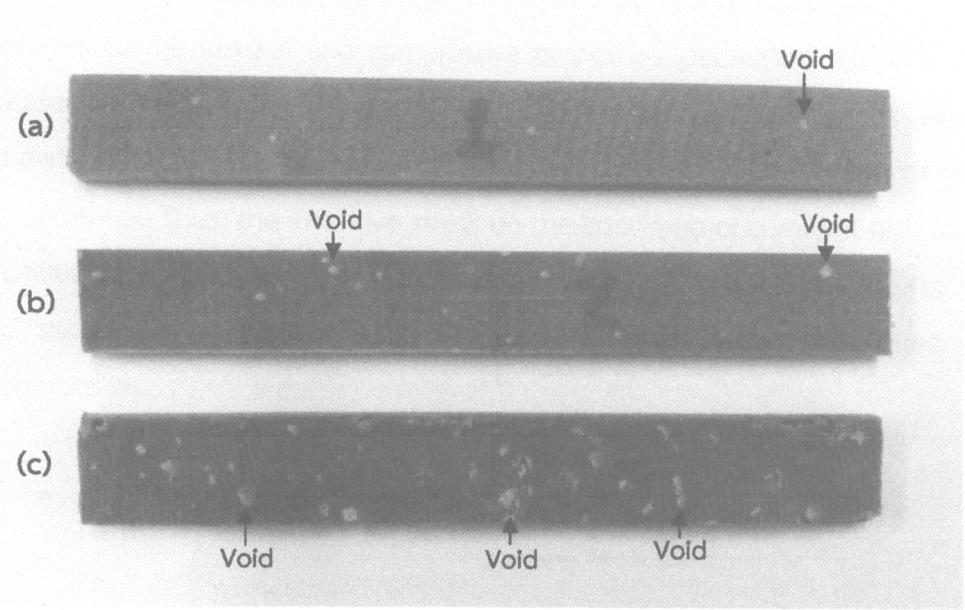

Figure 12.5 Composite samples produced from dies (a) 9 mm × 22 mm, (b) 17 mm × 36 mm, and (c) 25 mm × 50 mm

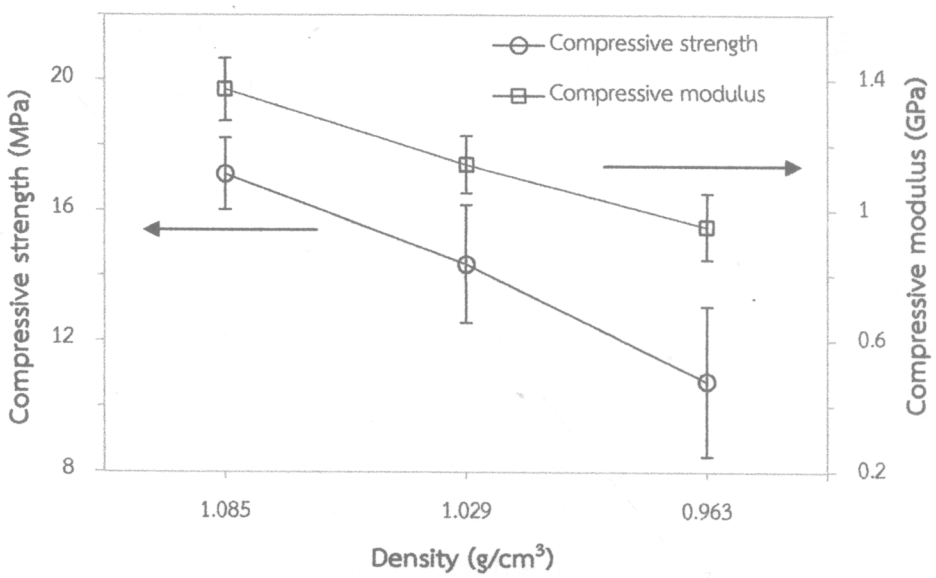

Figure 12.6 Effect of extruded density on compressive strength and modulus of rPP/RWF composites

Figure 12.7 shows the tensile strength and modulus of rPP/RWF composites with different density. Both the tensile strength and modulus exhibited a similar behavior to the flexural and compressive properties, decreased sharply with the decrease of the density. Potential mechanisms causing these trends were discussed earlier for flexural properties. The increase of voids means that mass of the specimen decreases. Thus, the intensive stress on the specimen occurred at high and large porosities, resulting in poor bearing the stress transfer. The ANOVA results in Table 12.1 showed a significant effect of the density on the tensile properties of rPP/RWF composites.

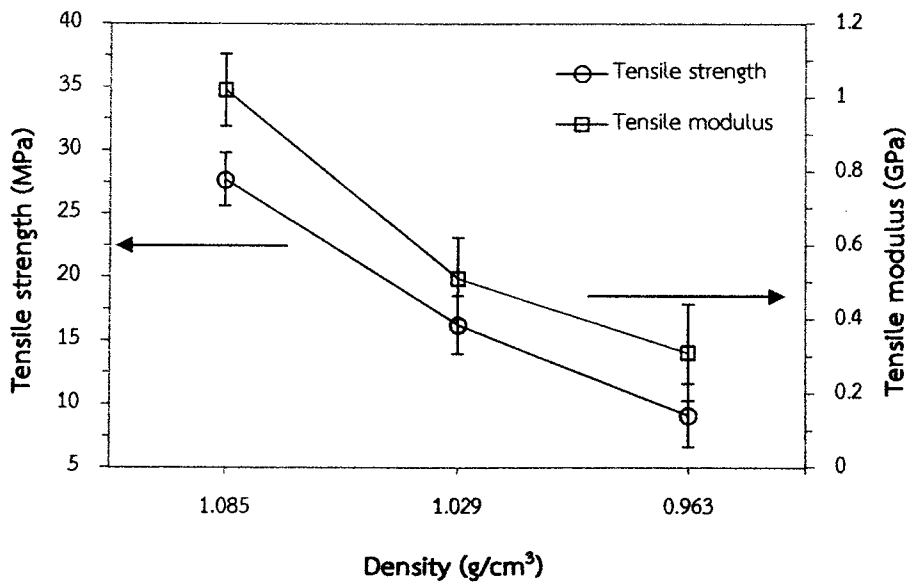

Figure 12.7 Effect of extruded density on tensile strength and modulus of rPP/RWF composites

12.4.3 Screw and nail withdrawal strengths

Screw and nail withdrawal strengths of the rPP/RWF composites with three different densities are shown in Figure 12.8. The decrease of density from 1.085 g/cm^3 to 1.029 g/cm^3 insignificantly reduced both screw and nail withdrawal strengths of the composites, whereas the composites with density 0.963 g/cm^3 steadily decreased the screw and nail withdrawal strengths. This decrease is probably due to weak structures of composite materials. The increasing void and larger

porosity easily allow pulling out the screw and nail from the panel composites. Besides, the screw exhibited significantly higher withdrawal strengths than the nail. The ANOVA results in Table 12.1 also exhibited that the density significantly affected both screw and nail withdrawal strengths.

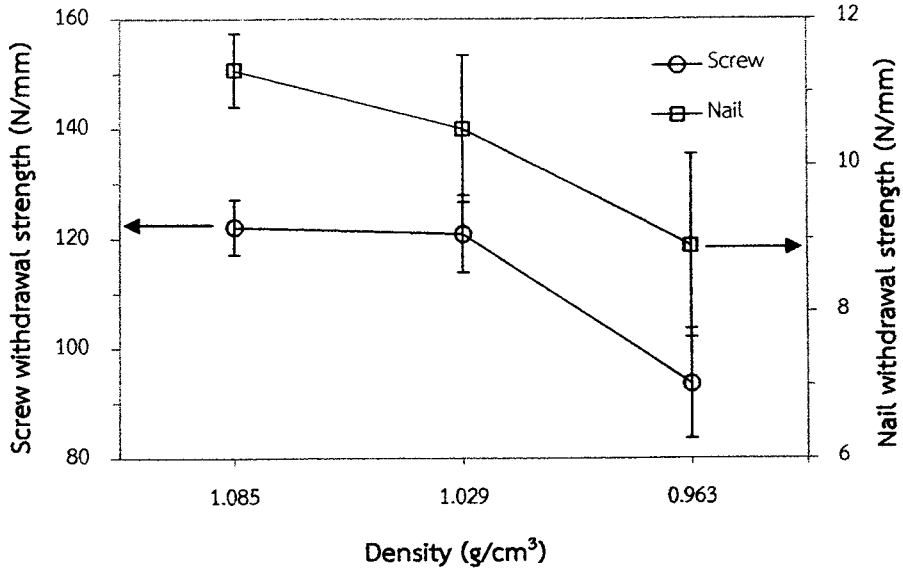

Figure 12.8 Effect of extruded density on screw and nail withdrawal strengths of rPP/RWF composites

12.4.4 Cost estimation

When the new materials are successfully developed, the cost calculation of the products manufactured from such materials is necessary. Generally, the cost of product consists of seven main types: (1) direct material; (2) indirect material; (3) energy; (4) overhead; (5) depreciation; (6) direct labor; and (7) indirect labor, as shown in Figure 12.9. This figure shows the example cost of hub front product, which could be seen that the main cost of the product is the direct material cost (64%) and the energy cost (18%) [21]. Likewise, flange final driven and heat sink products were found that the direct material costs are 32% and 58%, respectively, and the energy costs are 16% and 17%, respectively [21]. Therefore, this research particularly explores the direct material cost and energy cost (or energy cost

of processing) of decking board produced from new composite materials with dimensions of 25 mm × 50 mm × 1000 mm.

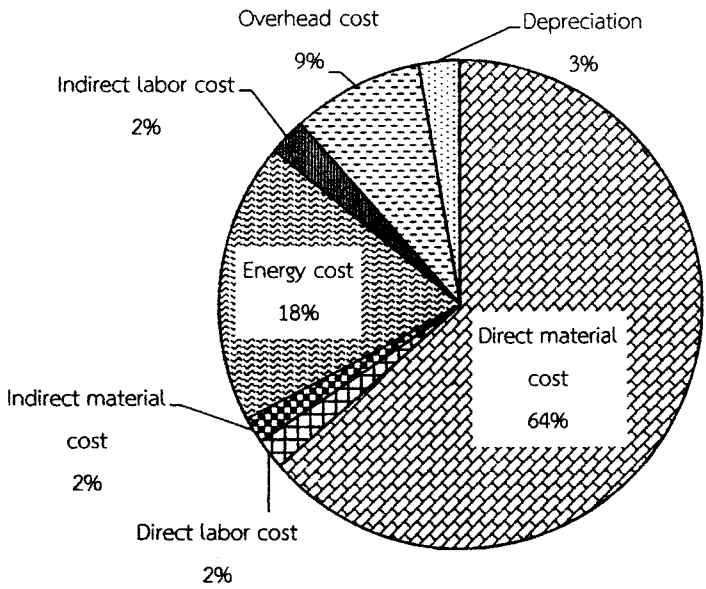

Figure 12.9 Cost per unit of hub front product [21]

Direct material cost of rPP/RWF composites. The materials used to produce the decking board include the five compositions: rPP (50.3 wt%); RWF (44.5 wt%); MAPP (3.9 wt%); UV stabilizer (0.2 wt%); and lubricant (1.0 wt%). The decking board with dimensions of 25 mm × 50 mm × 1000 mm had the weight of 1,356 g. Thus, the quantities of each material mixed is 682.068 g for rPP, 603.420 g for RWF, 52.884 g for MAPP, 2.712 g for UV stabilizer, and 13.56 g for lubricant, as shown in Table 12.2. Likewise, the prices of each material are shown in Table 12.2, such as 0.041 baht/g for rPP, 0.001 baht/g for RWF, etc. Therefore, the direct material cost of each material can be calculated by using:

$$\text{Cost}_{\text{material}} = \text{quantity} \times \text{price} \qquad (12.2)$$

The total cost of direct materials is 375.23 baht per piece.

Table 12.2 Direct material cost of rPP/RWF composites with dimensions of 25 mm × 50 mm × 1000 mm

Material	Quantity (g)	Price (Baht/g)	Cost (Baht)
rPP	682.068	0.041	27.964
RWF	603.420	0.001	0.603
MAPP	52.884	6.520	344.800
UV stabilizer	2.712	0.291	0.789
Lubricant	13.560	0.079	1.079
Total cost of direct materials			375.235

Energy cost in processing of rPP/RWF composites. The production of the WPC products was included with three stage processes: (1) preparing process; (2) mixing process; and (3) manufacturing process. The machines used in the preparing process are sieve machine and oven, as shown in Table 12.3. The sieve machine and oven used electric power are 0.37 and 2.17 kW, respectively, and they were consumed 0.5 and 0.28 hour, respectively. The other processes are also shown the details in Table 12.3. Furthermore, expense of electric energy for small business with voltage of 22-33 kV is 2.4649 baht per unit. Therefore, the energy cost of each machine can be calculated by using:

$$\text{Energy Cost}_{\text{processing}} = \text{electric power} \times \text{consumption} \times 2.4649 \quad (12.3)$$

The total energy cost of processing is 13.11 baht per piece.

The estimated cost of the decking board product with dimensions of 25 mm × 50 mm × 1000 mm based on the summation of direct material cost and energy cost in processing is approximately 388 baht per piece.

Table 12.3 Energy cost in processing of rPP/RWF composites with dimensions of 25 mm × 50 mm × 1000 mm

Machine	Electric power (kW)	Consumption (Hour)	Cost (Baht)
Preparing process			
Sieve machine	0.37	0.5	0.456
Oven	2.17	0.28	1.497
Mixing process			
Extruder machine	23.65	0.083	4.838
Pelletizer machine	1.50	0.083	0.306
Cooling machine	0.55	0.083	0.112
Manufacturing process			
Oven	2.17	0.15	0.802
Extruder machine	23.65	0.083	4.838
Vacuum pump	0.75	0.083	0.153
Cooling machine	0.55	0.083	0.112
Total energy cost in processing			13.114

12.5 Conclusions

The evaluation of extruded density of the composite materials is necessary, when the products are expanded to larger sizes. The effects of extruded density of the composites from recycled polypropylene and rubberwood flour were investigated experimentally. The physical and mechanical properties of the composites were significantly dependent on the density. The properties of flexural strength, and tensile strength and modulus significantly decreased with a decrease of the density. However, the hardness, flexural modulus, compressive properties, and screw and nail withdrawal strengths insignificantly reduced with a decrease of the density from 1.085 g/cm^3 to 1.029 g/cm^3, but significantly decreased for the density 0.963 g/cm^3 due to the increasing number of porosity, resulting in poor stress transfer in the composite materials. In addition, the estimated cost of the decking board product with dimensions of 25 mm × 50 mm × 1000 mm is approximately 388 baht per piece.

12.6 References

[1] S. Rimdusit, W. Smittakorn, S. Jittarom, and S. Tiptipakorn. "Highly Filled Polypropylene Rubber Wood Flour Composites." *Engineering Journal*, vol. 15, pp. 17–30, 2011.

[2] P. Petchpradab, T. Yoshida, T. Charinpanitkul, and Y. Matsumura. "Hydrothermal Pretreatment of Rubber Wood for the Saccharification Process." *Industrial and Engineering Chemistry Research*, vol. 48, pp. 4587–4591, 2009.

[3] C. Homkhiew, T. Ratanawilai, and W. Thongruang. "Composites from Recycled Polypropylene and Rubberwood Flour: Effects of Composition on Mechanical Properties." *Journal of Thermoplastic Composite Materials*, Epub ahead of print 14 February 2013. DOI: 10.1177/0892705712475019.

[4] S.L. Favaro, M.S. Lopes, A.G.V.d.C. Neto, R.R.d. Santana, and E. Radovanovic. "Chemical, Morphological, and Mechanical Analysis of Rice Husk/Post-Consumer Polyethylene Composites." *Composites Part A: Applied Science and Manufacturing*, vol. 41, pp. 154–160, 2010.

[5] N. Sombatsompop, W. Prapruit, K. Chaochanchaikul, T. Pulngern, and V. Rosarpitak. "Effects of Cross Section Design and Testing Conditions on the Flexural Properties of Wood/PVC Composite Beams." *Journal of Vinyl and Additive Technology*, vol. 16, pp. 33–41, 2010.

[6] H. Bouafif, A. Koubaa, P. Perre, and A. Cloutier. "Effects of Fiber Characteristics on the Physical and Mechanical Properties of Wood Plastic Composites." *Composites Part A: Applied Science and Manufacturing*, vol. 40, pp. 1975–1981, 2009.

[7] S. Ghahri, S.K. Najafi, B. Mohebby, and M. Tajvidi. "Impact Strength Improvement of Wood Flour–Recycled Polypropylene Composites." *Journal of Applied Polymer Science*, vol. 124, pp. 1074–1080, 2012.

[8] S. Butylina, M. Hyvärinen, and T. Kärki. "A Study of Surface Changes of Wood-Polypropylene Composites as the Result of Exterior Weathering." *Polymer Degradation and Stability*, vol. 97, pp. 337–345, 2012.

[9] N. Sombatsompop and K. Chaochanchaikul. "Effect of Moisture Content on Mechanical Properties, Thermal and Structural Stability and Extrudate Texture of Poly(Vinyl Chloride)/Wood Sawdust Composites." *Polymer International*, vol. 53, pp. 1210–1218, 2004.

[10] N. Petchwattana, S. Covavisaruch, and S. Chanakul. "Mechanical Properties, Thermal Degradation and Natural Weathering of High Density Polyethylene/Rice Hull Composites Compatibilized with Maleic Anhydride Grafted Polyethylene." *Journal of Polymer Research*, vol. 19, pp. 1–9, 2012.

[11] A. Nourbakhsh, A. Ashori, H.Z. Tabari, and F. Rezaei. "Mechanical and Thermo-Chemical Properties of Wood-Flour/Polypropylene Blends." *Polymer Bulletin*, vol. 65, pp. 691–700, 2010.

[12] M.A.S. Spinace, K.K.G. Fermoseli, and M.A.D. Paoli. "Recycled Polypropylene Reinforced with Curaua Fibers by Extrusion." *Journal of Applied Polymer Science*, vol. 112, pp. 3686–3694, 2009.

[13] M.N. Ichazo, C. Albano, J. Gonzalez, R. Perera, and M.V. Candal. "Polypropylene/Wood Flour Composites: Treatments and Properties." *Composite Structures*, vol. 54, pp. 207–214, 2001.

[14] M. Bengtsson, M.L. Baillif, and K. Oksman. "Extrusion and Mechanical Properties of Highly Filled Cellulose Fibre–Polypropylene Composites." *Composites Part A: Applied Science and Manufacturing*, vol. 38, pp. 1922–1931, 2007.

[15] K.B. Adhikary, S. Pang, and M.P. Staiger. "Dimensional Stability and Mechanical Behaviour of Wood-Plastic Composites based Recycled and Virgin High-Density Polyethylene." *Composites Part B: Engineering*, vol. 39, pp. 807–815, 2008.

[16] P.Y. Kuo, S.Y. Wang, J.H. Chen, H.C. Hsueh, and M.J. Tsai. "Effects of Material Compositions on the Mechanical Properties of Wood–Plastic Composites Manufactured by Injection Molding." *Materials and Design*, vol. 30, pp. 3489–3496, 2009.

[17] S.M.B. Nachtigall, G.S. Cerveira, and S.M.L. Rosa. "New Polymeric-Coupling Agent for Polypropylene/Wood-Flour Composites." *Polymer Testing*, vol. 26, pp. 619–628, 2007.

[18] H.P. San, L.A. Nee, and H.C. Meng. "Physical and Bending Properties of Injection Moulded Wood Plastic Composites Boards." *ARPN Journal of Engineering and Applied Sciences*, vol. 3, pp. 13–19, 2008.

[19] British Standard. "*Wood-Plastics Composites (WPC) Part 1: Test Methods for Characterisation of WPC Materials and Products*." 2007.

[20] A.R. Haftkhani, G. Ebrahimi, M. Tajvidi, and M. Layeghi. "Investigation on Withdrawal Resistance of Various Screws in Face and Edge of Wood-Plastic Composite Panel." *Materials and Design*, vol. 32, pp. 4100–4106, 2011.

[21] W. Chienwichai. "A Cost Model Development and Cost Comparison of Liquid Die Casting Process and Semi-Solid Die Casting Process for Machinery Parts Factory." M.E. thesis, Prince of Songkla University, Thailand, 2012.

CHAPTER 13

Conclusions and Recommendations

13.1 Conclusions

Wood-plastic composites (WPCs) were made from recycled polypropylene (rPP) and rubberwood flour (*Hevea brasiliensis*) as reinforcement. Post-consumer polypropylene and rubberwood waste were used as main materials. Some formulations of WPCs were also made with virgin polypropylene (vPP) for comparative studies. WPC panels were manufactured by using twin-screw extruder based on formulations designed with mixture experiment, the components being rPP, rubberwood flour (RWF), maleic anhydride-grafted polypropylene (MAPP), ultraviolet (UV) stabilizer, and lubricant (Lub). The experimental design and analysis were done with Design-Expert software (version 8.0.6, Stat-Ease, Inc.), according to D-optimal mixture design. Mechanical properties, morphology, durability, and dimensional stability of WPCs were investigated. Long-term water absorption, thickness swelling, and mechanical failure of WPCs with water immersion tests were also studied. Durability performances of WPCs were studied by exposing WPCs to natural weathering. These characterizations of WPCs were investigated to optimize the mixture ratios for composites made from rPP and RWF and to assess the effect of the compositions. In addition, to develop such composites as building products, creep behavior, lifetime prediction, and extruded density effects were also examined. The major findings from these studies are summarized in sequent sections.

13.1.1 Long-term water absorption of composites and optimal formulation

The long-term water immersion test of the PP/RWF composites over a period of 10 weeks (70 days) revealed that both water absorption (WA) and thickness swelling (TS) increased with wood flour content. At 45 wt% RWF, the rPP composites had initially higher WA and TS than the vPP composites; however, after 6 weeks of

immersion the vPP and rPP composites had closely similar saturation values. Besides, an addition of MAPP at 3 wt% reduced WA and TS, with no further benefit reached at 5 wt% MAPP: using more than 3 wt% MAPP may be unnecessary and uneconomical. In contrast, the addition of 1 wt% UV stabilizer increased the WA and TS of composites, and thus adding amount of UV stabilizer should be as small as possible. The flexural strength and modulus of composites reduced significantly with moisture uptake; however, at WA less than 3% its effects on flexural strength were not significant. The maximum strain of composites significantly increased with absorption. In addition, the regression models fitted were used for optimization of a desirability score, substituting for the multiple objectives modeled. The optimal formulation based on the water absorption was exhibited in Table 13.1.

Table 13.1 Optimal formulation based on each property

	Mixture component proportion (wt%)				
Characteristic	rPP	RWF	MAPP	UV	Lub
Water absorption	68.9	25.0	5.0	0.1	1.0
Natural weathering resistance	61.9	33.9	3.1	0.2	1.0
Creep behavior	50.5	44.9	3.5	0.1	1.0
Mechanical properties*	50.3	44.5	3.9	0.2	1.0

*The optimal formulation based on the mechanical properties has the density of 1.085 g/cm^3. These optimal formulations were produced using a twin-screw extruder (Model SHJ-36 from En Mach Co., Ltd, Nonthaburi, Thailand). The extruding conditions were as follows: (1) temperature profiles: 130–190 °C; (2) screw rotating speed: 50 rpm; (3) vacuum venting at 9 temperature zones: 0.022 MPa; and (4) melt pressure: 0.10-0.20 MPa. The samples were extruded through a rectangular die with the dimensions of 9 mm × 22 mm and cooled in ambient air.

13.1.2 Exposure to natural weathering of composites and optimal formulation

In natural weathering test, changes in the physical and mechanical properties of WPCs based on both virgin and recycled PP were investigated for a total of 360 days. The results demonstrated that the lightness and discoloration of unfilled PP and PP/RWF composites sharply increased after exposing 60 days and then it clearly decreased at 180 weathering days, but it again enhanced slightly after

exposing 240 days as the exposure times increased. Moreover, the composites based on virgin PP (vPP) show lower percentage change of L^* and loss percentage of hardness, flexural strength and modulus than those based on rPP, for the same plastic to wood ratio. The increasing RWF content from 25 to 45 wt% in vPP and rPP composites increased the percentage change of lightness and loss percentage of flexural strength and modulus, and maximum strain. For the effect of UV stabilizer, it was observed that the rPP/RWF composites adding 1 wt% UV stabilizer exhibited lower percentage change of lightness and loss percentage of hardness, flexural strength and modulus, and maximum strain than the composites without UV stabilizer. In addition, the regression models fitted were used to optimize a desirability score that balanced multiple physical and mechanical properties. The optimal formulation based on the exposure to the natural weathering was shown in Table 13.1.

13.1.3 Creep behavior of composites and optimal formulation

In the creep tests, the plastic grades and rubberwood flour contents showed a large impact on the creep behavior of the composites. The neat vPP and composites based on vPP exhibited lower creep deformation than those based on rPP, for the same plastic to wood ratio. The creep strain reduced as the wood flour level increased. It was clearly revealed that the addition of rubberwood flour in PP composites can be efficiently improved the poor creep stability of polyolefin. The additions of 5 wt% MAPP content increased the creep strain of composites. Likewise, the creep strain was significantly increased by an addition of 1 wt% UV stabilizer content. Further, the short-term flexural creep behavior could be well fitted by using the Burger model. Besides, the approximately optimal formulation jointly minimizing all creep characteristics was shown in Table 13.1. The joint optimization maximized a desirability score that balanced the multiple objectives, and the jointly optimal formulation was experimentally validated to produce low creep nearly as predicted.

13.1.4 Mechanical properties and optimal formulation

The mechanical and physical properties of PP/RWF composites affected plastic grades (virgin and recycled) and contents of wood flour, coupling agent, and UV stabilizer were also examined. The results revealed that the strengths (flexure, compression, and tension) of RWF reinforced rPP composites could be enhanced with increasing wood flour contents beyond 25 wt%, whereas those composites based on vPP show lower strengths than the unfilled vPP. The modulus and hardness of composites (both virgin and recycled plastics) increased linearly with wood flour loadings. The unfilled rPP and composites based on rPP exhibit lower mechanical properties than those based on vPP for the same plastic to wood ratio. The addition level of 4.0 wt% MAPP in the rPP/wood flour composites is suggested for economical benefit and good mechanical properties. The strength, modulus, and hardness of composites were reduced by an addition of 1 wt% UV stabilizer content. To limit the negative effects of the UV stabilizer on the mechanical properties of the composites, its use should be minimized. Moreover, the models fitted were used for optimization of a desirability score, substituting for the multiple objectives modeled. The optimal formulation found was exhibited in Table 13.1; the composite made with this formulation had good mechanical properties that closely matched the model predictions.

13.1.5 Time-temperature and stress dependent behaviors

The optimal composite formulation based on mechanical properties previously found was used to investigate experimentally and model numerically the time-temperature and stress dependent behaviors and to predict the lifetime of the building products. The creep was dependent on both temperature and stress, increasing with both of these. The Burger and Power law models were both able to fit well the creep data, but at high temperature and stress levels the Power law gave the poorer fit of these models. The HRZ model provided an approximate interpolation across temperatures or stresses of the Power law fits, and also fit these data well in cases where the Power law performed well. The master curves from time-temperature and time-stress superpositions were in good agreement with each

other. From the master curves the long-term creep was predicted with stresses 3 and 15 MPa at 25 °C, suggesting that the creep lifetime of rPP/RWF composites exceeds 10 years.

13.1.6 Effect of extruded density on mechanical properties

When the building composite products were expanded to have larger cross-section sizes, it is necessary to evaluate the effect of different extruded density on the physical and mechanical properties. The properties of flexural strength, and tensile strength and modulus significantly decreased with a decrease of the extruded density. However, the hardness, flexural modulus, compressive properties, and screw and nail withdrawal strengths insignificantly reduced with a decrease of the density from 1.085 g/cm^3 to 1.029 g/cm^3, but significantly decreased for the density 0.963 g/cm^3 due to the increasing number of porosity, resulting in poor stress transfer in the composite materials. In addition, the estimated cost of the decking board product with dimensions of 25 mm x 50 mm x 1000 mm is approximately 388 baht per piece, which composed of 375 baht for direct materials cost and 13 baht for energy cost in processing.

13.2 Recommendations for future work

The new information offered in this study will facilitate the development and manufacturing of the WPCs from recycled polypropylene and rubberwood flour, but there are still more work needed to investigate additional performances of the product in applications, for example, the studies in stress relaxation, fatigue, recovery, etc. Likewise, the manufacturing conditions of the composites should be also examined. From this study, it was observed that the optimal formulation on the mechanical and creep properties had almost 45 wt% RWF. Therefore, the increasing addition of RWF in the composites should be further investigated to improve the WPC performances and to reduce the cost. Furthermore, the study in the effects of the natural weathering was found that the lightness and discoloration of the composites sharply increased, and thus the addition of pigment filler is necessary. In addition, from the cost estimation of the composites it was

found that the MAPP is the most ex pensive, comparing to other components; thereby, other coupling agents should be further studied to replace as a cheaper coupling agent.

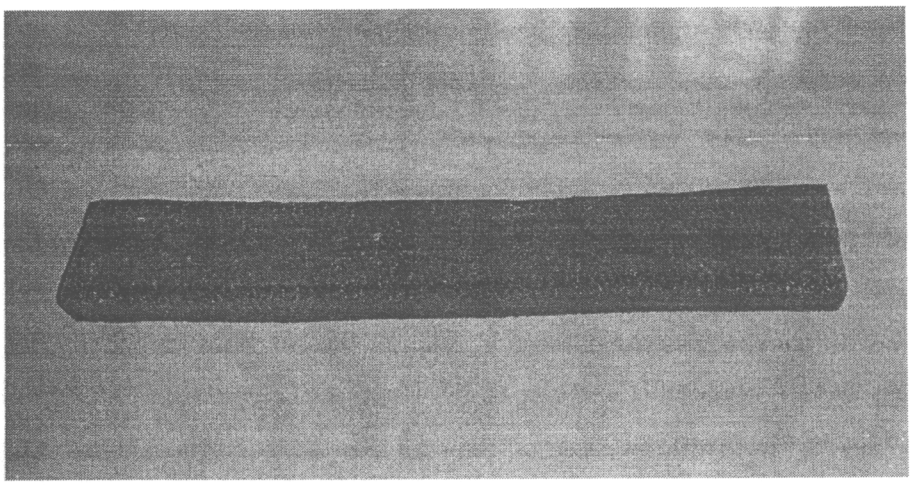

(a)

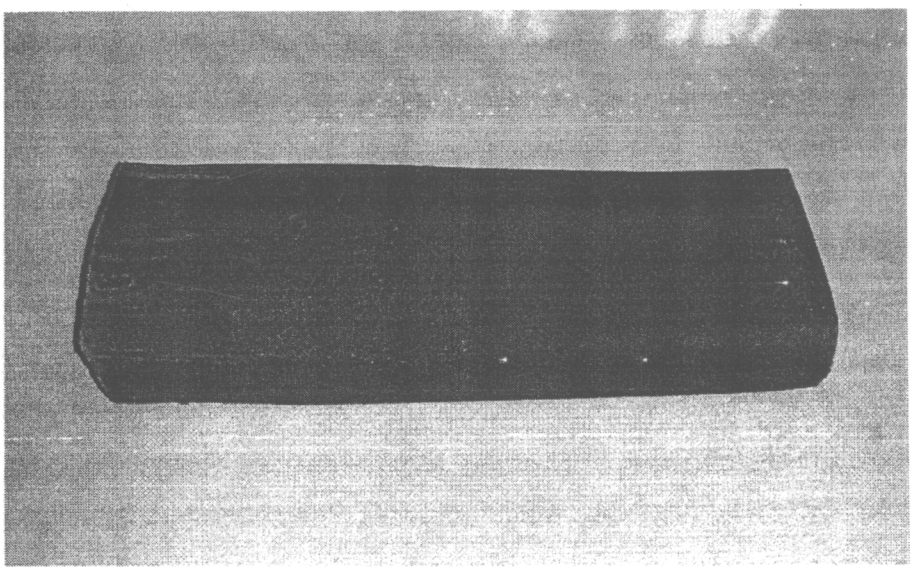

(b)

Figure 13.1 WPC decking products with cross-section sizes (a) 9 mm × 22 mm and (b) 25 mm × 50 mm

APPENDIX

Contents lists available at ScienceDirect

Composites: Part B

journal homepage: www.elsevier.com/locate/compositesb

The optimal formulation of recycled polypropylene/rubberwood flour composites from experiments with mixture design

Chatree Homkhiew[a], Thanate Ratanawilai[a,*], Wiriya Thongruang[b]

[a] Department of Industrial Engineering, Faculty of Engineering, Prince of Songkla University, Hat Yai, Songkhla 90112, Thailand
[b] Department of Mechanical Engineering, Faculty of Engineering, Prince of Songkla University, Hat Yai, Songkhla 90112, Thailand

ARTICLE INFO

Article history:
Received 4 April 2013
Received in revised form 8 July 2013
Accepted 12 August 2013
Available online 20 August 2013

Keywords:
A. Polymer–matrix composites (PMCs)
B. Mechanical properties
C. Statistical properties/methods
E. Extrusion

ABSTRACT

A mixture design was used in experiments, to determine the optimal mixture for composites of rubberwood flour (RWF) and reinforced recycled polypropylene (rPP). The mixed materials were extruded into panels. Effects were determined of the mixture components rPP, RWF, maleic anhydride-grafted polypropylene (MAPP), and ultraviolet (UV) stabilizer, on the mechanical properties. The overall composition significantly affected flexural, compressive, and tensile properties. The fractions of recycled polypropylene and rubberwood flour increased all the mechanical material properties; however, increasing one fraction must be balanced by decreasing the other, and the rubberwood flour fraction had a higher effect size. The fraction of MAPP was best kept in mid-range of the fractions tested, while the UV stabilizer fraction overall degraded the mechanical properties. Our results suggest that the fraction of UV stabilizer should be as small as possible to minimize its negative influences. The models fitted were used for optimization of a desirability score, substituting for the multiple objectives modeled. The optimal formulation found was 50.3 wt% rPP, 44.5 wt% RWF, 3.9 wt% MAPP, 0.2 wt% UV stabilizer, and 1.0 wt% lubricant; the composite made with this formulation had good mechanical properties that closely matched the model predictions.

1. Introduction

Wood waste is generated when wood is processed for various applications, such as in sawmills and in furniture making. The waste in the forms of flour, sawdust, and chips, has primarily been used as inexpensive filler in plastic industries, to reduce raw material costs and to increase the strength and modulus of various thermoplastics. Likewise, the wood particles show high specific strength and modulus that allow the production of low-density composites with higher filler content [1,2], and advantages associated with wood particles include their non-abrasive nature, low energy consumption, and biodegradability. Hence, these natural plant-based fillers offer several benefits over synthetic fillers [1]. Recent advances in natural fillers may lead to improved materials using renewable resources; this trend would also support global sustainability [3]. The mechanical properties of environmentally friendly plastic composites have been improved with wood waste from various tree species including eastern red cedar [4], maple [5], oak [4], pine [6], and rubberwood [7]. In addition, the increasing worldwide production and consumption of plastics has caused serious public concerns about effective and safe disposal [8]; however, plastic waste could be a promising raw material source for wood plastic composites (WPCs) [9]. The use of recycled plastics for producing WPCs would not only decrease the consumption of energy and natural resources, but also offers an effective and safe way to dispose of plastic waste [10]. Therefore, increasing the use of wood and plastic waste could reduce solid waste, lessen the amounts going to landfills, and decrease the cost of making WPCs [6,8].

A D-optimal mixture experimental design is a special type of statistical approach to experimentally find the individual effects and interactions of components in a mixture, and the fitted models can be used to find the optimal formulation of a composite material [11]. A D-optimal design can considerably reduce the number of experiments needed for scientific and technical information on the composition effects. It allows restricting the ranges of component fractions, and within this range of formulations helps fit the mathematical models, used to improve the characteristics of final goods [11,12]. Moreover, this method is appropriate for non-linear models [13].

The fractions of components in wood–plastic composites, such as polymer, filler and coupling agent, significantly affect their mechanical properties. Recently, several publications have assessed the effects of each material component on the thermal and mechanical properties. Mixture designs and factorial designs have been used in experiments on WPCs. Matuana et al. [14] used a four-factor central composite design to develop a response

* Corresponding author. Tel.: +66 74 287151; fax: +66 74 558829.
E-mail address: thanate.r@psu.ac.th (T. Ratanawilai).

1359-8368/$ - see front matter © 2013 Elsevier Ltd. All rights reserved.
http://dx.doi.org/10.1016/j.compositesb.2013.08.041

surface model and to study the foamability of rigid PVC/wood-flour composites. Stark and Matuana [15] applied a 2^4 factorial design to determine the effects of two hindered amine light stabilizers, a colorant, an ultraviolet absorber, and their interactions on the photo stabilization of wood flour/high-density polyethylene composites. Jun et al. [16] used a Box-Behnken design with response surface method to determine which variables influenced board performance significantly. Prior studies on the component effects and interactions, and optimization of the formulation for WPCs, seem not to have used a D-optimal mixture design. Here, a D-optimal mixture design was applied to model mechanical characteristics of WPCs. The main objective of this work was to optimize the mixture ratios for composites made from recycled polypropylene and rubberwood flour, based on mechanical properties determined experimentally. The new information will facilitate informed decisions regarding manufacture of such composites.

2. Materials and methods

2.1. Materials

Rubberwood flour (RWF) collected from a local furniture factory was used as lignocellulosic filler, and the size of the wood flour particles was smaller than 180 μm, after sieving through a standard sieve of 80 mesh. The chemical composition of RWF was, by weight: cellulose 39%; hemicellulose 29%; lignin 28%; and ash 4% [17]. Withaya Intertrade Co., Ltd. (Samutprakarn, Thailand) supplied recycled polypropylene (rPP) pellets with a melt flow index of 11 g/10 min at 230 °C, under the trade name WT170. The interfacial adhesion between wood flour and polymer was improved using maleic anhydride grafted polypropylene (MAPP), supplied by Sigma–Aldrich (Missouri, USA), with 8–10% of maleic anhydride (M_w = 9100, M_n = 3900) as a coupling agent. The ultraviolet (UV) stabilizer used was hindered amine light stabilizer additive, purchased from TH Color Co., Ltd. (Samutprakarn, Thailand) under the trade name MEUV008. Paraffin wax chosen as the lubricant (Lub) was supplied by Nippon Seiro Co., Ltd. (Yamaguchi, Japan).

2.2. Experimental design to optimize formulation

The responses of a process to various factors and parameters are effectively explored with designed experiments, using approaches such as the Taguchi method, factorial design, and mixture design [18,19]. The fractions of components in a mixture cannot be changed independently, and for this situation the mixture designs are appropriate. The nonnegative fractions must add up to 100%. For example, if $x_1, x_2, \ldots, x_l$ denote the fractions of l components of a mixture, then [18]

$$0 \leqslant x_i \leqslant 1 \quad i = 1, 2, \ldots, l$$

and $$x_1 + x_2 + \ldots + x_l = 1 \text{ (i.e., 100\%)}$$

The region of interest for the current experiments is not this simplex but has additional constraints added [18], so a D-optimal design was used to statistically evaluate the effects of component fractions on the mechanical properties, and the identified models were used to optimize the formulation. The optimized experimental design had mixture compositions for the manufacture of WPCs, the components being rPP (x_1), RWF (x_2), MAPP (x_3), UV (x_4), and Lub (x_5). The upper and lower limits of experimental range for the fractions are shown in Table 1. Despite the fraction of Lub being held constant, it is included as a variable because it contributes to the 100% in the mixture. The experimental design and analysis were done with Design-Expert software (version 8.0.6, Stat-Ease, Inc.), according to D-optimal mixture design. The design included 15 different formulations and 5 replicates to check the lack of fit. Thus, the total number of runs was 20, as shown in Table 2. After data collection, linear and quadratic models following Eqs. (1) and (2), respectively, were used to model the responses.

Table 1
Selected components and their constraints for the mixture design of experiments.

Component	Fraction restriction (wt%)
rPP (x_1)	$50 \leqslant x_1 \leqslant 70$
RWF (x_2)	$25 \leqslant x_2 \leqslant 45$
MAPP (x_3)	$3 \leqslant x_3 \leqslant 5$
UV stabilizer (x_4)	$0 \leqslant x_4 \leqslant 1$
Lub (x_5)	= 1

$$Y = \sum_{i=1}^{l} \beta_i x_i \tag{1}$$

$$Y = \sum_{i=1}^{l} \beta_i x_i + \sum \sum_{i<j}^{l} \beta_{ij} x_i x_j \tag{2}$$

where Y is the predicted response, β_i is the model response to a pure component in the blend, each β_{ij} scales an interaction between components, x_i, $x_j, \ldots, x_l$ are the fractions of components, and $x_ix_j, x_ix_k, \ldots, x_kx_l$ are the quadratic interactions of the fractions. Note that mixture models differ in appearance from the general polynomials applied in response surface work, because the constraint $\sum x_i = 1$ enables elimination of terms quadratic in a single fraction [18]. Because of this, Eq. (2) has the same power to fit data from mixtures as a general quadratic polynomial; such a polynomial can be rewritten in this form.

2.3. Composites processing

To minimize its moisture content, the rubberwood flour was carefully dried prior to use; in an oven at 110 °C for 8 h. WPCs were then manufactured in a two-stage process. In the first stage to produce WPC pellets, rubberwood flour and recycled polypropylene were dry-blended, and then melt-blended into wood–plastic composite pellets using a twin-screw extruder machine (Model SHJ-36 from En Mach Co., Ltd., Nonthaburi, Thailand). The 10 temperature zones of the extruder were set to a profile in range 130–170 °C, to reduce degradation of the mixture components, while the screw rotating speed was controlled at 70 rpm. The extruded strand passed through a water bath and was subsequently pelletized. In the second stage to produce WPC panels, the WPC pellets were again dried at 110 °C for 8 h. WPC pellets, MAPP, UV stabilizer, and lubricant compositions indicated in Table 2 were then dry-mixed, and added into the feeder of a twin-screw extruder. The processing conditions for extruding were as follows: (1) barrel temperatures: 130–190 °C; (2) screw rotation speed: 50 rpm; (3) melt pressure: 0.10–0.20 MPa depending on wood flour content; and (4) vacuum venting at nine temperature zones: 0.022 MPa. The samples were extruded through a 9 mm × 22 mm rectangular die and cooled in atmospheric air. Consequently, the specimens were machined following the standards of American Society for Testing and Materials (ASTM) for flexural, compressive, and tensile tests.

2.4. Mechanical properties

Flexural properties were measured in a three-point bending test at a cross-head speed of 2 mm/min, with nominal dimensions of 4.8 mm × 13 mm × 100 mm, and a span of 80 mm in accordance with ASTM D790-92. For compressive properties, prism specimens were used to determine the compressive strength and modulus.

Table 2
Experimental compositions and responses based on mixture experiment design.

Experiment run no.	Mixture component fraction (wt%)					Response (MPa)					
						Flexure		Compression		Tension	
	x_1	x_2	x_3	x_4	x_5	MOR	MOE	CS	CM	TS	TM
1	63.9	29.9	4.5	0.7	1.0	39.38	2120	12.43	978	24.86	833
2	70.0	25.0	3.0	1.0	1.0	36.84	1807	9.45	763	23.89	787
3	50.0	43.0	5.0	1.0	1.0	36.91	2429	8.89	1133	23.37	1058
4	54.9	38.9	4.5	0.7	1.0	41.62	2387	14.43	1018	26.17	967
5	59.5	34.5	5.0	0.0	1.0	43.51	1965	14.82	830	26.32	872
6	55.4	39.9	3.5	0.2	1.0	43.97	2472	16.44	1123	28.10	997
7	59.5	34.5	4.0	1.0	1.0	36.64	2119	9.03	945	23.79	961
8[a]	59.5	34.5	5.0	0.0	1.0	41.41	2040	15.61	915	27.42	867
9	50.0	44.3	4.3	0.5	1.0	40.44	2569	15.02	1287	26.84	1067
10	68.0	25.0	5.0	1.0	1.0	37.04	2007	8.21	826	23.29	738
11	50.0	45.0	3.0	1.0	1.0	39.66	2685	13.59	1202	23.97	993
12[a]	50.0	43.0	5.0	1.0	1.0	37.85	2485	10.23	1236	24.00	1083
13	60.3	35.3	3.0	0.5	1.0	40.23	2175	15.73	1151	25.38	879
14	64.9	30.4	3.5	0.2	1.0	41.01	1969	13.02	832	25.20	765
15[a]	70.0	25.0	3.0	1.0	1.0	36.94	1760	8.25	711	23.00	649
16	51.0	45.0	3.0	0.0	1.0	46.24	2601	17.96	1449	28.36	1087
17[a]	51.0	45.0	3.0	0.0	1.0	47.63	2740	18.20	1418	28.33	1074
18[a]	50.0	45.0	3.0	1.0	1.0	39.49	2676	11.74	1262	24.70	1024
19	70.0	25.0	4.0	0.0	1.0	38.95	1902	10.55	1006	24.65	760
20	69.0	25.0	5.0	0.0	1.0	38.44	1929	8.96	789	25.01	785

[a] Duplicate experiments.

Table 3
Tabulation of p-values from analysis of variance, for the quadratic and linear models, and for the individual interaction terms included in the quadratic models.[a]

Resource	MOR	MOE	CS	CM	TS	TM
Model	Quadratic	Quadratic	Quadratic	Quadratic	Quadratic	Linear
	<0.0001[a]	<0.0001[a]	<0.0001[a]	0.0002[a]	<0.0001[a]	<0.0001[a]
Linear mixture	<0.0001[a]	<0.0001[a]	<0.0001[a]	<0.0001[a]	<0.0001[a]	<0.0001[a]
x_1x_2	0.5289	0.0072[a]	0.1054	0.0958	0.9599	–
x_2x_3	0.8167	0.3759	0.3675	0.9867	0.3210	–
x_3x_4	0.6484	0.0844	0.0171[a]	0.4518	0.1583	–
x_2x_3	0.7577	0.5301	0.3433	0.9665	0.3374	–
x_2x_4	0.7047	0.0841	0.0196[a]	0.4440	0.1918	–
x_2x_4	0.5885	0.0195[a]	0.0273[a]	0.1605	0.1815	–
Lack of Fit	0.0628	0.4678	0.2521	0.0631	0.5874	0.6260

[a] P-value less than 0.05 is considered significant.

The displacement rate was a constant 0.5 mm/min, following ASTM standard D6108-97. Type-IV tensile bar specimens with dimensions of 115 mm × 19 mm × 4 mm were cut and machined from the extruded composite panels. The crosshead speed of tensile test was 5 mm/min, according to ASTM standard D638-99. The flexural, compressive and tensile measurements were carried out on an Instron Universal Testing Machine (Model 5582 from Instron Corporation, Massachusetts, USA) and performed at ambient conditions of 25 °C. Five replicates of each composite formulation were tested. Extrusion is directional and orients the fibers and polymer chains. The composite will not be similar in all directions (isotropic); instead, it has a preferred direction. The span in flexural testing was in the extrusion direction, and the same for tensile testing. The compression tests, however, compressed normal to the extrusion direction.

2.5. Morphological analysis

The interfacial morphology and phase dispersion of the wood flour in the polymeric matrix were assessed by imaging with a scanning electron microscope (SEM). The surfaces were prepared by sputter coating with gold, to prevent electrical charging, and were imaged with a FEI Quanta 400 microscope (FEI Company, Oregon, USA) at an accelerating voltage of 20 kV. Magnifications of 150× and 1000× were used.

Table 4
Model adequacy indicators for each modeled response of rPP/RWF composites.

Response	R^2	Adj-R^2	Pred-R^2	CV
MOR	0.9380	0.8841	0.5496	2.63
MOE	0.9838	0.9693	0.9237	2.51
CS	0.9490	0.9031	0.6751	8.15
CM	0.9258	0.8589	0.6135	7.94
TS	0.9533	0.9112	0.8004	2.04
TM	0.9153	0.8995	0.8577	4.72

3. Results and discussion

The D-optimal mixture design of experiments, with five fractions as (mutually dependent) variables (that sum to one), had 20 runs in a randomized order. The six determined responses were flexural strength (MOR) and modulus (MOE), compressive strength (CS) and modulus (CM), and tensile strength (TS) and modulus (TM). The results are summarized in Table 2.

3.1. Statistical analysis of the response surface model

Analysis of variance (ANOVA) of the response surface models indicated the quadratic model as the best fit with MOR, MOE, CS, CM, and TS, while TM was best fit with a linear model. These best

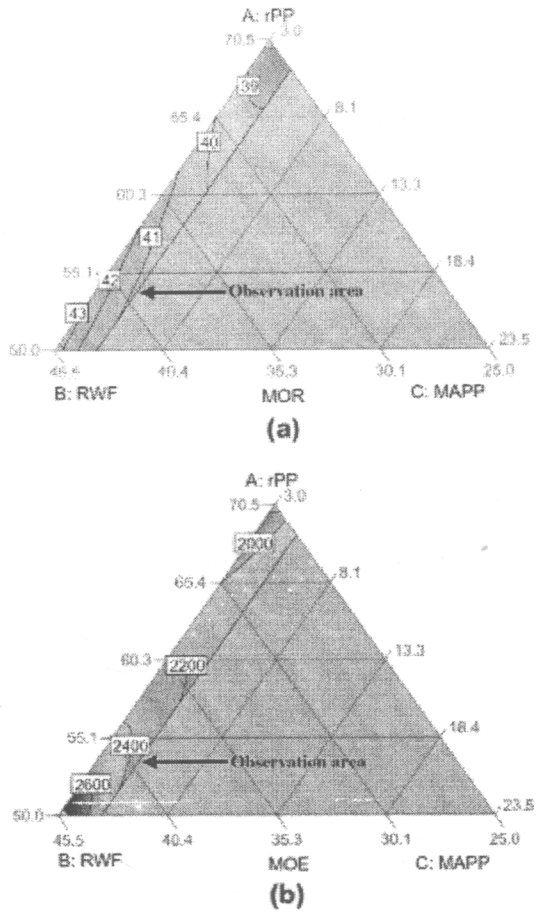

Fig. 1. Triangular contour plots for composition effects at fixed UV stabilizer fraction of 0.5 wt%, and Lab fraction 1 wt%: (a) MOR, and (b) MOE. The contours represent the models fit to experimental data.

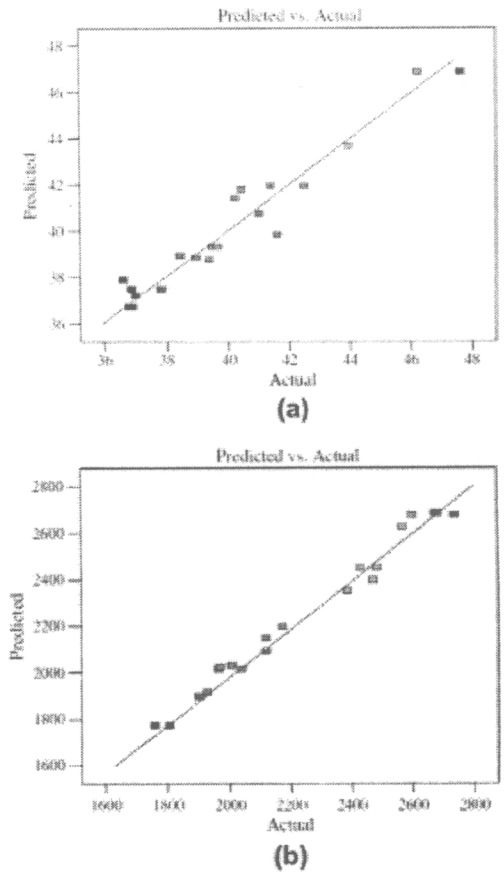

Fig. 2. Comparisons of model outputs to the fitted observed values for rPP/RWF composites. Model output was (a) MOR and (b) MOE.

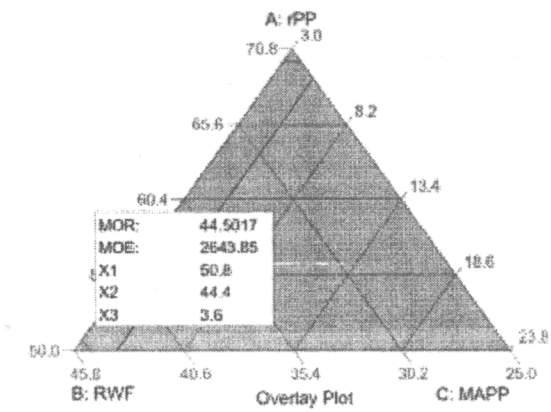

Fig. 3. The optimal formulation for flexural properties.

fit models had insignificant lack of fit and high coefficients of determination (both adjusted adj-R^2, and predicted pred-R^2). For example the quadratic model for the TS response had insignificant lack of fit with p-value 0.5874, and the coefficients of determination adj-R^2 = 0.9112 and pred-R^2 = 0.8004. The ANOVA analysis in Table 3 also indicates statistically significant quadratic terms in these models by p-values less than a significance threshold α (significance level α = 0.05 was used for markings in the table). In the linear models, fractions of rPP, RWF, MAPP, and UV stabilizer significantly influence ($P < 0.0001$) all the mechanical properties. No significant interaction effects were indicated on MOR, CM, or TS; while for modeling MOE there were significant interactions between rPP and RWF, and between MAPP and UV stabilizer. The CS was affected by significant interactions between rPP and UV stabilizer, RWF and UV stabilizer, and MAPP and UV stabilizer. The frequent interactions with UV stabilizer might indicate it reacted chemically with the other components. The insignificant p-values for lack of fit, at 95% confidence level, also suggest that the fits of the data are appropriate.

The fit of these empirical models was also checked by the coefficient of determination (R^2), the adj-R^2, the pred-R^2, and the coefficient of variation (CV); see Table 4. The R^2 values of the six response fits are in the range from 0.9153 to 0.9838. The extreme R^2 values of TM (0.9153) and MOE (0.9838) indicate that only 8.47% and 1.62%, respectively, of the total variability in observa-

Table 5
Predicted responses with optimized formulation of each property.

Property	Mixture component proportion (wt%)					Predicted response (MPa)		
	x_1	x_2	x_3	x_4	x_5	Strength	Modulus	Desirability
Flexure	50.8	44.4	3.6	0.2	1.0	44.50	2643	0.803
Compression	51.2	44.2	3.4	0.2	1.0	17.51	1333	0.886
Tension	50.0	44.8	4.0	0.2	1.0	28.47	1065	0.975

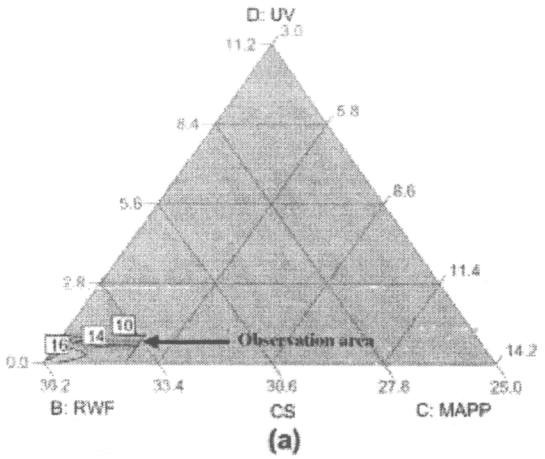

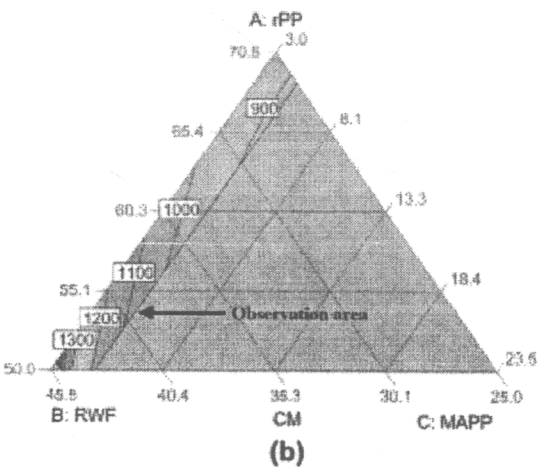

Fig. 4. Triangular contour plots for effects of the compositions on (a) CS with rPP fixed at 59.8 wt% and Lub at 1 wt%; and (b) CM with UV stabilizer fixed at 0.5 wt%, and Lub at 1 wt%.

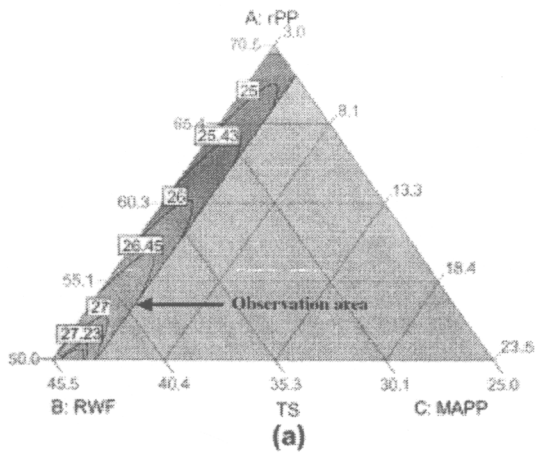

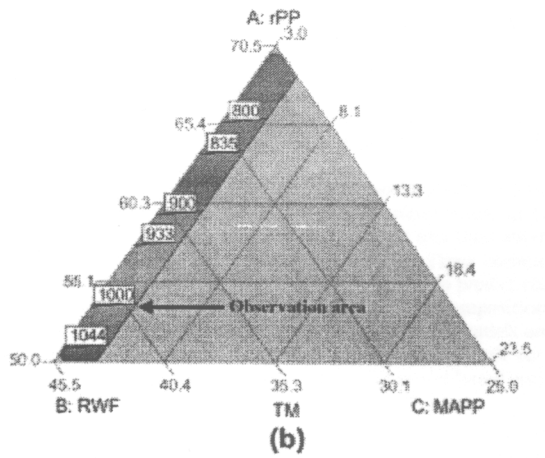

Fig. 5. Composition effects on (a) TS and (b) TM. The fractions held fixed were UV stabilizer at 0.5 wt% and Lub at 1 wt%. The contours represent the numerical models fitted to experimental observations.

tions was not explained by the models; R^2 values close to 1 indicate good fits [20]. The pred-R^2 value of MOE was 0.9237, meaning that the full model is estimated to explain about 92.37% of the variability in new data. The coefficients of variation, of MOR, MOE, CS, CM, TS, and TM, were estimated at 2.63%, 2.51%, 8.15%, 7.94%, 2.04%, and 4.72%, respectively, based on the replicates of experiments. The low CV values indicate that the determinations of material characteristics had a good precision, and can serve the fitting of parametric models. Basically, the coefficient of variation was used to measure the residual variation in the data [18].

3.2. Effect of composition on the flexural properties, and optimal formulation

The quadratic regression models fitted to experimental MOR and MOE values were:

$$\begin{aligned}\text{MOR} = {} & 39.04x_1 + 47.14x_2 + 107.71x_3 - 646.43x_4 + 2.09x_1x_2 \\ & - 77.5x_1x_3 - 668.48x_1x_4 - 102.86x_2x_3 - 555.13x_2x_4 \\ & + 728.26x_3x_4 \end{aligned} \quad (3)$$

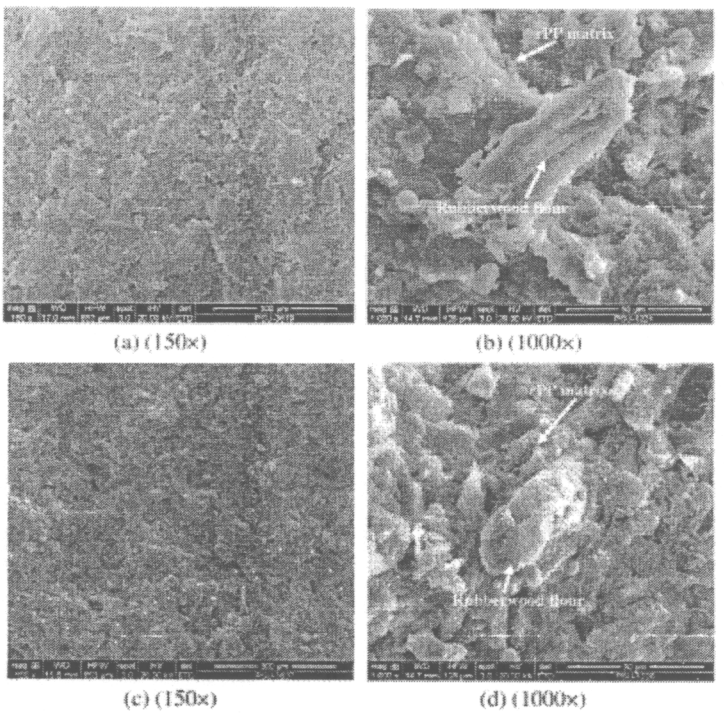

(a) (150×) (b) (1000×)

(c) (150×) (d) (1000×)

Fig. 6. Scanning electron micrographs of rPP/RWF composites with (a), (b) 25 wt% RWF and (c), (d) 45 wt% RWF. Magnifications were 150× and 1000×, from left to right.

$$MOE = 1803.43x_1 + 2743.06x_2 - 11575.14x_3 - 136983x_4 - 573.4x_1x_2 + 16071.92x_1x_3 + 145070x_1x_4 + 11237.53x_2x_3 + 145344.6x_2x_4 + 192792.7x_3x_4 \quad (4)$$

The equation of MOR shows a negative coefficient for fraction of UV stabilizer (x_4), and MOE shows negative coefficients for MAPP (x_3) and UV stabilizer (x_4). However, since these are quadratic models, also the quadratic interaction terms must be inspected, for example at some reasonable values of the other fractions. This is why linear models are much more interpretable, and even on inspecting them, the dependency between the fractions (they must sum to one) makes model interpretation difficult. The addition of UV stabilizer in the wood–plastic composites is known to reduce the flexural properties due to non-homogeneous spatial distribution of wood flour, polymer, and UV stabilizer [21]. The covered experimental regions of MOR and MOE are shown in Fig. 1a and b, respectively. In these triangular plots the three pure components (rPP, RWF, and MAPP) are represented by the corners, while the additive levels were fixed (UV stabilizer at 0.5 wt% and Lub at 1 wt%). The contours in the colored areas, that include the experimental observations, present the MOR and MOE regression fits varying from 39 to 43 MPa and 2000 to 2600 MPa, respectively. MOR and MOE clearly increase with the rubberwood flour content, and its good interfacial adhesion to recycled polypropylene contributes to this. MAPP acts as a compatibilizer providing a hydrophobic rich layer attached to wood flour [22]. Generally, the strength and modulus of wood flour reinforced composites depend on the properties of constituents and the interfacial adhesion [22]. The MAPP addition of about 3–4 wt% is close to optimal for MOE, based on the regression fit. Similar results were found in the work of Kuo et al. [23] who reported that the optimal content of MAPP was 3–4.5 wt% because the interfacial adhesion weakens at higher MAPP contents.

Fig. 2a and b shows the MOR and MOE model predictions vs. observations. The model outputs fit the actual observations quite well, with MOR model deviating from actual by less than about 5%, and MOE model being slightly more accurate. These correlations verified that the Eqs. (3) and (4) are adequate to predict the MOR and MOE responses. The numerically optimized composition, based on these model fits, is shown in Fig. 3. Since two models are optimized simultaneously, the software actually uses a single surrogate called "desirability" to balance them. The model-based optimal formulation is included in Table 5.

3.3. Effect of composition on the compressive properties, and optimal formulation

The quadratic regression models for the compressive properties CS and CM were:

$$CS = 9.76x_1 + 18.28x_2 + 287.82x_3 - 3776.11x_4 + 5.56x_1x_2 - 299.68x_1x_3 + 3956.09x_1x_4 - 314.6x_2x_3 + 3852.86x_2x_4 + 3278.65x_3x_4 \quad (5)$$

$$CM = 1014.25x_1 + 1461.58x_2 - 1406.56x_3 - 87880.43x_4 - 462.14x_1x_2 + 435.39x_1x_3 - 87388.18x_1x_4 - 1096.7x_2x_3 + 89032x_2x_4 + 155014.6x_3x_4 \quad (6)$$

Again these equations do not lend themselves to easy interpretation, due to interaction terms and dependencies between the model

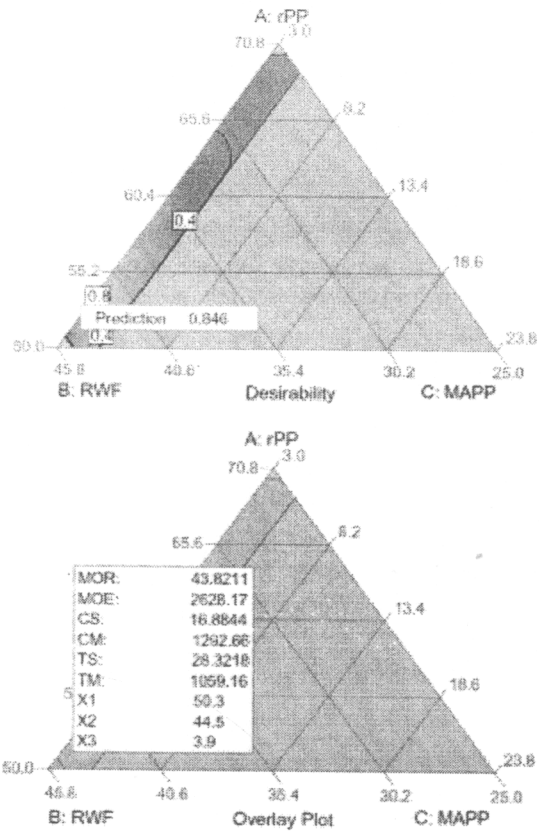

Fig. 7. The optimal formulation for overall desirability.

input variables. We resort to inspecting plots of the model outputs. Fig. 4a shows that CS (in range of 16–10 MPa) decreases for high fractions of the UV stabilizer. The reason for this phenomenon is probably similar to what was discussed in relation to flexural properties. In Fig. 4b, the CM values vary in range of 900–1300 MPa and increase with wood flour loading, since wood flour is stiffer than neat plastic [24]. Likewise, the optimal addition of MAPP for the compressive modulus is approximately 3–4 wt%. Too much MAPP relative to wood flour will cause self-entanglement, resulting in slippage with the PP molecules [25]. The optimal formulation based on these regression models is also included in Table 5.

3.4. Effect of composition on the tensile properties, and optimal formulation

The regression fits for the tensile strength (TS) and modulus (TM) were:

$$TS = 23.54x_1 + 28.64x_2 - 112.44x_3 - 989.02x_4 + 0.081x_1x_2 + 166.14x_1x_3 + 1059.37x_1x_4 + 159.72x_2x_3 + 973.37x_2x_4 + 914.15x_3x_4 \quad (7)$$

$$TM = 717.6x_1 + 1067.03x_2 + 1114.53x_3 + 687.04x_4 \quad (8)$$

By these equations, rPP (x_1) and RWF (x_2) increase the tensile properties; all terms containing these variables have positive coefficients. Of these two, RWF has the larger coefficient in the fit for TS and TM, so it should be maximized. The fractions of MAPP (x_3) and UV stabilizer (x_4) each have both positive and negative coefficients in the model for tensile strength, but both increase the tensile modulus. Fig. 5a and b show that TS and TM increase with the rubberwood flour content. The SEM micrographs in Fig. 6 show that the composites with 25 and 45 wt% of RWF had low porosity, good contact between the wood flour and the PP matrix, and good dispersion of wood flour. Stress transfer was therefore supported at these high rubberwood flour contents. The composition optimized based on these regression models is shown numerically in Table 5.

Table 6
Predicted and observed responses with the formulation optimized jointly for all the mechanical properties.

	Mixture component proportion (wt%)					Response (MPa)					
						Flexure		Compression		Tension	
	x_1	x_2	x_3	x_4	x_5	MOR	MOE	CS	CM	TS	TM
Predicted	50.3	44.5	3.9	0.2	1.0	43.82	2628	16.88	1292	28.32	1059
Observed						47.28	2527	17.11	1369	27.68	1024
						(2.92)[a]	(112)	(2.72)	(109)	(2.41)	(128)

[a] The values in parentheses are standard deviations from five replicates.

3.5. Optimal formulation of the overall mechanical properties

Multiobjective optimization using all of the regression models was performed with the Design-Expert software, using its default settings to construct a desirability score that balances all of the fitted models. The plot in Fig. 7 shows the formulation that was considered optimal, along with contours of the desirability score. The optimal formulation is given in Table 6, and can be compared with the formulations in Table 5: all the previous optima were at practically the same formulation, so a reasonable desirability score must also give this formulation. Table 6 also shows the model predicted responses for this formulation. Test samples with five replicates were prepared with this formulation, and the average material properties along with their standard deviations are included in Table 6. The maximum deviation between model prediction and experimental average occurs for MOR and is of the order 10%.

4. Conclusions

Design and analysis of a D-optimal mixture experiment were used to obtain the optimal formulation of an rPP/RWF composite. The formulation provides high values for all the material characteristics modeled. Analysis of variance revealed that all the component fractions experimentally varied, namely of rPP, RWF, MAPP, and UV stabilizer, statistically significantly affected every one of the mechanical properties (MOR, MOE, CS, CM, TS, and TM). In general, a high fraction of RWF improved all of these, and the optima found had close to 45% RWF that was the maximum in the experimental design. At this wood flour loading stress transfer was still supported by good dispersion and surface contact with the polymer, and the wood flour is much stiffer than the rPP matrix. The compatibilizer MAPP had negative effects on MOE and CM, while for TS a middle of the range value seemed optimal (Fig. 5a). The fraction of UV stabilizer overall degraded the mechanical properties. While the actual optimal composition may depend on a variety of factors, including the quality of raw materials and processing conditions, we have demonstrated the applicability of particular techniques to optimizing properties of composites. In this case, the optima for various mechanical properties agreed well, while in general the joint optimization of multiple responses will depend on their prioritization.

Acknowledgements

The authors would like to express their thanks to the Prince of Songkla Graduate Studies Grant, the Government budget Fund (Research Grant Code: 2555A11502062) for financial support throughout this work, and Rubberwood Technology and Management Research Group (ENG-54-27-11-0137-S) of Faculty of Engineering, Prince of Songkla University, Thailand. We would also like to thank Research and Development Office (RDO) and Assoc. Prof. Seppo Karrila for editing this article.

References

[1] Ashori A, Nourbakhsh A. Performance properties of microcrystalline cellulose as a reinforcing agent in wood plastic composites. Compos Part B: Eng 2010;41(7):578–81.

[2] Liu W, Drzal LT, Mohanty AK, Misra M. Influence of processing methods and fiber length on physical properties of kenaf fiber reinforced soy based biocomposites. Compos Part B: Eng 2007;38(3):352–9.

[3] Cheung HY, Ho MP, Lau KT, Cardona F, Hui D. Natural fibre-reinforced composites for bioengineering and environmental engineering applications. Compos Part B: Eng 2009;40(7):655–63.

[4] Kim JW, Harper DP, Taylor AM. Effect of wood species on the mechanical and thermal properties of wood–plastic composites. J Appl Polym Sci 2009;112(3):1378–85.

[5] Li T, Yan N. Mechanical properties of wood flour/HDI%bonomer composites. Compos Part A – Appl Sci Manuf 2007;38(1):1–12.

[6] Adhikary KB, Pang S, Staiger MP. Dimensional stability and mechanical behaviour of wood–plastic composites based recycled and virgin high-density polyethylene (HDPE). Compos Part B: Eng 2008;39(5):807–15.

[7] Homkhiew C, Ratanawilai T, Thongruang W. Effect of wood flour content and cooling rate on properties of rubberwood flour/recycled polypropylene composites. Adv Mater Res 2013;488–489:495–500.

[8] Ashori A, Sheshmani S. Hybrid composites made from recycled materials: moisture absorption and thickness swelling behavior. Bioresour Technol 2010;101(12):4717–20.

[9] Najafi SK, Hamidinia E, Tajvidi M. Mechanical properties of composites from sawdust and recycled plastics. J Appl Polym Sci 2006;100(5):3641–5.

[10] Khan ZA, Kamaruddin S, Siddiquee AN. Feasibility study of use of recycled high density polyethylene and multi response optimization of injection moulding parameters using combined grey relational and principal component analyses. Mater Des 2010;31(6):2925–31.

[11] Khosrowshahi YB, Salemi A. Influence of polyvinyl alcohol and carboxymethyl cellulose on the reliability of extruded ceramic body: application of mixture design method in fabricating reliable ceramic raschig rings. Int J Appl Ceram Technol 2011;8(6):1334–41.

[12] John RCS. Experiments with mixtures, ill-conditioning, and ridge regression. J Qual Technol 1984;16:81–96.

[13] Mannarswamy A, Munson-McGee SH, Andersen PK. D-optimal designs for the cross viscosity model applied to guar gum mixtures. J Food Eng 2010;97(3):403–9.

[14] Matuana LM, Mengeloglu F. Manufacture of rigid PVC/wood-flour composite foams using moisture contained in wood as foaming agent. J Vinyl Addit Technol 2002;8(4):264–70.

[15] Stark NM, Matuana LM. Ultraviolet weathering of photostabilized wood-flour-filled high-density polyethylene composites. J Appl Polym Sci 2003;90(10):2609–17.

[16] Jun Z, Xiang-Ming W, Jian-Min C, Kai Z. Optimization of processing variables in wood–rubber composite panel manufacturing technology. Bioresour Technol 2008;99(7):2384–91.

[17] Pothiprakdah P, Yoshida T, Chaiwanichsiri T, Matsumura Y. Hydrothermal pretreatment of rubber wood for the saccharification process. Ind Eng Chem Res 2009;48(9):4587–91.

[18] Montgomery DC. Design and analysis of experiments. 7th ed. John Wiley & Sons; 2009.

[19] Mirjalili F, Mozafari S, Ansari F. Assessing optimal dyeability and tensile properties of poly(propylene/poly(ethylene terephthalate) blends with a special cubic mixture experimental design. J Appl Polym Sci 2011;121(6):3201–10.

[20] Ahmadi M, Younesi H, Bahramifar N, Lorestani AAZ, Ghorbani F, Daneshi A, et al. Application of response surface methodology for optimization of lead biosorption in an aqueous solution by Aspergillus niger. J Hazard Mater 2008;154(1–3):694–702.

[21] Wechsler A, Hiziroglu S. Some of the properties of wood–plastic composites. Build Environ 2007;42(7):2637–44.

[22] Ashori A, Nourbakhsh A. Mechanical behavior of agro-residue-reinforced polypropylene composites. J Appl Polym Sci 2009;111(5):2616–20.

[23] Kuo PY, Wang SY, Chen JH, Huaeh HC, Tsai MJ. Effects of material compositions on the mechanical properties of wood–plastic composites manufactured by injection molding. Mater Des 2009;30(9):3690–98.

[24] García M, Hidalgo J, Garmendia I, García-Jaca J. Wood–plastics composites with better fire retardancy and durability performance. Compos Part A – Appl Sci Manuf 2009;40(11):1772–6.

[25] Mohanty S, Verma SK, Nayak SK, Tripathy SS. Influence of fiber treatment on the performance of sisal–polypropylene composites. J Appl Polym Sci 2004;94(3):1336–45.

Journal of Thermoplastic Composite Materials
http://jtc.sagepub.com/

Composites from recycled polypropylene and rubberwood flour: Effects of composition on mechanical properties

Chatree Homkhiew, Thanate Ratanawilai and Wiriya Thongruang

Journal of Thermoplastic Composite Materials published online 14 February 2013
DOI: 10.1177/0892705712475019

The online version of this article can be found at:
http://jtc.sagepub.com/content/early/2013/02/14/0892705712475019

Published by:
SAGE
http://www.sagepublications.com

JOURNAL OF THERMOPLASTIC COMPOSITE MATERIAL

Article

Journal of Thermoplastic Composite Materials
1–16

DOI: 10.1177/0892705712475019
jtc.sagepub.com
SAGE

Composites from recycled polypropylene and rubberwood flour: Effects of composition on mechanical properties

Chatree Homkhiew[1], Thanate Ratanawilai[1] and Wiriya Thongruang[2]

Abstract

The mechanical properties of composites from recycled waste plastic and waste sawdust are of interest in trying to convert these waste streams to useful products. The development of these composites from natural fiber is therefore receiving widespread attention due to the growing environmental awareness. The effects of compositions were investigated including different grades of plastic (virgin and recycled) and amounts of wood flour, coupling agent, and ultraviolet (UV) stabilizer on mechanical and physical properties of polypropylene/rubberwood flour (RWF) composites. Virgin polypropylene gave better mechanical properties than recycled (recycled polypropylene (rPP)), both in composites and as unfilled plastic. RWF content exceeding 25 wt% enhanced the strength of RWF-reinforced rPP composites. The modulus and hardness of composites increased linearly with wood flour loadings. Maleic anhydride-grafted polypropylene (MAPP) as a coupling agent increased the strength, modulus, and hardness of the composites. However, addition of 1 wt% UV stabilizer degraded the mechanical properties. Therefore, 4 wt% MAPP content is recommended to achieve good mechanical properties of rPP/RWF composites, while the amount of UV stabilizer should be as small as possible to avoid its negative influence.

[1] Department of Industrial Engineering, Faculty of Engineering, Prince of Songkla University, Hat Yai, Songkhla, Thailand
[2] Department of Mechanical Engineering, Faculty of Engineering, Prince of Songkla University, Hat Yai, Songkhla, Thailand

Corresponding author:
Thanate Ratanawilai, Department of Industrial Engineering, Faculty of Engineering, Prince of Songkla University, Hat Yai, Songkhla, 90112, Thailand.
Email: thanate.r@psu.ac.th

Keywords
Rubberwood flour, recycled polypropylene, wood–plastic composite, mechanical properties, statistical analysis

Introduction

Nowadays, wood–plastic composites (WPCs) have become popular. They are extensively used in automotive industry as door inner panels, seat backs, and headliners; in construction business as decking, cladding, and fencing; and in infrastructure as marina and boardwalk. This is due to recyclability, low density, low cost, low maintenance, and eco-friendliness with good mechanical properties. Moreover, softwood lumber is increasingly replaced as WPCs and plastic lumber in applications of deck building because of its better durability than softwood lumber,[1,2] and the demand for WPCs is also expected to expand nearly 12% each year between 2000 and 2010 in the United States.[2]

Numerous investigators have recently studied the thermal and mechanical properties of virgin plastics filled with cellulosic fibers in an attempt to reduce the cost and improve the properties of plastics,[3,4] whereas the utilization of postconsumer plastics in WPCs has been studied little. Lisperguer et al.[5] compared the WPCs manufactured from wood flour and virgin and/or recycled polystyrene (rPS). They reported that the mechanical properties of the composites based on virgin polystyrene were not better than those based on rPS. Najafi et al.[6] studied the mechanical properties of WPCs produced from sawdust and virgin or recycled plastics, namely high-density polyethylene (HDPE) and polypropylene (PP). The composites containing HDPE (recycled and virgin) exhibited lower stiffness and strength than those made from PP. Ashori and Sheshmani[7] investigated the effects of weight fraction of fibers in hybrid composites made from combinations of recycled newspaper fiber, poplar wood flour, and recycled polypropylene (rPP). The composites with a high fraction of recycled newspaper fiber showed maximum water absorption during the whole duration of immersion. Nourbakhsh et al.[8] also concluded that waste PP and waste wood are promising alternative raw materials for making low-cost WPCs.

Plastic wastes are the major constituent of municipal solid waste and a promising raw material source for WPCs.[6] Using recycled plastics to produce WPCs would not only decrease the consumption of energy and natural resources but also offer an effective and safe method of disposing plastic waste.[9] The development of new composites from postconsumer polymers, and a better understanding of the effects of composition on the physical and mechanical properties, will facilitate economic application of these composites in consumer products and accordingly decrease environmental impacts.[10,11]

Application of waste fiber as reinforcement or filler is increasing in WPCs. These fibers offer several advantages including biodegradability, renewable character, low cost, easy fiber surface modification, absence of associated health hazards, and low equipment wear during their processing.[10,12] Natural fibers have been extensively popularized and successfully used to improve the mechanical properties of plastic composites, with bagasse, bamboo, banana, flax, hemp, jute, kenaf, oil palm, pineapple,

sisal, wood, and other wastes as examples.[13,14] Yemele et al.[15] mixed bark and HDPE and examined the effects of wood species on mechanical properties. They found that black spruce bark composites had better strength than aspen bark composites. Rahman et al.[16] also investigated the effects of jute fiber content on the mechanical properties of reinforced PP. The tensile strength of the composites decreased with an increasing jute fiber loading, but the Young's modulus decreased only slowly. Reddy et al.[17] reported that an increase in the wheat straw and clay contents in a PP hybrid composite increased the flexural modulus and water absorption. Despite extensive research in the area of natural fiber-reinforced plastics, few studies have used rubberwood flour (RWF) to reinforce virgin plastics, and there is no prior report on RWF-reinforced posteonsumer PP.

The rubberwood (*Hevea brasiliensis*) flour is a waste fiber generated from sawmills and furniture industries, such as local factories in Thailand. These industries generally produced waste wood of about 36% and small branches of about 54%. Only 10% of the rubberwood ends up as the goods.[18] Most of the waste wood can be used as raw material to manufacture particle board and medium-density fiberboard. However, there is a great deal of interest in utilizing the waste fibers as reinforcement of plastic composites. The fillers (wood flour or wood fiber) are also a more important factor affecting the mechanical properties of the WPCs because the different wood species consisted of different contents and components, such as cellulose, hemicellulose, lignin, and extractants.[19] Hence, the effect of filler (RWF) and grade of plastic (virgin and rPP) on the composites are needed to be further studied. In the current work, the effects of material compositions (including different grades of plastic and the contents of RWF, coupling agent, and ultraviolet (UV) stabilizer) on the mechanical and physical properties of composites were investigated. The goal of this research was to determine the effects of composition on the mechanical and physical properties of RWF-reinforced rPP. The new information will facilitate informed decisions regarding manufacture of such composites.

Materials and methods

Materials

rPP pellets were obtained from Withaya Intertrade Co., Ltd (Samutprakarn, Thailand) under the trade name WT170. The material has a melt flow index of 11 g/10 min at 230°C. Virgin polypropylene (vPP), HIPOL J600 with a melt flow index of 7 g/10 min at 230°C was supplied by Mitsui Petrochemical Industries Co., Ltd (Tokyo, Japan). RWF, used as a lignocellulosic filler, was supplied by S.T.A. Furniture Group Co., Ltd (Songkhla, Thailand). Its chemical composition (by weight) was cellulose 39%, hemicellulose 29%, lignin 28%, and ash 4%.[18] The interfacial adhesion between filler and matrix was also modified using a coupling agent maleic anhydride-grafted polypropylene (MAPP), supplied by Sigma-Aldrich, Missouri, USA: 427845 Aldrich (8–10% of maleic anhydride, M_w = 9100, M_n = 3900). Hindered amine light stabilizer additive, chosen as the UV stabilizer, was supplied by TH Color Co., Ltd (Samutprakarn, Thailand) under the trade name MEUV008. A lubricant (Lub), paraffin wax, was purchased from Nippon Seiro Co., Ltd (Yamaguchi, Japan).

Table 1. Wood–plastic composite formulation (percentage by weight).[a]

Composite sample code	rPP	vPP	RWF	MAPP	UV	Lub
rPP100	100					
vPP100		100				
rP70R25M3U1	70		25	3	1	1
vP70R25M3U1		70	25	3	1	1
rP60R35M3U0.5	60.3		35.3	3	0.5	1
vP60R35M3U0.5		60.3	35.3	3	0.5	1
rP50R45M3U1	50		45	3	1	1
vP50R45M3U1		50	45	3	1	1
rP51R45M3U0	51		45	3	0	1
rP70R25M4U0	70		25	4	0	1
rP69R25M5U0	69		25	5	0	1
rP68R25M5U1	68		25	5	1	1

UV: ultraviolet; rPP: recycled polypropylene; RWF: rubberwood flour; MAPP: maleic anhydride-grafted polypropylene; vPP: virgin polypropylene.

[a] The selected formulations from the mixture experiment design were carried out. The rP70R25M3U1 means 70 wt% rPP, 25 wt% RWF, 3 wt% MAPP, and 1 wt% UV.

Preparation of the composites

Prior to compounding, the RWF was sieved (80 mesh) and dried in an oven at 110°C for 8 h. WPCs were then produced in a two-stage process. In the first stage, WPC pellets were produced: PP and wood particles were compounded into WPC pellets using a twin-screw extruder (Model SHJ-36 from En Mach Co., Ltd, Nonthaburi, Thailand). The barrel with 10 temperature zones was controlled at 130–170°C to reduce the degradation of the compositions, while the screw rotation speed was fixed at 70 r/min. In the second stage, WPC panels were produced and the WPC pellets were dried at 110°C for 8 h. WPC pellets, MAPP, UV stabilizer, and lubricant (formulations in Table 1) were then dry mixed and fed into a twin-screw extruder. The temperature profile in the extruding process was 130–190°C, with 50 r/min. Melt pressure at the die varied between 0.10 MPa and 0.20 MPa, depending on the wood flour content. Vacuum venting at nine temperature zones was also used to purge volatile compounds. The samples were then extruded through a rectangular 9 × 22 mm^2 die and cooled in atmospheric air. Subsequently, the specimens were machined according to American Society for Testing and Materials (ASTM) for mechanical and physical testing.

Testing

Mechanical properties. Tensile, compressive, and flexural tests were carried out in an Instron Universal Testing Machine (Model 5582, Instron Corporation, Massachusetts, USA), according to ASTM standards D638, D6108, and D790, respectively. The crosshead speed used for the type IV tensile specimens was 5 mm/min. The compressive test was also conducted using a constant displacement rate of 0.5 mm/min, and the prism

specimens were used to determine the compressive strength and modulus. For the flexural test, specimens with nominal dimensions of 4.8 × 13 × 100 mm^3, a span of 80 mm, and a crosshead speed of 2 mm/min were used. All the mechanical tests were performed at room temperature (25°C) with five replications.

Hardness testing. Hardness measurements were performed according to ASTM D2240 specification, using two durometers (Shore D scales) for the composites. The dimensions of the specimens tested were approximately 16 × 16 × 6.5 mm^3. The measurements were performed at room temperature (25°C).

Analysis

Morphological analysis. The interfacial morphology and phase dispersion of the wood flour in the polymeric matrix were analyzed with a scanning electron microscope. Scanning electron microscopic (SEM) imaging was performed using an FEI Quanta 400 microscope (FEI Company, Oregon, USA) at an accelerating voltage of 20 kV. The samples were sputter coated with gold to prevent electrical charging during the observation. Specimens were imaged at magnifications of 150× and 1000×.

Statistical analysis. Results, such as mean values and standard deviations, from five samples of each test were statistically analyzed. The effects of composition on the WPCs' properties were evaluated by analysis of variance (ANOVA) and student's *t* test. ANOVA indicated the significant differences between wood flour contents, and then a comparison of the means was done with Tukey's multiple comparison test. A two-sample *t* test was also used to detect significant differences between the levels of additives. All the statistical analyses used a 5% significance level ($\alpha = 0.05$).

Results and discussion

The specimens produced from the blends of PP and RWF were characterized. The mechanical and physical properties of WPCs are summarized in Tables 2 and 3. The average values and standard deviations of the flexural strength and modulus, compressive strength and modulus, tensile strength and modulus, and hardness were calculated from five replications.

Flexural properties

The flexural properties are important factors in decision making of WPCs' applications. Figure 1(a) and (b) shows the flexural strength and modulus, respectively, of the composites with virgin or rPP and different amounts of RWF. Generally, an increase in the wood flour content (without the coupling agent) clearly decreases the flexural strength, but the flexural modulus slightly increases.[20,21] It was found in the present work that an increase in RWF content in rPP increased the flexural strength. This is because of the reinforcing effect of the wood flour that distributes a uniform stress from a continuous

Table 2. Effects of RWF content on mechanical and physical properties of WPCs.[a]

Composite sample code	Flexural		Compressive		Tensile		
	Strength (MPa)	Modulus (GPa)	Strength (MPa)	Modulus (GPa)	Strength (MPa)	Modulus (GPa)	Hardness (Shore D)
rPP100	37.02[b]	1.27[b]	10.10[b]	0.79[b]	24.12[b]	0.55[b]	72.5[b]
vPP100	50.07[c]	1.67[c]	20.03[c]	0.97[c]	30.12[c]	0.69[c]	75.6[c]
rP70R25M3U1	36.94[b]	1.76[d]	8.25[b]	0.71[b]	23.00[b]	0.65[d]	73.2[b]
vP70R25M3U1	44.31[e]	1.93[c]	15.34[e]	1.06[c]	25.86[e]	0.84[e]	76.4[c]
rP50R45M3U1	39.66[d]	2.68[f]	13.59[d]	1.20[d]	23.97[b]	0.99[d]	75.2[d]
vP50R45M3U1	43.41[e]	2.66[e]	16.77[e]	1.40[e]	27.93[g]	1.09[g]	78.3[e]
rP60R35M3U0.5[h]	40.23	2.17	15.73	1.15	25.38	0.88	74.3
vP60R35M3U0.5[h]	44.85	2.31	19.63	1.28	28.41	0.99	77.8

rPP: recycled polypropylene; RWF: rubberwood flour; WPC: wood–plastic composite; vPP: virgin polypropylene.
[a] Means within each property with the same letter (suffixes b, d, and f for rPP and c, e, and g for vPP) are not significantly different (Tukey's test, $\alpha = 0.05$).
[h] rP60R35M3U0.5 and vP60R35M3U0.5 were not analyzed to compare the statistical effect of rubberwood content, but they were employed to show the trend of increasing RWF content.

Table 3. Effect of MAPP and UV stabilizer content on mechanical and physical properties of WPCs.[a]

Composite sample code	Flexural		Compressive		Tensile		
	Strength (MPa)	Modulus (GPa)	Strength (MPa)	Modulus (GPa)	Strength (MPa)	Modulus (GPa)	Hardness (Shore D)
rP70R25M3U1	36.94[b]	1.76[b]	8.25[b]	0.71[b]	23.00[b]	0.65[b]	73.2[b]
rP68R25M5U1	37.04[b]	2.01[c]	8.21[b]	0.83[b]	23.29[b]	0.74[c]	73.7[c]
rP70R25M4U0	38.95[b]	1.90[b]	10.55[b]	1.01[b]	24.65[b]	0.76[b]	73.6[b]
rP69R25M5U0	38.44[b]	1.93[b]	8.96[c]	0.79[c]	25.01[b]	0.78[b]	73.8[b]
rP69R25M5U0	38.44[b]	1.93[b]	8.96[b]	0.79[b]	25.01[b]	0.78[b]	73.8[b]
rP68R25M5U1	37.04[b]	2.01[b]	8.21[b]	0.83[b]	23.29[c]	0.74[c]	73.7[b]
rP51R45M3U0	46.24[b]	2.60[b]	17.96[b]	1.45[b]	28.36[b]	1.09[b]	76.1[b]
rP50R45M3U1	39.66[c]	2.68[b]	13.59[c]	1.20[c]	23.97[c]	0.99[b]	75.2[c]

UV: ultraviolet; MAPP: maleic anhydride-grafted polypropylene; WPC: wood–plastic composite.
[a] Means within each couple of formulation with the same letter are not significantly different (student's t test, $\alpha = 0.05$).

plastic matrix to a dispersed wood flour phase.[22,23] Likewise, the flexural modulus of composites (both virgin and recycled plastics) linearly increased with wood flour loadings. Since RWF is a high modulus material compared to the plastic matrix, composites with higher wood flour concentration require a higher stress for the same deformation.[16] These results are verified by the statistical ANOVA. According to the one-way ANOVA of the composites between RWF and rPP or vPP in Table 4, the RWF

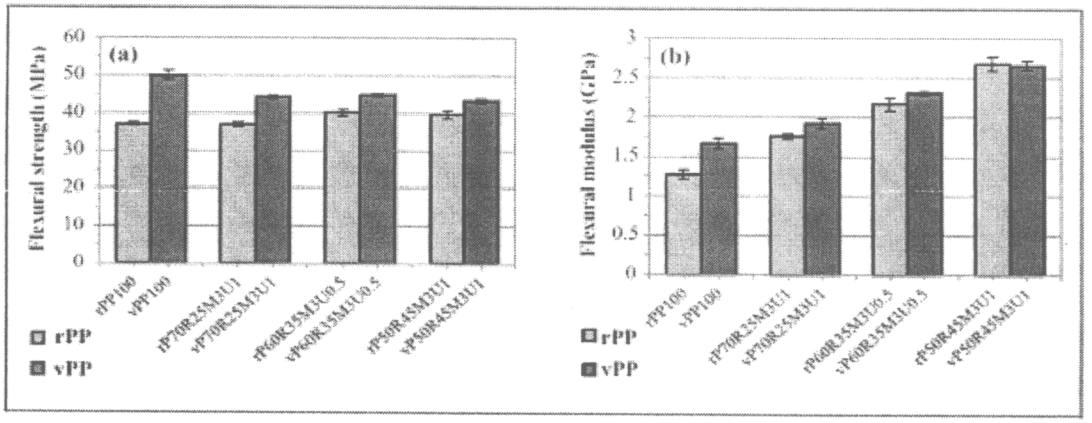

Figure 1. Effect of RWF content and plastic grade on (a) flexural strength and (b) flexural modulus for PP-RWF composites. RWF: rubberwood flour; PP: polypropylene.

Table 4. Results of one-way ANOVA for the effect of RWF content on mechanical and physical properties of PP-RWF composites.

	rPP/RWF composites		vPP/RWF composites	
Property	F_0	p Value	F_0	p Value
Flexural strength	4.60	0.003[a]	22.99	0.000[a]
Flexural modulus	112.55	0.000[a]	38.75	0.000[a]
Compressive strength	10.46	0.003[a]	13.15	0.001[a]
Compressive modulus	19.69	0.000[a]	9.88	0.004[a]
Tensile strength	0.96	0.417	17.46	0.000[a]
Tensile modulus	20.82	0.000[a]	178.66	0.000[a]
Hardness	112.99	0.000[a]	23.35	0.000[a]

ANOVA: analysis of variance; rPP: recycled polypropylene; RWF: rubberwood flour; PP: polypropylene; vPP: virgin polypropylene.
[a] The effect of RWF content is significant at $p < 0.05$.

content significantly ($p = 5\%$) affects the flexural strength and modulus of the composite materials. Tukey's test in Table 2 also indicates that unfilled rPP (suffix b) has insignificantly higher flexural strength than rPP composites with 25 wt% RWF (suffix b), but unfilled rPP and composites with 25 wt% RWF have significantly lower flexural strength than rPP composites with 45 wt% RWF (suffix d). Furthermore, unfilled vPP and composites based on vPP exhibit higher flexural properties than those based on rPP, for the same plastic to wood ratio. This is probably due to the virgin plastic being stiffer than recycled plastic. The recycled plastic has the capacity to lower the melt viscosity, which is attributed to the decrease in molecular weight.[24]

The effects of different amounts of MAPP and UV stabilizer on the flexural strength and modulus are shown in Figure 2(a) and (b), respectively. The effects of 3 and 5 wt%

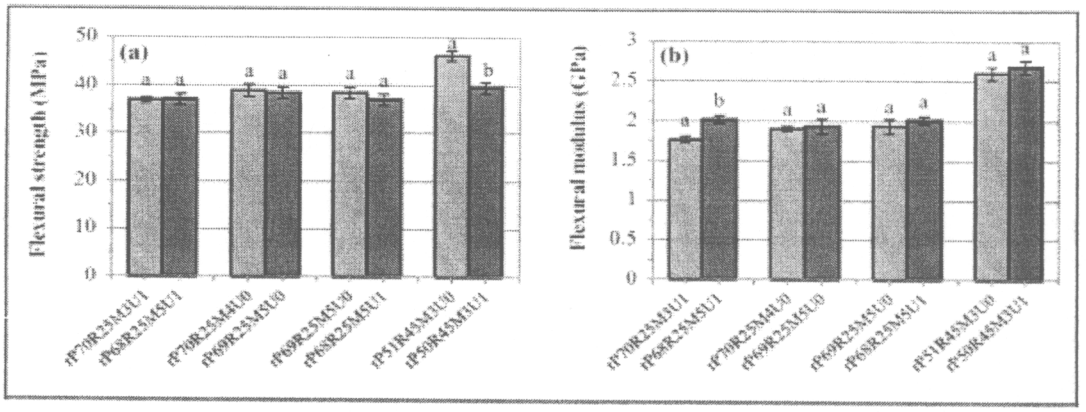

Figure 2. Influence of MAPP and UV stabilizer concentration on (a) flexural strength and (b) flexural modulus of rPP-rubberwood flour composites. UV: ultraviolet; rPP: recycled polypropylene; MAPP: maleic anhydride-grafted polypropylene.

MAPP additions on the flexural properties of rPP/RWF composites containing 25 wt% RWF show that the addition of 5 wt% MAPP gives higher flexural strength (not statistically significant) and modulus (significantly) than the 3 wt% MAPP addition. This was expected because MAPP can improve the compatibility between wood flour and rPP matrix,[8,21,22] improving the stress transfer from polymer to wood particles.[22] However, comparing additions of 4 and 5 wt% MAPP, the composites adding 4 wt% MAPP shows higher strength (not statistically significant) than composites adding 5 wt% MAPP in accordance with prior research.[22,25] Too much MAPP relative to wood flour causes self-entanglement and results in slippage with the PP molecules.[22] These trends conclude that addition of 3 wt% MAPP in composites shows lower flexural properties than those based on the addition of 4 and 5 wt% MAPP, and addition of 5 wt% MAPP exhibits lower flexural strength than those added with 4 wt% MAPP. Furthermore, adding 1 wt% UV stabilizer affects the flexural properties of the composites with 25 wt% RWF so that the strength is reduced (not statistically significantly), but the modulus increases slightly. Again, composites with 45 wt% RWF showed a significant decrease in strength with UV stabilizer content. This may be attributed to the nonhomogeneous spatial distribution of wood flour, polymer, and UV stabilizer.[26]

Compressive properties

Figure 3(a) and (b) shows variation in the compressive strength and modulus with different wood flour loadings, for PP/RWF composites with both virgin and recycled PP. Compressive strength of the composites decreases with the addition of 25 wt% RWF but increases clearly with the further addition of 35.3 wt% RWF. However, it was observed that the increase in RWF content to 45 wt% exhibits a slight reduction in the compressive strength. This decrease is probably because of weak interfacial bonding of the wood within the polymer, with microcrack formation at the interface.[22] Besides, the

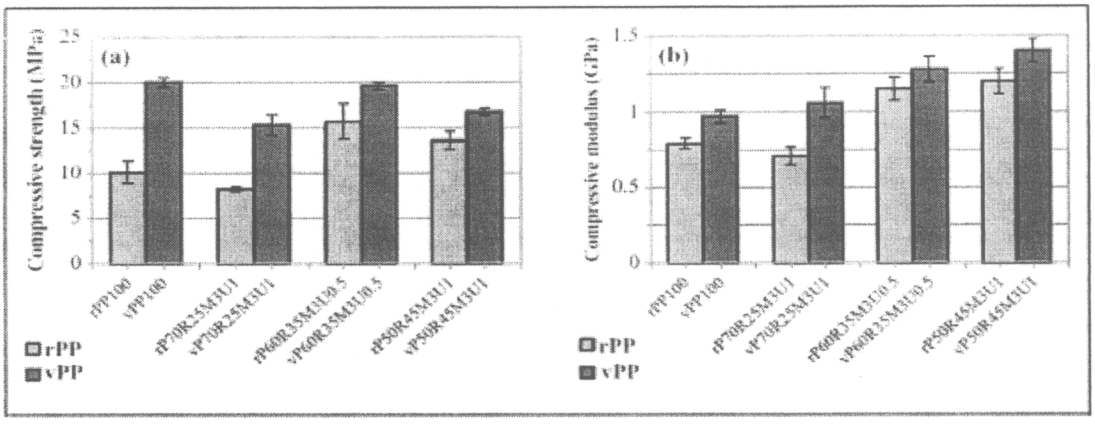

Figure 3. Effect of RWF content and plastic grade on (a) compressive strength and (b) compressive modulus for PP-RWF composites. RWF: rubberwood flour; PP: polypropylene.

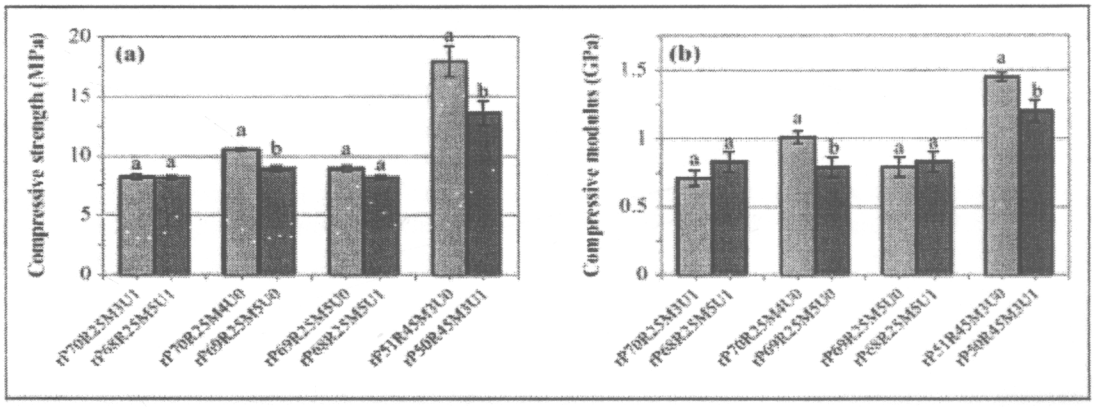

Figure 4. Influence of MAPP and UV stabilizer concentration on (a) compressive strength and (b) compressive modulus of rPP-rubberwood flour composites. UV: ultraviolet; rPP: recycled polypropylene; MAPP: maleic anhydride-grafted polypropylene.

compressive modulus exhibited a similar trend to the flexural modulus: the modulus increased progressively with wood flour content. Similar results were found by Garcia et al.,[27] reporting that the increase in compressive modulus caused the wood flour being stiffer than the neat plastics. In addition, composites based on vPP exhibit a trend similar to rPP/RWF composites with increased wood flour loading. The ANOVA results in Table 4 demonstrate that the effects of the wood flour concentration on the compressive properties are statistically significant, for both virgin and recycled PP composites.

The effects of MAPP and UV stabilizer contents on the compressive strength and modulus of WPCs are shown in Figure 4(a) and (b), respectively. As can be seen, the compressive properties (both strength and modulus) of composites with MAPP between 3 wt% and 5 wt% showed a similar trend to the flexural properties. However, for the coupling agent the MAPP between 4 wt% and 5 wt%, both the strength and the modulus

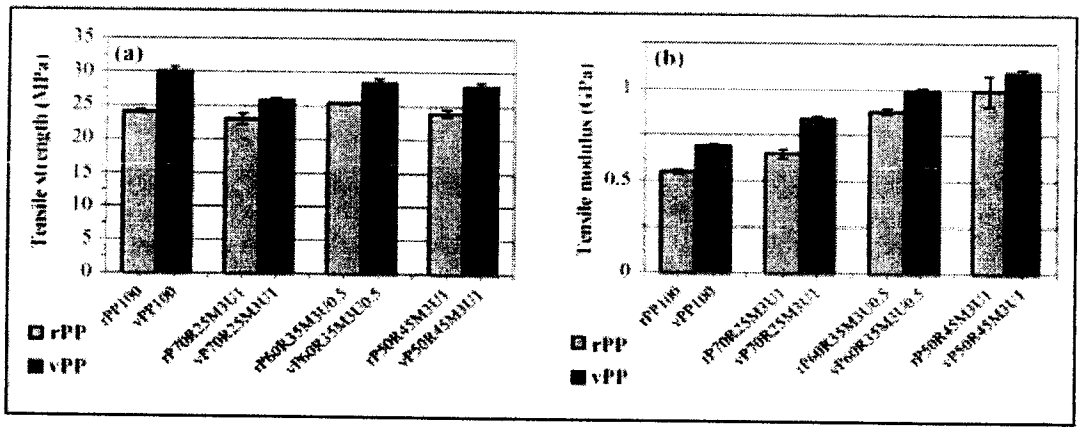

Figure 5. Effect of RWF content and plastic grade on (a) tensile strength and (b) tensile modulus for PP-RWF composites. RWF: rubberwood flour; PP: polypropylene.

of composites decreased significantly. Furthermore, the change in the compressive strength and modulus with different UV stabilizer concentrations, for 25 wt% RWF, is similar to that found in the flexural properties. The composites with 45 wt% RWF show a significant decrease in both strength and modulus with an increase (from 0 wt% to 1 wt%) in UV stabilizer. The reason for this phenomenon is probably similar to that shown in the flexural properties. Using 1 wt% of UV stabilizer may be unnecessary, and to reduce the negative effects on the mechanical properties, the amount of UV stabilizer should be minimized.[26]

Tensile properties

Figure 5(a) and (b) shows the tensile strength and modulus of PP/wood flour composites with different rubberwood contents. Both the tensile strength and modulus exhibited a behavior similar to the flexural properties, increasing slightly with wood flour content. These results can be substantiated by considering the scanning electron micrographs in Figure 6 (Figure 6(a) and (b) for 25 wt% RWF and Figure 6(c) and (d) for 45 wt% RWF). The composites are comprised of irregular short fibers. The composites containing 25 wt% and 45 wt% RWF had few voids, good dispersion of the fibers in the matrix, and strong interfacial adhesion between the wood flour and the PP matrix. Hence, stress transfer is supported by these high wood flour contents. According to this SEM study, the coupling agent used in the composites improves the compatibility between the wood flour and the PP matrix of all the formulations, resulting in the good interfacial bonding and enhancement of mechanical properties. In contrast, the previous work[20] found that rPP/RWF composites without the compatibilizer showed numerous cavities and weak interfacial adhesion, and these results in a decrease in the mechanical properties of the composites. Besides, the unfilled vPP and composites based on vPP exhibit higher tensile properties than those based on rPP, for the same plastic to wood flour ratio. Moreover, unfilled vPP has a higher tensile strength than the composites based on vPP.

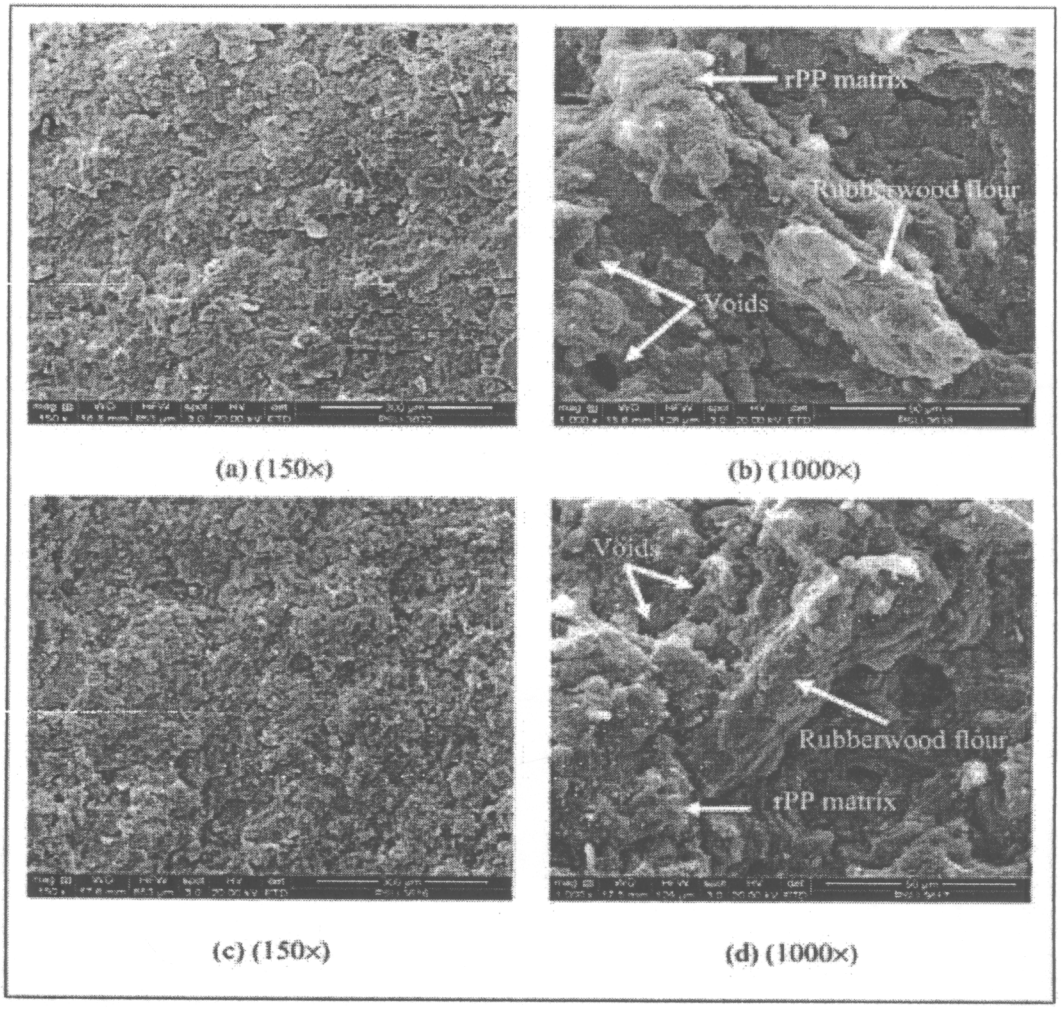

Figure 6. Scanning electron micrographs of rPP-rubberwood flour composites showing voids, dispersion of the fibers in the matrix, and interfacial adhesion based on various formulations (magnification ×150 and ×1000): (a and b) rP70R25M3U1 and (c and d) rP50R45M3U1. rPP: recycled polypropylene.

This is because high melt viscosity or low melt flow index (about 7 g/10 min) of vPP reduces the encapsulation of wood flour into the resin, resulting in poor dispersion and weak interfacial bonding between wood particles and polymer. The ANOVA results in Table 4 show a statistically significant effect of RWF content on the tensile properties of reinforced rPP or vPP, although the tensile strength effects on composites with rPP are not significant at 5% level.

Figure 7(a) and (b) (tensile strength and modulus, respectively) shows the influence of MAPP and UV concentrations on the tensile properties of rPP/RWF composites. The effects of these concentrations have similar trends as in the flexural and compressive

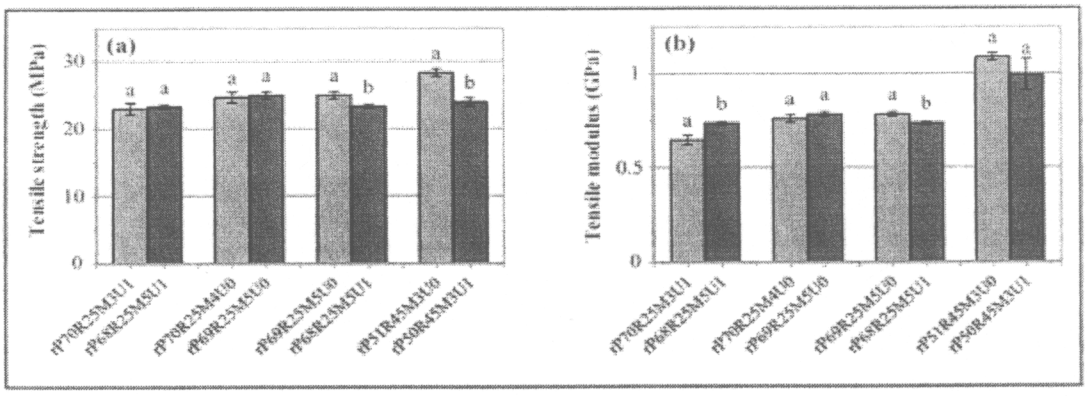

Figure 7. Influence of MAPP and UV stabilizer concentration on (a) tensile strength and (b) tensile modulus of rPP-rubberwood flour composites. UV: ultraviolet; rPP: recycled polypropylene; MAPP: maleic anhydride-grafted polypropylene.

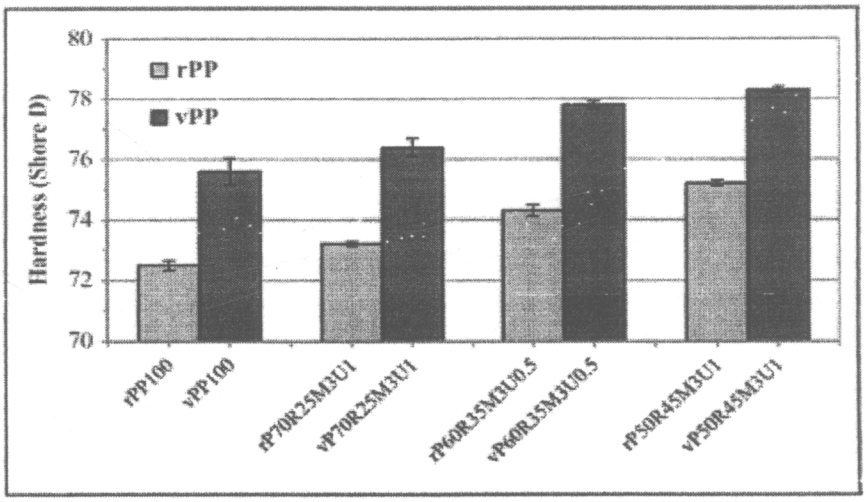

Figure 8. Effect of RWF content and plastic grade on hardness for PP-RWF composites. RWF: rubberwood flour; PP: polypropylene.

properties. Increasing MAPP content does not significantly increase the tensile properties, until between 3 wt% and 5 wt% MAPP, it significantly enhanced the tensile modulus. In contrast, an increase in UV stabilizer content reduced the tensile properties (both strength and modulus). Potential mechanisms causing these trends were discussed earlier for flexural properties.

Hardness

Figure 8 shows the hardness of both virgin and recycled PP/RWF composites with different amounts of wood flour. The average hardness (both for virgin and for recycled

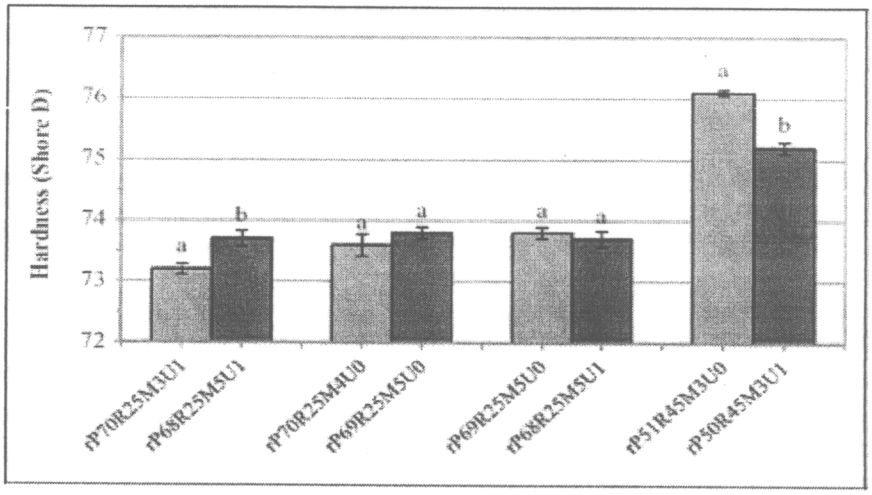

Figure 9. Influence of MAPP and UV stabilizer concentration on hardness of rPP-rubberwood flour composites. UV: ultraviolet; rPP: recycled polypropylene; MAPP: maleic anhydride-grafted polypropylene.

PP) greatly increased with the reinforcing filler. This is caused by the fact that the wood filler has a considerably higher hardness than the weak plastic matrix,[28] and adding RWF decreases flexibility, resulting in more rigid composites.[16,29] The virgin PP/RWF composites seem to have much higher hardness compared to the recycled PP since vPP has lower melt flow index than that of the rPP, leading to lower flexibility composites. Usually, composites with a less flexible matrix have a higher hardness.[29] Moreover, results of the ANOVA (Table 4) show that the hardness of PP/RWF composites was significantly affected by wood flour content.

Hardness of rPP/RWF composites with different coupling agents and UV stabilizer contents are presented in Figure 9. The addition of coupling agent to composites based on 25 wt% RWF showed a significant increase in hardness with MAPP concentration. This could be attributed to both better dispersion of the wood flour into the polymer with minimum voids and stronger coupling between the RWF and rPP.[16,29] When the UV stabilizer was added into the composites containing 45 wt% RWF, the hardness decreased significantly. This decrease is probably due to the negative interaction of mixtures (namely wood flour and UV stabilizer).

Conclusions

The influence of plastic grades (virgin and recycled) and contents of wood flour, coupling agent, and UV stabilizer on the mechanical and physical properties of PP/RWF composites was examined. The results demonstrated that the strengths (flexure, compression, and tension) of RWF-reinforced rPP composites could be enhanced with increasing wood flour contents beyond 25 wt%, whereas those composites based on vPP show lower strengths than the unfilled vPP due to poorer encapsulation of wood flour

into the resin. The modulus and hardness of composites (both virgin and recycled plastics) increased linearly with wood flour loadings due to the fact that wood flour is much stiffer than the PP matrices. The unfilled rPP and composites based on rPP exhibit lower mechanical properties than those based on vPP for the same plastic to wood ratio. The MAPP content affected on the mechanical and physical properties of the composites; however, the addition level of 4.0 wt% MAPP in the rPP/wood flour composites is suggested for economical benefit and good mechanical properties. The strength, modulus, and hardness of composites were reduced by an addition of 1 wt% UV stabilizer content. To limit the negative effects of the UV stabilizer on the mechanical properties of the composites, its use should be minimized. The overall result highlights the effects of composition and new information to facilitate the development of engineering performance of composite materials, making use of wastes and by-products from industry and lending technology toward another effective environmental conservation.

Funding

This work was financially supported from the graduate school of Prince of Songkla University, the Government budget Fund (Research Grant Code: 2555A11502062), and Rubberwood Technology and Management Research Group (ENG-54-27-11-0137-S) of Faculty of Engineering, Prince of Songkla University, Thailand.

Acknowledgments

We would like to thank the Research and Development Office (RDO) and Assoc. Prof. Seppo Karrila for editing this article.

References

1. Carroll DR, Stone RB, Sirignano AM, Saindon RM, Gose SC and Friedman MA. Structural properties of recycled plastic/sawdust lumber decking planks. *Res Conservat Recycl* 2001; 31(3): 241–251.
2. Ganguly I and Eastin IL. Trends in the US decking market: a national survey of deck and home builders. *Forest Chron* 2009; 85(1): 82–90.
3. Sombatsompop N, Prapruit W, Chaochanchaikul K, Pulngern T and Rosarpitak V. Effect of cross section design and testing conditions on the flexural properties of wood/PVC composite beams. *J Vinyl Addit Technol* 2010; 16(1): 33–41.
4. Bouafif H, Koubaa A, Perre P and Cloutier A. Effects of fiber characteristics on the physical and mechanical properties of wood plastic composites. *Compos A: Appl Sci Manufac* 2009; 40(12): 1975–1981.
5. Lisperguer J, Bustos X and Saravia Y. Thermal and mechanical properties of wood flour-polystyrene blends from postconsumer plastic waste. *J Appl Polym Sci* 2011; 119(1): 443–451.
6. Najafi SK, Hamidinia E and Tajvidi M. Mechanical properties of composites from sawdust and recycled plastics. *J Appl Polym Sci* 2006; 100(5): 3641–3645.
7. Ashori A and Sheshmani S. Hybrid composites made from recycled materials: moisture absorption and thickness swelling behavior. *Biores Technol* 2010; 101(12): 4717–4720.
8. Nourbakhsh A, Ashori A, Tabari HZ and Rezaei F. Mechanical and thermo-chemical properties of wood-flour/polypropylene blends. *Polym Bull* 2010; 65(7): 691–700.

9. Khan ZA, Kamaruddin S and Siddiquee AN. Feasibility study of use of recycled high density polyethylene and multi response optimization of injection moulding parameters using combined grey relational and principal component analyses. *Mater Des* 2010; 31(6): 2925–2931.
10. Favaro SL, Lopes MS, Vieira de Carvalho Neto AG, Santana RR and Radovanovic E. Chemical, morphological, and mechanical analysis of rice husk/post-consumer polyethylene composites. *Compos A: Appl Sci Manufac* 2010; 41(1): 154–160.
11. Dullius J, Ruecker C, Oliveira V, Ligabue R and Einloft S. Chemical recycling of post-consumer PET: alkyd resins synthesis. *Prog Org Coating* 2006; 57(2): 123–127.
12. Zabihzadeh SM. Influence of plastic type and compatibilizer on thermal properties of wheat straw flour/thermoplastic composites. *J Thermoplast Compos Mater* 2010; 23(6): 817–826.
13. Ashori A. Wood-plastic composites as promising green-composites for automotive industries! *Biores Technol* 2008; 99(11): 4661–4667.
14. Nahar S, Khan RA, Dey K, Sarker B, Das AK and Ghoshal S. Comparative studies of mechanical and interfacial properties between jute and bamboo fiber-reinforced polypropylene-based composites. *J Thermoplast Compos Mater* 2012; 25(1): 15–32.
15. Yemele MCN, Koubaa A, Cloutier A, Soulounganga P and Wolcott M. Effect of bark fiber content and size on the mechanical properties of bark/HDPE composites. *Compos A: Appl Sci Manufac* 2010; 41(1): 131–137.
16. Rahman MR, Huque MM, Islam MN and Hasan M. Improvement of physico-mechanical properties of jute fiber reinforced polypropylene composites by post-treatment. *Compos A: Appl Sci Manufac* 2008; 39(11): 1739–1747.
17. Reddy CR, Sardashti AP and Simon LC. Preparation and characterization of polypropylene–wheat straw–clay composites. *Compos Sci Technol* 2010; 70(12): 1674–1680.
18. Petchpradab P, Yoshida T, Charinpanitkul T and Matsumura Y. Hydrothermal pretreatment of rubber wood for the saccharification process. *Ind Eng Chem Res* 2009; 48(9): 4587–4591.
19. Li B, Jiang H, Guo L and Shi H. Comparative study on the effect of manchurian ash and larch wood flour on mechanical property, morphology, and rheology of HDPE/wood flour composites. *J Appl Polym Sci* 2008; 107(4): 2520–2530.
20. Homkhiew C, Ratanawilai T and Thongruang W. Effect of wood flour content and cooling rate on properties of rubberwood flour/recycled polypropylene composites. *Adv Mater Res* 2012; 488–489: 495–500.
21. Adhikary KB, Pang S and Staiger MP. Dimensional stability and mechanical behaviour of wood–plastic composites based recycled and virgin high-density polyethylene (HDPE). *Compos B: Eng* 2008; 39(5): 807–815.
22. Mohanty S, Verma SK, Nayak SK and Tripathy SS. Influence of fiber treatment on the performance of sisal-polypropylene composites. *J Appl Polym Sci* 2004; 94(3): 1336–1345.
23. Ratanawilai T, Lekanukit P and Urapantamas S. Effect of rubberwood and palm oil content on the properties of wood–polyvinyl chloride composites. *J Thermoplast Compos Mater*. Epub ahead of print 9 August 2012. DOI: 10.1177/0892705712454863.
24. Aurrekoetxea J, Sarrionandia MA, Urrutibeascoa I and Maspoch ML. Effects of recycling on the microstructure and the mechanical properties of isotactic polypropylene. *J Mater Sci* 2001; 36(11): 2607–2613.
25. Kuo PY, Wang SY, Chen JH, Hsueh HC and Tsai MJ. Effects of material compositions on the mechanical properties of wood–plastic composites manufactured by injection molding. *Mater Des* 2009; 30(9): 3489–3496.
26. Wechsler A and Hiziroglu S. Some of the properties of wood–plastic composites. *Build Environ* 2007; 42(7): 2637–2644.

27. Garcia M, Hidalgo J, Garmendia I and Garcia-Jaca J. Wood–plastics composites with better fire retardancy and durability performance. *Compos A: Appl Sci Manufac* 2009; 40(11): 1772–1776.
28. Kord B. Effect of wood flour content on the hardness and water uptake of thermoplastic polymer composites. *World Appl Sci J* 2011; 12: 1632–1634.
29. Rahman MR, Huque MM, Islam MN and Hasan M. Mechanical properties of polypropylene composites reinforced with chemically treated abaca. *Compos A: Appl Sci Manuf* 2009; 40(4): 511–517.

Applied Mechanics and Materials Vols. 368-370 (2013) pp 736-740
© (2013) Trans Tech Publications, Switzerland
doi:10.4028/www.scientific.net/AMM.368-370.736

Flexural creep behavior of composites from polypropylene and rubberwood flour

Chatree Homkhiew[a], Thanate Ratanawilai[b], Wiriya Thongruang[c]

[a,b]Department of Industrial Engineering, [c]Department of Mechanical Engineering,
Faculty of Engineering, Prince of Songkla University,
Hat Yai, Songkhla 90112, Thailand

[a]cha-190@hotmail.com, [b]thanate.r@psu.ac.th, [c]twiriya@me.psu.ac.th

Keywords: wood-plastic composites, polypropylene, rubberwood flour, flexural creep

Abstract. The effects of plastic grades and composition contents on creep behavior of extruded composites from polypropylene and rubberwood flour were investigated. Virgin polypropylene gave lower creep strain than recycled polypropylene, both in composites and as unfilled plastic. An increase of rubberwood flour content reduced the creep deformation of the composites, both virgin and recycled plastics. Maleic anhydride-grafted polypropylene as a coupling, 5 wt% addition increased the creep strain of the composite materials. Likewise, an addition of 1 wt% ultraviolet (UV) stabilizer content significantly enhanced the creep deformation. The results recommend that the amount of UV stabilizer should be as small as possible to limit its negative effects. Four-element Burger model offered a good fitting on the creep behavior of each composite formulation.

Introduction

Natural organic fibers have been often filled to plastic matrix for improving their strength and stiffness, increasing their durability and thermal stability. Recent advances, they create opportunities for improved materials from renewable resources, supporting global sustainability [1]. Polypropylene (PP) is one of the most well-know plastics that have been widely used in wood-plastic composite industries in the past few decades [2]. However, its use in some applications is limited by several disadvantages, such as low creep stability in long-term loading applications [3]. Reinforcement of natural fibers has demonstrated to be an effective response to increase the creep stability of PP. For example, wood flour was used to decrease the creep strain of PP [4], while addition of wood flour from *Eucalyptus saligna* resulted in an increase of the creep resistance of PP [5]. Despite the composites between the natural fiber and the PP were acceptably described for improving the creep behavior, there is no prior report of the positive effect of rubberwood flour (RWF) reinforced PP on the final creep deformation.

As recently reported, the natural organic fibers can considerably improve the mechanical, physical, and thermal properties of polyolefins, such as polypropylene [2, 6]. Therefore, the objective of the recent work was to assess the effects of material compositions (including different grades of plastic and the contents of rubberwood flour, coupling agent, and ultraviolet stabilizer) on the creep behavior of PP/RWF composites.

Experimental

Materials

Recycled polypropylene (rPP) pellets were purchased from Withaya Intertrade Co., Ltd (Samutprakarn, Thailand), with a melt flow index of 11 g/10 min at 230 °C. Virgin polypropylene (vPP) granules were procured from Mitsui Petrochemical Industries Co., Ltd (Tokyo, Japan), with a melt flow index of 7 g/10 min at 230 °C. Rubberwood flour, used as the reinforcement, was supplied by a local furniture factory (Songkhla, Thailand). The wood flour was sieved through a standard sieve of 80 mesh size and was dried in an oven at 110 °C for 8 h before compounding. Maleic anhydride-grafted polypropylene (MAPP), with 8-10% of maleic anhydride, used as a coupling agent was supplied by Sigma-Aldrich (Missouri, USA). Hindered amine light stabilizer additive, chosen as

the ultraviolet (UV) stabilizer, was supplied by TH Color Co., Ltd (Samutprakarn, Thailand) under the trade name MEUV008. A paraffin wax was purchased from Nippon Seiro Co., Ltd (Yamaguchi, Japan), used as lubricant (Lub).

Sample preparation

Wood-plastic composites (WPCs) were produced in a two-stage process. In the first stage to produce WPC pellets, RWF and PP were mixed into WPC pellets by using a twin-screw extruder (Model SHJ-36 from En Mach Co., Ltd, Nonthaburi, Thailand). The extruding temperature ranged from 130°C to 170 °C to reduce degradation of the compositions. In the second stage to produce WPC panels, WPC pellets, MAPP, UV stabilizer, and lubricant were dry-mixed and added into feeder of the twin-screw extruder according to the compositions given in Table 1. The 10 temperature zones of extruder were set to profile in the range of 130-190 °C, while the screw rotating speed was maintained at 50 rpm. The samples were then extruded through a 9 mm × 22 mm rectangular die and cooled in atmospheric air. Consequently, the specimens were machined following the standards of ASTM for creep and flexural tests.

Table 1 Wood-plastic composite formulation (percent by weight) and creep strain of PP and PP/RWF composites (T = 25 °C, σ = 19 MPa)

Composite sample code	Composition (wt%)						Creep strain (%)		
	rPP	vPP	RWF	MAPP	UV	Lub	C_g	C_{ve6000}	C_{a6000}
rPP100	100						1.27	0.52	1.79
vPP100		100					1.07	0.44	1.51
rP70R25M3U1	70		25	3	1	1	1.03	0.40	1.43
vP70R25M3U1		70	25	3	1	1	0.94	0.38	1.32
rP60R35M3U0.5	60.3		35.3	3	0.5	1	0.88	0.34	1.22
vP60R35M3U0.5		60.3	35.3	3	0.5	1	0.78	0.27	1.05
rP50R45M3U1	50		45	3	1	1	0.70	0.25	0.95
vP50R45M3U1		50	45	3	1	1	0.68	0.23	0.91
rP68R25M5U1	68		25	5	1	1	1.07	0.43	1.50
rP69R25M5U0	69		25	5	0	1	0.96	0.33	1.29

Note. The selected formulations from the mixture experiment design were carried out. The rP70R25M3U1 means 70 wt% rPP, 25 wt% RWF, 3 wt% MAPP, and 1 wt% UV.

Characterization

Three-point bending creep tests of PP and PP/RWF composites were carried out on an Instron Universal Testing Machine (Model 5582 from Instron Corporation, Massachusetts, USA) in Figure 1a, according to ASTM D2990 standard. Testing specimens of dimensions 4.8 mm × 13 mm × 100 mm and a span of 80 mm were employed for studying. All the tests were conducted under a constant load of 19 MPa and performed at ambient conditions of 25 °C. The creep test duration is 100 min (6000 sec). Modulus of elastic (MOE) was also measured in a three-point flexural test at a cross-head speed of 2 mm/min, according to ASTM D790 standard. Five replications of each formulation were tested.

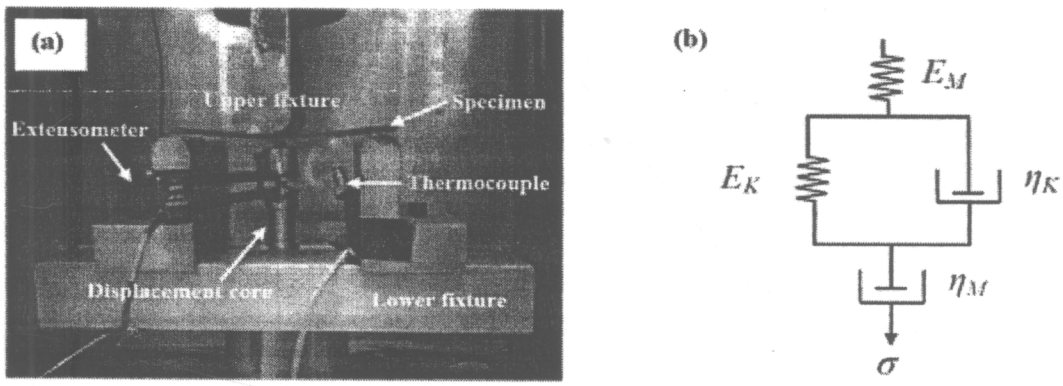

Fig. 1 (a) Test apparatus of creep and (b) schematic of the four-element Burger model.

Creep modeling

Basically, creep strain, $\varepsilon(\sigma, t, T)$, depends on stress ($\sigma$), time ($t$), and temperature ($T$) [7]. It consists of three main elements: (1) elastic deformation (stress-temperature dependence) $\varepsilon_e(\sigma, T)$; (2) viscoelastic deformation (stress-time-temperature dependence) $\varepsilon_{ve}(\sigma, t, T)$; and (3) viscoplastic deformation (stress-time-temperature dependence) $\varepsilon_p(\sigma, t, T)$ [7]:

$$\varepsilon(\sigma,t,T) = \varepsilon_e(\sigma,T) + \varepsilon_{ve}(\sigma,t,T) + \varepsilon_p(\sigma,t,T) \quad (1)$$

To describe and predict the short-term creep behavior, many models were developed and applied by using the constitutive relation of polymeric materials [8]. The four-element Burger model (Figure 1b) is a mathematical model that has been revealed to give a satisfactory prediction and description [8-10]. This model is combinations of Maxwell and Kelvin-Voigt models, which consists of elastic and viscous elements [8, 10]. The mathematical equation for Burger model can be expressed as follows:

$$\varepsilon(t) = \frac{\sigma}{E_M} + \frac{\sigma}{E_K}\left[1 - \exp\left(-t\frac{E_K}{\eta_K}\right)\right] + t\frac{\sigma}{\eta_M} \quad (2)$$

where ε is strain accumulated following time (t), when a certain stress (σ) is employed. E_M represents the elastic modulus of the spring in the Maxwell element, which defines the instantaneous elastic deformation that can be immediately recovered when stress is removed. E_K and η_K represent the elastic modulus of the spring and the viscosity of the dashpot, respectively, in the Kelvin element, which associate with the stiffness and viscous or oriented flow of amorphous polymer chains in the short term. η_M represents the viscosity of the dashpot in the Maxwell element, which defines the viscous flow [11].

Results and Discussion

Effect of composition on creep behavior

The short-term flexural creep behavior of PP and PP/RWF composites with different RWF and additive contents is shown in Figure 2, while the values of the instantaneous creep strain (C_e), of the viscoelastic creep strain after 6000 s (C_{ve6000}), and of the total creep strain after 6000 s (C_{e6000}) are also exhibited in Table 1. As can be seen in Figure 2a, the neat PP (both virgin and recycled) presented the highest creep in the duration of testing, and an increase of rubberwood flour content in the composites showed the decreased creep tendency. This behavior is probably due to an increase in modulus of elastic (MOE) of composites with high wood flour content [12], as shown in Table 2. The MOE of composites (both virgin and recycled plastics) increased with wood flour loadings. Since RWF is a high modulus material compared to the plastic matrix, composites with higher wood flour content require a higher stress for the same deformation [13, 14]. MOE thus has positive effect on decreasing deformation and effective improvement in creep behavior. In addition, unfilled rPP and composites based on rPP show higher creep strain than those based on vPP, for the same plastic to wood ratio. This is probably because of the virgin plastic being stiffer than recycled plastics [13]. However, the two types of plastic with 45 wt% RWF seem to have the same creep behavior, in good agreement with the values of MOE.

The effects of different amounts of MAPP and UV stabilizer on the creep strain are shown in Figure 2b. The effects of 3 wt% MAPP (rP70R25M3U1) and 5 wt% MAPP (rP68R25M5U1) additions on the creep behavior of rPP/RWF composites with 25 wt% RWF show that an increase in the coupling agent content insignificantly increases the creep strain. Generally, the addition of coupling agent in the wood-plastic composites reduced the creep deformation because of the improved filler dispersion and the stronger interfacial adhesion between wood flour and polymer matrix [5, 15, 16]. However, too much MAPP relative to wood flour will causes self-entanglement, resulting in slippage with the PP molecules [13, 17]. Furthermore, addition of 1 wt% UV stabilizer affects the creep strain of the composites with 25 wt% RWF so that the creep strain is significantly

increased. This is due to non-homogeneous spatial distribution of wood flour, polymer, and UV stabilizer [13, 18]. Using 1 wt% of UV stabilizer may be unnecessary, and to decrease the negative effects on the creep behavior the amount of UV stabilizer should be as small as possible [13, 18].

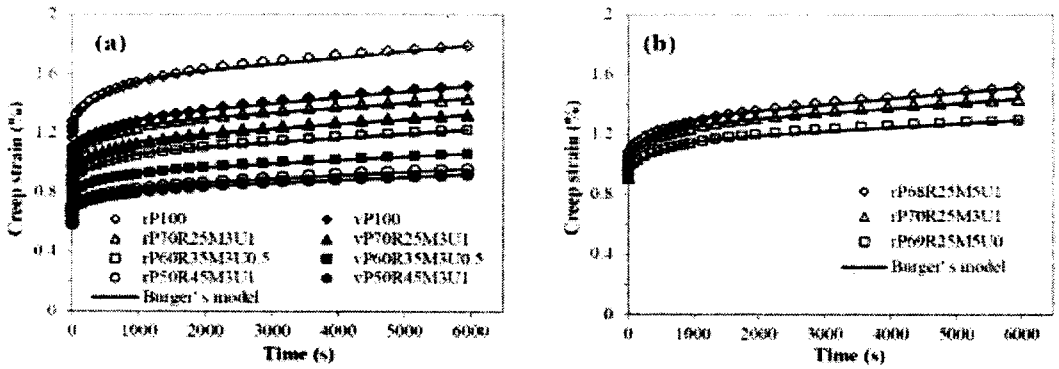

Fig. 2 Creep strain (dot) as a function of times at 25 °C, affected by (a) rubberwood flour contents and (b) additive contents; solid lines represent Burger fit.

Creep modeling analysis

Figures 2a and 2b also show fit of creep curves using Burger model with the solid lines. It can be seen that Burger model provided a good fitting with the experimental data of each formulation. Similar results were found in the work of Liu et al. [9] and Tamrakar et al. [10] who reported that the Burger model offered a good fitting for the creep curves of the composites. The first instantaneous creep arises from the elastic modulus or the spring (E_M) and later time-dependent deflection participates with the spring (E_K) and dashpot (η_K), and last time-dependent deformation comes from the viscous dashpot flow (η_M) [8]. The short-term creep curves were modeled with the Burger equation and the parameters are summarized in Table 2. According to these results, viscosity increased with an increase of the rubberwood flour content and a decrease of the UV stabilizer concentration, and lower flow occurred in the dashpot and permanent deflection also reduced. In the Maxwell spring part, the modulus (E_M) of composites from both virgin and recycled plastics exhibited the enhanced values with the wood flour loading. This is attributed to the stiffness of the composite materials with higher RWF content, and thus reduced the instantaneous elastic deformation during creep experiments. The viscous flow (η_M) values tend to also enhance with the increase of the wood flour content. This is caused by the fact that increasing additions of wood flour content reduced the amount of polymer chains in the plastic composites, resulting in the increase of the viscosity. The retardant elasticity (E_K) and viscosity (η_K) revealed a similar trend on wood flour, coupling agent, and UV stabilizer content, increasing with wood flour content and with a decrease of coupling agent and UV stabilizer content. It could be concluded that the deformation of the Kelvin-Voigt element decreased with increasing wood flour content and enhanced with increasing MAPP and UV stabilizer content.

Table 2 Modulus of elastic and Burger's model parameters

Composite sample code	MOE (GPa)	E_M (MPa)	E_K (MPa)	η_M (MPa·s)	η_K (MPa·s)
rPP100	1.27 (0.06)*	14.89	71.42	4.55E + 05	3.57E + 04
vPP100	1.67 (0.06)	17.64	95.47	4.67E + 05	4.77E + 04
rP70R25M3U1	1.76 (0.03)	18.32	95.95	5.73E + 05	4.79E + 04
vP70R25M3U1	1.93 (0.06)	20.12	103.26	5.82E + 05	5.16E + 04
rP60R35M3U0.5	2.17 (0.08)	21.46	118.01	6.49E + 05	5.90E + 04
vP60R35M3U0.5	2.31 (0.02)	24.20	138.68	8.25E + 05	6.93E + 04
rP50R45M3U1	2.68 (0.08)	27.02	162.39	8.31E + 05	8.11E + 04
vP50R45M3U1	2.66 (0.05)	27.73	165.21	9.50E + 05	8.26E + 04
rP68R25M5U1	2.01 (0.04)	17.67	94.52	4.85E + 05	4.72E + 04
rP69R25M5U0	1.93 (0.09)	19.70	110.46	7.34E + 05	5.52E + 04

*The values in parentheses are standard deviations from five replications.

Conclusions

The effects of plastic grades and contents of wood flour, coupling agent, and UV stabilizer on the creep behavior of PP/RWF composites were investigated. The plastic grades and rubberwood flour contents showed a large impact on the creep behavior of the composites. The neat vPP and composites based on vPP exhibited lower creep deformation than those based on rPP, for the same plastic to wood ratio. The unfilled PP (both virgin and recycled) demonstrated the highest creep strain in range of time studied. The creep strain reduced as the wood flour level increased, due to the resulting increase in stiffness [4]. It was clearly revealed that the addition of rubberwood flour in PP composites can be efficiently improved the poor creep stability of polyolefin. The MAPP and UV stabilizer content also affected the creep deformation of such materials. The additions of 5 wt% MAPP content increased the creep strain of composites, because of the resulting slippage of the PP molecules [13, 17]. Likewise, the creep strain was significantly increased by an addition of 1 wt% UV stabilizer content. To reduce negative effects on the creep behavior the amount of UV stabilizer should be as small as possible. Besides, the short-term flexural creep behavior could be well fitted by using the Burger model, and the data of modeling offered an understanding of the deformation mechanism for three elements: elastic, viscoelastic, and viscoplastic deformation.

Acknowledgements

The authors would like to thanks the Prince of Songkla Graduate Studies Grant, the Government budget Fund (Code: 2555A11502062) for financial support throughout this work, and Rubberwood Technology and Management Research Group (ENG-54-27-11-0137-S) of Faculty of Engineering, Prince of Songkla University, Thailand.

References

[1] H.Y. Cheung, M.P. Ho, K.T. Lau, F. Cardona and D. Hui: Compos Part B Eng Vol. 40 (2009), p. 655-663.

[2] C. Homkhiew, T. Ratanawilai and W. Thongruang: Adv Mater Res Vol. 488-489 (2012), p. 495-500.

[3] A. Dorigato and A. Pegoretti: Polym Int Vol. 59 (2010), p. 719-724.

[4] S. Y. Lee, H. S. Yang, H. J. Kim, C. S. Jeong, B. S. Lim and J. N. Lee: Compos Struct Vol. 65 (2004), p. 459-469.

[5] A. J. Nunez, P. C. Sturm, J. M. Kenny, M. I. Aranguren, N. E. Marcovich and M. M. Reboredo: J Appl Polym Sci Vol. 88 (2003), p. 1420-1428.

[6] C. R. Reddy, A. P. Sardashti and L. C. Simon: Compos Sci Technol Vol. 70 (2010), p. 1674-1680.

[7] A. Dorigato, A. Pegoretti and J. Kolarik: Polym Compos Vol. 31 (2010), p 1947-1955.

[8] K. Banik, J. Karger-Kocsis and T. Abraham: Polym Eng Sci Vol. 48 (2008), p 941-948.

[9] H. Liu, F. Yao, Y. Xu and Q. Wu: Bioresour Technol Vol. 101 (2010), p. 3295-3297.

[10] S. Tamrakar, R. A. Lopez-Anido, A. Kiziltas and D. J. Gardner: Compos Part A-Appl S Vol. 42 (2011), p. 834-842.

[11] G. Gong, J. Pyo, A. P. Mathew and K. Oksman: Compos Part A-Appl S Vol. 42 (2011), p. 1275-1282.

[12] N. E. Marcovich and M. A. Villar: J Appl Polym Sci Vol. 90 (2003), p. 2775-2784.

[13] C. Homkhiew, T. Ratanawilai and W. Thongruang: J Thermoplast Compos Mater, Epub ahead of print 14 February 2013.DOI: 10.1177/0892705712475019.

[14] M. R. Rahman, M. M. Huque, M. N. Islam and M. Hasan: Compos Part A-Appl S Vol. 39 (2008), p. 1739-1747.

[15] J. Mingyin, X. Ping, Z. Yongsheng and W. Kejian: J Wuhan Univ Technol-Mater Vol. 24 (2009), p. 440-447.

[16] M. Bengtsson, P. Gatenholm and K. Oksman: Compos Sci Technol Vol. 65 (2005), p. 1468-1479.

[17] S. Mohanty, S. K. Verma, S. K. Nayak and S. S. Tripathy: J Appl Polym Sci Vol. 94 (2004), p. 1336-1345.

[18] A. Wechsler and S. Hiziroglu: Build Environ Vol. 42 (2007), p. 2637-2644.

Applied Mechanics and Materials Vols. 368-370 (2013) pp 785-790
© (2013) Trans Tech Publications, Switzerland
doi:10.4028/www.scientific.net/AMM.368-370.785

Optimal formulation of recycled polypropylene/rubberwood flour composites on hardness property

Chatree Homkhiew[a], Thanate Ratanawilai[b], Wiriya Thongruang[c]

[a,b]Department of Industrial Engineering, [c]Department of Mechanical Engineering, Faculty of Engineering, Prince of Songkla University, Hat Yai, Songkhla 90112, Thailand

[a]cha-190@hotmail.com, [b]thanate.r@psu.ac.th, [c]twiriya@me.psu.ac.th

Keywords: wood-plastic composites, mixture experimental design, rubberwood flour, hardness

Abstract. Mixture experimental design was applied to determine the optimal mixture for composites between rubberwood flour (RWF) and recycled polypropylene (rPP). Experiments were conducted based on a D-optimal mixture design and analyzed using response surface methodology. Analysis of variance revealed that compositions including rPP, RWF, maleic anhydride grafted polypropylene (MAPP), and ultraviolet (UV) stabilizer significantly affected hardness property. Contour plots of the response surface demonstrated that an increase of RWF content steadily enhanced hardness value, but hardness property sharply decreased with an increase of rPP loading. An addition of the UV stabilizer in the composites showed a slight decrease of the hardness value. This result recommends that amount of UV stabilizer used should be minimized. With this experimental design, the optimal formulation of rPP/RWF composites found was 50.0 wt% rPP, 45.0 wt% RWF, 3.9 wt% MAPP, 0.1 wt% UV stabilizer, and 1.0 wt% Lubricant.

Introduction

Natural fibers from maple, oak, pine, and rubberwood are reinforcement materials, which have been extensively popularized and used in composite industries. It was used as a replacement for synthetic fillers such as glass fiber, carbon fiber, and inorganic filler. Compared to these materials, natural fibers provide low cost, low density, recyclability, and their non-abrasive natures. A large amount of natural fibers (wood wastes) is generated at different processing in wood applications such as in sawmills and in furniture making [1]. The wastes in the form of flour, sawdust, and chips have primary been used as inexpensive filler in composites. In addition, an increase of plastic production and consumption results in plastic wastes to be the major constituent of municipal solid waste; however, it is a promising raw material for producing wood-plastic composites (WPCs) [2, 3]. The use of recycled plastics for producing WPCs would not only offer a safe and effective disposal of plastic wastes, but also reduces the consumption of natural resources [4, 5]. Therefore, increasing the use of recycled plastics by blending with wood wastes provides the chance of lessening wastes going to landfill, decreasing solid waste disposals, and reducing the costs of making the WPCs [1, 6].

Applications and end-products of WPCs, such as decking and part of cars, have made. It is necessary to evaluate hardness characteristic of such materials. Because the hardness property is a measurement of the wear resistance, and harder materials resist a better friction and wear [7]. Thereby, the hardness property has to be taken into account in the design of WPCs for final products.

Nowadays, most of the experiment on composite formulations is still conducted by changing the contents of each composition at a time, and the other compositions are constantly fixed in order to investigate the effects of such specific composition. Mixture experimental design by using D-optimal is an important method to mediate an effect on the dependent compositions of interest [8]. It also decreases the number of experiments but increases the scientific information of compositions, which are the important values to determine the mathematical equation for improving the properties of end-products [9, 10]. Therefore, the D-optimal mixture experimental design was applied to determine the model parameters in WPCs. The main purposes of present research were to investigate the effect of compositions and to determine the optimal mixture ratios by designing mixture experiment for composites from recycled polypropylene and rubberwood flour based on hardness property.

Experimental

Materials

Recycled polypropylene (rPP) pellets were purchased from Withaya Intertrade Co., Ltd (Samutprakarn, Thailand). Rubberwood flour (RWF) was supplied from local furniture factory (Songkhla, Thailand). Maleic anhydride grafted polypropylene (MAPP) was used as a coupling agent, manufactured by Sigma-Aldrich (Missouri, USA). It contains 8-10% of maleic anhydride. Hindered amine light stabilizer (MEUV008) was purchased from TH Color Co., Ltd (Samutprakarn, Thailand), chosen as ultraviolet (UV) stabilizer. Paraffin wax was procured from Nippon Seiro Co., Ltd (Yamaguchi, Japan), used as lubricant (Lub).

Experimental design to optimize formulation

Mixture experimental design was used to study the hardness property of rPP/RWF composites using Design Expert software (version 8.0.6, Stat-Ease, Inc., Minneapolis, USA), according to a D-optimal design. In mixture experiments, the components are the variables of mixture, and their levels cannot be changed independently [11]. When interesting region for experiment is not a simplex due to irregular experiment region [11], D-optimal design is appropriate method to statistically evaluate the effect of compositions and to optimize the formulation. The rPP (x_1), RWF (x_2), MAPP (x_3), and UV stabilizer (x_4) were four key variables studied, while the hardness was the variable response obtained in the study. The intervals selected to conduct the experiment design were: 50-70 wt% rPP, 25-45 wt% RWF, 3-5 wt% MAPP, 0-1 wt% UV stabilizer, and 1 wt% Lub. The design included 15 formulations and 5 replications to evaluate lack of fit. Thus, the total number of runs was 20 in Table 1.

Table 1 Experimental compositions and response based on mixture experimental design

Experiment run No.	Mixture Proportion (wt%)					Hardness (Shore D)	Experiment run No.	Mixture Proportion (wt%)					Hardness (Shore D)
	x_1	x_2	x_3	x_4	x_5			x_1	x_2	x_3	x_4	x_5	
1	63.9	29.9	4.5	0.7	1.0	73.3 (0.40)**	11	50.0	45.0	3.0	1.0	1.0	75.2 (0.19)
2	70.0	25.0	3.0	1.0	1.0	73.2 (0.17)	12*	50.0	43.0	5.0	1.0	1.0	74.9 (0.44)
3	50.0	43.0	5.0	1.0	1.0	74.8 (0.38)	13	60.3	35.3	3.0	0.5	1.0	74.3 (0.39)
4	54.9	38.9	4.5	0.7	1.0	75.5 (0.40)	14	64.9	30.4	3.5	0.2	1.0	74.6 (0.10)
5	59.5	34.5	5.0	0.0	1.0	74.6 (0.53)	15*	70.0	25.0	3.0	1.0	1.0	72.9 (0.37)
6	55.4	39.9	3.5	0.2	1.0	74.7 (0.46)	16	51.0	45.0	3.0	0.0	1.0	76.1 (0.09)
7	59.5	34.5	4.0	1.0	1.0	74.9 (0.60)	17*	51.0	45.0	3.0	0.0	1.0	75.8 (0.24)
8*	59.5	34.5	5.0	0.0	1.0	75.0 (0.39)	18*	50.0	45.0	3.0	1.0	1.0	74.9 (0.33)
9	50.0	44.3	4.3	0.5	1.0	75.3 (0.51)	19	70.0	25.0	4.0	0.0	1.0	73.6 (0.36)
10	68.0	25.0	5.0	1.0	1.0	73.7 (0.26)	20	69.0	25.0	5.0	0.0	1.0	73.8 (0.19)

Note: *duplicate experiments, ** the values in parentheses are standard deviations from five replications.

Preparation of wood-plastic composites

Before compounding, RWF was sieved through a standard sieve of 80 mesh size and dried in an oven at 110 °C for 8 h. RWF and rPP were then mixed into WPC pellets by using a twin-screw extruder (Model SHJ-36 from En Mach Co., Ltd, Nonthaburi, Thailand). The extruding temperature ranged from 130°C to 170 °C to reduce degradation of the compositions. After compounding, the WPC panels were also prepared. WPC pellets, MAPP, UV stabilizer, and lubricant were dry-mixed and added into feeder of the twin-screw extruder according to the compositions given in Table 1. The 10 temperature zones of extruder were set to profile in range of 130-190 °C, while the screw rotating speed was controlled at 50 rpm. The samples were then extruded through a 9 mm × 22 mm rectangular die and cooled in atmospheric air. Consequently, the specimens were machined following the standard of American Society for Testing and Materials (ASTM) for hardness test.

Composite characterization

Hardness measurement of the composites was tested according to ASTM D2240 standard by using mechanical Shore D Durometer (Model GS-702G from teclock corporation, Nagano, Japan). The rectangular specimens with dimensions of 16 mm × 16 mm × 6.5 mm were tested. The test was characterized at room temperature (25 °C). Average of five specimens was measured and calculated.

Results and Discussion

Statistical analysis of response surface model

The statistical significance of linear model was analyzed by analysis of variance (ANOVA), as given in Table 2. The results revealed that the model was statistically significant at 5% significance level, indicating by p-value less than α (α = 0.05). This result indicates that at least one of the four variables contributes the hardness response. For the linear mixture, variables of rPP, RWF, MAPP, and UV stabilizer significantly affect hardness property. In addition, the ANOVA also showed that lack of fit was not significant for the model. This concludes that the regression model fits the data.

Table 2 Analysis of variance and model adequacy for hardness of rPP/RWF composites

Response	Model	Linear mixture	Lack of fit	R^2	Adj-R^2	Pred-R^2	CV %
Hardness	<0.0001*	<0.0001*	0.0510	0.8336	0.8024	0.7663	0.53

*P-value less than 0.05 is considered significant.

The fit of the model was also checked by determination coefficient (R^2), adjusted determination coefficient (adj-R^2), predicted determination coefficient (pred-R^2), and coefficient of variation (CV). The R^2 value of hardness (0.8336) reveals that about 83.36% of variability in observation is explained by the four key compositions of composites, whereas only 16.64% of the total variability couldn't be explained. A closer to 1 of R^2 value indicates good fits [12]. Also the adj-R^2 value of hardness (0.8024) is large and very close to the ordinary R^2. This indicates that there is a less chance of insignificant terms included in the model [13]. The pred-R^2 value of hardness was 0.7663 meaning that this model could be expected to explain about 76.63% of the variability in predicting new data. This result also revealed that pred-R^2 of 0.7663 is in reasonable agreement with the adj-R^2 of 0.8024. At the same time, the coefficient of variation found was 0.53%. The low value of CV indicates the good relative dispersion of the experimental points from the predictions of the models [14]. Basically, the coefficient of variation was used to measure the residual variation in the data [11].

Model adequacy checking

Model adequacy checking is always necessary to verify the fitted model to ensure that it provides an adequate approximation [13]. Figure 1a displays a normal probability plot of residuals. The plot of these points is reasonably attached close to a straight line, supporting the conclusion that only rPP, RWF, MAPP, and UV stabilizer significantly affect. Likewise, there is no strong indication of nonnormality and possible presence of outliers, which is the very much larger residual than any of the others [11]. The predicted hardness vs. actual hardness is also shown in Figure 1b. It illustrates the linear correlation between the predicted value and observation data, which was well fitted. These correlations verified that the model is adequate to predict the hardness value. From model adequacy checking, the overall predictive capability of model based on the residuals is very satisfactory.

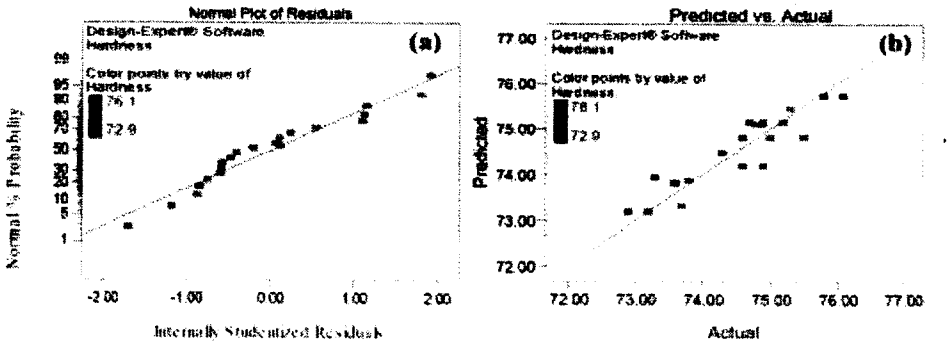

Fig. 1 (a) Normal probability plot of residuals and (b) plot of predicted versus actual hardness.

Effect of compositions on hardness

Significant linear model of the hardness property, affected by the WPC compositions, was obtained from the hardness response. The equation calculated from the regression data was:

$$\text{Hardness} = 73.74x_1 + 75.82x_2 + 75.12x_3 + 62.02x_4 \quad (1)$$

The linear equation of hardness shows positive coefficient of all the compositions, revealing the positive effect on the hardness property. The rubberwood flour (x_2) yielded the highest positive effect as compared with the other compositions. The covered experimental regions of hardness property are shown in Figures 2a and 2b. As seen in Figure 2a, the region is triangular contour plot, in which three compositions (rPP, RWF, and MAPP) were placed at the corners, while the other materials were fixed (UV stabilizer at 0.5 wt% and Lub at 1 wt%). The clear area in triangular contour plot reveals the hardness values varying in range of 73.66 to 75.38 shore D. The hardness value sharply increased with enhancing RWF content but greatly decreased with increase of rPP loading. This is because of higher hardness of rubberwood filler than the weak polymer matrix [3, 7]. In addition, flexibility of the composites was reduced by an increase of RWF content, resulting in more rigid composites [15, 16]. The enhancing addition of MAPP (from 3 wt% to 5 wt%) unaffected the hardness property as shown in the contour plot (Figure 2a). Generally, addition of the coupling agent to the composites increases the hardness with MAPP concentration. This is due to both stronger coupling between the RWF and rPP and better dispersion of the wood flour into the plastic matrix with minimum voids [3, 15, 16]. Furthermore, the effect of UV stabilizer addition is also exhibited in the contour plot (Figure 2b), in which two compositions fixed were the rPP at 59.8 wt% and the Lub at 1 wt%. The area in triangular contour plot presents the hardness values varying in range of 74.2 to 74.8 shore D. The hardness value of rPP/RWF composites slightly reduced with increasing addition of the UV stabilizer. This decrease is attributed due to the negative interaction of mixtures (namely wood flour and UV stabilizer) [3]. In the previous work, Homkhiew et al. [3] found that composites containing 45 wt% RWF and 1 wt% UV stabilizer showed a higher decrease of hardness value than composites with 25 wt% RWF and 1 wt% UV.

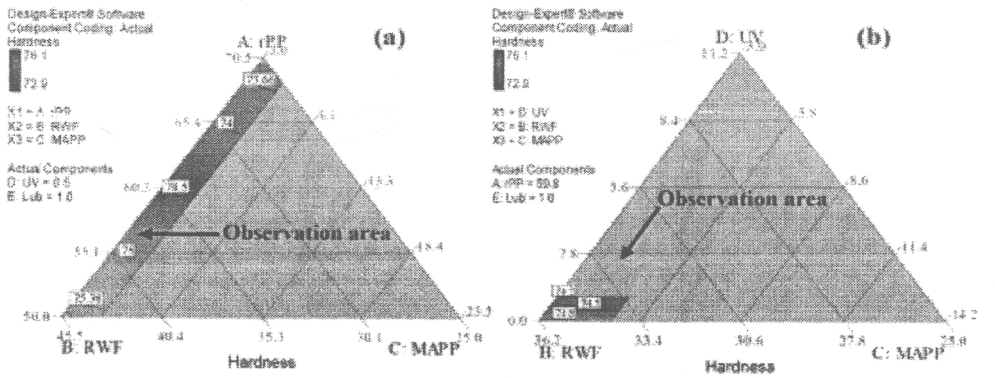

Fig. 2 Triangular contour plots for effects of the compositions on hardness (a) fixed UV stabilizer at 0.5 wt%, Lub at 1 wt% and (b) fixed rPP at 59.8 wt%, Lub at 1 wt%.

Optimal formulation of hardness

An optimal formulation of rPP/RWF composites was conducted to obtain maximum of the hardness value. It was generated by the software, which was produced, analyzed, and presented as a graphical optimization. The optimized point of mixture ratio on desirability and overlay plot is represented in Figures 3a and 3b, respectively. The desirability plot shows a point that maximizes the desirability function to be 0.887, revealing satisfactory value. The desirability level is close to 1, indicating a good hardness response. The obtained desirability exhibited that this point can represent the desired formulation. Likewise, the overlay plot in Figure 3b shows the point of optimal formulation, which is the same point with the desirability plot. The optimal formulation found was 50.0 wt% rPP, 45.0 wt% RWF, 3.9 wt% MAPP, 0.1 wt% UV stabilizer, and 1.0 wt% Lub. Besides, to confirm the accuracy of the model and predicted response, a measurement of the closeness of hardness response obtained from the predicted value and observed result was also validated in Table

3. This result confirmed that the predicted hardness value was not significantly different from the measured value. Concluding that the earlier propose formulation of rPP/RWF composites for the hardness property is reasonable and can be well applied in the WPC industries.

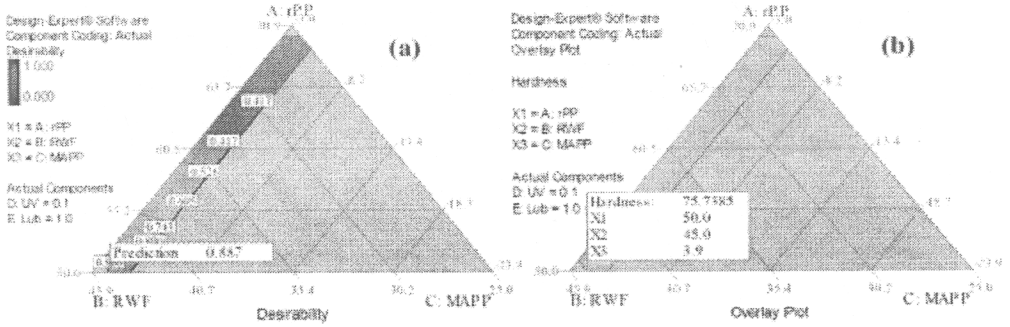

Fig. 3 (a) Desirability plot and (b) overlay plot of hardness for the optimal formulation.

Table 3 Predicted and observed responses with optimized formulation

Mixture component proportion (wt%)					Hardness (Shore D)	
x_1	x_2	x_3	x_4	x_5	Predicted	Observed
50.0	45.0	3.9	0.1	1.0	75.73	75.56 (0.40)*

* The value in parentheses is standard deviation from five replications.

Conclusions

Mixture experimental design, response surface, and optimization methods were applied to determine the optimal formulation based on maximum of the hardness property. Analysis of variance demonstrated that the compositions including rPP, RWF, MAPP, and UV stabilizer significantly affected the hardness property. Model adequacy checking also revealed that the overall predictive capability of model based on the residuals was very strong. From the contour plots, the hardness value sharply enhanced with increasing RWF content but greatly reduced with increase of rPP loading. This is due to the polymer matrix to be a considerably lower hardness than the rigid rubberwood filler [3, 7]. The addition of the UV stabilizer in the composites showed the negative effect, which slightly decreased the hardness value. This result is attributed due to the negative interaction of mixtures [3]. The optimal formulation of rPP/RWF composites using D-optimal mixture design based on maximum hardness value was found to be 50.0 wt% rPP, 45.0 wt% RWF, 3.9 wt% MAPP, 0.1 wt% UV stabilizer, and 1.0 wt% Lub with the desirability function to be 0.887.

Acknowledgements

The authors would like to thanks the Prince of Songkla Graduate Studies Grant, the Government budget Fund (Code: 2555A11502062) for financial support throughout this work, and Rubberwood Technology and Management Research Group (ENG-54-27-11-0137-S) of Faculty of Engineering, Prince of Songkla University, Thailand.

References

[1] A. Ashori and S. Sheshmani: Bioresour Technol Vol. 101 (2010), p. 4717-4720.
[2] S. K. Najafi, E. Hamidinia and M. Tajvidi: J Appl Polym Sci Vol. 100 (2006), p. 3641-3645.
[3] C. Homkhiew, T. Ratanawilai and W. Thongruang: J Thermoplast Compos Mater, Epub ahead of print 14 February 2013.DOI: 10.1177/0892705712475019.
[4] Z. A. Khan, S. Kamaruddin and A. N. Siddiquee: Mater Design Vol. 31 (2010), p. 2925-2931.
[5] T. Ratanawilai, N. Thanawattanasirikul and C. Homkhiew: Sci Asia Vol. 38 (2012), p. 289-294.
[6] K. B. Adhikary, S. Pang and M. P. Staiger: Compos Part B Eng Vol. 39 (2008), p. 807-815.
[7] B. Kord: World Appl Sci J Vol. 12 (2011), p. 1632-1634.
[8] M. S. Jang, J. E. Park and H. Y. Park: Food Sci Biotechnol Vol. 20 (2011), p. 409-417.

[9] Y. B. Khosrowshahi and A. Salem: Inter J Appl Ceramic Technol Vol. 8 (2011), p. 1334-1343.
[10]R. C. S. John: J Quali Technol Vol. 16 (1984), p. 81-96.
[11]D. C. Montgomery: *Design and analysis of experiments*, 7 ed: John Wiley & Sons, Inc., 2009.
[12]M. Amini, H. Younesi, N. Bahramifar, A. A. Z. Lorestani and F. Ghorbani: J Hazard Mater Vol. 154 (2008), p. 694-702.
[13]R. H. Myers: *Response surface methodology*, 3 ed: John Wiley & Sons, Inc., 2009.
[14]I. Eren and F. Kaymak-Ertekin: J Food Eng Vol. 79 (2007), p. 344-352.
[15]M. R. Rahman, M. M. Huque, M. N. Islam and M. Hasan: Compos Part A-Appl S Vol. 39 (2008), p. 1739-1747.
[16]M. R. Rahman, M. M. Huque, M. N. Islam and M. Hasan: Compos Part A-Appl S Vol. 40 (2009), p. 511-517.

Fig. 3 (a) Desirability plot and (b) overlay plot of hardness for the optimal formulation.

Table 3 Predicted and observed responses with optimized formulation

Mixture component proportion (wt%)					Hardness (Shore D)	
x_1	x_2	x_3	x_4	x_5	Predicted	Observed
50.0	45.0	3.9	0.1	1.0	75.73	75.56 (0.40)*

* The value in parentheses is standard deviation from five replications.

Conclusions

Mixture experimental design, response surface, and optimization methods were applied to determine the optimal formulation based on maximum of the hardness property. Analysis of variance demonstrated that the compositions including rPP, RWF, MAPP, and UV stabilizer significantly affected the hardness property. Model adequacy checking also revealed that the overall predictive capability of model based on the residuals was very strong. From the contour plots, the hardness value sharply enhanced with increasing RWF content but greatly reduced with increase of rPP loading. This is due to the polymer matrix to be a considerably lower hardness than the rigid rubberwood filler [3, 7]. The addition of the UV stabilizer in the composites showed the negative effect, which slightly decreased the hardness value. This result is attributed due to the negative interaction of mixtures [3]. The optimal formulation of rPP/RWF composites using D-optimal mixture design based on maximum hardness value was found to be 50.0 wt% rPP, 45.0 wt% RWF, 3.9 wt% MAPP, 0.1 wt% UV stabilizer, and 1.0 wt% Lub with the desirability function to be 0.887.

Acknowledgements

The authors would like to thanks the Prince of Songkla Graduate Studies Grant, the Government budget Fund (Code: 2555A11502062) for financial support throughout this work, and Rubberwood Technology and Management Research Group (ENG-54-27-11-0137-S) of Faculty of Engineering, Prince of Songkla University, Thailand.

References

[1] A. Ashori and S. Sheshmani: Bioresour Technol Vol. 101 (2010), p. 4717-4720.
[2] S. K. Najafi, E. Hamidinia and M. Tajvidi: J Appl Polym Sci Vol. 100 (2006), p. 3641-3645.
[3] C. Homkhiew, T. Ratanawilai and W. Thongruang: J Thermoplast Compos Mater, Epub ahead of print 14 February 2013.DOI: 10.1177/0892705712475019.
[4] Z. A. Khan, S. Kamaruddin and A. N. Siddiquee: Mater Design Vol. 31 (2010), p. 2925-2931.
[5] T. Ratanawilai, N. Thanawattanasirikul and C. Homkhiew: Sci Asia Vol. 38 (2012), p. 289-294.
[6] K. B. Adhikary, S. Pang and M. P. Staiger: Compos Part B Eng Vol. 39 (2008), p. 807-815.
[7] B. Kord: World Appl Sci J Vol. 12 (2011), p. 1632-1634.
[8] M. S. Jang, J. E. Park and H. Y. Park: Food Sci Biotechnol Vol. 20 (2011), p. 409-417.

Journal of Composite Materials
http://jcm.sagepub.com/

Minimizing the creep of recycled polypropylene/rubberwood flour composites with mixture design experiments

Chatree Homkhiew, Thanate Ratanawilai and Wiriya Thongruang

Journal of Composite Materials published online 12 December 2013
DOI: 10.1177/0021998313514257

The online version of this article can be found at:
http://jcm.sagepub.com/content/early/2013/12/12/0021998313514257

Published by:
SAGE
http://www.sagepublications.com

On behalf of:

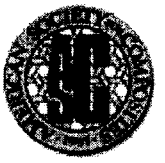

American Society for Composites

Article

JOURNAL OF COMPOSITE MATERIALS

Journal of Composite Materials
0(0) 1–10

DOI: 10.1177/0021998313514257
jcm.sagepub.com
SAGE

Minimizing the creep of recycled polypropylene/rubberwood flour composites with mixture design experiments

Chatree Homkhiew[1], Thanate Ratanawilai[1] and Wiriya Thongruang[2]

Abstract

Composites of rubberwood flour (RWF) and recycled polypropylene (rPP) were produced into panel samples by using a twin-screw extruder. The effects on creep behavior of mixture fractions of rPP, RWF, maleic anhydride-grafted polypropylene (MAPP), and ultraviolet (UV) stabilizer were studied in a D-optimal mixture design. Creep was significantly affected by the composition. Increasing the fraction of RWF decreased creep, while MAPP and UV stabilizer increased it. The models fitted were used to optimize a desirability score that balanced multiple creep characteristics. The model-based optimal formulation 50.5 wt% rPP, 44.9 wt% RWF, 3.5 wt% MAPP, 0.1 wt% UV stabilizer, and 1.0 wt% lubricant was experimentally validated to have low creep closely matching the model predictions.

Keywords

Wood-plastic composites, recycled polypropylene, rubberwood flour, mixture experimental design, creep behavior

Introduction

Wood-plastic composites (WPCs) have been extensively developed and used in non-structural applications.[1] For example, WPCs are increasingly used to replace softwood lumber in deck building, to improve durability.[2,3] The advantages of WPCs include high specific strength and stiffness, resistance to water absorption, and positive impact on environmental issues. These have stimulated the development of WPC materials for also structural applications.[1,4,5] However, these composites are poorly suited for some applications due to long-term creep under loading. This study is aimed to evaluate and improve the creep characteristics of specific WPCs.

Waste materials locally available in southern Thailand were used as raw materials because of both environmental benefits and low cost. Rubberwood (*Hevea brasiliensis*) waste is mainly produced by sawmills and furniture industry, both prevalent in southern Thailand. Of their total wood intakes, these industries generally generate about 34% wood wastes and about 54% rejects of plantation wastes, while only 12% of the rubberwood ends up in the products.[6] Most of the wood waste can be used in medium-density fiberboard and particle board.[7] However, the use of wood waste as reinforcement in plastic composites is of great interest, with environmental and economic benefits. The advantages of wood particles include biodegradability, low health hazard during handling, and non-abrasive nature,[8,9] when substituted for synthetic fillers such as glass fiber, carbon fiber, and other inorganic fillers. In addition, plastic waste is one of the major constituents of global municipal solid waste.[10] In 2008, at least 33.6 million tons post-consumer plastics were generated in the USA, of which 28.9 million tons went to landfills,

[1]Department of Industrial Engineering, Faculty of Engineering, Prince of Songkla University, Thailand
[2]Department of Mechanical Engineering, Faculty of Engineering, Prince of Songkla University, Thailand

Corresponding author:
Thanate Ratanawilai, Department of Industrial Engineering, Faculty of Engineering, Prince of Songkla University, Hat Yai, Songkhla 90112, Thailand.
Email: thanate.r@psu.ac.th

2.6 million tons to combustion and energy recovery, and only 2.2 million tons to recycling[11,12]—only a tiny fraction of plastic waste is recycled. Blending post-consumer plastics with wood flour to create value-added products could increase the value of plastic waste and impact its reuse practices.[11] Plastic waste is a promising raw material for WPCs because of low cost[10] and properties similar to virgin materials. For example, composites made from recycled high-density polyethylene (rHDPE) have similar or, in some cases, better mechanical properties than composites made from virgin HDPE.[13,14] The mechanical properties of composites are not better with virgin polystyrene than with recycled polystyrene.[15] Ashori[16] studied the potential of municipal solid waste materials for making wood plastic composites. Waste wood and paper can replace inorganic fillers in thermoplastic composites, and these composites can be reclaimed and recycled repeatedly. Ashori and Sheshmani[17] made hybrid composite materials with a combination of recycled newspaper fiber (RNF) and poplar wood flour as reinforcement, and with recycled polypropylene (rPP) as the polymer matrix. They found that the composites with a high fraction of RNF had high water absorption. Madhoushi et al.[18] studied the effects of sanding dust loading and nanoclay content on the physical and mechanical properties of polypropylene. Addition of sanding dust significantly decreased tensile and flexural properties of the composites, and flexural, tensile, and withdrawal strength of fasteners were improved by the addition of 2 wt% nanoclay in the matrix. Nourbakhsh and Ashori[19] evaluated the effects of the fiber content and compatibilizing agent concentration on the mechanical properties and water absorption of composites from poplar fiber and rHDPE. The compatibilizer polyethylene-grafted maleic anhydride improved the flexural properties that now increased with wood content. In another study, no statistically significant differences were found in mechanical properties of composites, on comparing recycled plastics (HDPE and polypropylene) with virgin plastics.[20] Polypropylene waste and wood waste are promising alternative raw materials for making low cost WPCs.[21] To reduce solid waste disposal in landfills and have low cost WPC products[13] with good mechanical properties and low creep deformation, suitable WPC formulations need to be developed.

Design of experiments contributes to efficiently finding the best formulations. Typical designs include Taguchi method, factorial design, and mixture design.[22] The fractions of components in a mixture cannot be changed independently because they must add up to 100%, and mixture designs make use of this fact.[22] A D-optimal mixture experimental design allows to fit models that can be used to optimize the formulation of a composite material.[23] It also allows placing restrictions on the formulations, such as lower or upper limits on the fractions of some components.[23,24] Mixture designs have recently been applied in food and pharmaceutical industries to find optimal formulations because they appear efficient in providing useful models with a comparatively small number of experiments. However, prior studies on WPCs seem not to have used D-optimal mixture designs. A four-factor central composite design was applied to develop a response surface model and to study the foamability of rigid PVC/wood-flour composites.[25] A 2^4 factorial design was used to determine the effects of two hindered amine light stabilizers (HALS), a colorant, an ultraviolet absorber, and their interactions, on the photostabilization of wood flour/HDPE composites.[26] A Box-Behnken design with response surface method was adopted to determine which variables influenced board performance significantly.[27] In the current study, a D-optimal mixture design was used to model the creep of WPCs. The ultimate goal of this work was to optimize the composite formulation using rPP and rubberwood flour (RWF) for minimal creep.

Materials and methods

Materials

rPP pellets, with a melt flow index of 11 g/10 min at 230°C, were purchased from Withaya Intertrade Co., Ltd (Samutprakarn, Thailand). RWF, used as a natural reinforcement, was collected from a local furniture factory (Songkhla, Thailand). Its chemical composition (by dry weight) was cellulose 39%; hemicellulose 29%; lignin 28%; and ash 4%.[6] The interfacial bonding between wood flour filler and polymer matrix was also modified, using maleic anhydride-grafted polypropylene (MAPP) with 8–10% of maleic anhydride, supplied by Sigma-Aldrich (Missouri, USA). HALS additive under the trade name MEUV008, chosen as the ultraviolet (UV) stabilizer, was supplied by TH Color Co., Ltd (Samutprakarn, Thailand). Paraffin wax, chosen as the lubricant (Lub), was purchased from Nippon Seiro Co., Ltd (Yamaguchi, Japan).

Experimental design to optimize formulation

The D-optimal design of mixture experiments was created with Design-Expert software (version 8.0.6, Stat-Ease, Inc.) to statistically evaluate and model the effects of component fractions on creep properties and to optimize the formulation. The optimal experimental design of WPC formulations specified the component fractions of rPP (x_1), RWF (x_2), MAPP (x_3), UV (x_4), and Lub (x_5). The upper and lower limits of experimental range

Table 1. Constraints for the mixture design of experiments.

Component	Proportion restriction (wt%)
rPP (x_1)	$50 \leq x_1 \leq 70$
RWF (x_2)	$25 \leq x_2 \leq 45$
MAPP (x_3)	$3 \leq x_3 \leq 5$
UV stabilizer (x_4)	$0 \leq x_4 \leq 1$
Lub (x_5)	$=1$

Table 2. Experimental compositions in mixture experimental design and measured responses.

	Mixture proportion (wt%)					Creep strain (%)		
Run no.	x_1	x_2	x_3	x_4	x_5	C_e	C_{ve6000}	C_{t6000}
1	63.9	29.9	4.5	0.7	1.0	0.98	0.33	1.31
2	70.0	25.0	3.0	1.0	1.0	1.03	0.42	1.45
3	50.0	43.0	5.0	1.0	1.0	0.77	0.27	1.04
4	54.9	38.9	4.5	0.7	1.0	0.75	0.25	1.00
5	59.5	34.5	5.0	0.0	1.0	0.80	0.37	1.17
6	55.4	39.9	3.5	0.2	1.0	0.74	0.29	1.03
7	59.5	34.5	4.0	1.0	1.0	0.78	0.31	1.09
8[a]	59.5	34.5	5.0	0.0	1.0	0.89	0.38	1.27
9	50.0	44.3	4.3	0.5	1.0	0.67	0.27	0.94
10	68.0	25.0	5.0	1.0	1.0	1.07	0.43	1.50
11	50.0	45.0	3.0	1.0	1.0	0.70	0.25	0.95
12[a]	50.0	43.0	5.0	1.0	1.0	0.71	0.36	1.07
13	60.3	35.3	3.0	0.5	1.0	0.88	0.34	1.22
14	64.9	30.4	3.5	0.2	1.0	0.90	0.38	1.28
15[a]	70.0	25.0	3.0	1.0	1.0	1.03	0.40	1.43
16	51.0	45.0	3.0	0.0	1.0	0.70	0.32	1.02
17[a]	51.0	45.0	3.0	0.0	1.0	0.69	0.26	0.95
18[a]	50.0	45.0	3.0	1.0	1.0	0.73	0.25	0.98
19	70.0	25.0	4.0	0.0	1.0	0.94	0.42	1.36
20	69.0	25.0	5.0	0.0	1.0	0.96	0.33	1.29

[a]Duplicate experiment.

for the compositions are shown in Table 1. Despite the fraction of Lub being held constant, it is included as a variable because it contributes to the 100% in the mixture. The total number of runs was 20, as shown in Table 2, including 15 different formulations and five duplications to evaluate reproducibility or variances.

Composites processing

Before compounding, the RWF was sieved through an 80 mesh standard sieve (particles smaller than 180 μm pass) and dried in an oven at 110°C for 8 h to minimize moisture content. WPCs were then produced in a two-stage process. In the first stage, WPC pellets were produced: rPP and RWF were dry-blended, and then melt-blended into wood-plastic composite pellets using a twin-screw extruder machine (Model SHJ-36 from En Mach Co., Ltd, Nonthaburi, Thailand). The extrusion barrel with 10 temperature zones was controlled at 130–170°C to avoid degradation of the components, while the screw rotating speed was maintained at 70 rpm. The extruded strand passed through a water bath and was subsequently pelletized. In the second stage, WPC panels were produced: the WPC pellets were again dried at 110°C for 8 h. WPC pellets, MAPP, UV stabilizer, and lubricant compositions indicated in Table 2 were then dry-mixed and added into the feeder of the twin-screw extruder. The temperature profile for extruding was 130–190°C, with 50 rpm screw feed. Melt pressure at the die varied between 0.10 and 0.20 MPa, depending on wood flour content. Vacuum venting at nine temperature zones was also used to purge volatile compounds. The samples were extruded through a rectangular 9 mm × 22 mm die and cooled in atmospheric air. The specimens were machined for flexural creep testing, following the standard of American Society for Testing and Materials (ASTM).

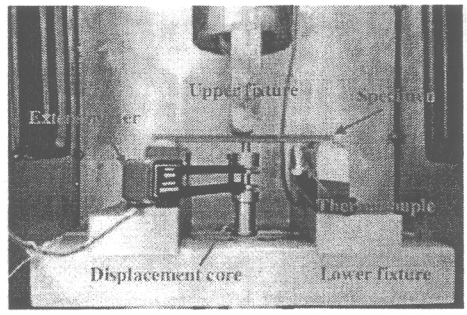

Figure 1. Test apparatus of three-point bending creep.

Characterization

Three-point bending creep tests of rPP/RWF composites were carried out on an Instron Universal Testing Machine (Model 5582 from Instron Corporation, MA, USA) in Figure 1, according to ASTM D2990 standard. All the tests were performed on 13 mm × 4.8 mm × 100 mm (width × thickness × length) rectangular samples, and a test span of 80 mm. Before the creep tests, the specimens were equilibrated for 15 min, and the tests were conducted at a temperature of 25°C (ambient conditions). The total time of the testing was 100 min (6000 s) under a constant stress of 19 MPa. Five replications of each formulation were tested.

Morphological analysis

The formation of cracks and interfacial morphology between the wood flour and the polymeric matrix were analyzed with a scanning electron microscope (SEM). The fracture surface of the specimen before creep testing was fractured in liquid nitrogen. Likewise, the fracture surface of the specimen after creep testing was fractured by the creep characterization. SEM imaging was performed using a FEI Quanta 400 microscope (Oregon, USA) at an accelerating voltage of 20 kV. The samples (fracture surfaces) before and after creep tests were sputter-coated with gold to prevent electrical charging during the observation. Specimens were imaged at magnifications of 150× and 2500×.

Results and discussion

The D-optimal mixture design of experiments, with five fractions as (mutually dependent) variables (that sum to one), had 20 runs in a randomized order. The three determined responses were the values of the instantaneous creep strain (C_e), of the viscoelastic creep strain after 6000 s (C_{ve6000}), and of the total creep strain after 6000 s (C_{t6000}), and the results are summarized in Table 2.

Statistical analysis of the response surface model

The data for C_e, C_{ve6000}, and C_{t6000} were fit with linear models by multiple linear regression, with no statistical need for quadratic, special cubic, and cubic models. For example, a summary of modeling the C_{t6000} response is shown in Table 3. The sequentially fit linear model is significant (p-value less than $\alpha = 0.05$), but the higher order terms are not. The adjusted coefficient of determination (adj-R^2) and predicted coefficient of determination (pred-R^2) shown in Table 4 have fairly good values at 0.8780 and 0.8413, respectively. The values in Table 4 came from an analysis of variance (ANOVA) on the significant effects relative to the creep responses. The ANOVA shows statistical

Table 3. Fit summary of C_{t6000} response.

Source	Sequential p-value	Lack of fit p-value	Adj-R^2	Pred-R^2	
Linear	<0.0001*	0.1125	0.8780	0.8413	Suggested
Quadratic	0.2092	0.1415	0.9045	0.7242	
Special cubic	0.2454	0.1161	0.9279	−13.77	
Cubic	0.1161	–	0.9497	–	Aliased

*$P < 0.05$ indicates that model terms are significant.

Table 4. P-values from analysis of variance and model adequacy indicators for each modeled response.

Source	C_e (%)	C_{ve6000} (%)	C_{t6000} (%)
Model	Linear	Linear	Linear
	<0.0001*	0.0006*	<0.0001*
Linear mixture	<0.0001*	0.0006*	<0.0001*
Lack of fit	0.3331	0.3590	0.1125
R^2	0.9143	0.6555	0.8973
Adj-R^2	0.8982	0.5909	0.8780
Pred-R^2	0.8742	0.4296	0.8413
CV (%)	4.99	12.03	5.52

*$P < 0.05$ indicates that model terms are significant.

significance of these linear models, indicated by p-values less than α ($\alpha = 0.05$). This result implies that each modeled output, C_e, C_{ve6000}, and C_{t6000}, was significantly affected by at least one of the four controlled variables. The R^2 value for C_{ve6000} is relatively poor, partly because its determination was "noisy" with a high CV.

The R^2 values of the C_e, C_{ve6000}, and C_{t6000} are 0.9143, 0.6555, and 0.8973, indicating that 8.57%, 34.45%, and 10.27%, respectively, of the total variability in observations is not explained by the models; R^2 values close to 1 indicate good fits.[28] R^2 values will always increase when a variable is added to the model,[29] and the computed adj-R^2 should be close to R^2 value of the model selected. This indeed is the case for the fitted models, indicating it is unlikely that the models have insignificant terms included.[30] The pred-R^2 value of C_e was 0.8742, meaning that the fitted model is estimated to explain about 87% of variability in new cases, and this is in reasonable agreement with the adj-R^2 of 0.8982. For C_{ve6000} all of R^2, adj-R^2, and pred-R^2 have relatively low or poor values, because C_{ve6000} was calculated as $C_{t6000} - C_e$ and this increased its relative inaccuracy. The coefficients of variation (CV), of C_e, C_{ve6000}, and C_{t6000} were estimated at 4.99%, 12.03%, and 5.52%, respectively, based on the residual variation. Low CV values indicate good precision of the determinations.

Model adequacy checking

Model adequacy checking is always necessary with a fitted model.[30] Figure 2(a) displays normal probability plots of the residuals for elastic creep strain C_e, and the visually good fit with a straight lines suggests the residuals are about normally distributed. The interpretation is that the residuals are Gaussian measurement noise, while the explanatory variables (fractions of rPP, RWF, MAPP, and UV stabilizer) explain the

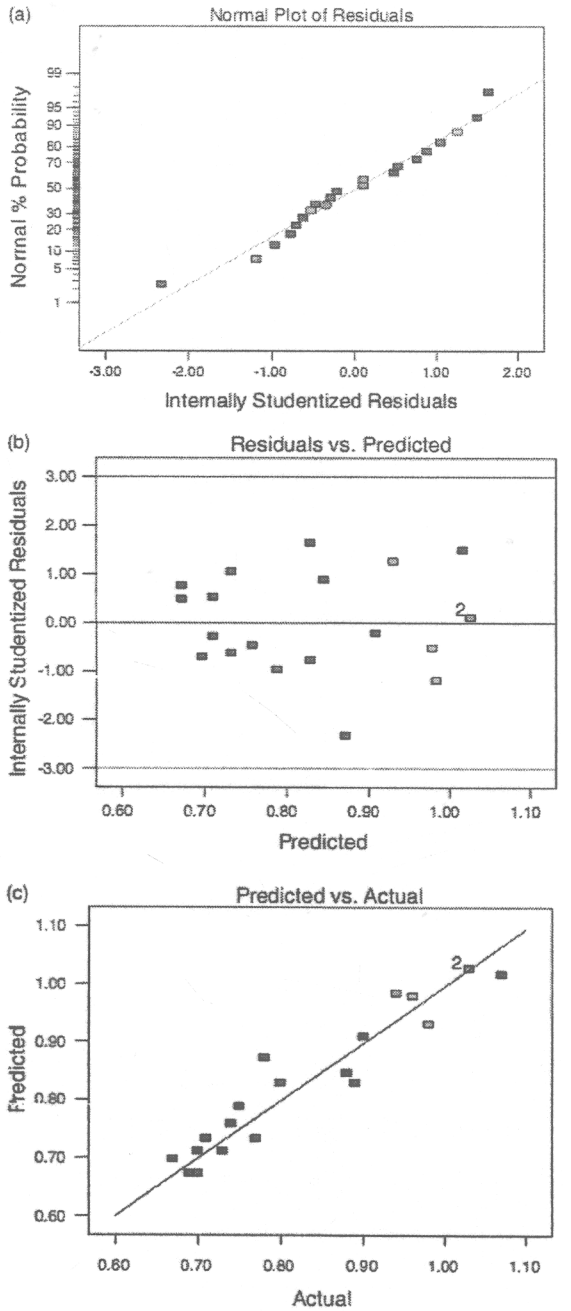

Figure 2. Model adequacy checking for elastic creep strain: (a) normal probability plot of residuals, (b) plot of residuals versus predicted values, and (c) plot of predicted versus actual values.

deterministic part of the relationship. Likewise, the presence of outliers is not strong indication, as such a failed experiment would give a large residual disabling the good straight line fit in a probability plot.[22] A plot of the residuals vs. the predicted values for the model of

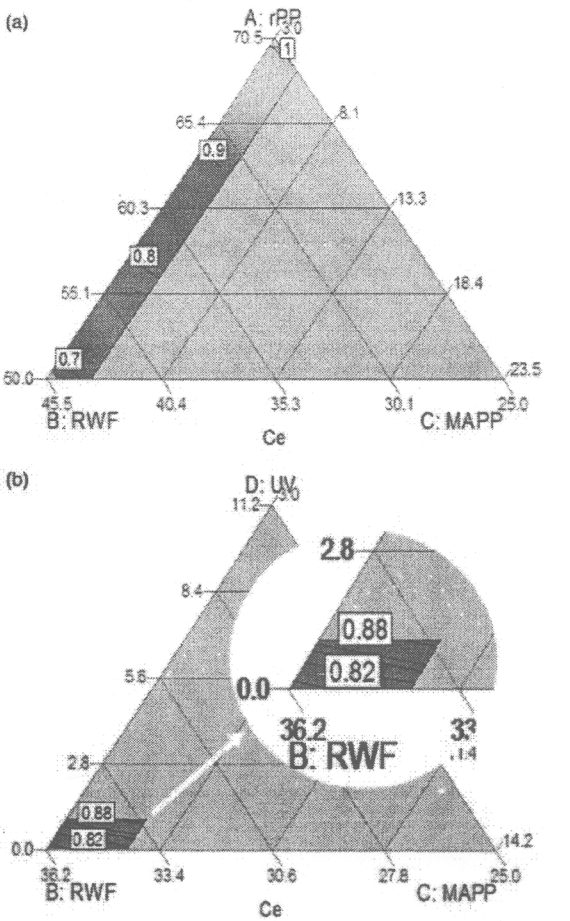

Figure 3. Triangular contour plots for effects of the compositions on elastic creep strain: (a) fixed UV stabilizer at 0.5 wt% and Lub at 1 wt% and (b) fixed rPP at 59.8 wt% and Lub at 1 wt%.

C_e is shown in Figure 2(b). There is no obvious pattern remaining, and therefore no suggestion for adding some nonlinear terms to the fit.[22] Figure 2(c) shows the C_e model predictions vs. observations. The model outputs fit the actual observations quite well, with C_e model deviating from actual by less than about 5%, in alignment with the estimated CV. The model adequacy was similarly checked for C_{ve6000} and C_{t6000}, with essentially similar conclusions.

Effect of composition on the elastic creep strain, and optimal formulation

The linear regression model fitted to experimental C_e value was

$$C_e = 0.99x_1 + 0.66x_2 + 0.89x_3 + 1.78x_4 \qquad (1)$$

Table 5. The optimal formulations that minimize each creep characteristic, with predicted responses.

Property (%)	Mixture proportion (wt%)					Predicted response	Desirability
	rPP	RWF	MAPP	UV	Lub		
C_e	50.0	45.0	3.9	0.1	1.0	0.67	0.996
C_{ve6000}	50.0	45.0	3.0	1.0	1.0	0.26	0.906
C_{t6000}	50.1	45.0	3.5	0.3	1.0	0.95	0.962

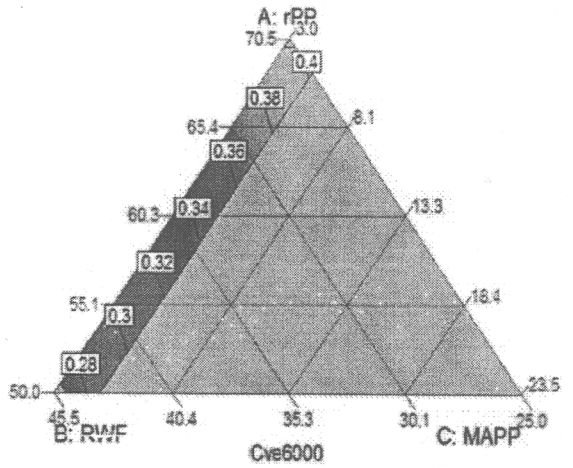

Figure 4. Triangular contour plot for effects of the compositions on viscoelastic creep strain. Constant fractions of UV stabilizer at 0.5 wt% and Lub at 1 wt%.

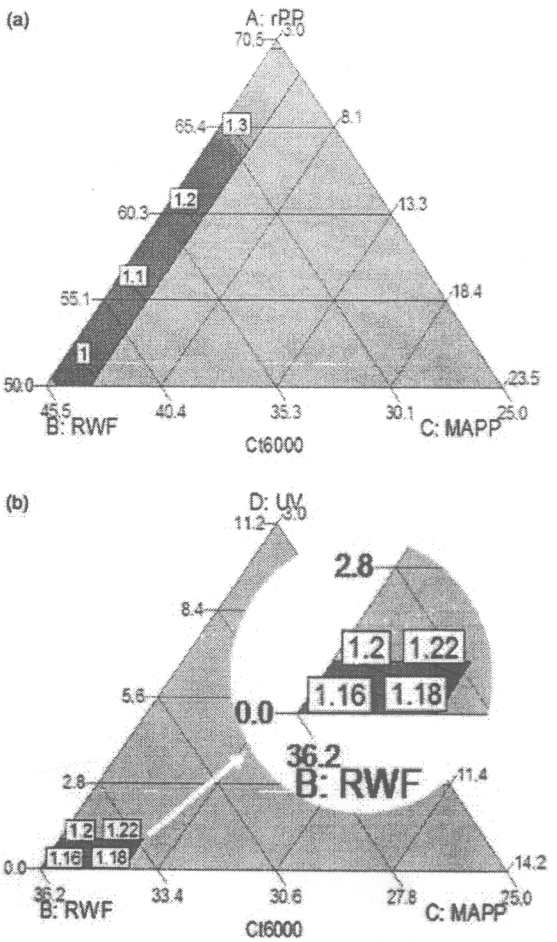

Figure 5. Triangular contour plots for effects of the compositions on total creep strain: (a) fixed UV stabilizer at 0.5 wt% and Lub at 1 wt% and (b) fixed rPP at 59.8 wt% and Lub at 1 wt%.

in which all coefficients are positive. RWF (x_2) has the smallest coefficient so it should be maximized to minimize creep. The UV stabilizer (x_4) has the largest coefficient, so its addition should be as small as possible. The experimentally covered formulations are shown in Figure 3(a) and (b), with color coding for the modeled C_e. In the triangular contour plot of Figure 3(a), the three pure components (rPP, RWF, and MAPP) are represented by the corners, while the additive levels were fixed (UV stabilizer at 0.5 wt% and Lub at 1 wt%). The contours in the colored areas, that include the experimental observations, present the C_e regression fits varying from 0.7% to 1%. The creep C_e clearly decreases with increasing RWF content. High wood flour content increases the modulus of elasticity (MOE) of composites,[31] so that higher stress is required for the same deformation.[7,32] The choice of MAPP content between 3 and 5 wt% barely affected the C_e. Generally, the addition of coupling agent in the WPCs decreases the creep strain due to the improved filler dispersion and improved interfacial adhesion between wood flour and polymer matrix,[33–35] whereas too much MAPP relative to wood flour will cause self-entanglement, resulting in slippage with the PP molecules.[7,36] This slippage in the WPC structures leads to easier creep deformation of the WPC specimens. The triangular contour plot in Figure 3(b) also shows that addition of 1 wt% UV stabilizer slightly increased the elastic creep strain from 0.82% to 0.88% because UV stabilizer has some chemical reactions with the other components.[37] Likewise, it is known to reduce the flexural properties but to increase creep strain, due to non-homogeneous spatial distribution of wood flour, polymer, and UV stabilizer.[38] Therefore, the load-bearing capacity of WPC specimens decreased, resulting in increase of the creep deformation. Using 1 wt% of UV stabilizer may be unnecessary, and its fraction should be minimized to minimize creep.

The numerically optimized compositions for each creep characteristic, based on fitted models, are

shown in Table 5. In all three cases, the formulations have about 50.0 wt% of rPP and 45.0 wt% of RWF, with minor variation in MAPP and UV stabilizer fractions. Since the requirements of optimizing the different creep characteristics are not in much of a conflict, they can be approximately optimized simultaneously.

Effect of composition on the viscoelastic creep strain, and optimal formulation

The linear regression model for the viscoelastic creep strain (C_{ve6000}) was

$$C_{ve6000} = 0.40x_1 + 0.27x_2 + 0.45x_3 + 0.26x_4 \quad (2)$$

with positive coefficients. In Figure 4 C_{ve6000} (in the range of 0.28 to 0.40%) increases for high fractions of rPP, because the mobility of polymer chains increased in the WPCs and contributed to viscoelasticity. The concentration effect of MAPP on C_{ve6000} was insignificant, similar to elastic creep strain. The optimal composition minimizing viscoelastic creep strain coincided with formulation 11, see Table 5.

Effect of composition on the total creep strain, and optimal formulation

The linear regression fit for the total creep strain (C_{t6000}) was

$$C_{t6000} = 1.39x_1 + 0.93x_2 + 1.33x_3 + 2.04x_4 \quad (3)$$

with positive coefficients. RWF (x_2) has the lowest coefficient, while UV stabilizer (x_4) had the largest

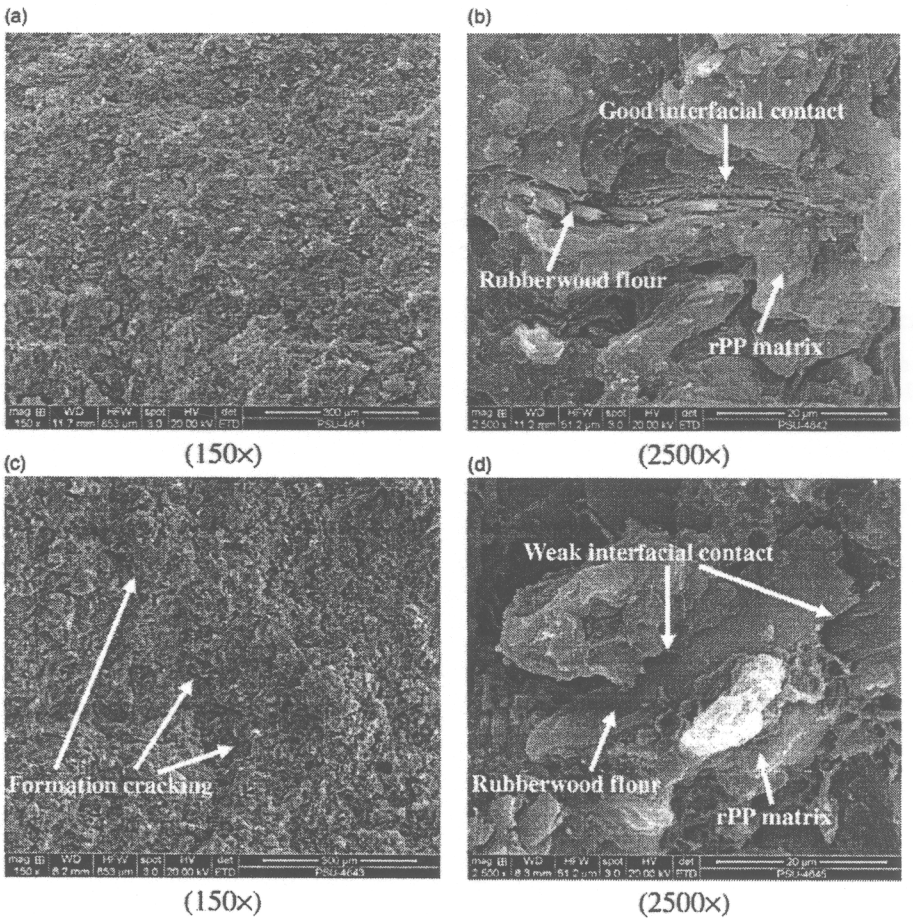

Figure 6. SEM micrographs of rPP-rubberwood flour composites showing formation of cracks and interfacial contact between wood flour and plastic matrix (Magnification 150× and 2500×): (a), (b) before creep testing and (c), (d) after creep testing.

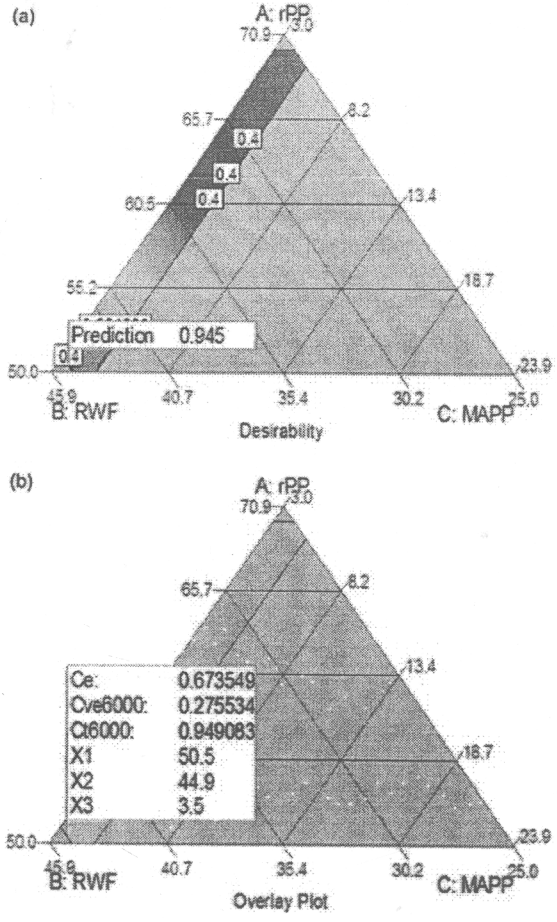

Figure 7. The optimal formulation for overall desirability.

coefficient. Figure 5(a) shows that total creep strain varies in range of 1.0–1.3% and decreases with RWF loading. RWF had a lower coefficient than rPP because wood flour is stiffer than the neat plastic.[39] Therefore, the deformation of the composites is reduced with increased wood flour content. Furthermore, the addition of increasing wood flour replaced the plastic matrix. It reduced the volume and mobility of the macromolecules chains in the composite structures, resulting in decrease of the creep deformation. The creep of WPCs is mainly caused from the plastic matrix, and the chains mobility leads to eventual failure of the WPC specimens. Figure 5(b) presents the effects of MAPP and UV stabilizer contents on the total creep strain. The total creep strain slightly increases with MAPP and UV stabilizer concentrations, with reasons similar to what was discussed in relation to C_e. The optimal formulation based on the numerical model is also shown in Table 5. In addition, the microstructure analysis of the composites before and after creep

Table 6. Predicted and observed responses with the formulation optimized jointly for all the creep characteristics.

	Mixture component proportion (wt%)					Creep strain (%)		
	rPP	RWF	MAPP	UV	Lub	C_e	C_{ve6000}	C_{t6000}
Predicted	50.5	44.9	3.5	0.1	1.0	0.67	0.27	0.95
Observed						0.71	0.29	1.00
						(0.01)	(0.02)	(0.03)

Note: The values in parentheses are standard deviations from five replicates.

experiment was also observed from the SEM micrographs in Figure 6 (Figure 6(a) and (b) before creep testing and 6(c) and (d) after creep testing). Irregular short fibers are seen in the composites. The composites before creep testing exhibited no crack formation and good interfacial contact between RWF and PP matrix. According to this SEM study, the coupling agent used in the composites improves the compatibility, resulting in the good interfacial adhesion and enhancement of creep performance.[7] In contrast, the composites after creep testing had large cracks and poor interfacial contact. This is due to great extension of the composites bearing load for long time, and the wood flour was pushed out from the plastic matrix, resulting in failure of the composites.

Optimal formulation for all creep characteristics

Multiobjective optimization using all of the regression models was performed with the Design-Expert software, using its default settings to construct a desirability score that balances all of the fitted models. The plot in Figure 7 shows the formulation that was considered optimal, along with contours of the desirability score. The optimal formulation found was 50.5 wt% rPP, 44.9 wt% RWF, 3.5 wt% MAPP, 0.1 wt% UV stabilizer, and 1.0 wt% Lub, corresponding to a high desirability of 0.945. All the previous optima, in Table 5, were at practically the same formulation. The model predictions were validated experimentally, and the results are given in Table 6 for the jointly optimal formulation. The maximum deviations between model predictions and experimental averages are of the same order as the earlier estimated CV accuracies of determinations.

Conclusions

Design and analysis of D-optimal mixture experiments were used to efficiently obtain the optimal formulation of rPP/RWF composites that minimizes creep. All the

component fractions experimentally varied, namely of rPP, RWF, MAPP, and UV stabilizer, which significantly affected all the creep characteristics (C_c, C_{tc6000}, and C_{t6000}). In general, a high fraction of RWF reduced all of these, and the optima found had 45 wt% RWF which was the maximum in the experimental design. At this wood flour loading, the modulus of elasticity was maximized, so that a comparatively high stress is required for a given creep deformation. Increasing the fraction of MAPP from 3 to 5 wt% only slightly affected the creep strain, lacking statistical significance. The addition of 1 wt% UV stabilizer slightly increased creep. The approximately optimal formulation minimizing jointly all creep characteristics was 50.5 wt% rPP, 44.9 wt% RWF, 3.5 wt% MAPP, 0.1 wt% UV stabilizer, and 1.0 wt% Lub. The joint optimization maximized a desirability score that balanced the multiple objectives, and the jointly optimal formulation was experimentally validated to produce low creep nearly as predicted.

Funding

The authors gratefully acknowledge the financial support from the graduate school of Prince of Songkla University, the Government budget Fund (Research Grant Code: 2555A11502062), and Rubberwood Technology and Management Research Group (ENG-54-27-11-0137-S) of Faculty of Engineering, Prince of Songkla University, Thailand.

Conflict of Interest

None declared.

Acknowledgement

We thank the Research and Development Office (RDO) and Assoc. Prof. Seppo Karrila for editing this article.

References

1. Tamrakar S, Lopez-Anido RA, Kiziltas A, et al. Time and temperature dependent response of a wood-polypropylene composite. *Compos A: Appl Sci Manuf* 2011; 42: 834–842.
2. Carroll DR, Stone RB, Sirignano AM, et al. Structural properties of recycled plastic/sawdust lumber decking planks. *Resour Conserv Recycl* 2011; 31: 241–251.
3. Ganguly I and Eastin IL. Trends in the US decking market: a national survey of deck and home builders. *Forest Chroni* 2009; 85: 82–90.
4. Klyosov AA. *Wood-plastic composites*. 1. Hoboken, NJ: John Wiley & Son, Inc, 2007.
5. Ratanawilai T, Lekanukit P and Urapantamas S. Effect of rubberwood and palm oil content on the properties of wood-polyvinyl chloride composites. *J Thermoplast Compos Mater* 2012; DOI: 10.1177/0892705712454863.
6. Petchpradab P, Yoshida T, Charinpanitkul T, et al. Hydrothermal pretreatment of rubber wood for the saccharification process. *Ind Eng Chem Res* 2009; 48: 4587–4591.
7. Homkhiew C, Ratanawilai T and Thongruang W. Composites from recycled polypropylene and rubberwood flour: effects of composition on mechanical properties. *J Thermoplast Compos Mater* 2013; DOI: 10.1177/0892705712475019.
8. Peng X, Fan M, Hartley J, et al. Properties of natural fiber composites made by pultrusion process. *J Compos Mater* 2011; 46: 237–246.
9. Francucci G, Rodriguez ES and Vazquez A. Experimental study of the compaction response of jute fabrics in liquid composite molding processes. *J Compos Mater* 2011; 46: 155–167.
10. Cui Y, Lee S, Noruziaan B, et al. Fabrication and interfacial modification of wood/recycled plastic composite materials. *Compos A: Appl Sci Manuf* 2008; 39: 655–661.
11. Ratanawilai T, Thanawattanasirikul N and Homkhiew C. Mechanical and thermal properties of oil palm wood sawdust reinforced post-consumer polyethylene composites. *ScienceAsia* 2012; 38: 289–294.
12. Themelis NJ, Castaldi MJ, Bhatti J, et al. Energy and economic value of nonrecycled plastics (NRP) and municipal solid wastes (MSW) that are currently landfilled in the fifty States. *EEC Study of non-recycled plastics*. Earth Engineering Center, Columbia University, 2011, p.8.
13. Adhikary KB, Pang S and Staiger MP. Dimensional stability and mechanical behaviour of wood-plastic composites based recycled and virgin high-density polyethylene (HDPE). *Compos B: Eng* 2008; 39: 807–815.
14. Selke SE and Wichman I. Wood fiber/polyolefin composites. *Compos A: Appl Sci Manuf* 2004; 35: 321–326.
15. Lisperguer J, Bustos X and Saravia Y. Thermal and mechanical properties of wood flour-polystyrene blends from postconsumer plastic waste. *J Appl Polym Sci* 2011; 119: 443–451.
16. Ashori A. Municipal solid waste as a source of lignocellulosic fiber and plastic for composite industries. *Polym Plas Technol Eng* 2008; 47: 741–744.
17. Ashori A and Sheshmani S. Hybrid composites made from recycled materials: moisture absorption and thickness swelling behavior. *Biores Technol* 2010; 101: 4717–4720.
18. Madhoushi M, Chavooshi A, Ashori A, et al. Properties of wood plastic composite panels made from waste sanding dusts and nanoclay. *J Compos Mater* 2013; DOI: 10.1177/0021998313489899.
19. Nourbakhsh A and Ashori A. Preparation and properties of wood plastic composites made of recycled high-density polyethylene. *J Compos Mater* 2009; 43: 877–883.
20. Najafi SK, Hamidinia E and Tajvidi M. Mechanical properties of composites from sawdust and recycled plastics. *J Appl Polym Sci* 2006; 100: 3641–3645.
21. Nourbakhsh A, Ashori A, Tabari HZ, et al. Mechanical and thermo-chemical properties of wood-flour/polypropylene blends. *Polym Bull* 2010; 65: 691–700.
22. Montgomery DC. *Design and analysis of experiments*. 7th ed. New York, NY: John Wiley & Sons, Inc, 2009.

23. Khosrowshahi YB and Salem A. Influence of polyvinyl alcohol and carboxymethyl cellulose on the reliability of extruded ceramic body: application of mixture design method in fabricating reliable ceramic raschig rings. *Inter J Appl Cera Technol* 2011; 8: 1334–1343.
24. John RCS. Experiments with mixtures, ill-conditioning, and ridge regression. *J Qual Technol* 1984; 16: 81–96.
25. Matuana LM and Mengeloglu F. Manufacture of rigid PVC/wood-flour composite foams using moisture contained in wood as foaming agent. *J Vinyl Addit Technol* 2002; 8: 264–270.
26. Stark NM and Matuana LM. Ultraviolet weathering of photostabilized wood-flour-filled high-density polyethylene composites. *J Appl Polym Sci* 2003; 90: 2609–2617.
27. Jun Z, Xiang-ming W, Jian-min C, et al. Optimization of processing variables in wood–rubber composite panel manufacturing technology. *Biores Technol* 2008; 99: 2384–2391.
28. Amini M, Younesi H, Bahramifar N, et al. Application of response surface methodology for optimization of lead biosorption in an aqueous solution by Aspergillus niger. *J Hazard Mater* 2008; 154: 694–702.
29. Eren I and Kaymak-Ertekin F. Optimization of osmotic dehydration of potato using response surface methodology. *J Food Eng* 2007; 79: 344–352.
30. Myers RH, Montgomery DC and Anderson-Cook CM. *Response surface methodology: process and product optimization using designed experiments*, 3rd ed. Hoboken, NJ: John Wiley & Sons, Inc, 2009.
31. Marcovich NE and Villar MA. Thermal and mechanical characterization of linear low-density polyethylene/wood flour composites. *J Appl Polym Sci* 2003; 90: 2775–2784.
32. Rahman MR, Huque MM, Islam MN, et al. Improvement of physico-mechanical properties of jute fiber reinforced polypropylene composites by post-treatment. *Compos A: Appl Sci Manuf* 2008; 39: 1739–1747.
33. Mingyin J, Ping X, Yongsheng Z, et al. Creep behaviour of wood flour/poly(vinyl chloride) composites. *J Wuhan Univer Technol-Mater* 2009; 24: 440–447.
34. Bengtsson M, Gatenholm P and Oksman K. The effect of crosslinking on the properties of polyethylene/wood flour composites. *Compos Sci Technol* 2005; 65: 1468–1479.
35. Nunez AJ, Sturm PC, Kenny JM, et al. Mechanical characterization of polypropylene-wood flour composites. *J Appl Polym Sci* 2003; 88: 1420–1428.
36. Mohanty S, Verma SK, Nayak SK, et al. Influence of fiber treatment on the performance of sisal–polypropylene composites. *J Appl Polym Sci* 2004; 94: 1336–1345.
37. Homkhiew C, Ratanawilai T and Thongruang W. The optimal formulation of recycled polypropylene/rubberwood flour composites from experiments with mixture design. *Compos B: Eng* 2014; 56: 350–357.
38. Wechsler A and Hiziroglu S. Some of the properties of wood–plastic composites. *Build Environ* 2007; 42: 2637–2644.
39. Garcia M, Hidalgo J, Garmendia I, et al. Wood–plastics composites with better fire retardancy and durability performance. *Compos A: Appl Sci Manuf* 2009; 40: 1772–1776.

Journal of Thermoplastic Composite Materials
http://jtc.sagepub.com/

Long-term water absorption and dimensional stability of composites from recycled polypropylene and rubberwood flour

Chatree Homkhiew, Thanate Ratanawilai and Wiriya Thongruang

Journal of Thermoplastic Composite Materials published online 7 January 2014
DOI: 10.1177/0892705713518789

The online version of this article can be found at:
http://jtc.sagepub.com/content/early/2014/01/06/0892705713518789

Published by:
SAGE
http://www.sagepublications.com

Article

JOURNAL OF THERMOPLASTIC COMPOSITE MATERIALS

Journal of Thermoplastic Composite Materials
1–18

DOI: 10.1177/0892705713518789
jtc.sagepub.com
SAGE

Long-term water absorption and dimensional stability of composites from recycled polypropylene and rubberwood flour

Chatree Homkhiew[1], Thanate Ratanawilai[1] and Wiriya Thongruang[2]

Abstract

The present study aims to investigate the moisture absorption of polypropylene (PP)/rubberwood flour (RWF) composites and its effects on dimensional stability. The compositions included different grades of plastic, and the amounts of wood flour, maleic anhydride-grafted polypropylene (MAPP), and ultraviolet (UV) stabilizer were varied. The composite materials were manufactured into panels by a twin-screw extruder. Long-term water absorption (WA), long-term thickness swelling (TS), and degradation of flexural properties of the composites were studied for a range of water immersion times. The WA and TS of the samples increased with RWF content and immersion time. Recycled PP gave higher WA and TS than virgin PP, for the composites with 45 wt% RWF. Increasing MAPP content from 3 to 5 wt% had no significant effect on WA and TS, whereas the addition of 1 wt% UV stabilizer increased them. A MAPP content of 3 wt% is recommended for moisture resistance, while the amount of UV stabilizer should be kept as low as possible. Flexural strength and modulus of composites also decreased with moisture uptake; however, <3% WA did not significantly affect the flexural strength. In contrast, the maximum strain of composites consistently increased with WA.

[1] Department of Industrial Engineering, Faculty of Engineering, Prince of Songkla University, Songkhla, Thailand
[2] Department of Mechanical Engineering, Faculty of Engineering, Prince of Songkla University, Hat Yai, Songkhla, Thailand

Corresponding author:
Thanate Ratanawilai, Department of Industrial Engineering, Faculty of Engineering, Prince of Songkla University, Hat Yai, Songkhla 90112, Thailand.
Email: thanate.r@psu.ac.th

Keywords
Wood–plastic composites, recycled polypropylene, rubberwood flour, water absorption, flexural property

Introduction

Natural organic fibers are potential replacements for glass or carbon fibers, inorganic fillers, and other traditional materials in composites.[1,2] The advantages of natural fibers include low cost, low density, low energy consumption, biodegradability, and non-abrasive nature.[1,3] Likewise, they can have high specific strength and modulus, allowing the production of low-density composites with high filler content.[4,5] Recent advances in natural fillers create opportunities to improve materials from renewable resources, supporting global sustainability.[6] Natural wood fibers in the form of flour, sawdust, and chips are available as waste streams from sawmills and furniture factories. In plastics industries, they have been primarily used as inexpensive reinforcement to enhance the modulus of several thermoplastics, and as fillers substituting for more costly raw materials. There have been numerous studies on producing thermoplastic composites with plant fibers, plant flour, or wood flour including eastern red cedar,[7] flax,[8] maple,[9] oak,[7] pine,[10] and rubberwood.[11] In addition, the increasing global production and consumption of plastics significantly contributes to municipal solid waste.[12] In 2008, at least 33.6 million tons of postconsumer plastics were generated in the United States, of which 85.8% went to landfills, 7.7% to combustion and energy recovery, and only 6.5% to recycling[13,14]—only a tiny fraction of plastic wastes are recycled. Effective and safe disposal has also become a serious public concern.[15] However, plastic wastes could be used as raw materials for wood–plastic composites (WPCs).[16] Increasing the opportunities to use plastic wastes has motivated the current study. The WPCs produced from recycled plastic would not only provide effective and safe disposal of plastic wastes but also the consumption of energy and natural resources would be reduced.[13,17] There are potential benefits on both environment and economics in recycling combinations of wood and plastic wastes.[10,15]

Rubberwood (*Hevea brasiliensis*) is used in large amounts by sawmills and furniture industry in southern Thailand, and these produce large quantities of waste in the forms of sawdust and wood chips. In these industries only 10% of the rubberwood ends up in the products, while the rest is wood waste about 36% and small branches about 54%.[18] Most of the wood wastes are used to produce medium-density fiberboard and particleboard.[19] However, the utilization of wood waste as reinforcement in plastic composites is great interest, with both environmental and economic benefits. Wood as reinforcement of plastic composites has many advantages over synthetic fillers,[20] but its hydrophilic nature is a disadvantage that impacts the performance of the WPCs.[12,21] The end-use applications of WPCs such as dimensional stability were limited by the amount of water absorption (WA).[2] This varies by the wood species, partly because they have different contents of cellulose, lignin, hemicellulose, and extractants.[22] Hence, the effects of filler (rubberwood flour; RWF) and grade of plastic (virgin or recycled) on the composite properties

need to be characterized. The objective of this work was to determine the effects of material compositions (including different grades of plastic; and contents of RWF, coupling agent, and ultraviolet (UV) stabilizer) on the long-term WA, and the resulting thickness swelling (TS), and degradation of flexural properties, of RWF-reinforced polypropylene (PP) composites. Data created from this work would help better understanding of properties of such samples so that developed products can be used for most suitable applications in the form of value-added material.

Materials

RWF supplied by a local furniture factory (Songkhla, Thailand) was used as reinforcement. The main chemical constituents were cellulose (39%), hemicellulose (29%), lignin (28%), and ash (4%).[18] The wood flour was screened through a standard sieve of mesh size 80 (passing particles smaller than 180 μm) and was dried in an oven at 110°C for 8 h before compounding. Recycled polypropylene (rPP) pellets, WT170 with a melt flow index of 11 g/10 min at 230°C, were supplied by Withaya Intertrade Co. Ltd (Samutprakarn, Thailand). Virgin polypropylene (vPP) granules, HIPOL J600 with a melt flow index of 7 g/10 min at 230°C, were procured from Mitsui Petrochemical Industries Co. Ltd (Tokyo, Japan). The coupling agent used was maleic anhydride-grafted polypropylene (MAPP), supplied by Sigma-Aldrich (St Louis, Missouri, USA), with 8–10% of maleic anhydride. Hindered amine light stabilizer additive, chosen as the UV stabilizer, was supplied by TH Color Co. Ltd (Samutprakarn, Thailand) under the trade name MEUV008. A paraffin wax lubricant (Lub) was purchased from Nippon Seiro Co. Ltd (Yamaguchi, Japan).

Manufacturing of the samples and testing

WPCs were manufactured in a two-stage process. In the first stage, to produce WPC pellets RWF and PP were mixed and pelletized using a twin-screw extruder (Model SHJ-36 from En Mach Co. Ltd, Nonthaburi, Thailand). Barrel temperatures of the 10 zones were controlled at 130–170°C from feeding to die zones, to reduce degradation of the compositions, while the screw rotation speed was controlled at 70 r min^{-1}. In the second stage, to produce WPC panels, the WPC pellets were carefully dried prior to use, in an oven at 110°C for 8 h. The WPC pellets, MAPP, UV stabilizer, and Lub (formulations in Table 1) were then dry mixed and added into the feeder of a twin-screw extruder. The extruding conditions were as follows: (1) temperature profiles: 130–190°C; (2) screw rotating speed: 50 r min^{-1}; (3) vacuum venting at 9 temperature zones: 0.022 MPa; and (4) melt pressure: 0.10–0.20 MPa depending on wood flour content. The samples were extruded through a rectangular die with the dimensions of 9 × 22 mm^2 and cooled in ambient air. After cooling, the specimens were cut according to ASTM standard for physical and mechanical testing.

Density. All samples were oven dried at 50°C for 24 h. After oven drying, the samples were cooled in a desiccator containing calcium chloride and then weighed (a precision of 0.001 g).

Table 1. Wood–plastic composite formulations (percent by weight).

Composite sample code[a]	rPP	vPP	RWF	MAPP	UV	Lub	Density (g cm^{-3})
rP100	100						0.886 (0.065)[b]
vP100		100					0.816 (0.092)
rP70R25M3U1	70		25	3	1	1	0.986 (0.070)
vP70R25M3U1		70	25	3	1	1	0.953 (0.069)
rP60R35M3U0.5	60.3		35.3	3	0.5	1	1.015 (0.036)
vP60R35M3U0.5		60.3	35.3	3	0.5	1	0.985 (0.063)
rP50R45M3U1	50		45	3	1	1	1.085 (0.033)
vP50R45M3U1		50	45	3	1	1	1.009 (0.060)
rP68R25M5U1	68		25	5	1	1	0.972 (0.089)
rP69R25M5U0	69		25	5	0	1	0.914 (0.072)

rPP: recycled polypropylene; vPP: virgin polypropylene; RWF: rubberwood flour; MAPP: maleic anhydride-grafted polypropylene; UV: ultraviolet; lub: lubricant.

[a]The sample codes summarize the formulation, as in rP70R25M3U1 having 70 wt% rPP, 25 wt% RWF, 3 wt% MAPP, and 1 wt% UV.

[b]The values in parentheses are standard deviations from five replications.

After that, the dimensions of the composite samples were measured using a digital vernier caliper (a precision of 0.01 mm) and the volume calculated. The full dry density (δ_0) of PP/RWF composites was computed using:

$$\delta_0(\text{g cm}^{-3}) = \frac{M_o}{V_o} \tag{1}$$

where M_0 is the full dry weight (in grams) and V_o is the volume (in cubic centimeter) of the composite.

Water absorption and dimensional stability. WA tests were carried out according to ASTM D570-88 specifications. Specimens (4.8 × 13 × 26 mm^3) were cut from the extruded panels and used to measure the WA and TS. Five specimens of each formulation were dried in an oven at 50°C for 24 h. The weight and thickness of dried specimens were measured to a precision of 0.001 g and 0.01 mm, respectively. The specimens were then immersed in water at ambient room temperature. After 1 week, soaked specimens were removed from the water, thoroughly dried with tissue papers, and immediately weighed and measured to determine the weight and thickness. Then, the specimens were immersed in water again and stored at ambient room temperature for 10 weeks, during which time the measurements were repeated at 1-week interval. The percentage of WA can be calculated using:

$$WA_t(\%) = \frac{W_t - W_0}{W_0} \times 100 \tag{2}$$

where WA_t is the WA at time t, W_0 is the initial dry weight, and W_t is the soaked weight of specimen at a given time t.

The percentage of TS was calculated using:

$$TS_t(\%) = \frac{T_t - T_0}{T_0} \times 100 \tag{3}$$

where TS_t is the TS at any time t, T_0 is the initial dry thickness, and T_t is the soaked thickness of specimen at a given time t.

Flexure testing. Three-point flexure test was carried out on an Instron universal testing machine (model 5582; Instron Corporation, Norwood, Massachusetts, USA) at a cross-head speed of 2 mm min^{-1} with nominal dimensions of 4.8 × 13 × 100 mm^3, a span of 80 mm in accordance with ASTM D790-92 standards. The testing was performed at ambient room temperature of 25°C with 5 samples in each formulation to obtain an average value. From flexural strength test, the modulus of rupture (MOR) can be calculated using:

$$MOR\ (\text{MPa}) = \frac{3P_{max}L}{2bd^2} \tag{4}$$

where P_{max} is the maximum load (in newton), L is the span (in millimeter), b is the width of the specimen (in millimeter), and d is the thickness of the specimen (in millimeter).

The modulus of elasticity (MOE) can also be calculated using:

$$MOE\ (\text{MPa}) = \frac{P_{pl}L^3}{4\delta_{pl}bd^3} \tag{5}$$

where L is the span (in millimeter), P_{pl} is the incremental load (in newton), δ_{pl} is the incremental bending distance (in millimeter) in the range where the relation is linear, b is the width of the specimen (in millimeter), and d is the thickness of the specimen (in millimeter).

The measurements of flexural strength and modulus were repeated at 1-week interval, for otherwise continuously soaked samples. The degradation of the flexural properties was determined for a total of 6 weeks, at which time the samples were water saturated and no longer absorbing.

Morphological analysis

Morphological analysis of the samples was carried out using a scanning electron microscope (SEM) to assess the interfacial adhesion and phase dispersion of wood flour in the polymeric matrix. SEM imaging was carried out with an FEI Quanta 400 microscope (FEI Company, Hillsboro, Oregon, USA) at an accelerating voltage of 20 kV. Prior to SEM observations, all samples were sputter coated with gold to prevent electrical charging during the imaging. Specimens were imaged at magnifications of 150× and 1000×.

Statistical analysis

The effects of WA on the bending properties of RWF-reinforced PP composites were evaluated by analysis of variance (ANOVA) and Tukey's multiple comparison test. The ANOVA revealed significant differences between WA amounts and degradation of flexural properties in each week, whereas comparison of the mean values was carried out with Tukey's multiple comparison tests. Results, such as mean and standard deviations from five samples of each test, were statistically analyzed. All the statistical analyses used a 5% significance level ($\alpha = 0.05$).

Results and discussion

Density of WPCs

Densities of the WPCs at various mix ratios and different plastic grades are shown in Figure 1. The density of the composites ranges from 0.816 g cm^{-3} for the entirely vPP panel to 1.085 g cm^{-3} for the 45 wt% rubberwood-rPP composite panels with 3 wt% MAPP. The density of WPC increased linearly with the wood fiber loading; the R^2 values of linear fits are 0.992 and 0.943 for vPP and rPP composites, respectively. The density of produced WPCs is over 0.8 g cm^{-3}, which can be compared with high-density fiberboard (0.8–1.040 g cm^{-3}). These are high-density boards that could be of interest as structure materials, among other applications. Generally, the bulk density of most wood species is in the range of 0.32–0.72 g cm^{-3}. Wood with density exceeding 0.8 g cm^{-3} is considered high density wood.[23] Furthermore, the WPCs from rPP had higher densities than those from vPP at all mix ratios, although both types of PP gave a similar trend for the density increase with wood flour loading. The effect of UV stabilizer was to increase the density of PP/RWF composites, at 1 wt% addition level. This is probably because the UV stabilizer has higher density than the rPP.

Long-term WA behavior

The long-term WA of the PP/RWF composites was monitored by full water immersion over a period of 10 weeks as shown in Figure 2. Composites made from vPP and rPP with 45 wt% RWF absorbed the most water, having moisture ratios of 9.80 and 10.33% (relative to solids by weight), respectively, after 10 weeks. Generally, the WA increased with wood flour content[24] because of an increase of free OH groups with wood cellulose content. These free OH groups interact with polar water molecules, leading to the weight gain of the composites.[12] During immersion, the wood flour absorbed a significant quantity of water, while the plastics absorbed very little.[12] With the same wood flour contents up to 35%, the composites based on vPP and rPP had very similar WA. However, at 45 wt% RWF, the two types of plastics seemed to give different absorption behavior. This may be due to better encapsulation of wood flour into vPP, with good dispersion and strong interfacial bonding between wood particles and polymer, and consequently slower WA. Theoretically, the penetration of moisture into WPCs takes place by three different mechanisms. These are capillary transport of

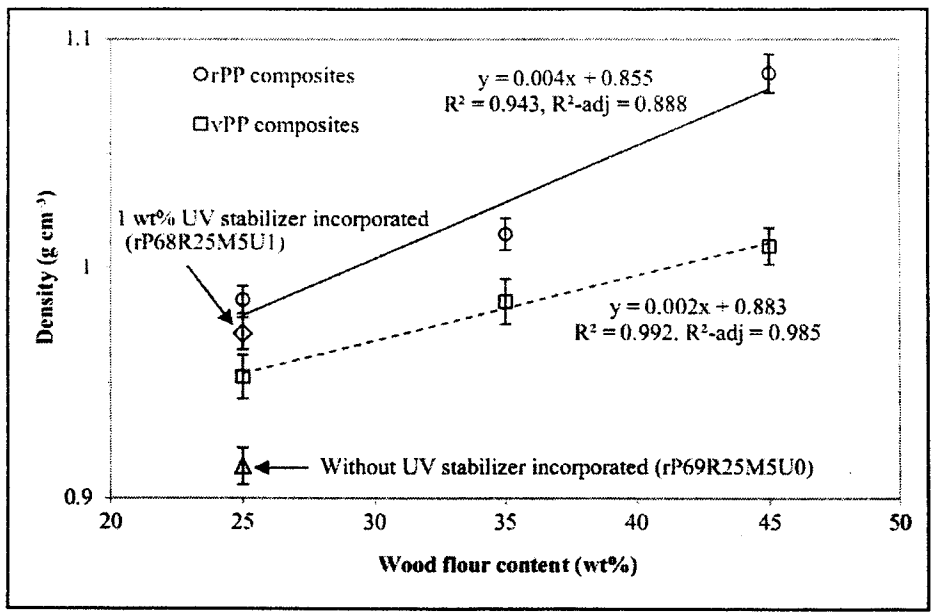

Figure 1. Averages of density as a function of wood flour loading, for the PP-RWF composites.
PP: polypropylene; RWF: rubberwood flour.

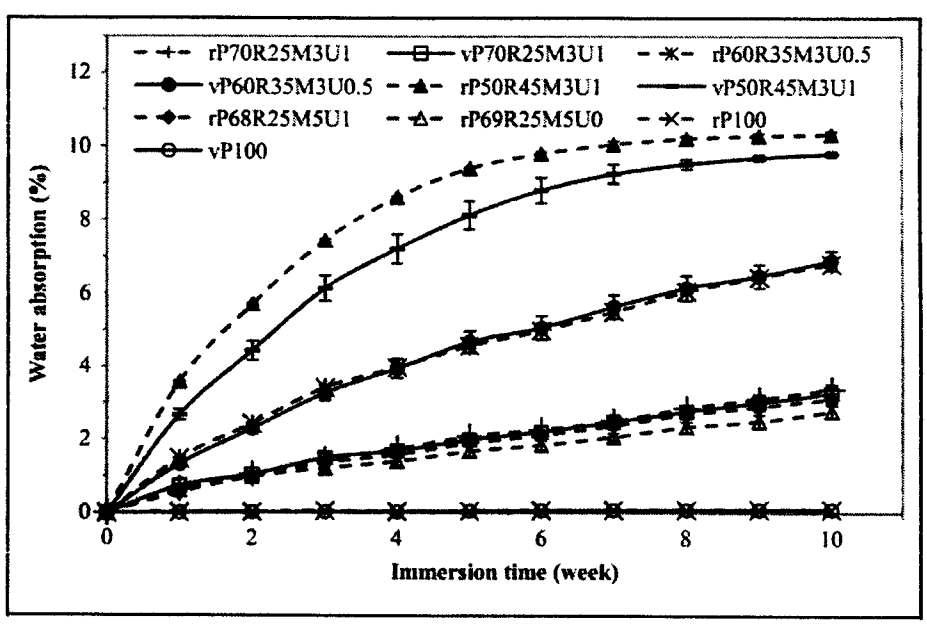

Figure 2. Effect of composition contents and plastic grades on long-term water absorption for PP-RWF composites.
PP: polypropylene; RWF: rubberwood flour.

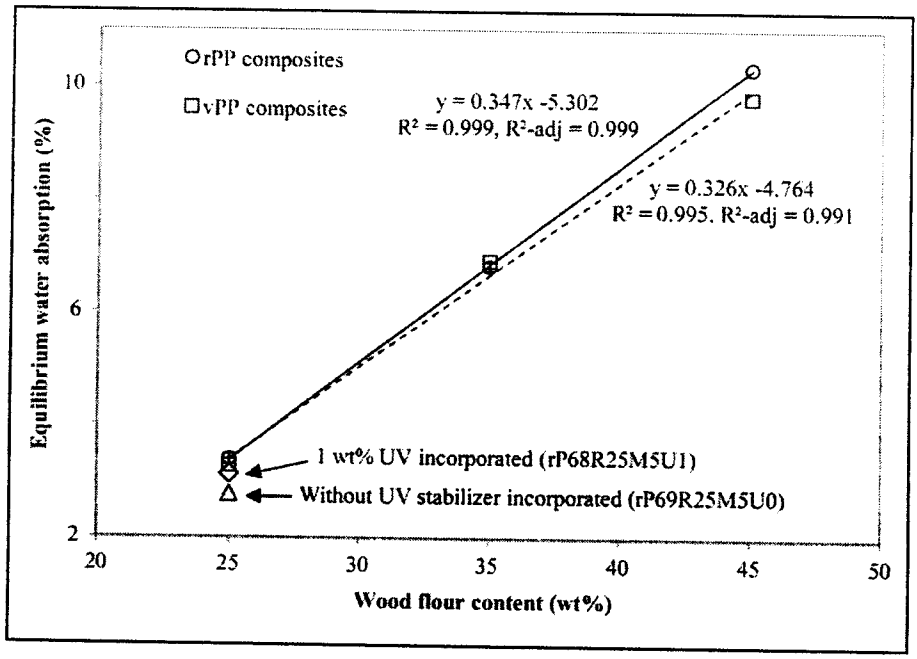

Figure 3. Averages of equilibrium water absorption is a practically linear function of wood flour loading, for the PP-RWF composites.
PP: polypropylene; RWF: rubberwood flour.

water in the pores, and flows at the interfaces between polymer and fibers, due to poor wettability and impregnation. The last mechanism is the diffusion of water molecules in the microgaps between polymer chains and transport by microcracks in the matrix.[25,26]

The effects of MAPP and UV stabilizer contents on the WA are also shown in Figure 2. MAPP addition of 5 wt% in rPP/RWF composites containing 25 wt% RWF (case rP68R25M5U1) gave a lower WA (not statistically significant) than the addition of 3 wt% MAPP (case rP70R25M3U1). Similar results have been reported by Adhikary et al.[12] that the coupling agent can increase adhesion in WPCs by improving compatibility between the wood particles and the polymer. Then, the plastic can cover more of the wood surfaces, resulting in lower WA. Furthermore, adding 1 wt% UV stabilizer (case rP68R25M5U1) increased the equilibrium moisture content (EMC) from 2.78 to 3.13% without UV stabilizer (case rP69R25M5U0), as shown in Figure 3. This may be attributed to the nonuniform spatial distribution of wood flour, polymer, and UV stabilizer,[19,27] which results in higher WA. In Figure 3, the linear correlation between EMC and wood flour content was high, for both vPP and rPP composites (R^2 = 0.995 and 0.999, respectively). However, the composite board density and EMC were less well correlated, with the R^2 value being 0.781. The WA behavior is complex and can be influenced by several factors, for example, wood content, virgin or recycled plastics, UV stabilizer, and coupling agent.

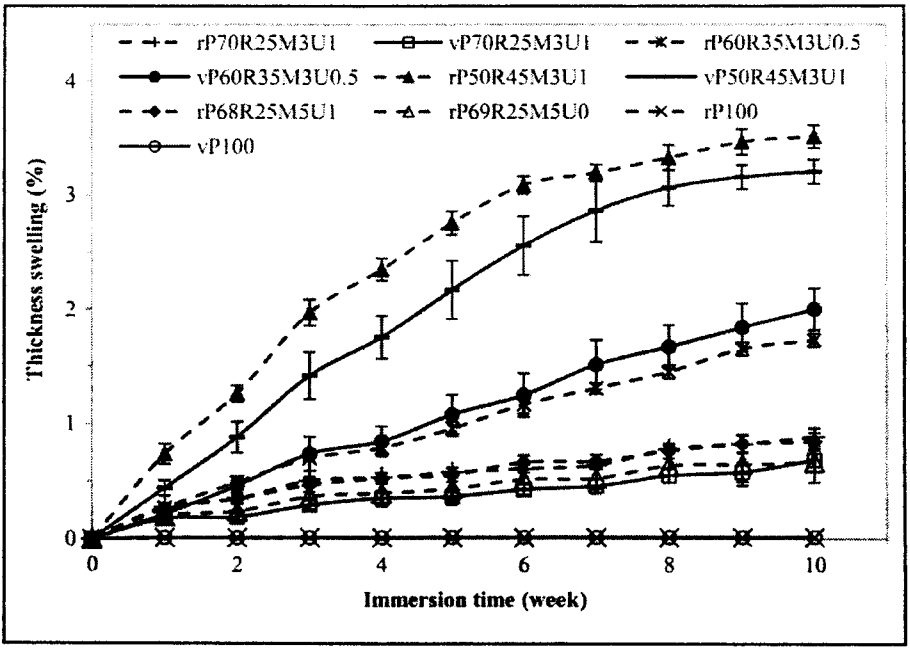

Figure 4. Thickness swelling as function of water immersion time for PP-RWF composites. Solid lines show virgin polymer and dashed lines represent recycled polymer.
PP: polypropylene; RWF: rubberwood flour.

Long-term TS behavior

The TS of vPP and rPP composites with various contents of RWF are represented in Figure 4. The TS of virgin and recycled composites was the highest with 45 wt% RWF at 3.20 and 3.51%, respectively, corresponding also to the highest WA. However, the rPP composites containing 45 wt% RWF had more TS than the vPP composites. These results can be compared with the scanning electron micrographs of PP composites with 45 wt% RWF in Figure 5 (Figure 5(a) and (b) for vPP and Figure 5(c) and (d) for rPP). Irregular short fibers were spread in the plastic matrix. The rPP composites showed less homogenous morphological structure, poorer dispersion of the fibers in the matrix, and weaker interfacial bonding between the wood flour and the polymer matrix than the vPP composites. Therefore, the rPP composites allow easier access of water to the cellulose.[12] With a similar trend to the WA, the TS of rPP/RWF composites increased with wood flour content and immersion time until saturation at equilibrium. For example, the rPP composites containing 25, 35, and 45 wt% RWF with addition of 3 wt% MAPP displayed equilibrium TS (ETS) values of 0.89, 1.73, and 3.51%, respectively. Likewise, the equilibrium TS of vPP composites with 25, 35, and 45 wt% RWF were 0.69, 2.0, and 3.20%, respectively, which have the same trends and qualitative as the rPP composites.

The effects of MAPP and UV stabilizer contents on the TS of WPCs are also shown in Figure 4. As can be seen, the rPP/RWF composites with 3 wt% MAPP (case rP70R25M3U1) yielded the same TS as the composites with 5 wt% MAPP (case

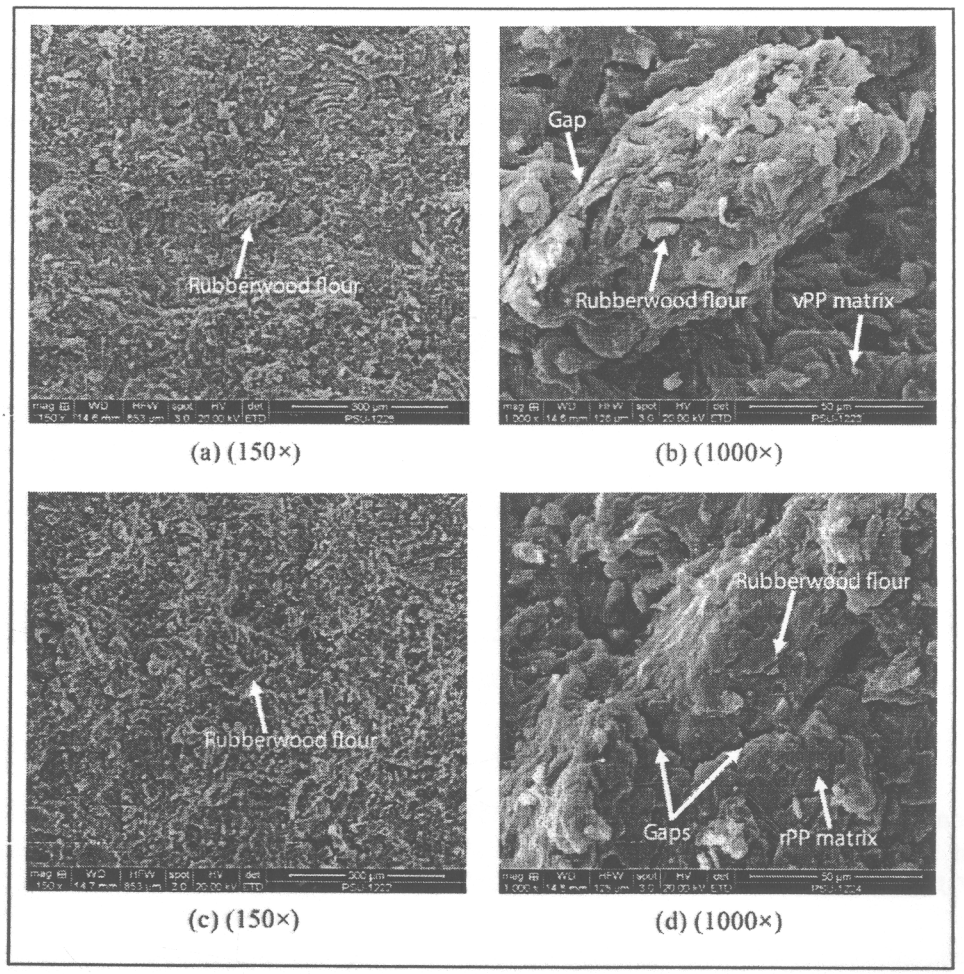

Figure 5. Scanning electron micrographs of 45 wt% RWF composites based on (a and b) virgin polypropylene and (c and d) recycled polypropylene. Magnifications of 150 × and 1000 × from left to right.
RWF: rubberwood flour.

rP68R25M5U1) and had similar trend with WA. In 3–5 wt% range, changes in MAPP content had no effect on the WA and TS of rPP/RWF composites, so using MAPP in excess of 3 wt% may be unnecessary. However, at the same wood flour content, the WA and TS significantly decreased with addition of 3–5 wt% coupling agent to the composites, compared with the composites without MAPP.[12,26] As the coupling agent improves the interfacial adhesion between wood flour and polymer matrix, the penetration of moisture into WPCs is limited.[28] In addition, the change in the TS with different UV stabilizer concentrations was similar to that found in the WA. The composites with 25 wt% RWF showed an insignificant increase in ETS with an increase in UV stabilizer from 0 wt% (case rP69R25M5U0) to 1 wt% (case

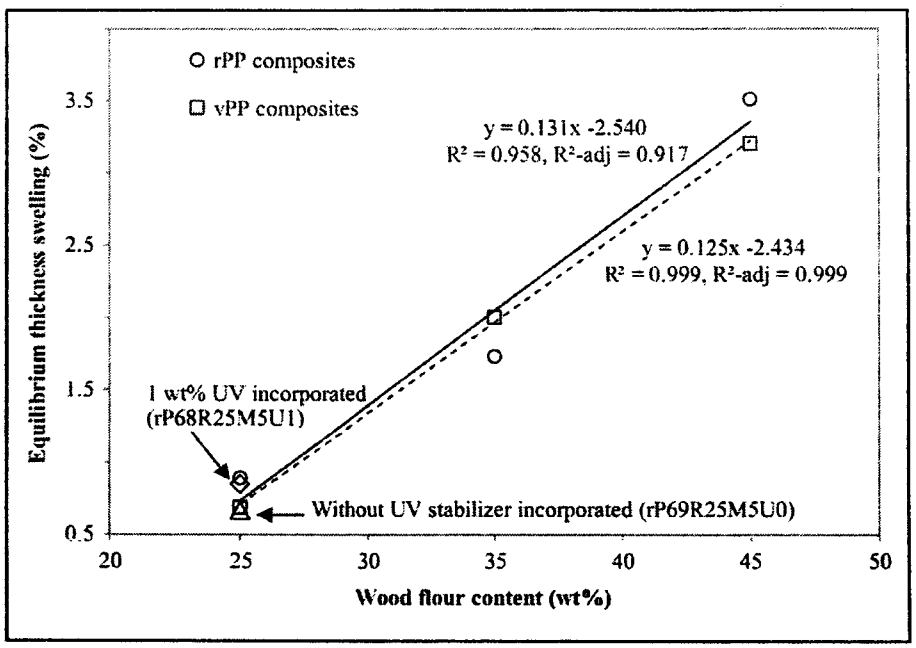

Figure 6. Averages of equilibrium thickness swelling of the PP-RWF composites as a function of wood flour loadings.
PP: polypropylene; RWF: rubberwood flour.

rP68R25M5U1), as shown in Figure 6. The mechanisms causing this phenomenon were discussed earlier in relation to WA. Using 1 wt% of UV stabilizer may be unnecessary and to reduce the negative effects on the TS and WA, the amount of UV stabilizer should be minimized.

The relationships between ETS and wood flour content of the vPP and rPP composites are also shown in Figure 6, with strong linear correlations (R^2 = 0.999 and 0.958, respectively). When the wood flour content in the composites is increased, the number of free OH groups contributed by wood cellulose is also increased. Therefore, the WA increased, resulting in increased TS.[2,12,29] The relationship between the ETS and EMC of the PP/RWF composites is also linear with an R^2 value of 0.997. The empirical equation obtained from the linear correlation between ETS and equilibrium WA (EMC) was:

$$\text{ETS}(\%) = 0.334\text{EMC}(\%) - 0.208 \quad \text{for EMC} > 0.63\% \tag{6}$$

Since the ETS should be positive value, the minimum EMC should be greater than 0.63%.

Degradation in mechanical properties

The flexural properties are important for decision making on WPC applications. The degradation of flexural strength and modulus of the composites, with vPP or rPP and

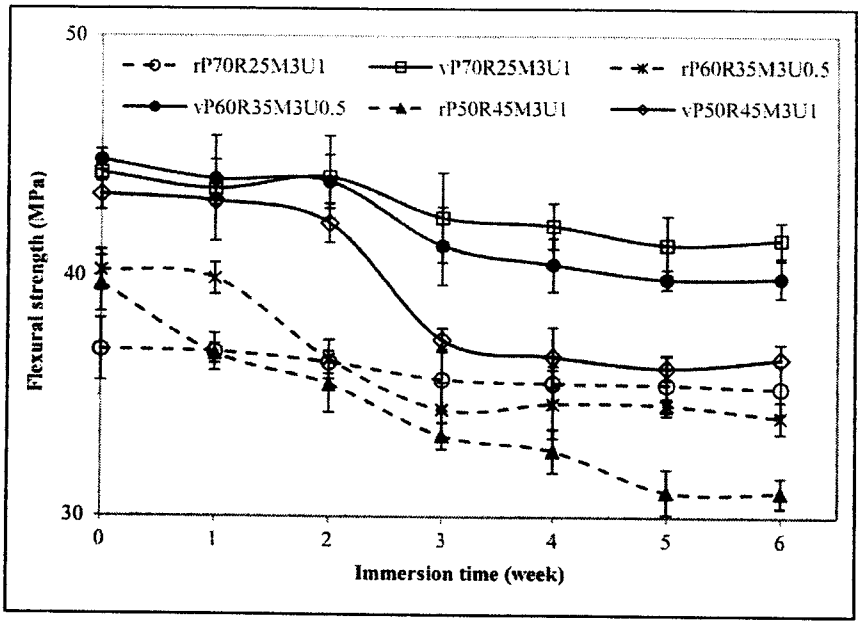

Figure 7. Effect of water immersion time on flexural strength of virgin (solid lines) and recycled (dashed lines) PP composites containing different RWF loadings.
PP: polypropylene; RWF: rubberwood flour.

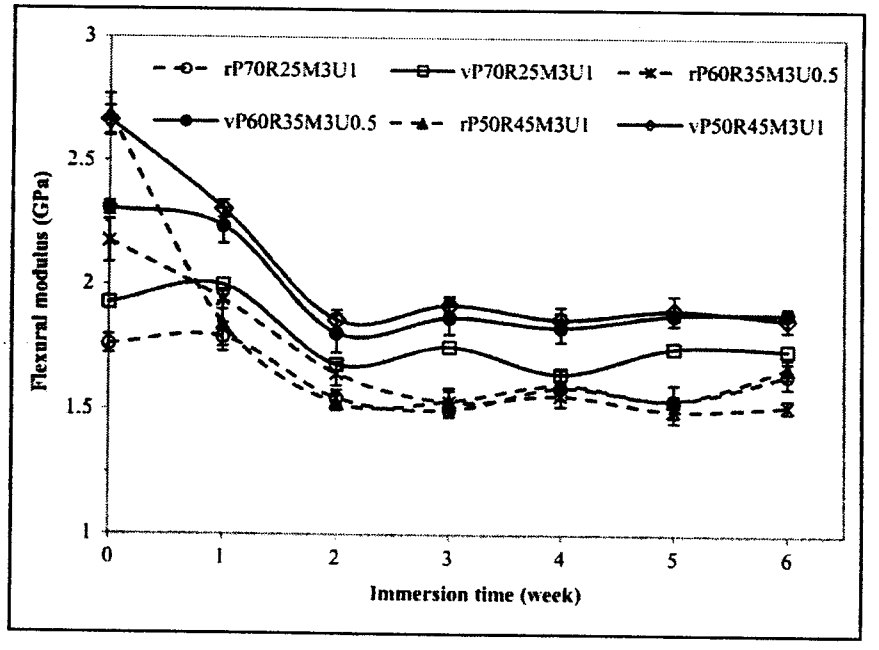

Figure 8. Effect of water immersion time on flexural modulus of virgin and recycled PP composites containing different RWF loadings.
PP: polypropylene; RWF: rubberwood flour.

different amounts of RWF, are shown in Figures 7 and 8. Both the flexural strength and modulus of vPP or rPP/RWF composites decreased with immersion time and moisture uptake. Moreover, the composites with high wood flour contents lost flexural properties sharply. The water molecules reduced the strength of interfacial adhesion between RWF and PP.[2] When water molecules infiltrate into the composite, the wood flour tends to swell resulting in localized yielding of the polymer matrix and loss of adhesion between the wood flour and matrix.[2,30] The flexural modulus also significantly decreased rather than the strength. In fact, wood flour has hard filler in comparison with the plastic matrix increased the stiffness of the composites. Wood flour plasticizes when wet becoming ductile decreasing the stiffness of composites.[30] These qualitative observations were assessed for statistical validity by analysis of variance (ANOVA). According to one-way ANOVA of data as shown in Tables 2 and 3, the WA does not significantly affect the flexural strength of vPP or rPP composites containing 25 wt% RWF. In contrast, with 35 and 45 wt% RWF, the flexural strength is significantly affected by WA. Initially for up to 2 weeks, the flexural strength decreased only slightly (not significant), but after 2 weeks it decreased significantly and then stabilized. The flexural strength depends on crack formation or fracture mechanism of the composites. When WPCs are soaked in water, the wood flour absorbs water and swells, while PP hardly absorbs water or swells.[30] Hence, the swelling of wood flour mainly causes microcracks and reduces adhesion of wood particles to the plastic matrix. However, the initial WA (for up to 2 weeks) is only around 1–3%, and the swelling of wood flour is not sufficient to generate microcracks[30]; in the current study, <3% absorption did not significantly affect flexural strength. Tukey's test values shown in Table 3 also indicates that, for vPP composites with 45 wt% RWF (case vP50R45M3U1), for up to 2 weeks, the decrease in flexural strength was not significant (indicated as footnote "[a]" in Table 3), but these initial flexural strengths were significantly higher than those at 3–6 weeks (indicated as footnote "[b]" in Table 3). Besides, an increase in maximum strain of the vPP or rPP composites with different amounts of RWF is also shown in Figure 9. The maximum strain increased significantly with immersion time and WA: the initial increase was rapid and then stabilized after 2 weeks. The reason for this phenomenon is probably similar as described earlier. When wood flour wets, it plasticizes and becomes ductile,[30] and this increases the maximum strain. The composites with high wood flour contents had sharper increases in the maximum strain because of this. The composites based on vPP had higher maximum strains than those based on rPP at equal wood contents. vPP being stiffer than rPP may be the reason for this. The molecular weight of recycled plastic decreases with repeated recycling. Short chains have more chain ends per mass than long chains, and these ends act as crystal defects that initiate failure during flexural loading, at comparatively lower elongation.[31]

Conclusions

WPCs were prepared from RWF and rPP or vPP. The density of WPCs increased linearly with wood flour content because these natural fibers have a higher density than the polymer matrix. Long-term WA and TS behavior of vPP or rPP/RWF were experimentally observed. Both WA and TS increased with wood flour content because wood cellulose absorbs water, while the plastic matrix in the composites does not. At 45 wt%

Table 2. Effect of moisture content on flexural properties of the rPP-RWF composites.

	rP70R25M3U1				rP60R35M3U0.5				rP50R45M3U1			
Time (weeks)	WA (%)	MOR (MPa)	MOE (GPa)	Maximum ε (%)	WA (%)	MOR (MPa)	MOE (GPa)	Maximum ε (%)	WA (%)	MOR (MPa)	MOE (GPa)	Maximum ε (%)
0	0	36.9^{a}	$1.76^{a,b}$	3.09^{a}	0	40.2^{a}	2.18^{a}	2.79^{a}	0	39.7^{a}	2.69^{a}	2.07^{a}
1	0.67^{a}	36.9^{a}	1.79^{a}	$3.38^{a,b}$	1.48^{a}	39.9^{a}	1.94^{b}	$3.15^{b,c}$	3.58^{a}	$36.8^{a,b}$	1.84^{b}	3.07^{b}
2	1.06^{b}	36.4^{a}	$1.55^{b,c}$	$3.76^{a,b,c}$	2.44^{b}	$36.6^{a,b}$	1.64^{c}	$3.82^{a,b}$	5.71^{b}	35.5^{b}	1.53^{c}	3.45^{c}
3	1.46^{c}	35.7^{a}	1.50^{c}	4.30^{c}	3.43^{c}	34.5^{b}	1.53^{c}	$4.00^{b,c}$	7.46^{c}	$33.4^{b,c}$	1.53^{c}	$3.60^{b,c}$
4	1.76^{d}	35.6^{a}	$1.59^{a,b,c}$	$4.26^{b,c}$	$3.98^{c,d}$	34.7^{b}	1.56^{c}	$4.07^{b,c}$	$8.63^{c,d}$	$32.8^{b,c}$	$1.60^{b,c}$	$3.60^{b,c}$
5	2.10^{e}	35.5^{a}	$1.54^{b,c}$	4.31^{c}	$4.58^{d,e}$	34.7^{b}	1.50^{c}	4.29^{c}	9.41^{d}	31.1^{c}	1.54^{c}	3.51^{bc}
6	2.28^{f}	35.4^{a}	$1.64^{a,b,c}$	$4.15^{a,b,c}$	5.00^{e}	34.2^{b}	1.52^{c}	$4.14^{b,c}$	9.80^{d}	31.0^{c}	$1.67^{b,c}$	$3.46^{b,c}$
p Value	0.000	0.879	0.001	0.000	0.000	0.000	0.000	0.000	0.000	0.000	0.000	0.000

Note: Means within each column with the same letter are not significantly different (Tukey's test, $\alpha = 0.05$).

rPP: recycled polypropylene; RWF: rubberwood flour; WA: water absorption; MOR: modulus of rupture; MOE: modulus of elasticity; maximum ε: maximum strain.

Table 3. Effect of moisture content on flexural properties of the vPP-RWF composites.

	vP70R25M3U1				vP60R35M3U0.5				vP50R45M3U1			
Time (weeks)	WA (%)	MOR (MPa)	MOE (GPa)	Maximum ε (%)	WA (%)	MOR (MPa)	MOE (GPa)	Maximum ε (%)	WA (%)	MOR (MPa)	MOE (GPa)	Maximum ε (%)
0	0	44.3^{a}	1.93^{a}	3.99^{a}	0	44.8^{a}	2.31^{a}	3.23^{a}	0	43.4^{a}	2.66^{a}	2.36^{a}
1	0.74^{a}	43.7^{a}	2.00^{a}	$4.18^{a,b}$	1.33^{a}	$44.1^{a,b}$	2.24^{a}	3.72^{a}	2.67^{a}	43.1^{a}	2.31^{b}	3.42^{b}
2	1.05^{a}	44.1^{a}	1.68^{b}	$4.66^{a,b,c}$	2.30^{b}	$44.0^{a,b,c}$	1.81^{b}	4.44^{b}	4.44^{b}	42.2^{a}	1.86^{c}	4.00^{c}
3	1.51^{b}	42.4^{a}	$1.75^{b,c}$	$4.86^{b,c}$	3.28^{c}	$41.3^{a,b,c}$	1.87^{b}	4.56^{b}	6.15^{c}	37.4^{b}	1.92^{c}	3.92^{c}
4	$1.70^{b,c}$	42.1^{a}	1.64^{b}	5.16^{c}	$3.96^{c,d}$	$40.5^{b,c}$	1.83^{b}	4.60^{b}	$7.23^{c,d}$	36.7^{b}	1.86^{c}	$3.90^{b,c}$
5	$2.01^{c,d}$	41.3^{a}	$1.75^{b,c}$	4.99^{c}	$4.69^{d,e}$	39.9^{c}	1.88^{b}	4.59^{b}	$8.15^{d,e}$	36.2^{b}	1.90^{c}	$3.77^{b,c}$
6	2.22^{d}	41.5^{a}	$1.74^{b,c}$	5.20^{c}	5.07^{e}	$39.9^{b,c}$	1.89^{b}	4.46^{b}	8.82^{e}	36.6^{b}	1.87^{c}	$3.87^{b,c}$
p Value	0.000	0.050	0.001	0.000	0.000	0.001	0.000	0.000	0.000	0.000	0.000	0.000

Note: Means within each column with the same letter are not significantly different (Tukey's test, $\alpha = 0.05$).

vPP: virgin polypropylene; RWF: rubberwood flour; WA: water absorption; MOR: modulus of rupture; MOE: modulus of elasticity; maximum ε: maximum strain.

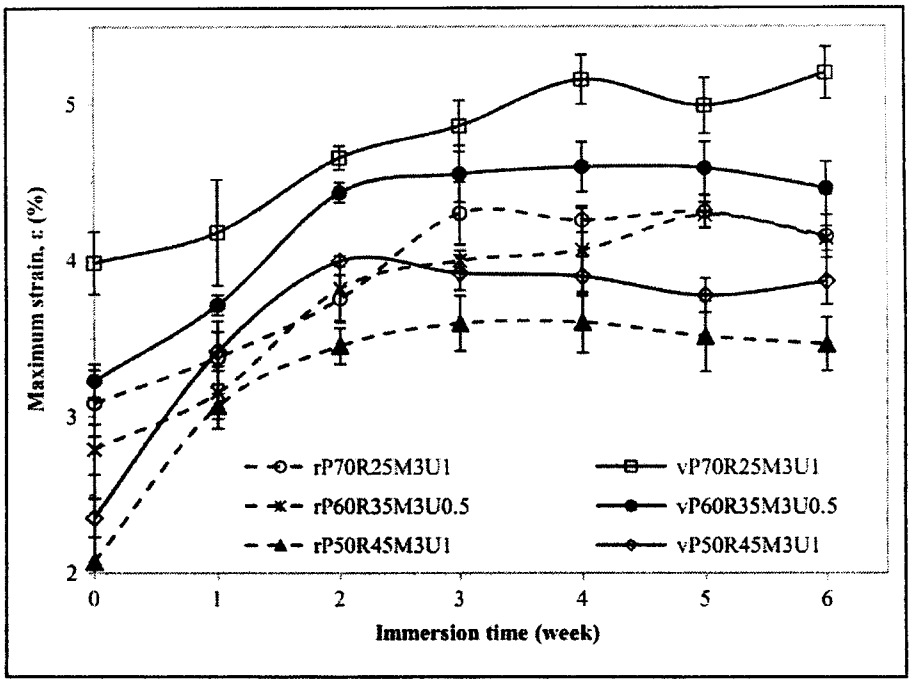

Figure 9. Effect of water immersion time on maximum strain of virgin and recycled PP composites containing different RWF loadings.
PP: polypropylene; RWF: rubberwood flour.

RWF, the rPP composites had initially higher WA and TS than the vPP composites; however, after 6 weeks of immersion the vPP and rPP composites had closely similar saturation values. The initially different absorption rate between the two types of plastic was attributed to poorer encapsulation of wood flour into the rPP matrix, with poor dispersion and weak interfacial adhesion. The coupling agent MAPP at 3 wt% reduced WA and TS, with no further benefit, reached at 5 wt% MAPP using more than 3 wt% MAPP may be unnecessary and uneconomical. The WA and TS of composites were increased by an addition of 1 wt% UV stabilizer. These negative effects of the UV stabilizer on the WA and TS of the composites should be minimized, by minimal use of the stabilizer. The flexural strength and modulus of composites decreased significantly with moisture uptake; however, at WA <3%, its effects on flexural strength were not significant. The composites with high wood flour loadings suffered a sharp decrease in the flexural properties with absorption of water, which reduced the interfacial adhesion between wood flour and plastic matrix. The maximum strain of composites significantly increased with absorption due to the water plasticizing wood particles.

Acknowledgements

The authors thank the Rubberwood Technology and Management Research Group (ENG-54-27-11-0137-S) of Faculty of Engineering, Prince of Songkla University, Thailand. The

authors would also thank the Research and Development Office and Associate Prof. Dr Seppo Karrila for editing this article.

Funding

The authors would like to express their thanks to the Prince of Songkla Graduate Studies Grant, the Government budget Fund (Research Grant Code: 2555A11502062) for financial support throughout this work.

References

1. Kaymakci A, Ayrilmis N, Ozdemir F, et al. Utilization of sunflower stalk in manufacture of thermoplastic composite. *J Polym Environ* 2013; 21: 1135–1142.
2. Law TT and Ishak ZAM. Water absorption and dimensional stability of short kenaf fiber-filled polypropylene composites treated with maleated polypropylene. *J Appl Polym Sci* 2011; 120(1): 563–572.
3. Mirzaei B, Tajvidi M, Falk RH, et al. Stress-relaxation behavior of lignocellulosic high-density polyethylene composites. *J Reinf Plast Compos* 2011; 30(10): 875–881.
4. Ashori A and Nourbakhsh A. Performance properties of microcrystalline cellulose as a reinforcing agent in wood plastic composites. *Compos B: Eng* 2010; 41(7): 578–581.
5. Liu W, Drzal LT, Mohanty AK, et al. Influence of processing methods and fiber length on physical properties of kenaf fiber reinforced soy based biocomposites. *Compos B: Eng* 2007; 38(3): 352–359.
6. Cheung HY, Ho MP, Lau KT, et al. Natural fibre-reinforced composites for bioengineering and environmental engineering applications. *Compos B: Eng* 2009; 40(7): 655–663.
7. Kim JW, Harper DP and Taylor AM. Effect of wood species on the mechanical and thermal properties of wood-plastic composites. *J Appl Polym Sci* 2009; 112(3): 1378–1385.
8. Barkoula NM, Garkhail SK and Peijs T. Effect of compounding and injection molding on the mechanical properties of flax fiber polypropylene composites. *J Reinf Plast Compos* 2010; 29(9): 1366–1385.
9. Li T and Yan N. Mechanical properties of wood flour/HDPE/ionomer composites. *Compos A: Appl Sci Manufac* 2007; 38(1): 1–12.
10. Adhikary KB, Pang S and Staiger MP. Dimensional stability and mechanical behaviour of wood-plastic composites based recycled and virgin high-density polyethylene (HDPE). *Compos B: Eng* 2008; 39(5): 807–815.
11. Homkhiew C, Ratanawilai T and Thongruang W. Effect of wood flour content and cooling rate on properties of rubberwood flour/recycled polypropylene composites. *Adv Mater Res* 2012; 488–489: 495–500.
12. Adhikary KB, Pang S and Staiger MP. Long-term moisture absorption and thickness swelling behaviour of recycled thermoplastics reinforced with pinus radiata sawdust. *Chem eng J* 2008; 142(2): 190–198.
13. Ratanawilai T, Thanawattanasirikul N and Homkhiew C. Mechanical and thermal properties of oil palm wood sawdust reinforced post-consumer polyethylene composites. *ScienceAsia* 2012; 38(3): 289–294.
14. Themelis NJ, Castaldi MJ, Bhatti J, et al. Energy and economic value of nonrecycled plastics (NRP) and municipal solid wastes (MSW) that are currently landfilled in the fifty States. *EEC Study of non-recycled plastics*, Earth Engineering Center, Columbia University, 2011.

15. Ashori A and Sheshmani S. Hybrid composites made from recycled materials: moisture absorption and thickness swelling behavior. *Biores Technol* 2010; 101(12): 4717–4720.
16. Najafi SK, Hamidinia E and Tajvidi M. Mechanical properties of composites from sawdust and recycled plastics. *J Appl Polym Sci* 2006; 100(5): 3641–3645.
17. Khan ZA, Kamaruddin S and Siddiquee AN. Feasibility study of use of recycled high density polyethylene and multi response optimization of injection moulding parameters using combined grey relational and principal component analyses. *Mater Des* 2010; 31(6): 2925–2931.
18. Petchpradab P, Yoshida T, Charinpanitkul T, et al. Hydrothermal pretreatment of rubber wood for the saccharification process. *Ind Eng Chem Res* 2009; 48(9): 4587–4591.
19. Homkhiew C, Ratanawilai T and Thongruang W. Composites from recycled polypropylene and rubberwood flour: effects of composition on mechanical properties. *J Thermoplast Compos Mater*. Epub ahead of print 14 February 2013. DOI:10.1177/0892705712475019.
20. Mishra S and Aireddy H. Evaluation of dielectric behavior of bio-waste reinforced polymer composite. *J Reinf Plast Compos* 2011; 30(2): 134–141.
21. Stokke DD and Gardner DJ. Fundamental aspects of wood as a component of thermoplastic composites. *J Vinyl Addit Technol* 2003; 9(2): 96–104.
22. Li B, Jiang H, Guo L, et al. Comparative study on the effect of manchurian ash and larch wood flour on mechanical property, morphology, and rheology of HDPE/wood flour composites. *J Appl Polym Sci* 2008; 107(4): 2520–2530.
23. Ratanawilai T, Lekanukit P and Urapantamas S. Effect of rubberwood and palm oil content on the properties of wood-polyvinyl chloride composites. *J Thermoplast Compos Mater*. Epub ahead of print 9 August 2012. DOI:10.1177/0892705712454863.
24. El-Saied H, Basta AH, Hassanen ME, et al. Behaviour of rice-byproducts and optimizing the conditions for production of high performance natural fiber polymer composites. *J Polym Environ* 2012; 20(3): 838–847.
25. Lin Q, Zhou X and Dai J. Effect of hydrothermal environment on moisture absorption and mechanical properties of wood flour-filled polypropylene composites. *J Appl Polym Sci* 2002; 85(14): 2824–2832.
26. Shakeri A and Ghasemian A. Water absorption and thickness swelling behavior of polypropylene reinforced with hybrid recycled newspaper and glass fiber. *Appl Compos Mater* 2010; 17(2): 183–193.
27. Wechsler A and Hiziroglu S. Some of the properties of wood–plastic composites. *Build Environ* 2007; 42(7): 2637–2644.
28. Yang HS, Kim HJ, Park HJ, et al. Water absorption behavior and mechanical properties of lignocellulosic filler–polyolefin bio-composites. *Compos Struct* 2006; 72(4): 429–437.
29. Tajvidi M and Takemura A. Recycled natural fiber polypropylene composites: water absorption/desorption kinetics and dimensional stability. *J Polym Environ* 2010; 18(4): 500–509.
30. Tamrakar S and Lopez-Anido RA. Water absorption of wood polypropylene composite sheet piles and its influence on mechanical properties. *Const Build Mater* 2011; 25(10): 3977–3988.
31. Aurrekoetxea J, Sarrionandia MA, Urrutibeascoa I, et al. Effects of recycling on the microstructure and the mechanical properties of isotactic polypropylene. *J Mater Sci* 2001; 36(11): 2607–2613.

Journal of Reinforced Plastics and Composites
http://jrp.sagepub.com/

Optimizing the formulation of polypropylene and rubberwood flour composites for moisture resistance by mixture design

Chatree Homkhiew, Thanate Ratanawilai and Wiriya Thongruang

Journal of Reinforced Plastics and Composites published online 20 January 2014
DOI: 10.1177/0731684413518362

The online version of this article can be found at:
http://jrp.sagepub.com/content/early/2014/01/17/0731684413518362

Published by:
SAGE
http://www.sagepublications.com

Original Article

JOURNAL OF
REINFORCED
PLASTICS &
COMPOSITES

Journal of Reinforced Plastics and Composites
0(00) 1–14

DOI: 10.1177/0731684413518362
jrp.sagepub.com
SAGE

Optimizing the formulation of polypropylene and rubberwood flour composites for moisture resistance by mixture design

Chatree Homkhiew[1], Thanate Ratanawilai[1] and Wiriya Thongruang[2]

Abstract

D-optimal mixture experimental design was used to determine the optimal mixture of composites from rubberwood (*Hevea brasiliensis*) flour and recycled polypropylene and to systematically analyze the effects of composition, namely recycled polypropylene, rubberwood flour, maleic anhydride-grafted polypropylene, and ultraviolet stabilizer fractions. Panel samples were extruded, and their properties were characterized. The overall compositions significantly affected water absorption, thickness swelling, flexural strength and modulus, and maximum strain. Water absorption and thickness swelling increased with the fraction of rubberwood flour. At long immersion times, flexural strength and modulus decreased, but maximum strain increased with high fraction of rubberwood flour. The fraction of maleic anhydride-grafted polypropylene only slightly affected water absorption and flexural properties, while the ultraviolet stabilizer fraction had a clear negative effect increasing water absorption and decreasing flexural properties. The models fitted were used for optimization of a desirability score, substituting for the multiple objectives modeled. The optimal formulation found was 68.9 wt% recycled polypropylene, 25.0 wt% rubberwood flour, 5.0 wt% maleic anhydride-grafted polypropylene, 0.1 wt% ultraviolet stabilizer, and 1.0 wt% lubricant. This formulation of the composites can be used for most suitable applications based on the moisture resistance.

Keywords

Wood–plastic composites, rubberwood flour, recycled polypropylene, statistical method, water absorption

Introduction

In the recent decades, plastic waste has globally become a significant contributor to municipal solid waste.[1] In 2008, at least 33.6 million tons of postconsumer plastics were generated in the United States, of which 28.9 million tons went to landfills, 2.6 million tons to combustion and energy recovery, and only 2.2 million tons to recycling.[2] The plastic waste typically includes polyethylene (PE), polypropylene (PP), polyvinyl chloride (PVC), polyethylene terephthalate (PET), and polystyrene (PS).[3] Of all these plastic types, PE and PP significantly contribute to landfills and have similarities in their structure and properties.[4] However, when PE (virgin or recycled) was blended with sawdust, it had lower stiffness and strength than similar composites with PP (virgin or recycled).[5] Due to the availability of plastic waste and increased environmental awareness, there have been many studies on natural fiber-reinforced recycled thermoplastics. For example, Cui et al.[1] fabricated composites from postconsumer high-density polyethylene and wood fiber and found that wood fiber content affected the flexural strength,

[1]Department of Industrial Engineering, Prince of Songkla University, Hat Yai, Songkhla, Thailand
[2]Department of Mechanical Engineering, Prince of Songkla University, Hat Yai, Songkhla, Thailand

Corresponding author:
T Ratanawilai, Department of Industrial Engineering, Prince of Songkla University, Hat Yai, Songkhla 90112, Thailand.
Email: thanate.r@psu.ac.th

modulus, and impact strength. Boukehili and Nguyen-Tri[6] manufactured composites from recycled polypropylene (rPP) and short bamboo fiber. They found that chemical treatment of fiber significantly improves the impermeability to helium gas and reduces the amount of water absorption. Kazemi et al.[4] produced composites from wood sawdust and blends of postconsumer PE and PP. The wood flour in composites increased tensile, flexural, and torsion moduli in comparison to the recycled plastic blends. Nourbakhsh et al.[7] also concluded that polypropylene waste and wood waste are promising alternative raw materials for making low-cost wood–plastic composites (WPCs). Hence, the use of recycled plastics may effectively dispose of plastic waste and also reduce the cost of products.[8]

The rubberwood industries of Thailand generate a large amount of wood waste in the forms of flour, sawdust, and chips at different stages of wood processing. Generally, rubberwood waste is dumped in landfills or burned, but some is used in medium-density fiberboard and particle board.[9] Rubberwood waste as reinforcement in plastic composites is of great interest both for economic and for environmental reasons. Natural fiber (wood waste)-reinforced thermoplastics also offers many advantages including biodegradability, renewable character, low cost, absence of associated health hazards, and low wear of processing equipment,[10–13] when compared with synthetic fibers.[14,15] Natural fibers have successfully improved the mechanical properties of plastic composites, as the following examples demonstrate. Homkhiew et al.[9] investigated the effects of rubberwood content on the mechanical properties of recycled PP composites and found that the modulus and hardness of composites increased linearly with an increase of wood flour loadings in the range of 25–45 wt% wood flour. Karmarkar et al.[16] also reported that the tensile strength and modulus linearly increased with an increase of wood fiber from 10 to 50 wt% in PP composites. However, the hygroscopic nature of natural fibers is a disadvantage influencing the performance of the WPCs, when exposed to environmental conditions.[17] The water-absorption characteristics WPCs limit their end-use applications,[17,18] as several mechanical and physical properties, such as dimensional stability, are affected. Likewise, water absorption (WA) is one of the key parameters in quality assessment of WPCs.[19] The WA of WPCs varies by the wood species, partly because they have different contents of cellulose, lignin, hemicelluloses, and extractants.[20] Hence, the effects of filler on the composite properties need to be characterized, and this has not been done previously for rubberwood flour (RWF) in relation to moisture resistance.

Statistical experimental design, such as mixture design, factorial design, and Taguchi method, is a well-established concept for planning and execution of informative experiments.[21] Recently, WPCs have been studied with designed experiments. For example, Jun et al.[22] used a Box–Behnken design with response surface method to determine which variables influenced board performance significantly. Matuana and Mengeloglu [23] used a four-factor central composite design to develop a response surface model and to study the foamability of rigid PVC/wood-flour composites. Stark and Matuana[24] applied a 2^4 factorial design to determine the effects of two hindered amine light stabilizers, a colorant and an ultraviolet (UV) absorber, and their interactions on the photostabilization of wood flour/high-density polyethylene composites. However, the fractions of components in a mixture cannot be changed independently since they must add up to 100%, and the methods for mixture designs have been created with this in mind.[25] Mixture designs have been successful in many applications, particularly in food and pharmaceutical industries, whereas prior studies on WPCs seem not to have used a mixture design.

Experiments with mixture design enable statistical estimation of individual effects and interactions of components in a mixture, and the fitted models can be used to find the optimal formulation of a composite material.[26] Hence, a mixture experimental design was applied to model physical and mechanical characteristics of WPCs. The main objective of this work was to optimize the mixture ratios for composites made from rPP and RWF, based on experimentally determined WA and flexural failure. The new information created from this work would help better understand the properties of components, and the optimal formulation of the composites can be used for most suitable applications in condition of the water resistance.

Materials and methods

Materials

rPP pellets, WT170 with a melt flow index of 11 g/10 min at 230°C, were purchased from Withaya Intertrade Co., Ltd (Samutprakarn, Thailand) and used as the polymer matrix. They have the flexural strength and modulus about 37.02 MPa and 1.27 GPa, respectively. RWF obtained from the cutting process in local furniture industry (Songkhla, Thailand) was used as reinforcement. Maleic anhydride-grafted polypropylene (MAPP) with 8–10% of maleic anhydride was supplied by Sigma-Aldrich (Missouri, USA) and used as a coupling agent to improve the interfacial adhesion between filler and matrix. Hindered amine light stabilizer (MEUV008) was purchased from TH Color Co., Ltd (Samutprakarn, Thailand), chosen as UV stabilizer. Paraffin wax was procured from Nippon Seiro Co., Ltd (Yamaguchi, Japan) and used as lubricant (Lub).

Experimental design to optimize formulation

The region of interest for the current experiments has constraints that imposed on the component fractions,[25] and these can be incorporated in a D-optimal mixture design. The experimental results were used to statistically evaluate the effects of component fractions on WA and flexural failure by using analysis of variance (ANOVA), and the identified models were used to optimize the formulation by using response surface methodology. The experimental D-optimal mixture design and statistical analysis were done with Design-Expert software (version 8.0.6, Stat-Ease, Inc.). The formulations for the manufacture of WPCs were defined by component fractions for rPP (x_1), RWF (x_2), MAPP (x_3), UV stabilizer (x_4), and Lub (x_5). The upper and lower limits of experimental range are shown in Table 1. The ranges of rPP and RWF contents obtained from the previous preliminary study[27] and the other compositions were determined following the literature review. For example, Kuo et al.[10] reported that the optimal content of MAPP was 3–4.5 wt%. Despite the fraction of Lub being held constant, it is included as a variable because it contributes to the 100% in the mixture. The design included 15 different formulations and 5 replications to evaluate reproducibility and variances. Thus, the total number of runs was 20, as shown in Tables 2 and 3. After data collection, linear, quadratic, and special cubic models (see equations (1) to (3)) were used to model the responses.

$$Y = \sum_{i=1}^{l} \beta_i x_i \tag{1}$$

$$Y = \sum_{i=1}^{l} \beta_i x_i + \sum \sum_{i<j}^{l} \beta_{ij} x_i x_j \tag{2}$$

Table 1. Constraints for the mixture design of experiments.

Component	Fraction restrictions (wt%)
rPP (x_1)	$50 \le x_1 \le 70$
RWF (x_2)	$25 \le x_2 \le 45$
MAPP (x_3)	$3 \le x_3 \le 5$
UV stabilizer (x_4)	$0 \le x_4 \le 1$
Lub (x_5)	$=1$

Table 2. Experimental compositions based on mixture experimental design, and replicate averaged measured responses: WA and TS at 1, 5, and 10 weeks.

	Mixture component fraction (wt%)					Water absorption (%)			Thickness swelling (%)		
Run no.	x_1	x_2	x_3	x_4	x_5	W1	W5	W10	W1	W5	W10
1	63.9	29.9	4.5	0.7	1.0	0.97	2.97	4.77	0.24	0.70	1.28
2	70.0	25.0	3.0	1.0	1.0	0.77	2.22	3.64	0.28	0.58	0.89
3	50.0	43.0	5.0	1.0	1.0	2.65	7.28	9.87	0.49	1.63	2.72
4	54.9	38.9	4.5	0.7	1.0	1.99	6.12	8.59	0.43	1.39	2.60
5	59.5	34.5	5.0	0.0	1.0	2.06	5.13	7.56	0.30	1.00	1.99
6	55.4	39.9	3.5	0.2	1.0	1.94	5.80	8.34	0.50	1.43	2.53
7	59.5	34.5	4.0	1.0	1.0	1.06	4.67	6.90	0.40	1.11	1.91
8[a]	59.5	34.5	5.0	0.0	1.0	1.55	4.75	7.10	0.31	1.17	2.15
9	50.0	44.3	4.3	0.5	1.0	2.58	7.14	9.45	0.66	1.92	3.07
10	68.0	25.0	5.0	1.0	1.0	0.56	1.91	3.13	0.26	0.56	0.85
11	50.0	45.0	3.0	1.0	1.0	3.39	8.92	10.50	0.75	2.39	3.15
12[a]	50.0	43.0	5.0	1.0	1.0	3.08	8.05	9.70	0.43	1.92	2.63
13	60.3	35.3	3.0	0.5	1.0	1.48	4.58	6.81	0.27	0.96	1.73
14	64.9	30.4	3.5	0.2	1.0	0.97	3.39	5.28	0.29	0.89	1.60
15[a]	70.0	25.0	3.0	1.0	1.0	0.67	2.10	3.39	0.23	0.58	0.93
16	51.0	45.0	3.0	0.0	1.0	2.70	7.77	10.02	0.60	2.11	3.37
17[a]	51.0	45.0	3.0	0.0	1.0	2.91	8.12	10.31	0.61	2.27	3.47
18[a]	50.0	45.0	3.0	1.0	1.0	3.58	9.41	10.33	0.74	2.75	3.51
19	70.0	25.0	4.0	0.0	1.0	0.68	1.80	2.95	0.28	0.48	0.75
20	69.0	25.0	5.0	0.0	1.0	0.61	1.69	2.78	0.20	0.44	0.67

[a]Duplicate experiments.

$$Y = \sum_{i=1}^{l} \beta_i x_i + \sum \sum_{i<j}^{l} \beta_{ij} x_i x_j + \sum \sum_{i<j<k} \sum \beta_{ijk} x_i x_j x_k \quad (3)$$

where Y is the predicted response, i, j, k, and l mean rPP, RWF, MAPP, and UV stabilizer, respectively, β_i is the model response to a pure component in the blend, each β_{ij} scales an interaction between components, each β_{ijk} scales an interaction of three components, x_i, x_j, ..., x_l are the fractions of components, terms with x_ix_j, x_jx_k, ..., x_kx_l are the quadratic interactions of the fractions, and the last sum in equation (3) consists of cubic interactions.

Preparation of composites

Prior to compounding, the rubberwood (*Hevea brasiliensis*) flour was sieved through a standard sieve of mesh size 80 (passing particles smaller than 180 μm) and was dried in an oven at 110°C for 8 h to minimize the moisture content. The WPCs were then manufactured in a two-stage process. In the first stage, WPC pellets were produced: rPP and RWF were dry-blended and melt-blended into WPC pellets using a twin-screw extruder (Model SHJ-36 from En Mach Co., Ltd, Nonthaburi, Thailand). The 10 temperature zones of the extruder were set to a profile in the range of 130–170°C to reduce degradation of the mixture components, while the screw-rotating speed was maintained at 70 rpm. The extruded strand passed through a water bath and was subsequently pelletized. In the second stage, WPC panels were produced: the WPC pellets were again dried in the oven at 110°C for 8 h. WPC pellets, MAPP, UV stabilizer, and lubricant compositions, indicated in Tables 2 and 3, were then dry-mixed and fed into the twin-screw extruder. The processing conditions for extruding were as follows: (a) temperature profiles: 130–190°C; (b) screw-rotating speed: 50 rpm; (c) melt pressure: 0.10–0.20 MPa depending on wood flour content; and (d) vacuum venting at nine temperature zones: 0.022 MPa. The WPC panels were extruded through a 9 mm × 22 mm rectangular die and cooled in ambient air. These specimens were machined following the standards of American Society for Testing and Materials (ASTM) for physical and mechanical testing.

Table 3. The experimental compositions and replicate averaged measured flexural properties.

Run no.	Mixture component fraction (wt%)					MOR (MPa)		MOE (GPa)		Max. ε (%)	
	x_1	x_2	x_3	x_4	x_5	W1	W6	W1	W6	W1	W6
1	63.9	29.9	4.5	0.7	1.0	38.7	36.8	1.90	1.67	3.23	3.80
2	70.0	25.0	3.0	1.0	1.0	37.2	35.8	1.76	1.65	3.03	3.81
3	50.0	43.0	5.0	1.0	1.0	37.5	29.7	2.10	1.63	2.92	3.11
4	54.9	38.9	4.5	0.7	1.0	39.7	34.2	2.03	1.62	3.12	3.66
5	59.5	34.5	5.0	0.0	1.0	41.9	32.5	1.87	1.50	3.52	3.74
6	55.4	39.9	3.5	0.2	1.0	40.7	32.5	1.96	1.59	3.41	3.61
7	59.5	34.5	4.0	1.0	1.0	36.3	32.8	1.94	1.49	2.82	3.67
8[a]	59.5	34.5	5.0	0.0	1.0	40.1	31.9	1.82	1.47	3.63	3.79
9	50.0	44.3	4.3	0.5	1.0	40.3	33.5	2.04	1.70	3.09	3.60
10	68.0	25.0	5.0	1.0	1.0	36.8	36.6	1.75	1.65	3.14	3.78
11	50.0	45.0	3.0	1.0	1.0	35.9	30.7	1.85	1.65	2.97	3.20
12[a]	50.0	43.0	5.0	1.0	1.0	37.4	28.6	2.10	1.64	2.75	2.77
13	60.3	35.3	3.0	0.5	1.0	39.9	34.2	1.94	1.52	3.15	4.14
14	64.9	30.4	3.5	0.2	1.0	40.8	37.0	1.86	1.53	3.70	4.42
15[a]	70.0	25.0	3.0	1.0	1.0	36.9	35.4	1.79	1.64	3.38	4.15
16	51.0	45.0	3.0	0.0	1.0	44.6	33.3	2.12	1.63	3.49	3.90
17[a]	51.0	45.0	3.0	0.0	1.0	43.1	34.6	2.11	1.65	3.50	3.94
18[a]	50.0	45.0	3.0	1.0	1.0	36.8	31.0	1.84	1.67	3.07	3.46
19	70.0	25.0	4.0	0.0	1.0	38.9	38.9	1.81	1.54	3.50	4.81
20	69.0	25.0	5.0	0.0	1.0	38.6	38.1	1.83	1.75	3.59	4.90

[a]Duplicate experiments.

WA and dimensional stability tests

WA and thickness swelling tests were carried out according to ASTM D570-88 specifications. Before testing, five replicate specimens of each formulation were dried in an oven at 50°C for 24 h. The weight and thickness of each specimen were measured to a precision of 0.001 g and 0.01 mm, respectively. The specimens were then submerged in water at ambient room temperature. After 1, 5, and 10 weeks, soaked specimens were removed from the water, thoroughly dried the surface with tissue papers, and immediately weighed and measured to determine the weight and thickness. The percentage of WA at any given time was calculated following

$$WA_t(\%) = \frac{W_t - W_0}{W_0} \times 100 \quad (4)$$

where WA_t is the WA at time t, W_0 is the initial dry weight, and W_t is the soaked weight of specimen at a given time t.

The percentage of thickness swelling (TS) at any given time was calculated following

$$TS_t(\%) = \frac{T_t - T_0}{T_0} \times 100 \quad (5)$$

where TS_t is the thickness swelling and T_t is the soaked thickness of specimen, both at the given time t, while T_0 is the initial dry thickness.

Flexural test of WPCs

Flexural properties of the samples were determined with an Instron Universal Testing Machine (Model 5582 from Instron Corporation, Massachusetts, USA) in accordance with ASTM D790-92. In the destructive flexural tests (three point bending), specimens with nominal dimensions of 4.8 mm × 13 mm × 100 mm, a span of 80 mm, and a cross-head speed of 2 mm/min were used. The testing was performed at ambient room temperature of 25°C with five samples of each formulation to obtain an average value. The measurements of flexural strength (MOR), modulus of elasticity (MOE), and maximum strain (max. ε) at failure were done at 1 and 6 weeks, and at the latter time, WA had reached its equilibrium so further testing was considered unnecessary.

Results and discussion

The D-optimal mixture design of experiments, with five fractions as (mutually dependent) variables (that sum to one), had 20 runs in a randomized order. The 12 determined responses were the values of the WA and thickness swelling at 1, 5, and 10 weeks and flexural strength, modulus, and maximum strain at 1 and 6 weeks. The results are summarized in Tables 2 and 3.

Statistical analysis of the response models

ANOVA of the alternative types of response models revealed that WA at 1, 5, and 10 weeks, TS at 1 and 5 weeks, and MOR at 1 and 6 weeks were best fit with quadratic models, instead of linear, special cubic, or cubic models, whereas MOE at both 1 and 6 weeks was best fit with special cubic model. The MOE at 6 weeks is shown as an example in Table 4. The sequential model sums of squares for quadratic and special cubic models are significant ($p < 0.05$), but not for the other model types. Moreover, the lack of fit is clearly insignificant for the special cubic model, suggesting that this model performs well. It also has the highest adjusted coefficient of determination (adj-$R^2 = 0.9726$) and predicted coefficient of determination (pred-$R^2 = 0.9484$), further indicating good fit.

The detailed ANOVAs in Tables 5 and 6 document the significant quadratic or cubic terms in models for each response, in terms of their p-values. The ANOVA shows the statistical significance ($p < 0.05$) of these terms supplementing linear models of the fractions, namely rPP, RWF, MAPP, and UV stabilizer. No interaction term was significant in models of WA, MOR, and MOE at 1 week or TS at 5 weeks. However, other response models had significant interactions, for example, between MAPP and UV stabilizer

Table 4. Fitted model summary for MOE at 6 weeks.

Source	Sequential p-value	Lack of fit p-value	Adj-R^2	Pred-R^2	
Linear	0.6971	0.0002*	−0.0884	−0.4177	
Quadratic	0.0056*	0.0023*	0.6382	−0.6377	
Special cubic	*0.0004**	*0.9391*	*0.9726*	*0.9484*	*Suggested*
Cubic	0.9391	–	0.9672	–	Aliased

*p-value less than 0.05 is considered significant.

Table 5. ANOVA and model adequacy for WA and TS responses.

	Water absorption			Thickness swelling		
Source	W1	W5	W10	W1	W5	W10
Model	<0.0001*	<0.0001*	<0.0001*	<0.0001*	<0.0001*	<0.0001*
Linear mixture	<0.0001*	<0.0001*	<0.0001*	<0.0001*	<0.0001*	<0.0001*
x_1x_2	0.1380	0.9034	0.0042*	0.0005*	0.0925	–
x_1x_3	0.1107	0.3851	0.4548	0.0007*	0.6560	–
x_1x_4	0.7164	0.0701	0.0246*	0.1941	0.2073	–
x_2x_3	0.1097	0.3679	0.5153	0.0010*	0.7388	–
x_2x_4	0.7422	0.0746	0.0242*	0.1839	0.2088	–
x_3x_4	0.2698	0.0205*	0.0065*	0.2339	0.1190	–
Lack of fit	0.4366	0.4456	0.2319	0.1650	0.5991	0.2126
R^2	0.9703	0.9906	0.9959	0.9810	0.9749	0.9727
Adj-R^2	0.9435	0.9821	0.9921	0.9639	0.9524	0.9675
Pred-R^2	0.8245	0.9526	0.9800	0.8801	0.8898	0.9584
C.V. (%)	13.29	6.65	3.54	8.14	11.79	8.39

ANOVA: analysis of variance.
*P-value less than 0.05 is considered significant.

Table 6. ANOVA and model adequacy for flexural properties.

	MOR		MOE		Max. strain	
Source	W1	W6	W1	W6	W1	W6
Model	<0.0001*	<0.0001*	<0.0001*	<0.0001*	<0.0001*	<0.0001*
Linear mixture	<0.0001*	<0.0001*	<0.0001*	0.0018*	<0.0001*	<0.0001*
x_1x_2	0.9169	0.0067*	0.1091	0.5197	–	–
x_1x_3	0.2973	0.0726	0.3808	0.2568	–	–
x_1x_4	0.1474	0.0124*	0.2373	0.0007*	–	–
x_2x_3	0.3236	0.0952	0.3308	0.5825	–	–
x_2x_4	0.1700	0.0127*	0.2523	0.0008*	–	–
x_3x_4	0.0968	0.0020*	0.8386	0.7737	–	–
$x_1x_2x_3$	–	–	0.5757	0.3760	–	–
$x_1x_2x_4$	–	–	0.0619	0.0039*	–	–
$x_1x_3x_4$	–	–	0.7685	0.5580	–	–
$x_2x_3x_4$	–	–	0.6719	0.3347	–	–
Lack of fit	0.6701	0.1192	0.7600	0.9391	0.6122	0.2335
R^2	0.9499	0.9514	0.9936	0.9913	0.8354	0.8382
Adj-R^2	0.9048	0.9077	0.9799	0.9726	0.8045	0.8079
Pred-R^2	0.8310	0.8449	0.7753	0.9484	0.7360	0.7354
C.V. (%)	1.86	2.51	0.91	0.78	3.86	5.90

ANOVA: analysis of variance.
*p-value less than 0.05 is considered significant.

for WA at 5 weeks and between rPP and RWF, rPP and UV stabilizer, RWF and UV stabilizer, and MAPP and UV stabilizer for MOR at 6 weeks. The frequent interactions with UV stabilizer might indicate that it reacted chemically with the other components or affected their distribution and interactions. In addition, the ANOVA also showed that lack of fit was not significant for any of the response surface models at 95%

confidence level. The regression models fit the data in a statistically sound manner.

Tables 5 and 6 also include the coefficient of determination (R^2), adj-R^2, pred-R^2, and coefficient of variation (C.V.). The R^2 values of the 12 response fits are in the range from 0.8354 to 0.9959. The R^2 values of maximum strain at 1 week (0.8354) and WA at 10 weeks (0.9959) indicate that only 16.46% and 0.41%, respectively, of the total variability in observations are not explained by the models; R^2 values close to 1 indicate good fits.[28] Also, the adj-R^2 values in the range from 0.8045 to 0.9921 suggest good fits and the same goes for pred-R^2 values. The pred-R^2 value of WA at 10 weeks was 0.9800 meaning that the fitted model would explain about 98% of the variability in new data. The coefficients of variation of all response fits based on the replications of experiments show low values in the range from 0.78 to 13.29%. The low-C.V. values indicate that the determinations of material characteristics had a good precision and can serve the fitting of parametric models.

Model adequacy checking

Model adequacy checking is performed to verify the appropriate approximation of the fitted model.[29] Figure 1(a) displays the normal probability plots of the residuals for WA at 10 weeks (WAW10). The good linear fit in this plot indicates that the residuals (approximation errors remaining in the model) are close to normally distributed. Basically, normally distributed residuals are a requirement for the validity of least squares regression, so the model is adequate. Likewise, there is no indication of possible outliers, such as faulty experiment cases with particularly large residuals.[25] The plot of residuals versus predicted values in Figure 1(b) exhibits no obvious patterns that would suggest adding a term to the model, to account for that pattern. If the residuals had such structure, the model would not be appropriate.[25] Figure 1(c) shows model predictions versus observations. The model outputs fit the actual observations quite well, with WAW10 model deviating from actual by less

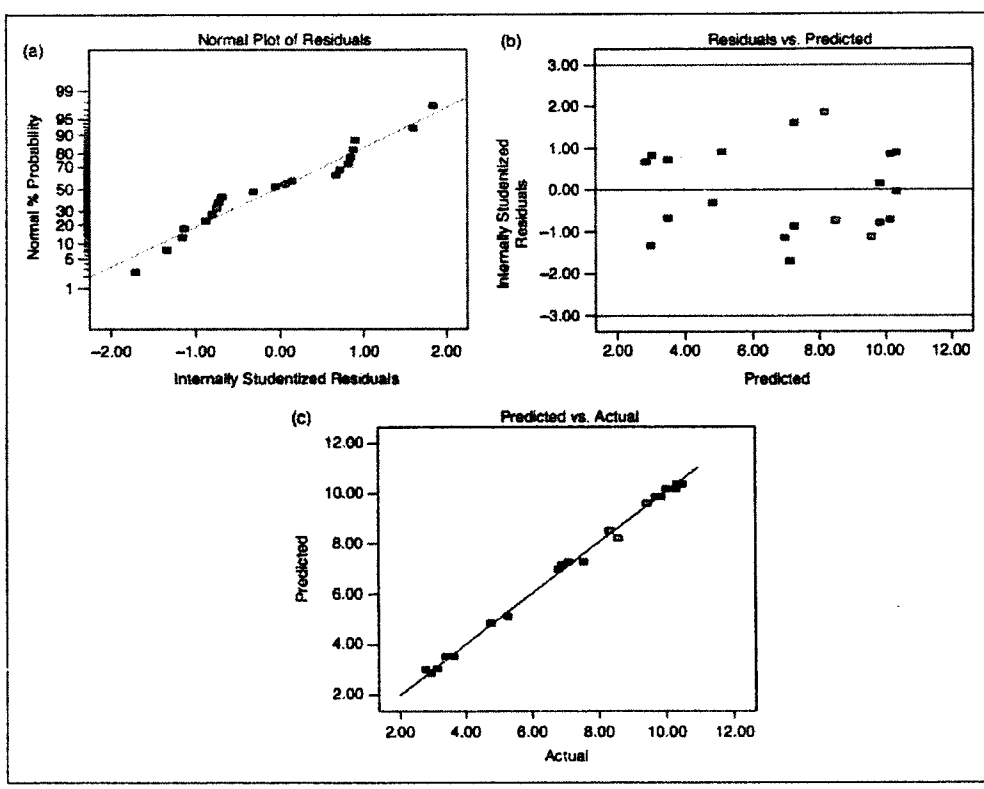

Figure 1. Model adequacy checking for water absorption at 10 weeks; (a) normal probability plot of residuals, (b) plot of residuals versus predicted values, and (c) plot of predicted versus actual values.

than about 5%. These adequacy checks of the WAW10 response model indicated accuracy with the model type or its fit to data. Similar checking for the other modeled responses gave no indications of problems with the fitted models either. This type of checking cannot guarantee predictive capability, but suggests that the models are sound approximations for interpolating within the experimental range.

Effect of composition on WA and optimal formulation

The quadratic regression models for WAW1, WAW5, and WAW10 were

$$\begin{aligned}\text{WAW1} = {} & 0.73x_1 + 2.99x_2 + 120.23x_3 + 115.96x_4 \\ & - 1.18x_1x_2 - 129.92x_1x_3 - 121.13x_1x_4 \\ & - 129.82x_2x_3 - 109.74x_2x_4 - 346.98x_3x_4 \quad (6)\end{aligned}$$

$$\begin{aligned}\text{WAW5} = {} & 1.8x_1 + 8.23x_2 + 91.78x_3 + 907.58x_4 \\ & + 0.13x_1x_2 - 96.75x_1x_3 - 942.92x_1x_4 - 100.05x_2x_3 \\ & - 926.36x_2x_4 - 1171.62x_3x_4 \quad (7)\end{aligned}$$

$$\begin{aligned}\text{WAW10} = {} & 2.99x_1 + 10.38x_2 + 57.33x_3 + 861.54x_4 \\ & + 2.80x_1x_2 - 60x_1x_3 - 890.01x_1x_4 - 51.83x_2x_3 \\ & - 894.58x_2x_4 - 1056.74x_3x_4 \quad (8)\end{aligned}$$

These equations show a positive coefficient for all the individual components, namely rPP (x_1), RWF (x_2), MAPP (x_3), and UV stabilizer (x_4), and the coefficients of rPP and RWF increased with immersion time. The rPP has the smallest coefficient in the fit for the WA due to hydrophobicity of this matrix polymer.[19] Contour plots of WAW1 and WAW10 are shown in Figure 2(a) and (b), respectively. In these triangular plots, the three pure components (rPP, RWF, and MAPP) are represented by the corners, while the additive levels were fixed (UV stabilizer at 0.5 wt% and Lub at 1 wt%). The contours in the colored areas, which include the experimental observations, present the WAW1 and WAW10 regression fits varying from 0.5 to 2.5% and 2.9 to 9.5%, respectively. Both WAW1 and WAW10 clearly increase with an increase in the RWF content: the free OH groups of RWF cellulose increase the WA of the composites.[30,31] Likewise, the acceleration of water uptake of WPCs could be concluded on four factors such as lumen, hydrophilicity of wood cellulous, microcracks in wood flour, and adhesion between wood flour and polymer matrix.[31] Increasing the MAPP addition from 3 to 5 wt% slightly affects the WA. This is because the coupling agent increases bonding in WPCs, by improving interfacial adhesion between the wood particles and the polymer. Then the plastic can cover more of the wood surfaces, resulting in a lower WA.[32,33] Besides, Adhikary et al.[8] also concluded that the addition of MAPP significantly reduced the WA, when compared with the composites without MAPP. The composites, consisted of 50 wt% wood flour and 3 wt% MAPP, decreased the WA from 4.1% to 1.31% for the 24-h immersion tests.[8] Furthermore, adding 1 wt% UV stabilizer increased the moisture content in the rPP/RWF composites. This may be attributed to the nonuniform spatial distribution of wood flour, polymer, and UV stabilizer.[9,34] When WPCs experienced with the nonuniform spatial distribution and poor interfacial adhesion between the compositions, it allows easier access of water into the structure. Figure 3 displays the numerically optimized composition, based on these model fits. Since three models are optimized simultaneously, the software

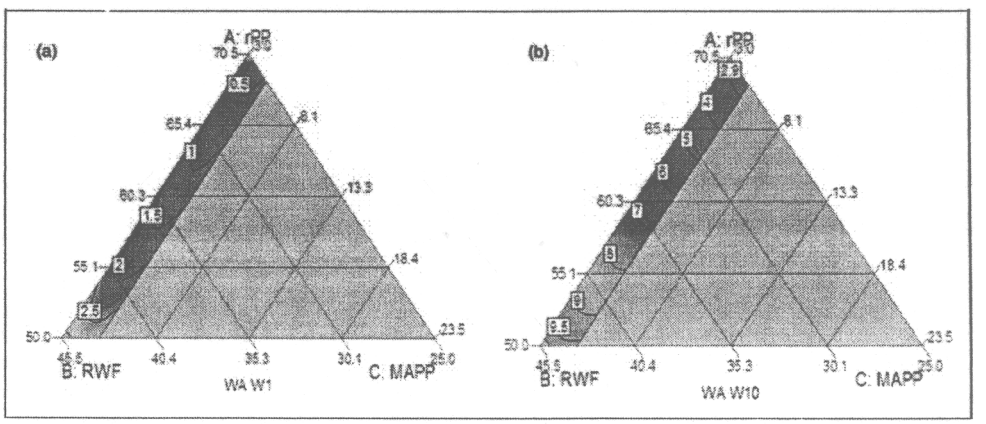

Figure 2. Triangular contour plots for effects of the compositions on water absorption at (a) 1 and (b) 10 weeks, with UV stabilizer fixed at 0.5 wt% and Lub at 1 wt%.

actually uses a single surrogate called "desirability" to balance them. This is reasonable because the three characteristics (WA at 1, 5, and 10 weeks) are not competing, but are in a good mutual agreement. The model-based optimal formulations are shown in Table 7, and the "overall" WA represented by the desirability was minimized by 69.3 wt% rPP, 25.0 wt% RWF, 4.6 wt% MAPP, 0.1 wt% UV stabilizer, and 1 wt% Lub, with a high-desirability score of 0.992 that indicates the agreement of the multiple objectives.

Effect of composition on thickness swelling and optimal formulation

The regression fits for the thickness swelling (TS) at 1, 5, and 10 weeks were

$$\begin{aligned} TSW1 = {} & 0.093x_1 + 0.67x_2 - 43.45x_3 + 63.68x_4 \\ & - 0.52x_1x_2 + 49.74x_1x_3 - 63.11x_1x_4 \\ & + 47.51x_2x_3 - 64.78x_2x_4 - 52.62x_3x_4 \quad (9) \end{aligned}$$

$$\begin{aligned} TSW5 = {} & 0.33x_1 + 2.33x_2 - 17.17x_3 + 273.76x_4 \\ & - 0.87x_1x_2 + 21.95x_1x_3 - 281.51x_1x_4 \\ & + 16.33x_2x_3 - 280.74x_2x_4 - 326.17x_3x_4 \quad (10) \end{aligned}$$

$$TSW10 = 0.95x_1 + 3.45x_2 - 0.71x_3 - 1.10x_4 \quad (11)$$

The equations of TS at all immersion times show positive coefficients for fraction of rPP (x_1) and RWF (x_2) and negative coefficient for fraction of MAPP (x_3) due to the decrease of WA and moisture penetration in the composite systems[35] when MAPP was added. Likewise, when the positive coefficients between rPP and RWF were compared, the RWF showed higher coefficients than the rPP due to nature of the hydrophilic filler.[19] Figure 4 shows that TS at 10 week (in range of 1 to 3%) increases with an increase in the RWF fraction. The wood flour expands and keeps absorbing water until the cell walls are saturated.[18] The addition of MAPP from 3 to 5 wt% affected the thickness swelling

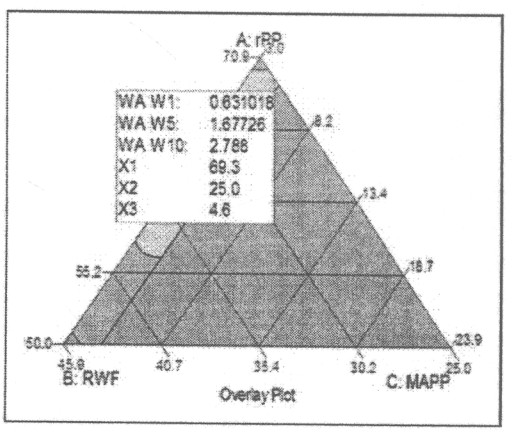

Figure 3. The optimal formulation for water absorption.

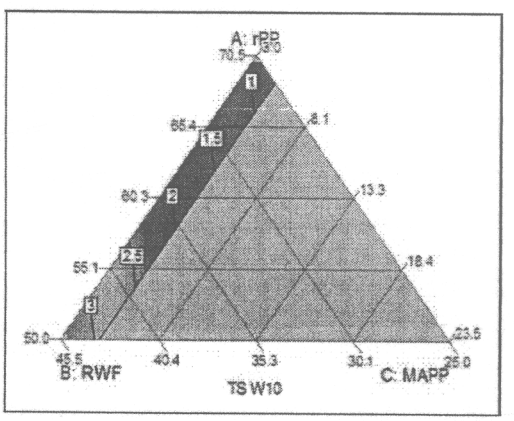

Figure 4. Triangular contour plots for effects of composition on thickness swelling at 10 weeks, with UV stabilizer fixed at 0.5 wt% and Lub at 1 wt%.

Table 7. Predicted optimal formulations and their responses, from multiobjective optimizations.

	Mixture component fraction (wt%)					Predicted response				
Property	x_1	x_2	x_3	x_4	x_5	W1	W5	W6	W10	Desirability
WA (%)	69.3	25.0	4.6	0.1	1.0	0.63	1.67	–	2.78	0.992
TS (%)	68.9	25.0	5.0	0.1	1.0	0.22	0.49	–	0.78	0.969
MOR (MPa)	69.4	26.4	3.1	0.1	1.0	40.4	–	37.7	–	0.678
MOE (GPa)	50.0	44.1	4.2	0.7	1.0	2.03	–	1.74	–	0.862
Max. strain (%)	69.8	26.2	3.0	0.0	1.0	3.70	–	4.77	–	0.968

Note: For example, the formulation in first row is optimal for a desirability score that balances WA at times W1, W5, and W10.

of composites, so that the swelling decreased with MAPP fraction. The reason is probably similar to what was discussed in relation to WA. The optimal formulation based on these numerical models, combined by a desirability score for optimization, is also included in Table 7.

Effect of composition on flexural strength and optimal formulation

The quadratic regression models fitted for the flexural strength MOR at 1 and 6 weeks were

$$\begin{aligned}\text{MOR W1} = {} & 40.35x_1 + 43.78x_2 + 247.09x_3 \\ & - 1498.46x_4 + 0.24x_1x_2 - 247.39x_1x_3 \\ & + 1542.49x_1x_4 - 232.7x_2x_3 + 1453.86x_2x_4 \\ & + 1649.2x_3x_4 \end{aligned} \quad (12)$$

$$\begin{aligned}\text{MOR W6} = {} & 37.82x_1 + 33.70x_2 - 437.66x_3 - 3328.49x_4 \\ & - 8.79x_1x_2 + 526.16x_1x_3 + 3484.81x_1x_4 \\ & + 481.2x_2x_3 + 3468.82x_2x_4 + 4344.19x_3x_4 \end{aligned} \quad (13)$$

The coefficients of rPP (x_1), RWF (x_2), MAPP (x_3), and UV stabilizer (x_4) decrease with the immersion time. The UV stabilizer fraction has the largest negative coefficient in the model fits, so it should be minimized. UV stabilizer in WPCs is known to reduce the flexural properties due to nonhomogeneous spatial distribution of wood flour, polymer, and UV stabilizer.[34] Therefore, ability of the stress transfer in the composite structure is reduced. The triangular contour plots in Figure 5(a) and (b) illustrate that an increase of wood flour loading slowly increased MOR at 1 week but greatly decreased MOR at 6 weeks, respectively. The water molecules reduced interfacial adhesion between RWF and polypropylene.[18] When water molecules infiltrate into the composite, the wood flour tends to swell, resulting in localized yielding of the polymer matrix and loss of adhesion between the wood flour and matrix.[18,36,37] Furthermore, the addition of MAPP about 3 wt% is close to optimal for MOR, based on the regression fit. Because MAPP acts as a compatibilizer providing a hydrophobic-rich layer attached to wood flour.[38] Thus, MOR increased with the RWF content after immersing for 1 week. Similar results were found in the work of Kuo et al.[10] who reported that the optimal content of MAPP was 3–4.5 wt% because the interfacial adhesion weakens at higher MAPP contents. The optimal composition based on the quadratic regression models is shown numerically in Table 7.

Effect of composition on flexural modulus and optimal formulation

The special cubic models fitted for the flexural modulus MOE at 1 and 6 weeks were

$$\begin{aligned}\text{MOE W1} = {} & 1.88x_1 + 2.15x_2 + 19.67x_3 - 64.10x_4 \\ & - 0.43x_1x_2 - 20.28x_1x_3 + 66.89x_1x_4 \\ & - 21.35x_2x_3 + 62.9x_2x_4 - 149.38x_3x_4 \\ & + 1.61x_1x_2x_3 + 16.71x_1x_2x_4 + 235.95x_1x_3x_4 \\ & + 332.38x_2x_3x_4 \end{aligned} \quad (14)$$

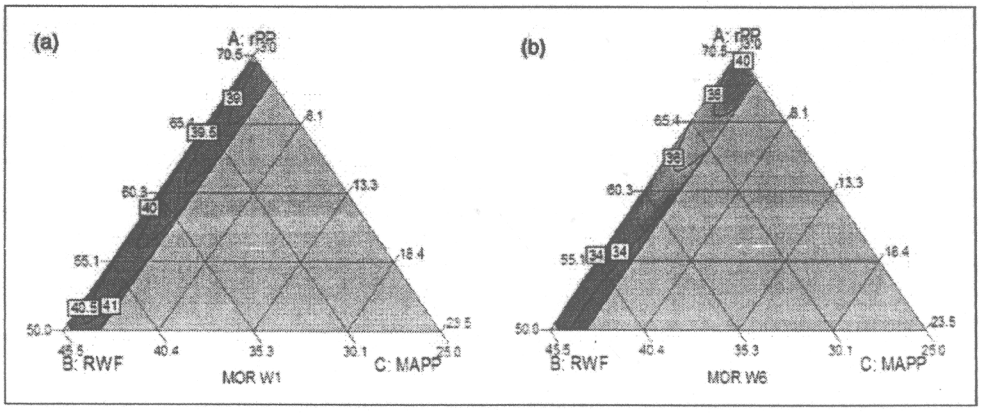

Figure 5. Triangular contour plots for effects of composition on MOR at (a) 1 and (b) 6 weeks, with UV stabilizer fixed at 0.5 wt% and Lub at 1 wt%.

$$\text{MOE W6} = 1.24x_1 + 1.67x_2 - 10.92x_3 - 211.79x_4 - 0.11x_1x_2 + 19.33x_1x_3 + 232.57x_1x_4 + 8.43x_2x_3 + 224.01x_2x_4 - 151.98x_3x_4 + 1.87x_1x_2x_3 - 23.9x_1x_2x_4 + 341.82x_1x_3x_4 + 563.41x_2x_3x_4 \quad (15)$$

These equations show kind of coefficients as flexural strength (MOR), decreasing with immersion time. Figure 6(a) shows that MOE at 1 week (in range of 1.85–2.05 GPa) increased for high fractions of wood flour. Since RWF is a high-modulus material compared to the plastic matrix, composites with higher wood flour concentration require a higher stress for the same deformation.[39] Likewise, fractions of MAPP about 3–4 wt% gave high-flexural modulus. This is because MAPP can improve the interfacial adhesion between wood flour and rPP matrix, leading to improve the stress transfer from polymer to wood particles.[40] However, too much MAPP relative to wood flour will cause self-entanglement, resulting in slippage with the PP molecules.[40] In Figure 6(b), when composites were soaked in water for 6 weeks, MOE at high 45 wt% RWF fraction was comparable to composites with 25 wt% RWF. The wood flour as hard filler, in comparison to the plastic matrix, increased the stiffness of the composites. With moisture wood flour plasticizes, becoming ductile, this decreased the stiffness of composites.[36] Figure 7 shows the optimal formulation based on the special cubic models for MOE and a desirability score combining their outputs. The optimal formulation is also included in Table 7.

Effect of composition on maximum strain and optimal formulation

The linear regression models for the maximum strain (max. ε) at 1 and 6 weeks were

$$\text{Max.}\varepsilon\ \text{W1} = 3.72x_1 + 3.48x_2 + 2.63x_3 - 7.75x_4 \quad (16)$$

$$\text{Max.}\varepsilon\ \text{W6} = 4.82x_1 + 3.87x_2 + 1.23x_3 - 9.29x_4 \quad (17)$$

The fraction of rPP (x_1) has the largest coefficients in the fit, so the maximum strain increased with high fraction of rPP. This is because rPP has high ductility and viscosity, resulting an increase of the maximum strain. In contrast, the maximum strain decreased with the

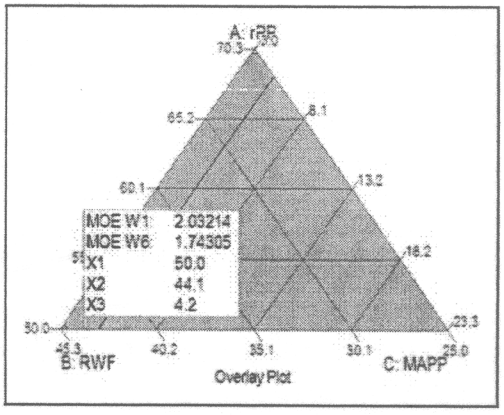

Figure 7. The optimal formulation for MOE.

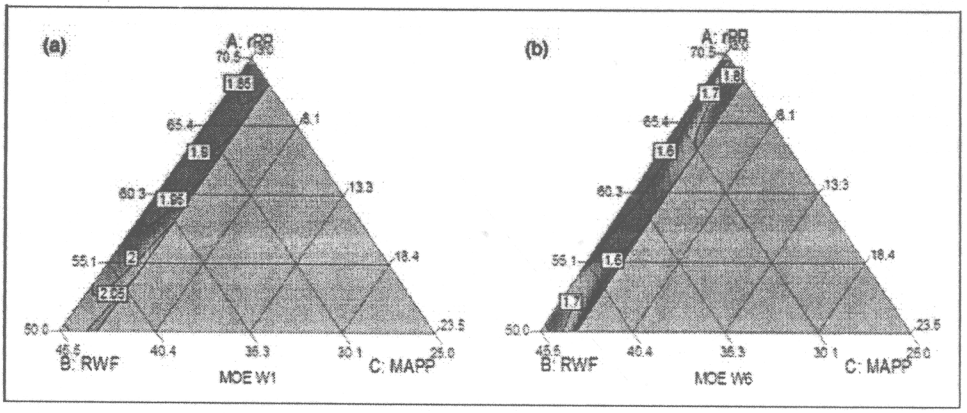

Figure 6. Triangular contour plots for effects of composition on MOE at (a) 1 and (b) 6 weeks, with UV stabilizer fixed at 0.5 wt% and Lub at 1 wt%.

fraction of UV stabilizer (x_4) that has a negative coefficient. The reason for this phenomenon is probably similar to that shown in the flexural strength. Using 1 wt% of UV stabilizer may be unnecessary and to reduce the negative effects on the mechanical properties, the amount of UV stabilizer should be minimized.[34] Again, the maximum strain increases with the WA and immersion time. The reason for this is probably similar as described earlier that ductile wet wood increases the maximum strain. Figure 8 shows that the maximum strain decreased with the RWF content. This is due to the increase in the stiffness and brittleness reducing the maximum strain. The stress concentrations at the fiber ends have been recognized as the leading cause for embrittlement.[8] The optimized composition based on these linear regression models is shown numerically in Table 7.

Optimal formulation of the overall properties based on WA

An optimal formulation for rPP/RWF composites was determined to minimize WA and thickness swelling and maximize flexural strength, modulus, and maximum strain. This multiobjective optimization, using all of the regression models, was performed with the Design-Expert software by constructing a desirability score that balances all of the fitted models in Figure 9. The optimal formulation was 68.9 wt% rPP, 25.0 wt% RWF, 5.0 wt% MAPP, 0.1 wt% UV stabilizer, and 1.0 wt% Lub. The optimal formulation is given in Table 8, along with the model-based responses. The overall formulations in Table 7 closely agree with this optimum.

Conclusions

Mixture experimental design, statistical model, and optimization were used to quantify the effects of rPP/RWF composite formulation and to optimize the formulation for moisture resistance. ANOVA revealed that all the component fractions experimentally varied, namely rPP, RWF, MAPP, and UV stabilizer, statistically significantly affected the WA, thickness swelling, flexural strength and modulus, and maximum strain. In general, a high fraction of RWF increased the WA and TS across immersion times due to the free OH

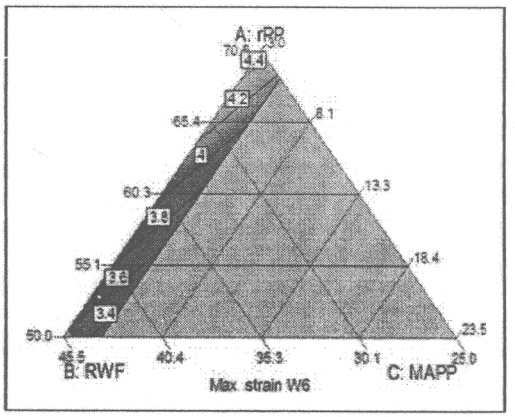

Figure 8. Triangular contour plots for effects of composition on the maximum strain at 6 weeks, with UV stabilizer fixed at 0.5 wt% and Lub at 1 wt%.

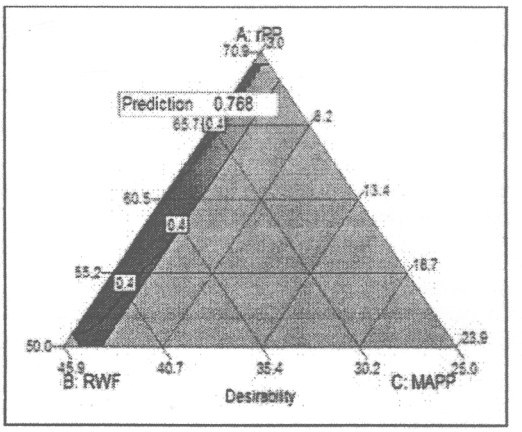

Figure 9. The optimal formulation for overall desirability.

Table 8. Predicted responses with the formulation optimized jointly for all properties.

	Mixture component fractions (wt%)					Predicted response			
Property	x_1	x_2	x_3	x_4	x_5	W1	W5	W6	W10
WA (%)						0.85	1.81	–	2.82
TS (%)						0.22	0.50	–	0.78
MOR (MPa)	68.9	25.0	5.0	0.1	1.0	38.9	–	38.5	–
MOE (GPa)						1.84	–	1.79	–
Max. strain (%)						3.56	–	4.41	–

groups in wood flour contributing WA. When the composites were soaked in water for 1 week, high fractions of RWF increased MOR and MOE but reduced maximum strain. In contrast, at 6 weeks, the MOR and MOE decreased but maximum strain increased with RWF loading. At the longer immersion time, water reduced the interfacial adhesion between RWF and rPP, and moisture plasticized the wood flour making it ductile. This decreased the strength and stiffness but increased the maximum strain of composites. Therefore, the optimum found had 25 wt% RWF, which was the minimum in the experimental design. The compatibilizer MAPP slightly affected WA and TS, which decreased with the MAPP content. The fraction of UV stabilizer also had negative effects on the WA, MOR, and maximum strain. This study demonstrated design and analysis of mixture experiments as an efficient tool to optimize the formulation of rPP/RWF composites for minimum WA and for maximum flexural properties.

Acknowledgements

The authors thank to the Prince of Songkla Graduate Studies Grant, the Government budget Fund (Research Grant Code: 2555A11502062) for financial support throughout this work, and Rubberwood Technology and Management Research Group (ENG-54-27-11-0137-S) of Faculty of Engineering, Prince of Songkla University, Thailand. We also thank Research and Development Office (RDO) and Associate Prof. Seppo Karrila for editing this article.

Funding

This research received no specific grant from any funding agency in the public, commercial, or not-for-profit sectors.

References

1. Cui Y, Lee S, Noruziaan B, et al. Fabrication and interfacial modification of wood/recycled plastic composite materials. *Composites Part A* 2008; 39: 655–661.
2. Themelis NJ, Castaldi MJ, Bhatti J, et al. Energy and economic value of nonrecycled plastics and municipal solid wastes that are currently landfilled in the fifty States. EEC study of non-recycled plastics, Earth Engineering Center, Columbia University, 2011.
3. Selke SE and Wichman I. Wood fiber/polyolefin composites. *Composites Part A* 2004; 35: 321–326.
4. Kazemi Y, Cloutier A and Rodrigue D. Mechanical and morphological properties of wood plastic composites based on municipal plastic waste. *Polym Compos* 2013; 34: 487–493.
5. Najafi SK, Hamidinia E and Tajvidi M. Mechanical properties of composites from sawdust and recycled plastics. *J Appl Polym Sci* 2006; 100: 3641–3645.
6. Boukehili H and Nguyen-Tri P. Helium gas barrier and water absorption behavior of bamboo fiber reinforced recycled polypropylene. *J Reinf Plast Compos* 2012; 31: 1638–1651.
7. Nourbakhsh A, Ashori A, Tabari HZ, et al. Mechanical and thermo-chemical properties of wood-flour/polypropylene blends. *Polym Bull* 2010; 65: 691–700.
8. Adhikary KB, Pang S and Staiger MP. Dimensional stability and mechanical behaviour of wood-plastic composites based recycled and virgin high-density polyethylene. *Composites Part B* 2008; 39: 807–815.
9. Homkhiew C, Ratanawilai T and Thongruang W. Composites from recycled polypropylene and rubberwood flour: effects of composition on mechanical properties. *J Thermoplast Compos Mater*. Epub ahead of print 14 February 2013. DOI: 10.1177/0892705712475019.
10. Kuo PY, Wang SY, Chen JH, et al. Effects of material compositions on the mechanical properties of wood–plastic composites manufactured by injection molding. *Mater Des* 2009; 30: 3489–3496.
11. Favaro SL, Lopes MS, Neto AGVC, et al. Chemical, morphological, and mechanical analysis of rice husk/post-consumer polyethylene composites. *Composites Part A* 2010; 41: 154–160.
12. Petchwattana N and Covavisaruch S. Influences of particle sizes and contents of chemical blowing agents on foaming wood plastic composites prepared from poly(vinyl chloride) and rice hull. *Mater Des* 2011; 32: 2844–2850.
13. Mirzaei B, Tajvidi M, Falk RH, et al. Stress-relaxation behavior of lignocellulosic high-density polyethylene composites. *J Reinf Plast Compos* 2011; 30: 875–881.
14. Khalid M, Ratnam CT, Chuah TG, et al. Comparative study of polypropylene composites reinforced with oil palm empty fruit bunch fiber and oil palm derived cellulose. *Mater Des* 2008; 29: 173–178.
15. Mishra S and Aireddy H. Evaluation of dielectric behavior of bio-waste reinforced polymer composite. *J Reinf Plast Compos* 2011; 30: 134–141.
16. Karmarkar A, Chauhan SS, Modak JM, et al. Mechanical properties of wood–fiber reinforced polypropylene composites: effect of a novel compatibilizer with isocyanate functional group. *Composites Part A* 2007; 38: 227–233.
17. Najafi SK, Kiaefar A, Hamidina E, et al. Water absorption behavior of composites from sawdust and recycled plastics. *J Reinf Plast Compos* 2007; 26: 341–348.
18. Law TT and Ishak ZAM. Water absorption and dimensional stability of short kenaf fiber-filled polypropylene composites treated with maleated polypropylene. *J Appl Polym Sci* 2011; 120: 563–572.
19. Khanjanzadeh H, Tabarsa T and Shakeri A. Morphology, dimensional stability and mechanical properties of polypropylene-wood flour composites with and without nanoclay. *J Reinf Plast Compos* 2012; 31: 341–350.
20. Li B, Jiang H, Guo L, et al. Comparative study on the effect of manchurian ash and larch wood flour on mechanical property, morphology, and rheology of HDPE/wood flour composites. *J Appl Polym Sci* 2008; 107: 2520–2530.

21. Martinello T, Kaneko TM, Velasco MVR, et al. Optimization of poorly compactable drug tablets manufactured by direct compression using the mixture experimental design. *Int J Pharm* 2006; 322: 87–95.
22. Jun Z, Xiang-Ming W, Jian-Min C, et al. Optimization of processing variables in wood–rubber composite panel manufacturing technology. *Bioresour Technol* 2008; 99: 2384–2391.
23. Matuana LM and Mengeloglu F. Manufacture of rigid PVC/wood-flour composite foams using moisture contained in wood as foaming agent. *J Vinyl Addit Technol* 2002; 8: 264–270.
24. Stark NM and Matuana LM. Ultraviolet weathering of photostabilized wood-flour-filled high-density polyethylene composites. *J Appl Polym Sci* 2003; 90: 2609–2617.
25. Montgomery DC. *Design and analysis of experiments*, 7th edn. Hoboken, NJ: John Wiley & Sons, Inc., 2009.
26. Khosrowshahi YB and Salem A. Influence of polyvinyl alcohol and carboxymethyl cellulose on the reliability of extruded ceramic body: application of mixture design method in fabricating reliable ceramic raschig rings. *Int J Appl Ceram Technol* 2011; 8: 1334–1343.
27. Homkhiew C, Ratanawilai T and Thongruang W. Effect of wood flour content and cooling rate on properties of rubberwood flour/recycled polypropylene composites. *Adv Mater Res* 2012; 488–489: 495–500.
28. Amini M, Younesi H, Bahramifar N, et al. Application of response surface methodology for optimization of lead biosorption in an aqueous solution by *Aspergillus niger*. *J Hazard Mater* 2008; 154: 694–702.
29. Myers RH, Montgomery DC and Anderson-Cook CM. *Response surface methodology: Process and product optimization using designed experiments*, 3th edn. Hoboken, NJ: John Wiley & Sons, Inc., 2009.
30. Shakeri A and Ghasemian A. Water absorption and thickness swelling behavior of polypropylene reinforced with hybrid recycled newspaper and glass fiber. *Appl Compos Mater* 2010; 17: 183–193.
31. Sathishkumar TP, Navaneethakrishnan P, Shankar S, et al. Mechanical properties and water absorption of snake grass longitudinal fiber reinforced isophthalic polyester composites. *J Reinf Plast Compos* 2013; 32: 1211–1223.
32. Adhikary KB, Pang S and Staiger MP. Long-term moisture absorption and thickness swelling behaviour of recycled thermoplastics reinforced with pinus radiata sawdust. *Chem Eng J* 2008; 142: 190–198.
33. Mohebby B, Younesi H, Ghotbifar A, et al. Water and moisture absorption and thickness swelling behavior in polypropylene/wood flour/glass fiber hybrid composites. *J Reinf Plast Compos* 2010; 29: 830–839.
34. Wechsler A and Hiziroglu S. Some of the properties of wood–plastic composites. *Build Environ* 2007; 42: 2637–2644.
35. Nourbakhsh A and Ashori A. Influence of nanoclay and coupling agent on the physical and mechanical properties of polypropylene/bagasse nanocomposite. *J Appl Polym Sci* 2009; 112: 1386–1390.
36. Tamrakar S and Lopez-Anido RA. Water absorption of wood polypropylene composite sheet piles and its influence on mechanical properties. *Constr Build Mater* 2011; 25: 3977–3988.
37. Masoodi R and Pillai KM. A study on moisture absorption and swelling in bio-based jute-epoxy composites. *J Reinf Plast Compos* 2012; 31: 285–294.
38. Ashori A and Nourbakhsh A. Mechanical behavior of agro-residue-reinforced polypropylene composites. *J Appl Polym Sci* 2009; 111: 2616–2620.
39. Rahman MR, Huque MM, Islam MN, et al. Improvement of physico-mechanical properties of jute fiber reinforced polypropylene composites by post-treatment. *Composites Part A* 2008; 39: 1739–1747.
40. Mohanty S, Verma SK, Nayak SK, et al. Influence of fiber treatment on the performance of sisal–polypropylene composites. *J Appl Polym Sci* 2004; 94: 1336–1345.

Elsevier Editorial System(tm) for Composites Part A
Manuscript Draft

Manuscript Number: JCOMA-13-856

Title: Time-temperature and stress dependent behaviors of composites between recycled polypropylene and rubberwood flour

Article Type: Research Paper

Keywords: A. Polymer-matrix composites (PMCs); B. Creep; C. Analytical modeling; E. Extrusion

Corresponding Author: Dr. Thanate Ratanawilai, Ph.D.

Corresponding Author's Institution: Prince of Songkla University

First Author: Chatree Homkhiew, Ph.D.

Order of Authors: Chatree Homkhiew, Ph.D.; Thanate Ratanawilai, Ph.D.; Wiriya Thongruang, Ph.D.

Abstract: The effects of time, temperature, and stress on the flexural creep of composites from recycled polypropylene (rPP) and rubberwood flour (RWF) were experimentally investigated and modeled numerically. Creep increased with time, temperature, and stress, as expected. Burger, Power law, and HRZ models fit the creep profiles well in general, but at high temperature and stress levels the Power law and HRZ models performed poorly. However, the HRZ model interpolated creep well across the applied stresses, or across the temperatures. The time-temperature superposition (TTS) and time-stress superposition (TSS) principles were used to model long-term creep. The master curves from TTS and TSS principles were in good agreement with each other. They predicted that the lifetime limitation by long-term creep exceeds 10 years for 15 MPa stress at 25 oC, and is irrelevant for 3 MPa stress at the same temperature. All these results pertain to a specific formulation of rPP/RWF composites.

Suggested Reviewers: Salim Hiziroglu
Natural Resource Ecology & Management, Oklahoma State University
salim.hiziroglu@okstate.edu

Narongrit Sombatsompop
School of Energy Environmenta and Materials , King's Mongkut University of Technology Thonburi
narongrit.som@kmutt.ac.th

Norma Marcovich
Materials Engineering, University of Mar del Plata
marcovic@fi.mdp.edu.ar

Kristiina Oksman
Engineering Sciences and Mathematics, Luleå University of Technology
kristiina.oksman@ltu.se

Time-temperature and stress dependent behaviors of composites between recycled polypropylene and rubberwood flour

Chatree Homkhiew[1], Thanate Ratanawilai[1]*, Wiriya Thongruang[2]

[1]Department of Industrial Engineering, Faculty of Engineering, Prince of Songkla University, Hat Yai, Songkhla 90112, Thailand

[2]Department of Mechanical Engineering, Faculty of Engineering, Prince of Songkla University, Hat Yai, Songkhla 90112, Thailand

* Corresponding author. Tel.: +6674 287151; Fax: +6674 558829.

E-mail addresses: thanate.r@psu.ac.th (T. Ratanawilai)

Abstract

The effects of time, temperature, and stress on the flexural creep of composites from recycled polypropylene (rPP) and rubberwood flour (RWF) were experimentally investigated and modeled numerically. Creep increased with time, temperature, and stress, as expected. Burger, Power law, and HRZ models fit the creep profiles well in general, but at high temperature and stress levels the Power law and HRZ models performed poorly. However, the HRZ model interpolated creep well across the applied stresses, or across the temperatures. The time-temperature superposition (TTS) and time-stress superposition (TSS) principles were used to model long-term creep. The master curves from TTS and TSS principles were in good agreement with each other. They predicted that the lifetime limitation by long-term creep exceeds 10 years for 15 MPa stress at 25 °C, and is irrelevant for 3 MPa stress at the same temperature. All these results pertain to a specific formulation of rPP/RWF composites.

Keywords: A. Polymer-matrix composites (PMCs); B. Creep; C. Analytical modeling; E. Extrusion

1. Introduction

In recent decades, reinforcing thermoplastics with inorganic fibers such as carbon, glass, graphite, and talc, has successfully produced high performance composites [1]. Also the reinforcement use of organic fibers in plastic composites, particularly use of wood flour, is of great interest due to several potential advantages, such as low cost, biodegradability, low health hazard during handling, and non-abrasive nature [2]. Therefore the use of wood flour to replace inorganic filler has an increasing trend in the plastic composite industries. Wood-plastic composites (WPCs) may have good moisture resistance and dimensional stability because of the continuous thermoplastic matrices [3]. They have been largely used as a replacement for softwood lumber as decking, railings, door and window frames, and other outdoor applications, where they have better durability than softwood lumber [4, 5].

Rubber tree (*Hevea brasiliensis*) is widely planted in Thailand for the production of latex, and is cut down when it becomes unproductive at about 25 years of age [6]. Rubberwood lumber is mainly used to produce furniture, toys, and packing materials. In these rubberwood industries, a large amount of wood waste in the forms of flour, sawdust, and chips, is generated at different stages of processing. Generally, rubberwood waste is dumped in landfills or burned, but some of the waste is also used to produce medium-density fiberboard and particle board [7]. The utilization of rubberwood waste as a filler in polymer composites could decrease environmental impacts from the waste, as well as add value when contributing to the composite properties.

The mechanical characteristics of WPCs include creep, i.e. time-dependent deformation under loading, due to their continuous thermoplastic matrices, and such creep is a critical issue in many engineering applications; for example biomedical, aerospace, and civil engineering infrastructure applications [8]. Hence, creep is an important material characteristic in the design of wood-plastic composite products, and relates to load-bearing capacity of end products. Likewise, durability and lifetime limitations of products, from intolerably large deformations, should be estimated at the design stage [9]. Environmental parameters, such as temperature and humidity, influence the creep of WPCs, because of temperature effects on the polymer and moisture effects on the wood filler [10]. Long term evaluation of creep would be prohibitively costly, so accelerated testing methods and mathematical models are used instead [10]. Acha et al. [8] investigated the effects of modifying the interfacial adhesion between jute and polypropylene on the creep behavior, and used the time-temperature superposition (TTS) to predict long-term creep deformation. Mosiewicki et al. [11] experimentally evaluated the creep of composites made from linseed oil -based polyester thermoset, and compared the results with Power law and Burger models; both models fit the data well. Chevali et al. [12] studied flexural creep behavior of nylon 6/6, polypropylene, high-density polyethylene, and their long fiber thermoplastic composites. The HRZ (for Hadid, Rechak, and Zouani, [13]) model provided an excellent fit to the experimental data, and the master curves obtained from TTS were able to predict the long-term creep. Banik et al. [14] investigated the influence of unidirectional and cross-ply polypropylene composites on the creep behavior, and both Burger and Findley power law models were satisfactory for fitting short-term creep behavior. Subramanian and Senthilvelan [15] experimentally evaluated the creep of leaf springs from glass-fiber-reinforced thermoplastic composites at various loads, and compared the results with the HRZ model. Despite extensive prior research on inorganic fiber and natural fiber reinforced plastics, only

a few studies on creep behavior have used rubberwood flour (RWF) to reinforce virgin plastics, and there is no prior report on the creep of RWF-reinforced postconsumer plastics that we focus on.

In our earlier work, the formulation of recycled polypropylene/RWF composites was optimized for select mechanical properties, but creep deformation was not investigated. The evaluation of creep is necessary for developing a new product subjected to long-term loading, when the materials are known to have viscoelastic time-dependent behavior. Therefore, creep must affect the design of WPCs and selecting their end-use applications. The objective of current work was to investigate the creep characteristics of composites made from recycled polypropylene and rubberwood flour, in particular the effects of temperature and stress levels. The Burger, Power law, and HRZ models were fit to short-term creep data. The time-temperature superposition and the time-stress superposition (TSS) principles were used to construct master curves of creep deformation, for predicting long-time creep.

2. Materials and experimental details

2.1 Materials

Rubberwood flour collected from local furniture factory was used as reinforcing filler. Before use it was sieved through a standard sieve of mesh size 80 (passing particles smaller than 180 μm) and dried in an oven at 110 °C for 8 h to minimize the moisture content. The main chemical constituents of rubberwood are: cellulose (39%), hemicellulose (29%), lignin (28%), and ash (4%) [16]. The matrix polymer was recycled polypropylene (rPP), purchased as pellets with a melt flow index of 11 g/10 min at 230 °C from Withaya Intertrade Co., Ltd (Samutprakarn, Thailand). Maleic anhydride grafted polypropylene (MAPP) with 8-10% of maleic anhydride, used as a coupling agent to improve interfacial bonding between wood flour and plastic matrix, was supplied by Sigma-Aldrich (Missouri, USA). TH Color Co., Ltd

(Samutprakarn, Thailand) supplied hindered amine light stabilizer additive, under the trade name MEUV008, chosen as the ultraviolet (UV) stabilizer. Paraffin wax used as lubricant (Lub) in processing was procured from Nippon Seiro Co., Ltd (Yamaguchi, Japan).

The composite formulation was held constant at 50.3 wt% rPP, 44.5 wt% RWF, 3.9 wt% MAPP, 0.2 wt% UV stabilizer, and 1.0 wt% Lub. In our prior work this formulation had the maximal 47.28 MPa flexural strength, and modulus 2527 MPa.

2.2 Preparation of composites samples

The WPCs were produced in a two-step process. In the first step to produce WPC pellets, RWF and rPP were blended and formed into composite pellets using a twin-screw extruder (Model SHJ-36 from En Mach Co., Ltd, Nonthaburi, Thailand). Barrel temperatures in ten zones were set in the range 130-170 °C from feed to die, to limit degradation of the raw materials, while the screw rotating speed was controlled at 70 rpm. The extrudate was passed through a water bath and was subsequently pelletized. In the second step to produce WPC panels, the WPC pellets were again dried prior to use, in an oven at 110 °C for 8 h. The WPC pellets, MAPP, UV stabilizer, and lubricant were dry-mixed, and fed to the twin-screw extruder. The extruding conditions were as follows: (1) temperature profiles: 130–190 °C; (2) screw rotating speed: 50 rpm; (3) vacuum venting at 9 temperature zones: 0.022 MPa; and (4) melt pressure: 0.10-0.20 MPa. The samples were extruded through a rectangular 9 × 22 mm^2 die and cooled in atmospheric air. Consequently, the specimens were machined, following the flexural creep testing standard of American Society for Testing and Materials (ASTM).

2.3 Characterization

Short-term creep tests of rPP/RWF composites were carried out using an Instron Universal Testing Machine (Model 5582 from Instron Corporation, Massachusetts, USA) with three-

point bending as shown in Figure 1, following ASTM D2990 standard. In all tests, the flexural strain was measured by an Instron extensometer with a travel of 5 mm and a gauge length of 10 mm. The specimens were 13 × 4.8 × 100 mm^3 (width × thickness × length), and the test span was 80 mm in the direction of extrusion. To evaluate the effects of various stress levels, creep tests were conducted at 25 °C ambient temperature at ten different stress levels: 3, 7, 11, 15, 19, 23, 27, 31, 35, and 39 MPa. Five levels of temperature in the range from 25 to 65 °C, were used with constant 19 MPa stress to assess temperature effects. This constant stress was approximately 40% of the ultimate flexural strength, from quasi-static tests at 25 °C. Before each creep test the specimens were equilibrated in an environmental chamber for 15 min. The loading duration of a test was 6000 sec (100 min), and there were five replicates at each test condition.

2.4 Creep models

Creep is the slow deformation of a material under constant stress. It is important in applications with long-term loading. When a material subjected to constant load creeps, its deflection continuously accumulates with time [14, 17]. Wood-reinforced plastics show this type of viscoelastic behavior. The creep strain of polymers or wood-plastic composites, $\varepsilon(\sigma, t, T)$, mainly depends on stress (σ), time (t), and temperature (T) [18, 19]. Conceptually this strain has three main components: (i) elastic deformation (stress-temperature dependence, reversible) $\varepsilon_e(\sigma, T)$; (ii) viscoelastic deformation (stress-time-temperature dependence, reversible) $\varepsilon_{ve}(\sigma, t, T)$; and (iii) viscoplastic deformation (stress-time-temperature dependence, irreversible) $\varepsilon_p(\sigma, t, T)$ [18, 19]:

$$\varepsilon(\sigma,t,T) = \varepsilon_e(\sigma,T) + \varepsilon_{ve}(\sigma,t,T) + \varepsilon_p(\sigma,t,T) \quad (1)$$

The modeling of experimental data helps bridge the gap between material properties and engineering designs [17]. For applications to predicting the creep behavior of WPCs, several models developed from the constitutive relations of polymeric materials [14] can be explored. If reinforced polymer materials are tested within their linearly viscoelastic range, simple rheological models are appropriate [14]. A simple constitutive model, the four-element Burger model, has given satisfactory descriptions and predictions [14, 20, 21]. It combines Maxwell and Kelvin-Voigt models; instantaneous deformation comes from the Maxwell spring; viscoelastic deformation from Kelvin units; and viscoplastic deformation from the Maxwell dashpot [22]. The mathematical description for response to constant stress is:

$$\varepsilon(t) = \frac{\sigma}{E_M} + \frac{\sigma}{E_K}\left[1 - \exp\left(-t\frac{E_K}{\eta_K}\right)\right] + t\frac{\sigma}{\eta_M} \tag{2}$$

where ε is the strain at time t, with constant stress σ. E_M and E_K are the elastic moduli, and η_M and η_K are the viscosities, of the Maxwell and Kelvin bodies, respectively [21]. Especially with non-linear creep behavior, empirical mathematical models have often been applied with satisfactory prediction, despite simple forms [14, 23]. An example of such simple model is the Power law model. Subramanian and Senthilvelan [15] and Hadid et al. [13] used the Power law model for the three-point bending creep of glass fiber reinforced thermoplastics. Also the American Society of Civil Engineers (ASCE) recommend this model for the analysis of composite materials under long-term structural loading, in their structural plastics design manual [15, 24]. The Power law equation is:

$$\varepsilon(t) = r_0 t^n \tag{3}$$

where ε is the creep strain at time t. r_0 is a coefficient, and n is the Power law exponent [23].

The two Power law parameters, the coefficient and the exponent, are significantly affected by the stress level [15]. This model was modified by Hadid et al. [13] to incorporate also stress dependence. This HRZ model has the form:

$$\varepsilon(t) = a \cdot \sigma^{b} \cdot t^{c \exp(e\sigma)} \tag{4}$$

where the model parameters a, b, c, and e are fit to data by non-linear regression. Subramanian and Senthilvelan [15], and Chevali et al. [12], used the HRZ model to fit experimental data, finding excellent fit to short-time flexural creep over a wide range of stresses.

2.5 Time-temperature and stress superposition

Time-temperature and stress superposition principles are widely used with viscoelastic materials such as wood-reinforced plastics. They are empirical relationships between time and temperature, or time and stress [25], stating that the effect of a constant temperature or stress change on a time-dependent response equals a uniform shift in logarithmic time-scale [25]. Then a single master curve at a reference temperature (or stress), using a logarithmic time scale, includes the creep curves obtained at different temperatures (or stresses); these are superposed on the master curve by a horizontal shift [11]. The master curve can be used to predict creep response at large time scales, even if experiments are limited to short times.

3. Results and discussion

3.1 Effect of the various stress levels

In service the plastic composites may be subjected to long-term stresses. The logarithmic re-scaling of time, according to the superposition principles, suggests accelerated testing by use of elevated stresses and/or temperatures, so a range of each was experimented with. The creep strain against time, with the specific composite formulation described earlier, is shown

at different stress levels ranging from 3 MPa to 39 MPa in Figure 2. The creep of the rPP/RWF composites was clearly dependent on the test stress, and increased with the stress level as expected. At the highest applied 39 MPa stress (83% of ultimate strength) the rate of creep deformation was the highest. At stresses close to the 47.28 MPa ultimate strength the mobility of the macromolecular chains strongly increases, and this mobility leads to eventual failure of the test specimen.

The creep was modeled with equations (2) and (3), for Burger and Power law models. The solid and dashed lines represent the fit for each stress level of Burger and Power law models, respectively, while symbols in the legend represent experimental averages across replicates. Both Burger and Power law models fit the experimental data overall well, but at 39 MPa stress level the Burger model is clearly better. This is not surprising since the Power law model is simpler with fewer parameters than the Burger model [11]. Also Hadid et al. [13] observed poorer fits at higher stress levels.

The fitted parameters of Burger and Power law models obtained from the rPP/RWF composites are shown in Table 1. All parameters (E_M, E_K, η_M, and η_K) in the Burger model decrease with stress level. The moduli (E_M and E_K) decrease because new mechanisms of molecular bond breaking and slippage emerge as stress is increased. The viscosities (η_M and η_K) similarly decrease due to increased polymer chain mobility. The Power law parameter r_0 is for instantaneous strain (time-independent) and relates to the elastic initial response, while the parameter n relates to viscous creep response (time-dependent) [11]. Both parameters increase with the stress level for the same molecular mobility reasons just discussed.

3.2 Effects of temperature

The short-term bending creep responses of rPP/RWF composites at five different temperatures are shown in Figure 3. The creep curves were still in the secondary creep stage at the end of the tests for temperatures from 25 °C to 55 °C, but the highest 65 °C temperature produced failure after 1500 sec (25 min), before the end of the test duration, and showed the tertiary creep stage. This indicates that 65 °C is a critical temperature for our recycled polypropylene composites containing 44.5 wt% of rubberwood flour. Both the instantaneous deformation and viscous creep increase with temperature, see Figure 5. Normally, thermoplastic materials are softened by an increase in temperature and creep deformation of matrix-dominant composites increases [1].

The curve fits with Burger and Power law models are included in Figure 3, with solid and dashed lines. The fits were otherwise good, but at high temperatures (55 °C and 65 °C) the Power law model performed poorly. The Power law model appears appropriate with small creep deformation only, while the Burger model fits all of the data well. This might be due to the better flexibility of Burger model, as it has more parameters, or due to this model actually describing some of the mechanisms determining the constitutive behavior [14].

The Burger parameters listed in Table 1 decrease with temperature. The moduli may decreasing due to softening of the composite materials [14]. Likewise, the viscosities decrease and contribute to creep deformation with increasing temperature [14]. This confirms increasing molecular mobility with temperature [11, 14]. The parameters of Power law model both increased with temperature due to the same reasons [11].

3.3 Empirical model for short-term creep

The creep of the rPP/RWF composites for stresses from 3 MPa to 39 MPa and temperatures ranging from 25 °C to 65 °C is shown in Figures 2 and 3. The Power law coefficient r_0 and

the exponent n increase with stress and temperature levels. This agrees with prior work in Subramanian and Senthilvelan [15], and Hadid et al. [13].

Figures 4 and 5 show the curve fits of the type used in the HRZ model, of the Power law parameters. The found HRZ model parameters (a, b, c, and e) are shown in these figures and listed in Table 2. Parameters a and b are determined by the instantaneous elastic strain immediately after load application, and depend on the degree of crystallinity and glass transition temperature [12, 15, 26]. Parameters c and e describe how the creep depends on stress, testing time, and relaxation of the composites [12, 15]. The HRZ and Power law fits are shown in Figures 6 and 7. The HRZ model fits the data almost as well as the Power law fits of individual curves, but performs poorly at the highest stress level tested. Similar lack of fit at high stresses was found by Hadid et al. [13] and Subramanian and Senthilvelan [15]. The HRZ model allows interpolation between the stresses and temperatures used experimentally.

3.4 Time-temperature and stress superposition

In order to predict the long-term creep behavior of the composites, the time-temperature superposition (TTS) and the time-stress superposition (TSS) principles were utilized, using master curves produced from the short-term creep tests accelerated by temperature and stress. In Figure 8, the creep data from different temperatures are superposed by horizontal shifts of log time scale. The reference temperature chosen was 25 °C, and the master curve constructed reveals long-term behavior at this temperature, based on accelerated testing. Figure 9 has similarly constructed master curve from the various stress levels, with 19 MPa as the reference stress whose long-term creep is revealed.

The creep of the rPP/RWF composites for stresses from 3 MPa to 39 MPa and temperatures ranging from 25 °C to 65 °C is shown in Figures 2 and 3. The Power law coefficient r_0 and

In order to show the lifetime creep deformation of rPP/RWF composites, Figure 10 displays master curves at reference temperature 25 °C with constant load 19 MPa as well as reference stresses at 3, 11, 15, and 19 MPa with temperature fixed at 25 °C, with the vertical lines indicating 1, 10, 100, and 1000 years [27]. The two master curves, accelerated by temperature and stress, agree well at 25 °C and 19 MPa. The highest temperature tested affected the curve from temperature acceleration, causing deviation of the two master curves at high strain. The two master curves predict a lifetime of less than 1 year at this stress level. However, at lower stress levels and 25 °C the predicted lifetimes of rPP/RWF composites exceed 10 years for 15 MPa stress and 1000 years for 3 MPa stress.

4. Conclusions

Creep deformation is an important characteristic of a composite material, when the end products are subjected to loading. The creep of a specific composite formulation from recycled polypropylene and rubberwood flour was investigated experimentally and modeled numerically. The creep was dependent on both temperature and stress, increasing with both of these. The Burger and Power law models were both able to fit well the creep data in general, but at high temperature and stress levels the Power law gave the poorer fit of these models. The HRZ model provided an approximate interpolation across temperatures or stresses of the Power law fits, and also fit these data well in cases where the Power law performed well. The master curves from time-temperature and time-stress superpositions were in good agreement with each other. From the master curves the long-term creep was predicted with stresses 3 and 15 MPa at 25 °C, suggesting that the creep-limited lifetime of rPP/RWF composites exceeds 10 years at the higher stress level, and is no longer a relevant limitation at the lower stress level.

Acknowledgements

The authors would like to express their thanks to the Prince of Songkla Graduate Studies Grant, the Government budget Fund (Research Grant Code: 2555A11502062) for financial support throughout this work, and Rubberwood Technology and Management Research Group (ENG-54-27-11-0137-S) of Faculty of Engineering, Prince of Songkla University, Thailand. We would also like to thank Research and Development Office (RDO) and Assoc. Prof. Seppo Karrila for editing this article.

References

[1] Park BD, Balatinecz JJ. Short term flexural creep behavior of wood-fi ber/polypropylene composites. Polym Compos. 1998; 19(4): 377-82.

[2] Peng X, Fan M, Hartley J, Al-Zubaidy M. Properties of natural fiber composites made by pultrusion process. J Compos Mater. 2011; 46(2): 237-46.

[3] Grubbstrom G, Holmgren A, Oksman K. Silane-crosslinking of recycled low-density polyethylene/wood composites. Compos A Appl Sci Manufac. 2010; 41(5): 678-83.

[4] Carroll DR, Stone RB, Sirignano AM, Saindon RM, Gose SC, Friedman MA. Structural properties of recycled plastic/sawdust lumber decking planks. Resour Conserv Recyc. 2001; 31(3): 241-51.

[5] Ganguly I, Eastin IL. Trends in the US decking market: A national survey of deck and home builders. The forestry chronicle. 2009; 85(1): 82-90.

[6] Rimdusit S, Smittakorn W, Jittarom S, Tiptipakorn S. Highly filled polypropylene rubber wood flour composites. Eng J. 2011; 15(2): 17-30.

[7] Homkhiew C, Ratanawilai T, Thongruang W. Composites from recycled polypropylene and rubberwood flour: Effects of composition on mechanical

properties. J Thermoplast Compos Mater. Epub ahead of print 14 February 2013.DOI: 10.1177/0892705712475019.

[8] Acha BA, Reboredo MM, Marcovich NE. Creep and dynamic mechanical behavior of PP–jute composites: Effect of the interfacial adhesion. Compos A Appl Sci Manufac. 2007; 38(6): 1507-16.

[9] Lai J, Bakker A. Analysis of the non-linear creep of high-density polyethylene. Polym. 1995; 36(1): 93-9.

[10] Chang FC, Lam F, Kadla JF. Using master curves based on time-temperature superposition principle to predict creep strains of wood-plastic composites. Wood Sci Technol. 2013; 47(3): 571-84.

[11] Mosiewicki MA, Marcovich NE, Aranguren MI. Creep behavior of wood flour composites made from linseed oil-based polyester thermosets. J Appl Polym Sci. 2011; 121(5): 2626-33.

[12] Chevali VS, Dean DR, Janowski GM. Flexural creep behavior of discontinuous thermoplastic composites: Non-linear viscoelastic modeling and time-temperature-stress superposition. Compos A Appl Sci Manufac. 2009; 40(6-7): 870-7.

[13] Hadid M, Rechak S, Zouani A. Empirical nonlinear viscoelastic model for injection molded thermoplastic composite. Polym Compos. 2002; 23(5): 771-8.

[14] Banik K, Karger-Kocsis J, Abraham T. Flexural creep of all-polypropylene composites: Model analysis. Polym Eng Sci. 2008; 48(5): 941-8.

[15] Subramanian C, Senthilvelan S. Short-term flexural creep behavior and model analysis of a glass-fiber-reinforced thermoplastic composite leaf spring. J Appl Polym Sci. 2011; 120(6): 3679-86.

polypropylene and rubberwood flour: Effects of composition on mechanical

[16] Petchpradab P, Yoshida T, Charinpanitkul T, Matsumura Y. Hydrothermal pretreatment of rubber wood for the saccharification process. Ind Eng Chem Res. 2009; 48(9): 4587-91.

[17] Schildmeyer AJ. Temperature and time dependent behaviors of a wood-polypropylene composite. Civil and environmental engineering. Master of science in civil engineering. Washington state university, 2006.

[18] Dorigato A, Pegoretti A, Kolarik J. Nonlinear tensile creep of linear low density polyethylene/fumed silica nanocomposites: Time-strain superposition and creep prediction. Polym Compos. 2010; 31(11): 1947-55.

[19] Kolarik J, Pegoretti A, Fambri L, Penati A. Prediction of nonlinear long-term tensile creep of heterogeneous blends: Rubber-toughened polypropylene-poly(styrene-co-acrylonitrile). J Appl Polym Sci. 2003; 88(3): 641-51.

[20] Liu H, Yao F, Xu Y, Wu Q. A novel wood flour-filled composite based on microfibrillar high-density polyethylene (HDPE)/nylon-6 blends. Biores Technol. 2010; 101(9): 3295-7.

[21] Tamrakar S, Lopez-Anido RA, Kiziltas A, Gardner DJ. Time and temperature dependent response of a wood-polypropylene composite. Compos A Appl Sci Manufac. 2011; 42(7): 834-42.

[22] Xu Y, Wu Q, Lei Y, Yao F. Creep behavior of bagasse fiber reinforced polymer composites. Biores Technol. 2010; 101(9): 3280-6.

[23] Hadid M, Rechak S, Tati A. Long-term bending creep behavior prediction of injection molded composite using stress-time correspondence principle. Mater Sci Eng A. 2004; 385(1-2): 54-58.

[24] American Society of Civil Engineers, Structural plastic design manual: ASCE Publications: New York, 1986.

[25] Chang FC. Lam F. Kadla JF. Application of time-temperature-stress superposition on creep of wood-plastic composites. Mech Time-Depend Mater. Epub ahead of print 6 October 2012. DOI: 10.1007/s11043-012-9194-9.

[26] Chevali VS. Janowski GM. Flexural creep of long fiber-reinforced thermoplastic composites: Effect of processing-dependent fiber variables on creep response. Compos A Appl Sci Manufac. 2010; 41(9): 1253-62.

[27] Goertzen WK. Kessler MR. Creep behavior of carbon fiber/epoxy matrix composites. Mater Sci Eng A. 2006; 421(1-2): 217-25.

prediction. Polym Compos. 2010; 31(11): 1947-55.

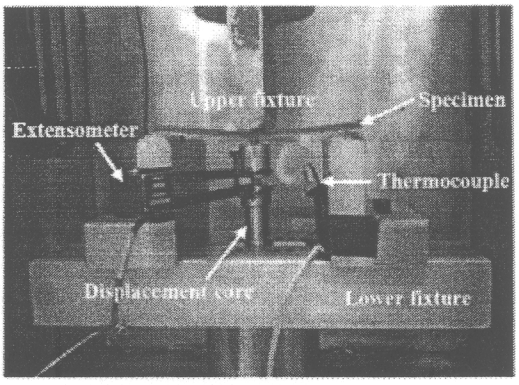

Fig. 1 Test apparatus for three-point bending creep

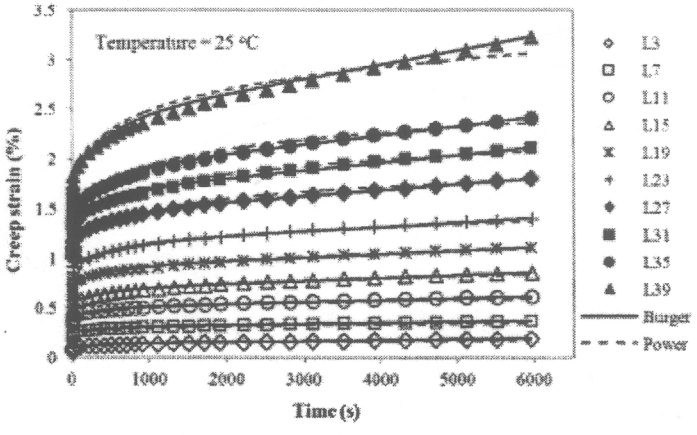

Fig. 2 Short-term flexural creep at different stress levels, fitted with Burger model (solid lines) and Power law model (dashed lines)

Table 1 Parameters of Burger model and Power law model

		Burger model				Power law model	
σ (MPa)	T (°C)	E_M (MPa)	E_K (MPa)	η_M (MPa·s)	η_K (MPa·s)	ε_0	n
3	25	2742	15268	6.62E + 07	7.83E + 06	0.079	0.089
7	25	2695	14815	6.27E + 07	7.41E + 06	0.158	0.091
11	25	2585	13679	5.79E + 07	6.84E + 06	0.260	0.095
15	25	2539	12714	5.53E + 07	6.36E + 06	0.358	0.098
19	25	2505	11970	5.35E + 07	5.49E + 06	0.457	0.101
23	25	2487	10705	5.09E + 07	4.82E + 06	0.561	0.103
27	25	2391	9879	4.51E + 07	4.45E + 06	0.722	0.105
31	25	2366	9847	4.04E + 07	4.43E + 06	0.814	0.108
35	25	2351	9025	3.85E + 07	4.06E + 06	0.903	0.111
39	25	2115	7422	2.69E + 07	3.34E + 06	1.108	0.117
19	35	2065	8004	3.49E + 07	4.00E + 06	0.583	0.104
19	45	1508	7691	2.84E + 07	3.85E + 06	0.771	0.106
19	55	1215	7386	1.56E + 07	3.69E + 06	0.905	0.109
19	65	967	7276	2.37E + 07	7.28E + 05	1.305	0.115

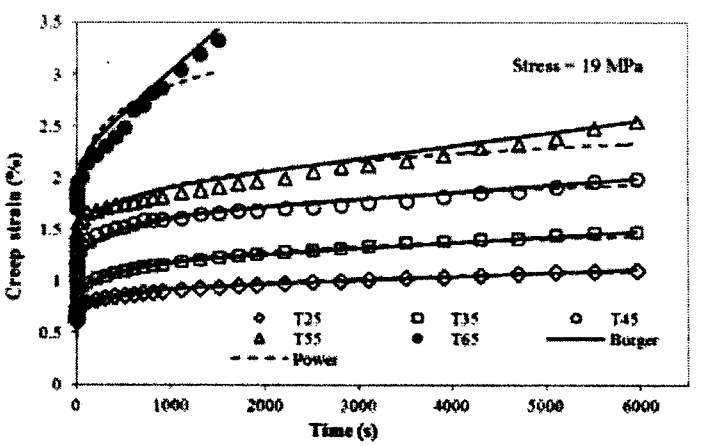

Fig. 3 Short-term flexural creep at different temperatures fitted with Burger model (solid lines) and Power law model (dashed lines)

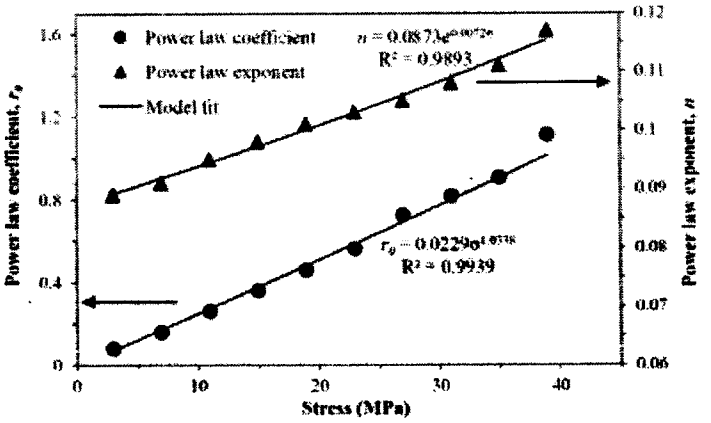

Fig. 4 Variation of Power law coefficient and exponent with stress level

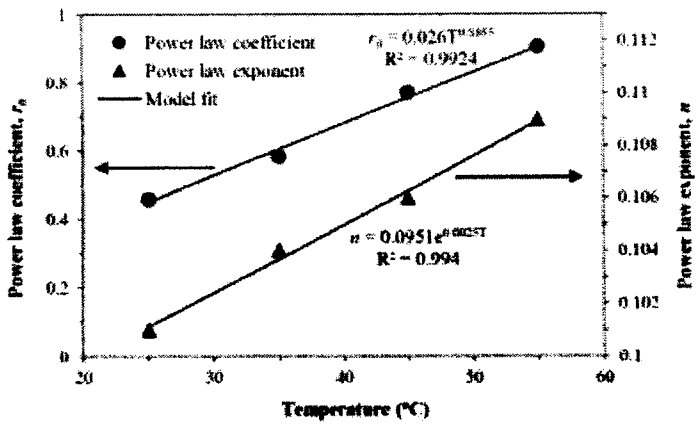

Fig. 5 Variation of Power law coefficient and exponent with temperature

Table 2 HRZ model parameters (*a*, *b*, *c*, and *e*) that allow interpolation of stress and temperature

Parameter	*a*	*b*	*c*	*e*
Stress dependence	0.023	1.034	0.087	0.0072
Temperature dependence	0.026	0.885	0.095	0.0025

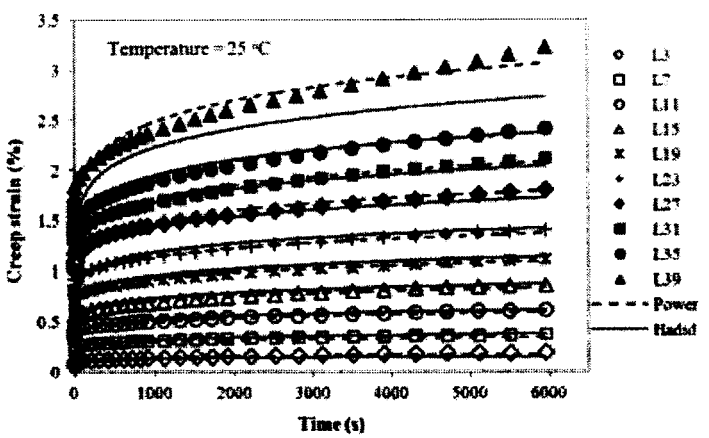

Fig. 6 Power law and HRZ model fits to the flexural creep curves at different stress levels

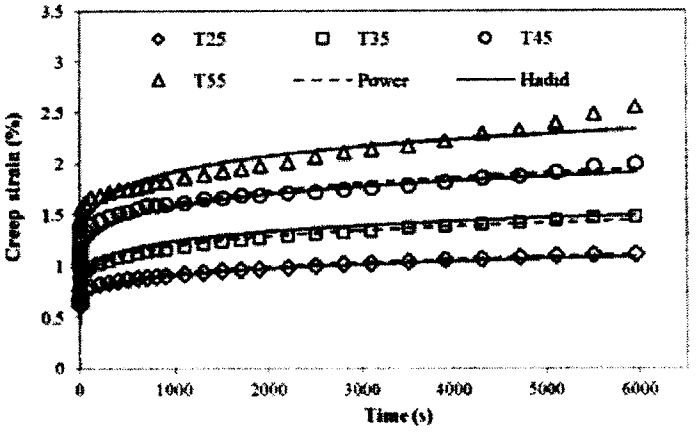

Fig. 7 Power law and HRZ model fits to the flexural creep curves at different temperatures

25

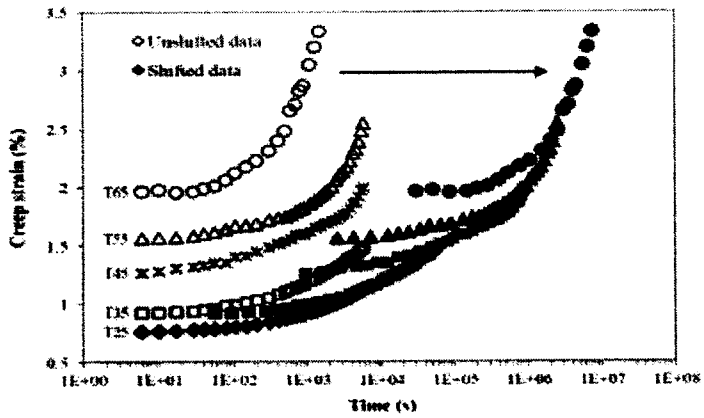

Fig. 8 Short-term creep curves superposed to a master curve; the reference temperature is 25 °C

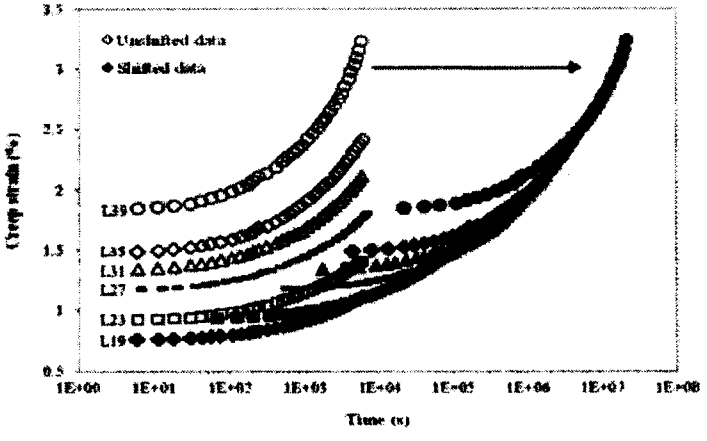

Fig. 9 Short-term creep curves superposed to a master curve; the reference stress is 19 MPa

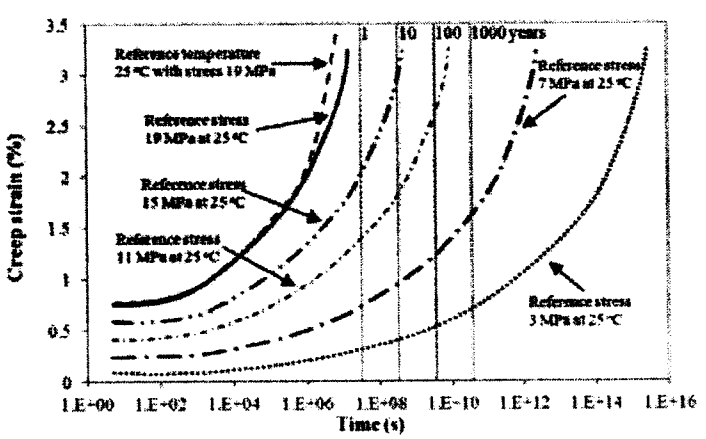

Fig. 10 Creep master curves for three-point flexure predict lifetimes